NASA CR-134553
BCAC D6-41244

# PROGRAM ON GROUND TEST OF MODIFIED QUIET, CLEAN, JT3D AND JT8D TURBOFAN ENGINES IN THEIR RESPECTIVE NACELLES

**Phase I Final Report**

N74-23349
NASA-CR-134553) PROGRAM ON GROUND TEST OF MODIFIED QUIET, CLEAN, JT3D AND JT8D TURBOFAN ENGINES IN THEIR RESPECTIVE NACELLES (Boeing Commercial Airplane Co., Seattle) 280 p HC $17.00 CSCL 21E
G3/28 Unclas 39185
281

September 1973

BOEING COMMERCIAL AIRPLANE COMPANY
A DIVISION OF THE BOEING COMPANY

prepared for

NATIONAL AERONAUTICS AND SPACE ADMINISTRATION

NASA Lewis Research Center
Contract NAS 3-16815

| 1. Report No. | 2. Government Accession No. | 3. Recipient's Catalog No. |
|---|---|---|
| NAS CR-134553 | | |

| 4. Title and Subtitle | 5. Report Date |
|---|---|
| PROGRAM ON GROUND TEST OF MODIFIED, QUIET, CLEAN, JT3D AND JT8D TURBOFAN ENGINES IN THEIR RESPECTIVE NACELLES–Phase 1 Final Report | September 1973 |
| | 6. Performing Organization Code |
| 7. Author(s) | 8. Performing Organization Report No. D6-41244 |
| 9. Performing Organization Name and Address<br>Boeing Commercial Airplane Company<br>P.O. Box 3707<br>Seattle, Washington 98124 | 10. Work Unit No. |
| | 11. Contract or Grant No. NAS 3-16815 |
| 12. Sponsoring Agency Name and Address<br>National Aeronautics and Space Administration<br>Washington, D.C. 20546 | 13. Type of Report and Period Covered<br>Contractor Report |
| | 14. Sponsoring Agency Code |

15. Supplementary Notes

Project Manager, A. A. Medeiros
JT3D/JT8D Refan Project
NASA Lewis Research Center, Cleveland, Ohio 44135

16. Abstract This report presents a summary of phase I of the "Program on Ground Test of Modified, Quiet, Clean JT3D and JT8D Turbofan Engines in their Respective Nacelles." This program is part of a joint DOT-NASA effort to reduce community noise levels of the commercial jet fleet. The program objective was preliminary development of three acoustically treated nacelle configurations for each of the 707, 727, and 737 series airplanes that would provide maximum noise reduction with minimum performance loss, modification requirements, and economic impact. Phase I included preliminary design, model testing, data analyses, and economic studies of proposed nacelle configurations. Funding limitations resulted in cancelling the 707 program, deleting the 737, and deferring a portion of the 727 program until phase II. The 707 nacelle configuration of prime interest at the time of cancellation had a treated, one-ring inlet, short fan ducts with simplified fan thrust reverser, and minimum change to the primary thrust reverser. The recommended 727 configuration had a treated inlet and nose dome, treated exhaust nozzle, and target-type thrust reverser. The 727 inlet is to be designed to accept the installation of a single treated ring, if required. The 737 configuration would also use a treated inlet and nose dome, treated exhaust nozzle, and target-type thrust reverser. Considerable additional development of these configurations will be necessary to complete the design. Economics were not a major influence, particularly, in the selection of the 727 and 737 nacelle configurations for further development. Modification of existing aircraft by installation of refanned engines/nacelles will cause minimum cash direct operating cost increases; however, the initial investment for the kit and installation is estimated to be sufficiently high to cause an unacceptable cash flow situation for the operators involved, thereby requiring other methods of financing.

| 17. Key Words (Suggested by Author(s)) | 18. Distribution Statement |
|---|---|
| Refan<br>Acoustic<br>Attenuation<br>Bypass | Unclassified–Unlimited |

| 19. Security Classif. (of this report) | 20. Security Classif. (of this page) | 21. No. of Pages | 22. Price* |
|---|---|---|---|
| Unclassified | Unclassified | 278 | |

*For sale by the National Technical Information Service, Springfield, Virginia 22151

# CONTENTS


| | | Page |
|---|---|---|
| 1.0 | SUMMARY | 1 |
| 2.0 | INTRODUCTION | 3 |
| 3.0 | 707 AIRPLANE | 7 |
| 3.1 | Airplane Description | 7 |
| 3.2 | Engine Definition | 7 |
| 3.3 | Model and Component Tests | 16 |
| 3.4 | Nacelle Preliminary Design | 23 |
| 3.5 | Airplane Modification | 39 |
| 3.6 | Maintenance Analysis and Support Equipment | 44 |
| 3.7 | Performance Comparison | 45 |
| 3.8 | Airplane and Community Noise Characteristics | 59 |
| 4.0 | 727 AIRPLANE | 75 |
| 4.1 | Airplane Description | 75 |
| 4.2 | Engine Definition | 75 |
| 4.3 | Model and Component Tests | 84 |
| 4.4 | Nacelle Preliminary Design | 100 |
| 4.5 | Airplane Modification | 129 |
| 4.6 | Maintenance Analysis and Support Equipment | 135 |
| 4.7 | Performance Comparison | 136 |
| 4.8 | Airplane and Community Noise Characteristics | 150 |
| 5.0 | 737 AIRPLANE | 173 |
| 5.1 | Airplane Description | 173 |
| 5.2 | Engine Definition | 179 |
| 5.3 | Model and Component Tests | 179 |
| 5.4 | Nacelle Preliminary Design | 183 |
| 5.5 | Airplane Modification | 211 |
| 5.6 | Maintenance Analysis and Support Equipment | 218 |
| 5.7 | Performance Comparison | 219 |
| 5.8 | Airplane and Community Noise Characteristics | 230 |
| 6.0 | ECONOMIC STUDIES | 251 |
| 6.1 | Objectives | 251 |
| 6.2 | Airplane/Fleet Operational Characteristics | 251 |
| 6.3 | Operating Costs | 254 |
| 6.4 | Fleet Modification Costs | 255 |
| 6.5 | Noise Comparisons | 258 |
| 6.6 | Market Characteristics | 261 |


 PRECEDING PAGE BLANK NOT FILMED

## CONTENTS (Concluded)

Page

7.0 SUMMARY OF RESULTS AND CONCLUSIONS . . . . . 267
7.1 707 Airplane . . . . . 267
7.2 727 Airplane . . . . . 267
7.3 737 Airplane . . . . . 268
7.4 Noise . . . . . 269
7.5 Economics . . . . . 269

APPENDIX A–REFERENCES . . . . . 271

APPENDIX B–DEFINITIONS . . . . . 272

APPENDIX C–SYMBOLS AND ABBREVIATIONS . . . . . 275

# 1.0 SUMMARY

The NASA sponsored Refan Program is one part of a joint DOT-NASA effort aimed at development of methods for reduction of environmental noise generated by the civil aviation jet fleet. The refan concept involves modification of existing engines and nacelles (engine installations) to achieve lower noise levels. The proposed engine modification involves a larger diameter fan and other associated hardware changes, thereby increasing the bypass ratio, increasing airflow, and reducing the noise-generating exhaust velocity. Nacelle modification, in addition to physical size increase to accept the larger engine, involves incorporation of acoustic treatment in the engine inlet and tailpipe. The program objective is to develop, design, manufacture, and test certifiable hardware which, if retrofit to the existing fleet, would reduce the community noise level to, or below, the FAR Part 36 limits for new airplanes. This is to be accomplished with minimum performance loss, at minimum retrofit cost, and minimum DOC increase.

Phase I of the program was authorized for the contractor under NASA contract NAS3-16815 "Program on Ground Test of Modified, Quiet, Clean JT3D and JT8D Turbofan Engines in Their Respective Nacelles" to investigate the concept as related to the JT3D and JT8D engines used on the contractor's airplanes. The objectives of this phase were to (1) provide documentation of planned installation of modified engines on their respective airplanes, (2) analyze the economic considerations and noise reduction tradeoffs involved in retrofitting the modified engines on their respective airplanes, (3) prepare a detailed proposal for phase II, (4) initiate model tests of nacelles and airplane configurations, and (5) initiate design of the nacelles.

This report covers the work accomplished during the contract period from 17 August 1972 through 11 July 1973. The JT3D work primarily considered the 707-320B airplane; the JT8D work considered the 727-200 and 737-200 airplanes. It is possible that the JT8D work could be applicable to all 727 and 737 airplanes produced to date.

Work completed under this program showed that the concept is technically practical and that noise reduction up to 13 to 20 EPNdB below the baseline airplane is attainable for the JT3D refanned engine installed on the 707 airplane and that reduction up to 8 to 13 EPNdB is attainable for the JT8D refanned engines installed on the 727 and 737 airplanes. These noise reductions are attainable with minimum performance loss.

The 707 nacelle configuration recommended for further investigation would have a treated inlet with one treated splitter ring, a short fan duct, a simplified cascade fan thrust reverser, a conical primary nozzle, and a modified primary thrust reverser. The selected airplane configuration would have an estimated $\Delta$OEW increase of 2565 lb (1163 kg), a range loss of 60 nmi (111 km),

and a reduction in takeoff field length of 1320 ft (426 m). Predicted range loss due to modification weight increase can be offset by increasing the maximum brake release gross weight within the present structural limits of the airplane and adding fuel in presently unused tank space.

The 727 nacelle modification recommended for further investigation would be either configuration 1, which has a treated inlet and treated tailpipe, or configuration 2, which has a treated inlet with a single treated splitter ring and treated tailpipe with a treated fan-primary divider. An exploratory model test of the new larger center-engine inlet and duct required for the modified engine has indicated that duct/engine compatibility can be attained with acceptable pressure recovery. Airplane configuration 1 would have an estimated ΔOEW increase of 3655 lb (1658 kg), a range loss of 220 nmi (407 km), and a reduction in takeoff field length of 1250 ft (381 m). The weight increase due to the proposed modification will affect airplane balance and ground handling characteristics. Several methods are shown for solving this problem. Baseline airplane range loss due to the modification weight increase can be compensated for in airline operation by increasing BRGW within presently certified limits.

The 737 nacelle modification recommended for further investigation would be similar to that for the 727 airplane. Additional modification required would be a tailpipe extension necessary to position the thrust reverser behind the flaps and rotation of the thrust reverser to achieve proper airflow patterns. Also, the inlet would be different due to inlet airflow angles and patterns. The larger nacelle will require an extended landing gear to maintain ground clearance. It would be expected that a 12 in. (0.305 m) extension will be sufficient. Airplane configuration 1 would have an estimated ΔOEW increase of 2380 lb (1080 kg), a range loss of 210 nmi (389 km), and a reduction in takeoff field length of 1290 ft (393 m). Presently available modifications will permit increasing the BRGW by up to 6000 lb (2727 kg) thereby permitting an airline operator to compensate for range loss if he so desires.

The results of economic studies show that the cost difference between configurations, particularly in the case of the 727 and 737 airplanes, was relatively small so that configuration selection would have to be based on considerations other than cost. These studies also showed that the initial investment for modification would create an unacceptable cash flow situation for the airlines that could only be solved by financial assistance. Airplane and engine modification projected costs are $1.5 to $2.2 million for the 707 series (depending upon the model), approximately $1.6 to $1.8 million for the 727 series, and approximately $1.5 to $1.5 million for the 737 series. Estimates of the cash (out-of-pocket) direct operating costs, of a representative average airplane, are less than 2.5% increase in DOC over the baseline airplanes.

From the work accomplished during phase I of the refan program, it is concluded that the noise reduction goals with minimum performance loss can be met for the 727 airplane using the configurations evaluated. Considerable development work would be necessary to define a final configuration for the 707 airplane. A configuration for the 737 airplane could be developed from the 727 configuration by making inlet and exhaust system changes.

## 2.0 INTRODUCTION

The largest portion of today's civil aviation fleet is powered by low bypass-ratio turbofan engines, and most of these airplanes are equipped with JT3D- or JT8D-series engines. More than 5000 JT3D engines and 6000 JT8D engines have been delivered to date, and approximately 3000 JT3D- and JT8D-powered airplanes are in service in the world airline fleet. These airplanes are expected to remain in service for a long time.

Estimated noise levels for the existing JT3D- and JT8D-powered fleets exceed the FAR Part 36 limits for new airplanes by as much as 11 EPNdB during takeoff (cutback) and by as much as 15 EPNdB during approach. Figure 1 presents a plot of estimated noise level versus gross weight for the two fleets. Achievement of the desired community noise levels represented by the FAR Part 36 limits required modification of the existing fleets.

Four approaches for reduction of noise levels from existing airplanes have been considered:

1) Nacelle treatment, with and without jet suppressors

2) A completely new engine

3) Replacement with new airplanes

4) Engine and nacelle modifications

Various studies, which considered the first three approaches, have been conducted under NASA and/or FAA contracts. The second and third approaches were found to be unacceptable in terms of cost. Considerable effort has been expended on the first approach, and evaluation is still being conducted. Recent studies and technical work have indicated that the fourth approach, engine and nacelle modification, is technically attractive because a revised engine cycle combined with an acoustically treated nacelle will provide greater noise attenuation with less performance loss than does nacelle treatment alone. The phase I development program was initiated to obtain data for further evaluation of this approach.

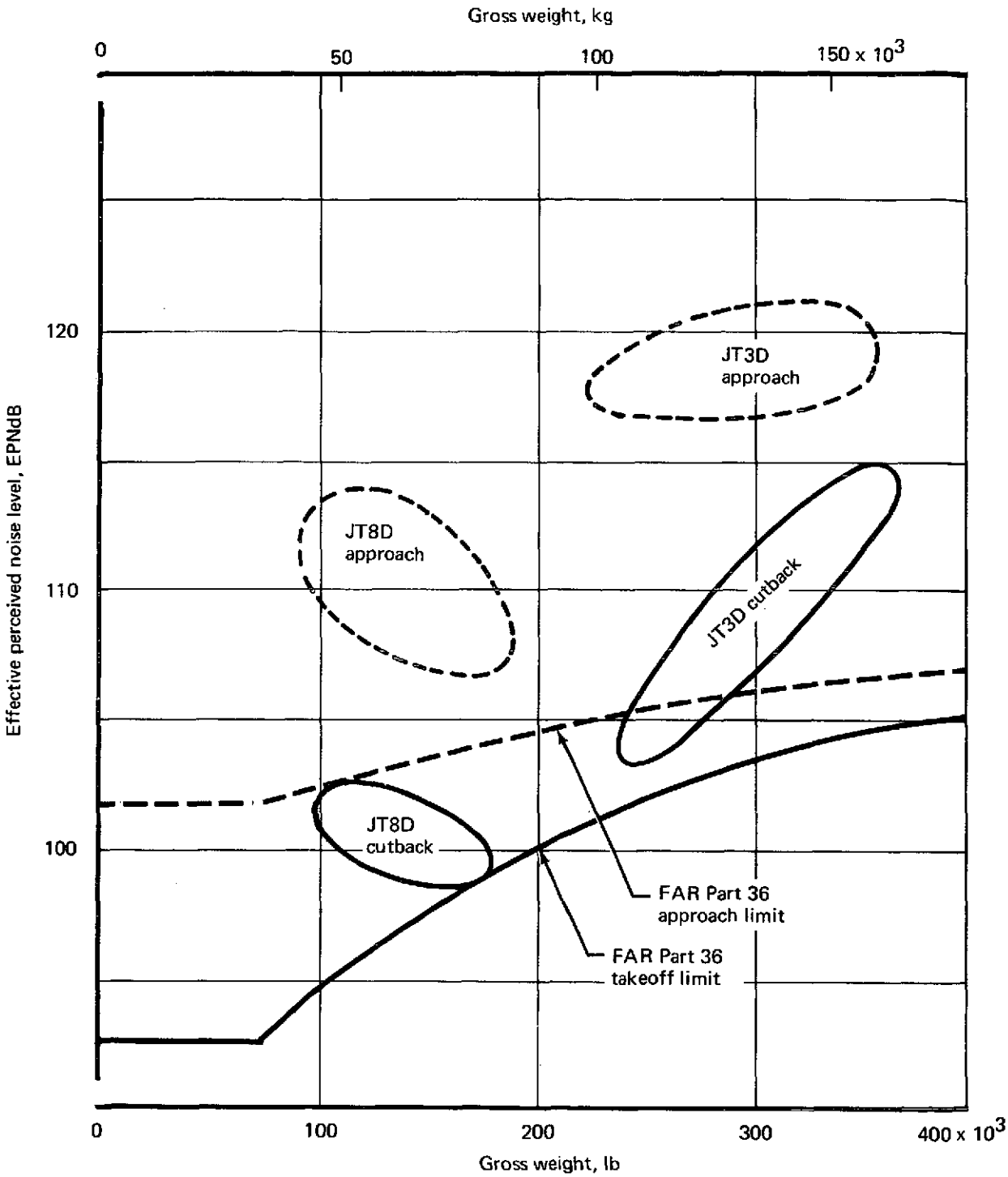


*FIGURE 1.—NOISE ESTIMATES—EXISTING JT3D/JT8D-POWERED AIRPLANES*

The refanned engine concept involves modification of existing engines by installing a larger diameter fan resulting in a higher bypass ratio and a larger total airflow. Extraction of more work from the primary gas flow to drive the larger fan results in a quieter primary exhaust. The higher total airflow provides increased thrust which allows a higher climb gradient and faster acceleration to climb speed, thereby reducing the area of noise exposure. The nacelle must be redesigned to accept the larger engine. Addition of acoustic treatment to the inlet and tailpipe of the modified nacelle will further reduce the noise level during all phases of engine operation.

This program was authorized by NASA contract NAS3-16815 for conduct of phase I of a two-part development program "Program on Ground Test of Modified, Quiet, Clean JT3D and JT8D Turbofan Engines in Their Respective Nacelles" as designed for installation on the applicable Boeing 707-, 727-, and 737-series airplanes. This contract was one of several independent contracts with the contractor, the engine manufacturer, the DC-8/DC-9 manufacturer, and several airlines. This phase I program included engine and nacelle configuration definition, preliminary design and analyses, model tests, preliminary economic analyses, and phase II program definition.

The phase I study consisted primarily of evaluating the refanned engine/nacelle design modifications for the reduction of environmental noise. The primary objective was to identify refanned engine/nacelle configurations that would achieve three levels of noise reduction and to evaluate the economic impact of each. Specific objectives to be accomplished were preliminary analysis of program cost/benefit relationships, preliminary selection of configurations for further development, definition of the effort necessary to develop the selected configurations through ground test of certifiable hardware, and preliminary definition of the effort necessary to continue development of the selected configuration through flight test.

The phase I effort was divided into nine separately identifiable tasks. Task I was the primary task of the program. In this task, design and analysis were conducted to establish the three acoustic nacelle configurations for each airplane series. Configuration descriptions will be found in the body of this report under the appropriate airplane sections.

Task II provided for cost/benefit analysis and documentation of the effect of this program on the civil fleet and the environment. This task is discussed in section 6.0 of this report, "Economic Studies."

Task III provided for definition of the phase II program through ground test and for preliminary definition of the effort necessary for continued development through flight test. These two items were submitted to NASA per schedule.

Task IV provided for component and model testing to support the efforts of task I. Discussion of the test programs for the three airplanes will be found in the body of this report under the respective airplane sections.

Task V provided for preliminary design of the selected nacelle configurations.

Task VI provided for the reporting function through the period of the program. Monthly technical, schedular, and financial reports were compiled and submitted.

Task VII provided means for ordering long-lead-time items in phase I so that phase II hardware would not be delayed. Delay in configuration definition removed any need for ordering long-lead-time items; therefore, no effort was expended under this task.

Tasks VIII and IX provided for design and manufacture of 20-in.-diameter scale models of the JT3D and JT8D modified-fan configurations. The JT3D scale model was terminated as a part of the 707 airplane termination. The JT8D model was scheduled for completion by the end of phase I, but delay in engine configuration definition resulted in a slide in the delivery schedule. At the time of preparing this report, the model was being fabricated.

This report presents the results of work accomplished during the phase I contract period of performance from 17 August 1972 to 11 July 1973. The 707 work considered primarily the 707-320B airplanes because these models are most numerous compared with the -100B and the -720B. The JT8D work considered only the -200 versions of the 727 and 737 airplanes, although it is possible that the resulting installations could be used on all airplanes produced to date.

The changes to the airplanes were limited to those required for satisfactory installation of the modified engines, subject to requirements for airplane safety, performance, noise reduction, reliability, durability, maintainability, cost, and fleet operational suitability.

This phase I contract was originally scheduled for completion in 8 months. Due to funding limitations after approximately 5 months, the 707 portion of the contract was terminated, and all work was stopped on the 707 with the exception of the 707 flutter model tests. At the same time, most of the 737 work and a portion of the 727 work was suspended or canceled. The full effect of these changes to the program are discussed in the appropriate sections of this report.

The phase I program was conducted using the English system of measurements, with conversion to the International System of Units (SI) (ref. 1) being made for this report where applicable. The SI units will be found in parentheses following the English units, in additional columns, or as secondary scales where appropriate.

# 3.0 707 AIRPLANE

## 3.1 AIRPLANE DESCRIPTION

The 707 airplane is a four-engine commercial airplane produced in three series. The primary series considered for this program is the 707-320B/C series. The 707-320B is the long-range intercontinental passenger version, and the -320C is a convertible passenger/cargo version. These two airplanes, for purposes of retrofit of refanned engines, are virtually identical. These 707-320B/C airplanes are the largest and the most numerous of the 707 model series.

The 707-320B was chosen as the baseline airplane. It has a range of approximately 6000 nmi (11 112 km) and can cruise at speeds of 375 kn (193 m/sec) indicated air speed or Mach 0.90 at altitudes up to 42 000 ft (12 802 m). The standard interior arrangement accommodates 149 passengers. The baseline 707-320B principal dimensions are shown in figure 2. Figure 3 illustrates the 707-320B modified with JT3D-9 refanned engines.

The 707-120B is the second series considered, and the 720B, a model similar to the 707, is the third series considered. Figures 4 and 5 illustrate the principal dimensions of the 707-120B and the 720B, respectively. Table 1 shows baseline aircraft physical characteristics for the three airplane series. Figure 6 shows the 707/JT3D weight/thrust growth history.

## 3.2 ENGINE DEFINITION

### 3.2.1 JT3D-3B (Baseline)

The Pratt & Whitney Aircraft JT3D-3B engine was selected for modification comparison and is the most numerous in-service engine on the 707 and 720 airplanes. The JT3D-3B is an axial-flow turbofan engine with multistage compressors and fan driven by a multistage reaction turbine designed for operation with fixed-area exhaust nozzles for the main engine and fan exit. The JT3D-3B is rated at 18 000 lb (80 064 N) sea-level static thrust. The performance characteristics are given in table 2. Figures 7 and 8 show typical views of the JT3D-3B engine.

### 3.2.2 JT3D-9 (Refanned)

The Pratt & Whitney Aircraft JT3D-9 (refanned) turbofan engine would be designed as a retrofit modification of the JT3D-3B/-7 commercial turbofan engine. The retrofit modification would include a new, single-stage, 2.2 bypass ratio fan of a larger diameter than the JT3D-3B fan

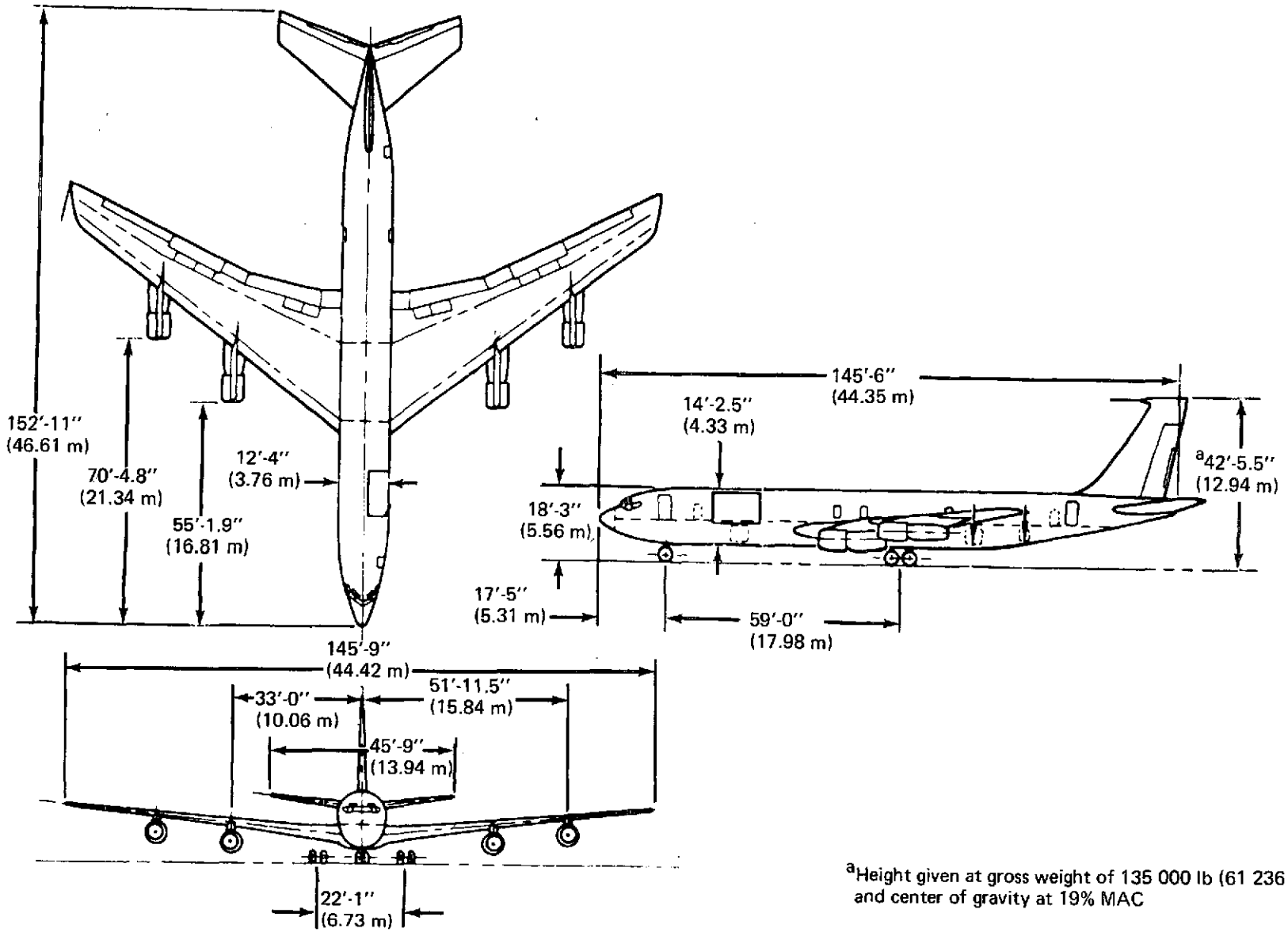


[a]Height given at gross weight of 135 000 lb (61 236 kg) and center of gravity at 19% MAC

*FIGURE 2.—707-320B/C/JT3D BASELINE AIRPLANE GENERAL ARRANGEMENT*

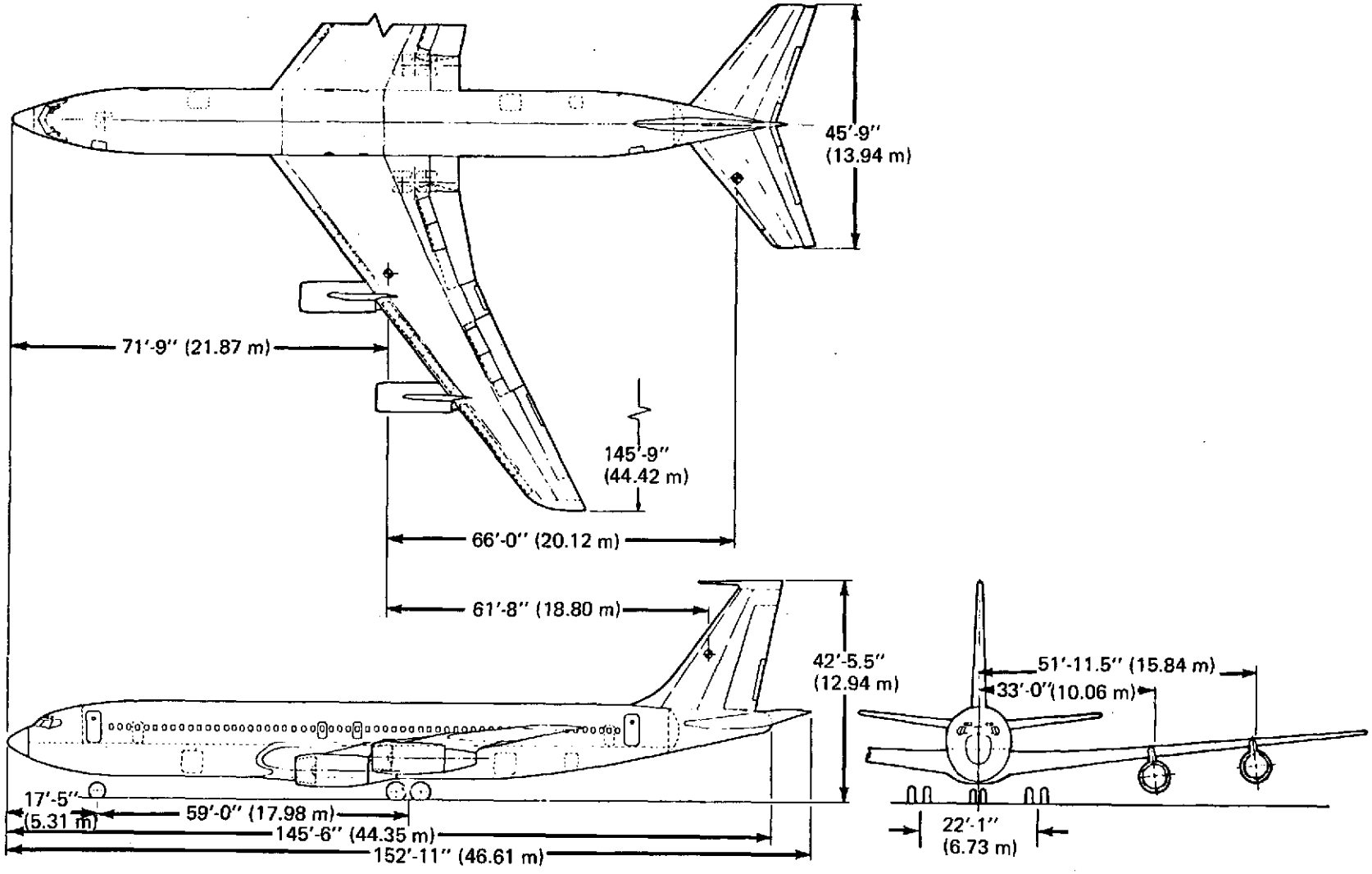


*FIGURE 3.—707-320B/JT3D-9 MODIFIED AIRPLANE GENERAL ARRANGEMENT*

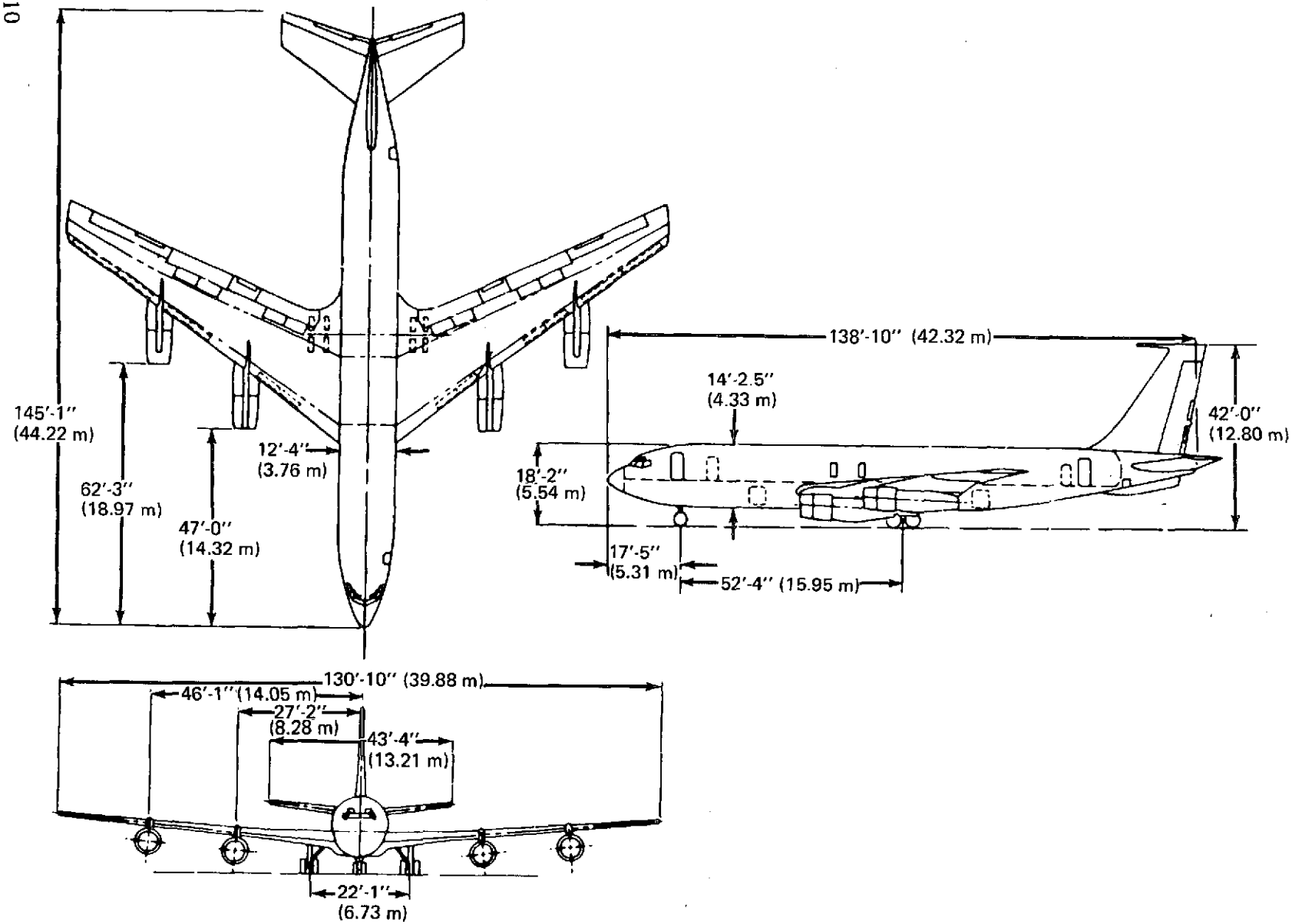


*FIGURE 4.—707-120B/JT3D AIRPLANE GENERAL ARRANGEMENT*

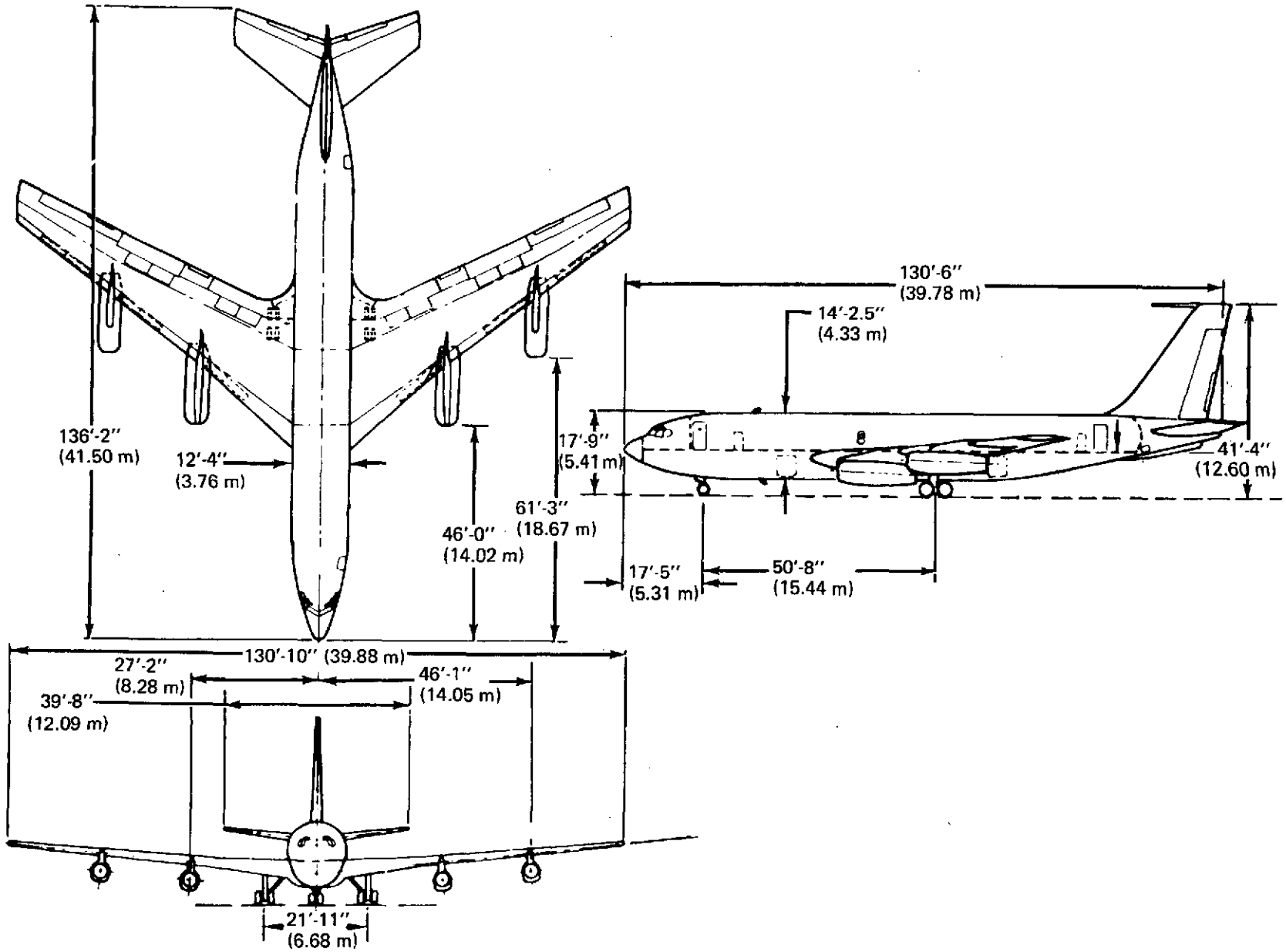


*FIGURE 5.—720B/JT3D AIRPLANE GENERAL ARRANGEMENT*

*TABLE 1.–707/720 BASELINE AIRPLANE CHARACTERISTICS*

| Item | 707-320B/C | 707-120B | 720B |
|---|---|---|---|
| Maximum taxi weight | 336 000 lb (152 409 kg) | 258 000 lb (117 028.8 kg) | 230 000 lb (104 328 kg) |
| Maximum landing weight | 247 000 lb (112 039.2 kg) | 190 000 lb ( 86 184 kg) | 175 000 lb ( 79 380 kg) |
| Operational empty weight | 145 000 lb ( 65 772 kg) | 131 000 lb ( 59 421.6 kg) | 122 000 lb ( 55 339.2 kg) |
| Number of passengers | 149 | 124 | 122 |
| Wing area | 2892 $ft^2$ (268.67 $m^2$) | 2433 $ft^2$ (226.03 $m^2$) | 2433 $ft^2$ (226.03 $m^2$) |
| Wingspan | 145 ft-9 in. (44.42 m) | 130 ft-10 in. (39.88 m) | 130 ft-10 in. (39.88 m) |
| Length | 152 ft-11 in. (46.61 m) | 145 ft-1 in. (42.22 m) | 136 ft-2 in. (41.50 m) |
| Height | 42 ft-5.5 in. (12.94 m) | 42 ft (12.80 m) | 41 ft-4 in. (12.60 m) |
| BL inboard engine | 33 ft (10.06 m) | 27 ft-2 in. (8.28 m) | 27 ft-2 in. (8.28 m) |
| BL outboard engine | 51 ft-11.5 in. (15.84 m) | 46 ft-1 in. (14.05 m) | 46 ft-1 in. (14.05 m) |
| Fin area | 337 $ft^2$ (31.31 $m^2$) | 353.8 $ft^2$ (32.87 $m^2$) | 328.3 $ft^2$ (30.50 $m^2$) |

*TABLE 2.–JT3D-3B/JT3D-9 UNINSTALLED ENGINE CHARACTERISTICS COMPARISON*

| Item | Baseline (JT3D-3B) | Refanned engine (JT3D-9) |
|---|---|---|
| Takeoff thrust–sea level, standard day | | |
| Static, lb (N) | 18 000 (80 068) | 20 750 (92 296) |
| 150 kn (77.2 m/sec), lb (N) | 15 300 (68 058) | 17 050 (75 842) |
| Maximum cruise–35 000 ft (10 668 m), Mach 0.80 | | |
| Thrust, lb (N) | 4400 (19 572) | 4715 (20 973) |
| TSFC, lb/hr/lb (kg/hr/daN) | 0.805 (0.821) | 0.766 (0.781) |
| Weights and dimensions | | |
| Basic engine weight, lb (kg) | 4350 (1973) | 4750 (2155) |
| Basic engine length, in. (m) | 83.683 (2.126) | 84.403 (2.144) |
| Fan tip diameter, in. (m) | 50.2 (1.275) | 56.6 (1.438) |

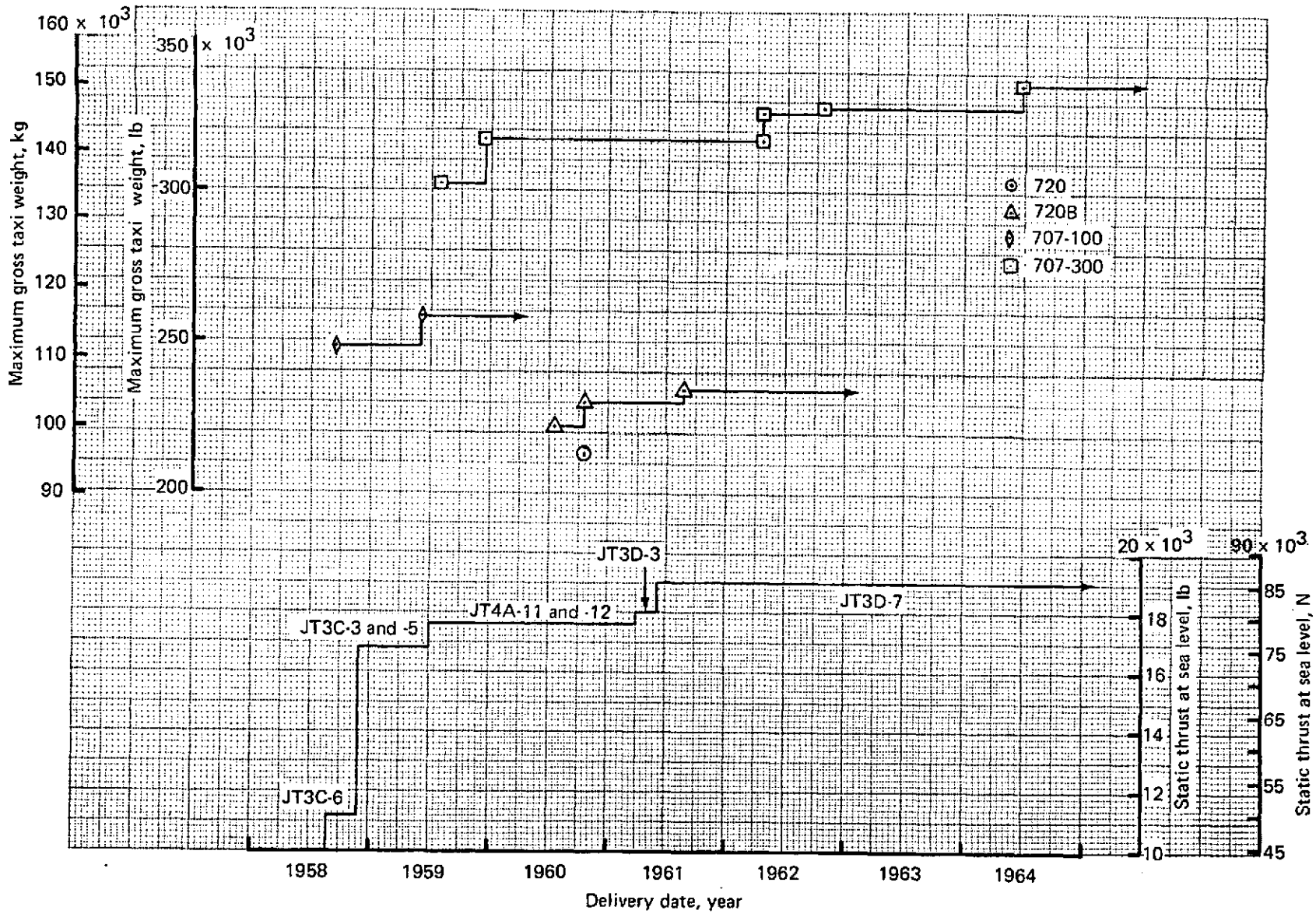


*FIGURE 6.—707/JT3D WEIGHT/THRUST GROWTH HISTORY*

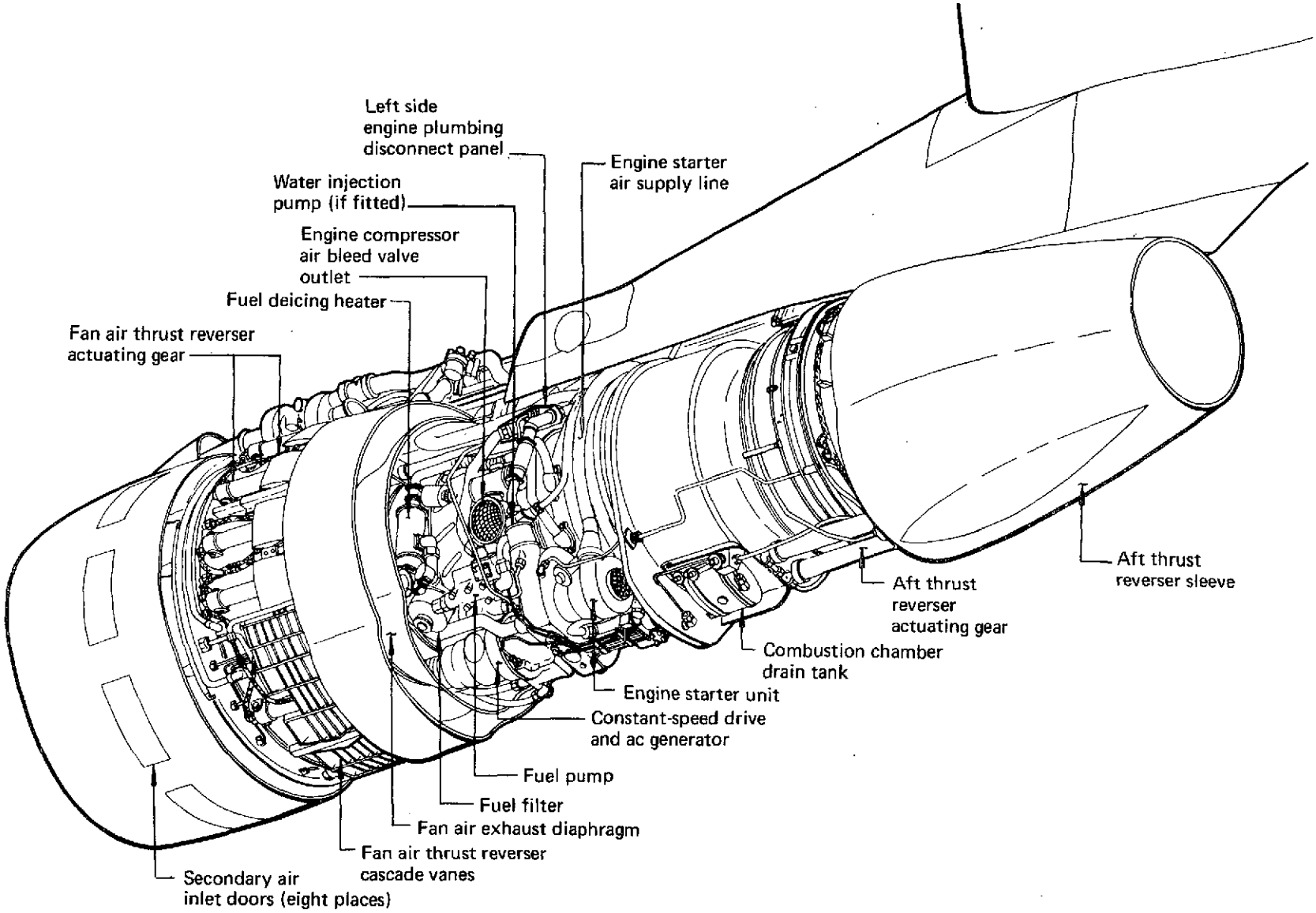


*FIGURE 7.—707/JT3D-3B ENGINE LOWER LEFT SIDE VIEW*

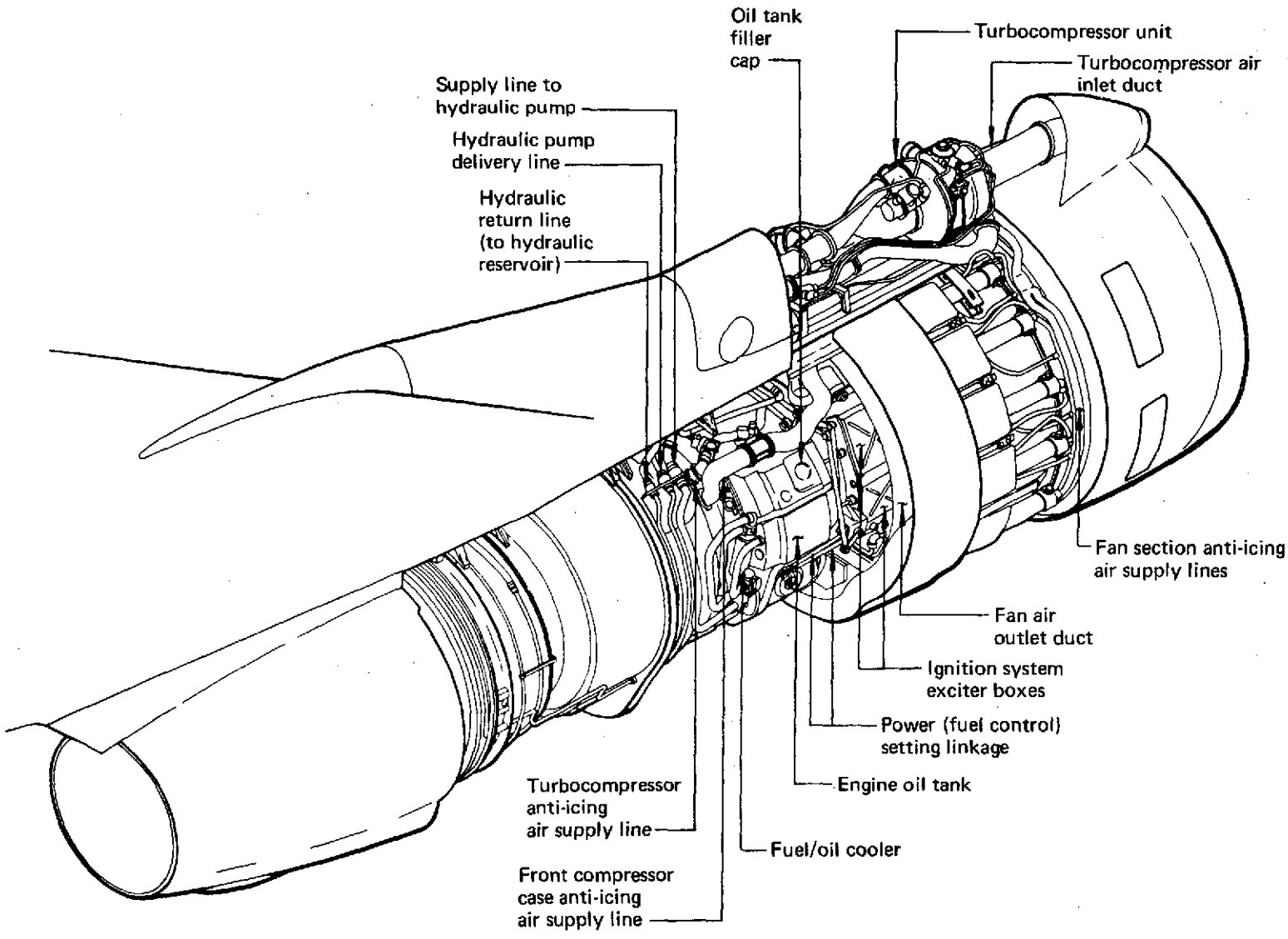


*FIGURE 8.—707/JT3D-3B ENGINE RIGHT SIDE VIEW*

stages; deletion of the inlet guide vanes; a new supercharging low-pressure compressor stage; the previously existing six-stage low-pressure compressors; and the previously existing three-stage low-pressure turbine modified by installation of a new final stage disc and blades. The high-pressure spool and can-annular combustor would be unchanged from the JT3D-3B. It would provide increased takeoff and cruise thrust, lower specific fuel consumption, and lower jet and fan noise. Figure 9 shows the JT3D-9 configuration.

The engine operating envelope for the JT3D-9 (shown in fig. 10) would be the same as for the JT3D-3B/-7 engines.

### 3.2.3 Uninstalled-Engine Performance Comparison

The takeoff and cruise performance characteristics of the uninstalled JT3D-9 engine are summarized in table 2. Performance of the uninstalled JT3D-3B engine is also shown for comparison. Uninstalled-engine performance comparison curves are shown in figures 11 and 12.

## 3.3 MODEL AND COMPONENT TESTS

### 3.3.1 General

The phase I test program was intended to provide critical test data required for phase I engine, nacelle, and airplane design decisions and to provide necessary nacelle design information for phase II. Tests were required in areas where neither applicable test data nor reliable analytical methods existed to confidently determine noise levels, airplane performance, costs, timing, and design feasibility.

The 707 program was curtailed in January 1973 due to reduction of available funding. This curtailment canceled all except the 707 flutter model tests and the reporting of results.

Nozzle system model noise tests were planned for determination of the noise-reduction potential of plug-type primary nozzles applied to JT3D-9 engines. Incremental noise level measurements from one-sixth-scale model nozzles of proposed configurations of refanned engine exhaust system noise suppressors were planned for comparison with the production JT3D nozzle. It was planned to measure sideline and forward- and aft-quadrant noise levels at combinations of fan and primary nozzle pressure ratios and temperatures representative of the JT3D refanned engine. Sufficient flight conditions were to be simulated to evaluate takeoff, cutback, approach, and sideline component noise. These tests were canceled.

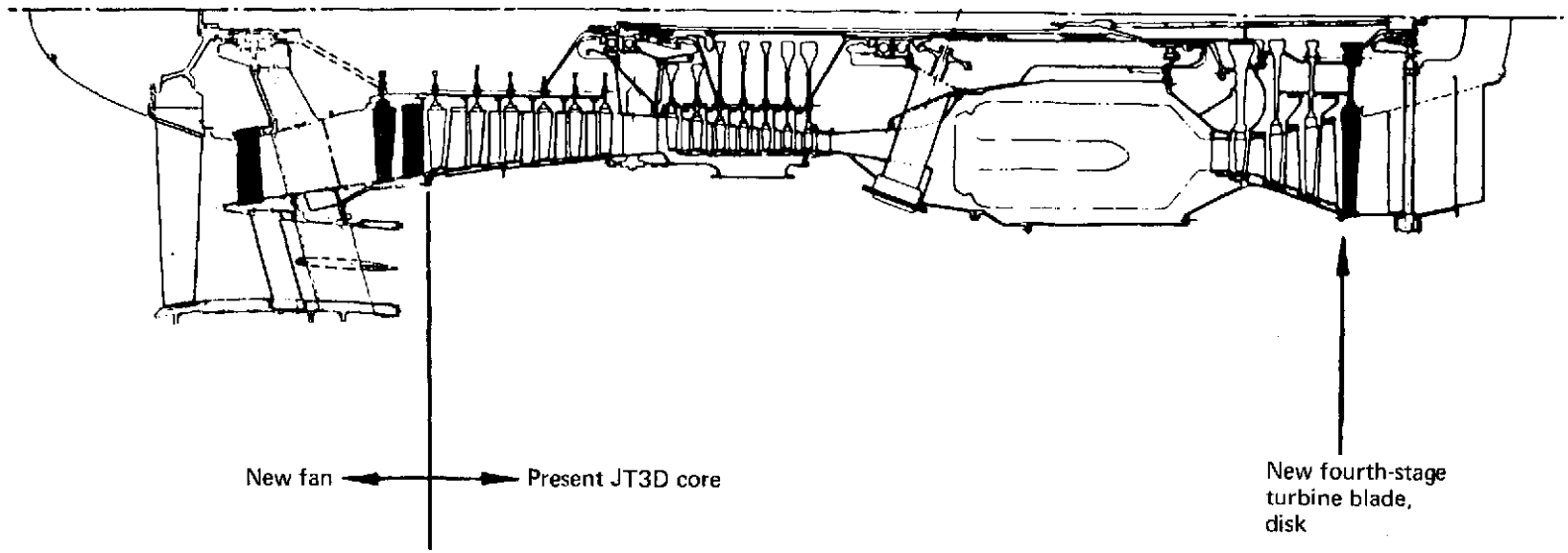


*FIGURE 9.—JT3D-9 ENGINE CONFIGURATION*

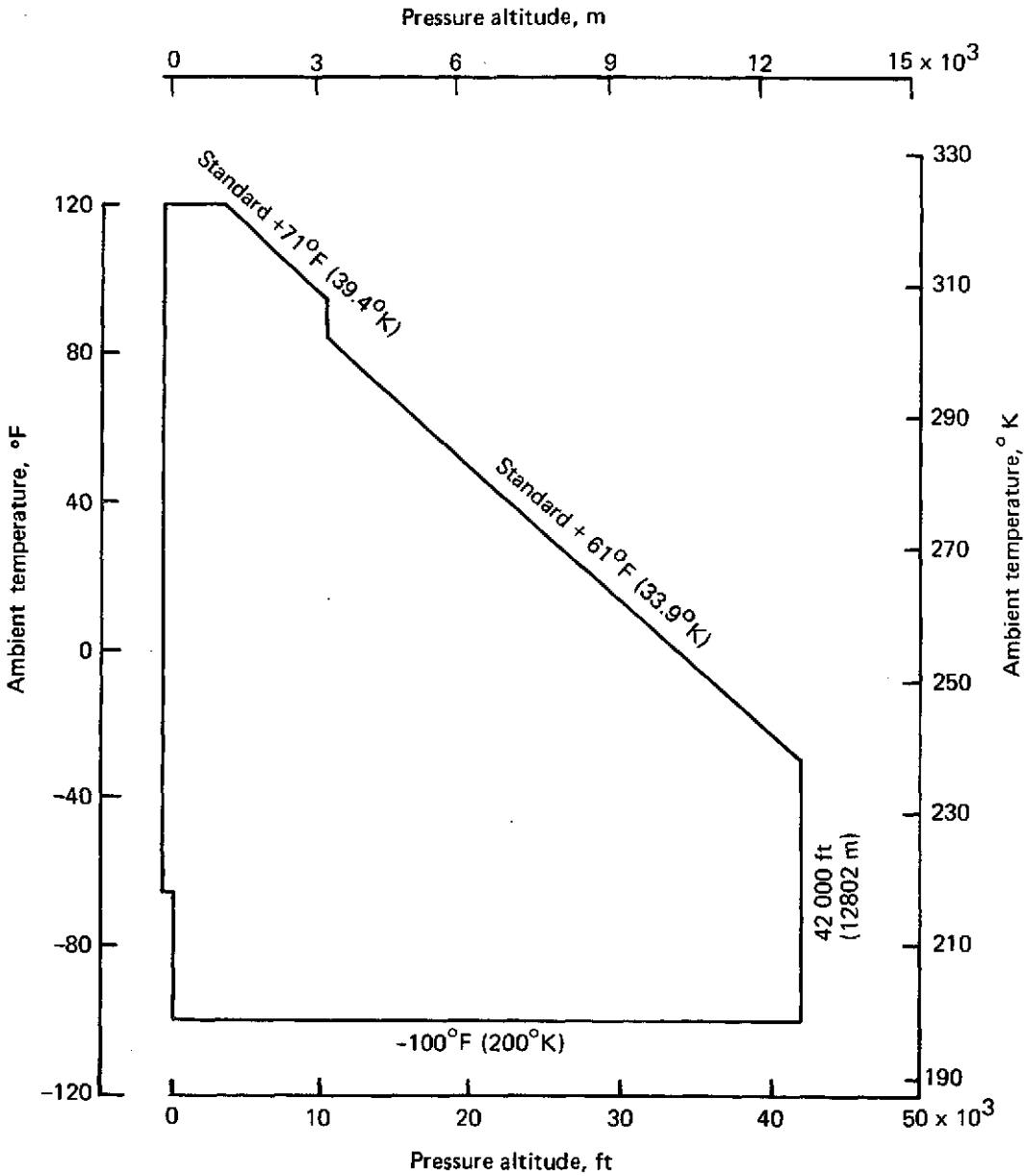


*FIGURE 10.–707/JT3D-9 OPERATING ENVELOPE*

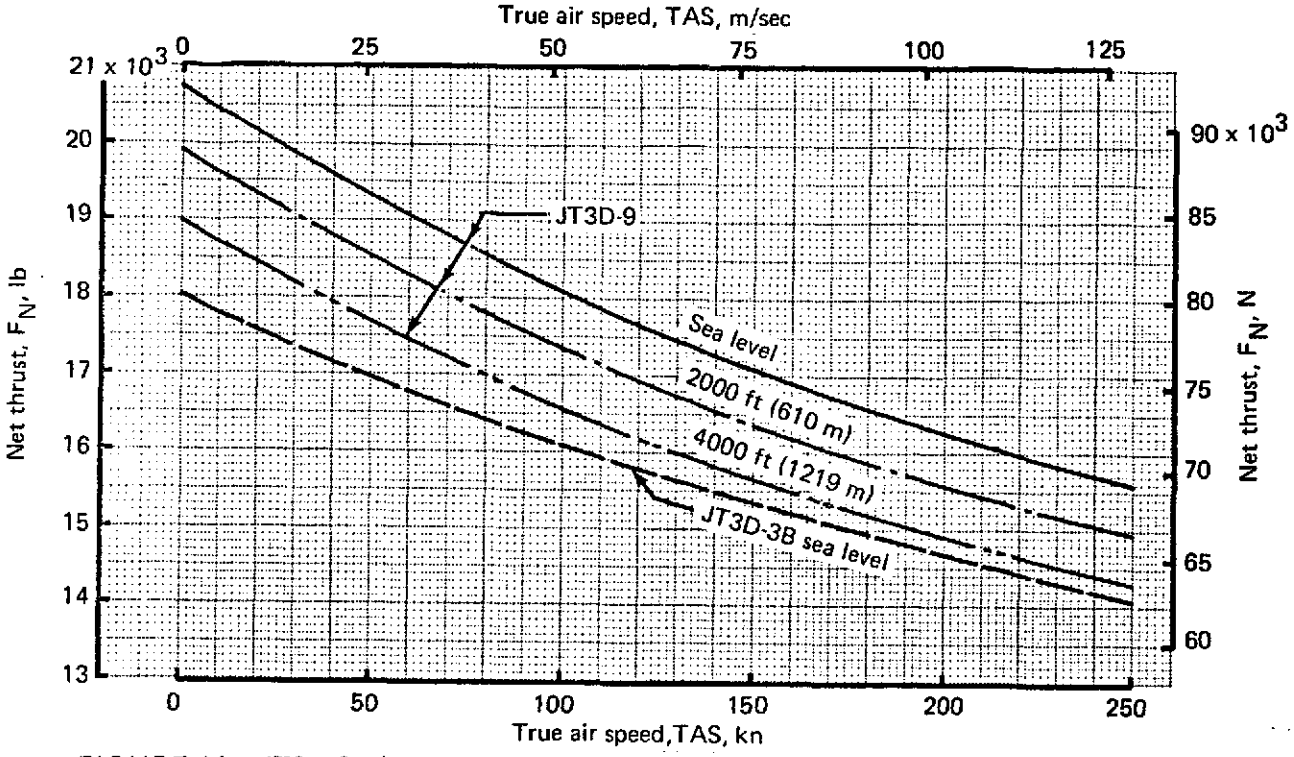


*FIGURE 11.–JT3D-3B/JT3D-9 UNINSTALLED ENGINE THRUST PERFORMANCE COMPARISON, STANDARD DAY*

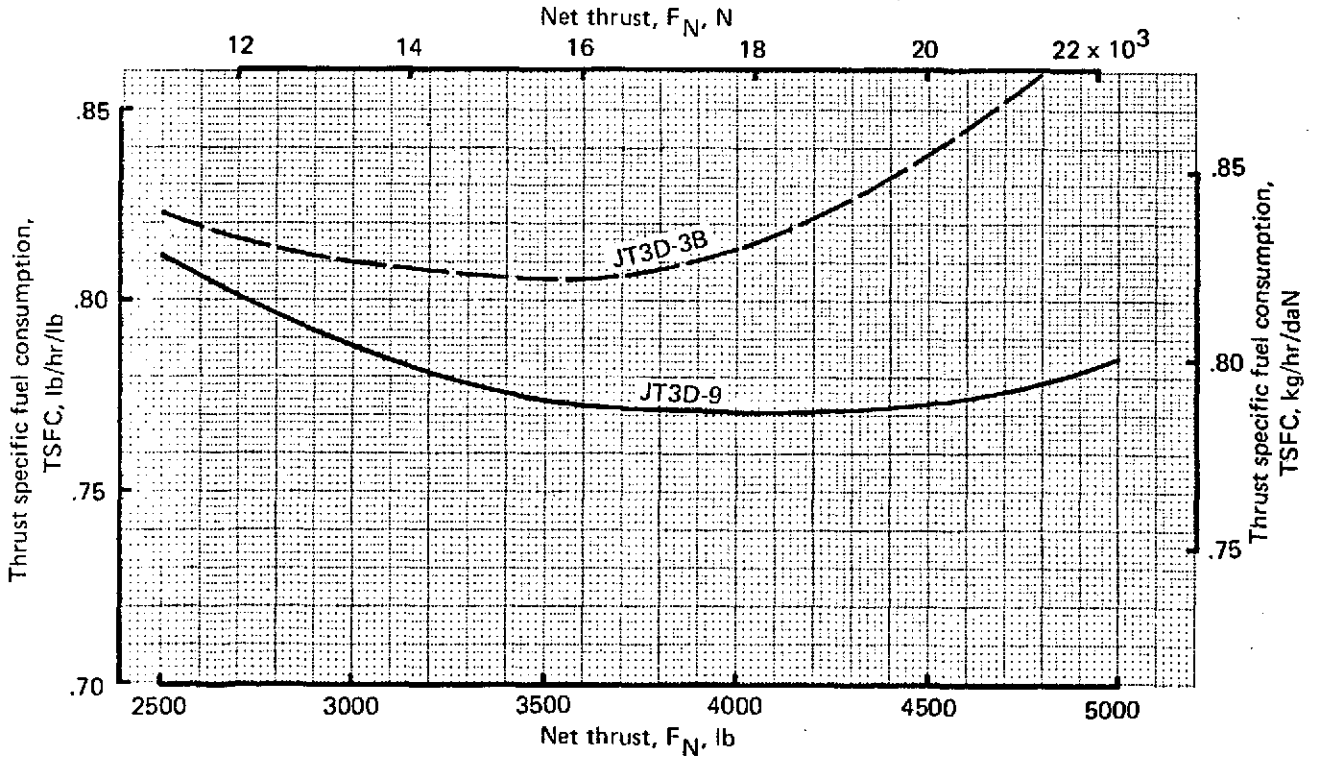


*FIGURE 12.–JT3D-3B/JT3D-9 UNINSTALLED ENGINE TSFC PERFORMANCE COMPARISON, STANDARD DAY, 35 000 FT (10 668 M), MACH 0.83*

Wind tunnel tests, using a high-speed model with flow-through nacelles representing refanned engine configurations, were planned for evaluation of aerodynamic interference drag and airplane high-speed stability characteristics relative to nacelle size and location on the wing. At termination of the 707 refan program, design of the model nozzle system and high-speed drag models was approximately 50% complete. Model fabrication had not started.

A test program for screening acoustic materials was planned for development of preliminary engineering data on acoustic characteristics, structural properties, and processing, plus weight and cost of selected new design concepts for metallic and nonmetallic acoustic liner systems. The intent was to obtain data for selection of the most promising materials at the earliest possible date for use in the JT3D/JT8D refan program. The candidate acoustic linings were a stainless steel single-layer lining and double-layer linings of three materials (polyimide, titanium, and Inconel 625). All acoustic material development and test work was canceled in January 1973 as a result of funding cuts. At 707 program termination, test materials had been received and the feasibility of processing test parts had been determined.

### 3.3.2 707 Flutter Model Tests

#### 3.3.2.1 Objective

The object of the 707 flutter model tests was to determine the effects of the proposed JT3D refan configurations on the flutter characteristics of the 707-120B, 707-320B, and the 720B airplanes.

#### 3.3.2.2 Model Description

The flutter model was basically the same as those used by the contractor in previous low-speed flutter tests of the 707/720-series airplanes. Figure 13 shows the flutter model installed in the wind tunnel. The bending and torsional stiffness of the wings, body, and tail surfaces were provided by single spars. The wing airfoil sections and body contours were essentially rigid and were attached to their respective spars, so they did not contribute to the stiffness of the spar. The existing -320B flutter model body was used in the tests for all the airplanes, and the -320B, -120B, and -720B wings were attached to the body as appropriate.

The model nacelles represented the modified configurations by means of flow-through cowls that were designed to give a velocity ratio corresponding to the airplane at a Mach number of 0.88 at the airplane design dive speed with the engines at maximum continuous thrust. The model nacelle struts were designed to give the mode shapes and frequencies of the side bending and pitch motions of the nacelles.

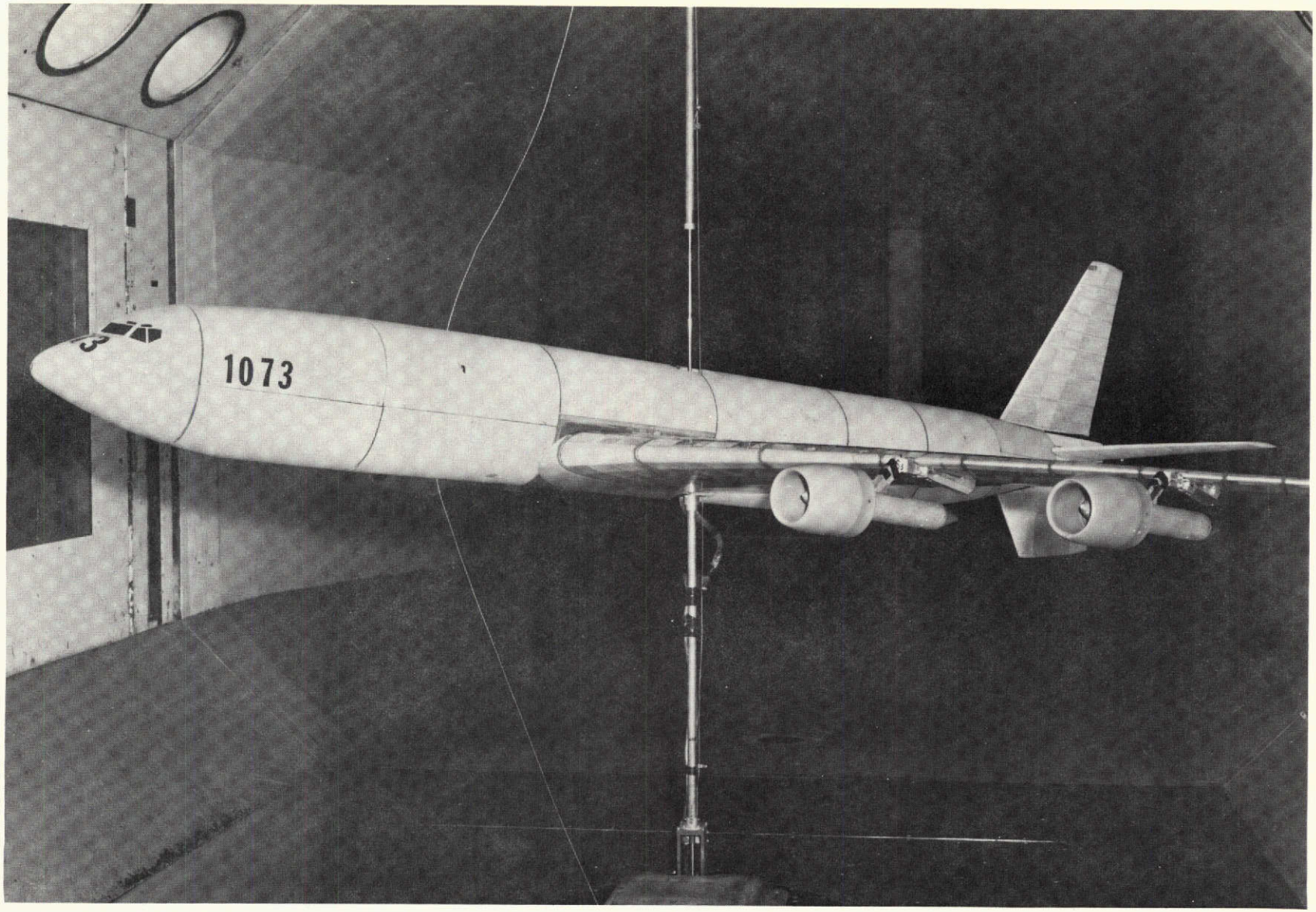


FIGURE 13.–707/JT3D-9 FLUTTER MODEL

The model was mounted on a rod that allowed pitch, yaw, and vertical translation. A cable supported 40% of the model weight to reduce Froude number effects.

#### 3.3.2.3 Test Description

To verify that the model had the correct dynamic characteristics, mode shapes and frequencies were obtained from vibration tests of both the cantilevered model wing and the complete model mounted on its support rod.

For each airplane, fuel load variations were evaluated to establish the critical fuel loading. At this critical fuel condition, the effect of the following parameters was investigated:

- Inboard and outboard nacelle side bending frequencies
- Inboard and outboard nacelle pitch frequencies
- Inboard and outboard nacelle streamwise center-of-gravity location
- Engine weight

#### 3.3.2.4 Results and Conclusions

All of the airplane models showed sensitivity to outboard nacelle side bending frequency, variation of which shows that there are two modes of flutter. One mode, involving primarily outboard nacelle side bending motions, exists at low nacelle frequencies. The other mode involving mainly wing bending and torsion exists at high nacelle frequencies. A flutter-free region exists between the two modes. Flutter speed is insensitive to inboard nacelle vertical bending frequency, decreases slightly with increasing inboard nacelle side bending frequency, and is benefited by increasing outboard nacelle vertical bending frequency. Besides outboard nacelle side bending frequency, two other significant parameters affect flutter speed. They are nacelle weight and outboard nacelle streamwise center-of-gravity location. Increasing nacelle weight increases flutter speed, as does moving the outboard nacelle center of gravity aft 10 in. (0.254 m) or more.

In general, the results show that the modified nacelles change the flutter characteristics of the airplane. This is due to the increased aerodynamic effect of the larger cowls. The flutter characteristics of the airplane modified with JT3D refanned engines will be satisfactory with suitable choice of nacelle frequencies and outboard nacelle streamwise location.

## 3.4 NACELLE PRELIMINARY DESIGN

This section discusses the five nacelle configurations investigated. Initially, preliminary design was conducted on the four basic nacelles illustrated in figure 14. Configuration 1 employs a fixed-geometry no-ring inlet and a short fan duct, configuration 2 has a one-ring inlet and a 3/4-length fan duct, configuration 3 is the same as configuration 2 but has two inlet rings, and configuration 4 has two inlet rings and a full-length fan duct. An additional configuration (1A), added as a result of further study, is identical to configuration 1, except as noted in section 3.4.5. These configurations are all discussed as variations from configuration 1.

Each configuration considers a different level of acoustic treatment. The performance loss and noise attenuation would be proportionate to the extent of acoustic treatment and treatment methods. The inlet acoustic treatment was designed to attenuate buzz-saw noise during takeoff and fundamental blade passage frequency noise during approach. This inlet treatment would consist of single-layer fiberglass/polyimide lining, except for the buzz-saw lining segment, which would be perforated sheet. The lining lengths, backing depths, and face sheet properties for each configuration are stated in the appropriate sections. Lining designs considered velocity gradients from sheared flow in the inlet.

The JT3D-9 nacelle was designed with a longer, fixed-geometry, treated inlet that included a revised lip design to eliminate the need for auxiliary blow-in doors. The inlet would be acoustically treated on the inner wall and would feature an acoustic splitter ring, or rings, in all but configuration 1. The ring would be supported by four struts. The acoustic treatment would consist of polyimide acoustic sandwich panels with limited use of perforated metal sheet. These panels would be integral with the basic inlet structure to withstand pressure and inertia loads.

The inlet structure would be of conventional aluminum skin and frame construction with intercostals and bulkheads. This structure would incorporate a 3-1/2° droop to transition between the acoustic ring leading edge and inlet throat.

For those configurations using inlet rings, the ring radial location was selected to produce maximum far-field attenuation of the fundamental blade passage frequency of approach power. Ring placement and ring lengths were also affected by geometric constraints to minimize inlet pressure losses.

The attenuation characteristics of the individual airflow passages were predicted for power settings corresponding to approach, cutback, and takeoff operation. The composite attenuation spectra were calculated by establishing the acoustic power at the inlet entrance for both untreated and treated configurations. Conservation of total power was observed in all cases.

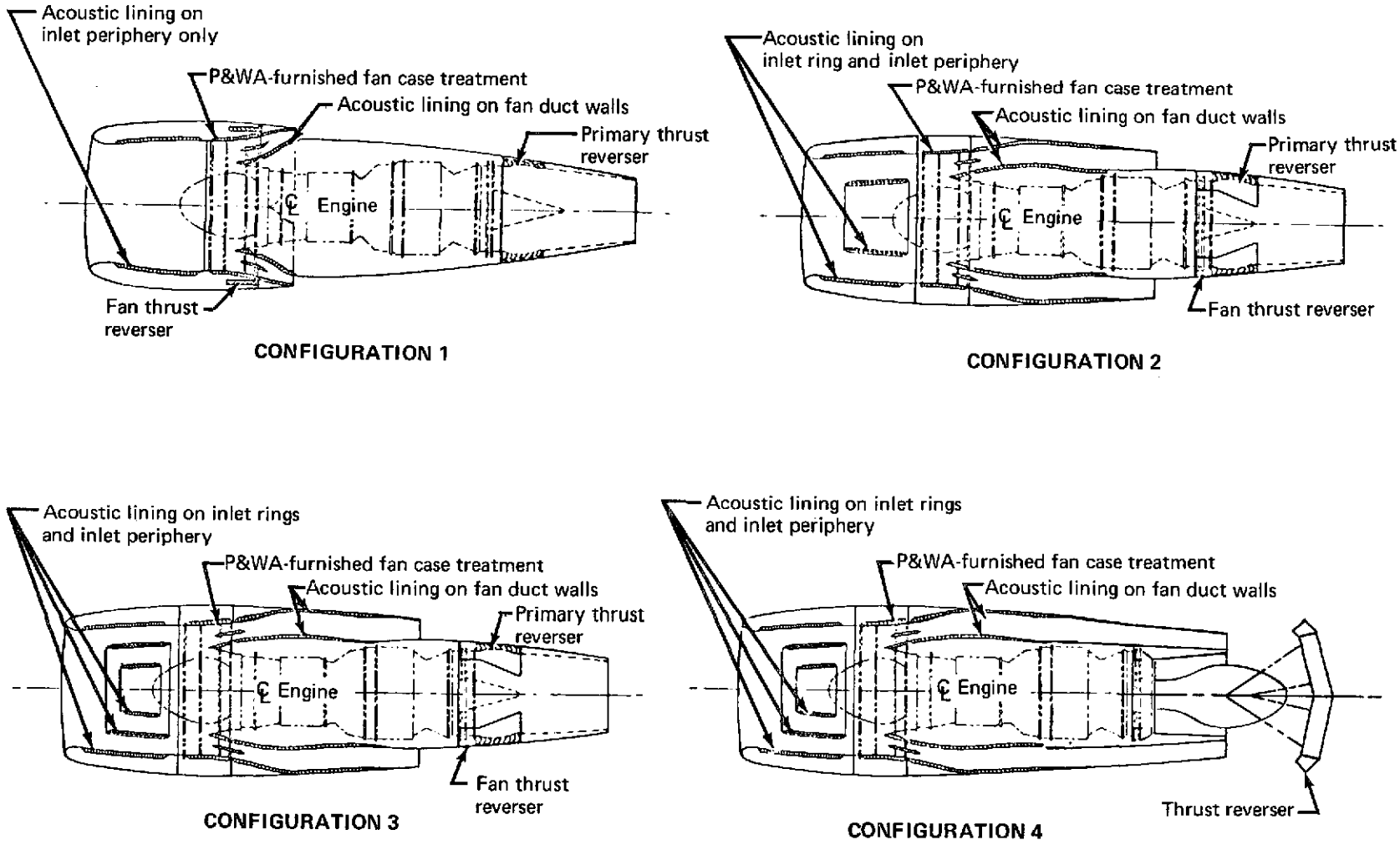


*FIGURE 14.—707/JT3D-9 MODIFIED NACELLE CONFIGURATIONS*

The fan duct acoustic lining was designed to operate with the engine fan case treatment as an acoustic attenuation system. The engine fan case design has single-layer, perforated-sheet linings tuned between the fundamental blade passage frequency and the second harmonic. The fan duct design has a double-layer fiberglass/polyimide lining designed to suppress both the fundamental and second harmonic blade passage frequencies at approach power.

### 3.4.1 Configuration 1

Configuration 1 was designed for minimum investment cost, minimum weight, minimum performance loss, and minimum maintenance requirements. The resulting overall arrangement is illustrated in figure 15. It features a clean, fixed-lip inlet; a short fan duct; a conical primary nozzle; a simplified cascade fan thrust reverser; minimum change to the existing primary reverser; replacement of the turbocompressor with a direct-bleed cabin air supply; and the same maintenance access as the existing 707 production nacelle.

The short fan duct would be fully acoustically treated. This treatment would prevent the use of a fan duct surface cooler and would require a ram air CSD oil cooler. The fan duct nozzles for the refanned JT3D-9 engine terminate at the same nacelle station as the JT3D-3B/-7 fan ducts, and the present accessory locations and access provisions were retained in the design. The side cowl contour was designed to permit blocking the fan duct during thrust reversal by translating the fan duct outer ring aft, thereby eliminating the need for annular blocker doors. (See fig. 16.) The fan reverser cascades would be translated with the blocker ring. Fan pressure would assist in rapidly driving the reverser to a full aft position. The existing primary thrust reverser would be retained, but the cascade vanes would be revised for the lower density primary exhaust flow. Hydraulic pressure was selected as the reverser actuation medium.

A precooler for cooling direct bleed air below fuel autoignition temperature would be mounted on the outer fan case. This bleed air would replace the existing turbocompressor. (See figs. 8 and 17.)

### 3.4.2 Configuration 2

The configuration 2 nacelle design includes a long, fixed-geometry treated inlet with one treated ring; a midlength treated fan duct; an untreated conical primary nozzle; a target-type fan thrust reverser; and a cascade-type primary thrust reverser. (See fig. 18.)

Access for maintenance of the fan case-mounted accessories would be provided by two fan cowl panels. These panels would be hinged to the engine at their upper edges and latched together at the bottom centerline. Access for maintenance of accessories on the lower portion of the engine

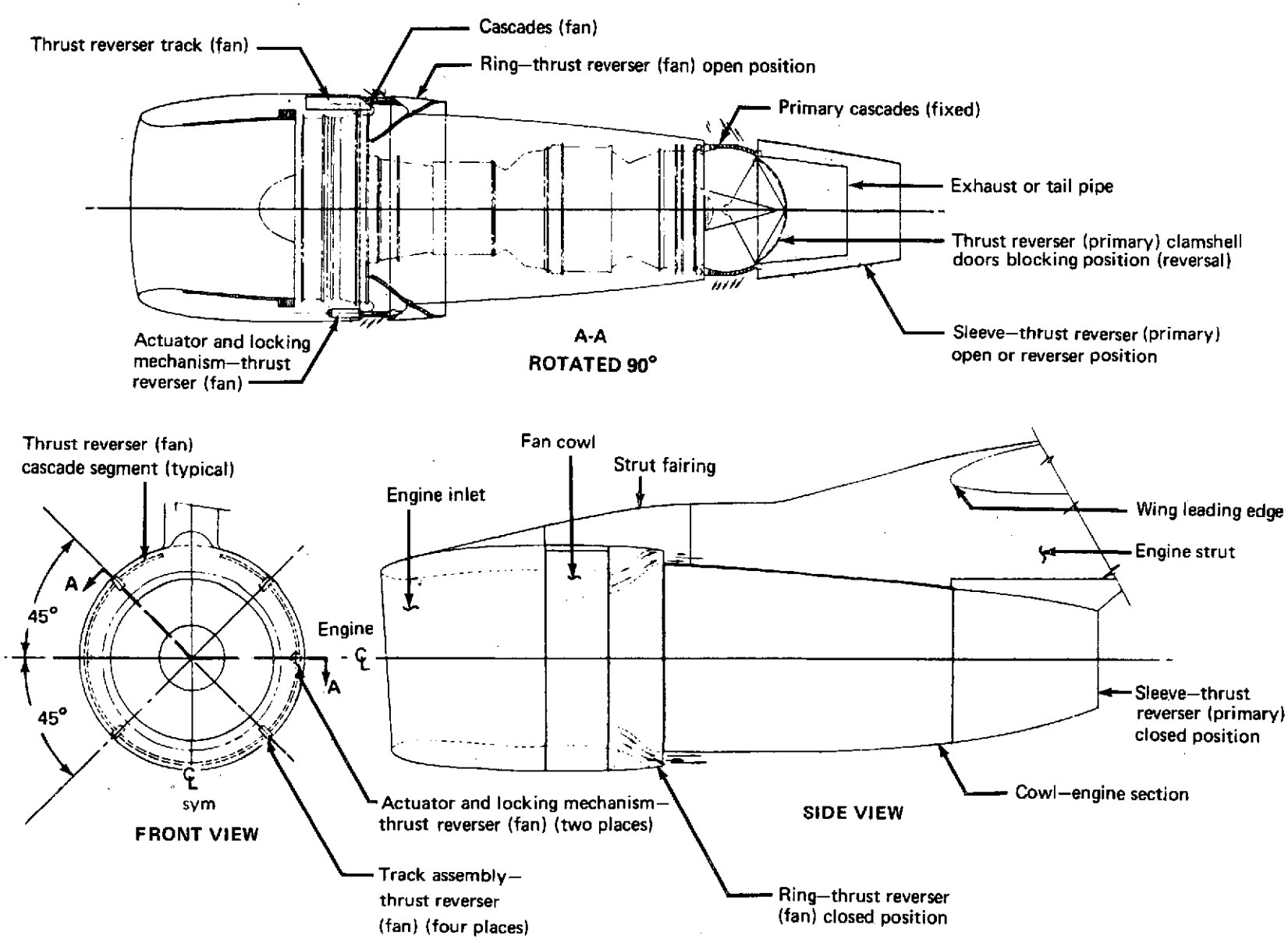


*FIGURE 15.—707/JT3D-9 CONFIGURATION 1 NACELLE*

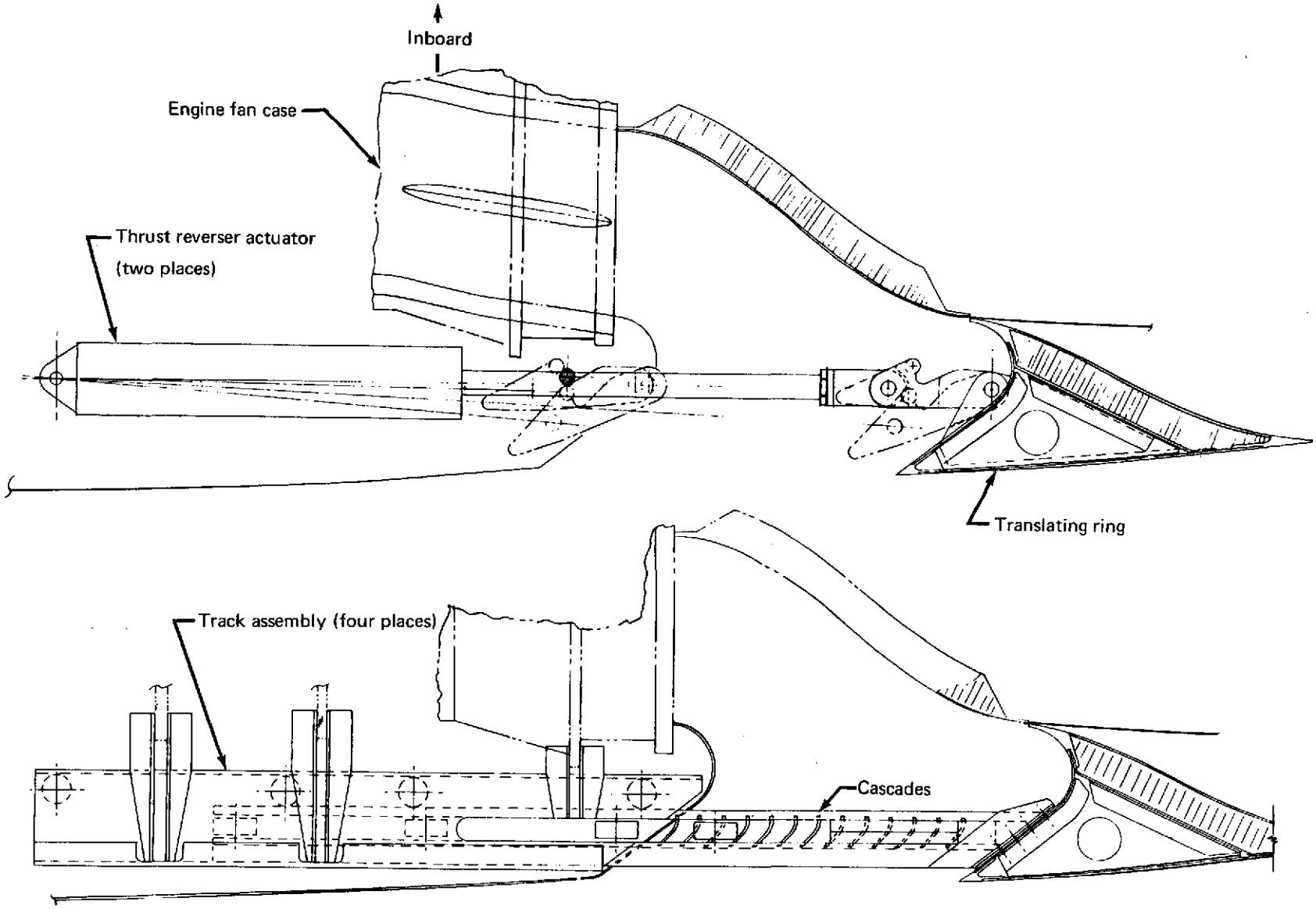


*FIGURE 16.—707/JT3D-9 CONFIGURATION 1 FAN THRUST REVERSER*

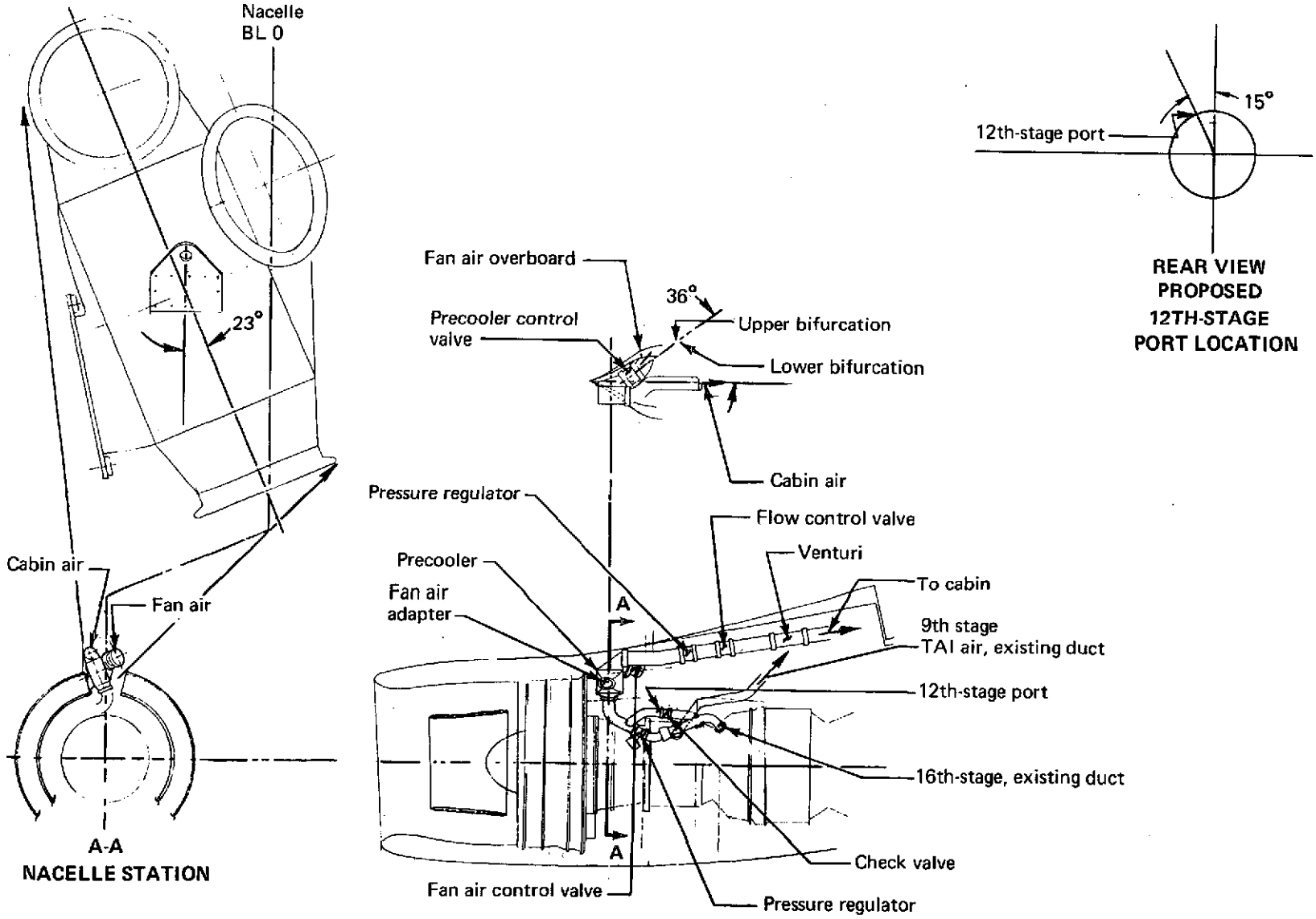


*FIGURE 17.—707/JT3D-9 PRECOOLER INSTALLATION*

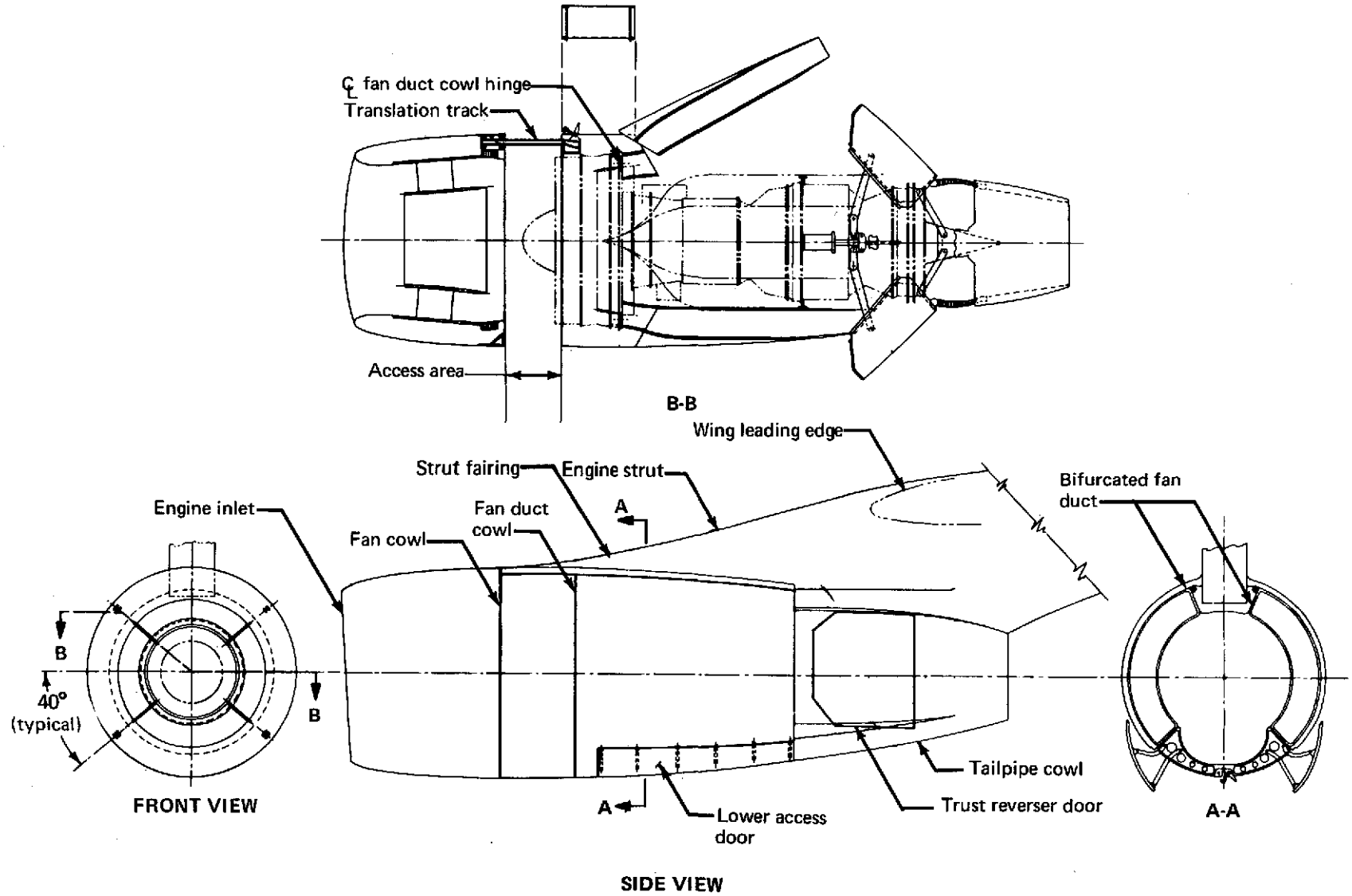


*FIGURE 18.—707/JT3D-9 CONFIGURATION 2 NACELLE*

would be by two hinged doors that covered the lower bifurcated area of the fan ducts. The aft fan duct upper section would be hinged from a forward adapter section to provide access to this area.

The fixed-lip inlet would be acoustically treated on the inner wall and feature an acoustic splitter ring supported by four struts, as shown in figure 19.

The inlet assembly would be supported from the engine by four latch points and 10 alignment pins attached to the fan case. These attachments would react the loads acting on the nose cowl.

The inlet structure would be of conventional aluminum skin and frame construction with intercostals and bulkheads. This structure incorporates a 3-1/2° droop for transition between the acoustic ring leading edge and inlet throat. The inlet was designed to translate forward to alleviate the limited access associated with the acoustic ring. Four tracks and a carriage system provide support for the inlet when translating and while extended forward from the engine fan case, as shown in figure 20. The inlet lip and leading edge of the acoustic ring and supporting struts would be anti-iced with engine bleed air.

In configuration 2, the fan ducts, as shown in figure 18, section A-A, are bifurcated on the top and bottom. The ducts would be approximately 83 in. (2.108 m) long with a break about 15 in. (0.381 m) aft of the fan case. The ducts would be constructed of polyimide acoustic panels and sheet metal. The forward adapter section that attaches to the fan case also would contain the fan duct hinging and allow the cowl to swing out, as shown in figure 21. This would permit access to the engine and airframe components.

Four, hinged, cowl panels and doors would provide aerodynamic fairing and service access to the engine. Two doors would be mounted on the lower surface of the fan ducts for access to that area.

The 707/JT3D-9 primary nozzle construction would be similar to that of the JT3D-3B but with no aft sleeve support tracks. The nozzle would be attached to the thrust reverser frame and would be 4.49 $ft^2$ (0.407 $m^2$) in area.

The configuration 2 thrust reverser would consist of two target-type doors that cover the primary reverser cascades when in the stowed position. During the reverse-thrust cycle, a four-bar linkage system would open and translate the target doors forward, uncovering the primary cascades and reversing the secondary air. An overcenter linkage system would be used to ensure positive retention in the stowed position. An interconnecting linkage for activating the clamshell door would also be used. Figure 22 shows the thrust reverser system.

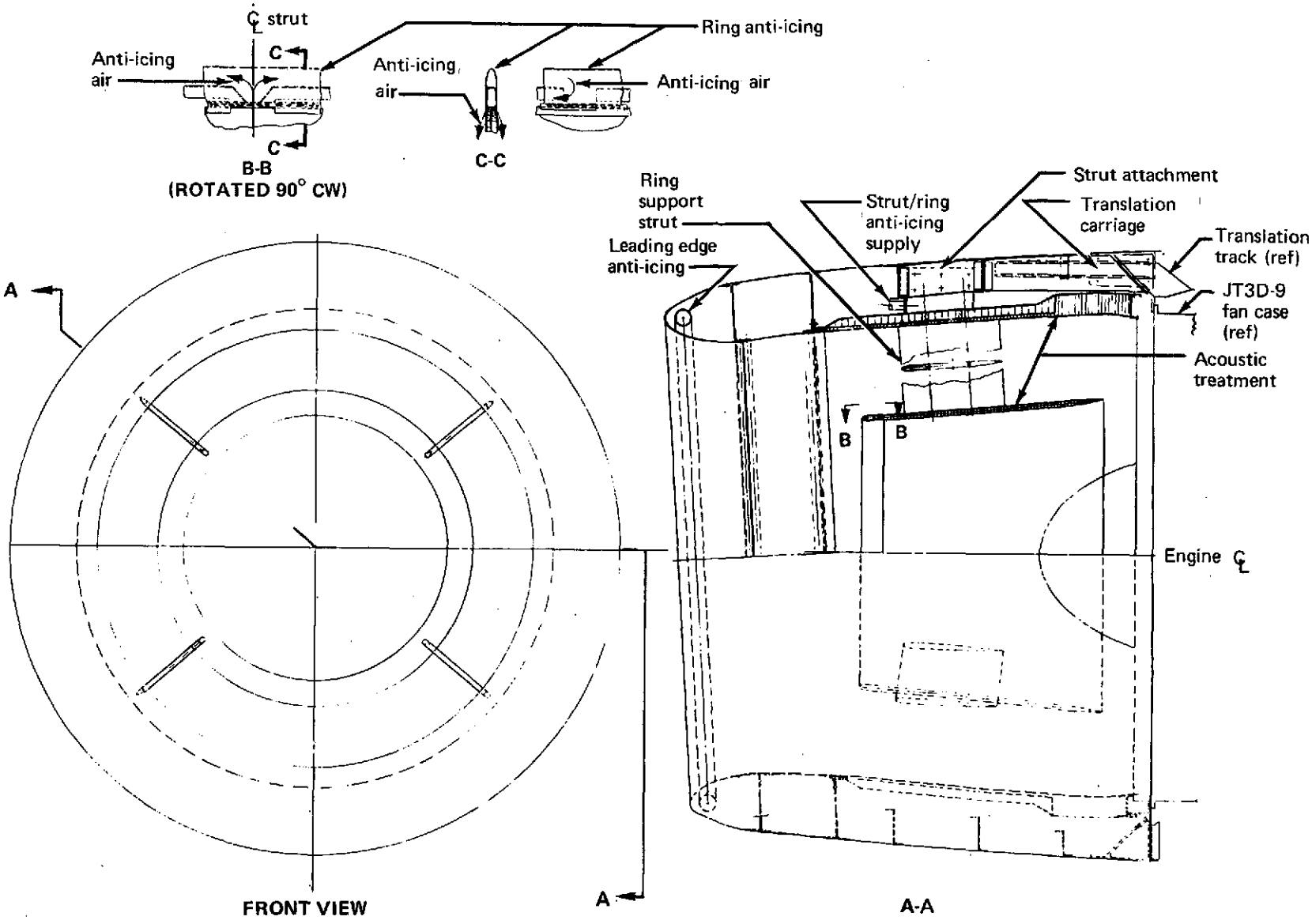


*FIGURE 19.—707/JT3D-9 CONFIGURATION 2 INLET*

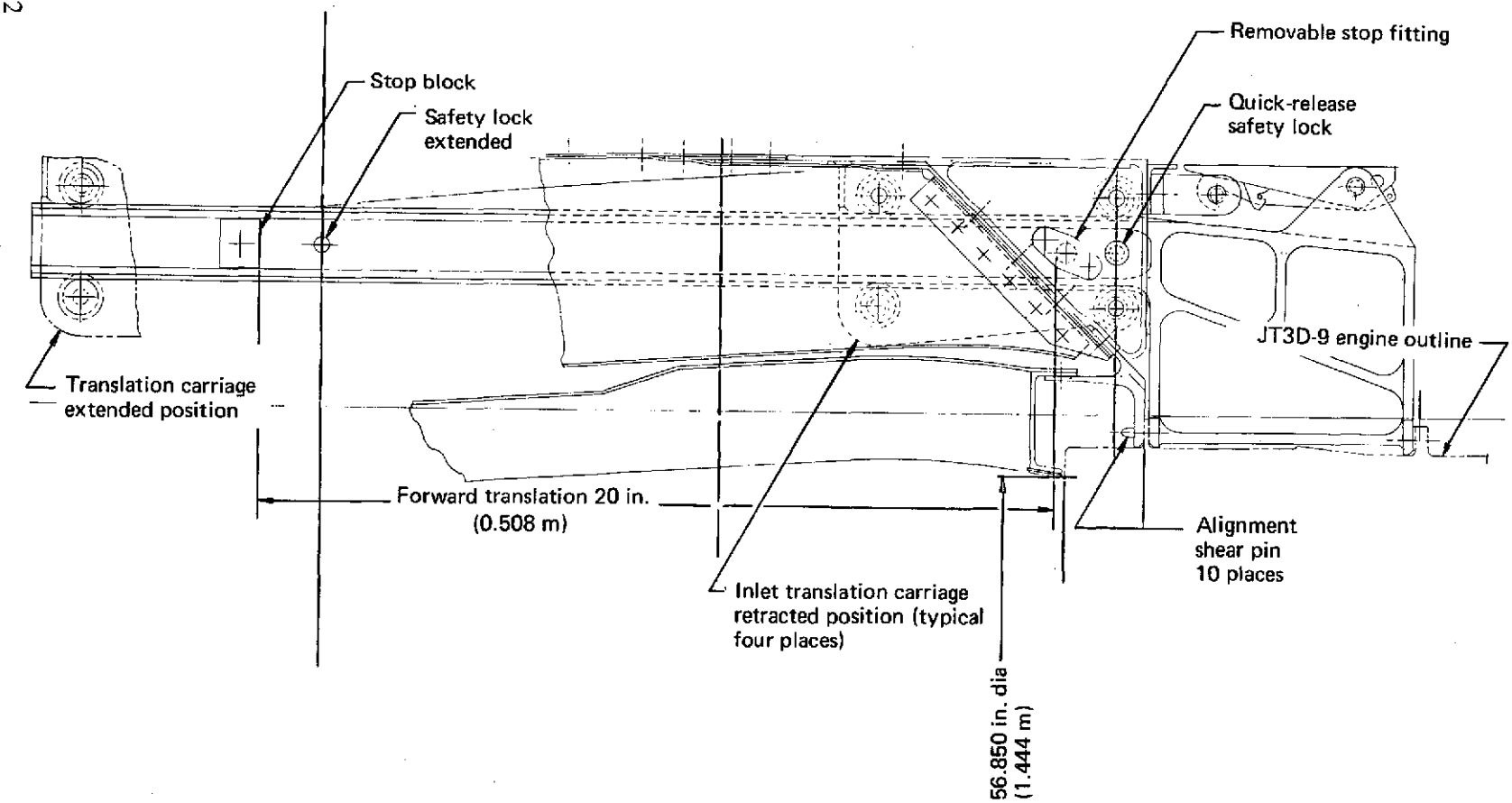


*FIGURE 20.—707/JT3D-9 BASELINE INLET INTERFACE*

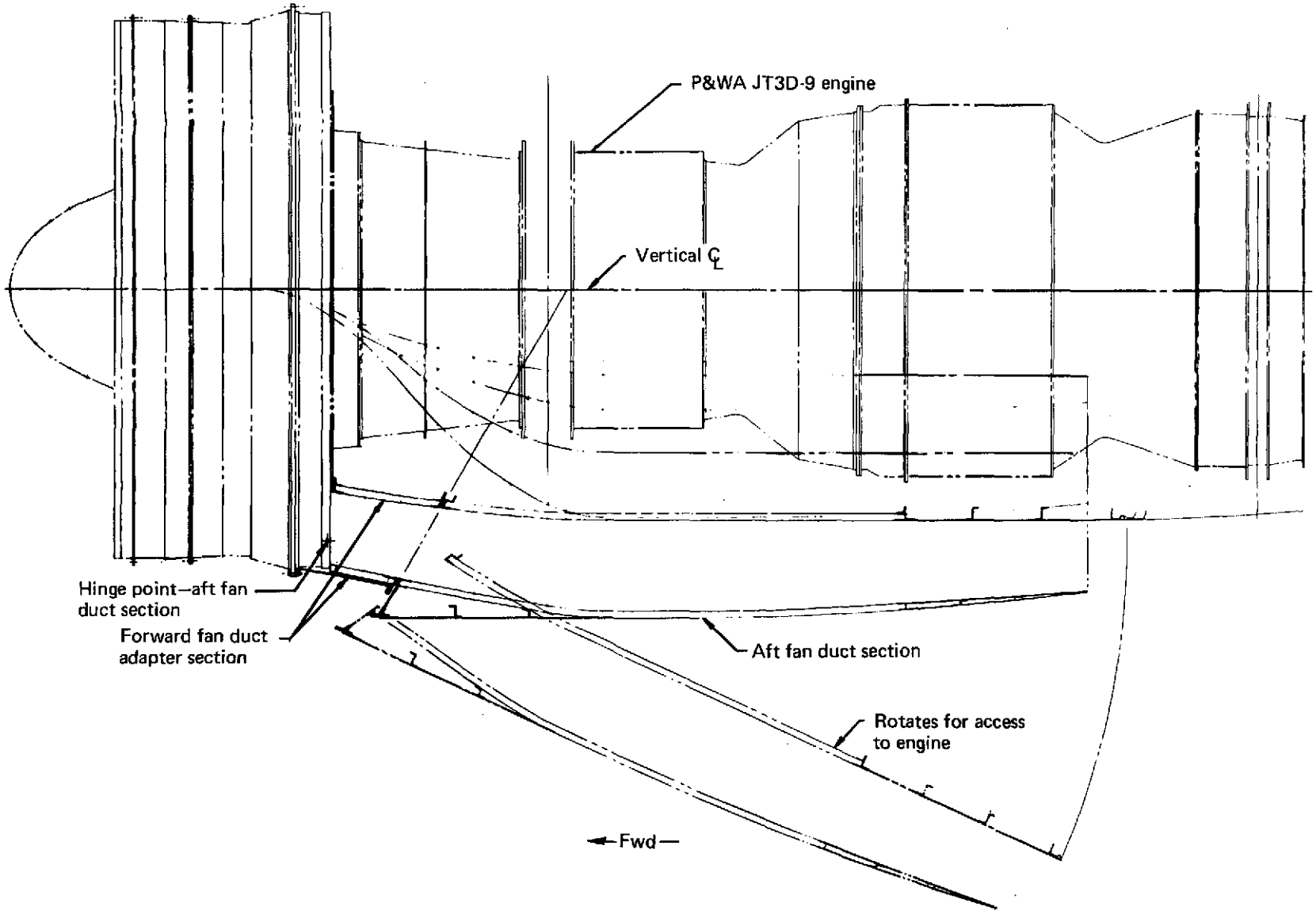


*FIGURE 21.—707/JT3D-9 CONFIGURATION 2 FAN DUCTS—PLAN VIEW*

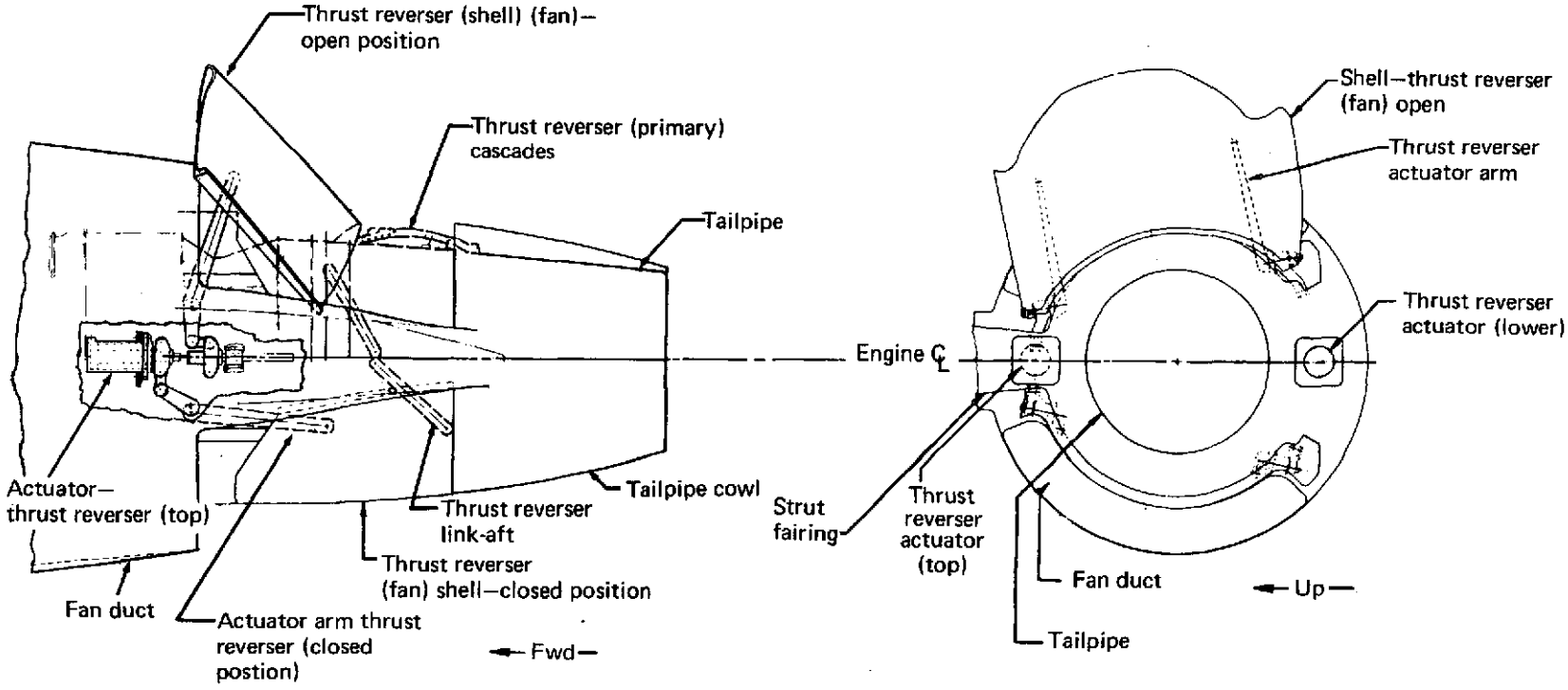


PLAN VIEW

END VIEW

*FIGURE 22.—707/JT3D-9 CONFIGURATION 2 FAN THRUST REVERSER*

A new independent hydraulic system was designed in each nacelle for operating the thrust reverser. This system is shown schematically in figure 23.

### 3.4.3 Configuration 3

The configuration 3 design was identical to configuration 2 in all respects, except that it would contain two treated splitter rings instead of one. The increased inlet weight would require an increase in strut structural weight.

### 3.4.4 Configuration 4

Configuration 4 is shown in figure 24. This design was developed for evaluation of a long-duct, fully treated nacelle. The design features a two-ring inlet; a long fan duct bifurcated for maintenance access, then recombined to obtain acoustic benefits of a coannular nozzle; a primary plug nozzle; and a single target-type thrust reverser to reverse both primary and secondary flow.

Successful development of this concept would have permitted maximum suppression of fan noise. The plug nozzle would have provided a reasonably small duct height for treatment of turbine tones and core engine machinery noise. The plug nozzle would also have reduced jet noise. (The nozzle noise test program would have evaluated potential jet noise reduction and established design criteria.) This nozzle also would have permitted a significant reduction in nozzle length. The external target-type thrust reverser would also have provided noise-reduction benefits during reversed-thrust operation and promised significant improvements in weight, operational reliability, and maintenance requirements. Studies of this type of thrust reverser system for the 707 airplane have emphasized the fact that successful development of this concept will require considerable wind tunnel testing and design ingenuity.

### 3.4.5 Configuration 1A

The configuration 1A design was identical in all respects to configuration 1, except that it incorporated a one-ring inlet and inlet translation like that featured in configuration 2.

### 3.4.6 Trade Studies

This section includes a general discussion of the various studies made on the 707 airplane nacelle packages; design considerations preceding the particular studies; and the reason nacelle configuration 1 was chosen as the recommended nacelle design.

A trade study was performed on configurations 1, 2, and 4. Configurations 3 and 1A were not included in the trade study. Table 3 shows the configurations included in the trade study.

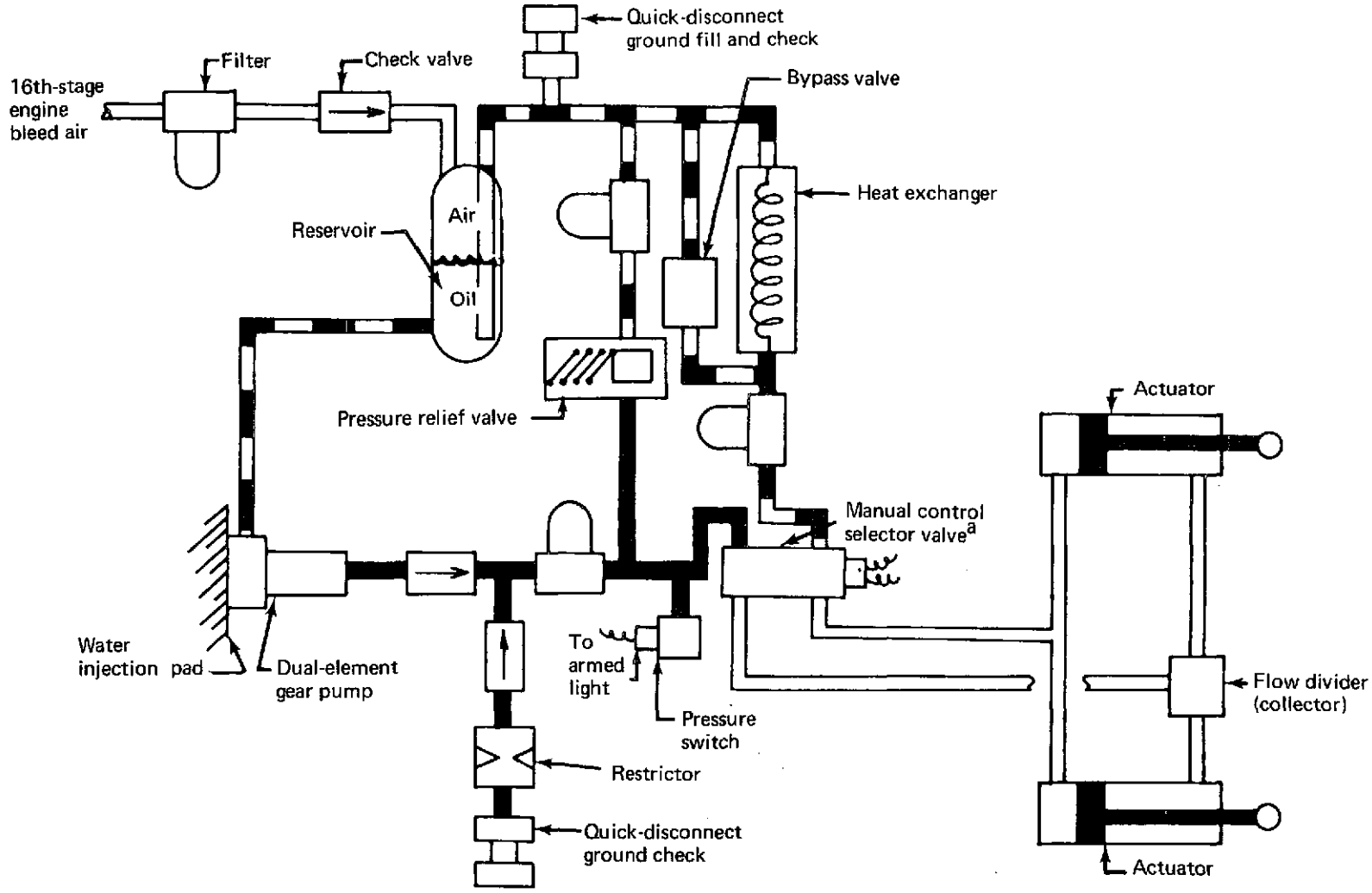


[a]Pressurization valve solenoid energized by reverse lever

*FIGURE 23.—707/JT3D-9 CONFIGURATION 2 THRUST REVERSER ACTUATION SYSTEM*

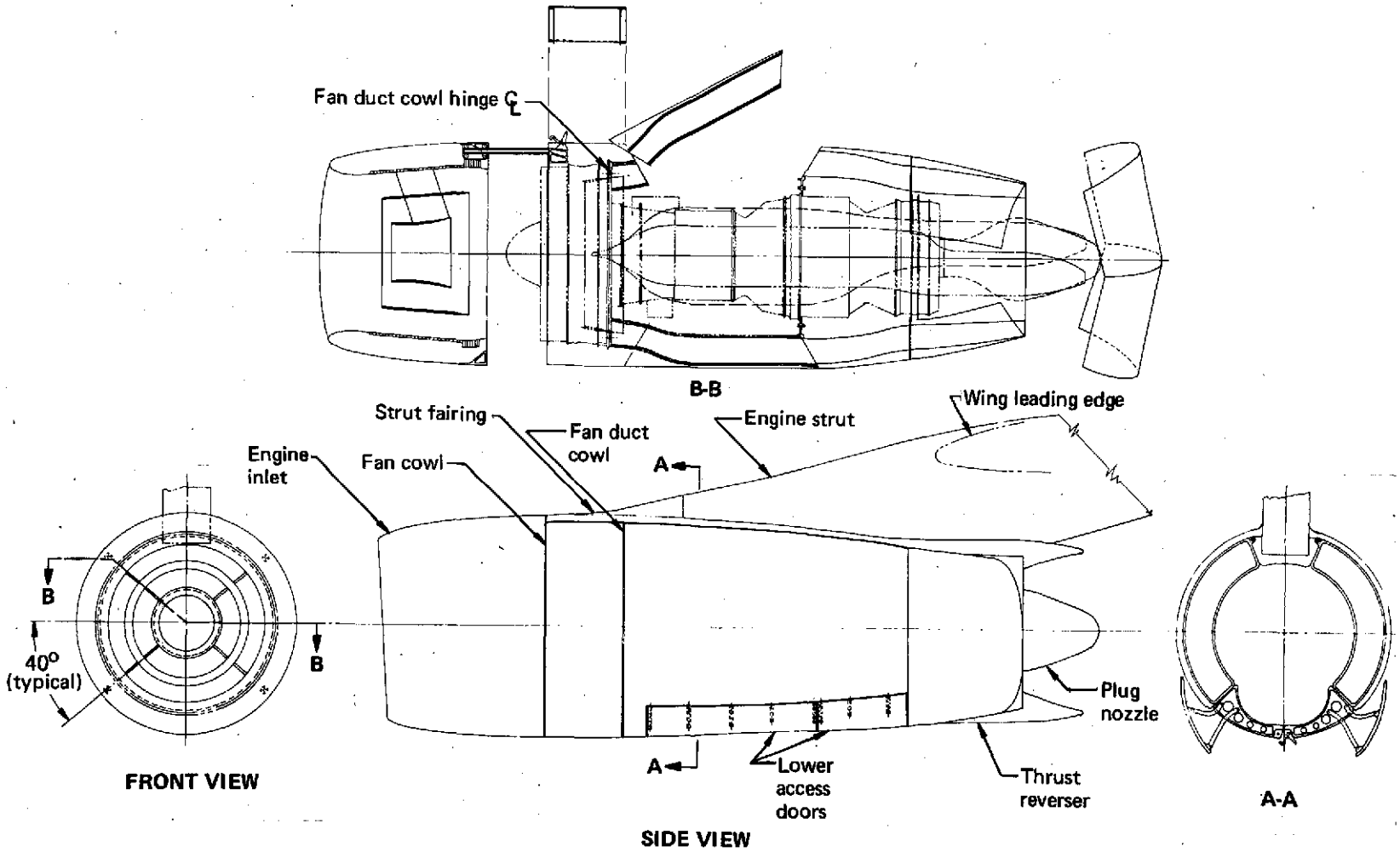


*FIGURE 24.—707/JT3D-9 CONFIGURATION 4 NACELLE*

*TABLE 3.—707/JT3D-9 NACELLE CONFIGURATION TRADE STUDY MATRIX*

| Number of inlet rings | Fan duct length | | |
|---|---|---|---|
| | Short | 3/4 | Full |
| 0 | X | X | |
| 1 | X | X | X |
| 2 | | X | X |

The no-ring, one-ring, and two-ring inlet configurations differ dimensionally, but they have the same geometrical shape and have the same type of acoustic treatment. The amount (area) of treatment in the three inlets will vary, since the rings will be treated on both inner and outer surfaces as shown in figure 36. The short and 3/4-length fan ducts correspond to those previously described in sections 3.4.2 and 3.4.4 (ref. figs. 21 and 24). The full-length fan duct would contain the same length, 63 in. (1.60 m), of acoustic treatment as the 3/4-length fan duct.

Table 4 shows the airplane weight increase for each nacelle configuration. The comparatively low weight increase with the full-length ducts would be due to the use of a single target-type thrust reverser for the combined primary and fan exhaust. This thrust reverser concept would be applicable only to the long-duct configuration and would require extensive development to ensure that it would be operationally satisfactory for the 707 airplane.

*TABLE 4.—707/JT3D-9 AIRPLANE OPERATING EMPTY WEIGHT INCREASE FOR TRADE STUDY NACELLES*

| Number of inlet rings | Fan duct length | | |
|---|---|---|---|
| | Short | 3/4 | Full |
| 0 | 2205 lb (1000.2 kg) | 3390 lb (1537.7 kg) | |
| 1 | 2530 lb (1147.6 kg) | 3705 lb (1680.6 kg) | 3030 lb (1374.4 kg) |
| 2 | | 3925 lb (1780.4 kg) | 3170 lb (1437.9 kg) |

Figure 25 shows the nacelle configuration effect on cruise-effective specific fuel consumption (considering nacelle/strut external drag), airplane OEW increase, and range loss. Comparison of these data for the single ring inlet shows that while the 3/4-length duct configuration would result in the largest OEW increase, the lower cruise-effective specific fuel consumption would result in a very small range loss. Addition of a second inlet ring would result in further increases in all three parameters.

Figure 26 shows the effect of nacelle configuration on flyover noise estimates at FAR Part 36 conditions for approach, takeoff, and takeoff with cutback. The results show that takeoff noise, with or without cutback, would be only slightly affected by nacelle configuration. Approach noise would be significantly reduced with the addition of a single inlet ring. Addition of a second ring would achieve only a small reduction over the one-ring inlet configuration.

From figures 25 and 26, it is apparent that the full-length duct would not have offered sufficient noise reduction over the 3/4-length duct to justify the additional range loss.

Table 5 compares noise reduction and range loss for the one-ring inlet nacelles with short and 3/4-length fan ducts. These two configurations are very similar in noise reduction and airplane performance; however, other considerations, such as initial kit costs, maintenance access, maintainability, and simplicity of thrust reverser design, favor a short fan duct nacelle configuration.

## 3.5 AIRPLANE MODIFICATION

### 3.5.1 Wing

The extent of wing modification required would depend on need for relocation of the nacelles to ensure adequate flutter margins. Fittings used for strut attachment or load distribution may require redesign for compatibility with the higher nacelle loads.

The primary influence of the JT3D-9 installation on the wing structure would be the change in nacelle aerodynamic loads, weight, and center of gravity, which affect the strength and flutter characteristics of the wing. Examination of the margins of safety at the critical wing station at 73.7% semispan indicated sufficient strength to allow a gross weight increase of 8000 lb (3628.8 kg). Based on this, no structural revision of the wing would be anticipated for the refanned configuration, even if flutter requirements had dictated a relocation of the nacelle.

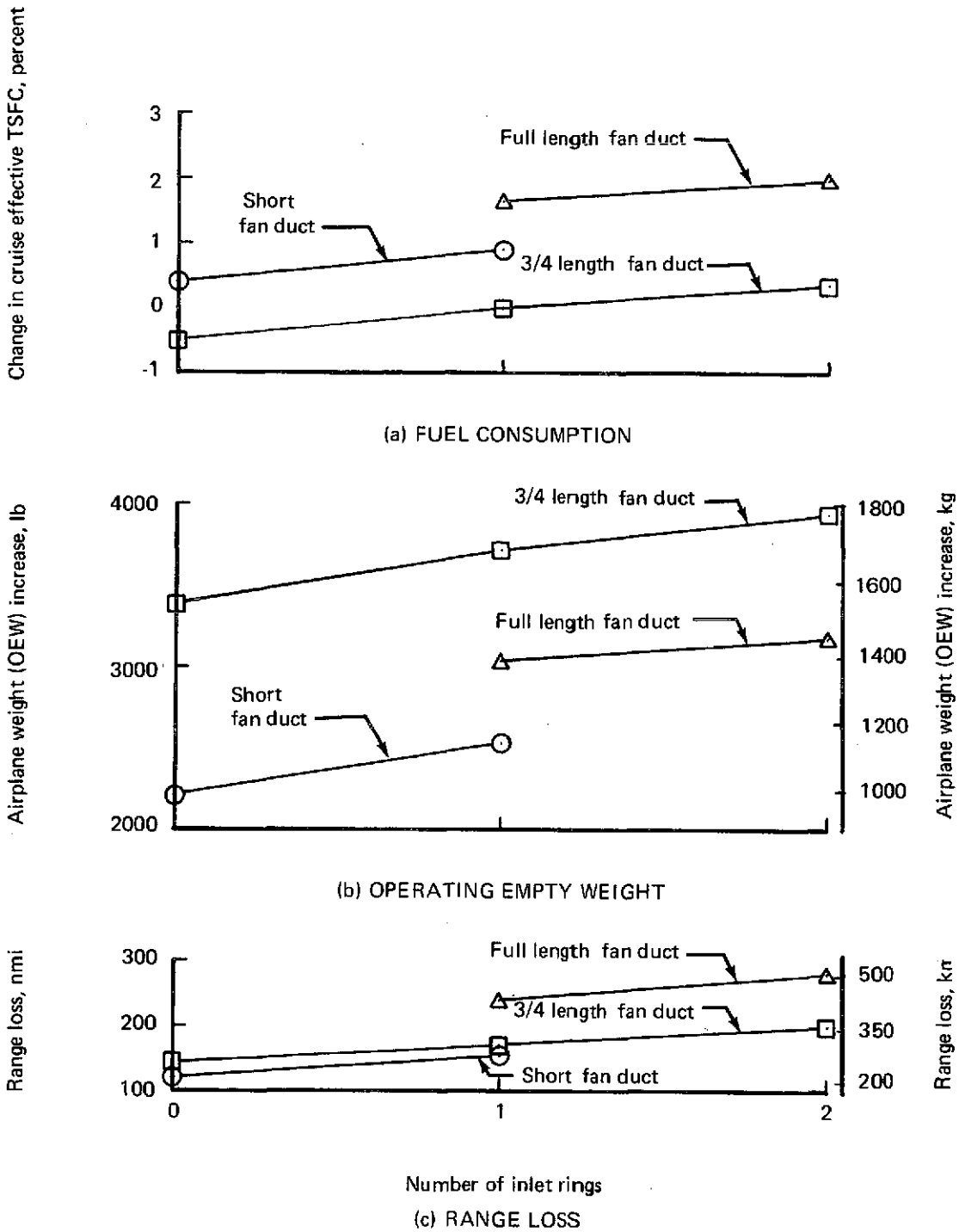


*FIGURE 25.—707/JT3D-9—EFFECT OF NACELLE CONFIGURATION ON FUEL CONSUMPTION, OPERATING EMPTY WEIGHT, AND RANGE, INCLUDING NACELLE/STRUT EXTERNAL DRAG, MACH 0.83, 35 000 FT (10 668 M)*

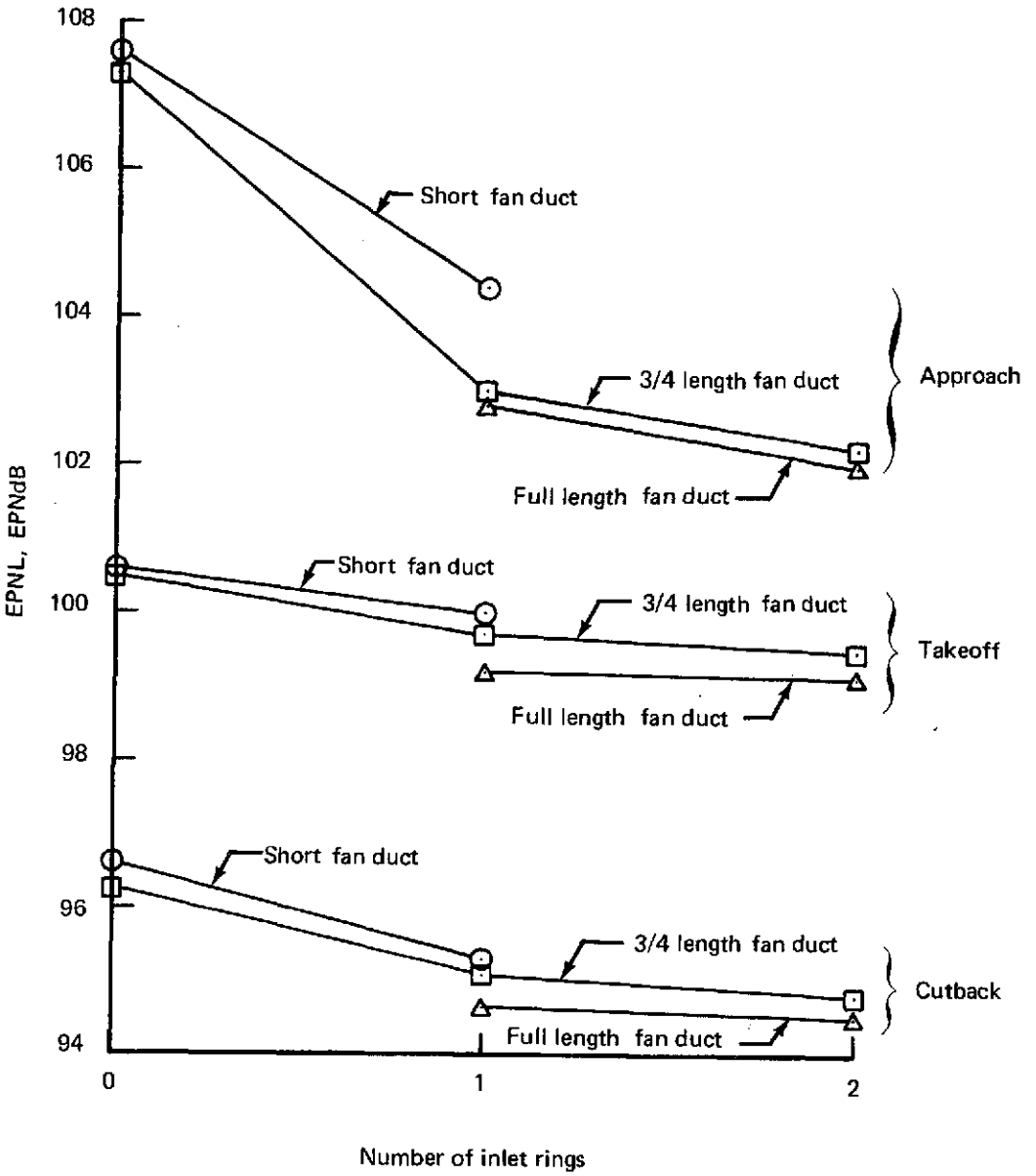


*FIGURE 26.–707/JT3D-9–EFFECT OF NACELLE CONFIGURATION ON FLYOVER NOISE AT FAR PART 36 CONDITIONS*

*TABLE 5.–COMPARISON OF NOISE REDUCTION AND RANGE LOSS FOR THE SHORT AND 3/4-LENGTH FAN DUCTS WITH ONE INLET RING*

| Condition | | One-ring inlet 3/4 fan duct | One-ring inlet Short fan duct |
|---|---|---|---|
| EPNL, EPNdB (per FAR Part 36) | | | |
| Takeoff | | 99.7 | 100.0 |
| Takeoff with cutback | | 95.1 | 95.3 |
| Approach | | 103.0 | 104.4 |
| Maximum sideline | | 92.1 | 92.5 |
| Noise contour area reduction (reference current airplane), % | | | |
| Full-power operational takeoff | 90 EPNdB | 86 | 85 |
| | 100 EPNdB | 94 | 93 |
| Cutback certification takeoff | 90 EPNdB | 90 | 88 |
| | 100 EPNdB | 93 | 92 |
| Range loss (reference current airplane) | | 170 nmi (314.84 kn) | 155 nmi (287.06 kn) |

### 3.5.2 Nacelle Struts

The engines and nacelles are mounted forward of, and below, the wing on nacelle struts (fig. 27). The primary functions of the struts are to position the engines and nacelles so that adequate wing flutter margins exist under all expected operational conditions, to minimize installed nacelle drag, to provide adequate nacelle ground clearance, and to transmit engine loads to the wing.

Four longitudinal members, four vertical members, and the skin panels comprise strut primary structure. Strut-to-wing attachment is made with four bolts. The secondary structure includes the fairing around the wing leading edge and over the wing upper surface and the trailing edge fairing, which fairs in the diagonal brace on the wing undersurface.

Inertia and air loads associated with the JT3D-9 installation were expected to require changes to both inboard and outboard nacelle struts to maintain adequate structural and flutter margins. The analysis of the magnitude of the required changes was not completed. It is anticipated that the outboard strut will be replaced and the inboard strut reinforced.

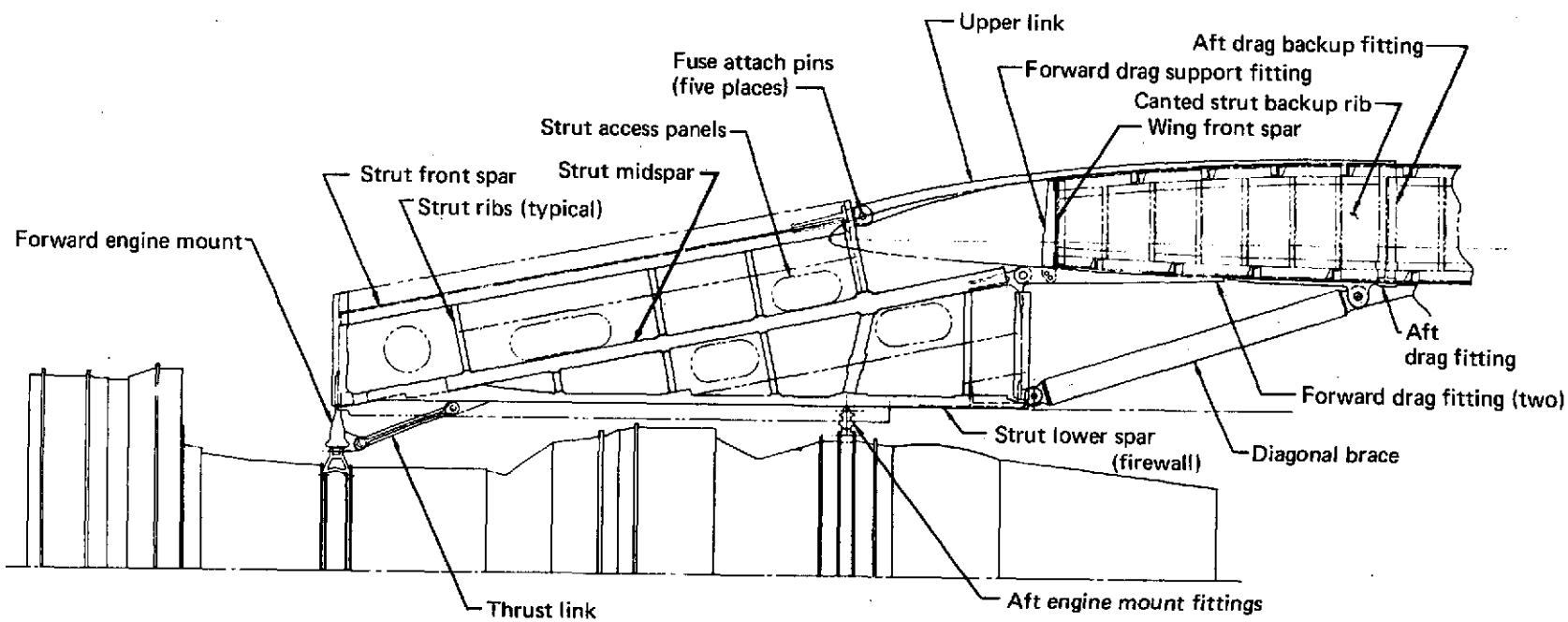


*FIGURE 27.–707/JT3D STRUT/WING BASIC STRUCTURE*

### 3.5.3 Fin and Aft Body

Directional control and $V_{MC}$ would be adversely affected by the increased thrust available from the refanned engines. (See sec. 3.7.4.) It was estimated that a 15% increase in rudder hinge moment would be required to maintain directional control. The rudder and actuator attachment fittings and basic airframe structures have sufficient strength to accommodate this change. The adequacy of the attachment fittings for required fatigue life was not analyzed.

## 3.6 MAINTENANCE ANALYSIS AND SUPPORT EQUIPMENT

### 3.6.1 Maintenance Analysis

The JT3D-9 installation design incorporated a majority of the JT3D-3B engine accessories; those new items incorporated were designed to meet a standard of maintainability equivalent to that of the remainder of the installation. The new engine installation will provide a standard of accessibility equal to (and, in some cases, better than) that of the baseline airplane. The larger cowl doors, hinged fan duct, and relocated oil tank and ignition exciters will provide better accessibility.

The inlet was designed for installation of an acoustic diffuser and an acoustic ring (or rings). The design provides for ease of inspection and replacement of the acoustic panels, when required. The airplane can be flown with the ring (or rings) removed, if necessary. The inlet assembly was designed with a track-and-carriage assembly to permit better access to the engine fan blades and other components for inspection and maintenance.

The target-type thrust reverser design was based on the currently used reverser with simplification and design improvement of the primary and fan reverser. This basic design has a minimum of moving parts and will have a high standard of maintainability.

Elimination of the turbocompressor, inlet guide vanes, and inlet blow-in doors will also improve maintainability.

### 3.6.2 Support Equipment

There are no changes expected for the ground support equipment, except those necessary for nacelle handling. No change is anticipated for the service equipment. No change is anticipated in either procedures or equipment involved with jacking, hoisting, and towing.

### 3.6.3 System Support

A minimum of special training would be required for certification of ground maintenance people, due to the high standard of commonality between the JT3D-3B/-7 and the JT3D-9 installations regarding accessories, instrumentation, and controls. A minimum of flight crew familiarization would be required because of the similarity in flight and handling characteristics between the refanned engine airplane and the baseline airplane.

Hardware would be designed to the certification rules of FAR Part 25 (flutter requirements). Changes to the airplane would be confined to those required for installation of the refanned engines.

## 3.7 PERFORMANCE COMPARISON

Each of the candidate nacelle configurations was analyzed to determine takeoff and cruise performance of modified 707-320B airplanes with constant BRGW and with BRGW increased within existing design limitations. This analysis indicates that the 707-320B airplane, modified with any one of four nacelle configurations, and using allowable BRGW increases, will have significantly improved takeoff and climb performance and a slight improvement in cruise performance and maximum range.

Table 6 presents a summary of airplane performance, modification cost estimates, and predicted noise levels for each configuration on an airplane with BRGW limited to that of the baseline airplane. Table 7 presents a similar summary in which the BRGW for the different configurations was estimated to increase within existing design growth limits.

The JT3D-9 uninstalled-engine performance is discussed in section 3.2.3. This performance must be adjusted to installed-engine performance by subtracting nacelle internal and external drag, and engine power and bleed extraction. Installed-engine performance, together with estimated weight changes, is then used to determine the modified-airplane performance.

### 3.7.1 Installed-Engine Performance

The nacelle installation losses include inlet, fan duct, and primary duct pressure losses; air bleed; and mechanical power extraction. The incremental effects of these losses on takeoff thrust and cruise fuel consumption are summarized in tables 8 and 9, respectively.

## TABLE 6.—707-320B PERFORMANCE SUMMARY—CONSTANT BRGW

| Parameter | 707-320B configuration | | | | | | | | | | | | | |
|---|---|---|---|---|---|---|---|---|---|---|---|---|---|---|
| | Baseline | | 1 | | | 1A | | | 2 | | | 3 | | |
| OEW, lb (kg)<br>ΔOEW, lb (kg)<br>Change, % | 145 000 (65 771) | | 147 025 (66 689)<br>+2025 (919)<br>+1.4 | | | 147 565 (66 934)<br>+2565 (1163)<br>+1.7 | | | 148 925 (67 551)<br>+3925 (1780)<br>+2.7 | | | 149 145 (67 651)<br>+4145 (1880)<br>+2.9 | | |
| Brake release gross weight, [a]lb (kg) | 333 600 (151 318) | | 333 600 (151 318) | | | 333 600 (151 318) | | | 333 600 (151 318) | | | 333 600 (151 318) | | |
| Takeoff field length, ft (m)<br>Change, % | 11 350 (3459) | | 9950 (3033)<br>-12.3 | | | 10 030 (3057)<br>-11.6 | | | 9990 (3045)<br>-12.0 | | | 10 130 (3088)<br>-10.7 | | |
| ATA range, nmi (km)<br>Change, % | 4770 (8834) | | 4750 (8797)<br>-0.4 | | | 4710 (8723)<br>-1.3 | | | 4730 (8760)<br>-0.8 | | | 4700 (8704)<br>-1.5 | | |
| Kit and installation cost, millions of dollars per aircraft | – | | 1.549 | | | 1.581 | | | 2.205 | | | 2.220 | | |
| Airplane quantity | – | | [b]385 | | | [b]385 | | | [c]222 | | | [c]222 | | |
| Cash DOC change from baseline, % | – | | -0.14 | | | 0.03 | | | 0.29 | | | 0.33 | | |
| Average range, nmi (km) | – | | 1515 (2806) | | | 1515 (2806) | | | 1515 (2806) | | | 1515 (2806) | | |
| FAR Part 36 noise, EPNdB | Limit | Measured | Limit | Predicted | Δ [f] | Limit | Predicted | Δ [f] | Limit | Predicted | Δ [f] | Limit | Predicted | Δ [f] |
| Takeoff | 103.7 | 115.0 | 103.7 | 98.3 | -16.7 | 103.7 | 97.7 | -17.3 | 103.7 | 97.2 | -17.8 | 103.7 | 96.6 | -18.4 |
| Cutback | 103.7 | 114.0 | 103.7 | 94.5 | -19.5 | 103.7 | 93.2 | -20.5 | 103.7 | 93.0 | -21.0 | 103.7 | 92.6 | -21.4 |
| Approach[d] | 106.3 | 120.5 | 106.3 | 105.1 | -15.4 | 106.3 | 103.0 | -17.5 | 106.3 | 101.9 | -18.6 | 106.3 | 99.1 | -21.4 |
| Sideline | 106.3 | 107.5 | 106.3 | 94.8 | -12.7 | 106.3 | 94.5 | -13.0 | 106.3 | 94.2 | -13.3 | 106.3 | 93.8 | -14.7 |
| 95 EPNdB contour area reduction,[e] % | – | | 88.7 | | | 91.0 | | | 92.1 | | | 93.7 | | |
| Relative footprint noise index | 1.0 | | 0.111 | | | 0.092 | | | 0.082 | | | 0.065 | | |

[a]Note constant gross weight

[b]Cost base includes 707-120B and 720B fleets

[c]Assumes 707-120B and 720B modified to configuration 1 (385 aircraft)

[d]Approach flaps—50°

[e]At baseline BRGW

[f]Δ from baseline measured noise level

## TABLE 7.—707-320B PERFORMANCE SUMMARY—INCREASED BRGW

| Parameter | 707-320B configuration | | | | | | | | | | | | | |
|---|---|---|---|---|---|---|---|---|---|---|---|---|---|---|
| | Baseline | | 1 | | | 1A | | | 2 | | | 3 | | |
| OEW, lb (kg)<br>ΔOEW, lb (kg)<br>Change, % | 145 000 (65 772) | | 147 025 (66 691)<br>2025 (919)<br>+1.40 | | | 147 565 (66 935)<br>2565 (1163)<br>+1.77 | | | 148 925 (67 552)<br>3925 (1780)<br>+2.71 | | | 149 145 (67 652)<br>4145 (1880)<br>+2.85 | | |
| Brake release gross weight, [a]lb (kg)<br>Change, % | 333 600 (151 321) | | 337 500 (153 090)<br>+1.17 | | | 338 100 (153 362)<br>+1.35 | | | 339 400 (153 952)<br>+1.74 | | | 339 600 (154 043)<br>+1.80 | | |
| Takeoff field length, ft (m)<br>Change, % | 11 350 (3459) | | 10 260 (3127)<br>-9.6 | | | 10 370 (3161)<br>-8.6 | | | 10 370 (3161)<br>-8.6 | | | 10 530 (3210)<br>-7.2 | | |
| ATA range, nmi (km)<br>Change, % | 4770 (8834) | | 4840 (8964)<br>+1.5 | | | 4810 (8908)<br>+0.8 | | | 4880 (9038)<br>+2.3 | | | 4850 (8982)<br>+1.7 | | |
| Kit and installation cost, millions of dollars per aircraft | – | | 1.549 | | | 1.581 | | | 2.205 | | | 2.220 | | |
| Airplane quantity | – | | [b]385 | | | [b]385 | | | [c]222 | | | [c]222 | | |
| Cash DOC change from baseline, % | – | | -0.14 | | | 0.03 | | | 0.29 | | | 0.33 | | |
| Average range, nmi (km) | – | | 1515 (2806) | | | 1515 (2806) | | | 1515 (2806) | | | 1515 (2806) | | |
| FAR Part 36 noise, EPNdB | Limit | Measured | Limit | Predicted | Δ [f] | Limit | Predicted | Δ [f] | Limit | Predicted | Δ [f] | Limit | Predicted | Δ [f] |
| Takeoff | 103.7 | 115.0 | 103.8 | 98.5 | -16.5 | 103.8 | 98.0 | -17.0 | 103.9 | 97.5 | -17.5 | 103.9 | 97.0 | -18.0 |
| Cutback | 103.7 | 114.0 | 103.8 | 94.7 | -19.3 | 103.8 | 93.8 | -20.2 | 103.9 | 93.3 | -20.7 | 103.9 | 93.0 | -21.0 |
| Approach[d] | 106.3 | 120.5 | 106.4 | 105.1 | -15.4 | 106.4 | 103.0 | -17.5 | 106.4 | 101.9 | -18.6 | 106.4 | 99.1 | -21.4 |
| Sideline | 106.3 | 107.5 | 106.4 | 94.8 | -12.7 | 106.4 | 94.5 | -13.0 | 106.4 | 94.2 | -13.3 | 106.4 | 93.8 | -13.7 |
| 95-EPNdB contour area reduction[e], % | – | | 88.7 | | | 91.0 | | | 92.1 | | | 93.7 | | |
| Relative footprint noise index | 1.000 | | 0.111 | | | 0.092 | | | 0.082 | | | 0.065 | | |

[a]Note modified airplane gross weight increase—does not apply to all 707-320B airplanes

[b]Cost base includes 707-120B and 720B fleets

[c]Assumes707-120B, 720B modified to configuration 1 (total of 385 aircraft modified)

[d]Approach flaps—50°

[e]At baseline BRGW

[f]Δ from baseline measured noise level

## TABLE 8.–707/JT3D-9 INSTALLED INCREMENTAL LOSSES $\Delta F_N/F_N$ AT TAKEOFF[a]

| Item | Configuration | | | | | | | |
|---|---|---|---|---|---|---|---|---|
| | 1 | | 1A | | 2 | | 3 | |
| | Loss | $\Delta F_N/F_N$, % | Loss | $\Delta F_N/F_N$, % | Loss | $\Delta F_N/F_N$, % | Loss | $\Delta F_N/F_N$, % |
| Inlet loss, $\Delta P/P$ | 0.004 | –0.8 | 0.007 | –1.6 | 0.007 | –1.6 | 0.012 | –2.6 |
| Power extraction | 32 hp (23.8 kW) | –0.1 | 32 hp (23.8 kW) | –0.1 | 32 hp (23.8 kW) | –0.1 | 32 hp (23.8 kW) | –0.1 |
| Bleed | 0 | 0 | 0 | 0 | 0 | 0 | 0 | 0 |
| Primary nozzle velocity coefficient, $\Delta C_{VE}$ | –0.002 | –0.2 | –0.002 | –0.2 | –0.002 | –0.2 | –0.002 | –0.2 |
| Fan nozzle velocity coefficient, $\Delta C_{VD}$ | –0.001 | –0.1 | –0.001 | –0.1 | –0.001 | –0.1 | –0.001 | –0.1 |
| Primary duct, $\Delta P/P$ | 0 | 0 | 0 | 0 | 0 | 0 | 0 | 0 |
| Fan duct, $\Delta P/P$ | 0.001 | –0.1 | 0.001 | –0.1 | 0.014 | –1.3 | 0.014 | –1.3 |
| Scrubbing drag | – | –2.1 | – | –2.1 | – | –0.5 | – | –0.5 |
| Total | | –3.4 | | –4.2 | | –3.8 | | –4.8 |

[a]Sea level, standard day

## TABLE 9.–707/JT3D-9 INSTALLED INCREMENTAL LOSSES $\Delta TSFC/TFSC$ AT CRUISE[a]

| Item | Configuration | | | | | | | |
|---|---|---|---|---|---|---|---|---|
| | 1 | | 1A | | 2 | | 3 | |
| | Loss | ΔTSFC/ TSFC, % | Loss | ΔTSFC/ TSFC, % | Loss | ΔTSFC/ TSFC, % | Loss | ΔTSFC/ TSFC, % |
| Inlet loss, $\Delta P/P$ | 0.003 | 0.4 | 0.007 | 0.8 | 0.007 | 0.8 | 0.010 | 1.2 |
| Power extraction | 32 hp (23.8 kW) | 1.8 | 32 hp (23.8 kW) | 1.8 | 32 hp (23.8 kW) | 1.8 | 32 hp (23.8 kW) | 1.8 |
| Bleed | 2.67 lb/sec (1.21 kg/sec) | | 2.67 lb/sec (1.21 kg/sec) | | 2.67 lb/sec (1.21 kg/sec) | | 2.67 lb/sec (1.21 kg/sec) | |
| Primary nozzle velocity coefficient, $\Delta C_{VE}$ | -0.002 | 0.4 | -0.002 | 0.4 | -0.002 | 0.4 | -0.002 | 0.4 |
| Fan nozzle velocity coefficient, $\Delta C_{VD}$ | -0.001 | 0.6 | -0.001 | 0.6 | -0.006 | 0.6 | -0.001 | 0.6 |
| Primary duct, $\Delta P/P$ | 0 | 0 | 0 | 0 | 0 | 0 | 0 | 0 |
| Fan duct $\Delta P/P$ | 0.003 | 0.2 | 0.003 | 0.2 | 0.016 | 1.2 | 0.016 | 1.2 |
| Scrubbing | | 5.7 | – | 5.7 | – | 1.4 | – | 1.4 |
| Total | | 9.1 | | 9.5 | | 6.2 | | 6.6 |

[a]Mach = 0.83, 35 000 ft (10 668 m), net thrust = 3350 lb (14 902 N)

Takeoff lapse rates ($F_N$ vs TAS) for these nacelle configurations at sea level, 2000 ft (609.6 m) and 4000 ft (1219.2 m) are compared in figure 28. The JT3D-3B sea-level takeoff lapse rate is shown for comparison. As shown, the JT3D-9 sea-level installed takeoff thrust is about 10% greater than the JT3D-3B and at 4000 ft (1219.2 m) is approximately the same as the JT3D-3B at sea level. The increased takeoff thrust of the JT3D-9 can be used to decrease takeoff field length requirements for a given airplane gross weight or to permit increased takeoff gross weight with a given runway length.

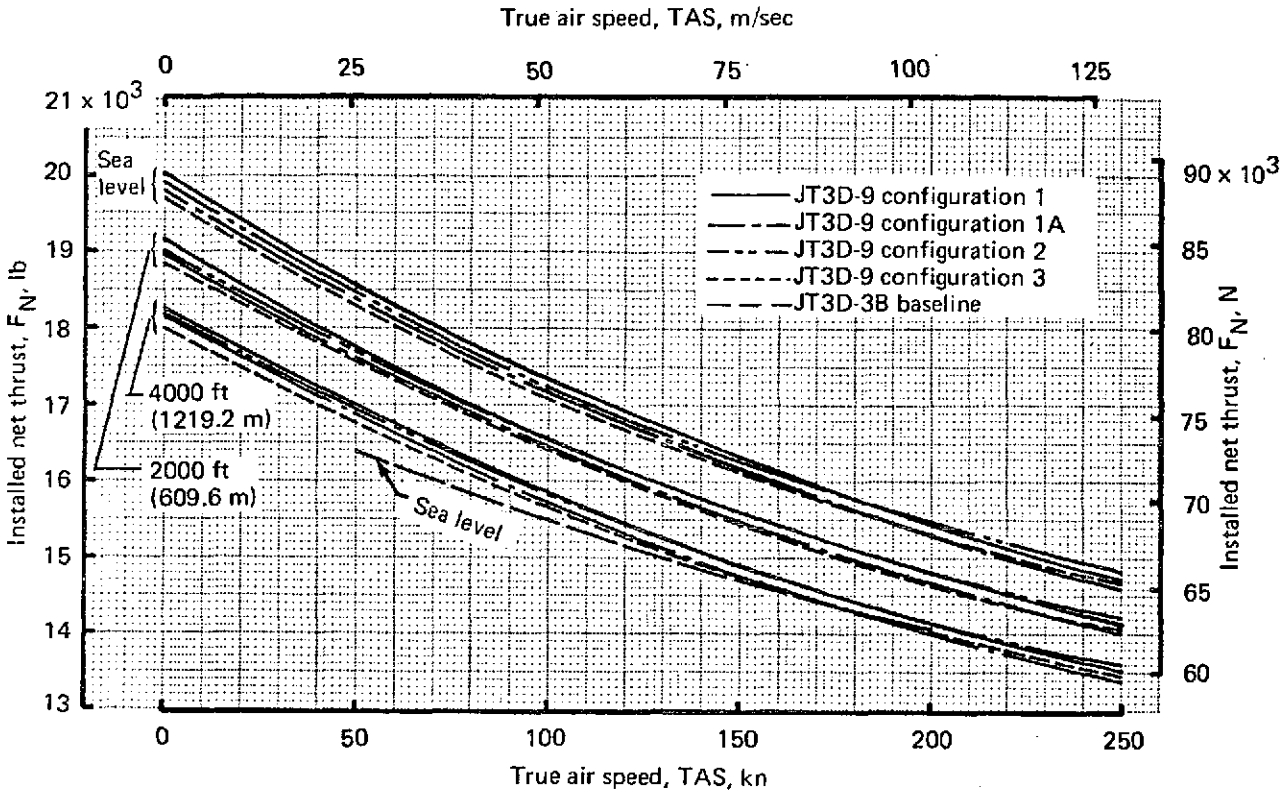


*FIGURE 28.—707/JT3D-3B/JT3D-9 INSTALLED-ENGINE THRUST PERFORMANCE COMPARISON, STANDARD DAY*

Thrust specific fuel consumption (TSFC vs $F_N$) for the JT3D-9 engine installed in each of the four nacelle configurations is compared in figure 29. The effect of nacelle external drag is included in this illustration. As shown, nacelle configuration 2 has the best performance. Each of these configurations exhibits improved thrust specific fuel consumption when compared with the JT3D-3B configuration.

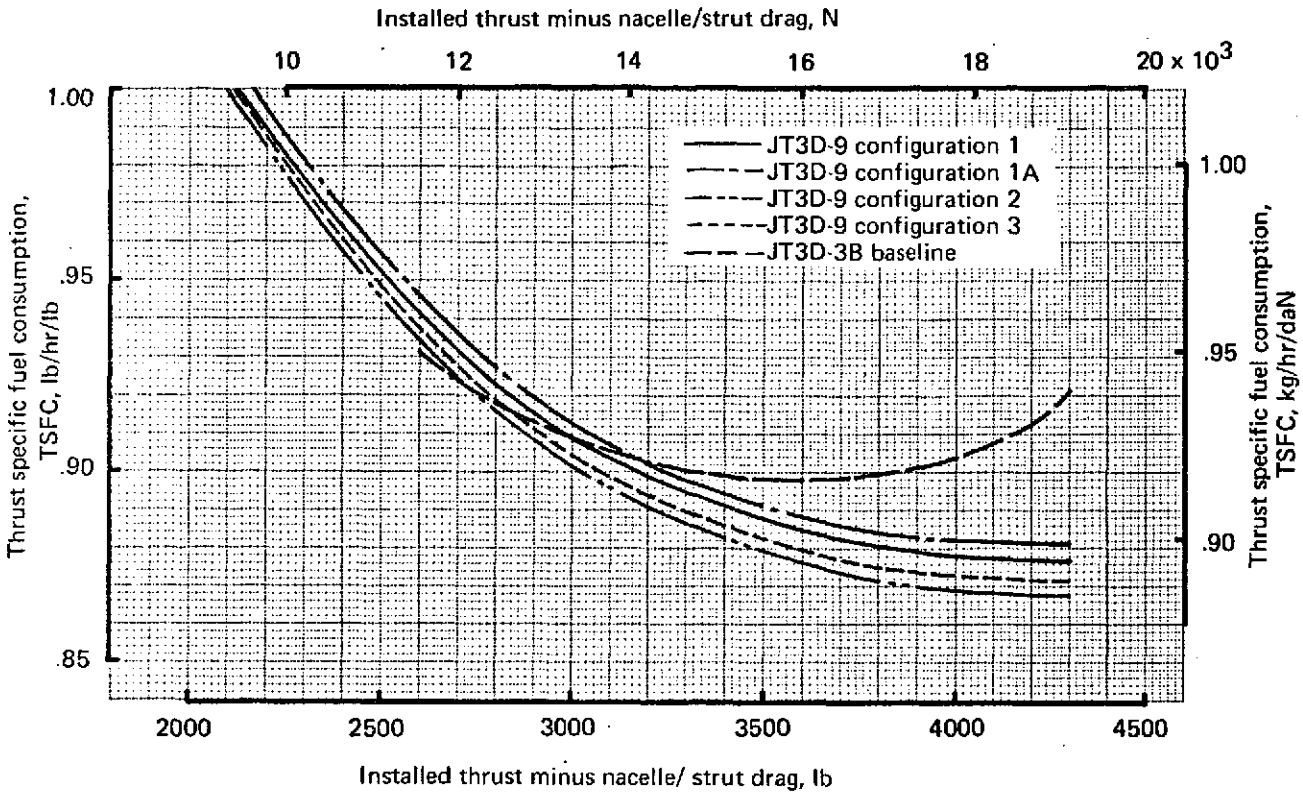


*FIGURE 29.–707/JT3D-3B/JT3D-9–INSTALLED-ENGINE TSFC PERFORMANCE COMPARISON, STANDARD DAY, 35 000 FT (10 668 M), MACH 0.83*

### 3.7.2 Weight and Balance

Installation of the JT3D-9 engines would cause the airplane operating empty weight (OEW) to increase. The operational weight breakdown for the baseline airplane is shown in table 10. Table 11 shows the items in the nacelle weight statement that are modified by the refanned engine installation. Airplane loadability is not degraded with installation of the JT3D-9 engines.

The 707-320B baseline airplane was selected as being typical of the 707 fleet. Its characteristics are listed below.

| | |
|---|---|
| Operating empty weight (OEW) | 145 000 lb (65 770 kg) |
| Maximum taxi weight | 336 000 lb (152 410 kg) |
| Maximum landing weight | 247 000 lb (112 040 kg) |
| Maximum zero-fuel weight | 230 000 lb (104 328 kg) |
| Seating capacity | 149 passengers |
| Fuel capacity | 23 855 gal (90.301 $m^3$) |
| Engine | JT3D-3B |

*TABLE 10.—707-320B BASELINE AIRPLANE WEIGHT BREAKDOWN*

| Component | lb | kg |
|---|---|---|
| Wing | 32 550 | 14 765 |
| Horizontal tail | 4 080 | 1 850 |
| Vertical tail | 2 090 | 945 |
| Body | 26 940 | 12 220 |
| Main landing gear | 11 680 | 5 300 |
| Nose landing gear | 1 030 | 465 |
| Nacelle and strut | 4 230 | 1 920 |
| Total structure | 82 600 | 37 465 |
| Engine | 17 400 | 7 890 |
| Engine accessories | 1 210 | 550 |
| Engine controls | 170 | 75 |
| Starting system | 260 | 120 |
| Fuel system | 2 430 | 1 100 |
| Thrust reverser | 3 480 | 1 580 |
| Total propulsion group | 24 950 | 11 315 |
| Instruments | 540 | 245 |
| Surface controls | 3 090 | 1 400 |
| Hydraulics | 1 150 | 520 |
| Pneumatics | – | – |
| Electrical | 4 100 | 1 860 |
| Electronics | 2 410 | 1 095 |
| Flight provisions | 820 | 375 |
| Passenger accommodations | 11 320 | 5 135 |
| Cargo handling | 1 500 | 680 |
| Emergency equipment | 880 | 400 |
| Air conditioning | 3 460 | 1 570 |
| Anti-icing | 380 | 170 |
| Total fixed equipment | 29 650 | 13 450 |
| Exterior paint | 100 | 45 |
| Manufacturer's empty weight | 137 300 | 62 275 |
| Standard and operational items | 7 700 | 3 495 |
| Operating empty weight | 145 000 | 65 770 |

*TABLE 11.–707-320B BASELINE/MODIFIED WEIGHT COMPARISON*

| Component | Configuration | | | | | |
|---|---|---|---|---|---|---|
| | Baseline (JT3D-3B) | | 1 (JT3D-9) | | 1A (JT3D-9) | |
| | lb | kg | lb | kg | lb | kg |
| Engines (four) | 17 400 | 7 895 | 19 000 | 8 620 | 19 000 | 8 620 |
| Inlets, inlet rings | 780 | 355 | 1 040 | 470 | 1 580 | 715 |
| Cowls, fan ducts, miscellaneous | 1 315 | 595 | 1 510 | 685 | 1 510 | 685 |
| Primary thrust reversers | 2 340 | 1 060 | 2 360 | 1 070 | 2 360 | 1 070 |
| Fan thrust reversers | 1 140 | 520 | 1 280 | 580 | 1 280 | 580 |
| Accessories | 2 085 | 945 | 1 805 | 820 | 1 805 | 820 |
| Engine mounts | 100 | 45 | 110 | 50 | 110 | 50 |
| Struts and contents | 2 230 | 1 010 | 2 310 | 1 045 | 2 310 | 1 045 |
| Total engine installation weight per airplane | 27 390 | 12 425 | 29 415 | 13 340 | 29 955 | 13 585 |
| Propulsion weight change per airplane | Ref | Ref | +2 025 | +915 | +2 565 | +1 160 |
| Airplane modifications | – | – | 0 | 0 | 0 | 0 |
| Ballast | – | – | 0 | 0 | 0 | 0 |
| Total OEW change | Ref | Ref | +2 025 | +915 | +2 565 | +1 160 |

| Component | Configuration | | | | | |
|---|---|---|---|---|---|---|
| | 2 (JT3D-9) | | 3 (JT3D-9) | | 4 (JT3D-9) | |
| Engine | 19 000 | 8 620 | 19 000 | 8 620 | 19 000 | 8 620 |
| Inlets, inlet rings | 1 580 | 715 | 1 720 | 780 | 1 720 | 780 |
| Cowls, fan ducts, miscellaneous | 2 850 | 1 290 | 2 850 | 1 290 | 3 790 | 1 720 |
| Primary thrust reversers | 2 300 | 1 045 | 2 300 | 1 045 | [a]2 540 | [a]1 150 |
| Fan thrust reversers | 1 280 | 580 | 1 280 | 580 | | |
| Accessories | 1 805 | 820 | 1 805 | 820 | 1 805 | 820 |
| Engine mounts | 110 | 50 | 110 | 50 | 110 | 50 |
| Struts and contents | 2 390 | 1 085 | 2 470 | 1 120 | 2 470 | 1 120 |
| Total engine installation weight per airplane | 31 315 | 14 205 | 31 535 | 14 305 | 31 435 | 14 260 |
| Propulsion weight change per airplane | +3 925 | +1 780 | +4 145 | +1 880 | +4 045 | +1 835 |
| Airplane modifications | 0 | 0 | 0 | 0 | 0 | 0 |
| Ballast | 0 | 0 | 0 | 0 | 0 | 0 |
| Total OEW change | +3 925 | +1 780 | +4 145 | +1 880 | +4 045 | +1 835 |

[a]Primary and fan target-type thrust reverser

The baseline airplane maximum taxi weight can be increased to offset the refan OEW weight penalty with no structural changes to the aircraft. Further maximum gross weight growth is limited by the existing fuel tank capacity. There are early 707-320B airplanes and other 707 models that cannot accept a gross weight increase without significant structural modifications. Further study will be necessary to determine the extent of modifications required for each model.

### 3.7.3 Airplane Performance

The takeoff and cruise performance for the modified airplanes relative to the baseline airplane performance is shown in figures 30 through 35. There is a slight range penalty for the modified airplanes due to the increased OEW. This range loss can be offset by increasing maximum brake release gross weight within the limits of the existing fuel tank capacity. Such an increase is possible without loss in takeoff performance because of the improved thrust of the refanned engines. Figures 30 and 31 compare takeoff performance. A payload/range comparison between the modified and the production airplanes is shown in figures 32 and 33, while figures 34 and 35 show the range/field length trade. From figures 34 and 35, it can be seen that, for a given field length, all the modified airplanes show range improvement.

This analysis applies only to the baseline 707-320B/C, 336 000-lb (152 410-kg) gross weight airplane. This airplane is typical of the 707-320B/C series produced after line number 362. Further study will be required to determine the extent of modifications required for earlier 707-320B/C airplanes and for other 707 models to achieve any desired gross weight increase.

### 3.7.4 Stability and Control

The ground and air minimum control speeds, $V_{MCG}$ and $V_{MCA}$, for the 707-320B, with the JT3D-3B baseline and JT3D-9 configuration 2 nacelles, are shown in table 12. They have been estimated using previously obtained FAA certification results.

*TABLE 12.—MINIMUM CONTROL SPEED COMPARISON—707-320B*[a]

| Engine | $V_{MCG}$ | | $V_{MCA}$ | |
|---|---|---|---|---|
| | KEAS | m/sec | KEAS | m/sec |
| JT3D-3B (baseline) | 119 | 61.2 | 117 | 60.2 |
| JT3D-9 (configuration 2) | 124 | 63.8 | 123 | 63.3 |

[a]Sea level, standard day

The increased thrust of the JT3D-9 with configuration 2 nacelles will bring the ground minimum control speed close to the rudder blowdown speed of 125 kn (64.3 m/sec) equivalent air speed. Rudder hinge moment capability must be increased by approximately 15% to restore an adequate margin between $V_{MCG}$ and rudder blowdown speed and achieve acceptable engine-out control characteristics.

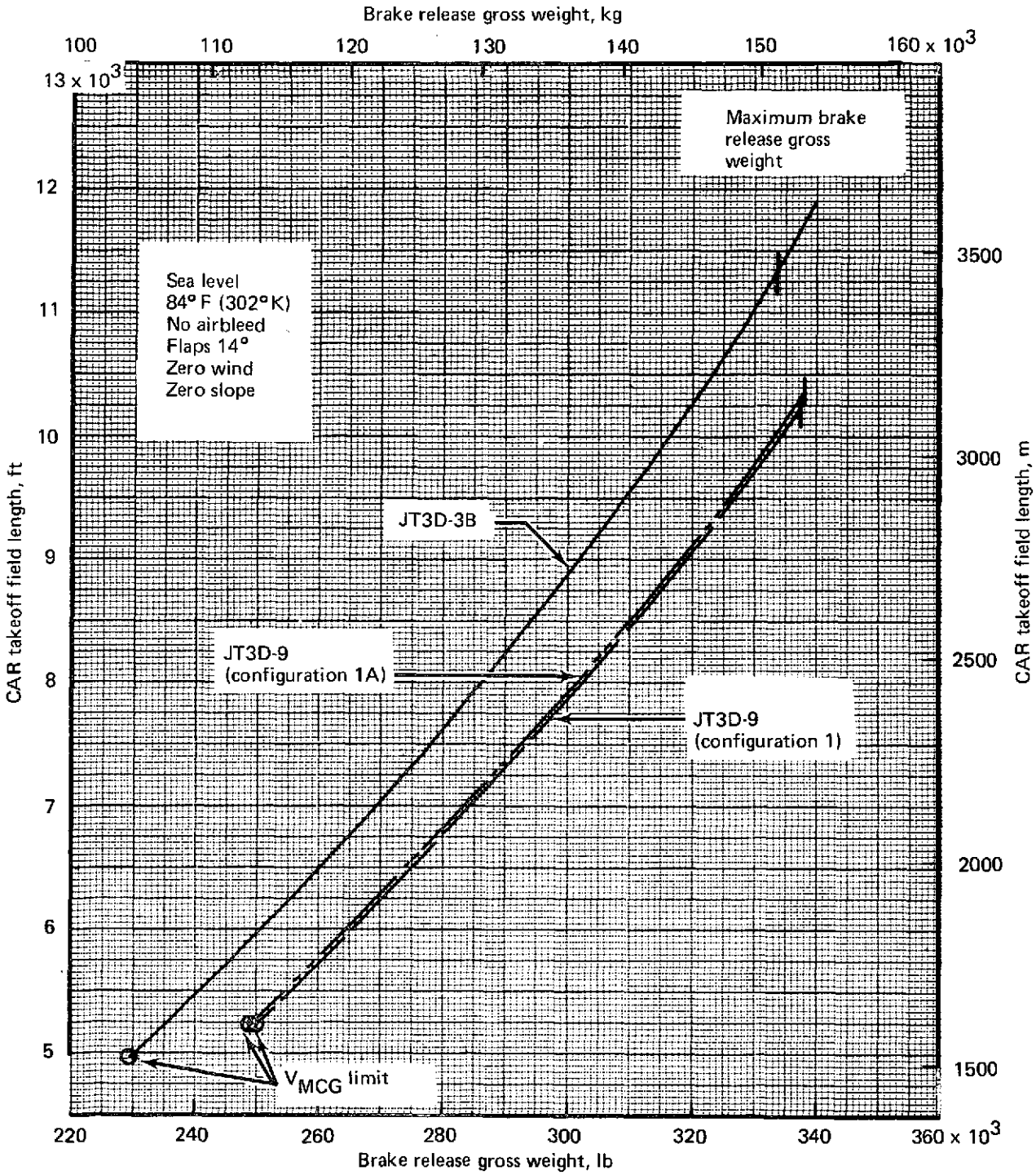


*FIGURE 30.—707/JT3D-9—CONFIGURATION 1 AND 1A TAKEOFF FIELD LENGTH COMPARISON*

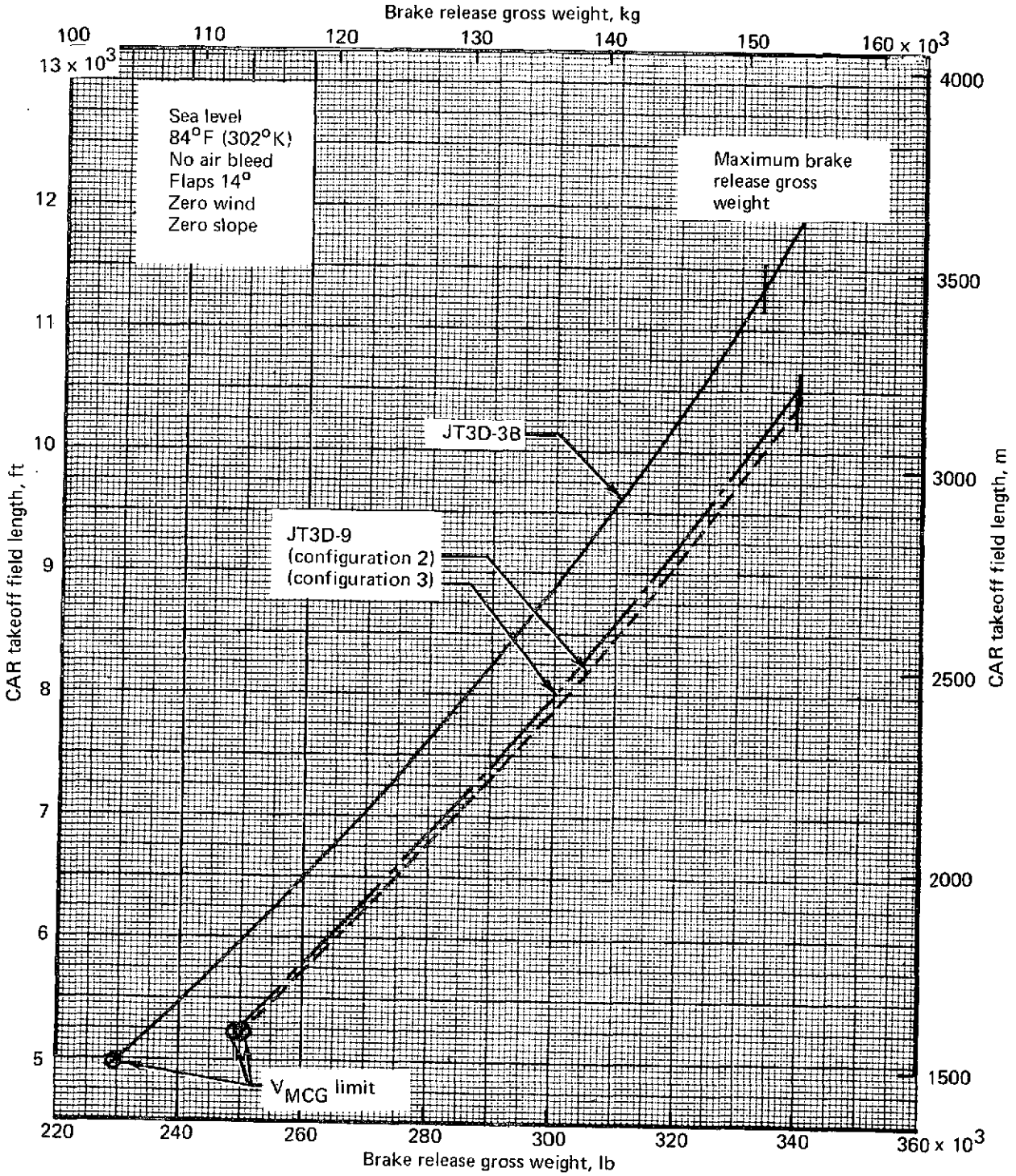


*FIGURE 31.—707/JT3D-9—CONFIGURATION 2 AND 3 TAKEOFF FIELD LENGTH COMPARISON*

| Configuration | Max BRGW | | OEW | |
|---|---|---|---|---|
| | lb | kg | lb | kg |
| Baseline | 333 600 | 151 318 | 145 000 | 65 770 |
| 1 | 337 500 | 153 087 | 147 025 | 66 689 |
| 1A | 338 100 | 153 359 | 147 565 | 66 934 |

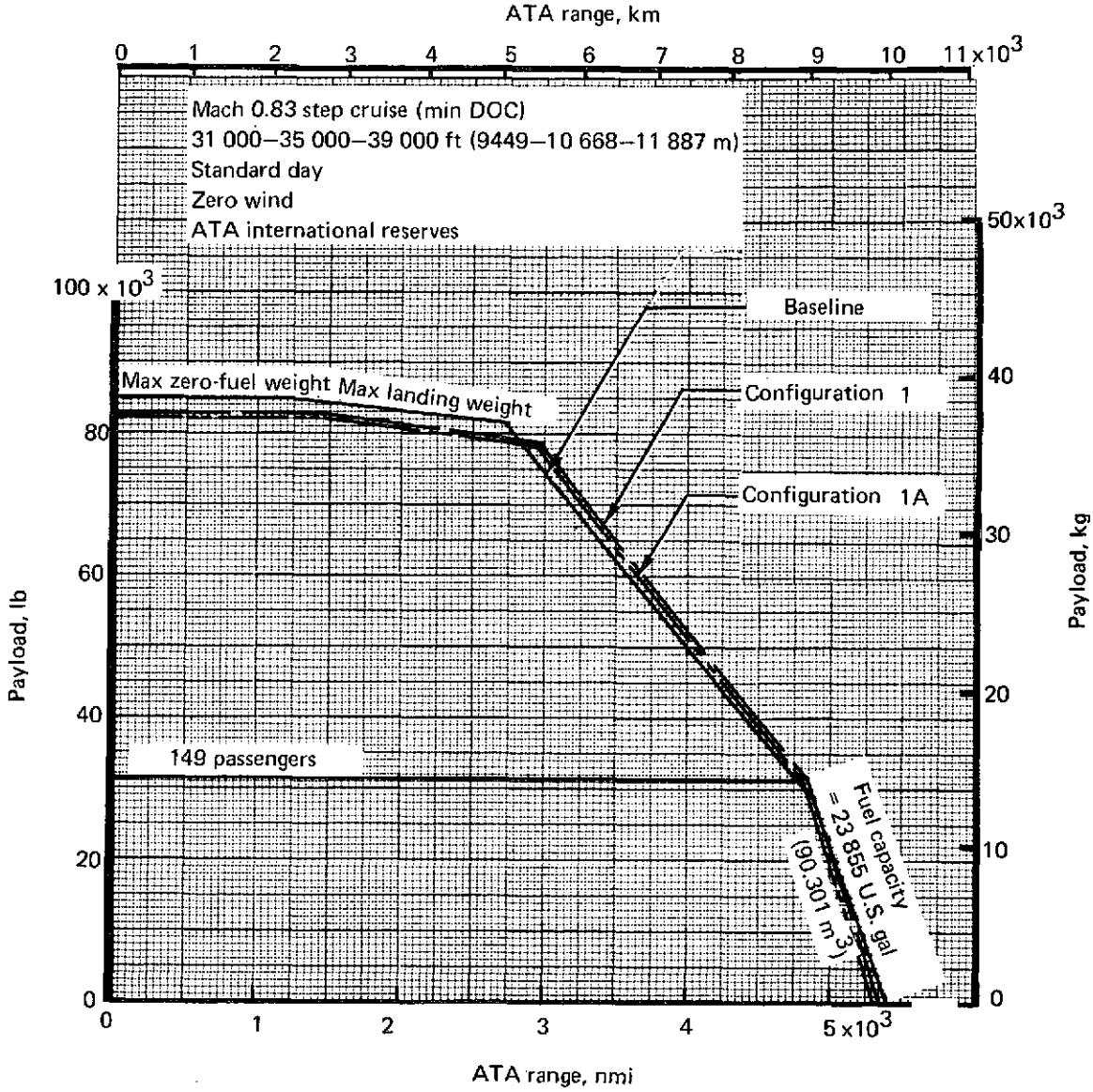


*FIGURE 32.–707/JT3D-9 CONFIGURATION 1 AND 1A PAYLOAD/RANGE COMPARISON*

| Configuration | Max BRGW | | OEW | |
|---|---|---|---|---|
| | lb | kg | lb | kg |
| Baseline | 333 600 | 151 318 | 145 000 | 65 770 |
| 2 | 339 400 | 153 948 | 148 925 | 67 550 |
| 3 | 339 600 | 154 039 | 149 145 | 67 650 |

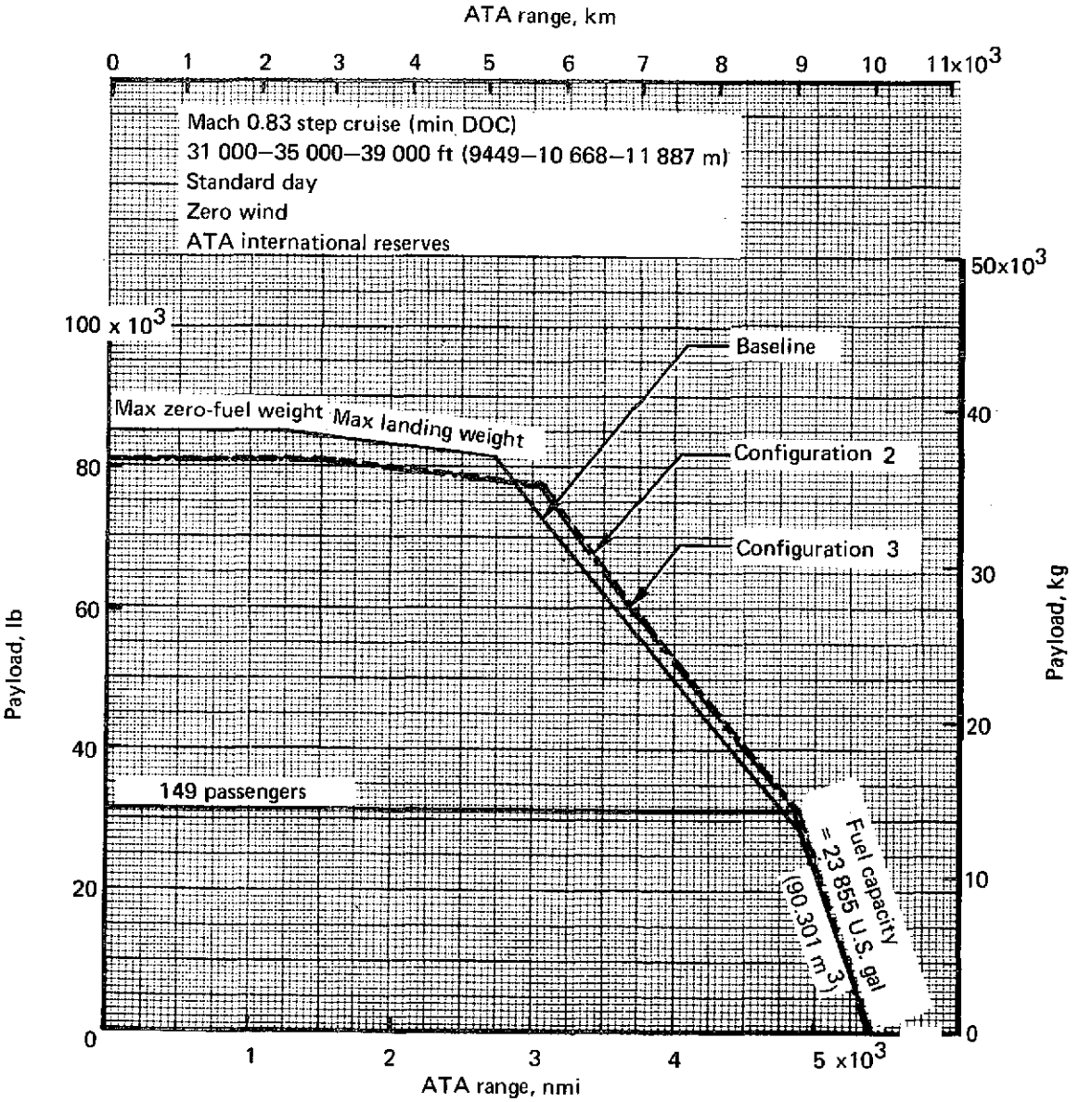


*FIGURE 33.–707/JT3D-9–CONFIGURATION 2 AND 3 PAYLOAD/RANGE COMPARISON*

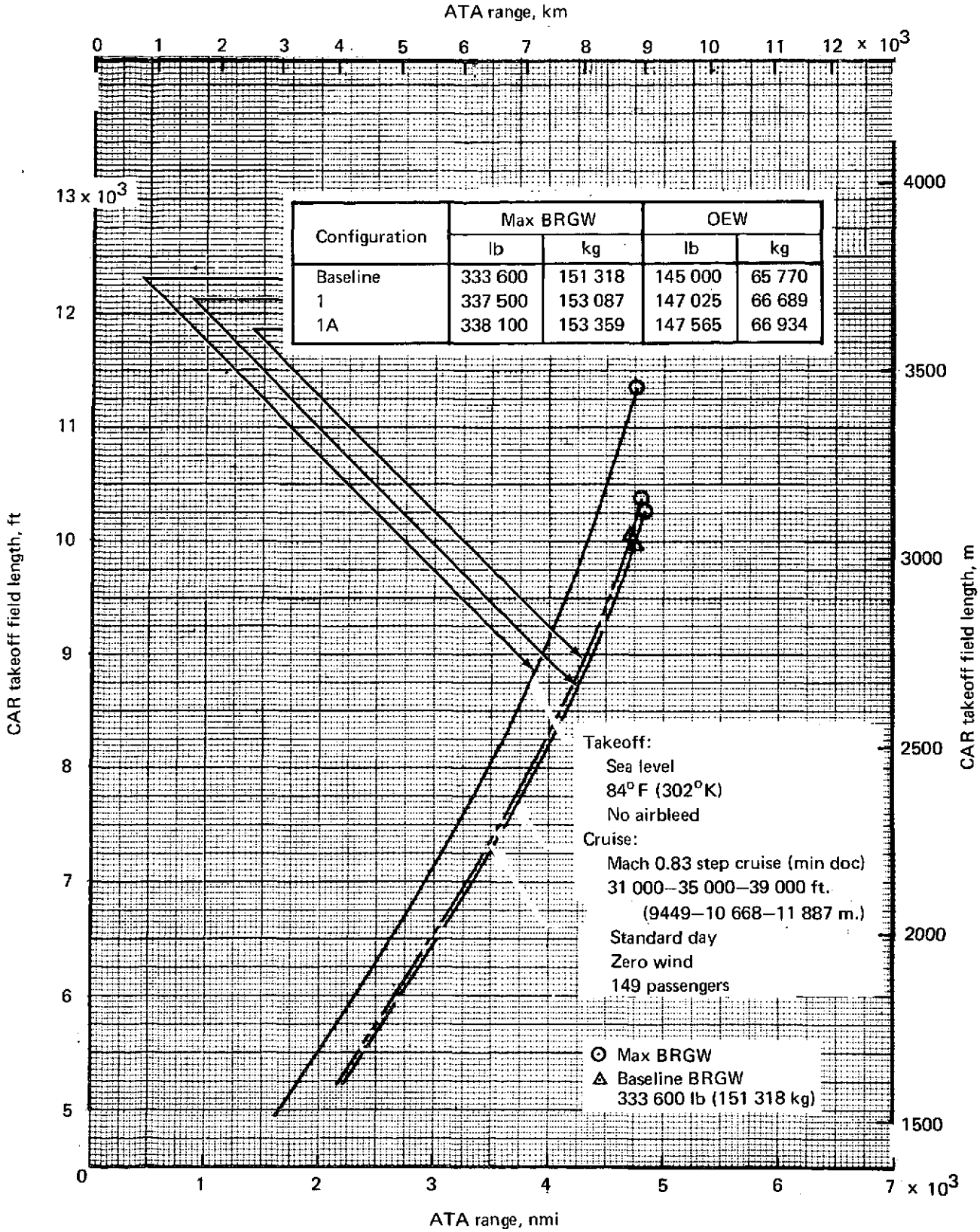


| Configuration | Max BRGW | | OEW | |
|---|---|---|---|---|
| | lb | kg | lb | kg |
| Baseline | 333 600 | 151 318 | 145 000 | 65 770 |
| 1 | 337 500 | 153 087 | 147 025 | 66 689 |
| 1A | 338 100 | 153 359 | 147 565 | 66 934 |

*FIGURE 34.–707/JT3D-9–CONFIGURATION 1 AND 1A FIELD LENGTH/RANGE COMPARISON*

| Configuration | Max BRGW | | OEW | |
|---|---|---|---|---|
| | lb | kg | lb | kg |
| Baseline | 333 600 | 151 318 | 145 000 | 65 770 |
| 2 | 339 400 | 153 948 | 148 925 | 67 550 |
| 3 | 339 600 | 154 039 | 149 145 | 67 650 |

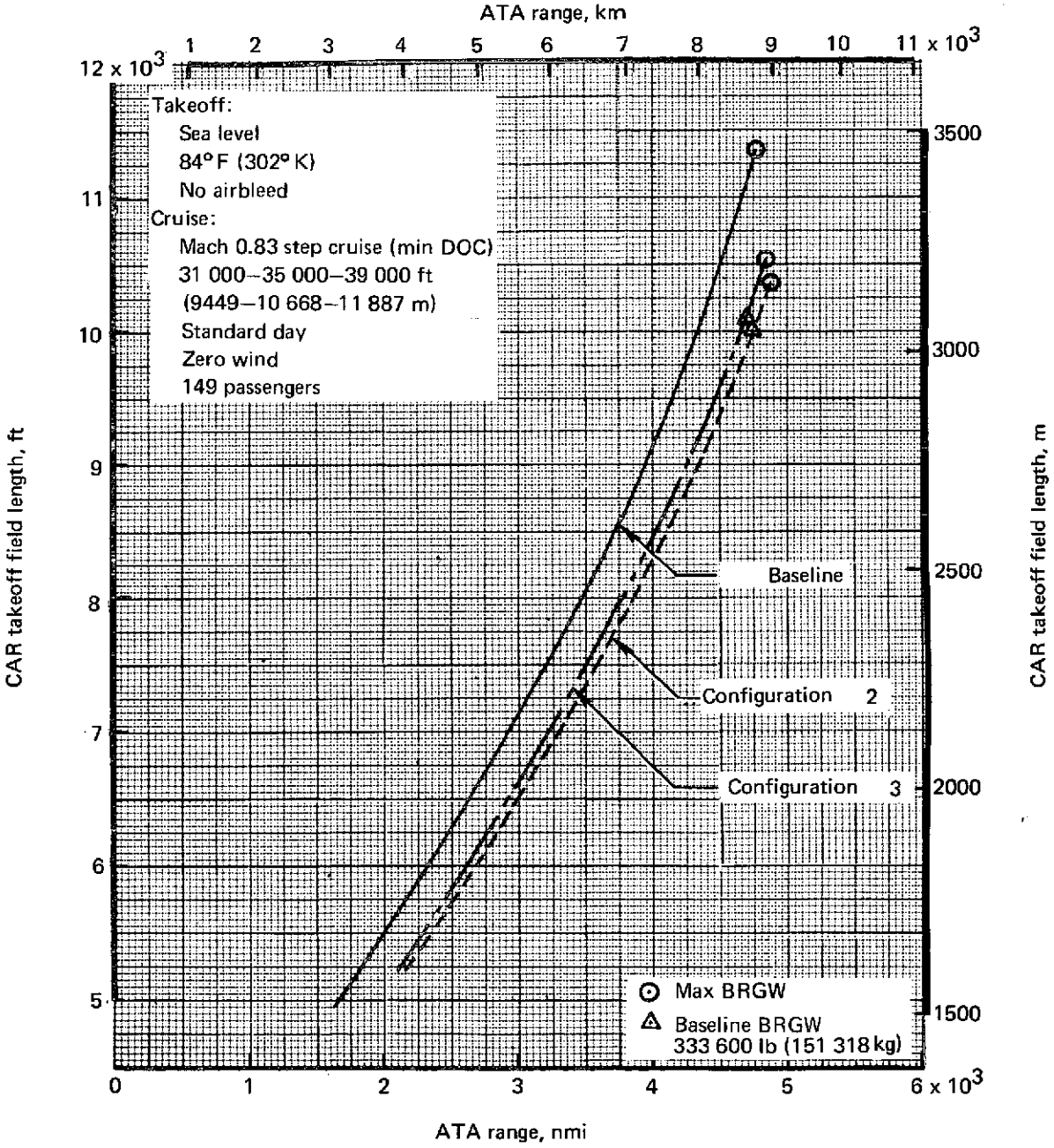


*FIGURE 35.–707/JT3D-9–CONFIGURATION 2 AND 3 FIELD LENGTH/RANGE COMPARISON*

Increased rudder hinge moment capability results in increased sideslip capability at speeds above the current rudder blowdown speed. This, in turn, requires additional lateral control power to balance the induced rolling moment. The most severe case is with flaps up, below 250 kn (128.8 m/sec), in which the outboard ailerons are locked out and rudder boost pressure is high (at 250 kn (128.8 m/sec), the rudder actuator hydraulic pressure is reduced). A minimum change to improve lateral control would be to increase the speed range for outboard aileron operation. Instead of locking out the ailerons with flap position, the lockout mechanism may be controlled by a dynamic pressure switch similar to that used to control the hydraulic pressure to the rudder.

Preliminary estimates of the effect of the modified nacelles on airplane speed stability show that, for adequate cruise speed stability, the aft center-of-gravity limit will be 33.7% MAC, compared to 35% MAC with the JT3D-3B engines. Wind tunnel tests would be required to confirm this estimated effect.

Preliminary estimates of the cruise dutch roll characteristics show no significant effect of the larger nacelles.

### 3.7.5 Flutter

The results of analyses and tests show that adding the modified nacelles degrades the flutter characteristics of the airplanes. This is due to the increased aerodynamic effect of the larger cowls.

All 707 models show a large sensitivity to outboard nacelle strut side bending frequency. The other nacelle strut frequencies (i.e., outboard nacelle strut vertical bending and inboard nacelle strut side and vertical bending) affect the flutter speeds to a lesser degree. The flutter speeds improve by moving the outboard nacelle center-of-gravity position aft, and increases in nacelle weight tend to improve the flutter characteristics.

The flutter characteristics of the 707-series airplanes with JT3D modified nacelles are expected to be satisfactory with suitable choices of nacelle strut frequencies and outboard nacelle streamwise location.

## 3.8 AIRPLANE AND COMMUNITY NOISE CHARACTERISTICS

Acoustic characteristics of the modified 707 airplane with JT3D-9 refanned engines were evaluated with four nacelle configurations. This section describes the acoustic linings designed for these nacelles, noise/thrust/altitude curves for the respective nacelles, noise levels predicted at FAR Part 36 conditions, EPNL contour areas, and a relative footprint noise index.

### 3.8.1 Nacelle Acoustic Preliminary Design

#### 3.8.1.1 Inlet Acoustic Design

Acoustic linings were analyzed for three inlet configurations (see fig. 36):

- Peripheral treatment (configuration 1)
- Peripheral treatment with one inlet ring (configurations 1A and 2)
- Peripheral treatment with two inlet rings (configuration 3)

Different segments of acoustic treatment were designed to attenuate buzz-saw noise during takeoff and the fundamental fan blade passage frequency during approach. This inlet treatment would consist of single-layer glass fiber/polyimide linings, except for the buzz-saw lining segment, which would be perforated sheet. The linings were designed considering velocity gradients from sheared flow in the inlet. The ring radial locations were selected to produce maximum far-field attenuation of the fundamental blade passage frequency at approach power. Ring placement and length were also affected by geometric constraints to minimize inlet pressure losses.

The flyover noise estimates presented in the following sections use an estimated effectiveness for each inlet configuration that assumes more detailed inlet acoustic design effort.

#### 3.8.1.2 Fan Duct Acoustic Design

Two fan duct acoustic linings were designed to work in conjunction with the engine fan case treatment. One was a 12-in. (0.305-m) long lining designed for a short fan duct. The other was a 63-in. (1.60-m) long lining designed for a 3/4-length fan duct. Both linings would be of double-layer glass fiber/polyimide designed to suppress both the fundamental and second harmonic fan blade passage frequencies at approach power.

### 3.8.2 Noise/Thrust/Altitude Curves

Level flyover noise was predicted for six different altitudes (300, 700, 1500, 3000, 6000, and 10 000 ft) (91.4, 213.4, 457.2, 914.4, 1829, and 3048 m). Figures 37 through 41 show the variation in EPNL as a function of altitude for approach, cutback, and takeoff power settings for the baseline airplane and the four modified-nacelle configurations. The true airspeeds shown are those required for maximum gross weight approach and takeoff.

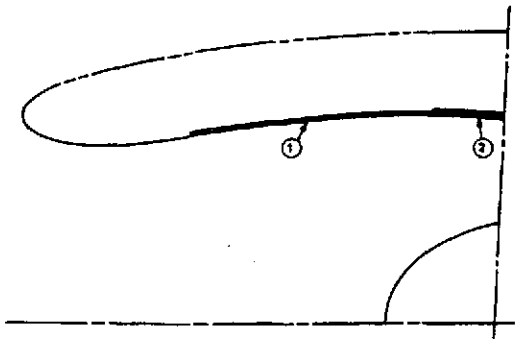

| Inlet configuration | Lining number | Number of plies | Backing depth, in. (m) | Length, in. (m) |
|---|---|---|---|---|
| No ring | 1 | 28 | 0.08 (0.002) | 27 (0.686) |
| | 2 | * | 1.43 (0.036) | 9 (0.229) |

CONFIGURATION 1

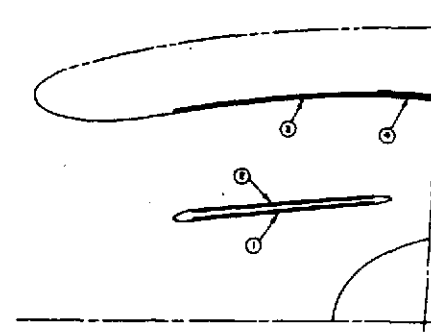

| Lining number | Number of plies | Backing depth, in. (m) | Length, in. (m) |
|---|---|---|---|
| 1 | 28 | 0.08 (0.002) | 24 (0.610) |
| 2 | 15 | 0.15 (0.0038) | 24 (0.610) |
| 3 | 14 | 0.16 (0.004) | 24 (0.610) |
| 4 | * | 1.43 (0.036) | 6 (0.152) |

CONFIGURATIONS 1A AND 2

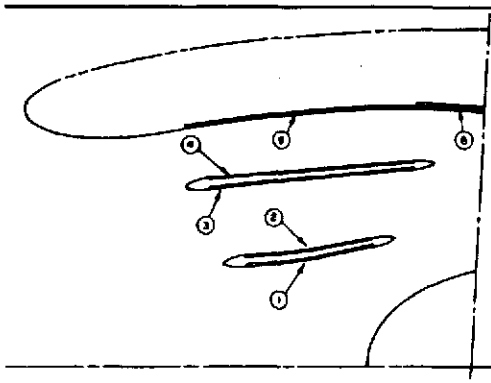

| Lining number | Number of plies | Backing depth, in. (m) | Length, in. (m) |
|---|---|---|---|
| 1 | 28 | 0.08 (0.002) | 13 (0.330) |
| 2 | 15 | 0.16 (0.004) | 13 (0.330) |
| 3 | 15 | 0.16 (0.004) | 24 (0.610) |
| 4 | 13 | 0.18 (0.0045) | 24 (0.610) |
| 5 | 12 | 0.19 (0.0048) | 24 (0.610) |
| 6 | * | 1.43 (0.036) | 6 (0.152) |

CONFIGURATION 3

| Duct type | Outer layer | Inner layer |
|---|---|---|
| Short fan duct | | |
| Number of facing sheet plies | 5 | 9 |
| Backing depth, in. (m) | 0.35 (0.00889) | 0.25 (0.00635) |
| Lining length, in. (m) | 12 (.3048) | |
| 3/4 length fan duct | | |
| Number of facing sheet plies | 5 | 13 |
| Backing depth, in. (m) | 0.25 (0.00635) | 0.20 (0.00508) |
| Lining length in. (m) | 63 (1.6002) | |

Fan Duct Lining Properties

*Perforated sheet: 20% open area,
hole diameter = 0.08 in. (0.002m),
sheet thickness = 0.063 in. (0.0016m)

*FIGURE 36.—707/JT3D-9 LINING DEFINITION*

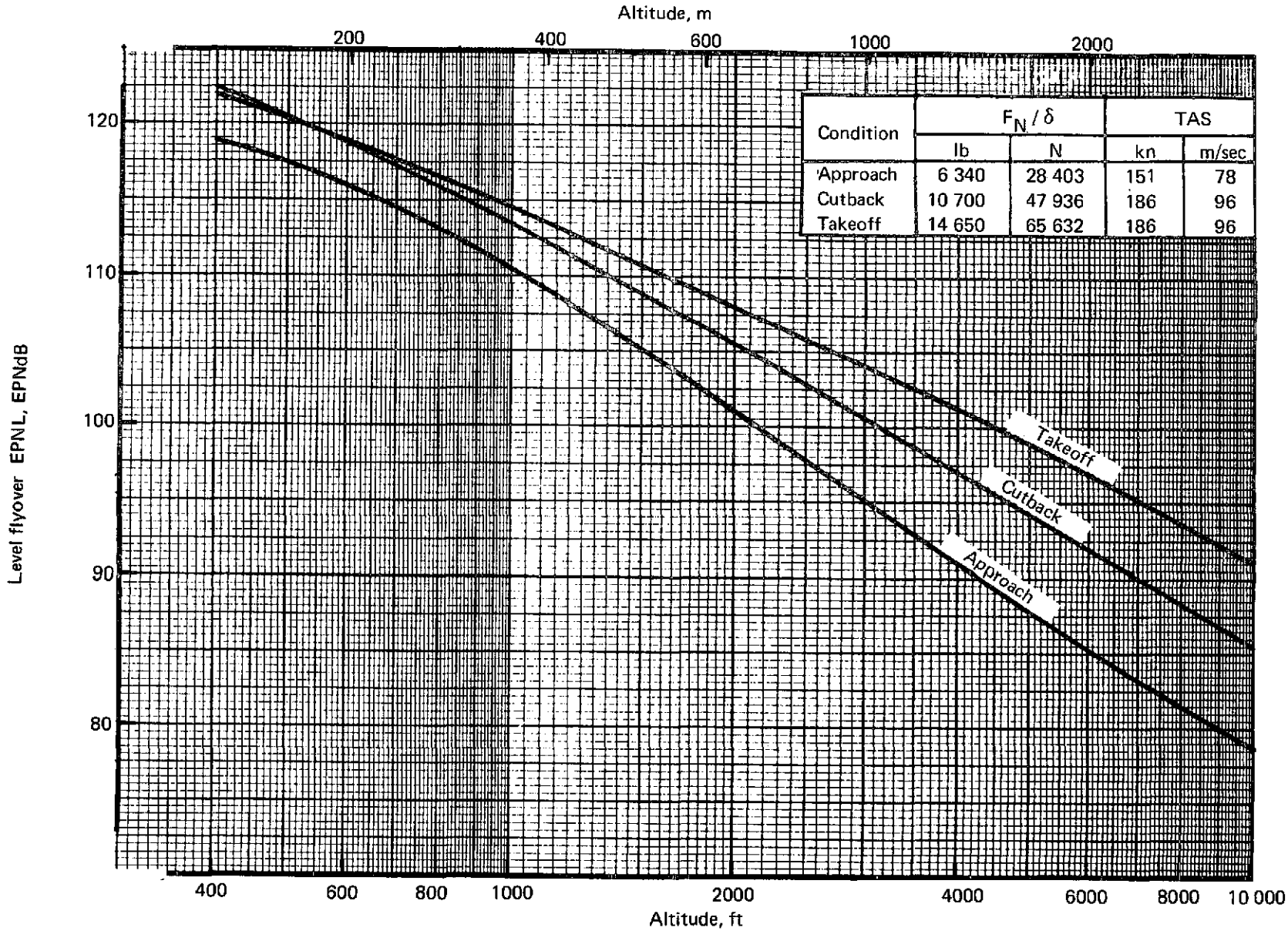


| Condition | $F_N/\delta$ | | TAS | |
|---|---|---|---|---|
| | lb | N | kn | m/sec |
| Approach | 6 340 | 28 403 | 151 | 78 |
| Cutback | 10 700 | 47 936 | 186 | 96 |
| Takeoff | 14 650 | 65 632 | 186 | 96 |

*FIGURE 37.—707/JT3D-3B PRODUCTION NACELLE NOISE/THRUST/ALTITUDE CURVES*

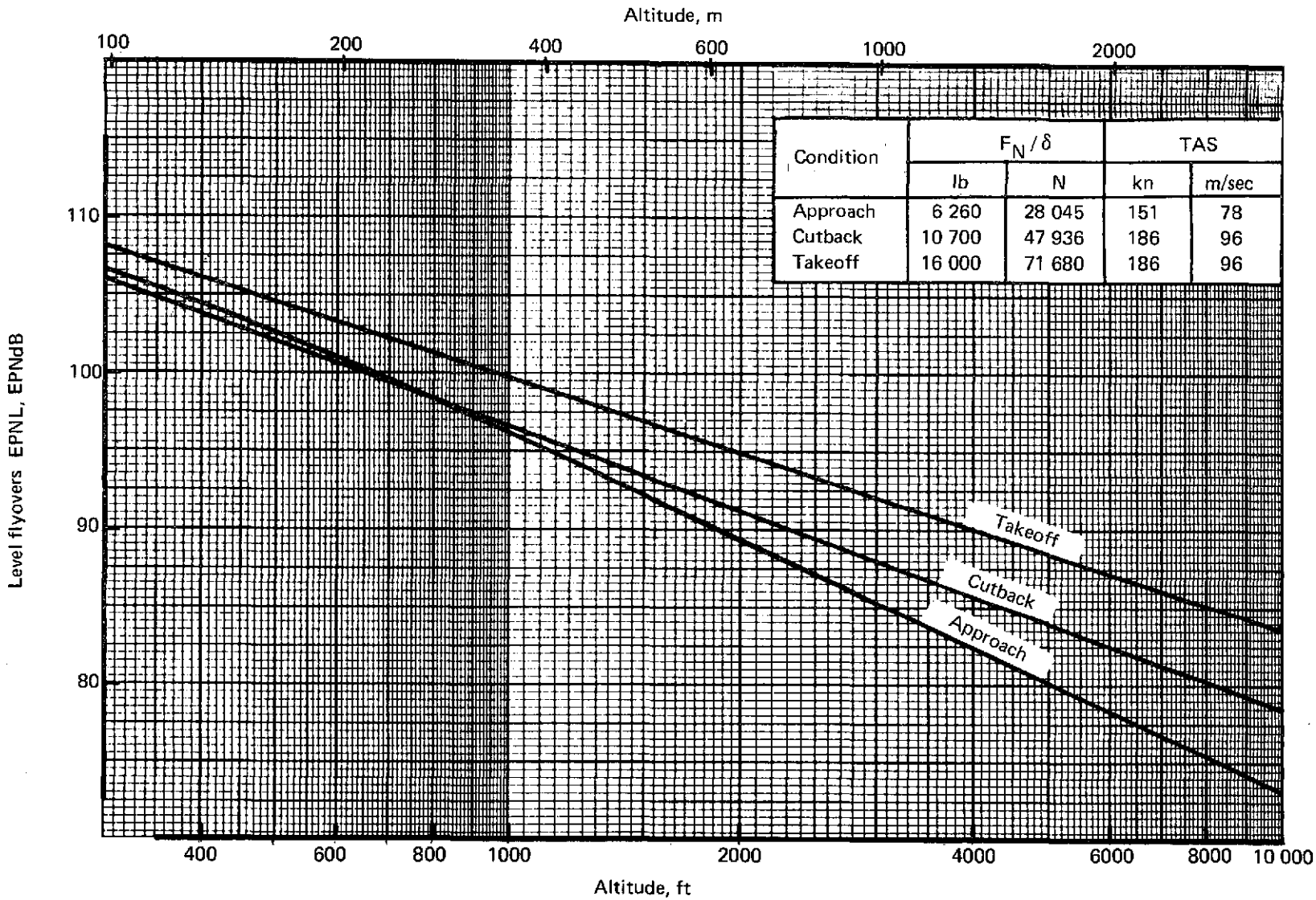


| Condition | $F_N/\delta$ | | TAS | |
|---|---|---|---|---|
| | lb | N | kn | m/sec |
| Approach | 6 260 | 28 045 | 151 | 78 |
| Cutback | 10 700 | 47 936 | 186 | 96 |
| Takeoff | 16 000 | 71 680 | 186 | 96 |

*FIGURE 38.—707/JT3D-9 CONFIGURATION 1 NOISE/THRUST/ALTITUDE CURVES*

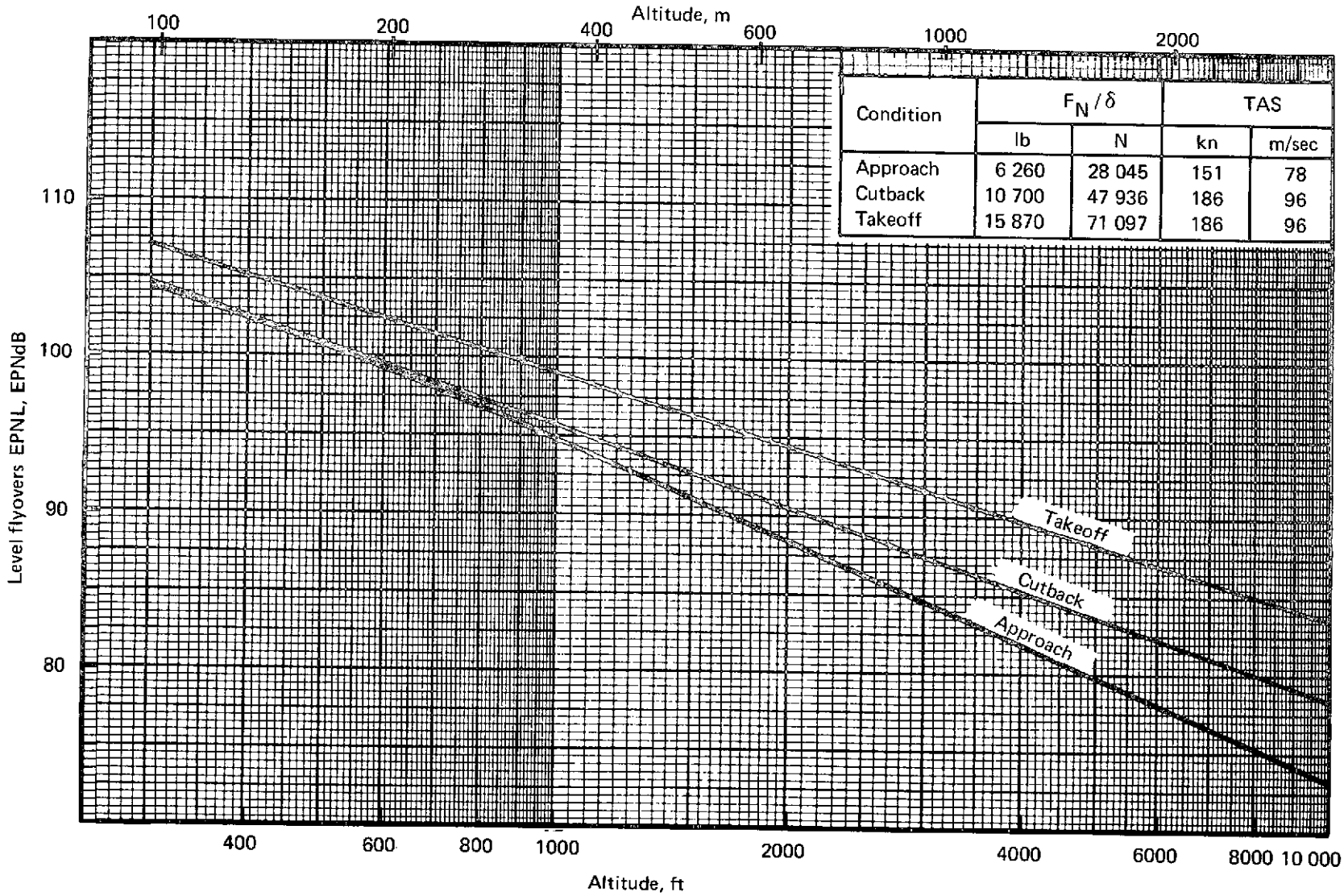


| Condition | $F_N/\delta$ | | TAS | |
|---|---|---|---|---|
| | lb | N | kn | m/sec |
| Approach | 6 260 | 28 045 | 151 | 78 |
| Cutback | 10 700 | 47 936 | 186 | 96 |
| Takeoff | 15 870 | 71 097 | 186 | 96 |

*FIGURE 39.—707/JT3D-9 CONFIGURATION 1A NOISE/THRUST/ALTITUDE CURVES*

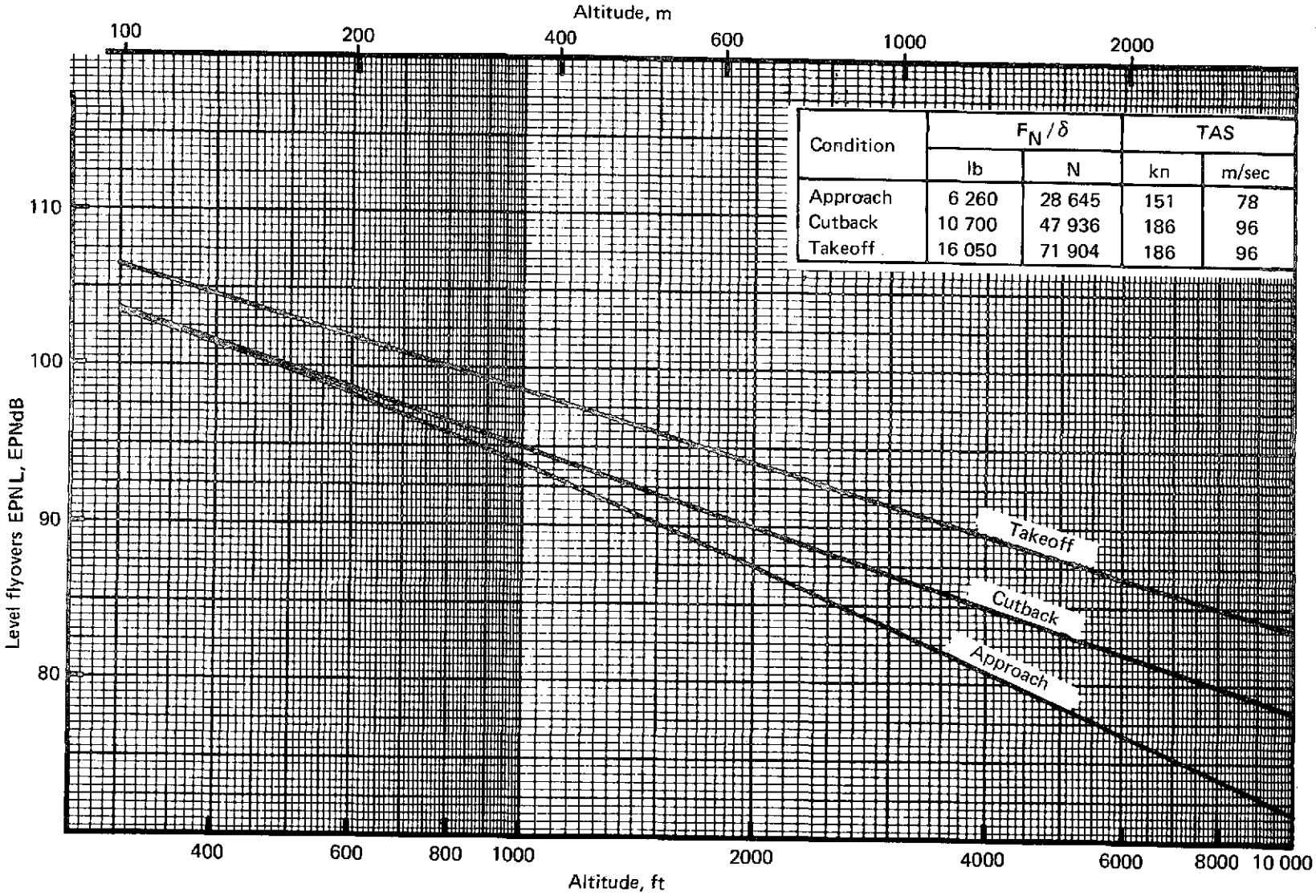


| Condition | $F_N/\delta$ | | TAS | |
|---|---|---|---|---|
| | lb | N | kn | m/sec |
| Approach | 6 260 | 28 645 | 151 | 78 |
| Cutback | 10 700 | 47 936 | 186 | 96 |
| Takeoff | 16 050 | 71 904 | 186 | 96 |

*FIGURE 40.—707/JT3D-9 CONFIGURATION 2 NOISE/THRUST/ALTITUDE CURVES*

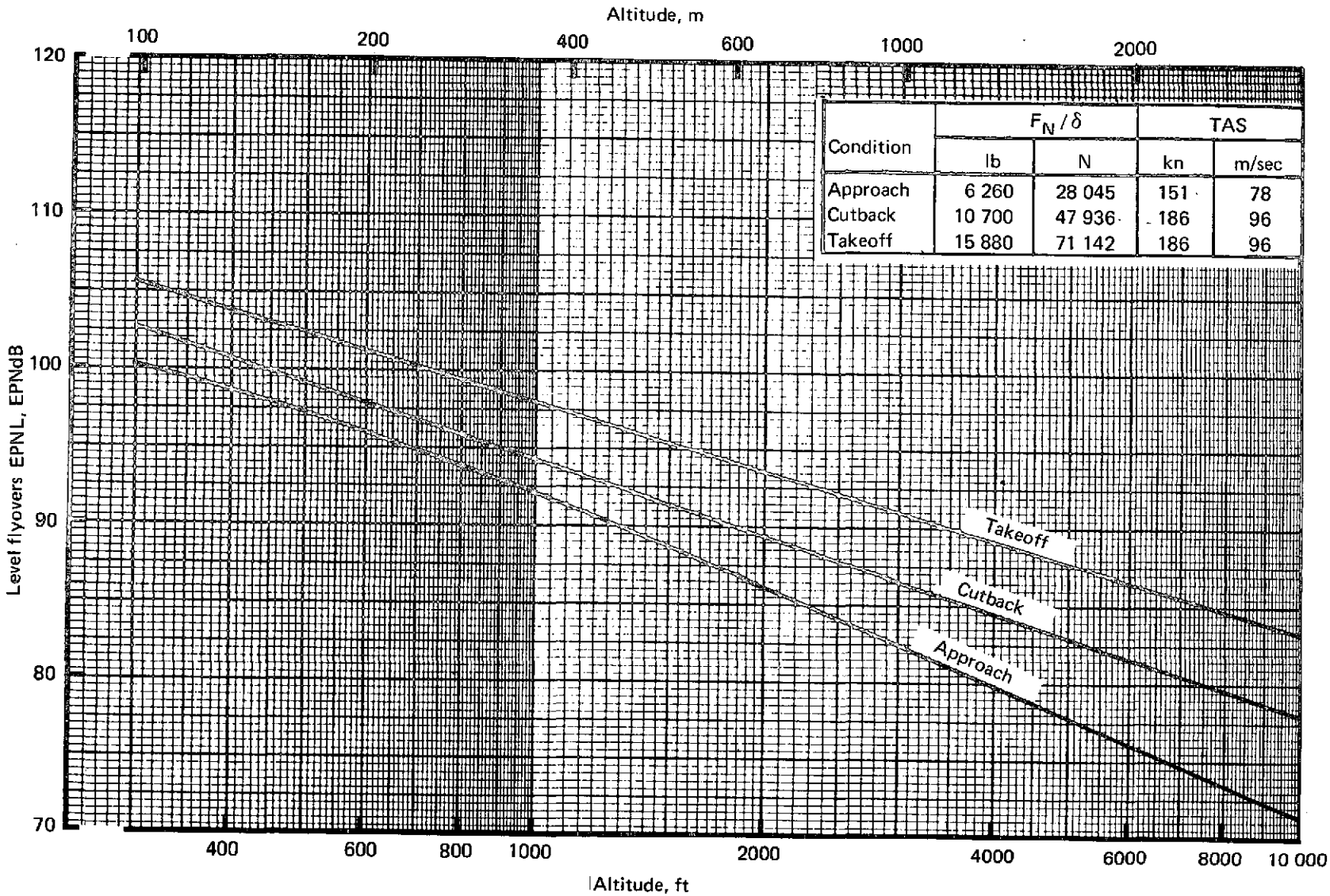


| Condition | $F_N/\delta$ | | TAS | |
|---|---|---|---|---|
| | lb | N | kn | m/sec |
| Approach | 6 260 | 28 045 | 151 | 78 |
| Cutback | 10 700 | 47 936 | 186 | 96 |
| Takeoff | 15 880 | 71 142 | 186 | 96 |

*FIGURE 41.–707/JT3D-9 CONFIGURATION 3 NOISE/THRUST/ALTITUDE CURVES*

### 3.8.3 Noise Levels at FAR Part 36 Conditions

The acoustic signature of the JT3D-9 was estimated using a contractor-developed engine-component noise-prediction program. The program used engine and airplane performance parameters as inputs to calculate sound pressure levels. The predicted component noise levels were matched as closely as possible to noise data supplied by the engine contractor.

Engine noise was predicted along a 150-ft (45.7-m) arc for the following components: primary jet, secondary jet, inlet fan, and aft fan noise. Fan noise attenuation estimates were applied at 150 ft (45.7 m) from the engine using empirically determined directivity indexes.

Noise components were extrapolated to flyover conditions using spherical divergence, standard air absorption, extra ground attenuation, relative jet velocity correction, and a correction for the number of engines. Flyover noise estimates for the FAR Part 36 conditions are listed in table 13. Included in the table are the 707-320B maximum brake release gross weights for each nacelle configuration and the corrected net thrust and true airspeeds for the respective FAR Part 36 conditions. Flyover noise levels for the current airplane are also included for comparison. Wherever applicable, the methods and techniques outlined in FAR Part 36 were used. A zero ambient noise floor was used for all flyover noise estimates. Cutback was initiated at 3.5 nmi (6.48 km) from brake release, assuming zero engine spool-down time.

### 3.8.4 Noise Contour Area Analysis

The EPNL contour information is presented in two forms: as relative footprint contour areas for different EPNL levels and as a single-number relative footprint noise index. Calculation methods for these two parameters are presented in the following sections.

#### 3.8.4.1 EPNL Contour Areas

Airplane noise exposure contours (footprints) were estimated with a contractor-developed computer program. The program used noise and airplane flight operations parameters as inputs to calculate ground plane coordinates of equal EPNL contours and the enclosed area within each contour.

Aircraft EPNLs were calculated as a function of distance, power setting, and flight speed. Flightpath operational procedures were simulated by flight profile segments described by airplane altitude, distance from brake release or touchdown, average power setting, and average flight speed.

## TABLE 13.—707-320B/JT3D-3B/JT3D-9 NOISE COMPARISONS AT FAR 36 MEASURING STATIONS

| Nacelle configuration | Condition | Approach 1 nmi (1.85 km) | | Takeoff (with cutback) 3.5 nmi (6.48 km) | | Takeoff (without cutback) 3.5 nmi (6.48 km) | | Sideline 0.35 nmi (0.65 km) | |
|---|---|---|---|---|---|---|---|---|---|
| | | English units | SI units | English units | SI units | English units | SI units | English units | SI units |
| Baseline (JT3D-3B) | BRGW | – | – | 333 600 lb | 151 288 kg | 333 600 lb | 151 288 kg | 333 600 lb | 151 288 kg |
| | LGW | 247 000 lb | 112 015 kg | – | – | – | – | – | – |
| | Flaps, deg | 50 | 50 | 14 | 14 | 14 | 14 | 14 | 14 |
| | Altitude | 370 ft | 112.8 m | 940 ft | 286.5 m | 940 ft | 286.5 m | – | – |
| | Sideline | – | – | – | – | – | – | 2126 ft | 648 m |
| | Thrust/δ | 6260 lb | 28 045 N | 10 700 lb | 47 936 N | 14 650 lb | 65 632 N | 14 650 lb | 65 632 N |
| | Velocity, TAS | 151 kn | 77.7 m/sec | 186 kn | 95.7 m/sec | 186 kn | 95.7 m/sec | 186 kn | 95.7 m/sec |
| | EPNL, EPNdB | 120.5 | 120.5 | 114.0 | 114.0 | 115.0 | 115.0 | 107.5 | 107.5 |
| | FAR 36, EPNdB | 106.3 | 106.3 | 103.7 | 103.7 | 103.7 | 103.7 | 106.3 | 106.3 |
| 1 (JT3D-9 refan) | BRGW | – | – | 337 500 lb | 153 056 kg | 337 500 lb | 153 056 kg | 337 500 lb | 153 056 kg |
| | LGW | 247 000 lb | 112 015 kg | – | – | – | – | – | – |
| | Flaps, deg | 50 | 50 | 14 | 14 | 14 | 14 | 14 | 14 |
| | Altitude | 370 ft | 112.8 m | 1170 ft | 356.6 m | 1170 ft | 356.6 m | – | – |
| | Sideline | – | – | – | – | – | – | 2126 ft | 648 m |
| | Thrust/δ | 6260 lb | 28 045 N | 10 700 lb | 47 936 N | 16 000 lb | 71 680 N | 16 000 lb | 71 680 N |
| | Velocity, TAS | 151 kn | 77.7 m/sec | 186 kn | 95.7 m/sec | 186 kn | 95.7 m/sec | 186 kn | 95.7 m/sec |
| | Δ EPNL, EPNdB[a] | (-15.4) | (-15.4) | (-19.3) | (-19.3) | (-16.5) | (-16.5) | (-12.7) | (-12.7) |
| | EPNL, EPNdB[b] | 105.1 | 105.1 | 94.7 | 94.7 | 98.5 | 98.5 | 94.8 | 94.8 |
| | FAR 36, EPNdB | 106.3 | 106.3 | 103.8 | 103.8 | 103.8 | 103.8 | 103.8 | 103.8 |
| 1A (JT3D-9 refan) | BRGW | – | – | 338 100 lb | 153 328 kg | 338 100 lb | 153 328 kg | 338 100 lb | 153 328 kg |
| | LGW | 247 000 lb | 112 015 kg | – | – | – | – | – | – |
| | Flaps, deg | 50 | 50 | 14 | 14 | 14 | 14 | 14 | 14 |
| | Altitude | 370 ft | 112.8 m | 1140 ft | 341.5 m | 1140 ft | 341.5 m | – | – |
| | Sideline | – | – | – | – | – | – | 2126 ft | 648 m |
| | Thrust/δ | 6260 lb | 28 045 N | 10 700 lb | 47 936 N | 15 870 lb | 71 098 N | 15 870 lb | 71 098 N |
| | Velocity, TAS | 151 kn | 77.7 m/sec | 186 kn | 95.7 m/sec | 186 kn | 95.7 m/sec | 186 kn | 95.7 m/sec |
| | Δ EPNL, EPNdB[a] | (-17.5) | (-17.5) | (-20.2) | (-20.2) | (-17.0) | (-17.0) | (-13.0) | (-13.0) |
| | EPNL, EPNdB[b] | 103.0 | 103.0 | 93.8 | 93.8 | 98.0 | 98.0 | 94.5 | 94.5 |
| | FAR 36, EPNdB | 106.3 | 106.3 | 106.3 | 106.3 | 106.3 | 106.3 | 106.3 | 106.3 |
| 2 (JT3D-9 refan) | BRGW | – | – | 339 400 lb | 153 917 kg | 339 400 lb | 153 917 kg | 339 400 lb | 153 917 kg |
| | LGW | 247 000 lb | 112 015 kg | – | – | – | – | – | – |
| | Flaps, deg | 50 | 50 | 14 | 14 | 14 | 14 | 14 | 14 |
| | Altitude | 370 ft | 112.8 m | 1160 ft | 353.5 m | 1160 ft | 353.5 m | – | – |
| | Sideline | – | – | – | – | – | – | 2126 ft | 648 m |
| | Thrust/δ | 6260 lb | 28 045 N | 10 700 lb | 47 936 N | 16 050 lb | 71 904 N | 16 050 lb | 71 904 N |
| | Velocity , TAS | 151 kn | 77.7 m/sec | 186 kn | 95.7 m/sec | 186 kn | 95.7 m/sec | 186 kn | 95.7 m/sec |
| | Δ EPNL, EPNdB[a] | (-18.6) | (-18.6) | (-20.7) | (-20.7) | (-17.5) | (-17.5) | (-13.3) | (-13.3) |
| | EPNL, EPNdB[b] | 101.9 | 101.9 | 93.3 | 93.3 | 97.5 | 97.5 | 94.2 | 94.2 |
| | FAR 36, EPNdB | 106.4 | 106.4 | 106.4 | 106.4 | 106.4 | 106.4 | 106.4 | 106.4 |
| 3 (JT3D-9 refan) | BRGW | – | – | 339 600 lb | 154 008 kg | 339 600 lb | 154 008 kg | 339 600 lb | 154 008 kg |
| | LGW | 247 000 lb | 112 015 kg | – | – | – | – | – | – |
| | Flaps, deg | 50 | 50 | 14 | 14 | 14 | 14 | 14 | 14 |
| | Altitude | 370 ft | 112.8 m | 1120 ft | 341.4 m | 1120 ft | 341.4 m | – | – |
| | Sideline | – | – | – | – | – | – | 2126 ft | 648 m |
| | Thrust/δ | 6260 lb | 28 045 N | 10 700 lb | 47 396 N | 15 880 lb | 71 142 N | 15 880 lb | 71 142 N |
| | Velocity, TAS | 151 kn | 77.7 m/sec | 186 kn | 95.7 m/sec | 186 kn | 95.7 m/sec | 186 kn | 95.7 m/sec |
| | ΔEPNL, EPNdB[a] | (-21.4) | (-21.4) | (-21.0) | (-21.0) | (-18.0) | (-18.0) | (-13.7) | (-13.7) |
| | EPNL, EPNdB[b] | 99.1 | 99.1 | 93.0 | 93.0 | 97.0 | 97.0 | 93.8 | 93.8 |
| | FAR 36, EPNdB | 106.4 | 106.4 | 103.9 | 103.9 | 103.9 | 103.9 | 106.4 | 106.4 |

[a] $\Delta EPNL = EPNL_{config} - EPNL_{baseline}$

[b] See calculation method in section 3.8.3

The profiles represent operation into and out of a sea-level airport on a standard + 18°F (10°K) day. The maximum brake release and landing gross weights were used for the calculation of the takeoff and approach data, respectively.

Two types of takeoff profiles were used: cutback certification profile and full-power operational profile.

The cutback certification profile represents the aircraft taking off and climbing at a speed of $V_2$ + 10 kn (5.2 m/sec), while maintaining takeoff power and takeoff flaps, to a point 3.2 nmi (5.95 km) from brake release. At 3.2 nmi (5.95 km) from brake release, the power on all engines is reduced to that power setting required for level flight with one engine inoperative. Climbout is continued at this reduced power setting, $V_2$ + 10 kn (5.2 m/sec) airspeed, and takeoff flaps.

The full-power operational profile represents the aircraft taking off from a sea-level airport on a standard + 18°F (10°K) day and climbing at $V_2$ + 10 kn (5.2 m/sec), while maintaining takeoff power and takeoff flaps (14°), to an altitude of 1500 ft (457 m). At this altitude, the flaps are retracted, and the aircraft is accelerated to an equivalent airspeed of 250 kn (129 m/sec) while at takeoff power. Climbout is then continued at an equivalent airspeed of 250 kn (129 m/sec) and maximum climb thrust rating. Table 14 presents this full power operational profile.

The approach profile represents the aircraft approaching the airport on a 3° glide slope, with landing flaps and gear down, at an approach speed of $V_{ref}$ + 10 kn (5.2 m/sec).

When the airplane location, power setting, and flight speed are known, simple geometric considerations are coupled with the EPNL/thrust/altitude curves to determine the noise at intersections of a ground plane grid surrouding the runway. At each intersection, noise from the various segments of the flightpath is estimated, entering the EPNL/thrust/altitude curve at a point corresponding to the shortest slant distance between the grid point and the appropriate flightpath segment. The EPNL is then corrected for approximate additional ground attenuation, aircraft noise shielding, and flight speed difference from reference speed. The maximum noise values during landing and takeoff are calculated at each grid point, and contours for prescribed noise levels are determined by linear interpolation within the grid. The area within each contour is then calculated.

The calculation of footprint areas includes a number of details that have not been universally agreed upon and that have significant effect on the shape and the area of the constant EPNL contours. However, it has been observed in a number of cases that different calculation details, while affecting contour areas, have a minor effect on the area ratios at different contours or configurations. Therefore, potentially misleading absolute footprint areas are not shown, but ratios of areas relative to an arbitrary reference value are shown.

*TABLE 14.–MODEL 707-320B OPERATIONAL PROFILE MBRGW = 333 600 LB (151 318 KG)*

| Nacelle configuration (a) | Distance from brake release | | Altitude | | Average power setting FN/δ | | Average flight speed | |
|---|---|---|---|---|---|---|---|---|
| | ft | m | ft | m | lb | N | KTAS | m/sec |
| Baseline JT3D-3B | 0 | 0 | 0 | 0 | 14 480 | 64 410 | 121.2 | 62.4 |
| | 9 710 | 2 960 | 0 | 0 | 14 540 | 64 677 | 179.8 | 92.5 |
| | 28 200 | 8 595 | 1 500 | 457 | 14 350 | 63 832 | 205.5 | 105.7 |
| | 35 800 | 10 912 | 1 500 | 457 | 13 910 | 61 875 | 242.5 | 124.8 |
| | 43 400 | 13 228 | 1 500 | 457 | 10 620 | 47 240 | 265.0 | 136.3 |
| | 83 500 | 25 451 | 4 000 | 1219 | 11 070 | 49 242 | 275.1 | 141.5 |
| | 126 500 | 38 557 | 6 500 | 1981 | 11 560 | 51 421 | 287.4 | 147.9 |
| | 186 000 | 56 693 | 9 500 | 2896 | 12 100 | 53 823 | 301.0 | 154.8 |
| | 254 000 | 77 419 | 12 500 | 3810 | 12 690 | 56 448 | 317.0 | 163.1 |
| | 338 500 | 103 175 | 16 000 | 4877 | 13 410 | 59 651 | 337.7 | 173.7 |
| | 490 000 | 149 352 | 20 000 | 6096 | | | | |
| 1 (JT3D-9 refan) | 0 | 0 | 0 | 0 | 15 890 | 70 682 | 121.7 | 62.6 |
| | 8 480 | 2 525 | 0 | 0 | 15 900 | 70 727 | 180.2 | 92.7 |
| | 24 190 | 7 373 | 1 500 | 457 | 15 620 | 69 481 | 208.2 | 107.1 |
| | 31 600 | 9 632 | 1 500 | 457 | 15 120 | 67 257 | 244.7 | 125.9 |
| | 36 950 | 11 262 | 1 500 | 457 | 12 780 | 56 848 | 265.0 | 136.3 |
| | 66 700 | 20 330 | 4 000 | 1219 | 13 180 | 58 628 | 275.1 | 141.5 |
| | 99 500 | 30 328 | 6 500 | 1981 | 13 630 | 60 629 | 287.4 | 147.9 |
| | 145 000 | 44 196 | 9 500 | 2896 | 14 140 | 62 898 | 301.0 | 154.8 |
| | 196 600 | 59 924 | 12 500 | 3810 | 14 730 | 65 522 | 317.0 | 163.1 |
| | 268 400 | 81 808 | 16 000 | 4877 | 15 450 | 68 725 | 337.7 | 173.7 |
| | 371 500 | 113 233 | 20 000 | 6096 | | | | |
| 1A (JT3D-9 refan) | 0 | 0 | 0 | 0 | 15 770 | 70 148 | 121.7 | 62.6 |
| | 8 660 | 2 640 | 0 | 0 | 15 780 | 70 193 | 180.2 | 92.7 |
| | 24 470 | 7 458 | 1 500 | 457 | 15 520 | 69 036 | 208.0 | 107.0 |
| | 31 890 | 9 720 | 1 500 | 457 | 15 020 | 66 812 | 244.7 | 125.9 |
| | 37 370 | 11 390 | 1 500 | 457 | 12 600 | 56 048 | 265.0 | 136.3 |
| | 67 500 | 20 574 | 4 000 | 1219 | 13 010 | 57 871 | 275.1 | 141.5 |
| | 101 500 | 30 937 | 6 500 | 1981 | 13 470 | 59 918 | 287.4 | 147.9 |
| | 147 400 | 44 928 | 9 500 | 2896 | 13 980 | 62 186 | 301.0 | 154.8 |
| | 199 800 | 60 899 | 12 500 | 3810 | 14 570 | 64 811 | 317.0 | 163.1 |
| | 274 200 | 83 576 | 16 000 | 4877 | 15 300 | 68 058 | 337.7 | 173.7 |
| | 379 700 | 115 733 | 20 000 | 6096 | | | | |
| 2 (JT3D-9 refan) | 0 | 0 | 0 | 0 | 15 940 | 70 905 | 121.7 | 62.6 |
| | 8 470 | 2 582 | 0 | 0 | 15 950 | 70 949 | 180.2 | 92.7 |
| | 24 080 | 7 340 | 1 500 | 457 | 15 710 | 69 882 | 208.4 | 107.2 |
| | 31 480 | 9 595 | 1 500 | 457 | 15 230 | 67 746 | 245.1 | 126.1 |
| | 36 730 | 11 195 | 1 500 | 457 | 12 850 | 57 160 | 265.0 | 136.3 |
| | 66 100 | 20 147 | 4 000 | 1219 | 13 260 | 58 983 | 275.1 | 141.5 |
| | 99 300 | 30 267 | 6 500 | 1981 | 13 730 | 61 074 | 287.4 | 147.9 |
| | 144 200 | 43 952 | 9 500 | 2896 | 14 260 | 63 432 | 301.0 | 154.8 |
| | 195 600 | 59 619 | 12 500 | 3810 | 14 870 | 66 145 | 317.0 | 163.1 |
| | 267 600 | 81 564 | 16 000 | 4877 | 15 620 | 69 481 | 337.7 | 173.7 |
| | 369 600 | 112 654 | 20 000 | 6096 | | | | |
| 3 (JT3D-9 refan) | 0 | 0 | 0 | 0 | 15 760 | 70 104 | 121.7 | 62.6 |
| | 8 590 | 2 618 | 0 | 0 | 15 770 | 70 148 | 180.2 | 92.7 |
| | 24 510 | 7 471 | 1 500 | 457 | 15 530 | 69 081 | 208.0 | 107.0 |
| | 31 930 | 9 732 | 1 500 | 457 | 15 030 | 66 857 | 244.7 | 125.9 |
| | 37 400 | 11 400 | 1 500 | 457 | 12 630 | 56 181 | 265.0 | 136.3 |
| | 67 500 | 20 574 | 4 000 | 1219 | 13 050 | 58 049 | 275.1 | 141.5 |
| | 101 400 | 30 907 | 6 500 | 1981 | 13 520 | 60 140 | 287.4 | 147.9 |
| | 147 200 | 44 867 | 9 500 | 2896 | 14 050 | 62 498 | 301.0 | 154.8 |
| | 199 400 | 60 777 | 12 500 | 3810 | 14 670 | 65 255 | 317.0 | 163.1 |
| | 273 600 | 83 393 | 16 000 | 4877 | 15 420 | 68 592 | 337.7 | 173.7 |
| | 378 900 | 115 489 | 20 000 | 6096 | | | | |

[a]Flaps 14°

### 3.8.4.2 Relative Footprint Noise Index

The relative footprint noise index (RFNI) is a single-number rating of a footprint contour map. It assesses the relative amount of community noise exposure caused by different types of aircraft or by different fleet mixes. The single-event EPNL footprint contours of the various configurations were evaluated in terms of this index. This index represents the ratio of two psychoacoustically weighted areas, that of the refanned engine configuration, and that of the baseline configuration with unmodified engines and with untreated nacelles. The calculation of the weighted areas is performed by integration over the region enclosed by the 90 EPNdB contour and outside the approximate airport boundary (1 square mile (2 589 988 $m^2$) in area).

RFNI calculations were made for the footprint contour maps corresponding to the full power operational takeoff profile described in detail above.

### 3.8.4.3 Results

Constant-EPNL contour areas were calculated in the range of 85 to 110 EPNdB. Five engine/nacelle configurations were investigated. The results are presented in figure 42 in the form of relative footprint area versus EPNL and in figure 43 where the gains relative to the JT3D-3B hardwall baseline are presented in the form of EPNL footprint area reduction. The RFNI has been calculated as described in section 3.8.4.2 and the results are presented in table 15.

*TABLE 15.–707-320B/JT3D-3B/JT3D-9 RELATIVE FOOTPRINT NOISE INDEX*

| Nacelle | RFNI (a) |
|---|---|
| JT3D-3B baseline | 1.000 |
| JT3D-9 configuration 1 | 0.111 |
| JT3D-9 configuration 1A | 0.092 |
| JT3D-9 configuration 2 | 0.082 |
| JT3D-9 configuration 3 | 0.065 |

[a]Based on 707-320B EPNL contours

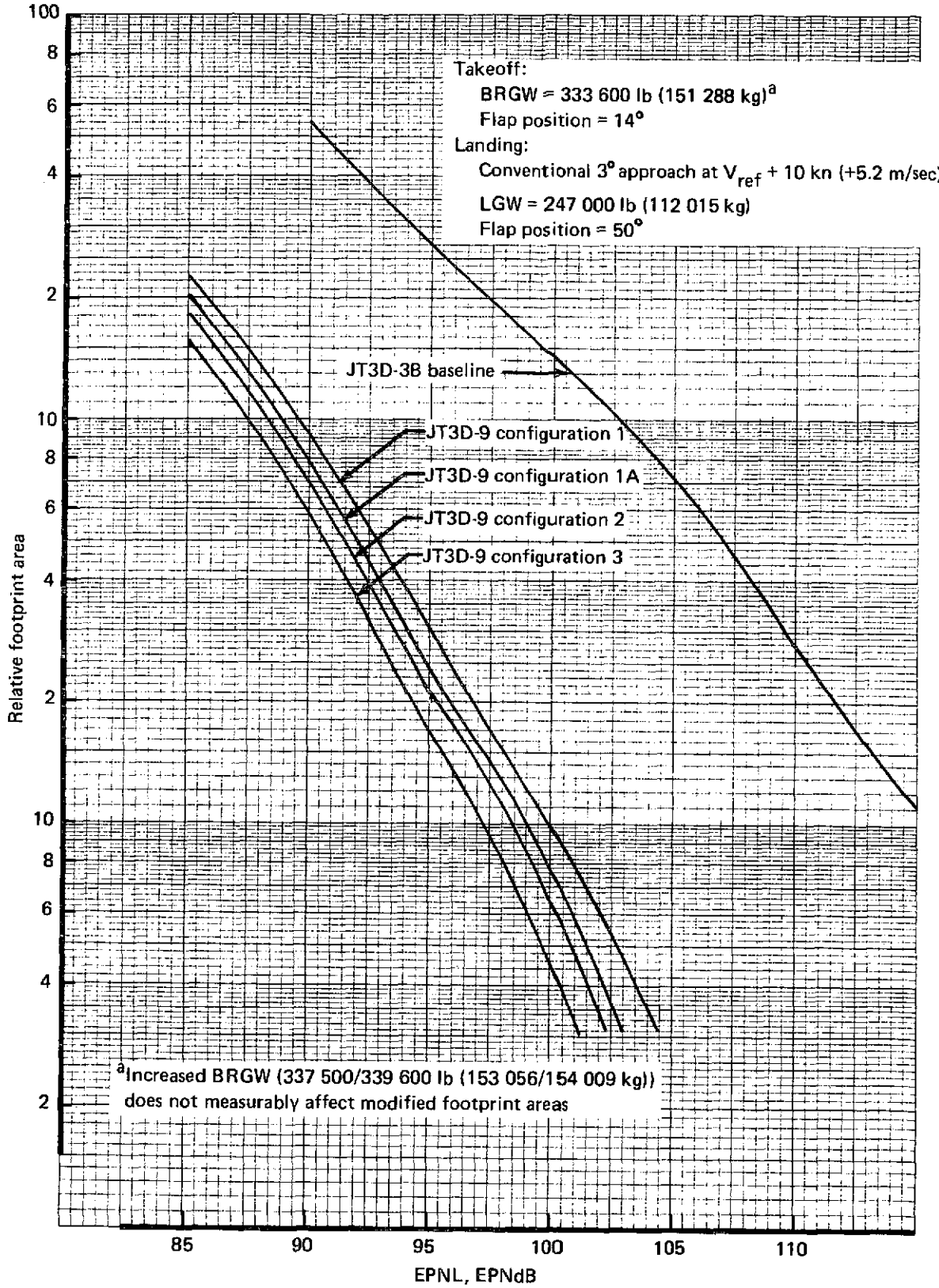


*FIGURE 42.—707-320B/JT3D-3B/JT3D-9 EPNL FOOTPRINT CONTOUR AREAS, FULL POWER OPERATIONAL PROFILE*

BRGW = 333 600 lb (151 288 kg)
Takeoff flaps = 14°
Conventional 3° approach at $V_{ref}$ + 10 kn (+5.2 m/sec)
LGW = 247 000 lb (112 015 kg)
Landing flaps = 50°

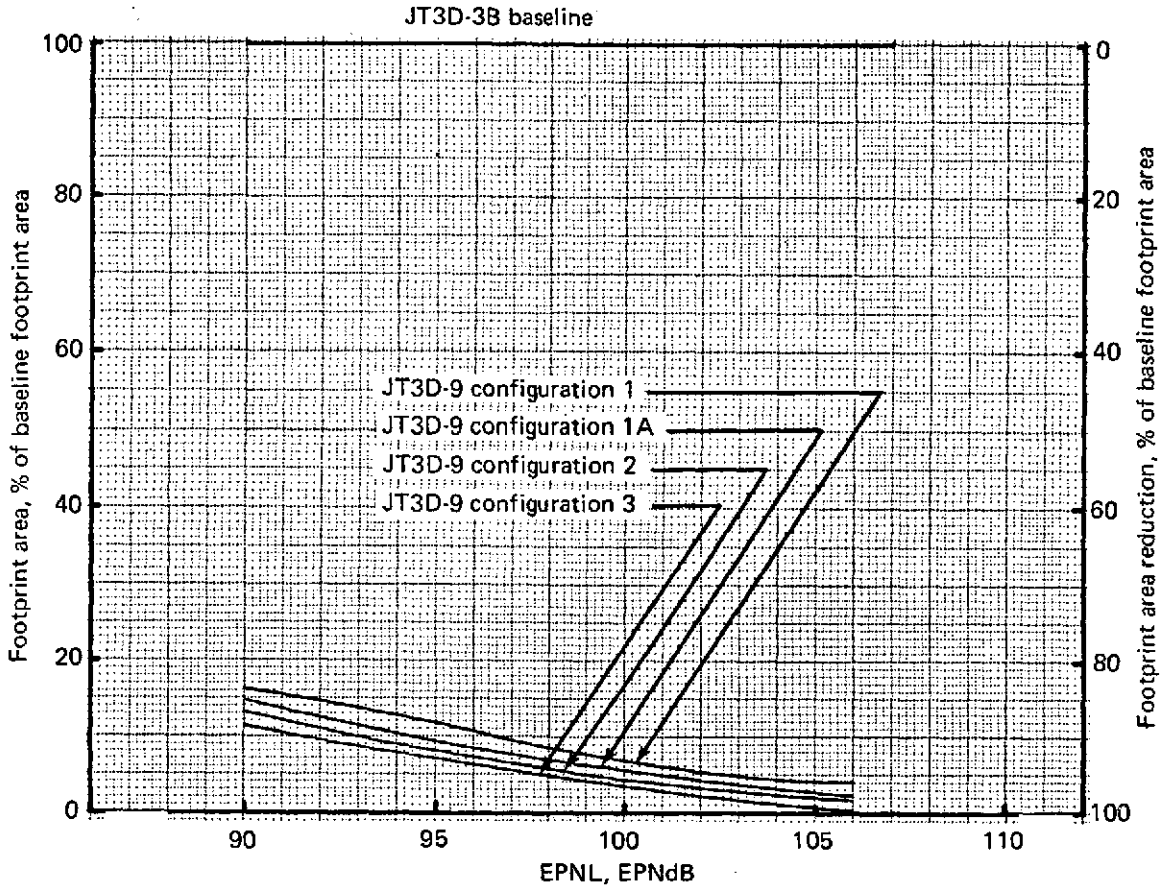


*FIGURE 43.—707-320B/JT3D-3B/JT3D-9 EPNL FOOTPRINT AREA REDUCTION, FULL POWER OPERATIONAL PROFILE*

# 4.0 727 AIRPLANE

## 4.1 AIRPLANE DESCRIPTION

The 727 airplane is a low-wing, three-engine, T-tail, commercial jet aircraft. The engines are located at the rear of the airplane with engines 1 and 3 mounted on struts protruding from the side of the body. Engine 2 is located on the body centerline with inlet air supplied through a center duct with the duct inlet located above the body and forward of the vertical fin.

By the end of 1972, more than a thousand 727 airplanes had been delivered or ordered. Two versions of the airplane have been built: the 727-100 and the 727-200. The 727-200 differs from the 727-100 in that it has 120-in. (3.048-m) body extensions inserted fore and aft of the wing. All 727 airplanes are equipped with versions of Pratt & Whitney Aircraft JT8D engines. A weight/thrust growth history of airplane and engine combinations is presented in figure 44.

The baseline airplane, against which the modified airplanes are compared, is the 727-200 standard airplane. It is a 172 500-lb (78 246-kg) maximum brake release gross weight airplane with JT8D-9 engines of 14 500 lb (64 496 N) sea-level static thrust and no acoustic treatment. This particular configuration was picked for the baseline because it represents the most widely used domestic version of the 727-200 airplane. Figure 45 shows the general arrangement of the 727-200 baseline airplane.

The modified airplane would be a 727-200 modified to accept Pratt & Whitney Aircraft JT8D-109 refanned engines with various levels of acoustic treatment. A general arrangement of the modified airplane, with the principal areas of modification shaded, is shown in figure 46. The airplane modifications include new nacelles, as defined in section 4.4, and airframe modifications, as defined in section 4.5.

## 4.2 ENGINE DEFINITION

### 4.2.1 JT8D-9 (Baseline)

The Pratt & Whitney Aircraft JT8D-9 is an axial-flow turbofan engine with multistage low- and high-pressure compressors, a two-stage fan, and a bypass ratio of 1.05. This engine was used as the baseline engine for comparison with the refanned JT8D-109 engine. Other series of this engine in airline operation are the JT8D-1, -7, -11, and -15.



PRECEDING PAGE BLANK NOT FILMED

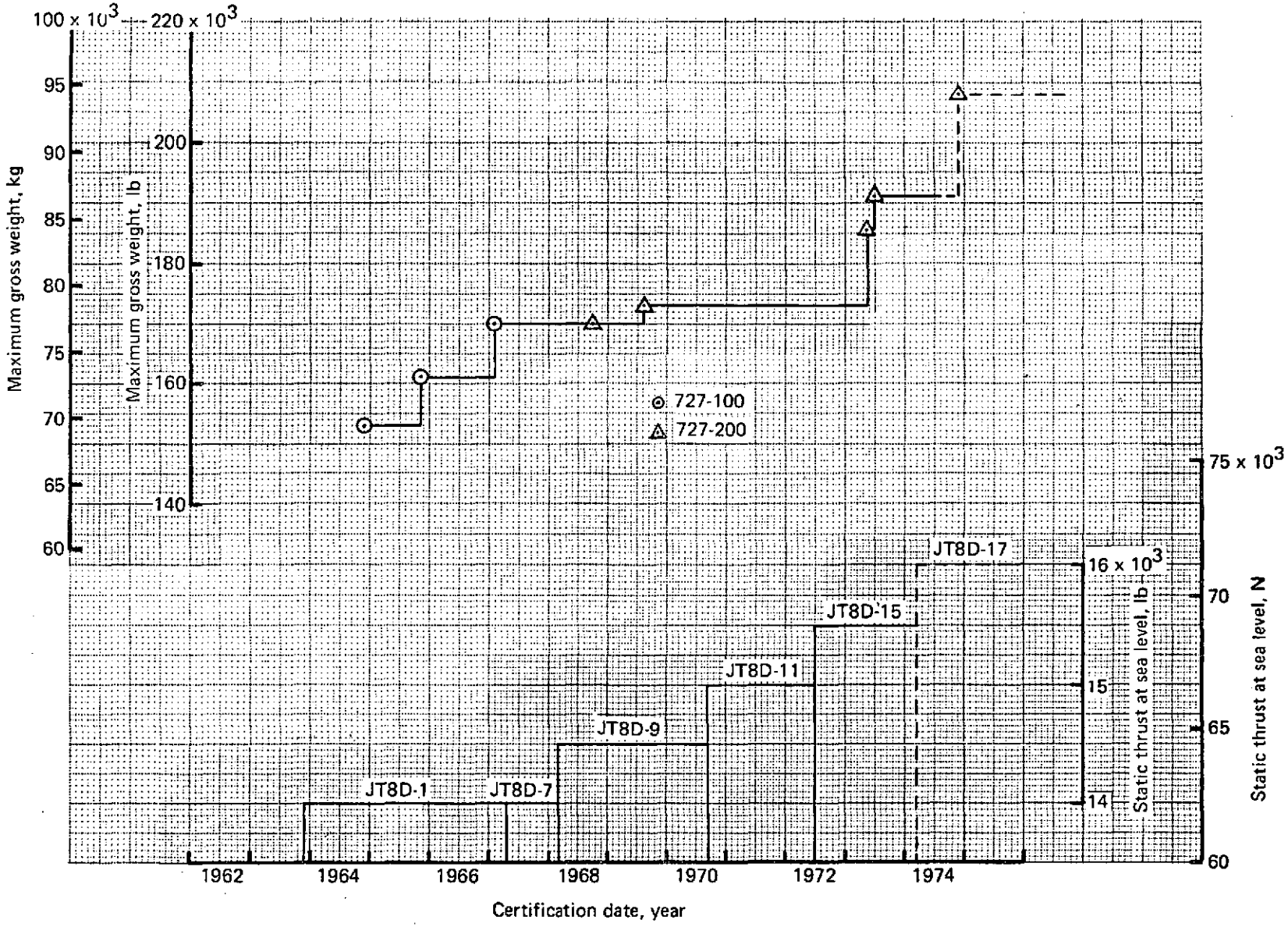


*FIGURE 44.—727/JT8D WEIGHT/THRUST GROWTH HISTORY*

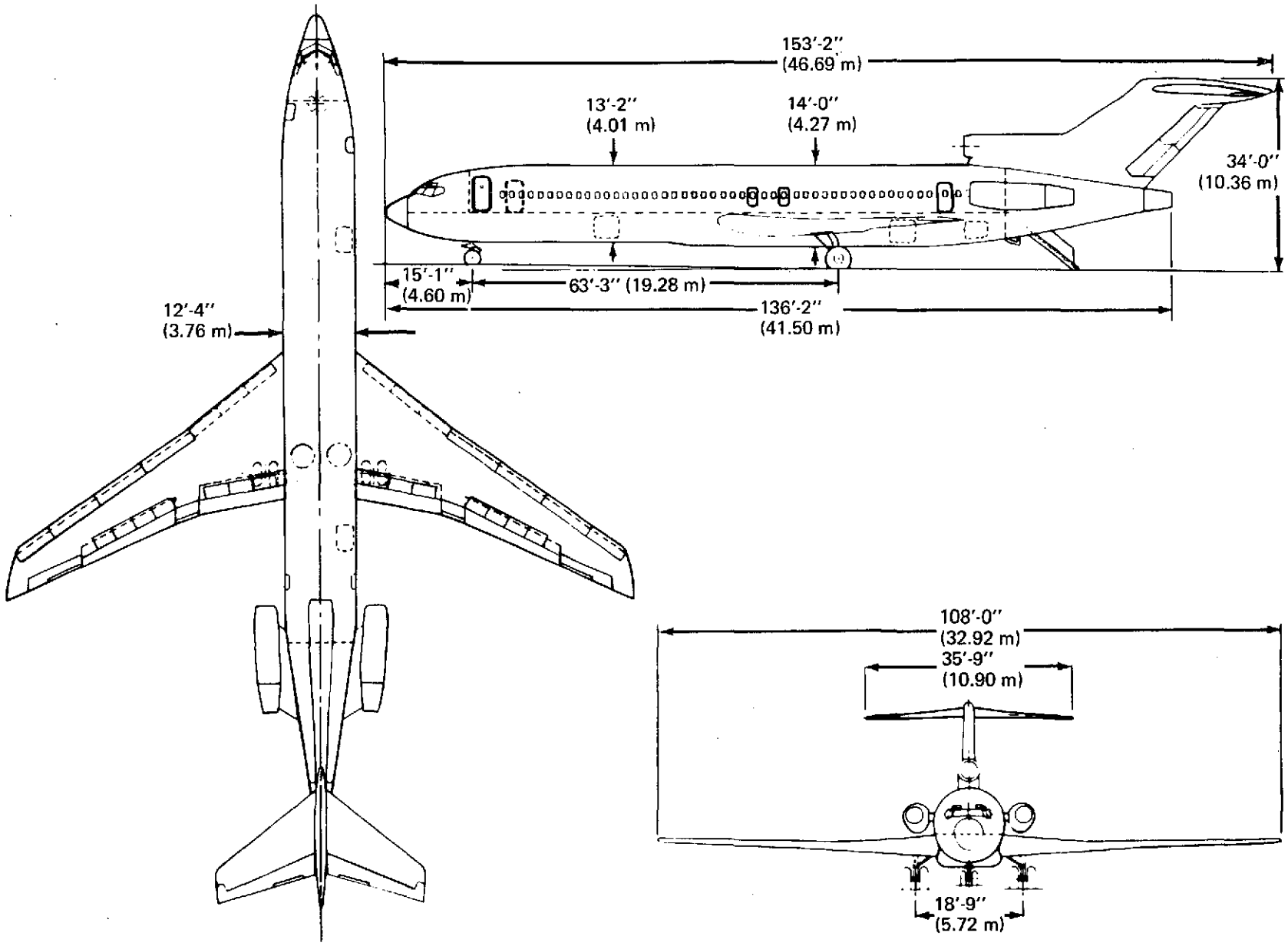


*FIGURE 45.–727-200 BASELINE AIRPLANE GENERAL ARRANGEMENT*

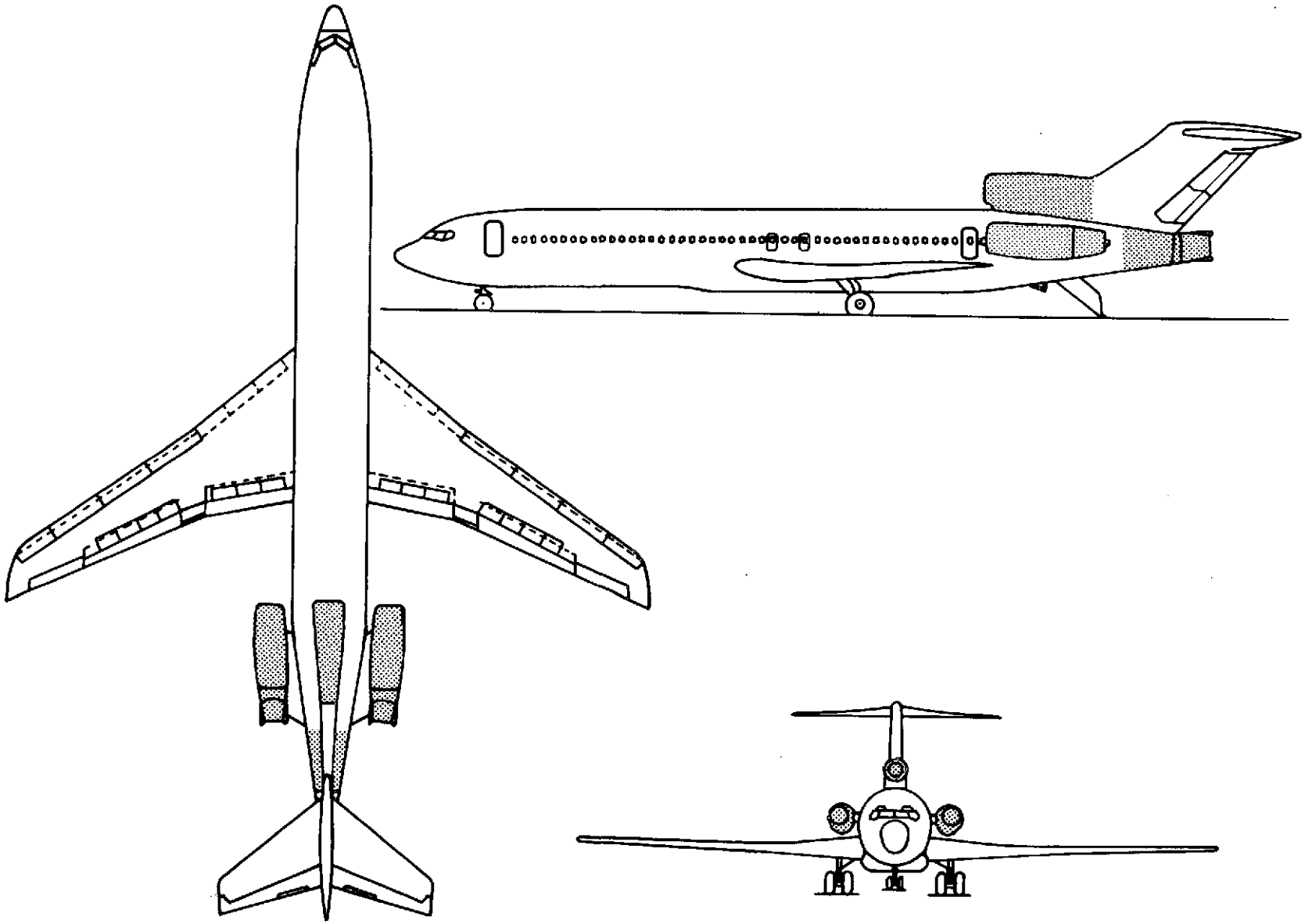

FIGURE 46.—727-200/JT8D-109 MODIFIED AIRPLANE GENERAL ARRANGEMENT

The 727-200/JT8D-9 operating envelopes are shown in figures 47 and 48. No changes are expected to be required to these envelopes for the refanned-engine installation.

### 4.2.2 JT8D-109 (Refanned)

The JT8D-109 engine was designed as a derivative of the basic JT8D turbofan engine, modified to incorporate a new, larger diameter, single-stage fan with a bypass ratio of 2.03 and two supercharging low-pressure compressor stages. The modifications would provide lower jet noise, increased takeoff and cruise thrust, and lower specific fuel consumption. A comparison of the configurations of the basic JT8D-9 and the JT8D-109 refanned engine is shown in figure 49.

The JT8D-9 engine core, with the exception of the two front fan stages and the fourth turbine stage, will be used in the JT8D-109 engine. Design interface requirements, such as flange loads, pressure limits, flow distortion, and flow areas for the inlet and exhaust systems, plus accessory and subsystem allowables, limitations, and subsystem requirements will be coordinated with the engine manufacturer. It has already been agreed that engine flange M will be moved forward 6 in. (0.1524 m) on the cylindrical section of the fan duct to provide design flexibility.

### 4.2.3 Uninstalled Engine Performance

Uninstalled performance of the JT8D-9 and JT8D-109 are compared in table 16. Uninstalled takeoff thrust lapse rates ($F_N$ vs TAS) are compared in figure 50. Figure 51 illustrates the relationship between the JT8D-109 and JT8D-9 uninstalled cruise TSFC (TSFC vs $F_N$).

*TABLE 16.–JT8D-9/JT8D-109 UNINSTALLED ENGINE CHARACTERISTICS COMPARISON*

| Item | Baseline (JT8D-9) | Refanned engine (JT8D-109) |
|---|---|---|
| Takeoff thrust–sea level, standard day | | |
| Static, lb (N) | 14 500 (64 499) | 16 600 (73 840) |
| 100 kn (51.4 m/sec), lb (N) | 13 200 (58 716) | 14 500 (64 499) |
| Maximum cruise–30 000 ft (9144 m), Mach 0.84 | | |
| Thrust, lb (N) | 4580 lb (20 373) | 4760 (21 174) |
| TSFC, lb/hr/lb (kg/hr/daN) | 0.800 (0.816) | 0.782 (0.797) |
| Weights and dimensions | | |
| Basic engine weight, lb (kg) | 3227 (1464) | 3797 (1722) |
| Basic engine length, in. (m) | 127.2 (3.231) | 119.9 (3.045) |
| Fan tip diameter, in. (m) | 40.9 (1.039) | 49.2 (1.250) |

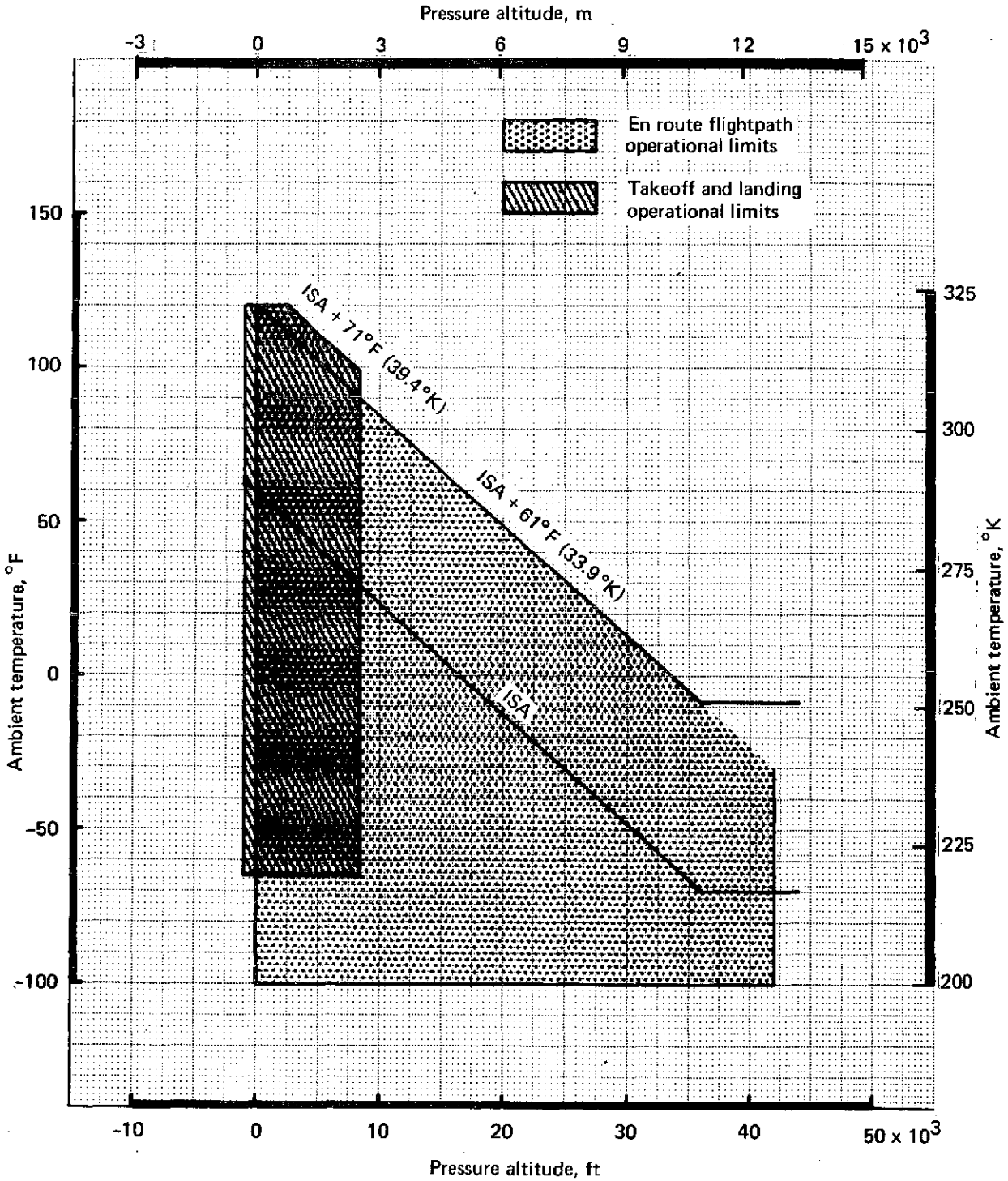


*FIGURE 47.—727-200/JT8D-9 BASELINE AIRPLANE—PRESSURE ALTITUDE/TEMPERATURE ENVELOPE*

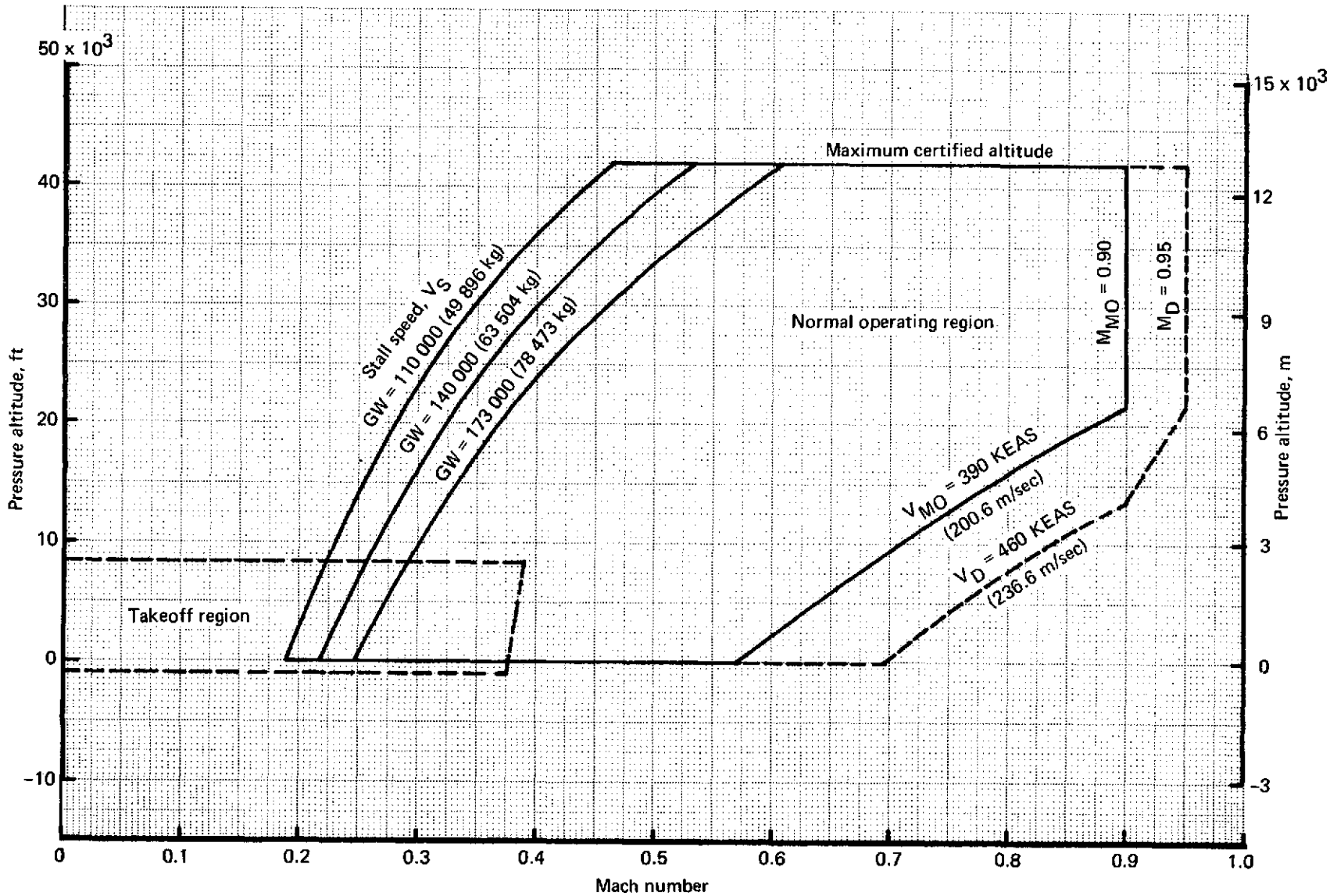


*FIGURE 48.—727-200/JT8D-9 BASELINE AIRPLANE—PRESSURE ALTITUDE/SPEED ENVELOPE, STANDARD DAY, FLAPS UP, GEAR UP*

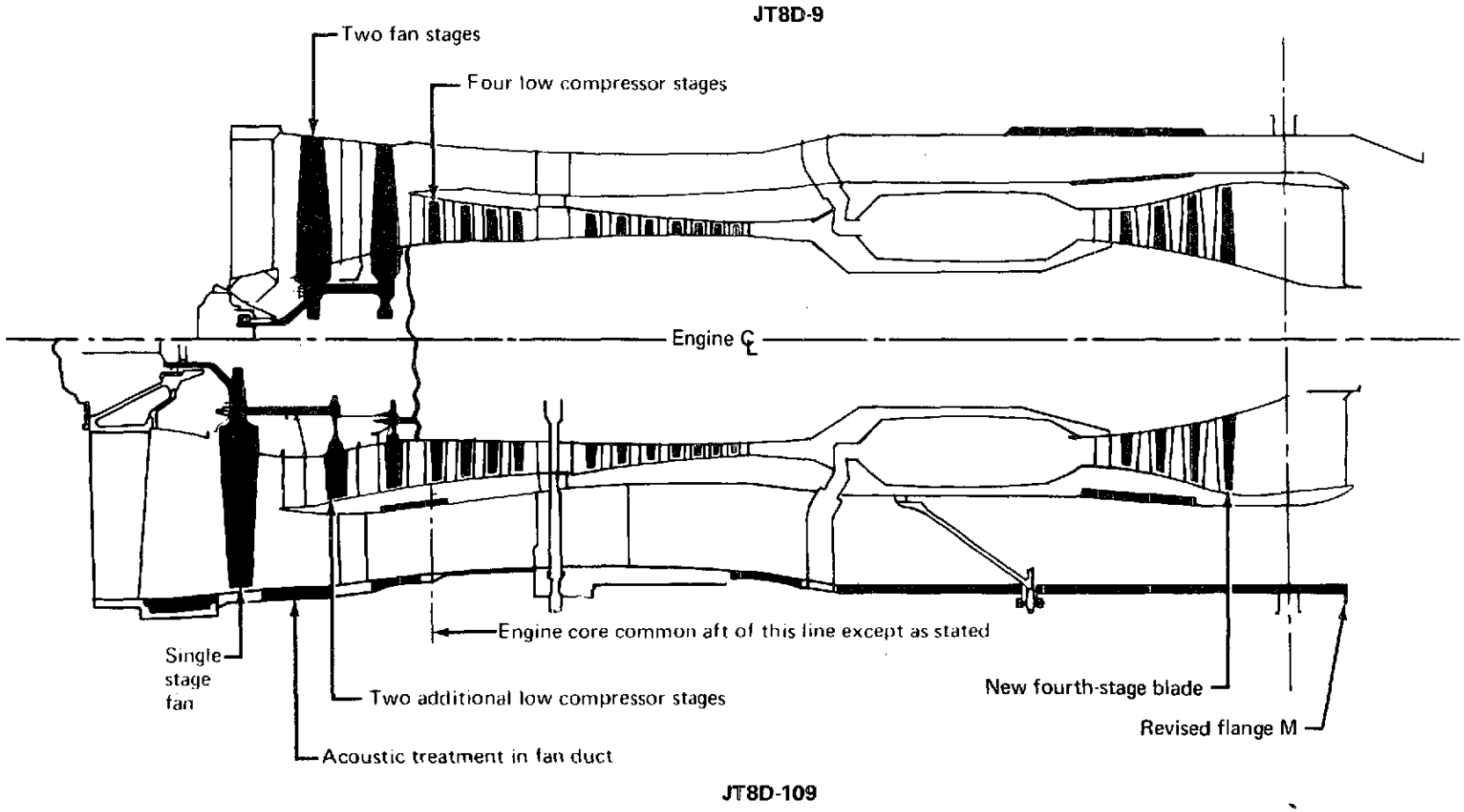


*FIGURE 49 –JT8D-9/JT8D-109 ENGINE CONFIGURATION COMPARISON*

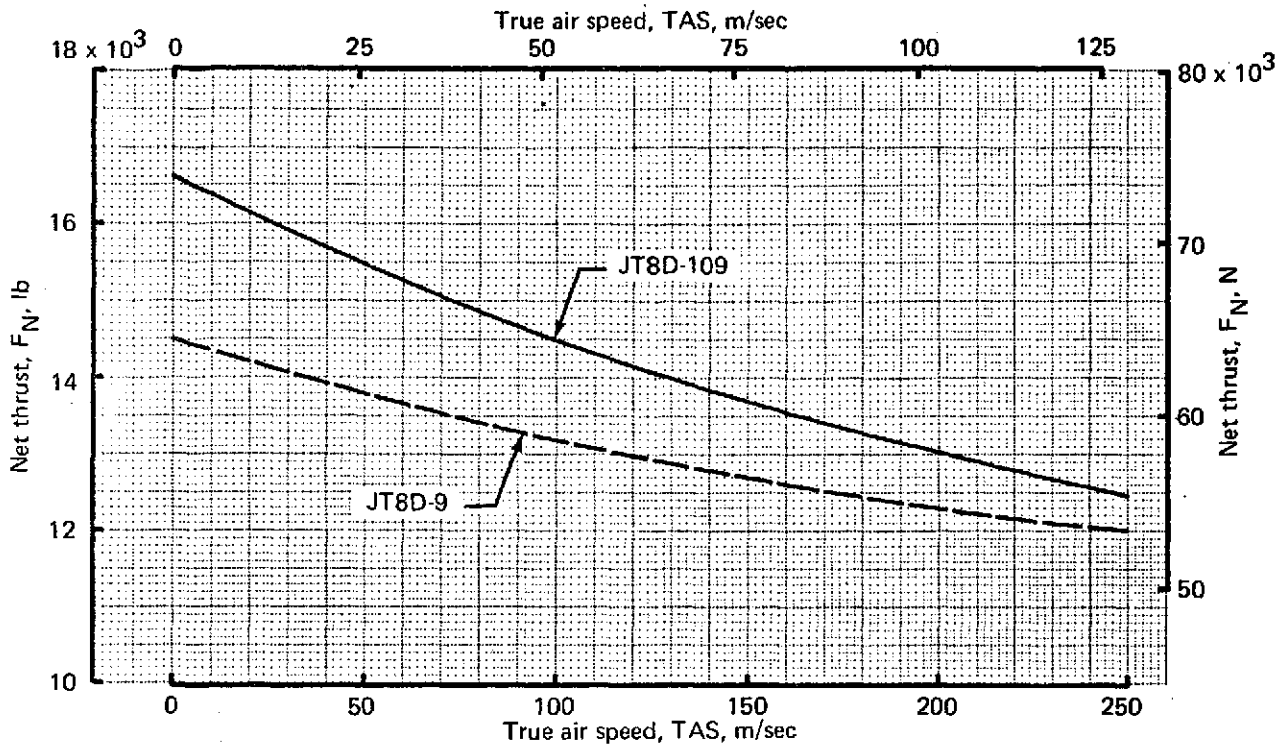


*FIGURE 50.–727/JT8D-9/JT8D-109 UNINSTALLED TAKEOFF LAPSE RATE COMPARISON, STANDARD DAY, SEA LEVEL*

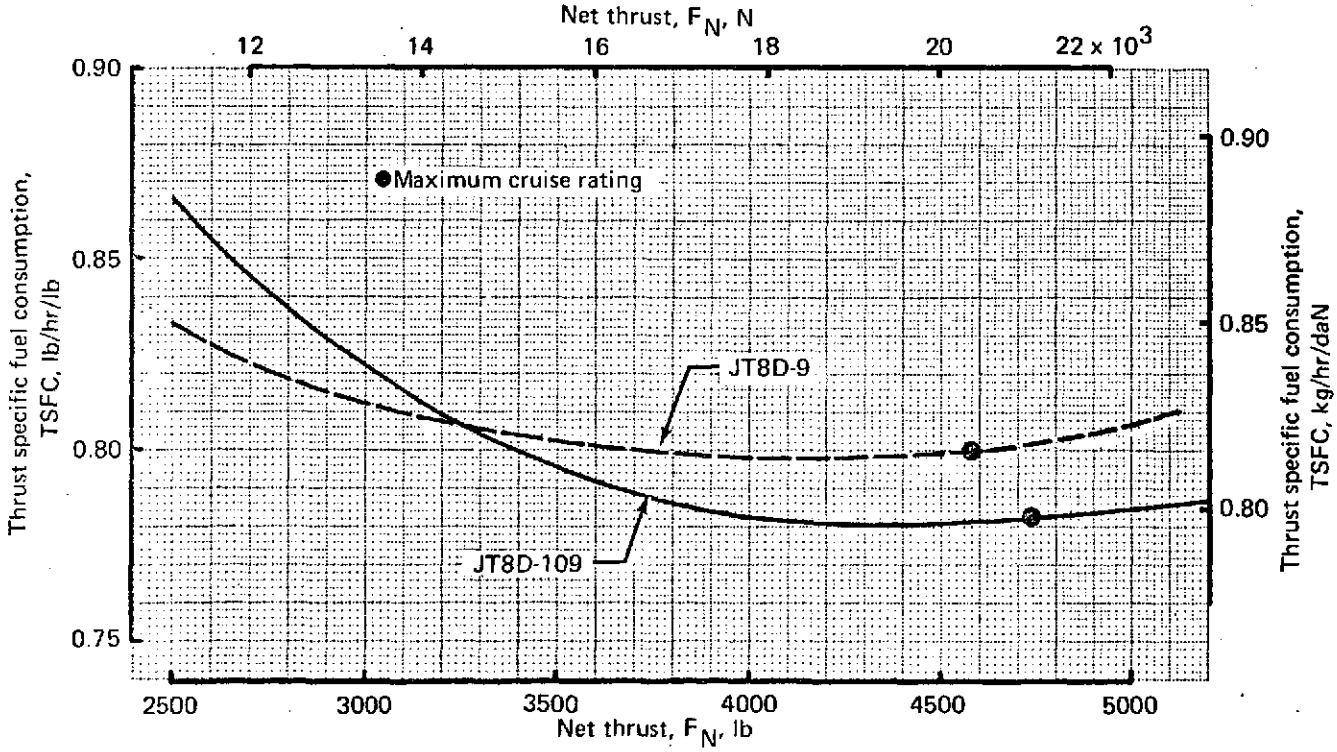


*FIGURE 51.–727/JT8D-9/JT8D-109 UNINSTALLED CRUISE PERFORMANCE COMPARISON, STANDARD DAY, 30 000 FT (9144 M), MACH 0.84*

### 4.2.4 Deteriorated Engine Performance

The engine performance data discussed in section 4.2.3 are for a newly manufactured engine. Since an important part of this program is the modification of existing engines (and airplanes), a study was conducted to determine the relative performance change of refanning a deteriorated JT8D-9 as compared to refanning a new JT8D-9. The comparisons quoted here were made at constant thrust (takeoff power).

As shown in figure 52, a deteriorated JT8D-9 engine was estimated to have an EGT 50° F (28° K) higher than a new JT8D-9. The refanned deteriorated JT8D-109 was estimated to have an EGT 20° F (11° K) to 36° F (20° K) higher than a new JT8D-109 and when fully deteriorated, the EGT was estimated to increase 50° F (28° K) relative to the new JT8D-109. The JT8D-9 and JT8D-109 were therefore estimated to experience similar EGT increases due to engine deterioration.

As shown in figure 53, the TSFC of a new JT8D-9 was estimated to increase 2% due to deterioration. The deteriorated JT8D-9, when refanned, would have a TSFC improvement of 2.5% to 3% depending on the extent of high pressure turbine work performed. Further deterioration, estimated as from 1.5% to 1.9% increase would still show a deteriorated JT8D-109 TSFC that is 1.7% lower than a deteriorated JT8D-9.

## 4.3 MODEL AND COMPONENT TESTS

### 4.3.1 General

Model nozzle tests were planned and models built to determine the performance of large and small plug nozzles with short and long splitters operating in a mixed-flow (hot primary, cold secondary) environment compared to a conical nozzle with short and long internal splitters. Cancellation of funds for this test after only the baseline model configuration had been run precluded further testing.

Scale-model fan acoustic tests were planned to provide early test data for substantiating JT8D-109 refanned engine fan performance and noise predictions. Estimates of fan noise for the full-scale refanned engine were to be obtained from incremental noise differences found by testing 0.2994-scale fan models of the JT8D-9 current engine and JT8D-109 refanned engine. Work on the scale fan models was stopped prior to start of noise tests, due to shortage of funds. All hardware fabrication for the two-stage JT8D-9 scale-model fan was complete at this point, but the JT8D-109 refanned-engine model was still in the early design stages.

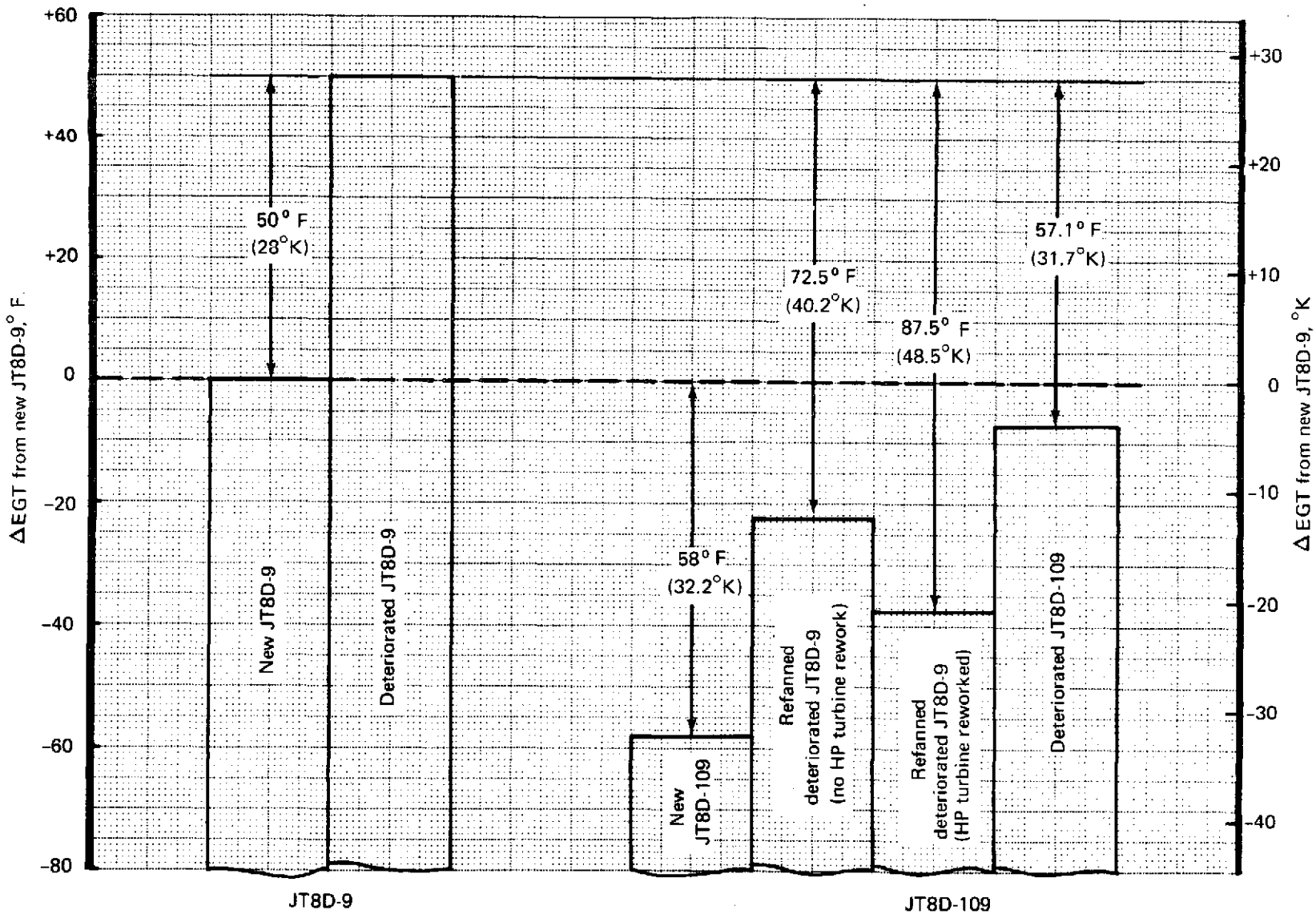


*FIGURE 52.–JT8D-9/-109 COMPARISON OF NEW AND DETERIORATED ENGINE EXHAUST GAS TEMPERATURES, SEA LEVEL, STATIC, TAKEOFF, CONSTANT $F_N$*

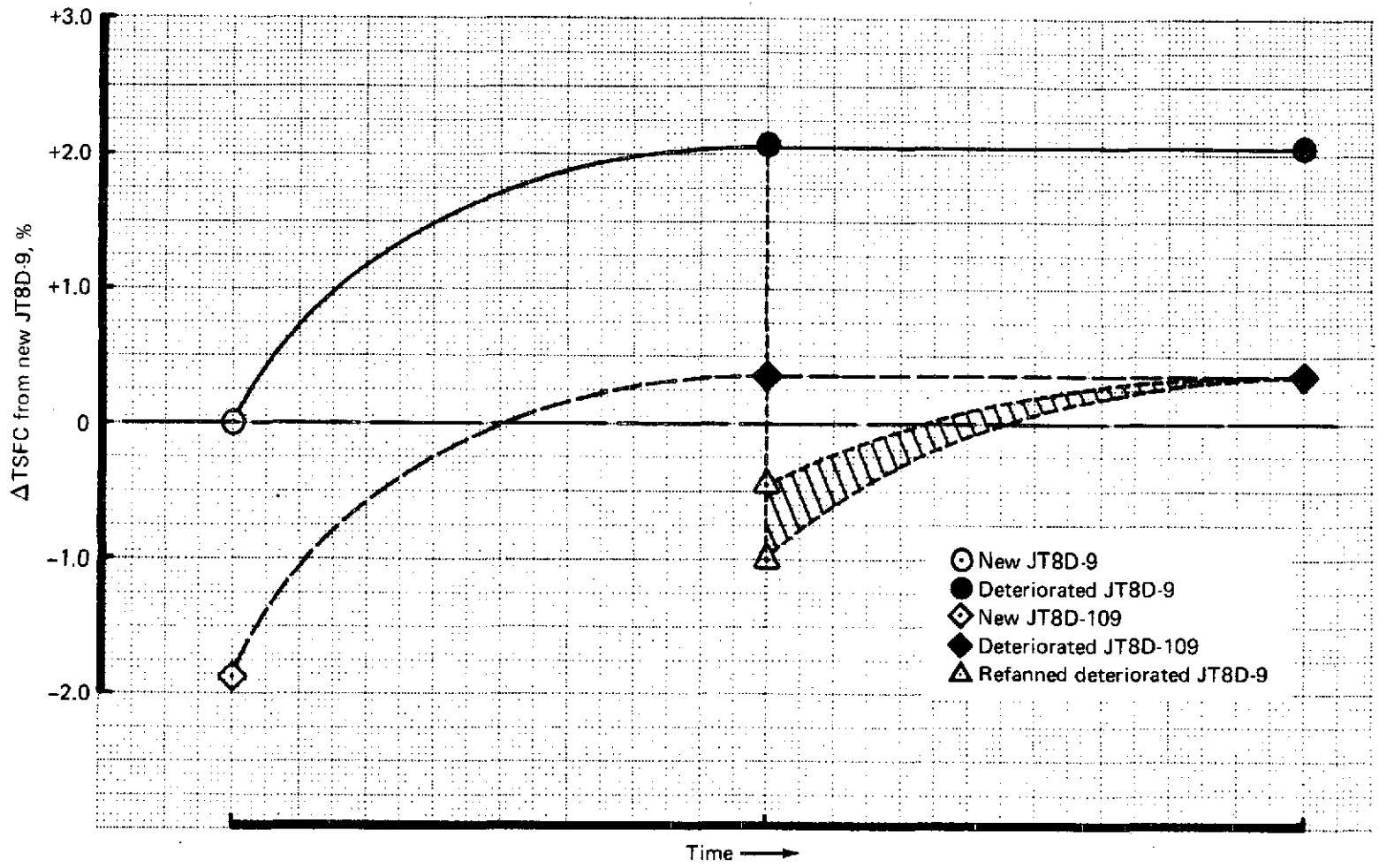


*FIGURE 53.—JT8D-9 AND JT8D-109 DETERIORATION OF TSFC's WITH TIME, 30 000 FT (9144 M) MACH 0.84, CONSTANT $F_N$*

### 4.3.2 Nozzle Acoustic Tests

#### 4.3.2.1 Objectives

The objectives of the model nozzle system acoustic tests were to evaluate the jet noise characteristics of conical and plug nozzles for the refanned engine cycle and to investigate the effects of airplane forward velocity on jet noise.

#### 4.3.2.2 Model Description

Relative velocity effects tests were to be performed on 1/20th-scale models of the JT8D-9 baseline nozzle, a modified conical nozzle, two modified plug nozzles, and three single-flow conical nozzles. One-eighth scale models of the above JT8D-9 and JT8D-109 configurations were also fabricated but were not tested because of funding limitations.

#### 4.3.2.3 Results

At the time of preparation of this report, analyses of the acoustic data had not been completed. Preliminary analyses indicate that the relative velocity effect on jet noise is somewhat less than that calculated by a $(V_{j\ rel})^8$ curve. For the conical nozzles, the relative velocity effects approximate a $(V_{j\ rel})^5$ curve at a given absolute velocity. Figure 54 presents preliminary data. The refanned-engine nozzle evaluation shows that the JT8D-109 nozzle is about 9 to 13 dB quieter statically and 9 to 14 dB quieter in flight than the JT8D-9, depending on the power setting. The JT8D-109 static benefit is just as predicted; the JT8D-109 flight benefit is about 1 dB less than predicted. This is due to a smaller relative velocity correction on the refanned engine compared to the JT8D-9 baseline engine.

### 4.3.3 727 Center-Engine Inlet and Duct Model Test

#### 4.3.3.1 Objectives

Program guidelines call for minimum modifications to the existing 727 airplane structure to accept the new center engine inlet and duct for the refanned JT8D engine. The refanned JT8D engines have a maximum cruise corrected airflow of approximately 480 lb/sec (217.7 kg/sec) as compared to 332 lb/sec (150.6 kg/sec) for existing JT8D-15 engines. The objective of this test was to explore, by wind tunnel testing, the aerodynamic design feasibility of a new center-engine inlet and duct which would meet the increased airflow requirement of the refanned JT8D engine and which could be fit into existing structure within the minimum modification requirement.

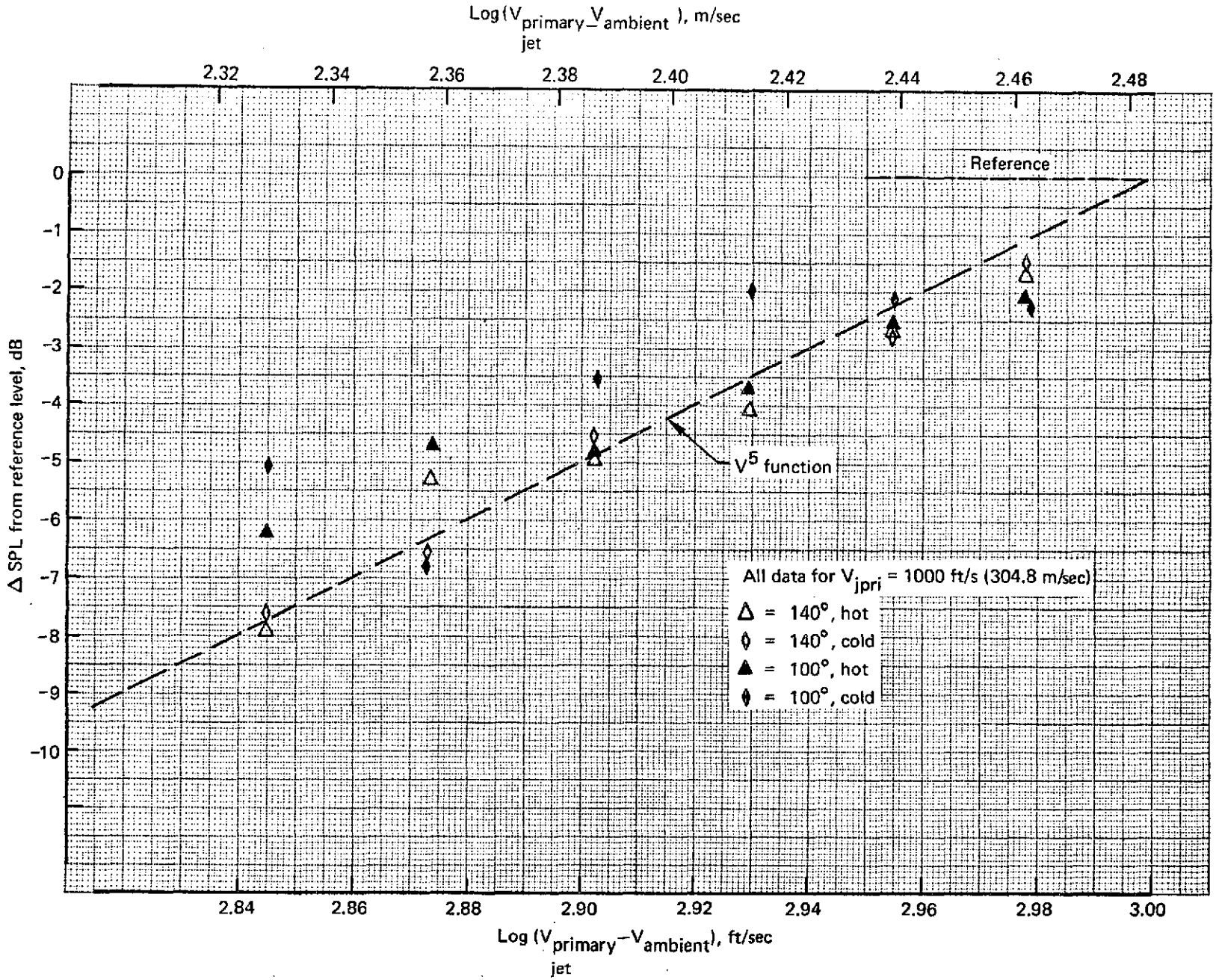


*FIGURE 54.—PRELIMINARY RESULTS OF JET NOISE MODEL TESTS*

### 4.3.3.2 Model Description

A 0.2994-scale fiberglass center duct model was designed and constructed. A comparison of the test model and 727-200 production inlet and center-duct geometry is shown in figure 55. The modified duct design was based on potential-flow/boundary-layer analyses.

The model was made in two halves so that it could be opened following testing to observe oil-flow patterns on the model surfaces. All model surfaces were of the hardwall type (i.e., without acoustic material). A 727 fuselage was simulated under the duct during a portion of the test. As shown in table 17, a total of six different vortex generator configurations were made for the model.

*TABLE 17.–727 CENTER INLET AND DUCT VORTEX GENERATOR TEST CONFIGURATIONS*

| Vortex generator configuration | 12 o'clock/second bend vortex generator | 6 o'clock/first bend vortex generator |
|---|---|---|
| 1 | Single row<br>90° sector–sta 1315 | Double rows<br>90° sector–sta 1160<br>120° sector–sta 1180 |
| 2 | Single row<br>90° sector–sta 1338 | Same as configuration 1 |
| 3 | Single row<br>90° sector–sta 1315 | Same as configuration 1 |
| 4 | Single row<br>90° sector–sta 1338<br>(5 sets) | Same as configuration 1 |
| 5 | Single row<br>90° sector–sta 1338<br>(5 sets) | None |
| 6 | Same as configuration 3 | Single row<br>120° sector–sta 1180 |

### 4.3.3.3 Test Description

The test was conducted in the Boeing 9- by 9-ft (2.75- by 2.75-m) low-speed wind tunnel. This tunnel is an open-circuit-type wind tunnel in which the test section airspeed can be varied from zero to approximately 165 kn (84.9 m/sec). Duct airflows were produced by using a turbojet engine to draw air through the model.

Test measurements consisted of tunnel total temperature and pressure, duct airflow, model wall static pressures, engine face steady-state total pressure, and engine face dynamic total pressure.

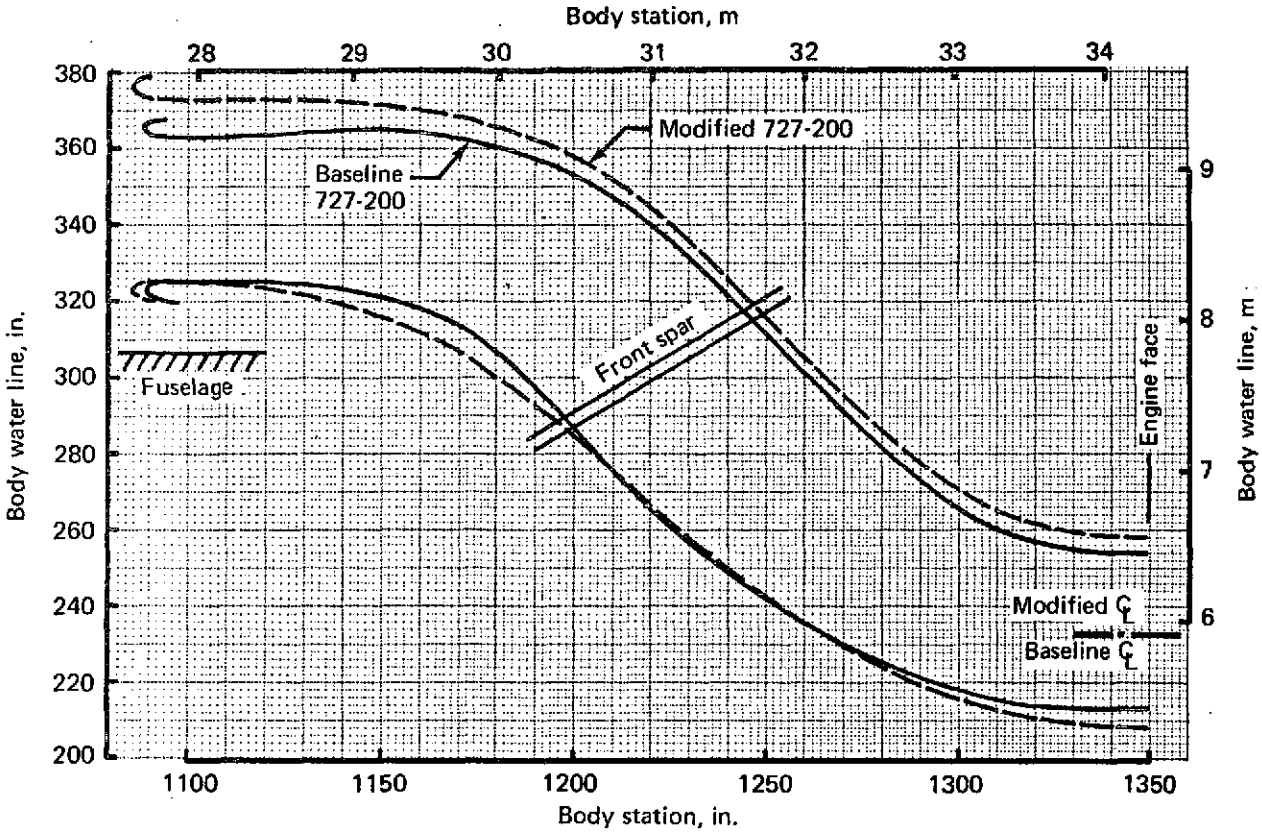


| Item | Modified 727-200 (JT8D-109) | Baseline 727-200 (JT8D-15) |
|---|---|---|
| Corrected airflow at cruise | 480 lb/sec (217.7 kg/sec) | 332 lb/sec (150.6 kg/sec) |
| Highlight diameter | 54 in. (1.372 m) | 43.70 in. (1.11 m) |
| Highlight area | 2290.23 in.$^2$ (1.478 m$^2$) | 1499.87 in.$^2$ (0.968 m$^2$) |
| Lip loading, corrected airflow/highlight area | 30.18 lb/sec-ft$^2$ (147.4 kg/sec-m$^2$) | 31.87 lb/sec-ft$^2$ (155.6 kg/sec-m$^2$) |
| Highlight Mach number | 0.386 | 0.413 |
| Throat diameter | 47.80 in. (1.21 m) | 38.33 in. (0.974 m) |
| Throat area | 1794.51 in.$^2$ (1.158 m$^2$) | 1153.90 in.$^2$ (0.744 m$^2$) |
| Throat Mach number | 0.532 | 0.596 |
| Highlight area/throat area | 1.276 | 1.30 |
| Lip contour | 2.258:1 ellipse | 2.111:1 ellipse |
| Lower lip height above fuselage | 15.7 in. (0.399 m) | 15.76 in. (0.4 m) |
| Engine face diameter | 50.1 in. (1.272 m) | 40.5 in. (1.03 m) |
| Nose dome diameter | 16.0 in. (0.406 m) | 12.0 in. (0.305 m) |
| Engine face area | 1770.298 in.$^2$ (1.142 m$^2$) | 1175.155 in.$^2$ (0.758 m$^2$) |
| Engine face Mach number | 0.543 | 0.579 |

*FIGURE 55.—727/JT8D BASELINE AND MODIFIED CENTER-ENGINE INLET AND DUCT GEOMETRY COMPARISON*

The model was instrumented with 66 static pressure ports. Steady-state total pressure was measured by using a four-arm (16 probes per arm) rotating rake. Measurements were taken at 10° increments. Steady-state recovery was computed by area averaging the measurements. Dynamic measurements were taken by making radial traverses at the engine face.

Data were taken for static, crosswind, forward speed, and angle-of-attack conditions over a range of center-duct airflows. Figures 56 and 57 show typical compressor face distortion maps for the duct without and with vortex generators.

#### 4.3.3.4 Results and Conclusions

Figure 58 shows center-duct pressure recovery without vortex generators versus corrected airflow at various forward speeds and zero angles of attack. Angles of attack within the 727 airplane operating regime (-15° to +5°) had little effect on inlet pressure recovery and distortion.

Test measurements and flow visualization indicated a secondary flow at the center-duct first bend, which produced a low total pressure region in the lower part of the annulus at the compressor face. At the upper wall, a flow separation region was indicated just in front of the compressor face. Installation of vortex generators along the duct wall improved the steady-state pressure distortion, as shown in figure 59. The better vortex generator configuration (no. 6), as shown in figure 60, incurred a total pressure recovery penalty of 0.25% at cruise.

The center duct was designed using the contractor's two-dimensional, compressible potential-flow/boundary-layer computer program. Predicted surface Mach number distributions, obtained by transforming the three-dimensional duct into an equivalent two-dimensional duct, were found to be in good agreement with the test results, as shown in figure 61.

The distortion and recovery comparisons of the modified and 727-200 baseline ducts are presented in table 18. The results indicate comparable duct performance.

A portion of the dynamic data taken during the test is presented in figure 62. Curve A shows the maximum dynamic pressure at the 6 o'clock measuring station, as a function of corrected airflow, for tunnel velocities equal to or greater than 25 kn (12.9 m/sec) and 0° inlet angle of attack. Curve B shows the maximum dynamic pressure at the 6 o'clock location, 0 kn (static) tunnel velocity and 0° angle of attack. A substantial difference between the static and forward speed conditions is apparent. Curves C and D show a similar trend, though a lower dynamic level, at the 12 o'clock location. Some dynamic data were taken, at tunnel forward speeds and various inlet angles of attack, with vortex generators installed. The data are shown as groups A′ and C′ for the 6

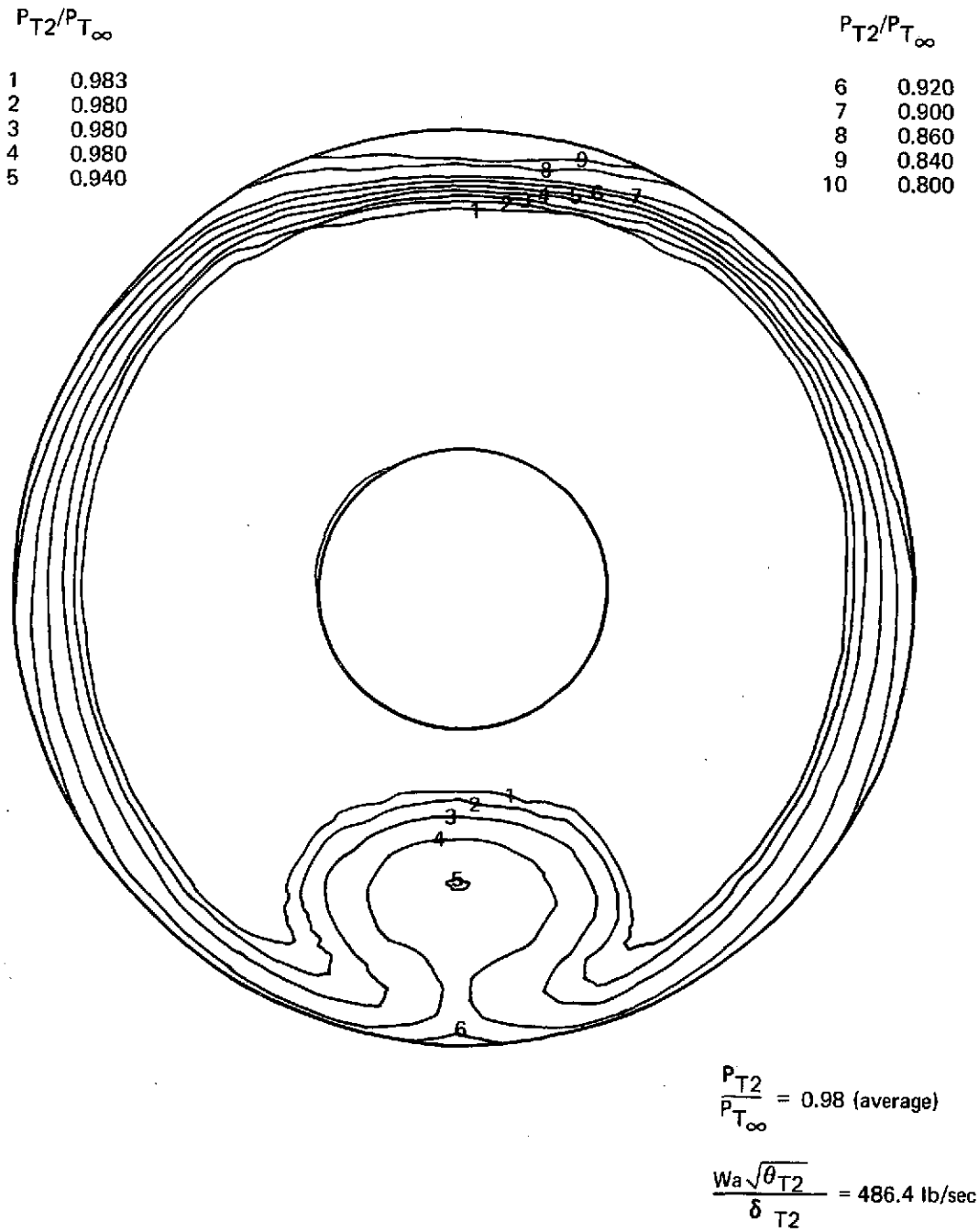


*FIGURE 56.—727/JT8D CENTER-DUCT PRESSURE RECOVERY MAP, 100 KN, NO VORTEX GENERATORS*

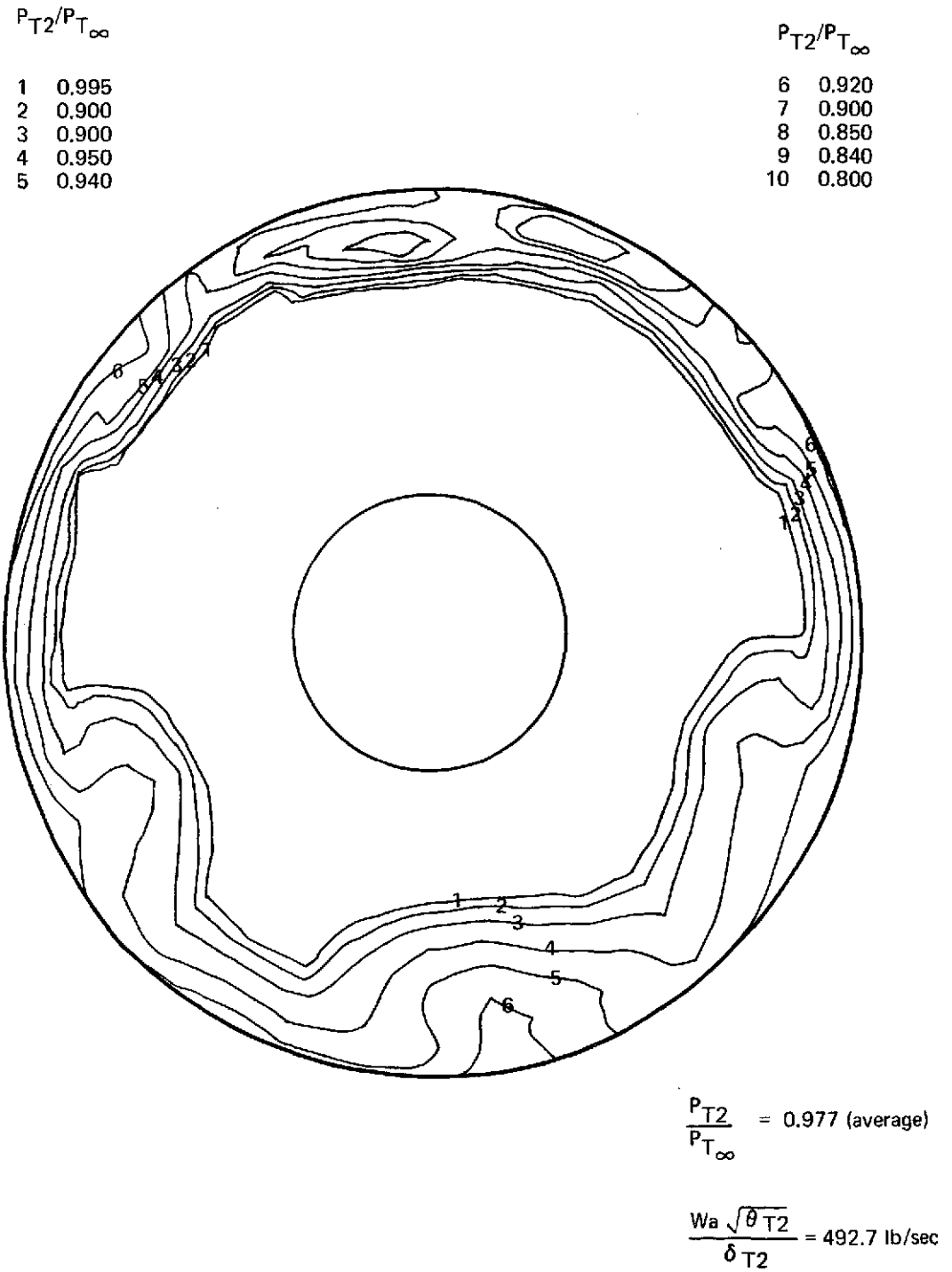


*FIGURE 57.–727/JT8D CENTER-DUCT PRESSURE RECOVERY MAP, VORTEX GENERATOR CONFIGURATION 6, 100 KN*

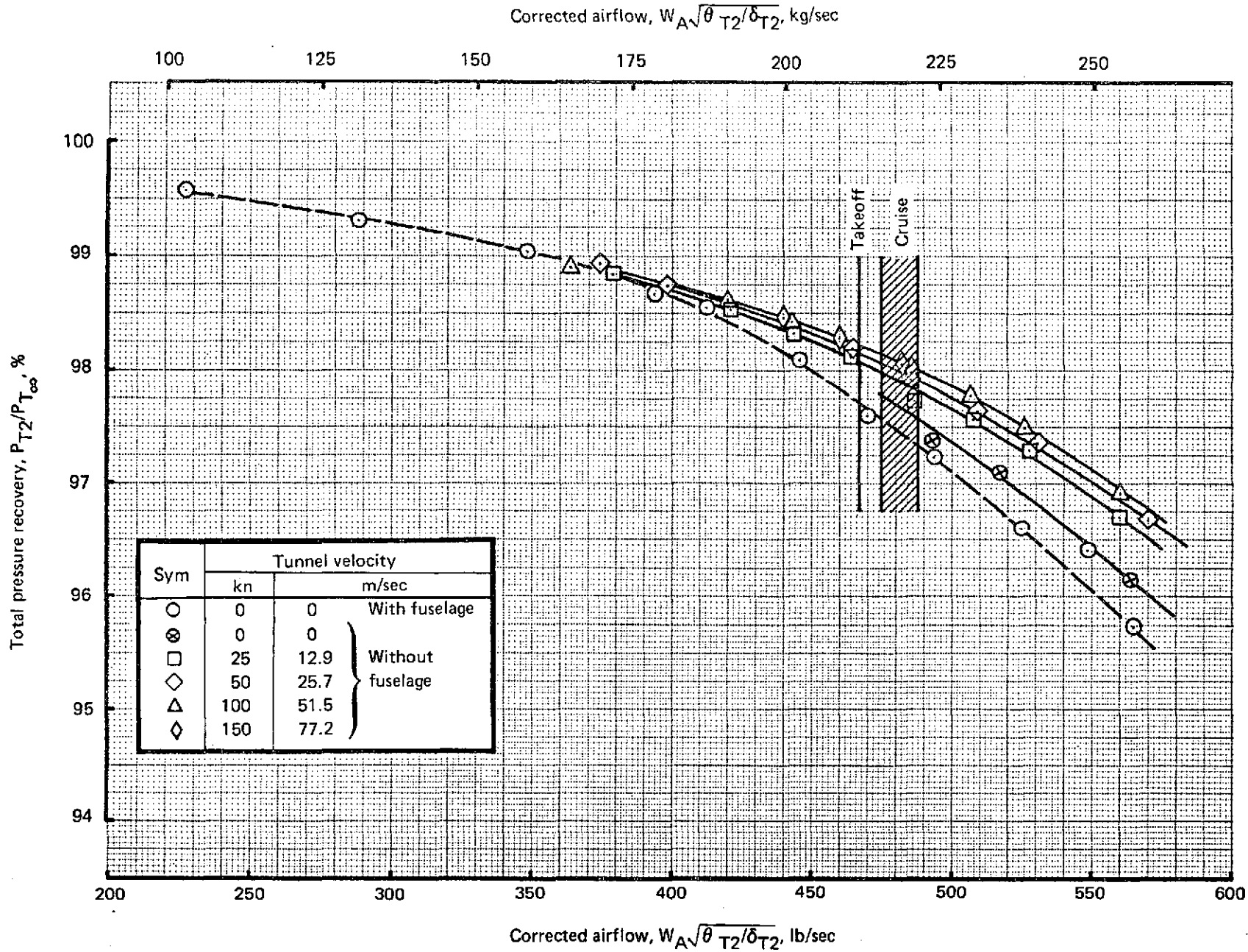


*FIGURE 58.—727/JT8D-109 MODIFIED INLET AND CENTER-DUCT PRESSURE RECOVERY WITHOUT VORTEX GENERATORS AT ZERO ANGLE OF ATTACK*

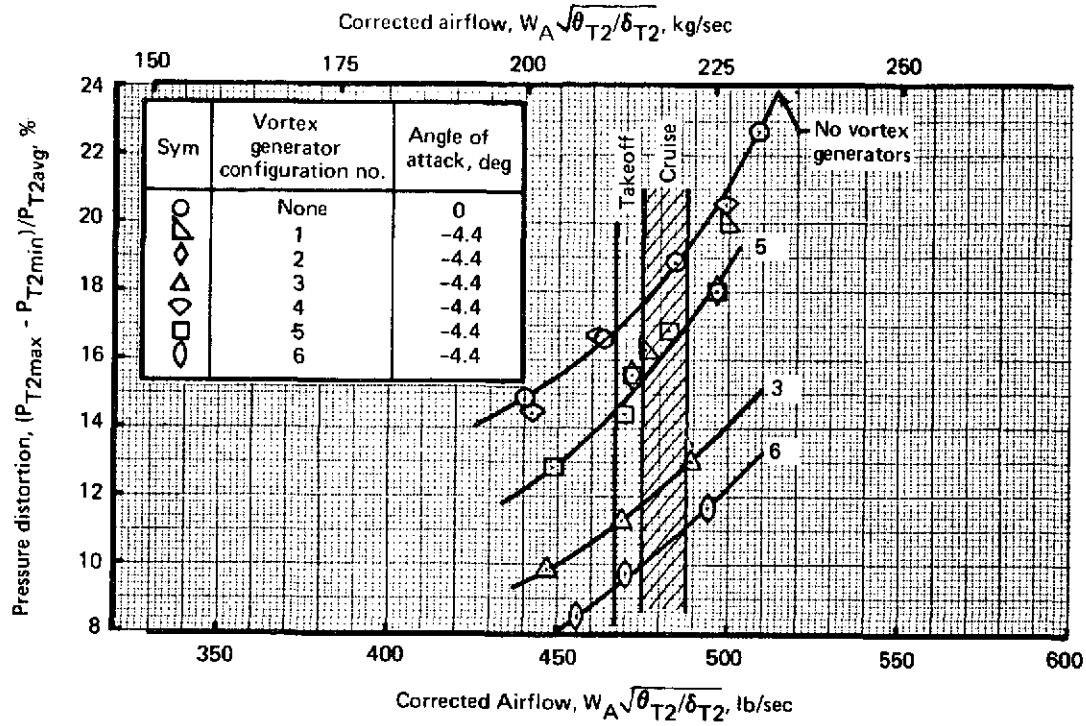


*FIGURE 59.—727/JT8D-109 MODIFIED INLET AND CENTER-DUCT DISTORTION WITH VORTEX GENERATORS, TUNNEL VELOCITY 165 KN (84.9 M/SEC)*

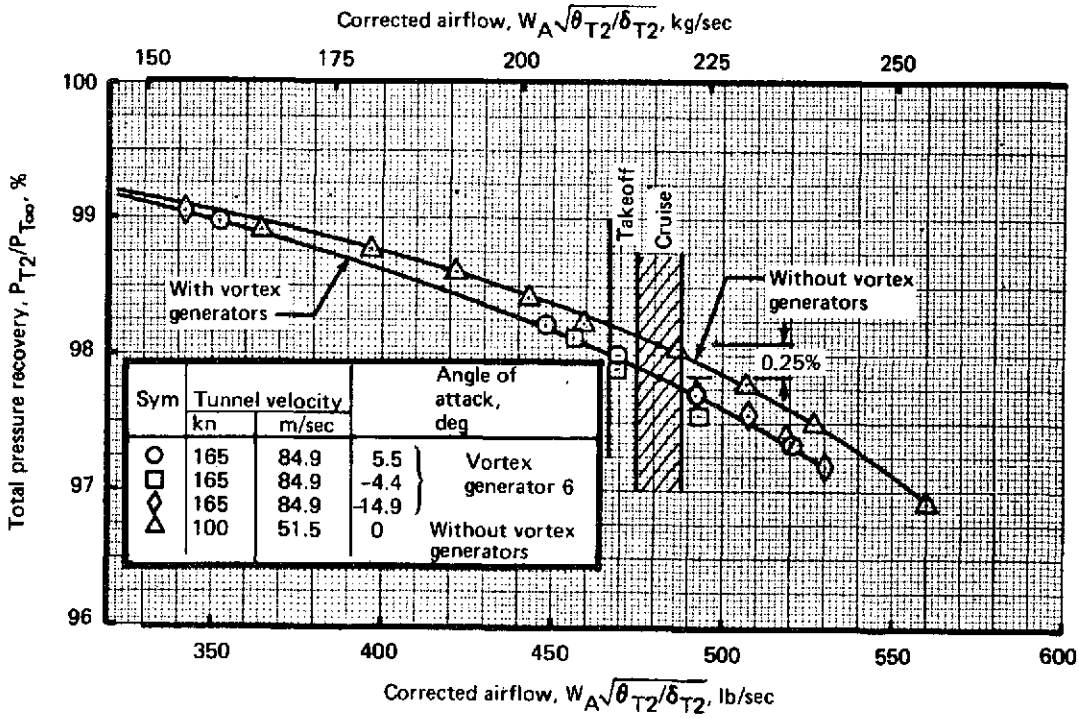


*FIGURE 60.—727/JT8D-109 MODIFIED INLET AND CENTER-DUCT PRESSURE RECOVERY WITH VORTEX GENERATORS, BOUNDARY LAYER INCLUDED*

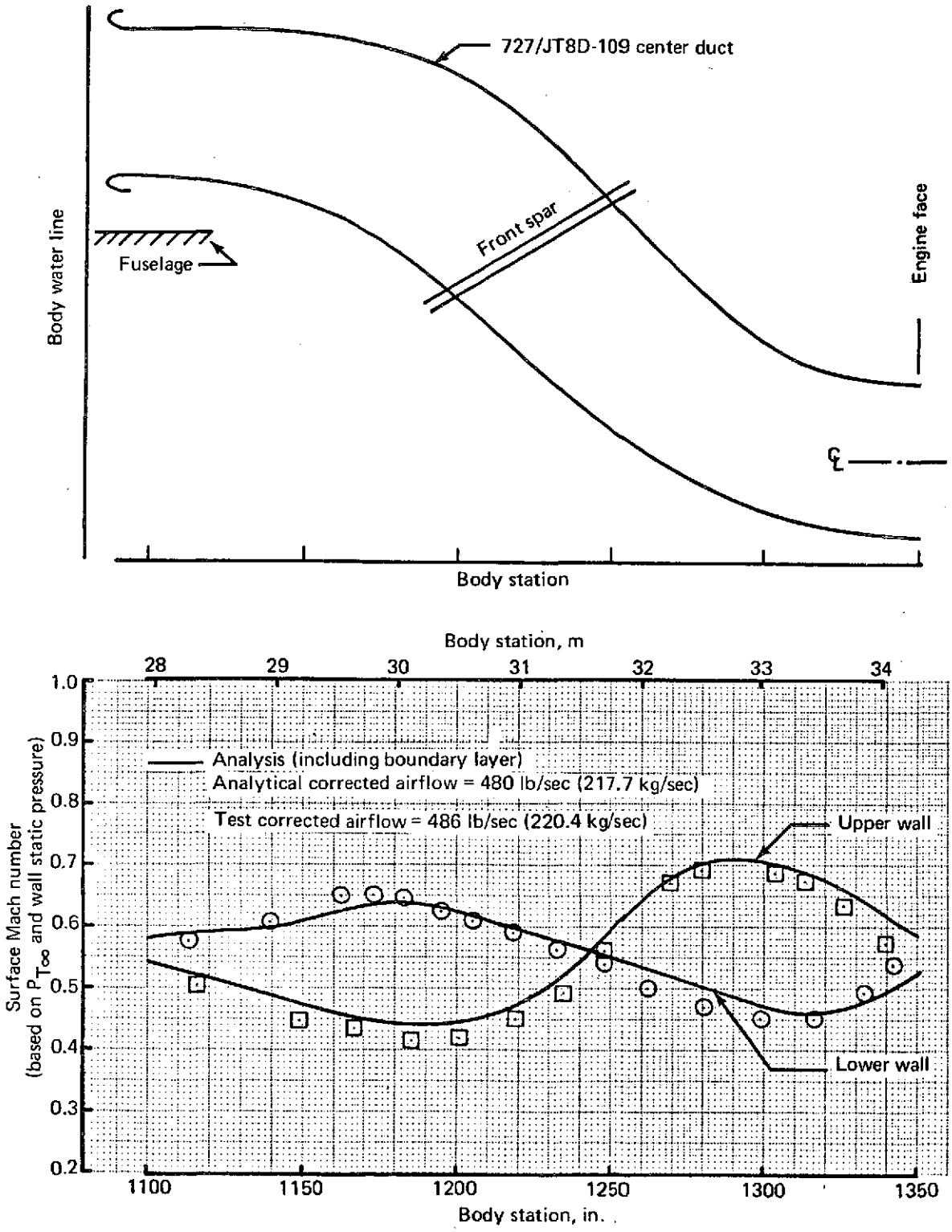


*FIGURE 61.—727/JT8D-109 CENTER-DUCT SURFACE MACH NUMBER COMPARISON, ANALYSIS VERSUS EXPERIMENTAL DATA, TEST WITHOUT VORTEX GENERATORS, TUNNEL VELOCITY 100 KN (51.5 M/SEC)*

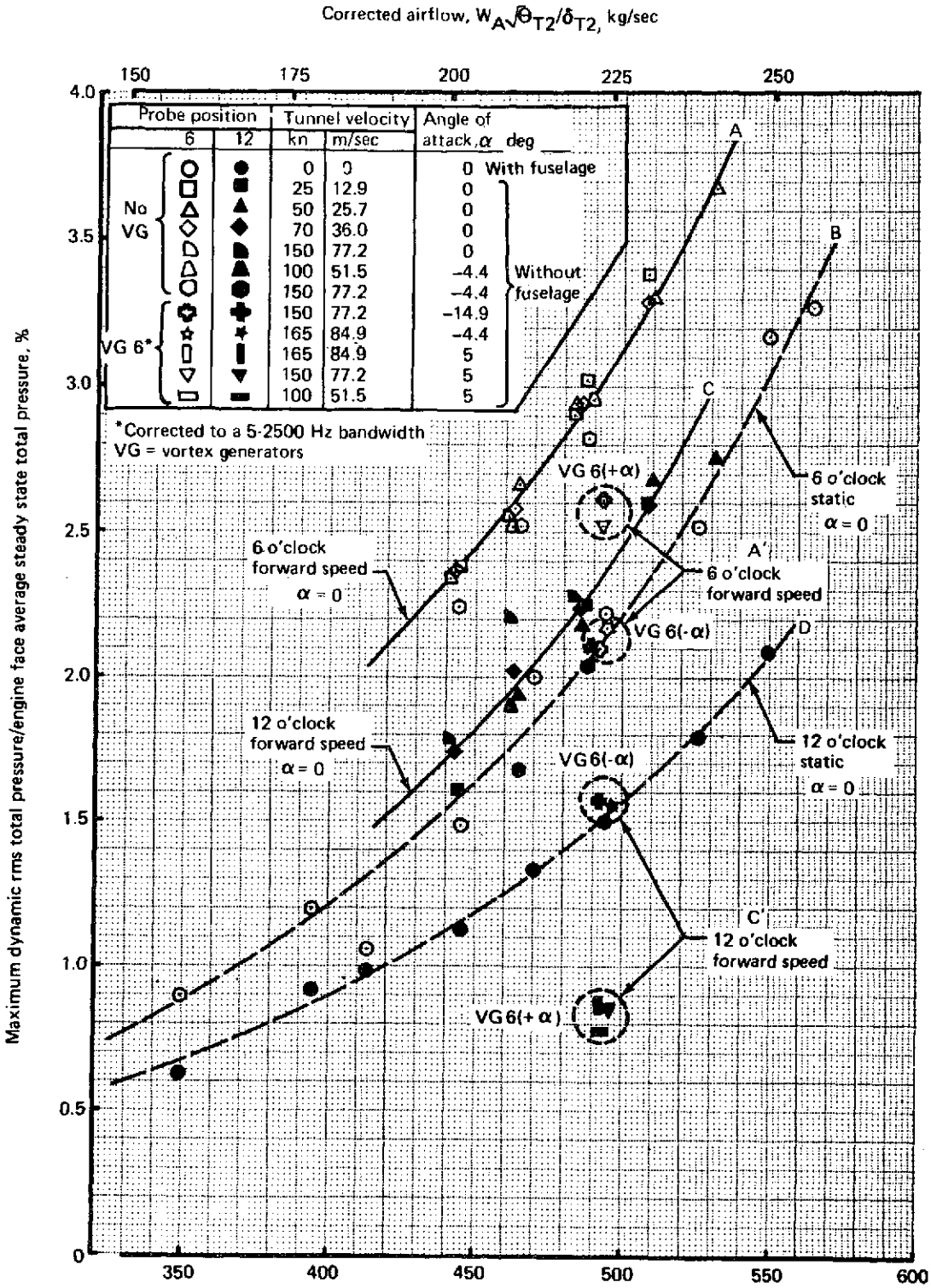


*FIGURE 62.—727/JT8D-109 ENGINE FACE MAXIMUM DYNAMIC PRESSURE VERSUS INLET AIRFLOW*

*TABLE 18.—727/JT8D BASELINE MODIFIED INLET AND CENTER-DUCT PERFORMANCE COMPARISON, MODEL TEST*

| Item | Baseline 727-200 | Modified 727-200 | |
|---|---|---|---|
| Engine | JT8D-15 | JT8D-109 | |
| Takeoff airflow | 325 lb/sec (147.4 kg/sec) | 467 lb/sec (211.8 kg/sec) | |
| Duct configuration | Production | Without vortex generators | With vortex generators (no.6) |
| Pressure recovery, 100 kn (51.5 m/sec) | [a]0.979 | [c]0.982 | [c]0.980 |
| Pressure distortion, 100 kn (51.5 m/sec)[b] | [a]0.146 | [c]0.170 | [c]0.096 |

[a]0.111-scale model test without vortex generators

[b]Pressure distortion = $(P_{T_{max}} - P_{T_{min}})/P_{T_{avg}}$

[c]0.2994-scale model test

and 12 o'clock locations, respectively. As shown, there is a substantial reduction in the maximum dynamic pressure when the vortex generators are installed. This is the first time center-duct dynamic data have been taken by the contractor; consequently, there are no past 727 data with which to compare.

Conclusions drawn concerning the test results are:

- Required airflow was achieved with acceptable pressure recovery.
- Performance of the tested center duct is comparable to that of the existing 727-200 center duct.
- Installation of vortex generators provides the capability for substantially reducing pressure distortion.
- The two-dimensional potential-flow/boundary-layer program is a useful tool for designing a center duct.
- A phase II model test of a redesigned center duct is necessary in order to optimize the vortex generator configuration for lower distortion and to evaluate duct lines changes required to resolve structural design problems.

### 4.3.4 JT8D Low-Frequency Noise Measurements

#### 4.3.4.1 Objective

The objective of this test was to obtain aft-quadrant low-frequency noise data at low power settings from a modified JT8D engine. These data were to be used for estimating the low-frequency core noise levels to be expected from the JT8D refanned engine.

#### 4.3.4.2 Test Setup

The test was conducted at the contractor's remote engine test site in Boardman, Oregon. The test engine was a modified JT8D-1. This test was primarily a contractor-funded nonacoustic research investigation. Noise measurement acquisition was funded by NASA. Microphones were placed at ground level along a 100-ft (30.48-m) sideline at 10° increments from 110° to 140° from the engine inlet.

#### 4.3.4.3 Test Procedure

A JT8D-1 engine was operated in its normal cycle and then modified to operate with a bypass ratio of approximately 3.0. The primary engine conditions then matched the JT8D-109 more closely than the JT8D-9. Acoustic data were recorded on a single-channel tape recorder. Data were taken at given power points from 6000 to 7730 $N_1$ with the engine in the normal bypass ratio and at six power points from 5500 to 7743 $N_1$ in the high bypass ratio. Engine vibration problems prohibited taking data at lower power settings. The resulting data were analyzed into 1/3-octave-band 20-Hz bandwidth spectra and OASPL levels from both 50 Hz to 1000 Hz and 50 Hz to 10 kHz.

#### 4.3.4.4 Results

Analyses of the data were concentrated on the frequency range from 50 to 1000 Hz. The resulting 100-ft (30.48-m) sideline OASPL directivities at high power settings when operating in the normal bypass ratio were characteristic of jet noise peaking at 140°. When operating in the high bypass ratio mode, however, directivities were exhibited that peaked at 120°. Two causes for this difference in low-frequency behavior were considered: (1) the short-duct fan stream, which is present when operating in the high bypass ratio but not in the normal bypass ratio, may have generated substantial jet noise, and (2) internally generated, low-frequency noise (core noise) increased in the high bypass ratio because of the increased turbine loading. Further analyses showed that the low-frequency levels of both engine bypass ratios at the high angles 130°-140°) correlated quite well when plotted against primary jet velocity. At lesser angles (110°-120°), however, the noise

data showed better correlation when plotted against turbine pressure ratio (see fig. 63). Analyses of some existing cold-flow jet noise data from a scale model, comparing short fan duct versus long fan duct noise generation, indicate that fan-stream jet noise is not the cause of the anomalous behavior observed in the high bypass ratio. However, further analyses of the short fan duct influence with hot primary flow is necessary to eliminate this as a definite possibility.

#### 4.3.4.5 Conclusions

- In the high bypass ratio, the JT8D-1 engine exhibited a substantial increase in low-frequency noise at 110°-120° from the engine inlet at a given primary jet velocity.

- Preliminary analyses of cold-flow model-scale data indicate that this increase in noise is not due to the short-duct fan stream, which is present in the high bypass ratio but not in the normal bypass ratio. However, further analyses of hot-flow data are necessary to eliminate this as a definite possibility.

- The low-frequency noise at 100°-120° could be correlated with turbine pressure ratio, indicating that turbine loading may be a reasonable correlating parameter for low-frequency core noise generation.

## 4.4 NACELLE PRELIMINARY DESIGN

Design studies and evaluations were made on three alternate nacelle configurations, which differed in the level of acoustic treatment. Side-engine nacelles for each configuration are shown schematically in figure 64.

Configuration 1 was the simplest nacelle, with acoustic treatment provided only on the nose dome and the diffuser wall of the inlet and on the inside of the tailpipe. Configuration 2 had treatment in the same areas a configuration 1 and, in addition, had an acoustically treated inlet ring and an acoustically lined splitter and plug in the exhaust system. Configuration 3 had treatment in the same areas as configuration 1 and, in addition, had two acoustically treated inlet rings and a fan and primary-stream mixer in the exhaust system.

It is emphasized that the performance and noise results for configurations 1 and 2 reflect currently used treatment methods. On the other hand, performance and noise estimates for configuration 3 are primarily attributable to an idealized mixer design, which is not available at this time. Realization of the noise and performance results for configuration 3 will require an intensive mixer technology development program. Such a program will need to address both the propulsion

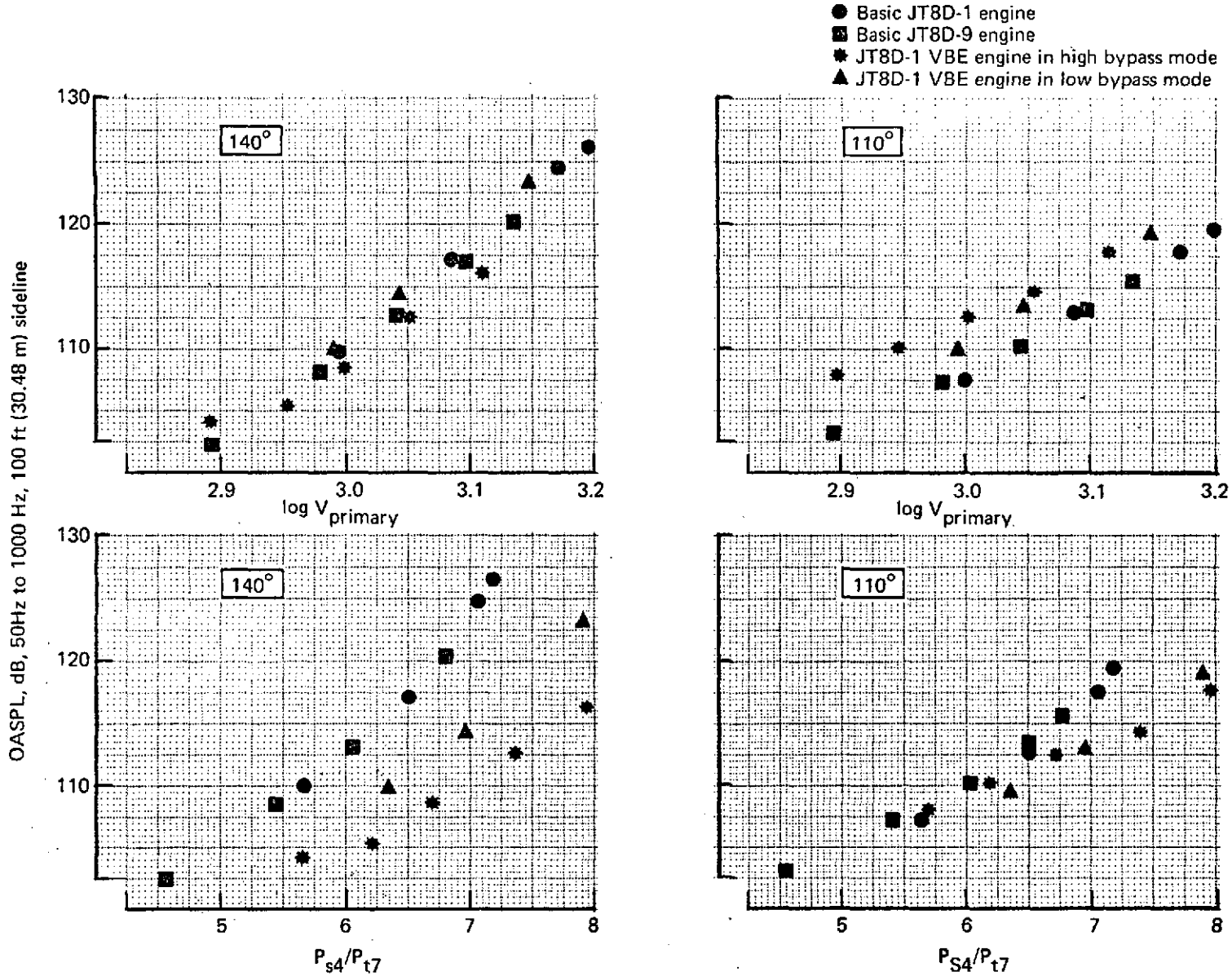


*FIGURE 63.–DIRECTIVITY AND POWER SETTING DEPENDENCE OF JT8D LOW-FREQUENCY NOISE*

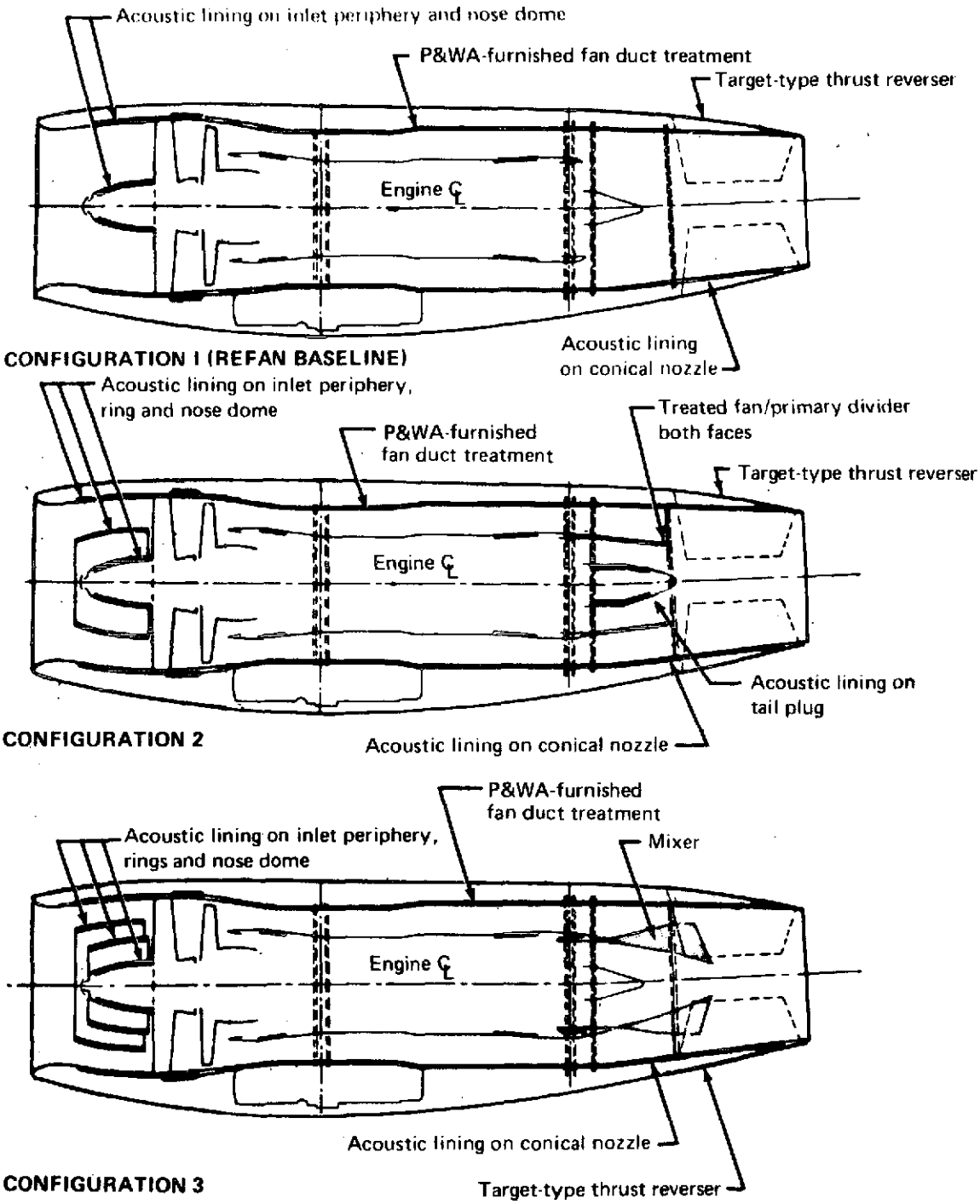


*FIGURE 64.—727/JT8D-109 NACELLE CONFIGURATIONS*

performance and noise aspects of mixers. The noise and installed-performance values quoted for configuration 3 are based on current best insight and must therefore be qualified preliminary estimates and not practicable options at this time.

### 4.4.1 Configuration 1

The nacelle general arrangement and aerodynamic design for configuration 1 are discussed in the following two sections.

#### 4.4.1.1 Nacelle General Arrangement

The configuration 1 nacelle and JT8D-109 engine installation design are shown in figures 65 and 66. The side engines retain the same upward cant as on the existing airplane. The engine centerline was moved outboard 5.5 in. (0.14 m) to preserve the side-engine mounts and firewall. However, because the relationship of the aft support points to the forward support points on the engine was changed, the toe-out angle of the engine in relation to the fuselage was increased slightly.

To retain the existing overhead firewall on the center-engine installation, the centerline of the new, larger diameter engine was lowered 4.5 in. (0.114 m). The inlet and center duct were enlarged to match the increased engine mass flow requirements. Also, the aft end of the center-duct was lowered to match the new engine position.

The thrust reverser and tailpipe were canted upward 3° 30′ with respect to the engine in all three positions. This yields a horizontal thrust line on the side engines and preserves airplane rotational capability on the center engine.

The side-engine mounts remained essentially the same, but the existing vibration isolators were changed to accommodate the greater nacelle weight and inertia of the refanned engine installation.

The new, longer engine required both center-engine mounts to be moved aft 8.8 in. (0.224 m). An all-new front engine mount assembly was required for the center engine, including forging, vibration isolators, cone bolts, and drag links. This assembly was attached to a relocated clevis fitting on the horizontal firewall. The aft mount, consisting of a vibration isolator and cone bolt, was suspended from a new cantilevered support structure.

The new side-engine inlets retained the same toe-in angle as the existing inlets, which require the inlets to be fabricated as opposite-hand assemblies. The inlet design consisted of an acoustically treated diffuser, an anti-iced inlet lip, and outer wall panels and supporting frames. The diffuser panel was a one-piece polyimide bonded fiberglass honeycomb part, and the remaining structure was aluminum sheet material. (See fig. 67 for configuration 1 side inlet construction.)

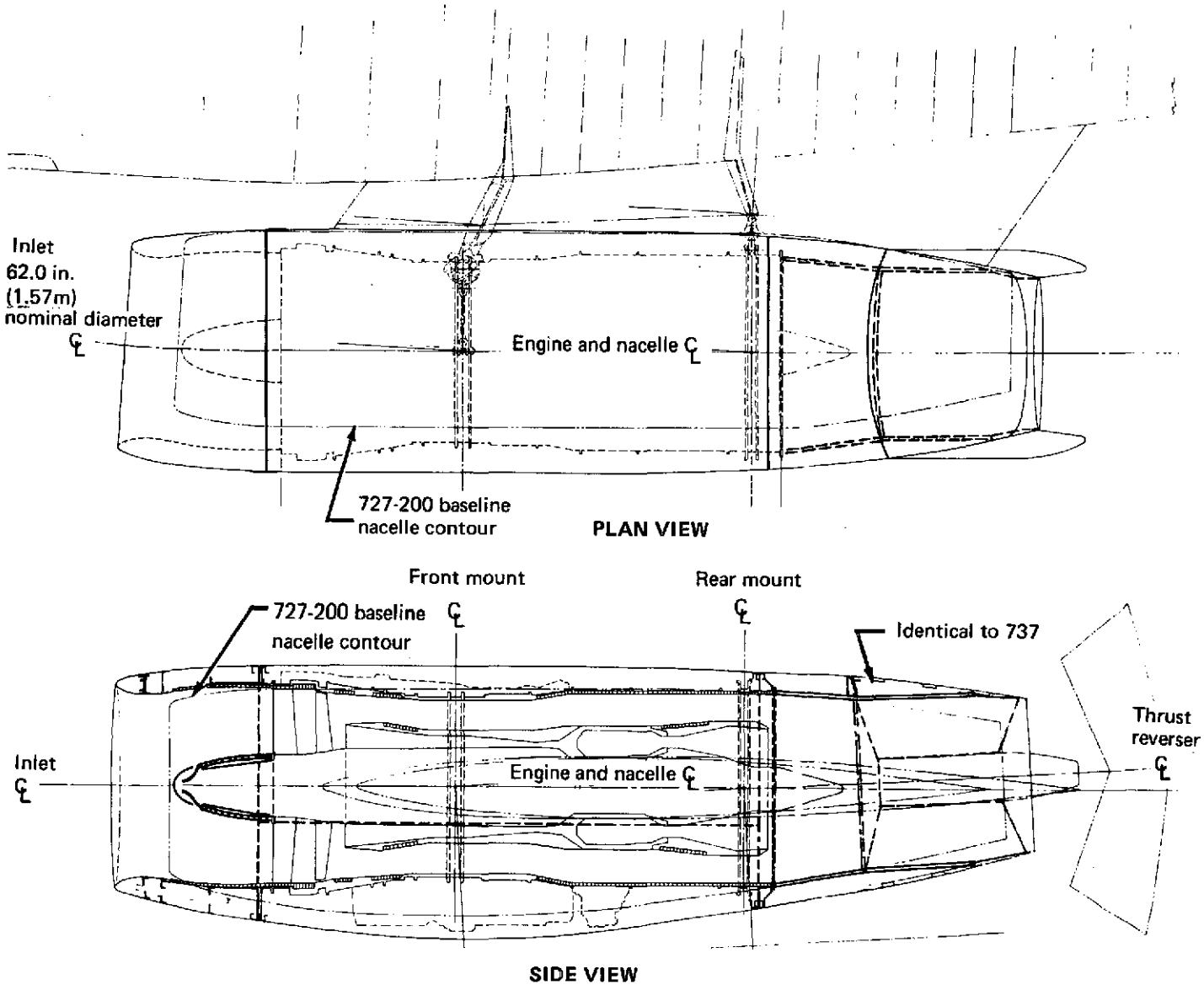


*FIGURE 65.—727/JT8D-109 CONFIGURATION 1 SIDE NACELLE*

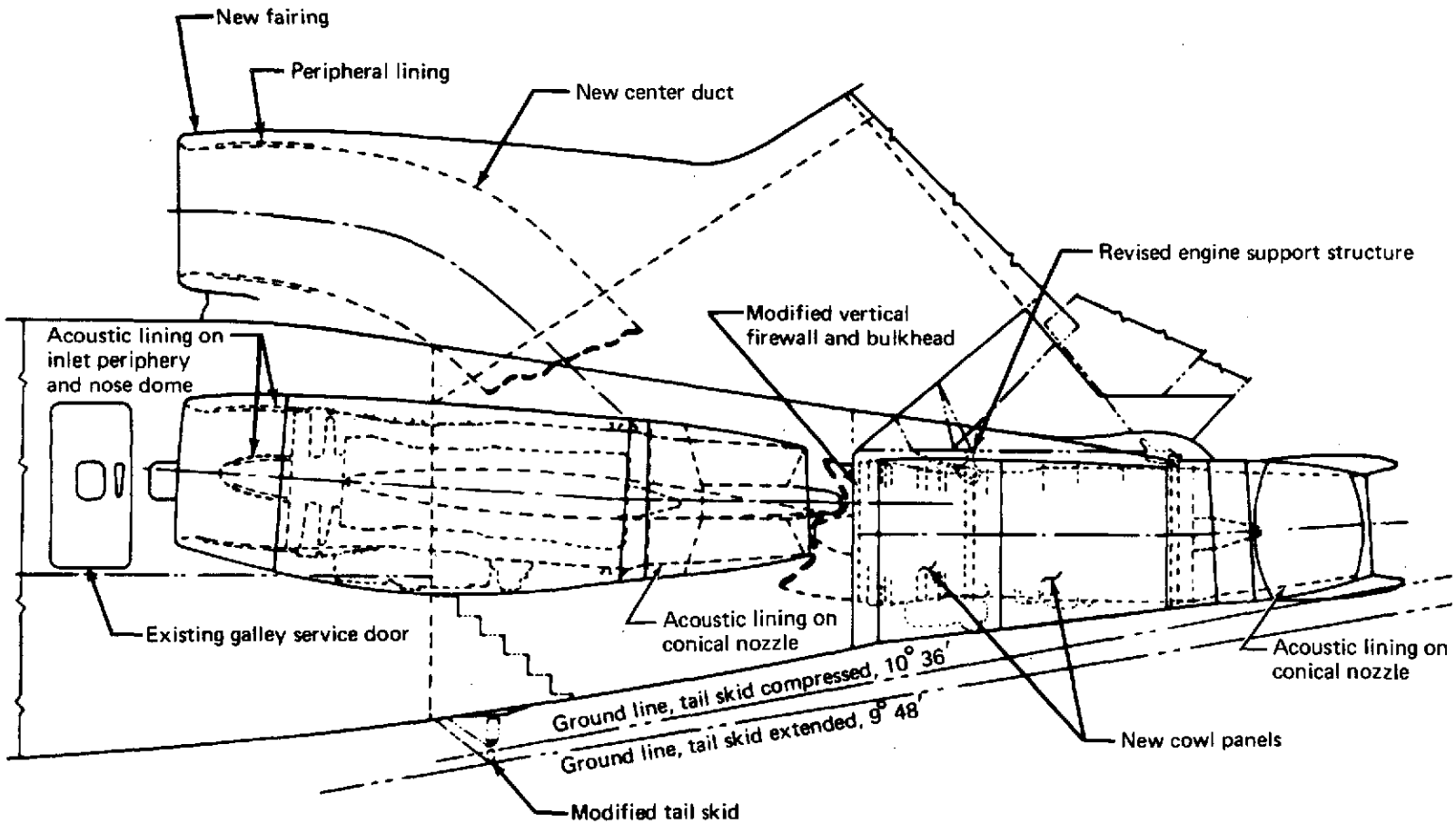


*FIGURE 66.—727/JT8D-109 CONFIGURATION 1 ENGINE INSTALLATION DESIGN*

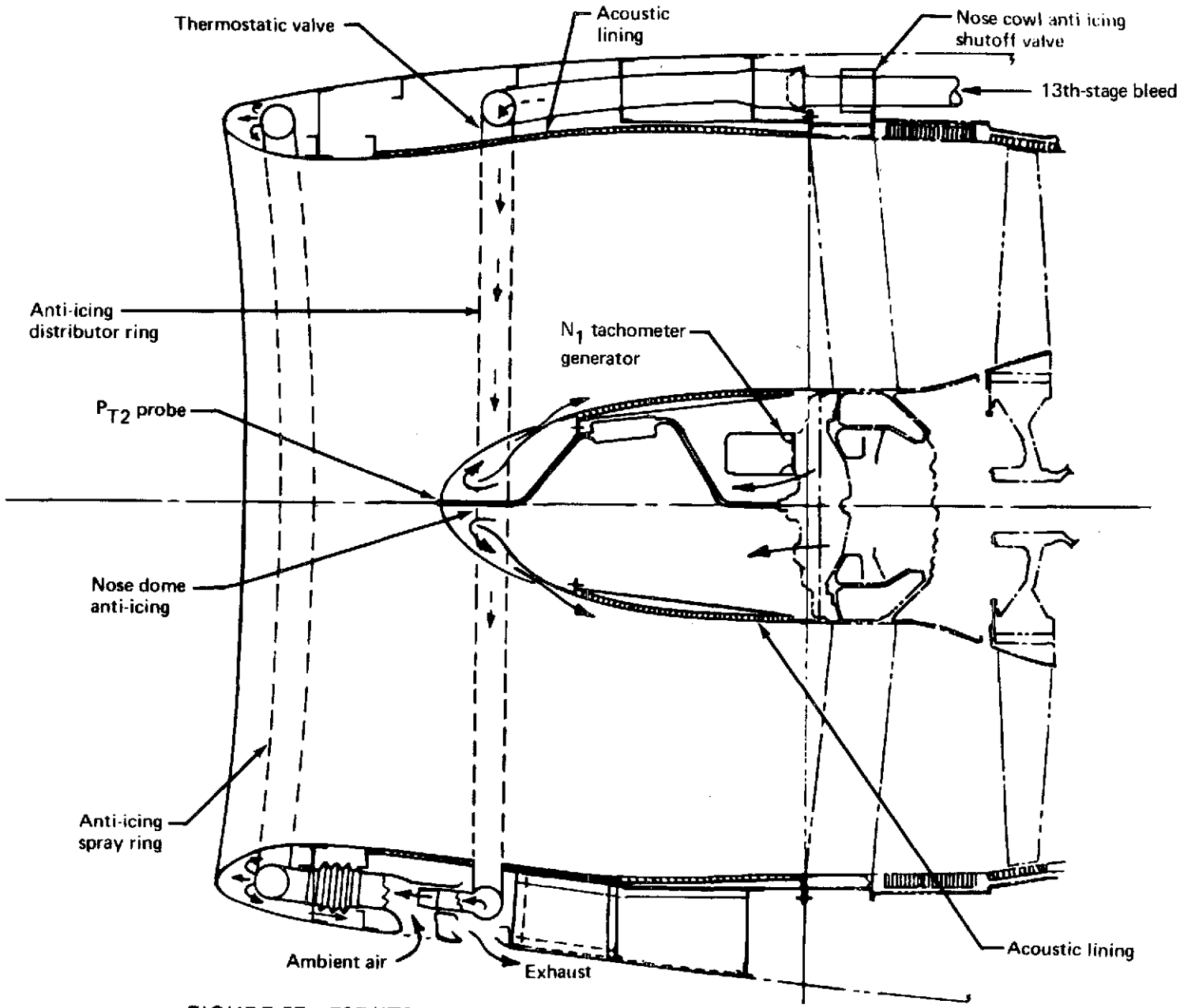


*FIGURE 67.–727/JT8D-109 CONFIGURATION 1 SIDE-INLET CONSTRUCTION*

The nose dome had a thermally anti-iced aluminum nose cap and a polyimide bonded fiberglass acoustic honeycomb body.

The center-engine inlet included an anti-iced aluminum inlet lip and a two-section inlet duct (center duct) joined at the tail fin front spar forging. The center duct was designed to be constructed of aluminum honeycomb, perforated as required for acoustic attenuation, except for rain impingement areas, which were constructed of anti-iced aluminum skin and stringers.

Fan air was directed through the integral long duct of the JT8D-109 engine, which was acoustically treated. Aft of the engine rear flange the fan air was free to mix with primary exhaust gases in the tailpipe as well as being exposed to the acoustic lining of the tailpipe.

The cowl panel arrangement on the JT8D-109 engine was the same as on the JT8D-9 engine. Side-engine cowling consisted of an inboard fixed panel with removable hinged upper and lower panels.

The center-engine cowling consisted of two forward and two aft panels, both hinged to the existing cowl support structure. Construction was structural honeycomb with phenol/epoxy materials. Fire protection was achieved with an intumescing paint applied to the inner surface of the cowls that, in the event of a fire, would foam to as much as 9 in. (0.23 m), protecting the structural integrity of the cowl and retarding the fire.

The exhaust system consisted of a two-segment tailpipe, a target-type thrust reverser, and the existing conical plug. The forward segment of the tailpipe was wedge shaped to cant the exhaust nozzle up 3°30′. This would, on the side engines, redirect the exhaust gases along the flightpath and, on the center engine, provide necessary ground clearance during rotation of the airplane.

The aft segment of the tailpipe provided the mounting for the thrust reverser. The flange between the fore-and-aft segments of the tailpipe would permit clocking the reverser between engine positions to obtain optimum exhaust gas distribution. Both segments of the tailpipe were constructed from Inconel 625 honeycomb with a perforated inner skin for acoustic treatment.

The target-type thrust reverser was a scaled-up version of the reverser used on 737 airplanes equipped with JT8D-9 engines and is shown in figure 68. The deflector doors were double-wall construction with an Inconel 625 inner skin and an aluminum outer skin.

Actuation was by means of two hydraulic actuators driving a four-bar linkage. The reverser was preloaded and locked in the stowed position by mechanical overcenter linkages. Secondary mechanically sequenced door locks were also included.

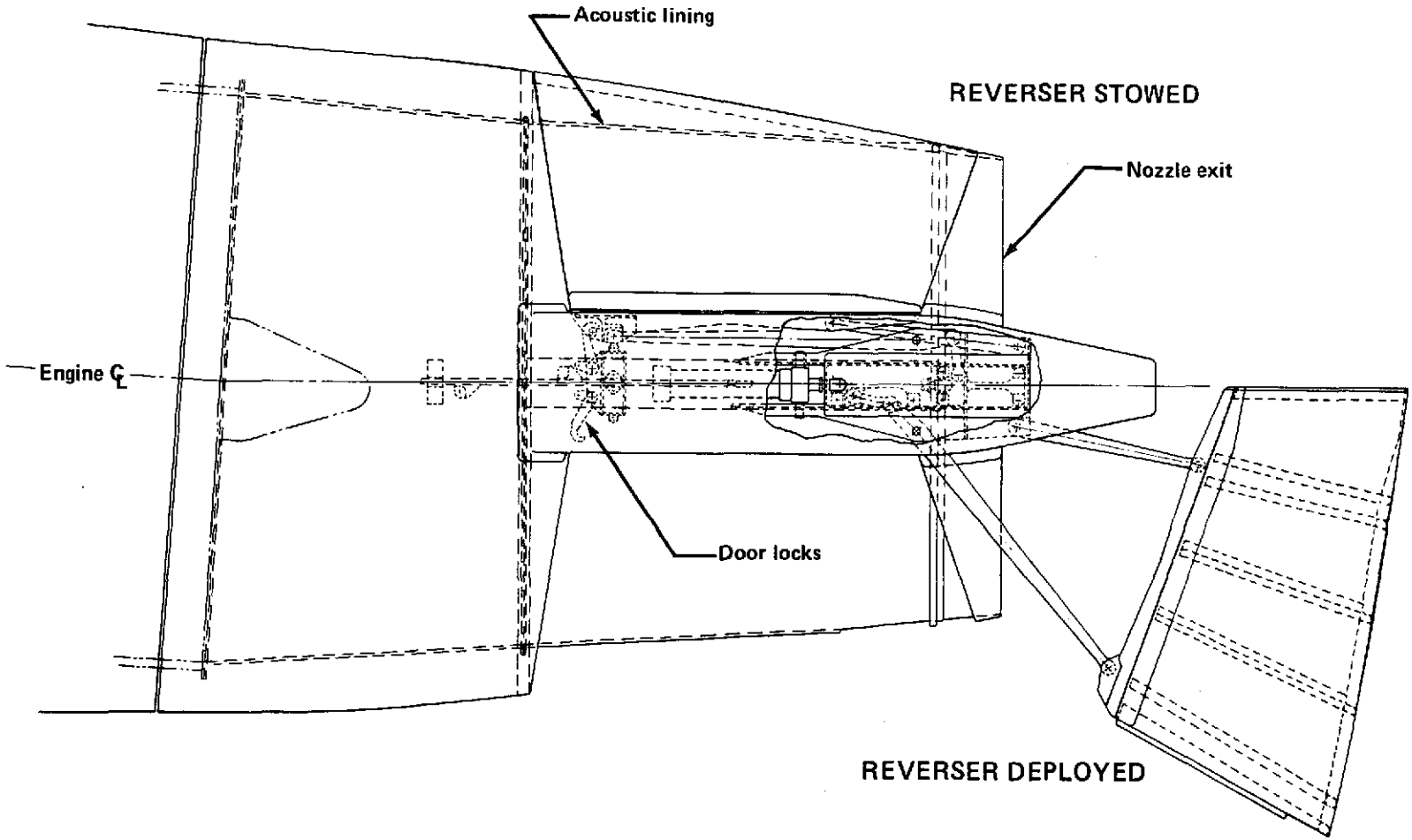


*FIGURE 68.—727/JT8D-109 TARGET-TYPE THRUST REVERSER*

The primary power source would be airplane hydraulic system A with alternate power available from the standby hydraulic system. As shown in figure 69, hydraulic power was isolated in flight by connection to the landing-gear-down line.

The existing mechanical interlock between the reverser and the power control levers was retained. Additional safety features included a fire shutoff valve and a manual shutoff feature to preclude operation during ground inspections. A double-switch system operated reverser-unlocked and reverser-deployed lights on the instrument panel.

The engine and nacelle subsystems furnished by the airframe manufacturer were retained to the maximum extent. This included such items as cooling and ventilation, vents and drains, fire protection, lubrication and fuel systems, CSD/generator, controls and instrumentation, engine starting, engine bleed air, and ice protection. In general, components were retained, but ducting, plumbing, and bracketry were completely new.

The lower fan pressure ratio of the JT8D-109 engine would result in a degraded cooling airflow through the existing precooler system and would produce precooler exhaust discharge temperatures over 600° F (588.72° K). To avoid routing this exhaust through the fuselage, the precooler was repositioned (rotated 90°), which would permit discharging the exhaust through the lower surface of the strut aft fairing. (See fig. 70.)

The control linkage from the airplane to the side engine was modified to accommodate the new location of the engine cross-shaft. On the center engine, the existing location of the control mechanism on the vertical firewall interfered with the new engine and center duct, as shown on figure 71. This required a new, relocated mechanism, complete with push-pull cables to control engine start and engine power. Use of the push-pull cables eliminated the necessity for a thrust-compensator linkage. Every effort was made to maximize parental commonality between the JT8D-9 installation and the JT8D-109 installation, as well as mutual commonality between engines 1, 2, and 3 on the 727 airplane and engines 1 and 2 on the 737 airplane. The bleed manifolds were symmetrical, with end connections to permit the use of the same manifold at all locations.

Table 19 illustrates the parental commonality, i.e., the equipment retained from the existing 727. Table 19 also shows some items of equipment that would be common to the 737/JT8D-109 installation. Table 20 illustrates the commonality of bleed air ducting between refanned engines for the 727 and 737 airplanes.

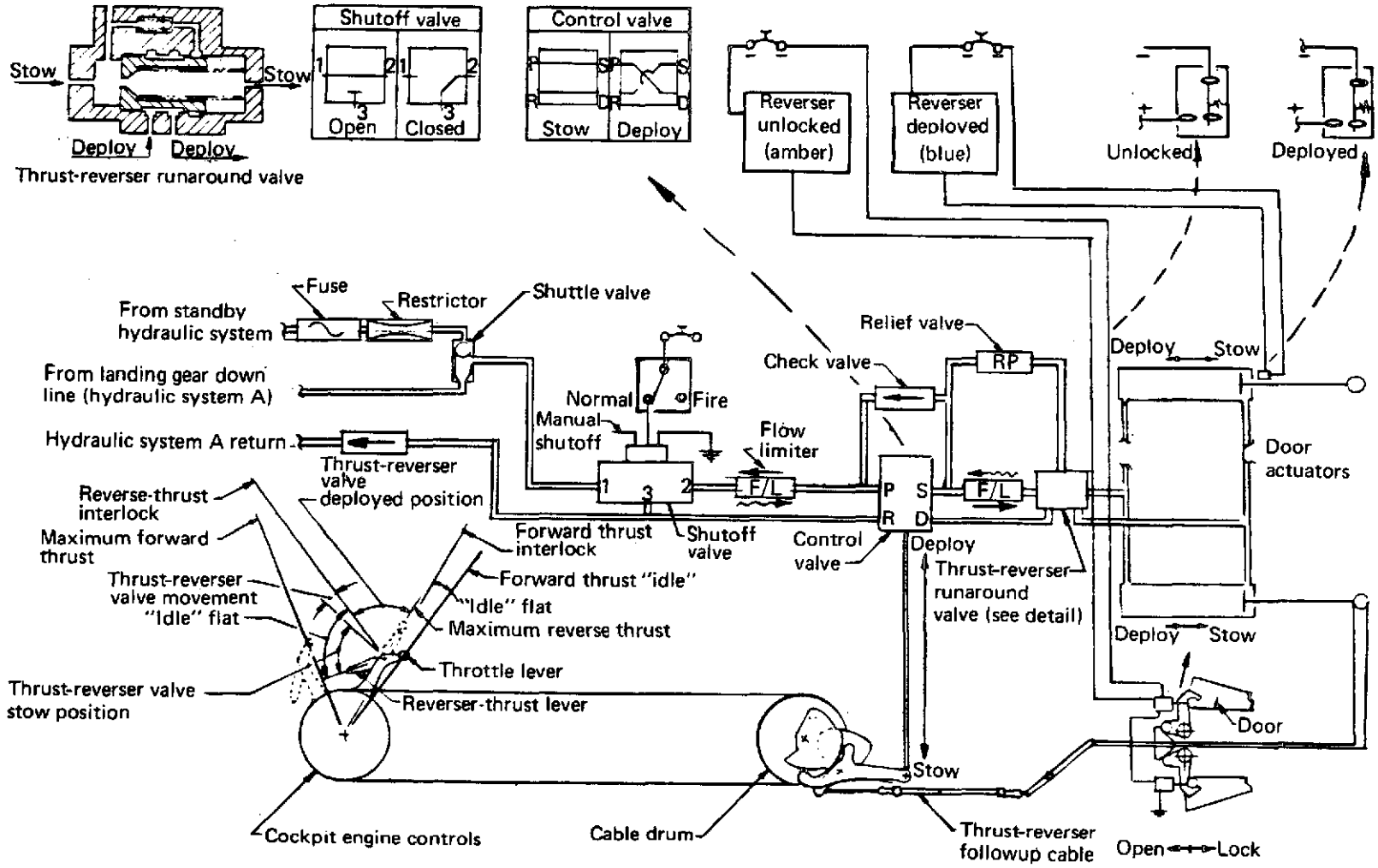


*FIGURE 69.—727/JT8D-109 THRUST-REVERSER HYDRAULIC/ELECTRICAL SYSTEM DIAGRAM*

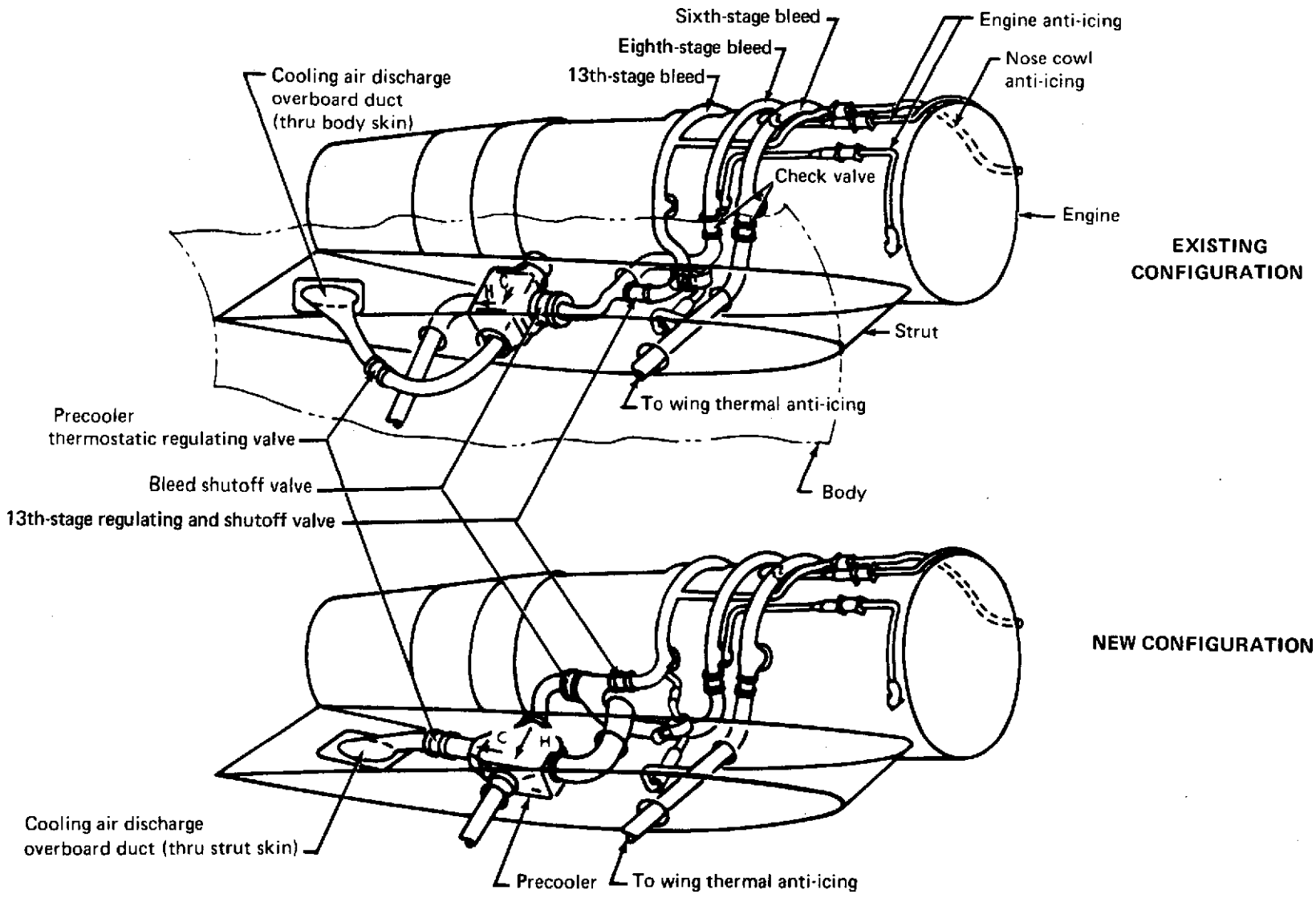


*FIGURE 70.—727/JT8D AIR CONDITIONING AND THERMAL ANTI-ICING COMPARISON*

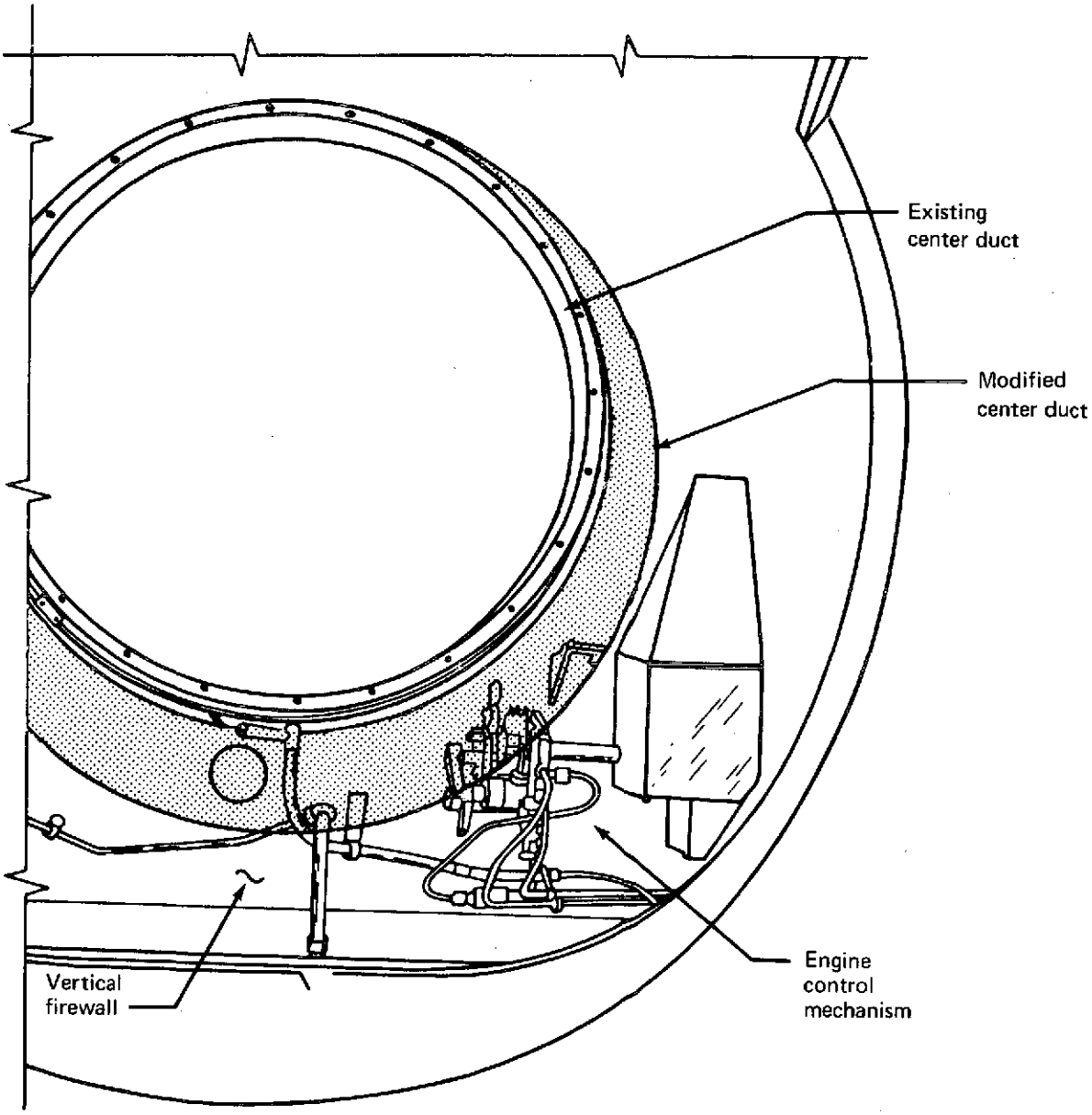


*FIGURE 71.–727/JT8D-109 ENGINE/CONTROL LINKAGE INTERFERENCE*

*TABLE 19.—727/737/JT8D MAJOR COMPONENT COMMONALITY*

| Component | 737 | | 727 | | |
|---|---|---|---|---|---|
| | Engine position | | | | |
| | 1 | 2 | 1 | 2 | 3 |
| Starter A/R ATS100-189 (existing) (or similar, if change was required) | X | X | X | X | X |
| Hydraulic pump (existing) 10-60246 or 10-61794 (customer optional) | X | X | X | X | |
| Constant-speed drive (CSD) | | | | | |
| (40AGD) 10-61223 (existing) | X | X | | | |
| (60 AGD) 10-61066 (existing) | | | X | X | X |
| Generator 10-61224 (existing) | X | X | X | X | X |
| Tach generators | | | | | |
| $N_1$ (existing) | X | X | X | X | X |
| $N_2$ (existing) | X | X | X | X | X |
| Precooler | | | | | |
| (new) | X | X | | | |
| 10-61426 (existing) | | | X | | X |
| CSD oil cooler, immersion | | | | | |
| (new) | | | X | X | X |
| (existing) | X | X | | | |

*TABLE 20.—727/737/JT8D NACELLE BLEED DUCT COMMONALITY*

| Duct position | 737 | | 727 | | |
|---|---|---|---|---|---|
| | Engine position | | | | |
| | 1 | 2 | 1 | 2 | 3 |
| 737 positions | 100% | 100% | | | |
| 727 side engine positions | | | 75% | | 75% |
| 727 center engine to side engine | | | 15% | 15% | 15% |
| 737 to 727 side engines | 10% | 10% | 10% | | 10% |

### 4.4.1.2 Nacelle Aerodynamic Design

*External aerodynamics.*—The JT8D-109 nacelle is designed to enclose the engine and accessory package with the minimum increase in size from the current installation. A comparison of external aerodynamic characteristics between the JT8D-109 and the JT8D-9 installation is shown in figure 72.

*Internal aerodynamics (side inlet).*—For configuration 1 the side-engine inlet is a conventional configuration with peripheral acoustic lining only. The inlet geometry results in a highlight diameter of 52.22 in. (1.326 m), a throat diameter of 46.70 in. (1.186 m), an engine compressor face diameter of 50.10 in. (1.273 m), and a 40.08-in. (1.02-m) centerline length, which will result in an inlet length/diameter (L/D) ratio of 0.8, as shown in figure 73. The contraction ratio (highlight-to-throat area) for this inlet is 1.25.

*Internal aerodynamics (design requirements).*—

a) Airflow—The engine inlet is sized from preliminary engine airflow data. These design inlet airflows and the resulting throat Mach numbers are shown below.

| Flight condition | Corrected airflow, $W_a$ lb/sec | Corrected airflow, $W_a$ kg/sec | Inlet throat Mach no. |
|---|---|---|---|
| Sea level static, takeoff thrust (standard day) | 467 | 211.8 | 0.548 |
| 13 000 ft (3962.4 m) static, takeoff thrust (standard day) | 491 | 222.7 | 0.593 |
| 35 000 ft (10 668 m), 0.8 M, maximum continuous thrust (standard day) | 489 | 221.8 | 0.589 |

b) Flow Field—In general, where a fixed geometry inlet is selected, the contraction ratio should not be less than 1.25 to ensure satisfactory performance over the normal range of inflow angles. For the side inlet the inflow angles relative to the body reference line are estimated to vary from 5° to 20° downflow at the inlet, depending on flap setting and forward speed.

Inlet aerodynamic losses can be subdivided into two categories: lip losses (a function of inlet velocity ratio, angle of attack, and lip geometry) and internal losses, which include acoustic treatment. The internal losses are only a function of wetted surface area and corrected airflow rate.

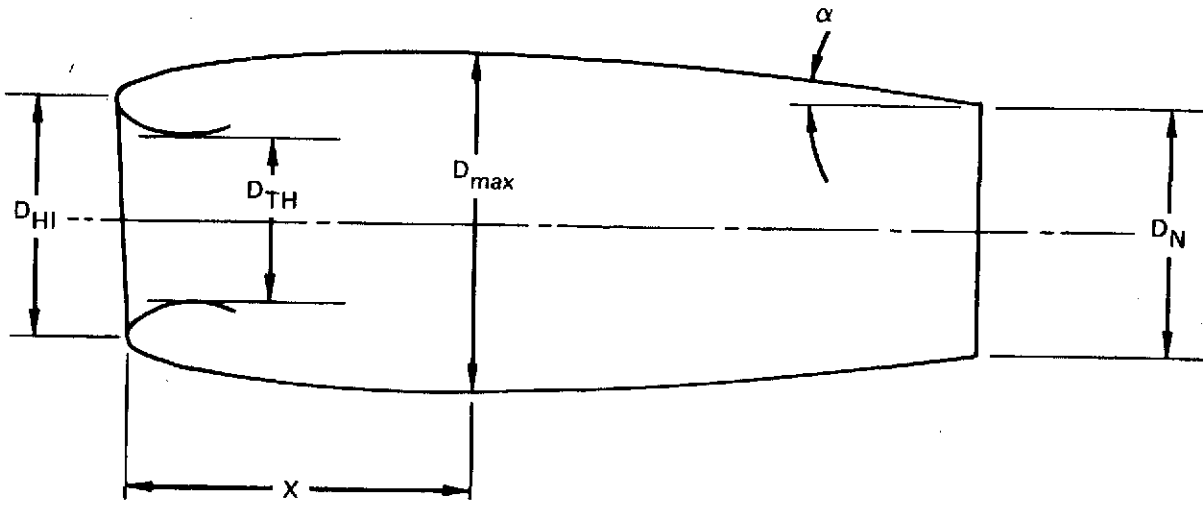


| | JT8D-9 | JT8D-9 | JT8D-109 | JT8D-109 |
|---|---|---|---|---|
| Nacelle length | 214.55 in. | 5.45 m | 234.13 in. | 5.947 m |
| Maximum diameter, $D_{max}$ | 50.0 in. | 1.27 m | 62.0 in. | 1.575 m |
| Maximum area, $A_{max}$ | 15.87 $ft^2$ | 1.474 $m^2$ | 23.0 $ft^2$ | 2.137 $m^2$ |
| Nozzle exit diameter, $D_N$ | 29.84 in. | 0.758 m | 38.544 in. | 0.979 m |
| Ratio, $D_{HI}/D_{max}$ | 0.784 | 0.784 | 0.844 | 0.844 |
| Length to maximum section, X | 25.0 in. | 0.635 m | 58.57 in. | 1.488 m |
| Tailpipe boattail angle, α | 10°30′ | 10°30′ | 12° | 12° |
| Throat diameter, $D_{TH}$ | 37.840 in. | .961 m | 46.70 in. | 1.186 m |
| Hilite diameter, $D_{HI}$ | 42.305 in. | 1.075 m | 52.22 in. | 1.326 m |

*FIGURE 72.--NACELLE AERODYNAMIC CHARACTERISTICS–727-200 AIRPLANE*

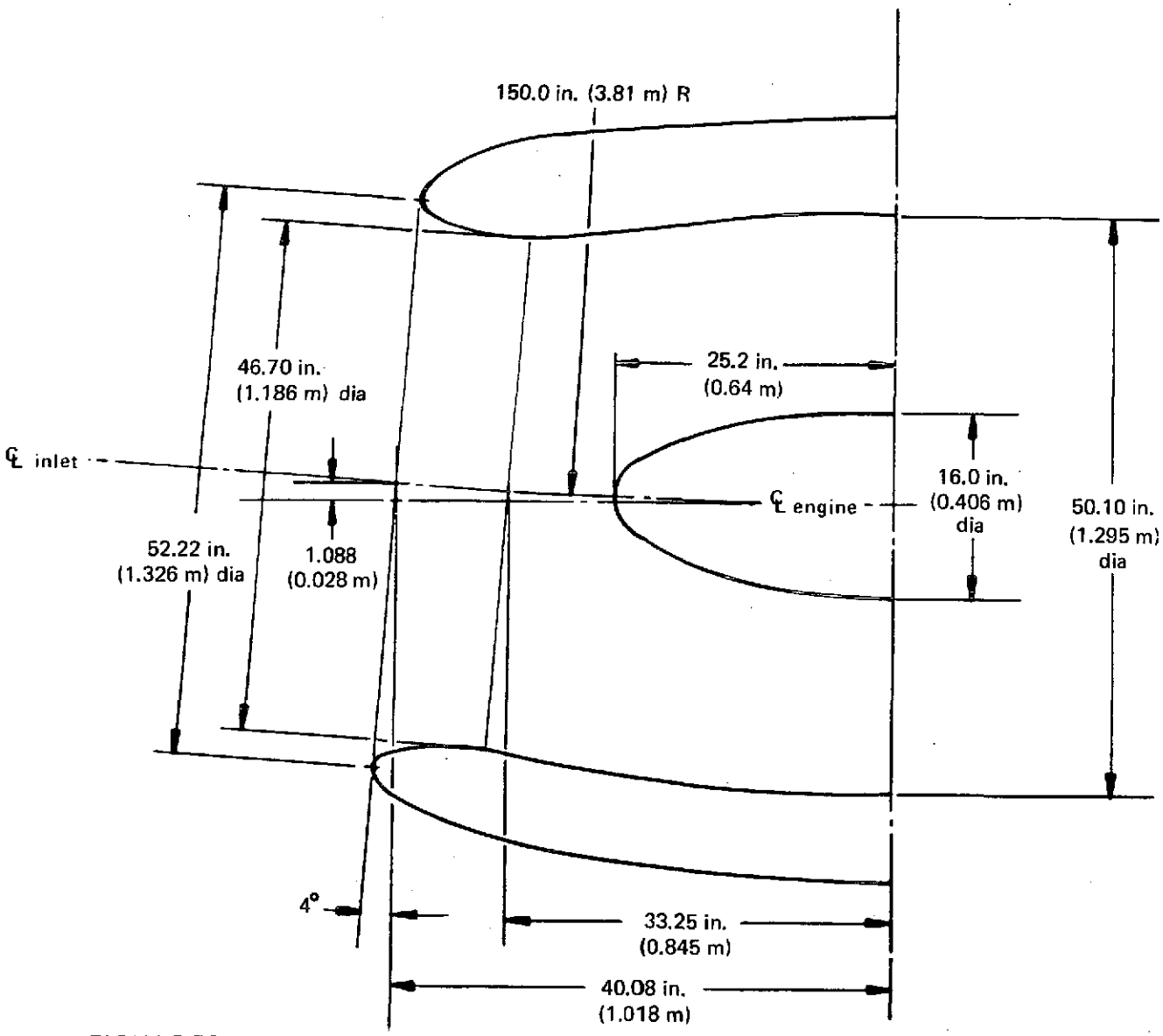


*FIGURE 73.–SIDE-INLET GEOMETRY –727-200 AIRPLANE, CONFIGURATION 1*

Estimated side inlet performance

| Flight condition | Pressure recovery $P_{T2}/P_{T0}$* |
|---|---|
| Sea level static, takeoff thrust | 0.990 |
| Sea level, ⩾ 50 kn (25.72 m/sec) takeoff thrust | 0.996 |
| 35 000 ft (10 668 m) 0.8 M, maximum cruise thrust | 0.996 |

*Internal aerodynamics (center inlet and duct).*– In order to meet the objective of retaining the maximum airplane structure and minimizing retrofit cost, the inlet aerodynamic design is constrained by increased duct offset and available duct cross-sectional area. The current design version for the center inlet and duct is described in section 4.4.1.1. The pertinent inlet geometry results in a highlight diameter of 54 in. (1.372 m) and a throat diameter of 47.8 in. (1.214 m). The contraction ratio for this inlet is 1.28. The minimum duct area is approximately 1700 in.$^2$ (1.096 m$^2$). In general, local wall Mach numbers vary from 0.45 to 0.6, with one location approaching 0.7.

The design requirements are:

a) Airflow-The engine inlet is sized from preliminary engine airflow data. These design inlet airflows and the resulting throat Mach numbers are shown in the following table.

| Flight condition | Corrected airflow, $W_a$ lb/sec | Corrected airflow, $W_a$ kg/sec | Inlet throat Mach no. |
|---|---|---|---|
| Sea level static, takeoff thrust (standard day) | 467 | 211.8 | 0.513 |
| 13 000 ft (3962.4 m) static, takeoff thrust (standard day) | 491 | 222.7 | 0.551 |
| 35 000 ft (10 668 m), 0.8 M, maximum continuous thrust (standard day) | 489 | 221.8 | 0.549 |

b) Flow Field–For the center inlet and duct, the inflow angle relative to the body reference line is estimated to vary from 5° to 15° downflow at the inlet, depending on flap setting and forward speed.

*The tabulated pressure recovery must be corrected upwards by 0.003 to be consistent with the baseline JT8D-9 performance data, which is referenced to a bellmouth inlet, as this reference bellmouth already accounts for 0.003 boundary layer loss.

The center inlet pressure recovery is estimated to be as shown in the following table.

Estimated center inlet and duct performance

| Flight condition | Pressure recovery $P_{T2}/P_{T0}$* |
|---|---|
| Sea level static, takeoff thrust | 0.975 |
| Sea level, ≥ 50 kn (25.72 m/sec), takeoff thrust | 0.978 |
| 35 000 ft (10 668 m) 0.8 M, maximum cruise thrust | 0.978 |

### 4.4.2 Configuration 2

The configuration 2 design shown in figure 74 was the same as configuration 1, except for the addition of an acoustically lined ring in the inlet, provision of hinges on the inlet/nose-cowl assembly, an acoustically lined splitter and plug in the tailpipe, and a revised anti-icing system.

#### 4.4.2.1 Nacelle General Arrangement

Side and center inlets were similar to those described in section 4.4.1.1, except for the addition of an acoustically lined ring supported on three struts in each inlet, as shown on figure 75. The ring was a double-faced panel of acoustic polyimide honeycomb construction. The ring leading edge was an Inconel 625 weldment anti-iced with bleed air, and the trailing edge would be a machined aluminum section. The struts, with leading edge weldments of Inconel 625, were anchored to longerons in the inlet structure.

To overcome the greatly reduced access to IGVs and fan blades with the addition of rings, the side-engine inlets were hinged at the engine face, as shown in figure 76. Inlet loads were transferred to the engine face by bolts, as before. To gain access to the engine face, the cowl doors were opened, the inlet bolts removed, and the inlet swung open on hinges.

The tailpipe was similar to that described in section 4.4.1.1, with the addition of an acoustically lined splitter and elongated, acoustically faced plug. The conical splitter was located behind the aft engine face, the forward end forming a continuation of the flow divider between primary and fan air on the engine. (See fig 74.) The splitter would be fabricated of a layer of Inconel 625 honeycomb adjacent to the primary duct and a layer of titanium honeycomb, adjacent

*The tabulated pressure recovery must be corrected upwards by 0.003 to be consistent with the baseline JT8D-9 performance data, which is referenced to a bellmouth inlet, as this reference bellmouth already accounts for 0.003 boundary layer loss.

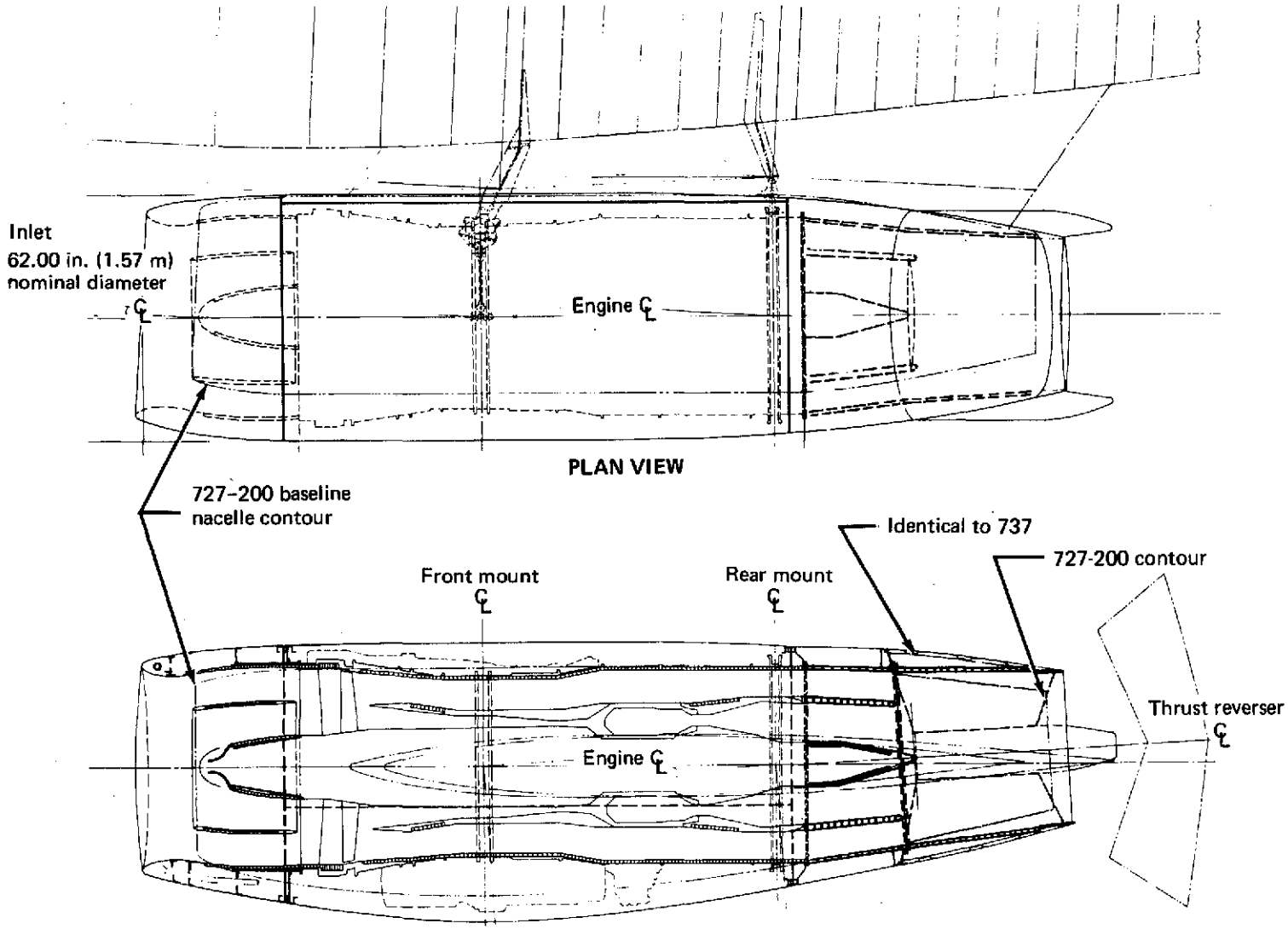


*FIGURE 74.–727/JT8D-109 CONFIGURATION 2 NACELLE*

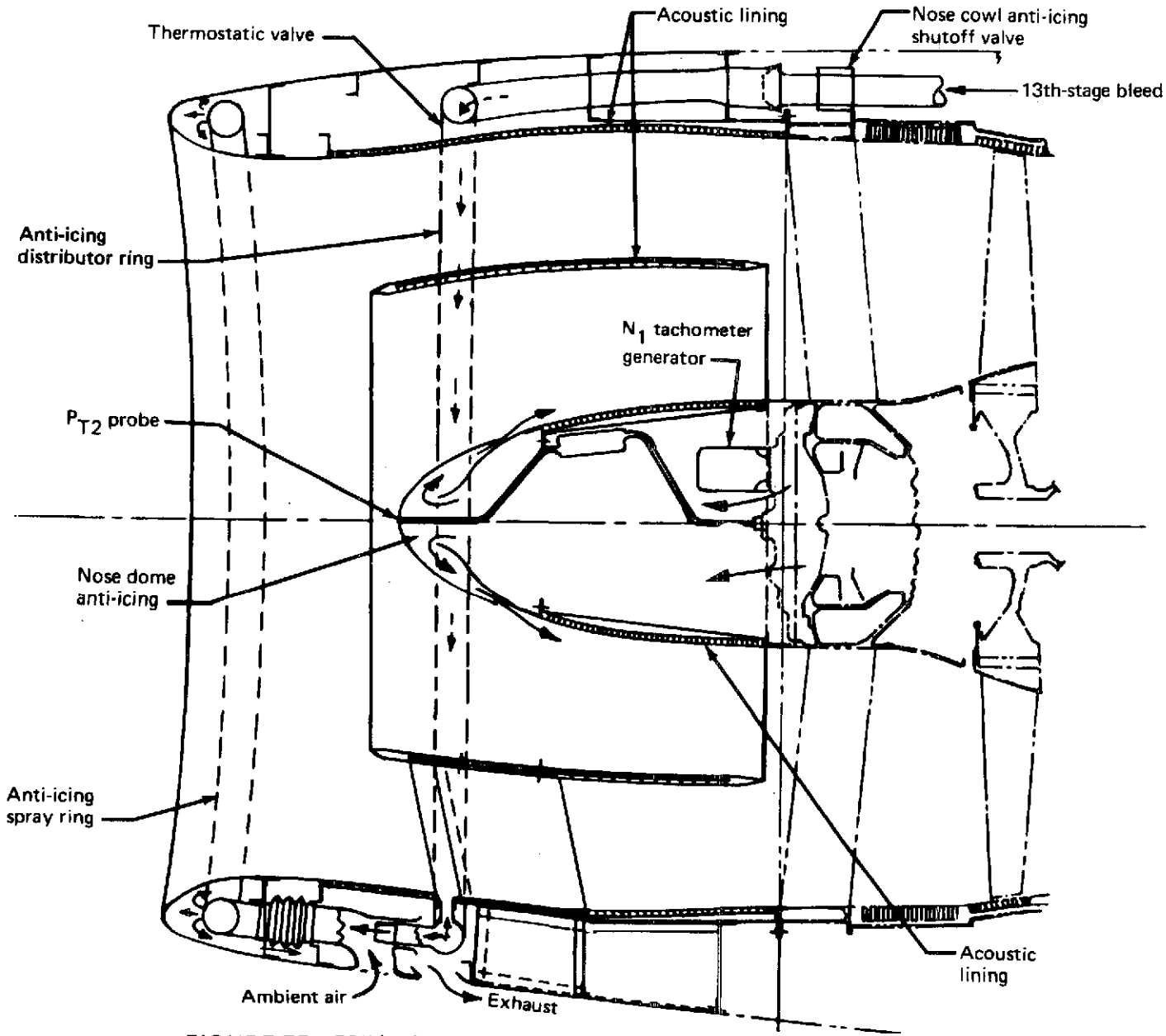


*FIGURE 75.—727/JT8D-109 CONFIGURATION 2 SIDE-INLET CONSTRUCTION*

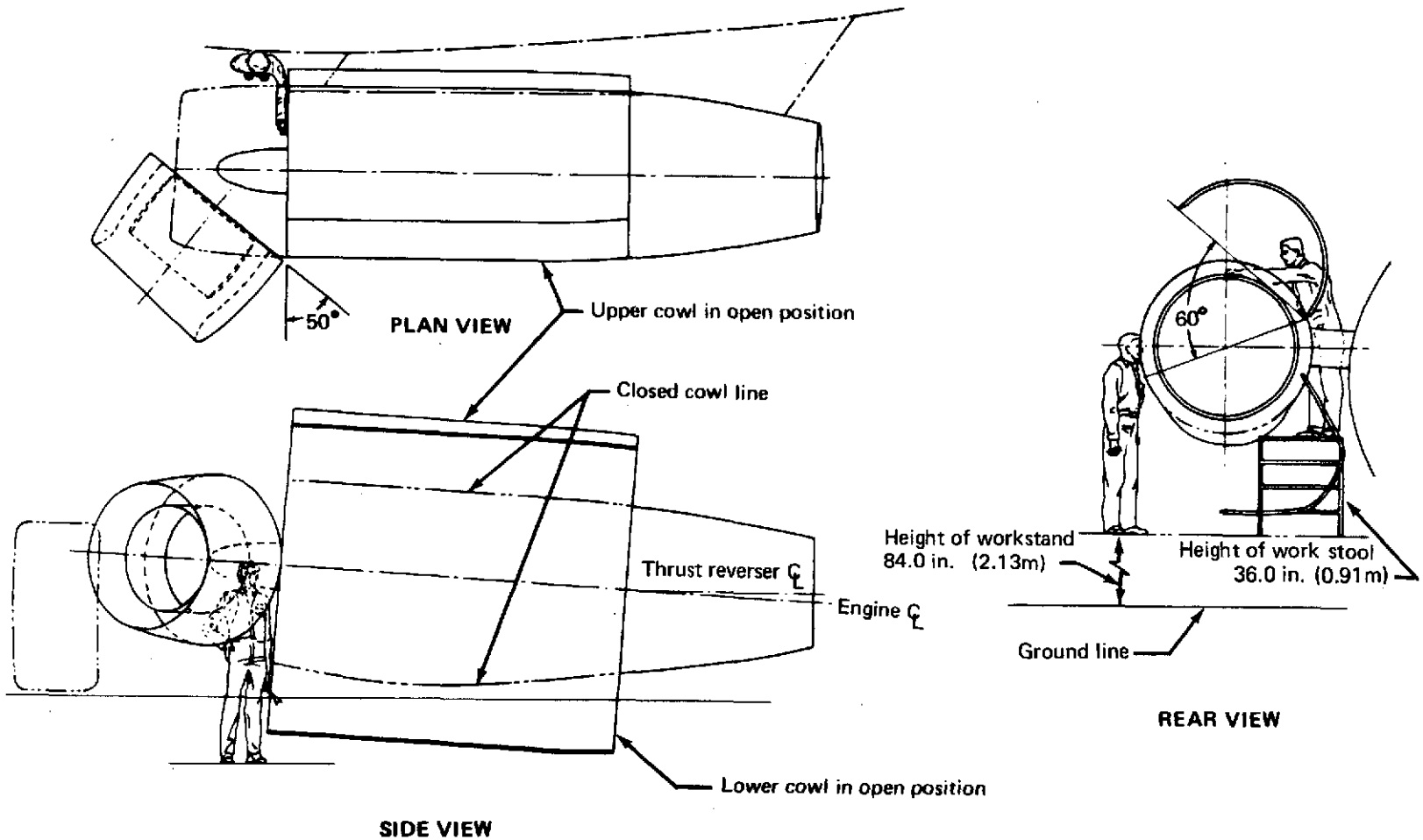


*FIGURE 76.—727/JT8D-109 CONFIGURATION 2 SIDE-ENGINE ACCESSIBILITY*

to the fan duct, with the faces exposed to the airflow perforated to acoustically treat the primary and fan flow. An elongated plug, fabricated of Inconel 625 honeycomb, with the outer face perforated to acoustically treat the primary flow, replaces the standard-size plug used on the modified nacelle baseline installation.

Anti-icing of the side-engine inlet for configuration 2 was the same as configuration 1, except that the supply line branched with one leg feeding hot air to the struts. The air was then routed through the struts and ring leading edge and exhausted into the inlet.

Anti-icing of the center-engine inlet for configuration 2 was the same as configuration 1. To anti-ice the inlet ring, an additional line was tapped from engine bleed and run forward into the inlet structure. The air was then fed to the struts and routed through the ring, as described for the side-engine inlet above.

#### 4.4.2.2 Nacelle Aerodynamic Design

The nacelle aerodynamic design for configuration 2 is the same as configuration 1. Incorporation of the single inlet ring did not necessitate any change in the inlet internal aerodynamics.

### 4.4.3 Configuration 3

The configuration 3 design shown in figure 77 was the same as configuration 1, except for the addition of two acoustically lined rings in the inlet, provision of hinges on the inlet/nose-cowl assembly, a mixer in the tailpipe, and a revised anti-icing system.

#### 4.4.3.1 Nacelle General Arrangement

Side- and center-engine inlets were similar to those described in section 4.4.1.1, except for the addition of two acoustically lined rings supported on three struts in each inlet, as shown in figure 78. The rings were double-faced panels of acoustic polyimide honeycomb construction. Ring leading edges were Inconel 625 weldments anti-iced with bleed air, and the trailing edges were machined aluminum sections.

To overcome the greatly reduced access to IGVs and fan blades with the addition of rings, the side-engine inlets were hinged at the engine face in the same manner as configuration 2, as shown in figure 76.

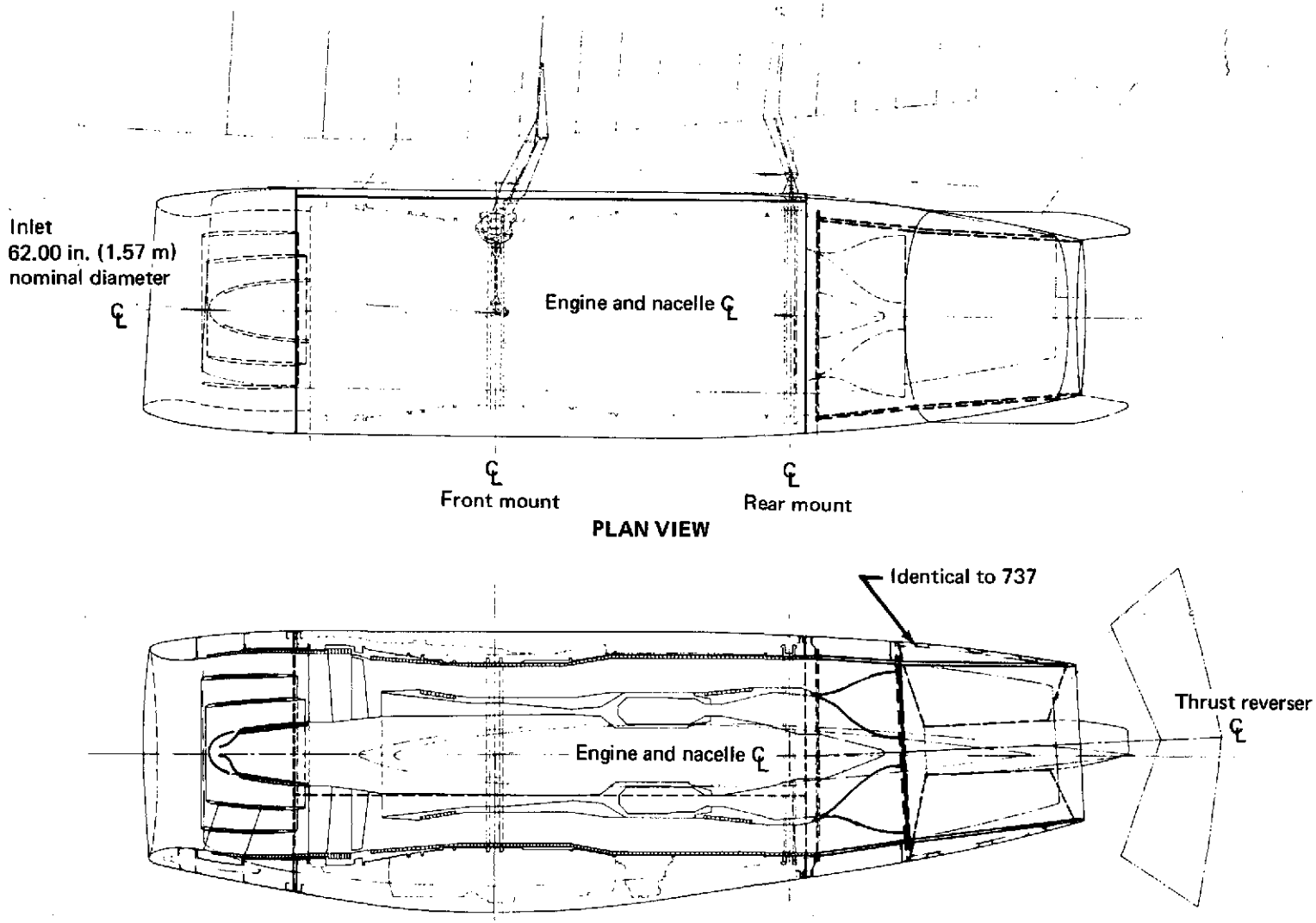


*FIGURE 77.–727/JT8D-109 CONFIGURATION 3 NACELLE*

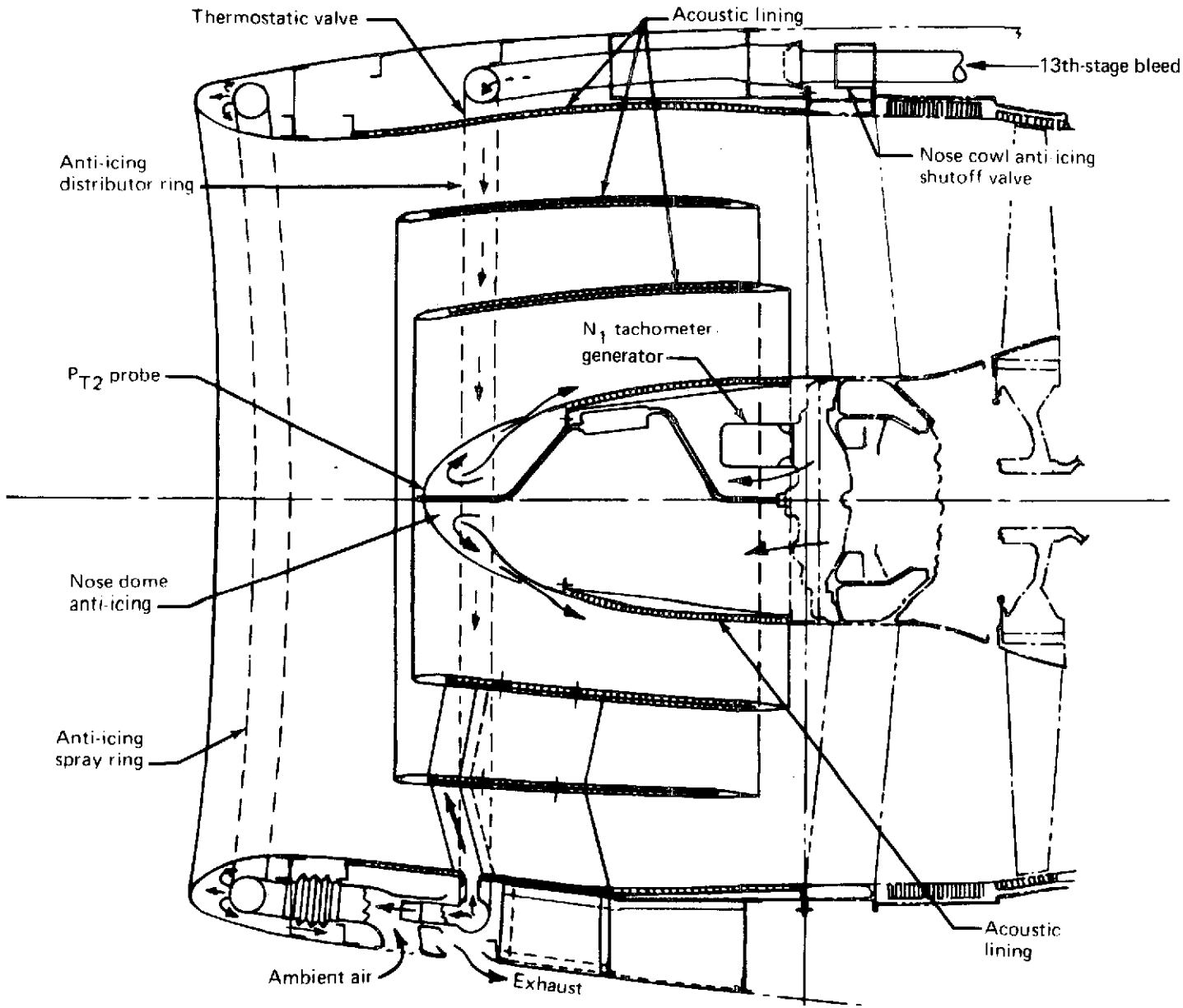


*FIGURE 78.—727/JT8D-109 CONFIGURATION 3 SIDE-INLET CONSTRUCTION*

The tailpipe was similar to that described in section 4.4.1.1 with the addition of an eight-lobe mixer attached to the engine fan and primary splitter. Mixer construction was of Inconel 625 sheet.

Anti-icing of the side-engine inlet for configuration 3 was the same as configuration 1, except that the supply line was branched with one leg feeding hot air to the struts. The air was then routed through the struts and ring leading edges and exhausted into the inlet.

Anti-icing of the center-engine inlet for configuration 3 was the same as configuration 1. To anti-ice the inlet ring, an additional line was tapped from engine bleed and run forward into the inlet structure. The air was then fed to the struts and routed through the rings, as described for the side-engine inlet above.

#### 4.4.3.2 Nacelle Aerodynamic Design

The nacelle aerodynamic design for configuration 3 is the same as configurations 1 and 2. Incorporation of the two inlet rings did not necessitate any change in the inlet internal aerodynamics.

### 4.4.4 Nacelle Design Studies

This section includes a general discussion of the various studies made on the 727 engine nacelle and inlet packages, the design considerations that preceded the particular studies, and the general reasons the airplane nacelle configuration 1 discussed in section 4.4.1 was chosen for further development from the available options.

On the 727 airplane, two separate engine installations must be discussed. One is the two side-mounted engines, and the other is the center-engine location. The side-mounted engines will be discussed first.

On the side engines, the original intent to reuse the existing nacelle-to-body strut and to reuse the existing engine mount system proved to be a feasible approach. The nacelle-to-body strut can be reused by trimming some of the panels and replacing some others.

One consideration was the strength of the side-engine mounts. The engine-mount structure appears to be satisfactory, if the vibration isolation units and the cone bolts are replaced with stronger units.

Other considerations were the effect of the larger diameter nacelle on aerodynamic drag and high angle of attack longitudinal stability and control characteristics. Wind tunnel testing is required to determine this effect.

On the center-engine installation, the three general design parameters were: ability to install a workable inlet air duct in the space presently available in the airplane, the retention of as much of the existing forward and upper firewall and engine-mount system as possible, and the maintenance of adequate ground clearance under the nacelle when the airplane is rotated to tail skid contact at takeoff. Further discussion is found in section 4.5.6.1.

#### 4.4.4.1 Side-Engine Inlet

Several different external and internal line combinations were investigated to check the feasibility of developing one basic inlet for both the 727 and the 737 airplanes. Coupled with this was a study of inlet length-to-diameter ratio to achieve the maximum performance recovery in various wind conditions. Due to the much different airflow patterns into the 727 and the 737 inlets, no single inlet geometry would provide acceptable pressure recovery on both airplanes. Therefore, different designs will be required for the 727 and 737 inlets.

Several different types of acoustic materials were considered, both for noise attenuation and for internal strength. The principal considerations of the airplane operators are the service life of the acoustic absorption panel and the ease of replacing the panel in case of irreparable damage.

The diffuser panel forming the outer wall of the inlet passage, both sides of all splitter rings, and the aft portion of the nose dome have acoustic treatment. This treatment consists of a pervious face sheet next to the air stream, a honeycomb core, and an impervious backing sheet, all made of polyimide impregnated fiberglass cloth material.

Various methods of constructing the anti-ice plenum chambers were investigated. The primary consideration was to obtain a durable lip that would be heat resistant, but would expand and contract with temperature fluctuations without materially affecting the adjoining aluminum structure. The design used will be similar to present production configurations.

Hinge types investigated for the hinged inlet concept ranged from hinge units that would accept flight loads to separately bolted units on which the hinges support the inlet only when open on the ground. Retention of the standard bolt circle with the hinges loaded only in the open position was selected.

#### 4.4.4.2 Engine Cowl Panels

The exterior lines of the cowl panels were defined by a combination of aerodynamic requirements, physical requirements to clear engine equipment, and requirements to mate with the existing engine-to-body strut, which would be reused.

The design parameters were: light weight for ease of handling, quick removal and replacement, minimum susceptibility to handling damage, stiff enough to provide a good base for all the engine penetrations that would be required at the middle of the panel, and economical to produce.

The materials and construction methods evaluated included conventional aluminum skin and stringers, conventional titanium skin and stringers, formed panels of aluminum honeycomb with aluminum face sheets, and fiberglass face sheets with fiberglass honeycomb. Since the engine cowls must be fire resistant, approximately two-thirds of the inner surfaces of these panels—with the exception of the panels of titanium construction—would require a lining of stainless steel or a coating of intumescing paint. Considering both weight and recurring and nonrecurring costs, the fiberglass honeycomb construction would be the most attractive.

#### 4.4.4.3 Engine System Component Arrangement

Arrangement of engine system components attached to the engine case or gear box pads is controlled by the engine manufacturer. Upon proper coordination with the engine manufacturer, some component attach points can be relocated to provide for more suitable installation. The effect of present bleed port and attach point locations on desired new design was investigated so that recommendations could be made to the engine contractor. After determining the optimum bleed port locations for the 727 and 737 airplane installations, several trades were made with the engine contractor and other interested contractors to finalize port locations.

In an effort to increase the surge margin of the center engine, an investigation was made of potential problems that might arise from using center engine bleed for air conditioning and pressurization. Two concepts were evaluated: bleeding the center engine and one side engine, and bleeding all three engines. In the first concept the second side engine would be used as backup in the same manner as the center engine is presently used. This evaluation showed that both concepts were practical from the standpoint of bleed sharing and performance. No recommendation can be made at this time since P&WA has not completed the analysis of the effect of center engine bleed on engine surge margin.

Because the larger engine diameter impinged on the existing control quadrants, several methods of routing the engine controls for the center engine were investigated.

#### 4.4.4.4 Tailpipe and Tailpipe Extensions

The geometric arrangement and the size of the tailpipe and tailpipe extension were controlled by engine size and by location on the airplane. The trade studies therefore dealt with material only. The baseline selection would be to use Inconel 625 sheet or Inconel 625 honeycomb. For the

temperature environment, titanium could be used in all places, except where there would be a direct impingement of unmixed primary exhaust gas. For hardwall versions, titanium could be used in all places in lieu of the Inconel 625. Thus, an extensive effort was made to develop a usable titanium honeycomb that could serve as a sound-suppression panel. If only titanium material was used, a weight saving of approximately 70 lb (32 kg) would be realized per nozzle. This would be doubly helpful on the 727 airplane, since a weight saving aft of the cg would also be reflected as less ballast forward or more flexible airplane loading.

#### 4.4.4.5 Mixers

As has been discussed in other sections of this summary, the initial studies indicated that enough thrust augmentation would be gained by inclusion of a properly designed mixer to minimize or offset the thrust losses that the mixer would generate. Again, this could be proved (or disproved) only by an extensive testing and study program.

The studies conducted include different methods to force the very early mixing of the primary exhaust with the secondary exhaust. This involved careful area matches at both inlet and exit of the mixers and different mixer shapes to generate the maximum coplanar shear areas between the two flows. Various types of vortex generators, to be used at the flow shear planes, were investigated in conjunction with the mixers.

Due to the high temperatures in the primary airflow, the only material that would appear to be acceptable for the mixer was Inconel 625.

#### 4.4.4.6 Thrust Reversers

Two basic types of thrust reversers were investigated. One was a target type similar to the reverser currently in use on the 737 airplane. The second type included internal clamshell doors that, when closed, would divert the exhaust gas through fixed, permanently exposed cascades.

On the target reverser, the basic trade studies conducted include: different methods and materials that could be used for both single-thickness and double-thickness target doors, different door and tailpipe shapes to obtain the best boattail angles and the least base area drag, hydraulic actuators and pneumatic air motor actuation systems, different sources of supply for a hydraulic system, and different gas deflection patterns that would affect system efficiency.

The options investigated for the exposed cascade reverser include different actuation systems, different methods of construction of the doors, different gas flow paths, and different types of cascade construction.

The target-type thrust reverser was selected as the most logical course to follow, since it will provide for installation of a maximum amount of acoustic lining in the exhaust system.

#### 4.4.4.7 Center-Engine Inlet

The center-engine inlet design was similar to the existing 727 center duct, which originates above the fuselage forward of the tail section and which directs the airflow to the inlet face of the engine.

The main design limitations were to provide sufficient airflow to the relocated and refanned center engine within acceptable pressure recovery and distortion limits, to clear the existing fin front spar fitting, to meet the noise-reduction requirements, to be compatible with anti-icing requirements, and to be cost effective in relation to weight and service life.

Several shapes were checked for flowpath characteristics, and—although a hard final shape was not defined—enough data were derived to allow verification that the duct could be installed within the established design limitations. (Ref. sec. 4.3.3.)

Different construction methods were evaluated. The best construction method appears to be aluminum honeycomb with aluminum skin and corrugation backing wherever duct anti-icing would be required.

The duct design will include a new flexible joint at the engine flange and slip joints on each side of the fin front spar. Figures 79 and 80 show cross sections through the two types of duct seals.

## 4.5 AIRPLANE MODIFICATION

The major portion of the airplane changes affected the aft body section in the area of attachment of the new engines. There were no design changes to the forward body or the wing structure, except to balance the added weight of the refanned engines. Systems changes were confined to those necessary to accommodate the refanned engine installations. Areas affected were tail skid, ventral airstairs, hydraulics, air conditioning, anti-icing, reverser indicating lights, and engine controls.

### 4.5.1 Fuselage and Inlet Fairing

To permit passage of the enlarged center duct, the aft body pressure bulkhead and several body frames were redesigned. The front spar fin forging was retained unchanged.

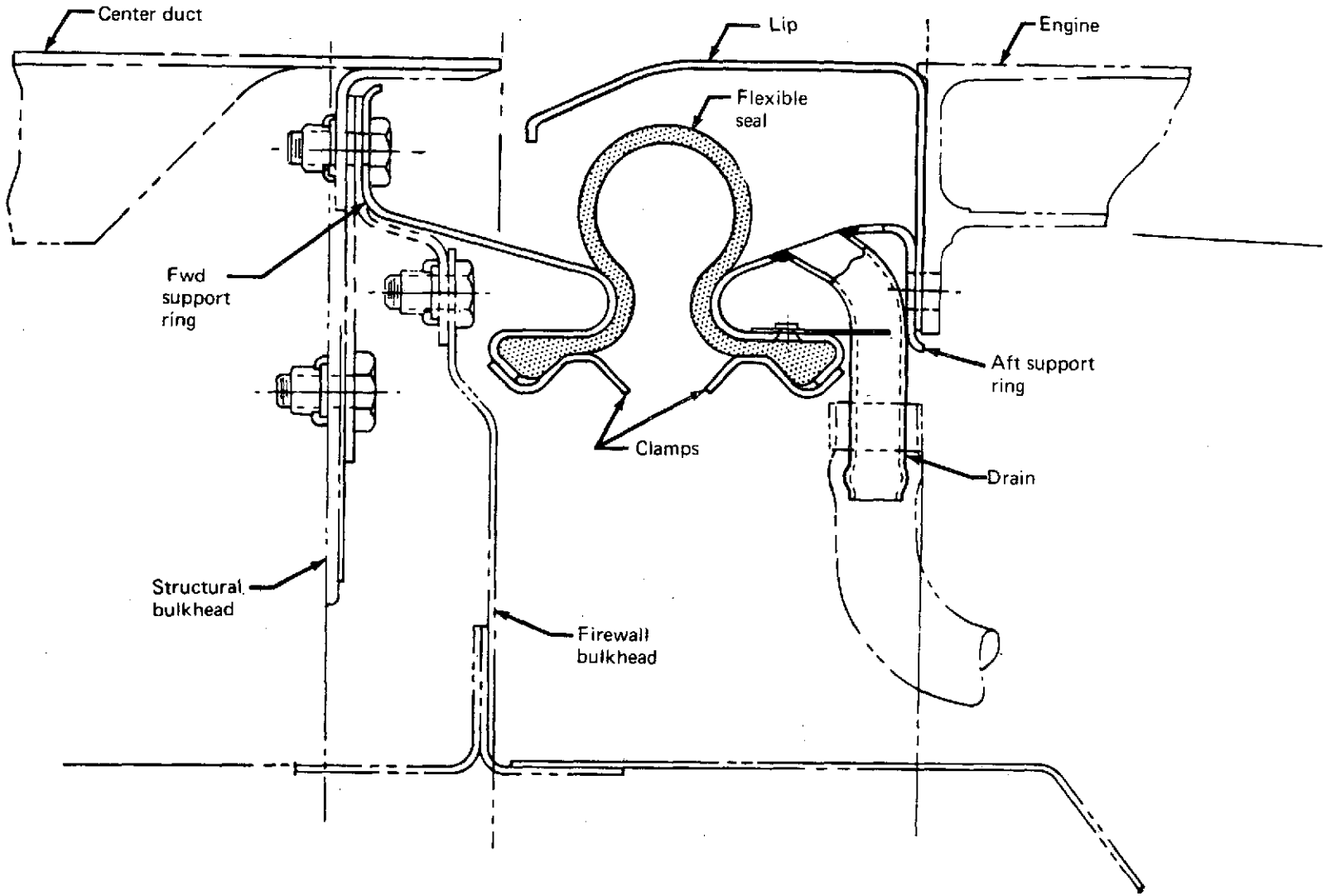


*FIGURE 79.—727/JT8D CENTER DUCT TO ENGINE FLEXIBLE SEAL ASSEMBLY*

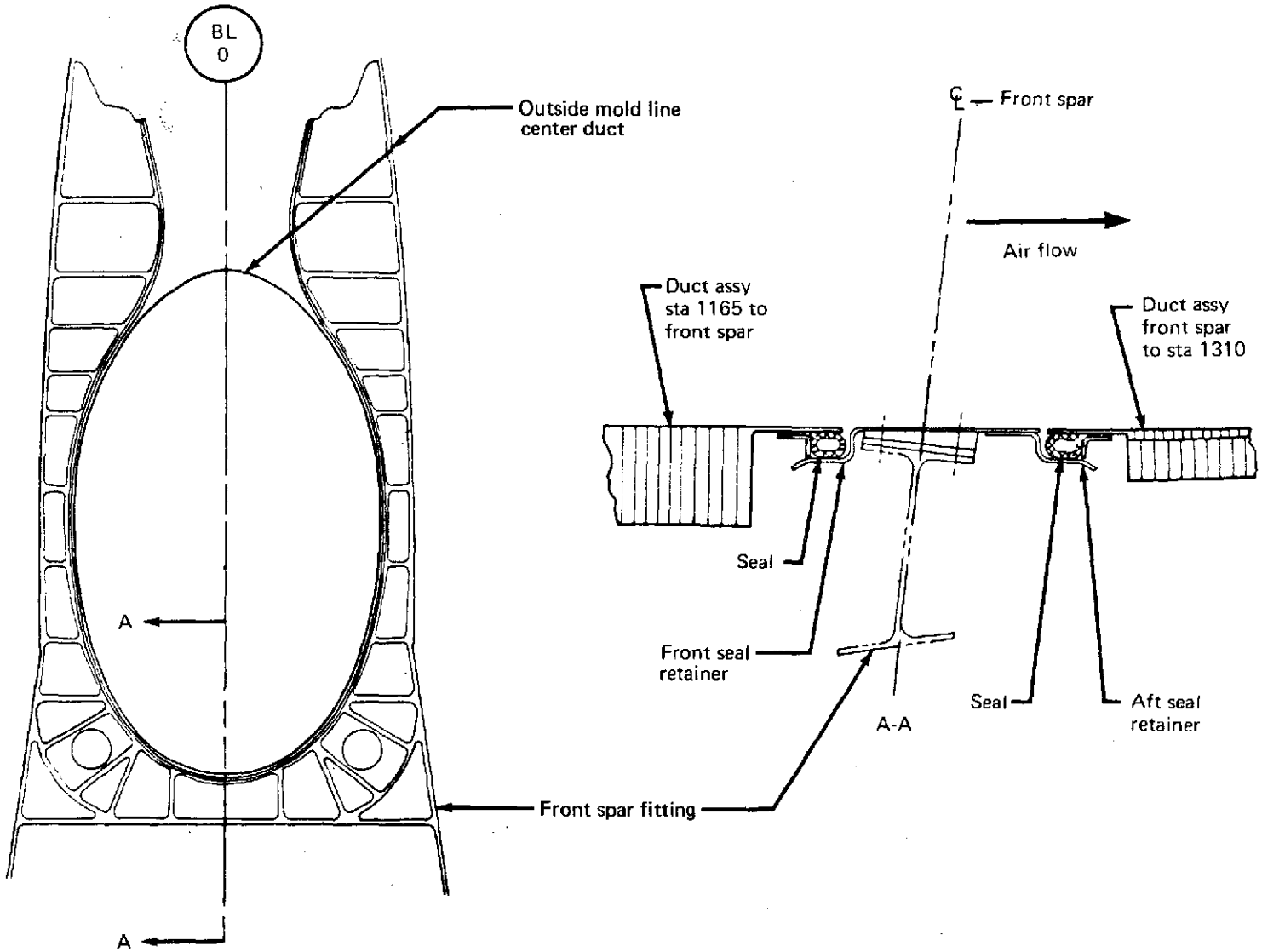


*FIGURE 80.—727/JT8D CENTER-DUCT SEAL AT FIN FRONT SPAR*

The center-engine inlet fairing was redesigned with aluminum frames and longitudinal channels providing support to nonmetallic honeycomb paneling to accommodate the larger inlet.

### 4.5.2 Firewalls and Engine Supports

While both the forward and overhead firewalls were retained on the center-engine installation, extensive changes were required. The center-duct opening in the forward or vertical firewall was redesigned to accept the new center duct, as shown in figure 71. Figure 81 shows the changes made to the overhead or horizontal firewall and the fin structure. This design included new front and aft engine-mount fittings and new internal fin structure to distribute the load. New thrust links and forward shock-mount fittings were also required.

### 4.5.3 Tail Skid

Lowering of the center engine, combined with its larger diameter, would allow the center-engine tailpipe to contact the ground during airplane rotation. Several studies were conducted to resolve this problem. The design selected limited the stroke of the tailskid cartridge when compressed. This slightly limited the airplane maximum rotation angle.

### 4.5.4 Ventral Stairs

To maintain clearance from the bottom of the new relocated center duct, several design changes to the ventral stairs were required. The stair-actuating torque tube and the uplock torque tube were offset from their pivot points to provide clearance for the bottom of the center duct. The stair ceiling panels were also revised to provide clearance for the larger duct.

### 4.5.5 Airframe Systems

Hydraulic system A, which is the basic airplane hydraulic system, was redesigned to provide power for the new target-type thrust reverser. Existing hydraulic system A is supplied by hydraulic pumps located on engines 1 and 2. A third pump was added on engine 3 to provide the required flow capacity necessary to give acceptable reverser extension and retraction times. As a safety feature, the airplane standby hydraulic system was interconnected to the reverser in the event of pressure loss in system A.

The air conditioning and anti-icing ducts forward of the center-engine vertical firewall were relocated to clear the new center duct. The four unused body duct openings left from precooler duct rerouting were covered by reskinning.

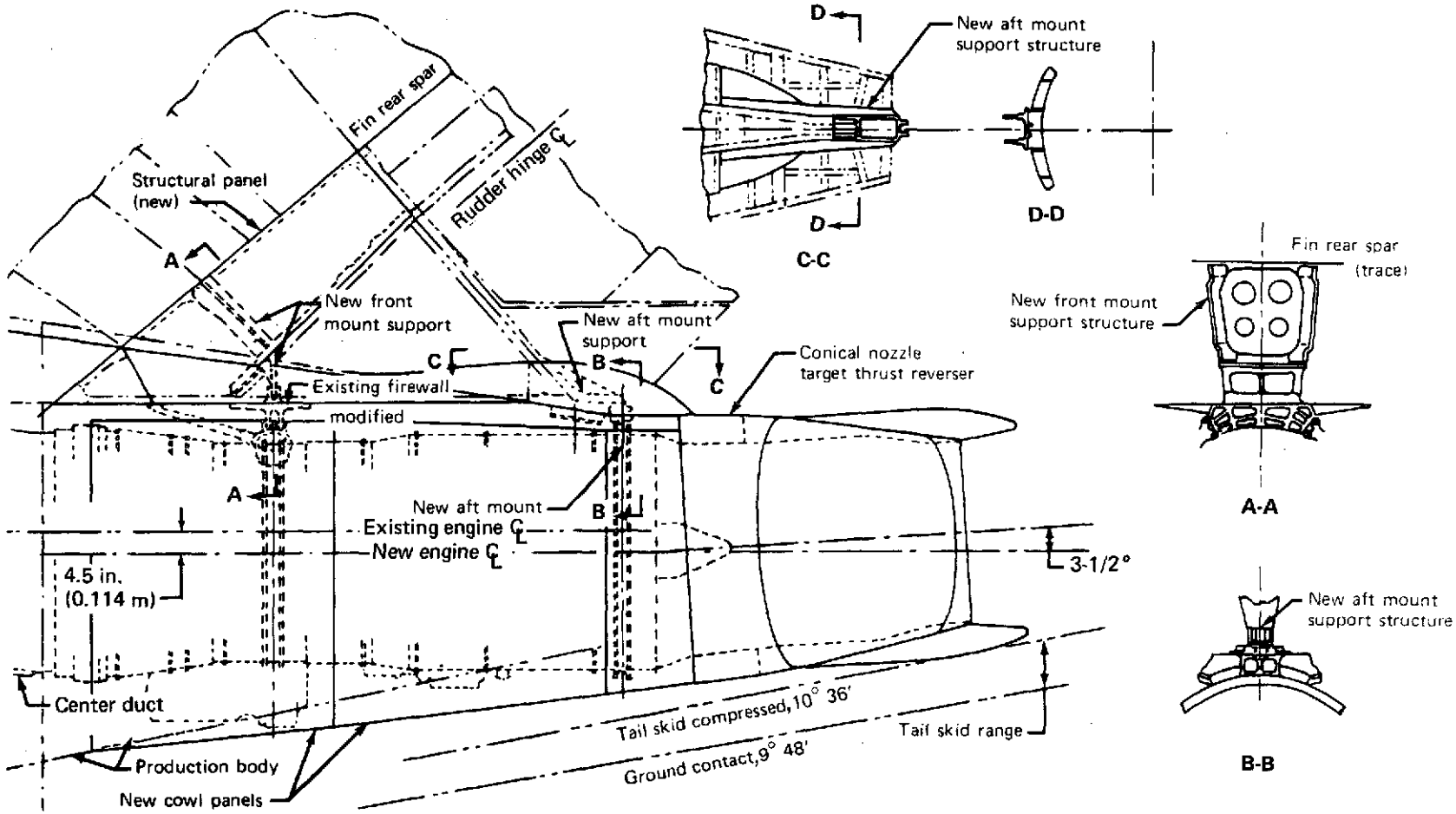


*FIGURE 81.—727/JT8D CENTER-ENGINE INSTALLATION COMPARISON*

The thrust reverser indication system was revised to add a thrust-reverser-deployed light in addition to the thrust-reverser-unlocked light.

### 4.5.6 Studies

Several studies were conducted that affected airplane structure and configuration. Three significant items considered were the center-engine position, tail skid, and evacuation through the aft service doors.

#### 4.5.6.1 Center-Engine Position

Several center-engine positions were considered within the following design constraints: minimum structural change for retrofit, compatibility with the center-duct configuration, and ground clearance during airplane rotation. The refanned engine would be approximately 11 in. (0.279 m) larger in diameter and 10 in. (0.254 m) longer on the front end. Designing an acceptable center-duct configuration precludes moving the aft end of the duct both down and forward. An acceptable compromise was made by lowering the engine to retain the horizontal firewall and maintaining the forward face location of the engine to preserve the vertical firewall and allow for satisfactory center-duct geometry. An acceptable airplane rotational capability was achieved by tilting the thrust reverser up 3°30′ from the horizontal. This also provided common thrust reversers and tailpipes on all three engine positions. The new engine-mount flange location did, however, necessitate redesigning the engine mounting structure on the airframe.

#### 4.5.6.2 Tail Skid

To limit aircraft rotation, various combinations of springs, crushable cartridges, and minor mechanism changes in the existing tail skid were studied as methods of absorbing the increased impact energy within a shorter stroke. The configuration chosen had a higher energy absorption cartridge, a spacer to limit the stroke, and a longer tip.

#### 4.5.6.3 Evacuation

Successful emergency evacuation from the aft service doors within the 90-sec time limit was studied. In addition to the inlet being larger on the refanned engine, the lip of the inlet would be 10 in. (0.254 m) closer to the doors. (See figs. 45 and 46.)

The modified airplane configuration was considered acceptable on the basis that a Dan-Air 727 airplane was certified with its aft service door 10 in. (0.254 m) closer to the engine inlet than that on the proposed refan configuration.

## 4.6 MAINTENANCE ANALYSIS AND SUPPORT EQUIPMENT

### 4.6.1 Maintenance Analysis

The JT8D-109 installation design incorporated a majority of the JT8D-9 engine accessories, and the new items incorporated were designed to meet a standard of maintainability equivalent to that of the original installation.

The new engine installation design provided a standard of accessibility equal to (and, in some cases, better than) that of the baseline airplane.

The inlet was designed for the installation of an acoustic diffuser and an acoustic ring (or rings). The design provided ease of inspection and replacement of the acoustic panels when required. The inlet was hinged to permit better access to the engine fan blades for inspection and maintenance. The airplane could be flown with the ring (or rings) removed, if necessary.

The target-type thrust reverser was based on the design currently in use on the 737. This basic design has a minimum of moving parts, with none inside the tailpipe, and has demonstrated a high standard of reliability.

### 4.6.2 Support Equipment

Except for dimensional changes, there would be no change in the requirements for ground support equipment from those used for the present 727 airplane. The proximity of the inlet to the galley door on the JT8D-109 side engine could cause some restriction in access for galley servicing. Studies and discussions with airline representatives indicated that the majority of existing galley service vehicles would be unaffected by this condition.

The increased weight and longer overall dimensions of the JT8D-109 engine and nacelle would necessitate modification of the present hoisting and handling equipment. No changes are expected for tie-down or towing.

The increased weight of the engines requires additional ballast (or equivalent loading of cargo, fuel, passengers, etc.) to ensure that jacking, taxiing, and towing characteristics would meet the same requirements as for the present 727-200.

### 4.6.3 System Support

Little special training would be required for certification of ground maintenance people because of the high standard of commonality between the JT8D-109 and the JT8D-9 installations regarding accessories, instrumentation, and controls. A minimum of flight crew familiarization would be required since the flight and handling characteristics of the modified airplane would be similar to the baseline airplane.

Hardware was designed to the certification rules of Civil Air Regulation CAR Part 4b—the same rules in effect at the time of initial certification. Design changes to the airplane were confined to those required for installation of the refanned engines.

## 4.7 PERFORMANCE COMPARISON

The information contained in this section describes and details estimated airplane characteristics that directly affect the airplane's operational capability.

The data deal primarily with a baseline airplane having a maximum taxi weight of 173 000 lb (78 473 kg). This baseline airplane, following some modification, is capable of operation at a higher gross weight of 183 000 lb (83 009 kg)—a gross weight more consistent with the increased thrust capability of the refanned JT8D-109 engine. Performance at both gross weights is therefore shown.

A detailed weight breakdown is provided for the baseline nacelle and for each of the modified-nacelle configurations. Performance comparisons on the basis of takeoff field length, payload versus range, and takeoff field length versus range are shown. The increase in airplane cruise drag for each of the modified-nacelle configurations is approximately 1.6% at a typical midcruise condition. Possible changes in handling characteristics, stability and control, and flutter stability are also discussed.

Table 21 presents a summary of airplane performance, modification cost estimate, and noise level predictions for each configuration as installed on an airplane with BRGW limited to that of the baseline airplane. Table 22 presents a similar summary in which the BRGW for the respective configurations is permitted to increase within presently planned growth limits.

### 4.7.1 Installed-Engine Performance

Nacelle installation losses include inlet losses, accessory power extraction, airbleed for aircraft systems, and exhaust nozzle losses. The installation losses and the incremental effects of these losses

## TABLE 21.—727-200 PERFORMANCE SUMMARY—CONSTANT BRGW

| Parameter | 727-200 configuration | | | | | | | | | | |
|---|---|---|---|---|---|---|---|---|---|---|---|
| | Baseline | | 1 | | | 2 | | | 3[a] | | |
| OEW, lb (kg)<br>ΔOEW, lb (kg)<br>Change, % | 99 000 (44 906) | | 102 655 (46 564)<br>+3655 (1658)<br>+3.69 | | | 103 365 (46 886)<br>+4365 (1980)<br>+4.41 | | | 103 500 (46 947)<br>+4500 (2041)<br>+4.55 | | |
| Brake release gross weight,[b] lb (kg) | 172 500 (78 245) | | 172 500 (78 245) | | | 172 500 (78 245) | | | 172 500 (78 245) | | |
| Takeoff field length, ft (m)<br>Change, % | 8370 (2551) | | 7120 (2170)<br>-14.9 | | | 7330 (2234)<br>-12.4 | | | 7380 (2249)<br>-11.8 | | |
| ATA range, nmi (km)<br>Change, % | 1355 (2509) | | 1135 (2102)<br>-16.2 | | | 1065 (1972)<br>-21.4 | | | 1080 (2000)<br>-20.3 | | |
| Kit and installation cost, millions of dollars per aircraft | - | | 1.634 | | | 1.740 | | | 1.785 | | |
| Airplane quantity | – | | [c]669 | | | [d]255 | | | [d]255 | | |
| Cash DOC change from baseline, % | – | | 1.77 | | | 2.35 | | | 1.94 | | |
| Average range, nmi (km) | – | | 473 (876) | | | 473 (876) | | | 473 (876) | | |
| FAR Part 36 noise, EPNdB | Limit | Measured | Limit | Predicted | Δ[h] | Limit | Predicted | Δ[h] | Limit | Predicted | Δ[h] |
| Takeoff | 99.0 | 107.4 | 99.0 | 96.8 | -10.6 | 99.0 | 96.2 | -11.2 | 99.0 | 91.4 | -16.0 |
| Cutback | 99.0 | 100.0 | 99.0 | 89.6 | -10.4 | 99.0 | 89.5 | -10.5 | 99.0 | 87.3 | -12.7 |
| Approach[e] | 104.4 | 108.2 | 104.4 | 97.2 | -11.0 | 104.4 | 95.2 | -13.0 | 104.4 | 94.7 | -13.5 |
| Sideline | 104.4 | [f]99.9 | 104.4 | 90.2 | - 9.7 | 104.4 | 89.3 | -10.6 | 104.4 | 84.4 | -15.5 |
| 95-EPNdB contour area reduction reduction,[g] % | – | | –78.5 | | | –82.5 | | | –93.7 | | |
| Relative footprint noise index | 1.0 | | 0.145 | | | 0.124 | | | 0.042 | | |

[a]Design goals only; effort discontinued because of funding
[b]Note constant BRGW
[c]Cost base includes 727-100 fleet
[d]Assumes 727-100 modified to configuration 1 (669 aircraft)
[e]Approach flaps–30°
[f]Sideline noise level based on cutback procedure
[g]At baseline BRGW
[h]Δ from baseline measured value

## TABLE 22.—727-200 PERFORMANCE SUMMARY—INCREASED BRGW

| Parameter | 727-200 configuration | | | | | | | | | | |
|---|---|---|---|---|---|---|---|---|---|---|---|
| | Baseline | | 1 | | | 2 | | | 3[a] | | |
| OEW, lb (kg)<br>Δ OEW, lb (kg)<br>Change, % | 99 000 (44 906) | | 102 815 (46 637)<br>3815 (1730)<br>+3.85 | | | 103 525 (46 960)<br>4525 (2053)<br>+4.57 | | | 103 660 (47 020)<br>4660 (2114)<br>+4.71 | | |
| Brake release gross weight,[b] lb (kg)<br>Change, % | 172 500 (78 246) | | 181 990 (82 551)<br>+5.50 | | | 182 500 (82 782)<br>+5.80 | | | 182 500 (82 782)<br>+5.80 | | |
| Takeoff field length, ft (m)<br>Change, % | 8370 (2551) | | 8670 (2643)<br>+3.6 | | | 9000 (2743)<br>+7.5 | | | 9080 (2768)<br>+8.5 | | |
| ATA range, nmi (km)<br>Change, % | 1355 (2509) | | 1540 (2852)<br>+13.6 | | | 1480 (2741)<br>+9.2 | | | 1495 (2769)<br>+10.3 | | |
| Kit and installation cost, millions of dollars per aircraft | – | | 1.634 | | | 1.740 | | | 1.785 | | |
| Airplane quantity | – | | [c]669 | | | [d]255 | | | [d]255 | | |
| Cash DOC change from baseline, % | – | | 1.77 | | | 2.35 | | | 1.94 | | |
| Average range, nmi (km) | – | | 473 (876) | | | 473 (876) | | | 473 (876) | | |
| FAR Part 36 noise, EPNdB | Limit | Measured | Limit | Predicted | (Δ)[h] | Limit | Prediction | (Δ)[h] | Limit | Predicted | (Δ)[h] |
| Takeoff | 99.0 | 107.4 | 99.4 | 97.6 | - 9.8 | 99.4 | 97.1 | -10.3 | 99.4 | 92.6 | -14.8 |
| Cutback | 99.0 | 100.0 | 99.4 | 91.7 | - 8.3 | 99.4 | 91.5 | - 8.5 | 99.4 | 89.4 | -10.6 |
| Approach[e] | 104.4 | 108.2 | 104.6 | 97.2 | -11.0 | 104.6 | 95.2 | -13.0 | 104.6 | 94.7 | -13.5 |
| Sideline | 104.4 | [f]99.9 | 104.6 | 90.0 | - 9.9 | 104.6 | 89.0 | -10.9 | 104.6 | 84.2 | -15.7 |
| 95-EPNdB contour area reduction,[g] % | – | | 78.5 | | | 82.5 | | | 93.7 | | |
| Relative footprint noise index | 1.000 | | 0.145 | | | 0.124 | | | 0.042 | | |

[a]Design goals only; effort discontinued because of funding
[b]Note modified airplane gross weight increase—does not apply to all 727-200 airplanes
[c]Cost base includes 727-100 fleet
[d]Assumes 727-100 modified to configuration 1 (total of 669 aircraft modified)
[e]Approach flaps–30°
[f]Sideline noise level based on cutback procedure
[g]At baseline BRGW
[h]Δ from baseline measured noise level

on takeoff thrust and cruise fuel consumption for configurations 1, 2, and 3 are summarized in tables 23 and 24 for the side-engine installation and tables 25 and 26 for the center-engine installation.

Accessory drive power extraction from the engine high pressure shaft on actual 727 nacelle installations varies from 50 hp (37.2 kW) to 70 hp (52.2 kW) throughout takeoff, climb, and cruise conditions. To simplify input, the contractor selected 60 hp (44.7 kW) as a representative value for all flight conditions. Use of this constant value, as opposed to a varying value, will result in no significant effect on engine performance prediction.

Takeoff lapse rates ($F_N$ vs TAS) for the three nacelle configurations are shown for the side and center engines in figures 82 and 83 for an 84° F (302° K) day at sea level and 5000 ft (1524 m). The JT8D-9 lapse rate is shown at both altitudes for comparison. The JT8D-109 has considerably more takeoff thrust than the JT8D-9 throughout the practical takeoff speed regime. The increased takeoff thrust of the JT8D-109 can be used to decrease takeoff field length requirements for a given airplane gross weight or to permit increased takeoff gross weight with a given runway length.

Thrust specific fuel consumption for the JT8D-109 for each of the three configurations is compared with that for the JT8D-9 in figure 84 for the side-engine installation and figure 85 for the center-engine installation. For the side-engine installation, configuration 1 shows a TSFC decrease of 0.7% from the JT8D-9 level at a nominal midcruise thrust of 4000 lb (17 793 N), while configurations 2 and 3 show increases of 0.9% and 0.0%, respectively. The center-engine JT8D-109 installations, when compared to the JT8D-9 in a like manner, show a decrease in TSFC of 1.5% and 0.5% for configurations 2 and 3, respectively. When two side engines and one center engine are averaged (to represent the average engine performance) for the airplane at the nominal midcruise thrust of 4000 lb (17 793 N), configuration 1 shows a net TSFC improvement over the JT8D-9 installation of 0.5%. Configurations 2 and 3 show TSFC increases of 1.1% and 0.2%, respectively, when compared to the JT8D-9 in a similar manner.

### 4.7.2 Weight and Balance

The installation of JT8D-109 engines would cause the airplane operating empty weight to increase. The operational weight breakdown for the baseline airplane is shown in table 27. Table 28 shows the items in the nacelle weight statement that would be modified by the refanned engine installation design. It should be noted that ballast would be required at the nose radome bulkhead to counteract the aft cg shift caused by the increased powerplant installation weight.

The 727-200 baseline airplane characteristics are listed in table 29. The baseline airplane has been selected as being typical of the 727-200 retrofit fleet.

*TABLE 23.–727/JT8D-109 SIDE-ENGINE INSTALLED INCREMENTAL LOSSES $\Delta F_N/F_N$ AT TAKEOFF[a]*

| Item | Configuration | | | | | |
|---|---|---|---|---|---|---|
| | 1 | | 2 | | 3 | |
| | Loss | $\Delta F_N/F_N$, % | Loss | $\Delta F_N/F_N$, % | Loss | $\Delta F_N/F_N$, % |
| Inlet loss, $\Delta P/P$ | 0.007 | -2.0 | 0.013 | -3.6 | 0.017 | -4.7 |
| Power extraction | 60 hp (44.7 kW) | -0.4 | 60 hp (44.7 kW) | -0.4 | 60 hp (44.7 kW) | -0.4 |
| Bleed | 2.18 lb/sec (0.99 kg/sec) | -3.8 | 2.18 lb/sec (0.99 kg/sec) | -3.8 | 2.18 lb/sec (0.99 kg/sec) | -3.8 |
| Nozzle velocity coefficient, $\Delta C_V$ | -0.003 | -0.3 | -0.009 | -0.9 | -0.005 | -0.5 |
| Total | | -6.5 | | -8.7 | | -9.4 |

[a]Sea level, standard day

*TABLE 24.–727/JT8D-109 SIDE-ENGINE INSTALLED INCREMENTAL LOSSES $\Delta TSFC/TSFC$ AT CRUISE[a]*

| Item | Configuration | | | | | |
|---|---|---|---|---|---|---|
| | 1 | | 2 | | 3 | |
| | Loss | ΔTSFC/TSFC, % | Loss | ΔTSFC/TSFC, % | Loss | ΔTSFC/TSFC, % |
| Inlet loss, $\Delta P/P$ | 0.001 | 0.1 | 0.007 | 0.8 | 0.001 | 1.2 |
| Power extraction | 60 hp (44.7 kW) | 0.5 | 60 hp (44.7 kW) | 0.5 | 60 hp (44.7 kW) | 0.5 |
| Bleed | 1.57 lb/sec (0.71 kg/sec) | 3.0 | 1.57 lb/sec (0.71 kg/sec) | 3.0 | 1.57 lb/sec (0.71 kg/sec) | 3.0 |
| Nozzle velocity coefficient, $\Delta C_V$ | -0.003 | 0.7 | -0.008 | 1.8 | -0.001 | 0.2 |
| Total | | 4.3 | | 6.1 | | 4.9 |

[a]Mach = 0.84, 30 000 ft (9144 m), net thrust = 4000 lb (17 793 N)

*TABLE 25.–727/JT8D-109 CENTER-ENGINE INSTALLED INCREMENTAL LOSSES $\Delta F_N/F_N$ AT TAKEOFF[a]*

| Item | Configuration | | | | | |
|---|---|---|---|---|---|---|
| | 1 | | 2 | | 3 | |
| | Loss | $\Delta F_N/F_N$, % | Loss | $\Delta F_N/F_N$, % | Loss | $\Delta F_N/F_N$, % |
| Inlet loss, $\Delta P/P$ | 0.022 | -6.0 | 0.028 | -7.6 | 0.032 | -8.7 |
| Power extraction | 60 hp (44.7 kW) | -0.4 | 60 hp (44.7 kW) | -0.4 | 60 hp (44.7 kW) | -0.4 |
| Nozzle velocity coefficient, $\Delta C_V$ | -0.003 | -0.3 | -0.009 | -0.9 | -0.005 | -0.5 |
| Total | | -6.7 | | -8.9 | | -9.6 |

[a]Sea level, standard day

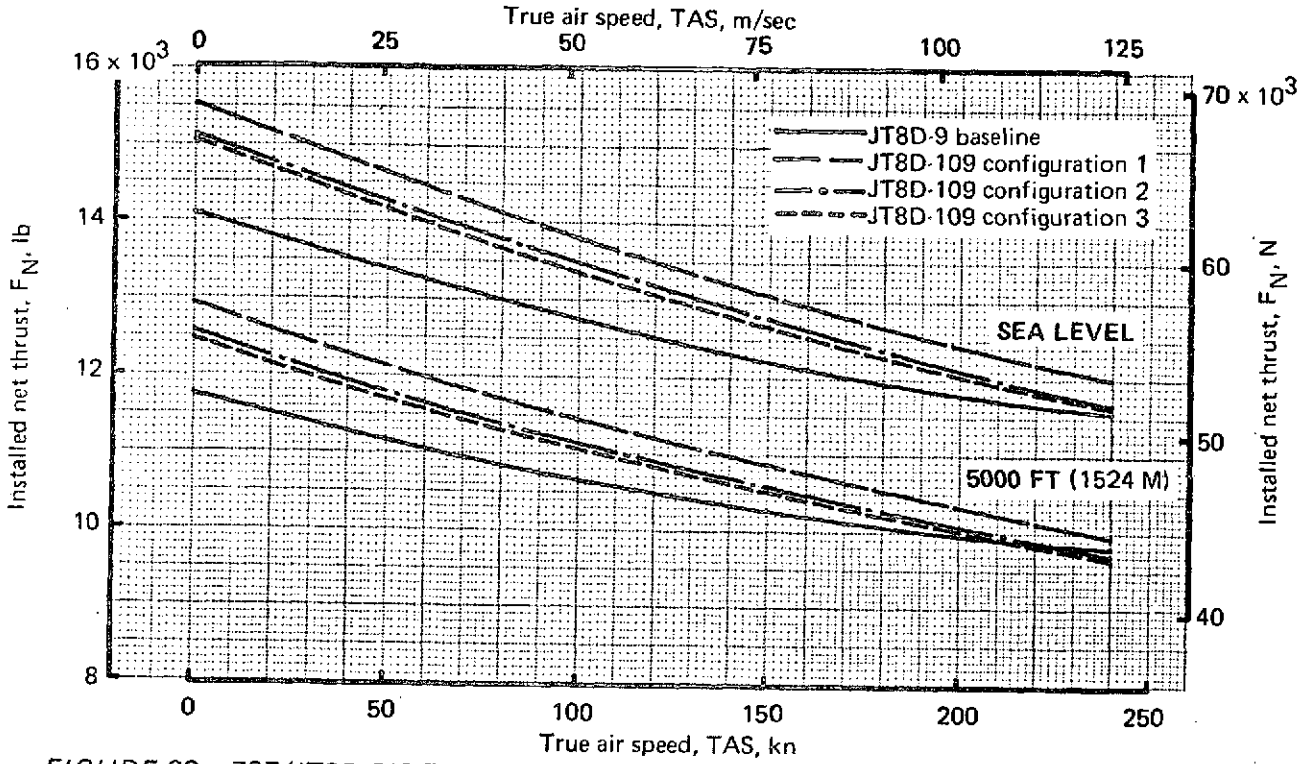


*FIGURE 82.—727/JT8D SIDE-ENGINE INSTALLED TAKEOFF THRUST LAPSE RATE COMPARISON, AIR CONDITIONING BLEED ON, 60 HP (44.7 KW) EXTRACTION, 84°F (302°K) DAY*

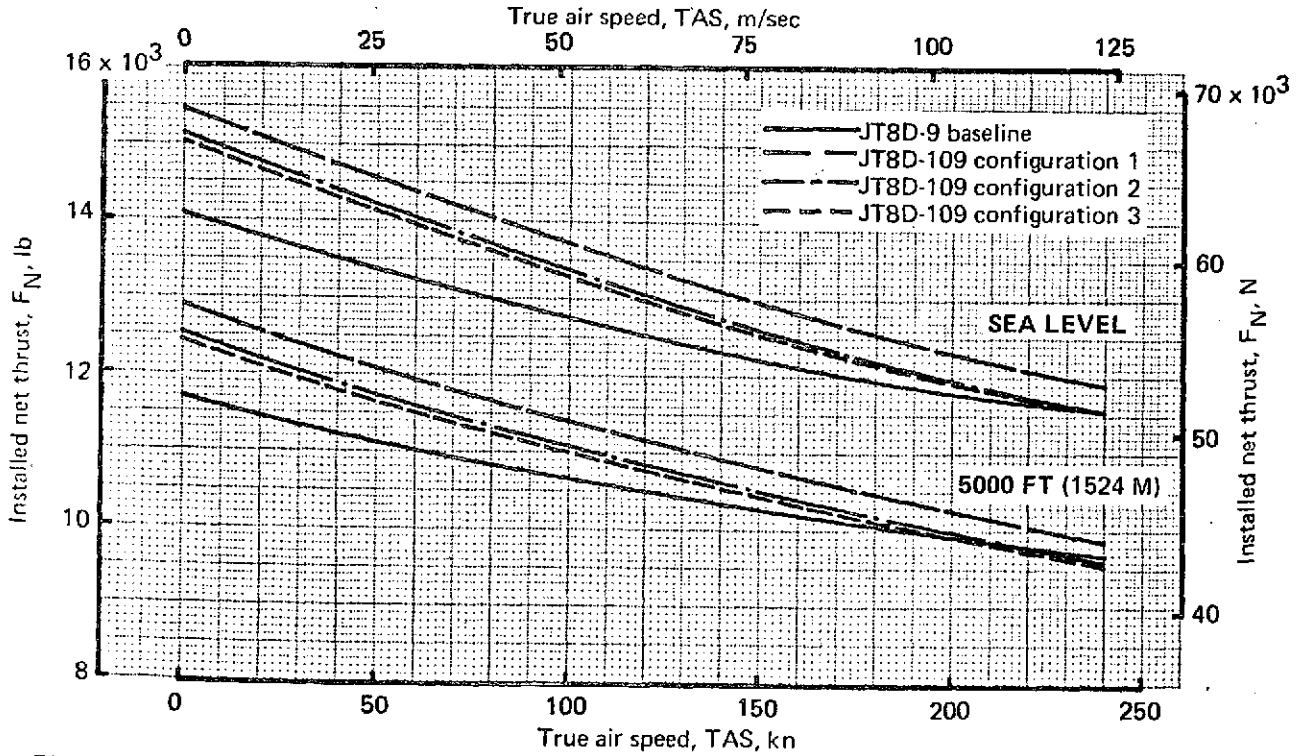


*FIGURE 83.—727/JT8D CENTER-ENGINE INSTALLED TAKEOFF THRUST LAPSE RATE COMPARISON, NO AIR CONDITIONING BLEED, 60 HP (44.7 KW) EXTRACTION, 84°F (302°K) DAY*

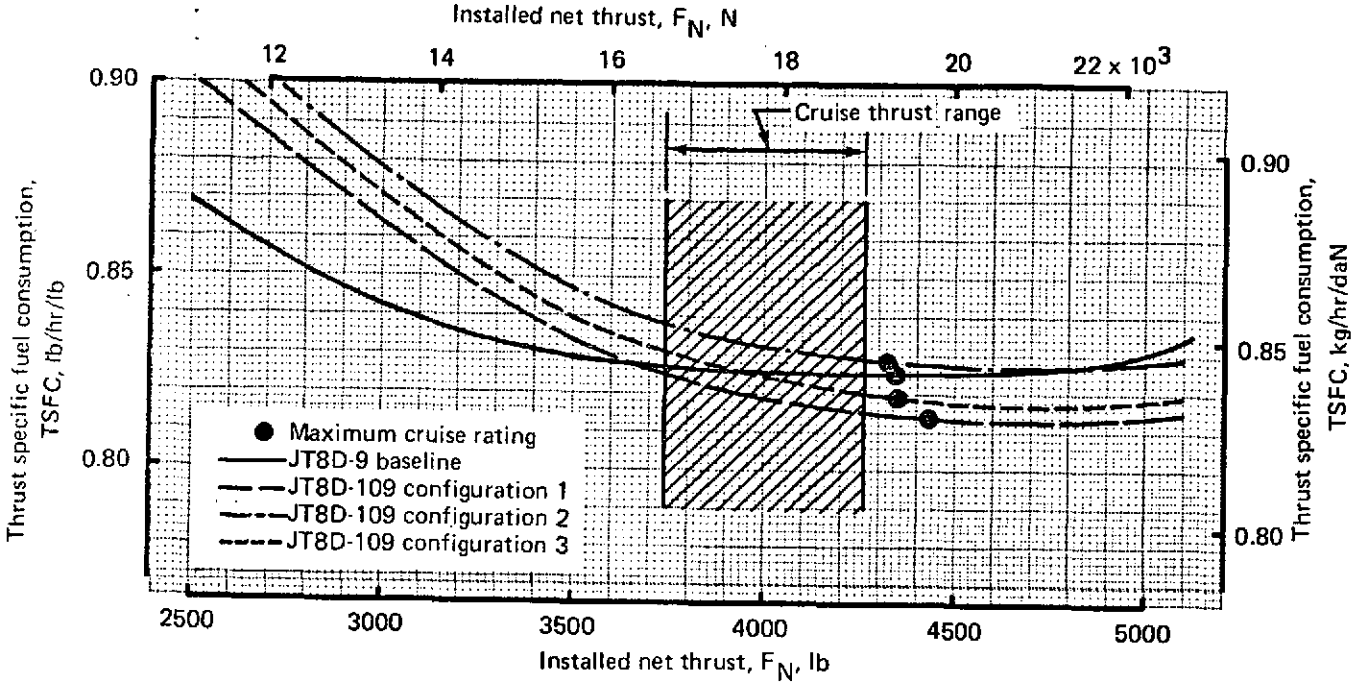


*FIGURE 84.–727/JT8D SIDE-ENGINE INSTALLED TSFC CRUISE PERFORMANCE, AIR CONDITIONING BLEED ON, 60 HP (44.7 KW) EXTRACTION, MACH 0.84 AT 30 000 FT (9144 M) STANDARD DAY*

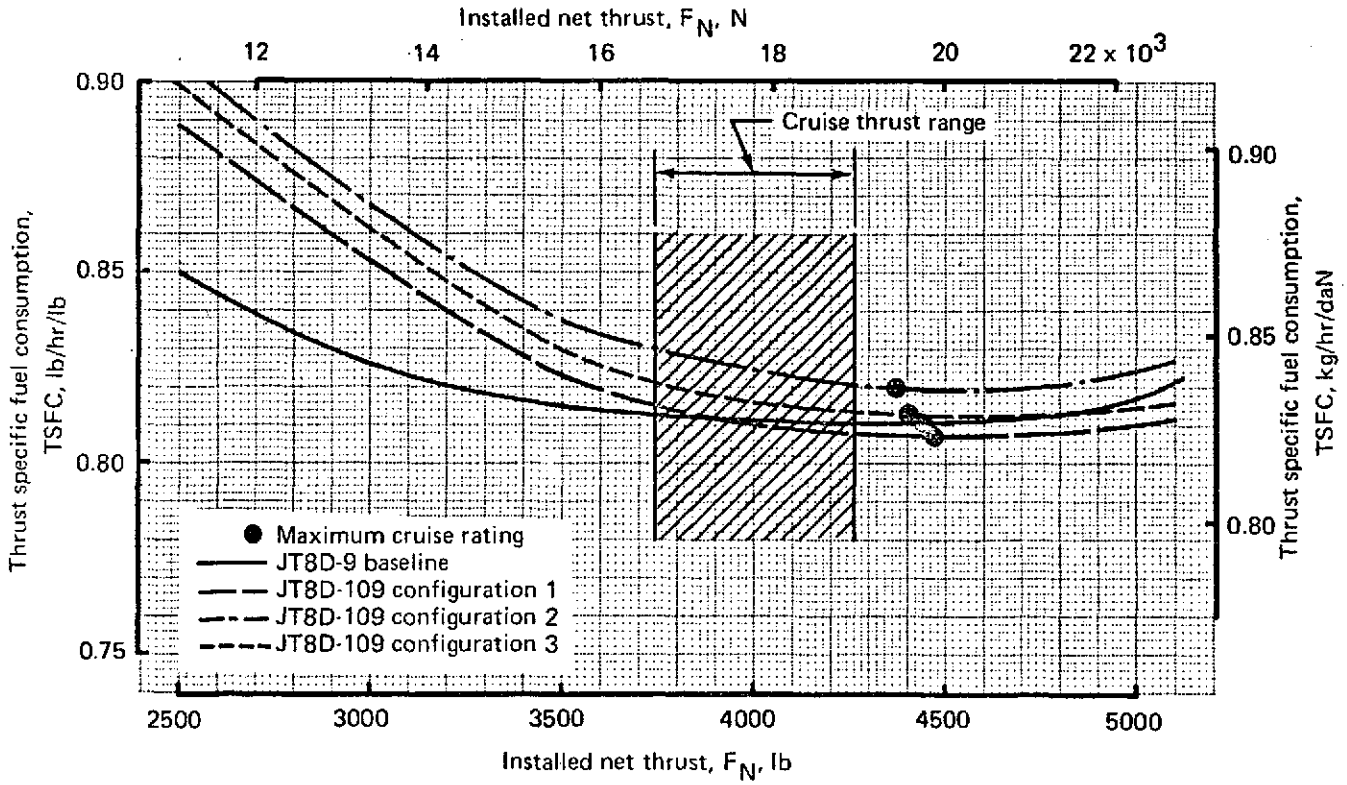


*FIGURE 85.–727/JT8D CENTER-ENGINE INSTALLED TSFC CRUISE PERFORMANCE, NO AIR CONDITIONING BLEED, 60 HP (44.7 KW) EXTRACTION, MACH 0.84 AT 30 000 FT (9144 M), STANDARD DAY*

*TABLE 26.—727/JT8D-109 CENTER-ENGINE INSTALLED INCREMENTAL LOSSES Δ TSFC/TSFC AT CRUISE[a]*

| Item | Configuration | | | | | |
|---|---|---|---|---|---|---|
| | 1 | | 2 | | 3 | |
| | Loss | ΔTSFC/TSFC, % | Loss | ΔTSFC/TSFC, % | Loss | ΔTSFC/TSFC, % |
| Inlet loss, ΔP/P | 0.019 | 2.1 | 0.025 | 2.7 | 0.029 | 3.2 |
| Power extraction | 60 hp (44.7 kW) | 0.5 | 60 hp (44.7 kW) | 0.5 | 60 hp (44.7 kW) | 0.5 |
| Nozzle velocity coefficient, $\Delta C_V$ | −0.003 | 0.7 | −0.008 | 1.8 | −0.001 | 0.2 |
| Total | | 3.3 | | 5.0 | | 3.9 |

[a]Mach = 0.84, 30 000 ft (9144 m), net thrust = 4000 lb (17 793 N)

Structurally, the baseline airplane maximum taxi weight can be increased up to 183 000 lb (83 009 kg) by making changes to the structure that weigh 160 lb (70 kg) and take 660 man-hours to incorporate. A kit is available to accomplish these changes, which include reinforcement of the body station 950 bulkhead; new brakes, wheels, and tires; higher level heat treatment of some gear components; and a change in fuel management to protect the wing from loss of fatigue life. For 727 airplane models other than this baseline, studies will be necessary to determine the extent of modifications required to accept any desired gross weight increase.

The installation of modified JT8D nacelles would result in a 2625 lb (1190 kg) to 3180 lb (1440 kg) weight increase and an aft OEW-cg shift of 7% to 8% MAC. A preliminary review of the 727 domestic fleet was made to scope the loadability problems resulting from the aft-cg shift.

The severity of the flight loadability problem is a function of OEW cg, passenger seating arrangement, and type of airline operation. Since these vary considerably from customer to customer, the magnitude of the problem would be different for each customer. This discussion considers a fleet-average airplane, having an average cg and interior arrangement.

The 7% to 8% MAC cg shift resulting from installation of the modified JT8D nacelle would cause the fleet-average airplane OEW cg to move 5% to 6% MAC aft of the flight-cg limit. A number of methods, listed below, would bring the cg back within the limits.

- Fixed ballast may be installed on the radome bulkhead to move the cg forward. This is the simplest fix, impacts operational procedures least, but penalizes payload/range performance and may require body monocoque reinforcement.

*TABLE 27.–727-200/JT8D BASELINE AIRPLANE WEIGHT BREAKDOWN*

| Component | lb | kg |
|---|---|---|
| Wing | 18 520 | 8 400 |
| Horizontal tail | 1 930 | 875 |
| Vertical tail | 2 220 | 1 005 |
| Body | 22 380 | 10 150 |
| Main landing gear | 6 520 | 2 955 |
| Nose landing gear | 1 140 | 515 |
| Nacelle and strut | 2 220 | 1 005 |
| Total structure | 54 930 | 24 915 |
| Engine | 9 680 | 4 390 |
| Engine accessories | 270 | 125 |
| Engine controls | 120 | 55 |
| Starting system | 150 | 70 |
| Fuel system | 1 210 | 550 |
| Thrust reverser | 1 580 | 715 |
| Total propulsion group | 13 010 | 5 900 |
| Instruments | 830 | 375 |
| Surface controls | 2 970 | 1 345 |
| Hydraulics | 1 430 | 650 |
| Pneumatics | – | – |
| Electrical | 2 420 | 1 100 |
| Electronics | 1 830 | 830 |
| Flight provisions | 890 | 405 |
| Passenger accommodations | 8 820 | 4 000 |
| Cargo handling | 1 090 | 405 |
| Emergency equipment | 1 100 | 500 |
| Air conditioning | 1 710 | 775 |
| Anti-icing | 490 | 220 |
| Auxiliary power unit | 850 | 385 |
| Total fixed equipment | 24 430 | 11 080 |
| Exterior paint | 100 | 45 |
| Options | 730 | 330 |
| Manufacturer's empty weight | 93 200 | 42 275 |
| Standard and operational items | 5 800 | 2 630 |
| Operating empty weight | 99 000 | 44 905 |

- Normal loading of passengers and baggage moves the cg forward, but a guaranteed high passenger load factor is required. For customers with existing aft-cg problems or customers with load factors that may at times be below the required number of passengers, other methods will be necessary to solve the problem.

- The forward cargo bay may be loaded with cargo or, if cargo is unavailable, with ballast to shift the cg forward.

## TABLE 28.–727-200/JT8D WEIGHT BREAKDOWN COMPARISON

| Component | Configuration | | | | | | | |
|---|---|---|---|---|---|---|---|---|
| | Baseline (JT8D-9) | | 1 (JT8D-109) | | 2 (JT8D-109) | | 3 (JT8D-109) | |
| | lb | kg | lb | kg | lb | kg | lb | kg |
| **Side engine** | | | | | | | | |
| Engine | 3 227 | 1464 | 3 797 | 1722 | 3 797 | 1722 | 3 797 | 1722 |
| Inlet | 120 | 54 | 181 | 82 | 266 | 121 | 308 | 140 |
| Cowl | 208 | 94 | 264 | 120 | 264 | 120 | 264 | 120 |
| Exhaust system | 524 | 238 | 607 | 275 | 678 | 308 | 671 | 304 |
| Accessories | 527 | 239 | 512 | 232 | 512 | 232 | 512 | 232 |
| Engine mounts | 131 | 59 | 145 | 66 | 145 | 66 | 145 | 66 |
| Strut and contents | 294 | 133 | 309 | 140 | 309 | 140 | 309 | 140 |
| Total weight per side engine | 5 031 | 2282 | 5 815 | 2638 | 5 971 | 2708 | 6 006 | 2724 |
| Total weight, side engines | 10 062 | 4564 | 11 630 | 5275 | 11 942 | 5417 | 12 012 | 5449 |
| **Center engine** | | | | | | | | |
| Engine | 3 227 | 1464 | 3 797 | 1722 | 3 797 | 1722 | 3 797 | 1722 |
| Center-inlet duct | 822 | 373 | 1 157 | 525 | 1 225 | 556 | 1 267 | 575 |
| Cowl | 232 | 105 | 275 | 125 | 275 | 125 | 275 | 125 |
| Exhaust system | 524 | 238 | 607 | 275 | 677 | 307 | 670 | 304 |
| Accessories | 527 | 239 | 512 | 232 | 512 | 232 | 512 | 232 |
| Engine mounts | 103 | 47 | 103 | 47 | 103 | 47 | 103 | 47 |
| Engine support beam | 264 | 120 | 305 | 138 | 305 | 138 | 305 | 138 |
| Total weight, center engine | 5 699 | 2585 | 6 756 | 3064 | 6 894 | 3127 | 6 929 | 3143 |
| Total engine installation weight per airplane | 15 761 | 7149 | 18 386 | 8340 | 18 836 | 8544 | 18 941 | 8591 |
| Propulsion weight change per airplane | Ref | Ref | +2 625 | +1191 | +3 075 | +1395 | +3 180 | +1442 |
| Airplane modifications | – | – | 100 | 45 | 150 | 68 | 150 | 68 |
| Ballast | – | – | 930 | 422 | 1 140 | 517 | 1 170 | 531 |
| Total OEW change | Ref | Ref | +3 655 | +1658 | +4 365 | +1980 | +4 500 | +2041 |

## TABLE 29.–727-200 CHARACTERISTICS

| Characteristic | Baseline airplane | Growth option |
|---|---|---|
| Operating empty weight | 99 000 lb (44 905 kg) | 99 160 lb (44 975 kg) |
| Operating empty weight | 40 % MAC (body station 932.5) | 40 % MAC (body station 932.5) |
| Maximum taxi weight | 173 000 lb (78 500 kg) | 183 000 lb (83 000 kg) |
| Maximum landing weight | | |
| 30° flaps | 150 000 lb (68 000 kg) | 154 500 lb (70 100 kg) |
| 40° flaps | 142 500 lb (64 650 kg) | 142 500 lb (64 650 kg) |
| Maximum zero-fuel weight | 136 000 lb (61 700 kg) | 138 000 lb (62 600 kg) |
| Passenger seating capacity | 134 (20 FC/114 TC) | 134 (20 FC/114 TC) |
| Fuel capacity | 7680 gal (29.000 $m^3$) | 7780 gal (29.400 $m^3$) |
| Interior | Two-class seating, typical galley and furnishings arrangement | Two-class seating, typical galley and furnishings arrangement |
| Engine | JT8D-9 | JT8D-9 |

- Seating may be restricted to prevent passengers from sitting in the aft portion of the airplane until the forward seats are filled.

- Wing center tank fuel may be carried as ballast to move the cg forward. Fuel used for ballast in unavailable for use during flight.

- Airplane configuration changes can be made to shift the cg forward. For example, deletion of the aft airstair results in a 1% MAC shift, or moving an 800-lb (360-kg) galley from an aft position to a forward position results in a 4% MAC shift.

- Removable ballast may be carried in the nose wheelwell.

While all of the methods listed above are technically feasible, most involve economic or operational penalties to the customer. Cost evaluation trade studies must be conducted to determine the loadability solutions that result in the least economic penalty to the various customer configurations.

The cg shift resulting from installation of the modified JT8D nacelle would also require that more attention be given during ground handling to ensure that the airplane would be stable with respect to ground tipping.

The methods discussed above in connection with the flight-cg problem can also be used to stabilize the airplane on the ground. For instance, the fleet-average airplane could be placed in a stable ground-handling condition with the addition of center-tank fuel.

In addition to the above methods in a static condition, the aft airstair can be deployed to prevent tipping. The present design allows the tail to drop 14 in. (0.356 m) before "bottoming out" to prevent further tipping, but the design could be modified so that the airstair would provide a positive tail stand. The airplane can also be stabilized through the use of special ground equipment such as a tail stand or an external weight to hang on the nose gear or forward body.

In the final analysis, a case-by-case examination by the airlines will be required to determine the most cost-effective operating procedure for a particular route.

The 727-100 has a less severe weight and balance problem, primarily because it has a more forward fleet-average OEW cg. However, some customer airplanes will require some balance correction, and in those cases the same methods used to correct the 727-200 balance may be applied to the 727-100.

### 4.7.3 Airplane Performance

The takeoff and cruise performance characteristics for modified configurations, relative to baseline airplane performance, are shown in figures 86 through 88.

The performance loss due to increased OEW of the modified configurations can be offset by the improved thrust of the refanned engines, which permits a heavier gross weight takeoff. Figure 86 shows that all three modified configurations can experience a significant gross weight increase without increasing takeoff field length. This weight increase can be used as additional fuel to improve the airplane's range capability. Figure 87 shows the payload/range comparison for the baseline and refanned engines, while figure 88 shows the range/field-length trade. These latter two figures show that the increased gross weight would enhance the range/payload situation for all configurations at the higher payload long-range missions, and that range can be increased for a given field length for configuration 1 and for a slightly increased field length for configurations 2 and 3.

This gross weight increase analysis applies only to the baseline 727-200, 172 500 lb (78 246 kg) gross weight airplane. Further studies will be necessary to determine the extent of modification required for other 727 models to achieve any desired gross weight increase.

### 4.7.4 Stability and Control

The larger nacelles of the modified configuration would affect the stall characteristics of the airplane. An assessment of the effect will be made upon completion of wind tunnel testing to be conducted during phase II of the program.

Preliminary estimates of cruise unaugmented dutch roll damping indicate a 1000-ft (305-m) reduction in the one yaw damper inoperative altitude placard. The baseline airplane placard is 30 000 ft (9144 m). A more detailed analysis will be made following wind tunnel testing.

The new nacelles are not expected to signifcantly change the static longitudinal stability (speed stability) characteristics of the airplane.

### 4.7.5 Flutter

The flutter analysis of the airplane with the modified JT8D-109 nacelle considered the effects of nacelle and strut weight, inertia, and pitch-and-roll frequency. This configuration shows satisfactory airplane flutter stability. Some changes in aft-fuselage/fin stiffnesses are expected, due to center-duct modifications. No significant changes in flutter speed or stability and control characteristics are expected, but this will be verified when the structural analysis is complete.

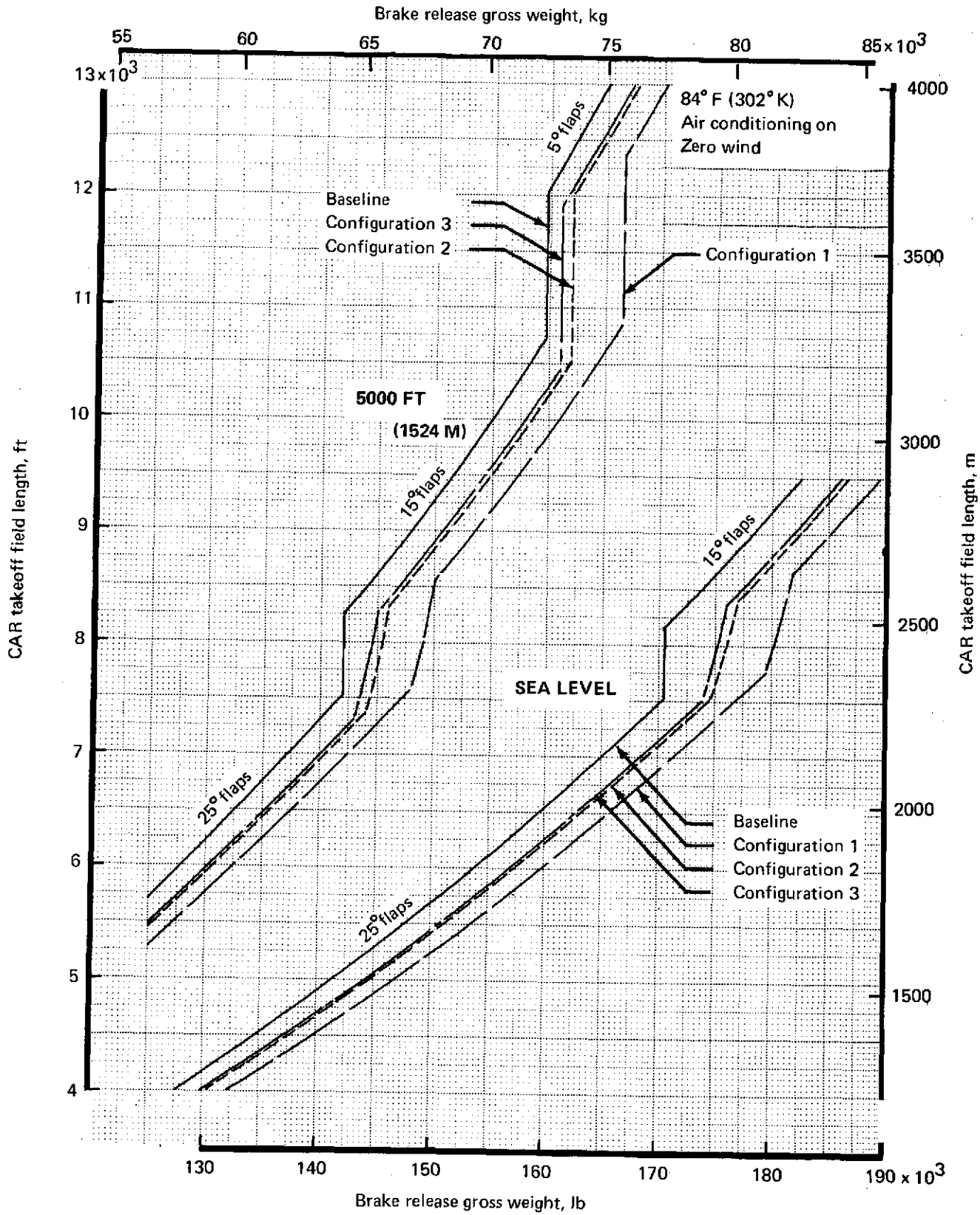


*FIGURE 86.—727/JT8D TAKEOFF FIELD LENGTH COMPARISON*

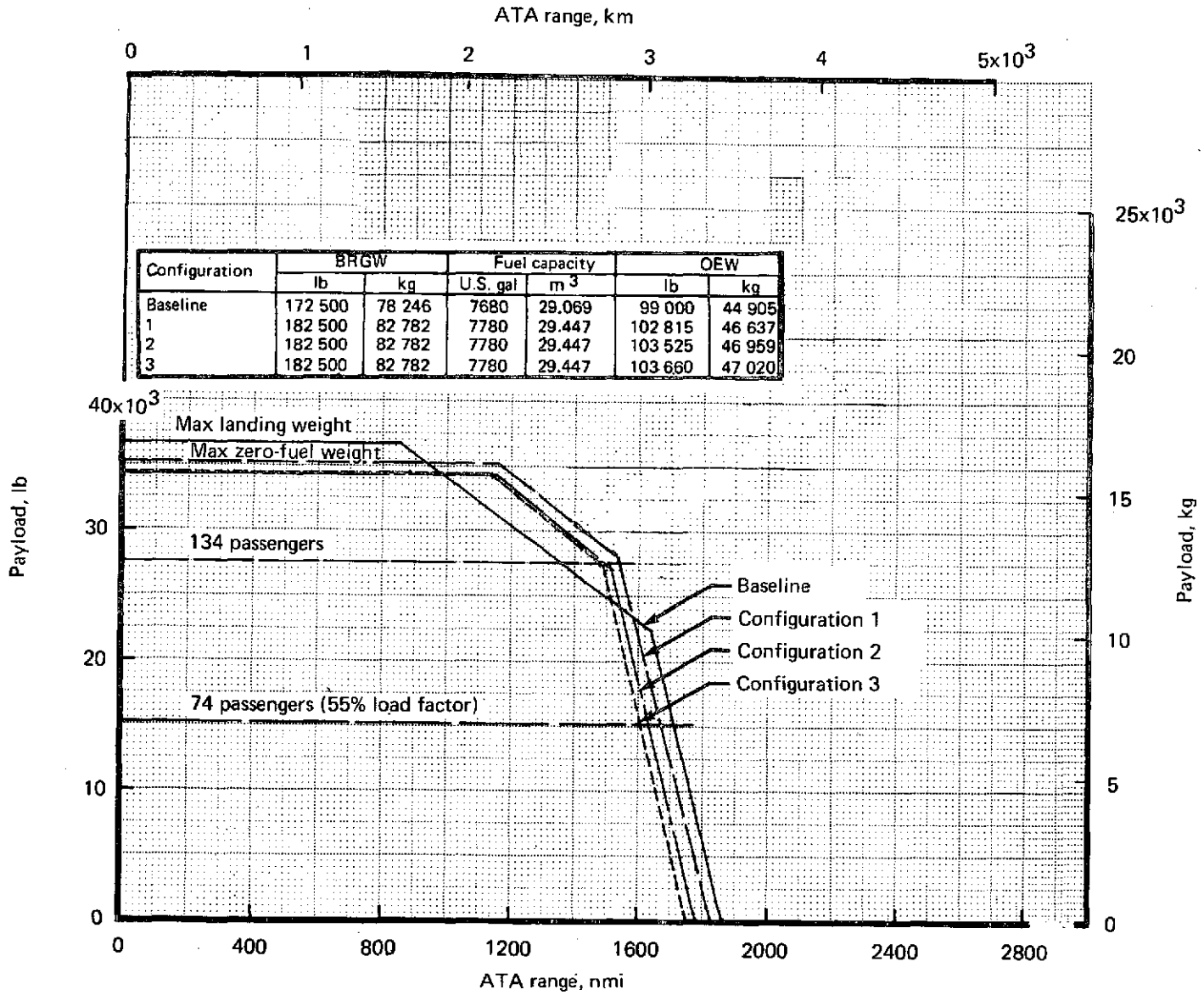


| Configuration | BRGW | | Fuel capacity | | OEW | |
|---|---|---|---|---|---|---|
| | lb | kg | U.S. gal | $m^3$ | lb | kg |
| Baseline | 172 500 | 78 246 | 7680 | 29.069 | 99 000 | 44 905 |
| 1 | 182 500 | 82 782 | 7780 | 29.447 | 102 815 | 46 637 |
| 2 | 182 500 | 82 782 | 7780 | 29.447 | 103 525 | 46 959 |
| 3 | 182 500 | 82 782 | 7780 | 29.447 | 103 660 | 47 020 |

*FIGURE 87.—727/JT8D PAYLOAD RANGE COMPARISON AT MACH 0.84, 30 000 FT (9144 M) ZERO WIND, ATA DOMESTIC RESERVES*

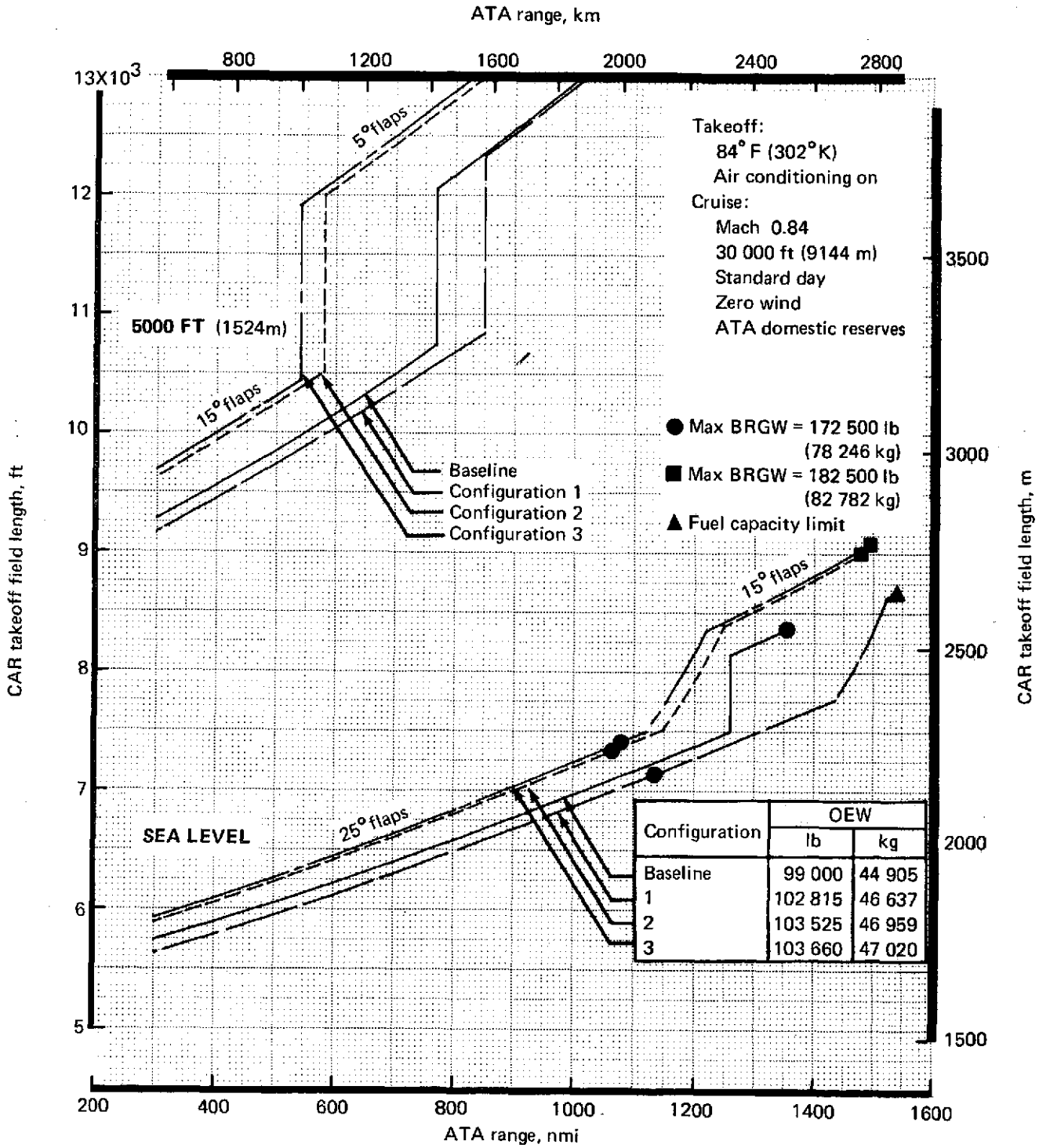


| Configuration | OEW | |
|---|---|---|
| | lb | kg |
| Baseline | 99 000 | 44 905 |
| 1 | 102 815 | 46 637 |
| 2 | 103 525 | 46 959 |
| 3 | 103 660 | 47 020 |

*FIGURE 88.–727/JT8D FIELD LENGTH RANGE COMPARISON (134 PASSENGERS)*

## 4.8 AIRPLANE AND COMMUNITY NOISE CHARACTERISTICS

The initial noise design analyses for all three JT8D-109 modified configurations on the 727-200 airplane are presented in this section. These analyses exclude low-frequency core noise and sources considered to be of secondary importance relative to total airplane noise. Also, any change in interior noise has not been investigated.

### 4.8.1 Nacelle Acoustic Preliminary Design

Initial designs were made for three levels of acoustic suppression designated configurations 1, 2, and 3. The main features of the configurations were as follows: in configuration 1 (see fig. 89), inlet acoustic treatment was applied to the inlet diffuser and nose dome, fan duct treatment was that prescribed by the engine contractor, and tailpipe treatment was peripheral. In configuration 2 (see fig. 90), the inlet treatment included, in addition to diffuser and nose dome treatment, a treated inlet ring; the fan duct treatment included, in addition to the engine-contractor-prescribed treatment, acoustic linings in areas judged amenable to additional treatment. The tailpipe treatment included peripheral acoustic lining on the outer wall, the external and internal surfaces of the primary/secondary-flow splitter, and the tail plug. In configuration 3 (see fig. 91), the inlet included in addition to diffuser and nose dome treatment, two treated inlet rings; the fan duct treatment was the same as that of configuration 2. The tailpipe acoustic treatment consisted of peripheral acoustic lining and a primary/secondary-flow mixer for jet noise reduction. Lining attenuation spectra are shown in figures 92 and 93.

Inlet and tailpipe acoustic treatments were designed for the JT8D-109 engine powering the 727-200. The design point was the FAR Part 36 approach point for a landing weight of 142 500 lb (64 637 kg). The aircraft was assumed in the landing configuration with 6310 lb (28 068 N) net thrust, 40° flap position, 139 kn (71.5 m/sec) true airspeed, and 370 ft (113 m) altitude at the FAR Part 36 approach point. The inlet and tailpipe linings were tuned for the fan fundamental blade passage frequency.

### 4.8.2 Noise/Thrust/Altitude Curves

EPNL levels were predicted as a function of altitude and thrust setting for the various configurations investigated. In order to provide a common basis for comparisons, all calculations were performed at constant true airspeed and each altitude corresponded to an airplane level flyover.

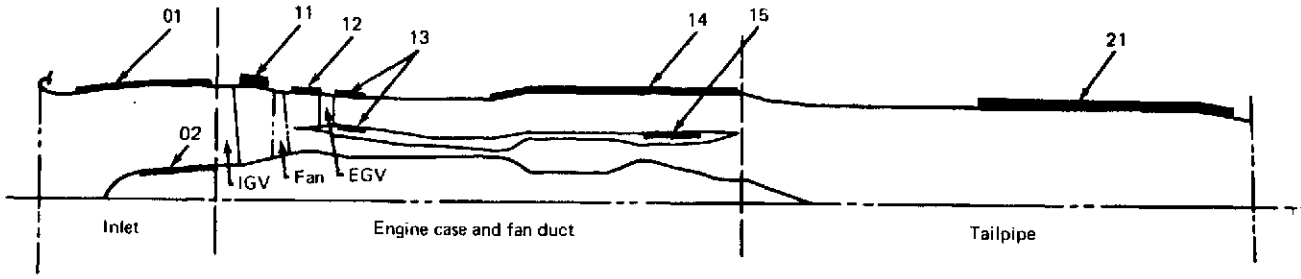


| Lining designation | Location | Face sheet type | Net active treatment area, ft$^2$ (m$^2$) | Core depth, in. (m) | Cell size, in. (m) | Design point, $R/\rho c$ | Open area, % | Hole dia., in. (m) | Face sheet thickness, in. (m) |
|---|---|---|---|---|---|---|---|---|---|
| Inlet | | | | | | | | | |
| 1-01 | Difusser | Polyimide | 31.6 (2.936) | 0.18* (0.0046) | 0.25 (0.0064) | 1.6 | | | |
| 1-02 | Nose dome | ↓ | 5.3 (0.492) | 0.18 (0.0046) | 0.25 (0.0064) | 1.6 | | | |
| Engine case and fan duct | | | | | | | | | |
| 1-11 | Fwd of fan | Perforated sheet | 6.6 (0.613) | 1.00 (0.0254) | 0.375 (0.0095) | | 20 | 0.050 (0.0013) | 0.016 (0.0004) |
| 1-12 | Aft of fan | ↓ | 6.2 (0.576) | 0.50 (0.0127) | 0.375 (0.0095) | | 12 | 0.050 (0.0013) | 0.016 (0.0004) |
| 1-13 | Aft of EGV | ↓ | 8.8 (0.818) | 0.25 (0.0064) | 0.375 (0.0095) | | 12 | 0.050 (0.0013) | 0.016 (0.0004) |
| 1-14 | Outer wall aft | ↓ | 61.7 (5.732) | 0.50 (0.0127) | 0.375 (0.0095) | | 12 | 0.050 (0.0013) | 0.016 (0.0004) |
| 1-15 | Inner wall aft | ↓ | 7.0 (0.650) | 0.50 (0.0127) | 0.375 (0.0095) | | 12 | 0.050 (0.0013) | 0.016 (0.0004) |
| Tailpipe | | | | | | | | | |
| 1-21 | Outer wall | Perforated sheet | 48.0 (4.459) | 0.25 | 0.375 (0.0095) | | 3.5 | 0.040 (0.0010) | 0.020 (0.0005) |

*Allow up to 2 in. (0.0508 m) core depth for buzz-saw treatment.

*FIGURE 89.—727/JT8D ACOUSTIC LINING DEFINITION, CONFIGURATION 1*

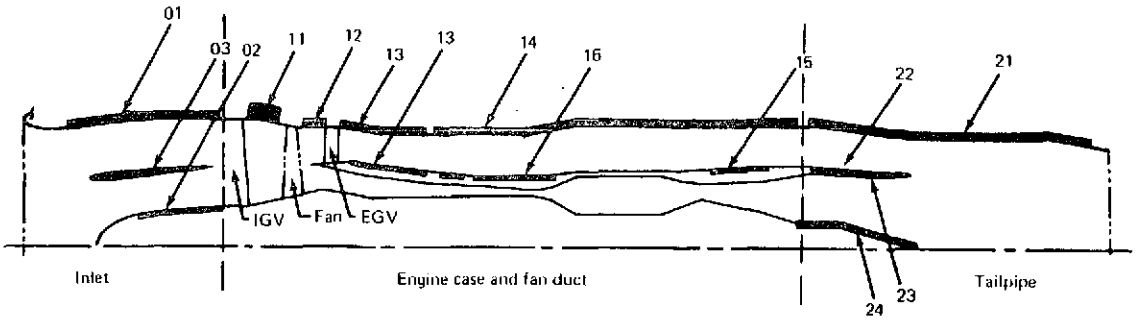


| Lining designation | Location | Face sheet type | Net active treatment area, ft$^2$ (m$^2$) | Core depth, in. (m) | Cell size, in. (m) | Design point, $R/\rho c$ | Open area, % | Hole dia., in. (m) | Face sheet thickness, in. (m) |
|---|---|---|---|---|---|---|---|---|---|
| | | | Inlet | | | | | | |
| 1-01 | Diffuser | Polyimide | 31.0 (2.880) | 0.21* (0.0053) | 0.25 (0.0064) | 1.3 | | | |
| 1-02 | Nose dome | | 4.0 (0.372) | 0.21 (0.0053) | 0.25 (0.0064) | 1.3 | | | |
| 2-03 | Ring | | 11.0, 11.0++ (1.022) (1.022) | 0.21 (0.0053) | 0.25 (0.0064) | 1.3 | | | |
| | | | Engine case fan duct | | | | | | |
| 2-11 | Fwd of fan | Perforated sheet | 8.2 (0.762) | 1.0 (0.0254) | 0.375 (0.0095) | | 20 | 0.050 (0.0013) | 0.016 (0.0004) |
| 2-12 | Aft of fan | | 6.2 (0.576) | 0.50 (0.0127) | 0.375 (0.0095) | | 12 | 0.050 (0.0013) | 0.016 (0.0004) |
| 2-13 | Aft of EGV | | 21.8 (2.025) | 0.25 (0.0064) | 0.375 (0.0095) | | 12 | 0.050 (0.0013) | 0.016 (0.0004) |
| 2-14 | Outer wall aft | | 78.1 (7.255) | 0.50 (0.0127) | 0.375 (0.0095) | | 12 | 0.050 (0.0013) | 0.016 (0.0004) |
| 2-15 | Inner wall aft | | 7.0 (0.650 | 0.50 (0.0127 | 0.375 (0.0095) | | 12 | 0.050 (0.0013) | 0.016 (0.0004) |
| 2-16 | Inner wall | | 11.7 (1.087) | 0.50 (0.0127) | 0.375 (0.0095) | | 12 | 0.050 (0.0013) | 0.016 (0.0004) |
| | | | Tailpipe | | | | | | |
| 2-21 | Outer wall | Perforated sheet | 48.0 (4.459) | 0.35 (0.0089) | 0.375 (0.0095) | | 6 | 0.040 (0.0010) | 0.020 (0.0005) |
| 2-22 | Splitter out | | 21.9 (2.035) | 0.35 (0.0089) | 0.375 (0.0095) | | 6 | 0.040 (0.0010) | 0.020 (0.0005) |
| 2-23 | Splitter in | | 19.4 (1.802) | 0.55 (0.0140) | 0.375 (0.0095) | | 6 | 0.040 (0.0010) | 0.020 (0.0005) |
| 2-24 | Tail plug | | 5.5 (0.511) | 0.55 (0.0140) | 0.375 (0.0095) | | 6 | 0.040 (0.0010) | 0.020 (0.0005) |

++ Treatment on both sides of ring.
*Allow up to 2 in. (0.0508 m) core depth for buzz-saw treatment.

*FIGURE 90.—727/JT8D ACOUSTIC LINING DEFINITION, CONFIGURATION 2*

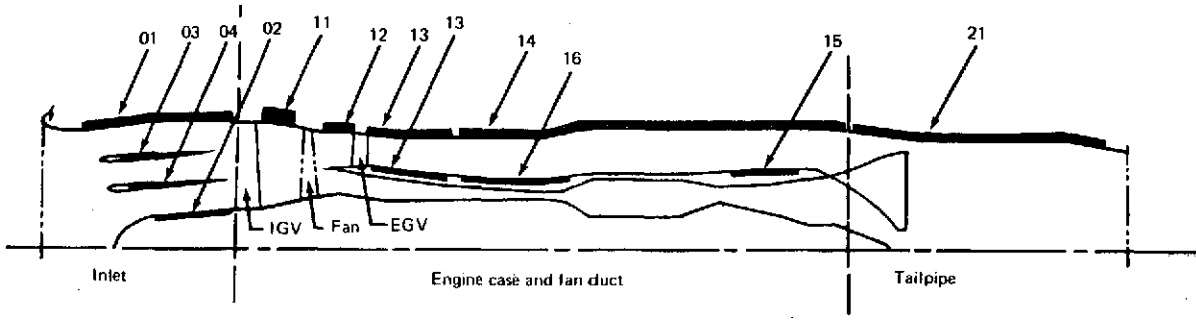


| Lining designation | Location | Face sheet type | Net active treatment area, ft$^2$ (m$^2$) | Core depth, in. (m) | Cell size, in. (m) | Design point, $R/\rho c$ | Open area, % | Hole dia., in. (m) | Face sheet thickness, in. (m) |
|---|---|---|---|---|---|---|---|---|---|
| | | | | Inlet | | | | | |
| 2-01 | Diffuser | Polyimide | 31.0 (2.880) | 0.23* (0.0058) | 0.25 (0.0064) | 1.1 | | | |
| 3-02 | Nose dome | ↓ | 4.0 (0.372) | 0.23 (0.0058) | 0.25 (0.0064) | 1.1 | | | |
| 3-03 | Outer ring | ↓ | 12.0, 12.0†† (1.115) (1.115) | 0.23 (0.0058) | 0.25 (0.0064) | 1.1 | | | |
| 3-04 | Inner ring | ↓ | 8.0, 8.0†† (0.743) (0.743) | 0.23 (0.0058) | 0.25 (0.0064) | 1.1 | | | |
| | | | | Engine case fan duct | | | | | |
| 3-11 | Fwd of fan | Perforated sheet | 8.2 (0.762) | 1.0 (0.0254) | 0.375 (0.0095) | | 20 | 0.050 (0.0013) | 0.016 (0.0004) |
| 3-12 | Aft of fan | ↓ | 6.2 (0.576) | 0.50 (0.0127) | 0.375 (0.0095) | | 12 | 0.050 (0.0013) | 0.016 (0.0004) |
| 3-13 | Aft of EGV | ↓ | 21.8 (2.025) | 0.25 (0.0064) | 0.375 (0.0095) | | 12 | 0.050 (0.0013) | 0.016 (0.0004) |
| 3-14 | Outer wall aft | ↓ | 78.1 (7.255) | 0.50 (0.0127) | 0.375 (0.0095) | | 12 | 0.050 (0.0013) | 0.016 (0.0004) |
| 3-15 | Inner wall aft | ↓ | 7.0 (0.650) | 0.50 (0.0127) | 0.375 (0.0095) | | 12 | 0.050 (0.0013) | 0.016 (0.0004) |
| 3-16 | Inner wall | | 11.7 (1.087) | 0.50 (0.0127) | 0.375 (0.0095) | | 12 | 0.050 (0.0013) | 0.016 (0.0004) |
| | | | | Tailpipe | | | | | |
| 3-21 | Outer wall | Perforated sheet | 48.0 (4.459) | 0.25 (0.0064) | 0.375 (0.0095) | | 4 | | |

†† Treatment on both sides of rings.

* Allow up to 2 in. (0.0508 m) core depth for buzz-saw treatment.

*FIGURE 91.–727/JT8D ACOUSTIC DEFINITION, CONFIGURATION 3*

$H_e$ = Effective duct height

$L/H = \frac{\text{Duct length}}{\text{Duct height}}$

$H/C = \frac{\text{Duct height}}{\text{Local speed of sound}}$

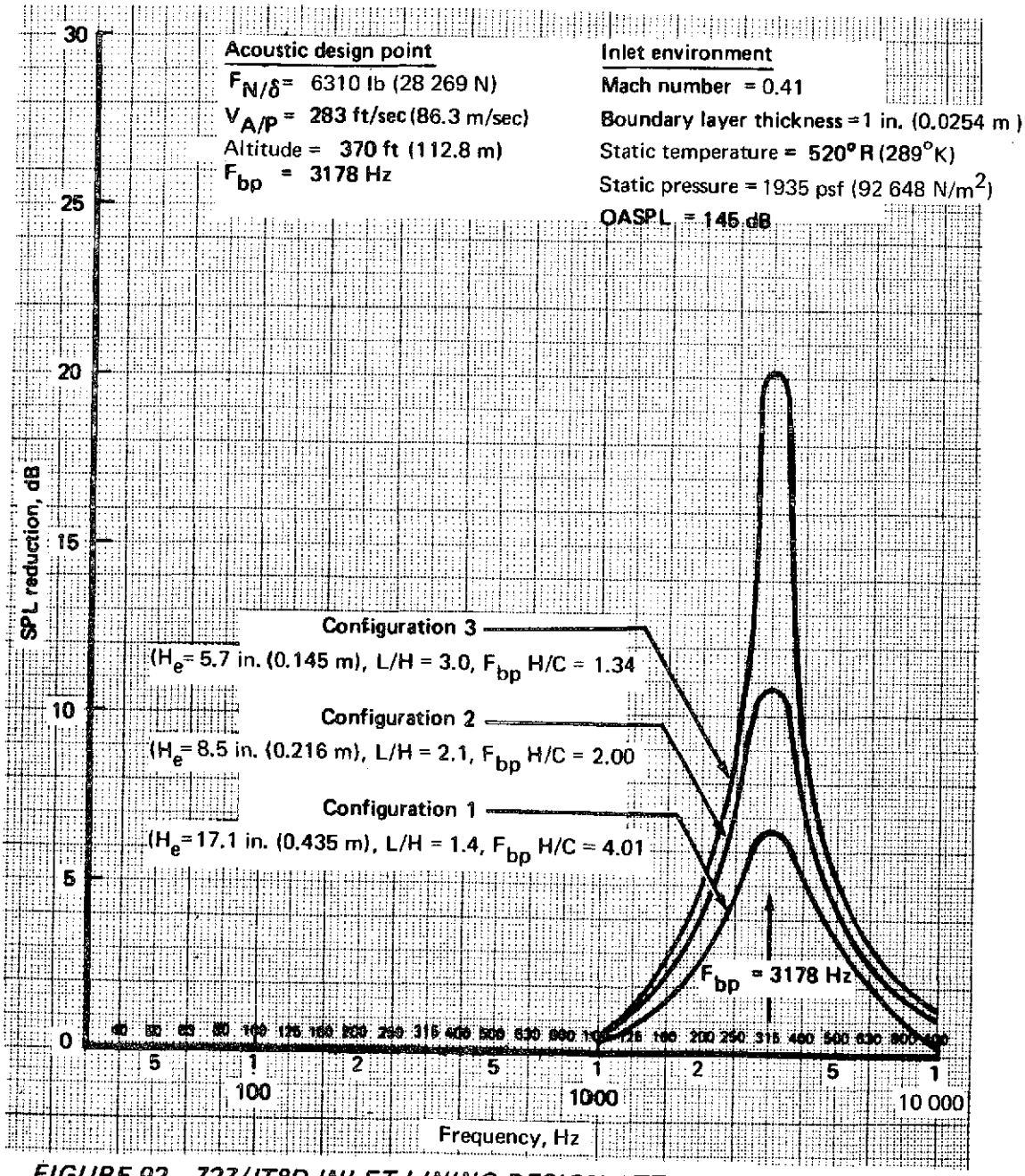


*FIGURE 92.–727/JT8D INLET LINING DESIGN ATTENUATION SPECTRA*

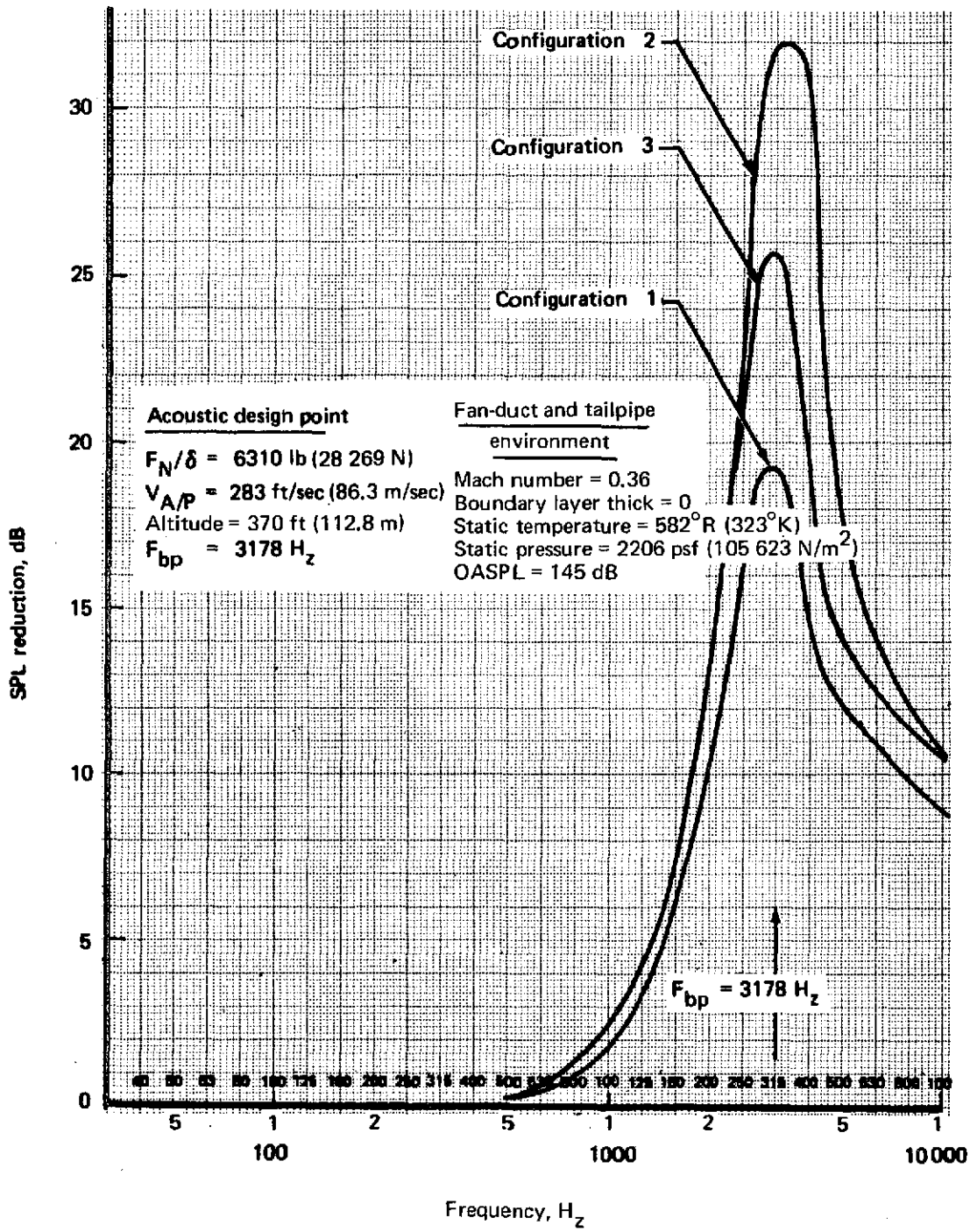


*FIGURE 93.—727/JT8D AFT FAN AND TAILPIPE LINING DESIGN ATTENUATION SPECTRA*

#### 4.8.2.1 Calculation Method

Airplane noise levels for the various configurations were predicted by using the contractor's prediction computer programs. These programs predicted EPNL levels by considering engine component noise sources and their attenuation. The component noise sources used were the inlet fan (including buzz-saw), exhaust fan, and jet. Each component noise source and attenuation prediction resulted in a complete matrix of one-third-octave-band sound pressure levels over appropriate directivity angles.

The source noise component SPL matrices were calculated from engine cycle data as a function of corrected net thrust for reference engine conditions. Untreated source noise estimates were based on semiempirical prediction models. Inlet and aft fan noise were related to the fan pressure ratio, fan rotor speed, fan geometry, and the inlet and fan duct design. The jet noise level varied with primary and secondary exhaust stream relative velocity, exhaust areas, and densities. Corrections were made to jet noise level to account for bypass ratio effects. For the mixer nozzle of configuration 3, complete mixing of the jet streams was assumed, and the noise was calculated for a single jet with mixed properties.

Lining attenuation matrices of each component were calculated for each power setting by using lining design parameters selected for the design condition. These design parameters were obtained using lining design computer programs in which nacelle internal geometry and aerodynamic and acoustic parameters were inputs. Attenuation matrices were then subtracted from the untreated SPLs to obtain the treated SPLs.

The SPL summation of resulting noise components was extrapolated to desired altitudes by considering spherical divergence, aircraft installation effects, atmospheric attenuation (SAE ARP866), and extra ground attenuation. These data were then combined with flight speed information to establish flyover time history and the resulting EPNL.

To incorporate airplane installation and in-flight effects, the noise prediction procedure described above was related to existing 727 flight data in two steps. First, SPL adjustments were made in each component, so that these components agree with JT9D-9 hardwall flight test data at critical angles and power settings. Then, a final, small EPNL adjustment was made, so that the procedure and the flight data agree on an EPNL basis. These component SPL and airplane EPNL adjustments were then applied to the JT8D-109 modified-nacelle configurations.

#### 4.8.2.2 Results

EPNL versus altitude plots were developed for a number of corrected net thrust values and are presented in figures 94 through 98. A comparison of figures 94 and 95 shows substantial EPNdB noise reduction due to the change in engine cycle without acoustic treatment attenuation. Addition of nacelle and engine acoustic treatment in the three refan configurations results in further reductions, depending on thrust, altitude, and configuration.

Comparison of the noise levels for the three modified-nacelle configurations with lining attenuation (figs. 96, 97, and 98) shows that, at low altitude, configuration 2 is 1 to 2 EPNdB lower than configuration 1, and configuration 3 is 0 to 2 EPNdB lower than configuration 2. At high altitudes, configuration 2 has a higher noise level than configuration 1, because configuration 2 requires higher jet velocities than configuration 1 to achieve the same corrected net thrust. Comparisons of configurations 1 and 2 with configuration 3 at high altitudes show reductions as large as 7 EPNdB resulting from the jet noise reduction attributed to the mixer. However, it is emphasized that the assumed mixer nozzle technology would require a development program if it is to be realized.

### 4.8.3 Noise Levels at FAR Part 36 Conditions

The noise estimates of phase I are probably optimistic by 1 to 4 EPNdB because of low frequency core noise; however, the more comprehensive estimates made in phase II are also expected to show very significant noise reduction relative to the baseline airplane.

#### 4.8.3.1 Calculation Method

For the hardwall baseline JT8D-9, the FAR Part 36 EPNLs were based on flight tests performed according to FAR Part 36 procedures. *Small differences exist between these EPNLs and the noise-thrust-altitude plots,* which were calculated from level flyover tests. The FAR Part 36 EPNLs for the JT8D-109 refanned engine were calculated by starting with the corresponding JT8D-9 baseline FAR Part 36 levels and superimposing the noise level increments, between hardwall baseline and modified airplane, derived analytically from the noise-thrust-altitude curves. (For the sideline FAR Part 36 JT8D-109 EPNLs, a more sophisticated method, which considers extra ground attenuation and shielding, was used to calculate the increments.) In this manner, the modified-airplane FAR Part 36 levels quoted represent the EPNL reductions analytically predicted for the modified airplanes with respect to the FAR Part 36 established JT8D-9 baseline flight data.

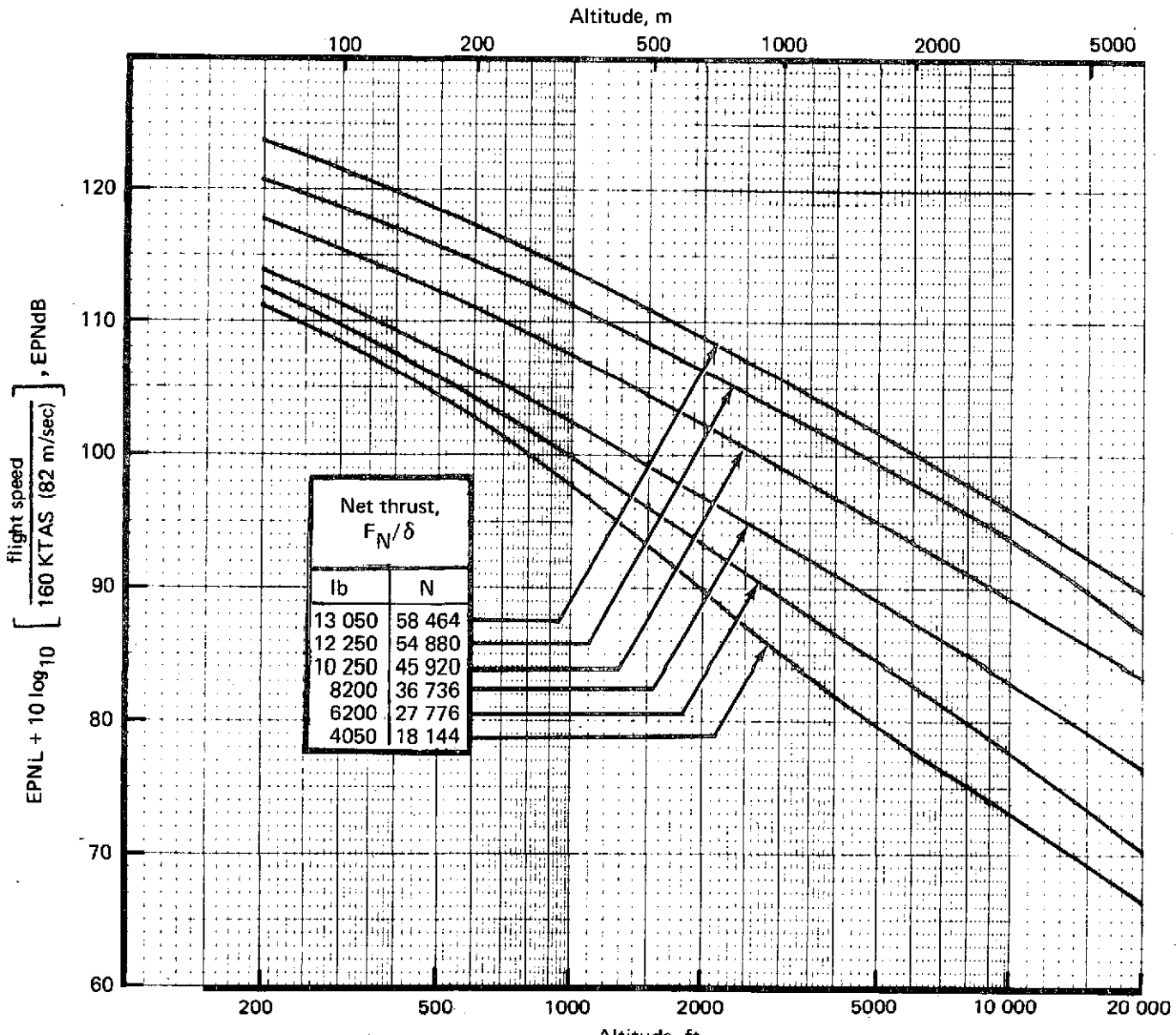


*FIGURE 94.—727/JT8D-9 BASELINE (HARDWALL) NOISE/THRUST/ALTITUDE CURVES, NOISE EXTRAPOLATION CONDITIONS, 77° F (298° K), RELATIVE HUMIDITY 70%*

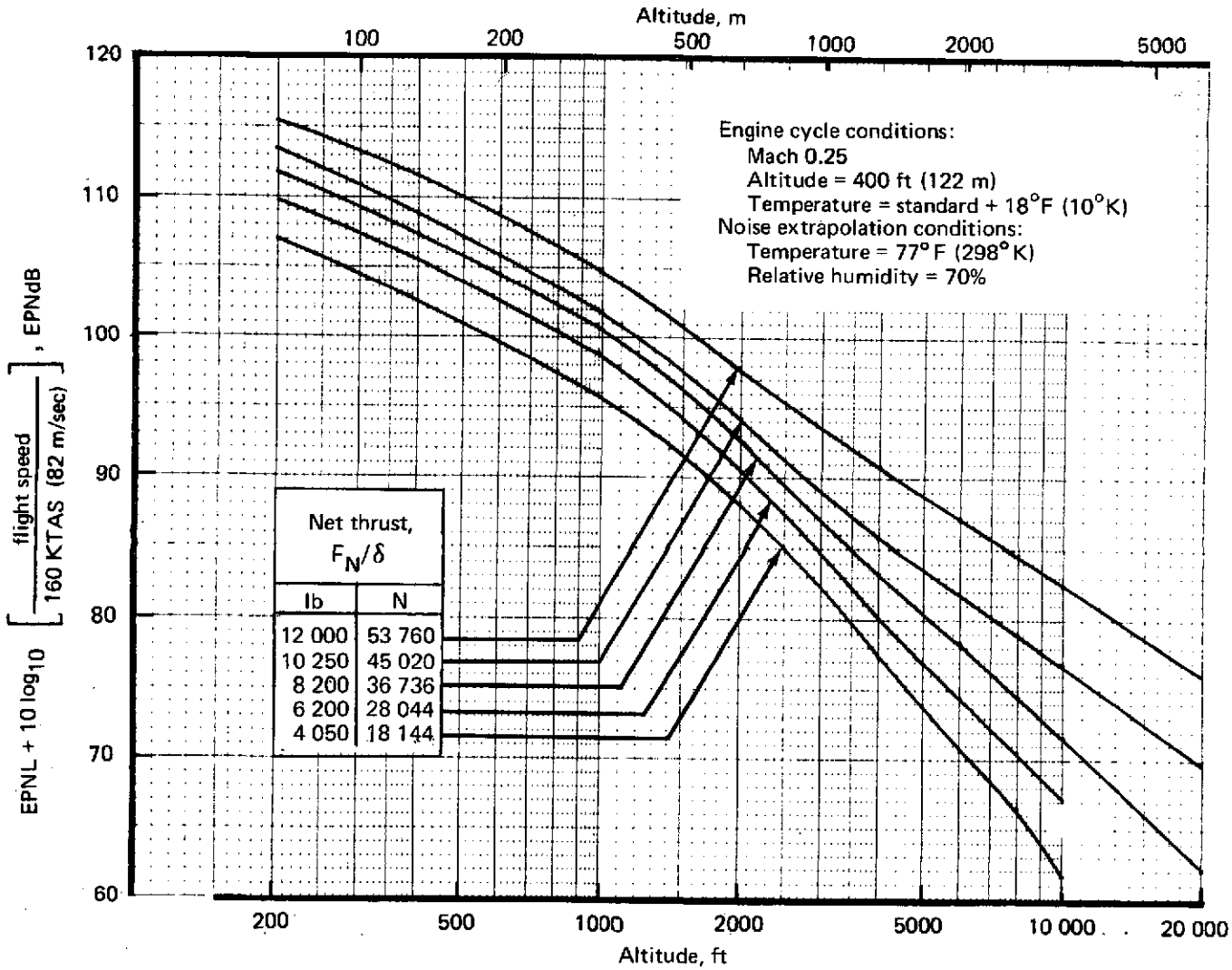


*FIGURE 95.—727/JT8D-109 CONFIGURATION 1 (HARDWALL)-NOISE/THRUST/ALTITUDE CURVES*

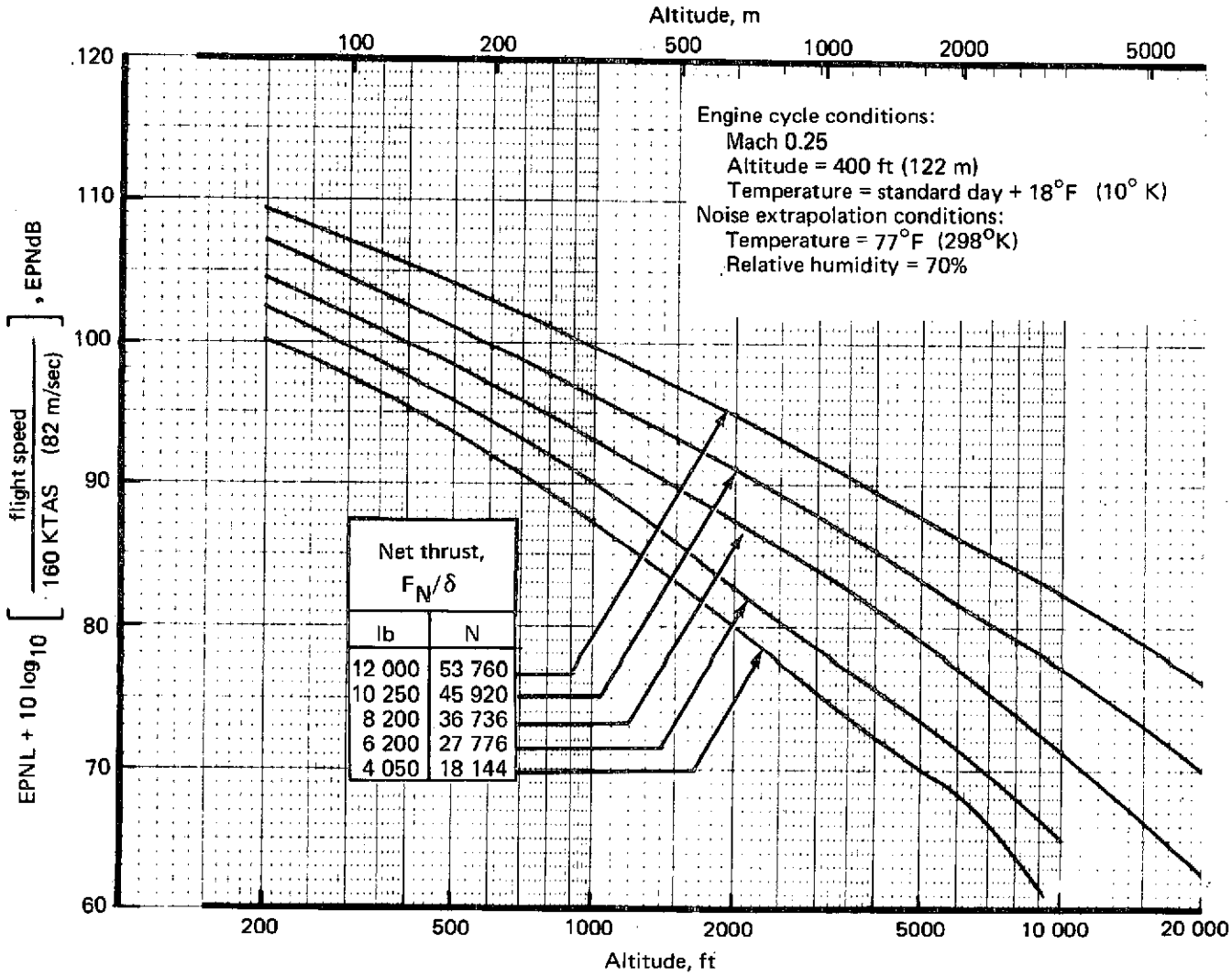


*FIGURE 96.—727/JT8D-109 CONFIGURATION 1—NOISE/THRUST/ALTITUDE CURVES*

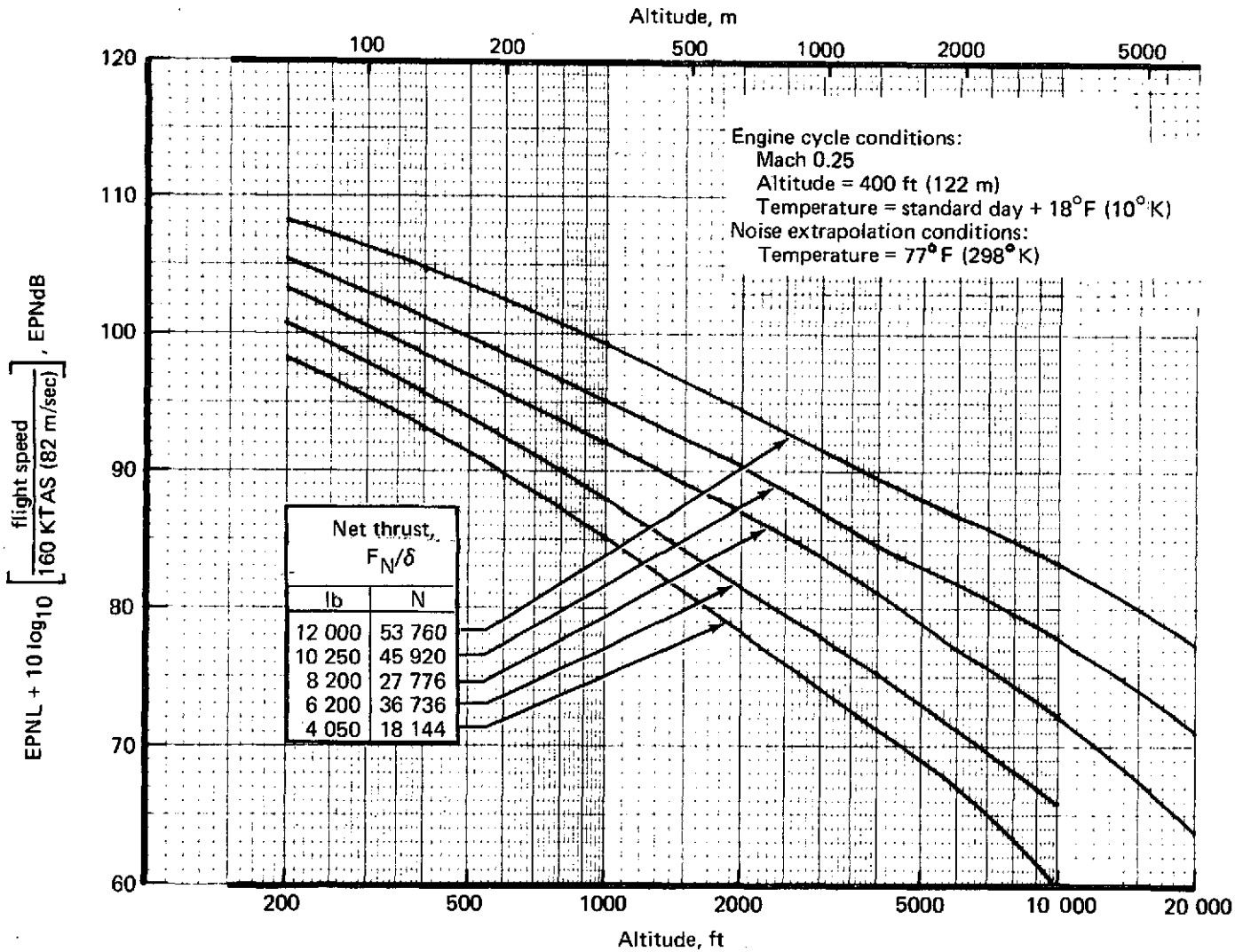


*FIGURE 97.—727/JT8D-109 CONFIGURATION 2—NOISE/THRUST/ALTITUDE CURVES*

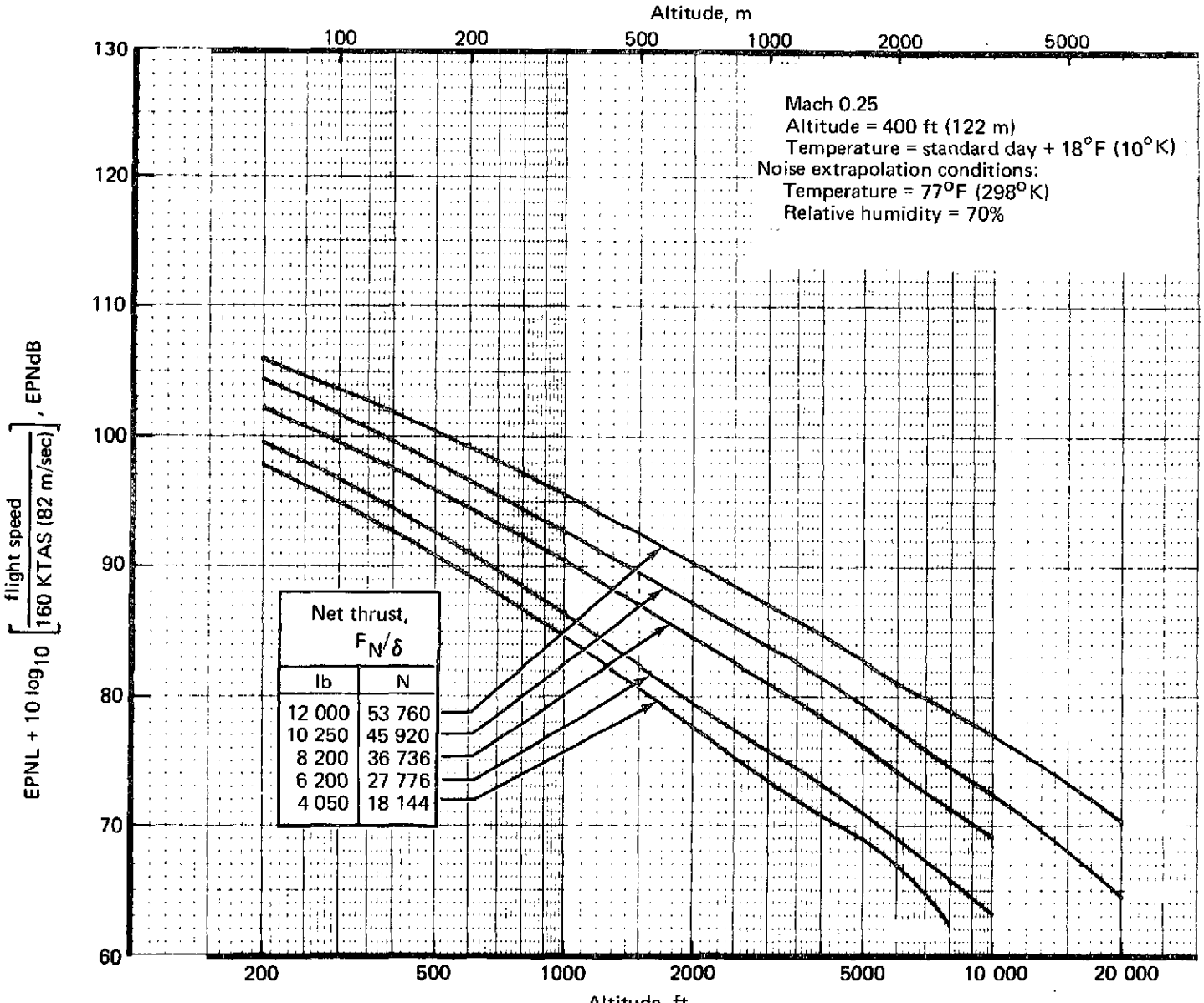


*FIGURE 98.—727/JT8D-109 CONFIGURATION 3—NOISE/THRUST/ALTITUDE CURVES*

#### 4.8.3.2 Results

The FAR Part 36 condition noise levels for the 727-200 at a maximum takeoff gross weight of 172 500 lb (78 245 kg) for the baseline and modified configurations are shown in table 30. Table 31 presents similar information for the modified configurations with the maximum brake release gross weight increased. Corresponding noise escalation is from 0 to 2 EPNdB, depending on the flight condition. It is shown that, based on this analysis, all three configurations meet FAR Part 36 requirements.

Configurations 1, 2, and 3 are progressively quieter. However, at takeoff and sideline, configurations 1 and 2 perform equally because the jet noise is dominant. On the other hand, the noise reductions resulting from the jet mixer in configuration 3 are demonstrated by the additional 5 EPNdB reduction in takeoff and sideline noise over that obtained with configuration 2. Although the prediction procedure for mixed jet noise is lacking the necessary supporting test data, the potential benefits are clear.

### 4.8.4 Noise Contour Area Analysis

The analysis was made in the same manner as for the 707 (sec. 3.8.4).

#### 4.8.4.1 EPNL Contour Areas

Constant-EPNL contour areas were calculated with the method described in section 3.8.4.1. Full power operational flight profiles are shown in table 32.

#### 4.8.4.2 Relative Footprint Noise Index

Relative footprint noise index (RFNI) calculations were made using the method described in section 3.8.4.2.

#### 4.8.4.3 Results

From the footprints derived with the types of takeoff profiles shown in table 32, constant-EPNL contour areas were calculated in the range of 85 to 110 EPNdB. Four engine/nacelle configurations were investigated: the JT8D-9 hardwall baseline and nacelle configurations 1, 2, and 3 for the JT8D-109 refanned engine using full power operational flight profiles. The JT8D-9 baseline and JT8D-109 configuration 1 were also investigated using a cutback certification profile.

*TABLE 30.–727/JT8D NOISE COMPARISONS AT FAR PART 36 MEASURING STATIONS, BRGW = 172 500 LB (78 245 KG)*

| Nacelle Configuration (a) | Condition | Approach 1 nmi (1.85 km) | | | | Takeoff (with cutback) 3.5 nmi (6.48 km) | | Takeoff (without cutback) 3.5 nmi (6.48 km) | | Sideline 0.25 nmi (0.46 km) | |
|---|---|---|---|---|---|---|---|---|---|---|---|
| | | English units | SI units | English units | SI units | English units | SI units | English units | SI units | English units | SI units |
| Hardwall baseline (JT8D-9) | BRGW | – | – | – | – | 172 500 lb | 78 229 kg | 172 500 lb | 78 229 kg | 172 500 lb | 78 229 kg |
| | LGW | 142 500 lb | 64 624 kg | 150 000 lb | 68 025 kg | – | – | – | – | – | – |
| | Flaps, deg | 40 | 40 | 30 | 30 | 5 | 5 | 5 | 5 | 5 | 5 |
| | Altitude | 370 ft | 112 | 370 ft | 112 | 1390 ft | 423.7 m | 1505 ft | 458.7 m | 800 ft | 243.8 m |
| | Sideline | – | – | – | – | – | – | – | – | 1520 ft | 463.3 m |
| | Thrust/δ | 6310 lb | 28 269 N | 4560 lb | 20 429 N | 8057 lb | 36 095 N | 12 420 lb | 55 642 N | 12 310 lb | 55 149 N |
| | Velocity, TAS | 139 kn | 71.6 m/sec | 145 kn | 74.7 m/sec | 177.5 kn | 91.4 m/sec | 178 kn | 91.6 m/sec | 176 kn | 90.6 m/sec |
| | EPNL, EPNdB | 109.5 | 109.5 | 108.2 | 108.2 | 100.0 | 100.0 | 107.4 | 107.4 | 99.9 | 99.9 |
| | FAR 36, EPNdB | 104.4 | 104.4 | 104.4 | 104.4 | 99.0 | 99.0 | 99.0 | 99.0 | 104.4 | 104.4 |
| 1 (JT8D-109 refan) | BRGW | – | – | – | – | 172 500 lb | 78 229 kg | 172 500 lb | 78 229 kg | 172 500 lb | 78 229 kg |
| | LGW | 142 500 lb | 64 624 kg | 150 000 lb | 68 025 kg | – | – | – | – | – | – |
| | Flaps, deg | 40 | 40 | 30 | 30 | 5 | 5 | 5 | 5 | 5 | 5 |
| | Altitude | 370 ft | 112.8 m | 370 ft | 112.8 m | 1556 ft | 474.3 m | 1685 ft | 513.6 m | 800 ft | 243.8 m |
| | Sideline | – | – | – | – | – | – | – | – | 1520 ft | 463.3 m |
| | Thrust/δ | 6310 lb | 28 264 N | 4560 lb | 20 429 N | 8100 lb | 36 228 N | 12 950 lb | 58 016 N | 12 840 lb | 57 523 N |
| | Velocity, TAS | 139 kn | 71.0 m/sec | 145 kn | 74.7 m/sec | 178.4 kn | 91.8 m/sec | 178.8 kn | 92.1 m/sec | 176.5 kn | 90.9 m/sec |
| | ΔEPNL, EPNdB[b] | –9.8 | –9.8 | –11.0 | –11.0 | –10.4 | –10.4 | –10.6 | –10.6 | –9.7 | –9.7 |
| | EPNL, EPNdB | (99.7) | (99.7) | (97.2) | (97.2) | (89.6) | (89.6) | (96.8) | (96.8) | (90.2) | (90.2) |
| | FAR 36, EPNdB | 104.4 | 104.4 | 104.4 | 104.4 | 99.0 | 99.0 | 99.0 | 99.0 | 104.4 | 104.4 |
| 2 (JT8D-109 refan) | BRGW | – | – | – | – | 172 500 lb | 78 229 kg | 172 500 lb | 78 229 kg | 172 500 lb | 78 229 kg |
| | LGW | 142 500 lb | 64 624 kg | 150 000 lb | 68 025 kg | – | – | – | – | – | – |
| | Flaps, deg | 40 | 40 | 30 | 30 | 5 | 5 | 5 | 5 | 5 | 5 |
| | Altitude | 370 ft | 112.8 m | 370 ft | 112.8 m | 1473 ft | 449.0 m | 1605 ft | 489.2 m | 800 ft | 243.8 m |
| | Sideline | – | – | – | – | – | – | – | – | 1520 ft | 463.3 m |
| | Thrust/δ | 6310 lb | 28 269 N | 4560 lb | 20 429 N | 8080 lb | 36 198 N | 12 660 lb | 56 717 N | 12 540 lb | 56 170 N |
| | Velocity, TAS | 139 kn | 71.6 m/sec | 145 kn | 74.7 m/sec | 177.9 kn | 91.6 m/sec | 178.3 kn | 91.8 m/sec | 176.2 kn | 90.7 m/sec |
| | Δ EPNL, EPNdB[b] | –11.8 | –11.8 | –13.0 | –13.0 | –10.5 | –10.5 | –11.2 | –11.2 | –10.6 | –10.6 |
| | EPNL, EPNdB | (97.7) | (97.7) | (95.2) | (95.2) | (89.5) | (89.5) | (96.2) | (96.2) | (89.3) | (89.3) |
| | FAR 36, EPNdB | 104.4 | 104.4 | 104.4 | 104.4 | 99.0 | 99.0 | 99.0 | 99.0 | 104.4 | 104.4 |
| 3 (JT8D-109 refan) | BRGW | – | – | – | – | 172 500 lb | 78 229 kg | 172 500 lb | 78 229 kg | 172 500 lb | 78 229 kg |
| | LGW | 142 500 lb | 64 624 kg | 150 000 lb | 68 025 kg | – | – | – | – | – | – |
| | Flaps, deg | 40 | 40 | 30 | 30 | 5 | 5 | 5 | 5 | 5 | 5 |
| | Altitude | 370 ft | 112.8 m | 370 ft | 112.8 m | 1455 ft | 443.5 m | 1585 ft | 483.1 m | 800 ft | 243.8 m |
| | Sideline | – | – | – | – | – | – | – | – | 1520 ft | 463.3 m |
| | Thrust/δ | 6310 lb | 28 260 N | 4560 lb | 20 429 N | 8075 lb | 36 176 N | 12 560 lb | 56 269 N | 12 450 lb | 55 776 N |
| | Velocity, TAS | 139 kn | 71.6 m/sec | 145 kn | 74.7 m/sec | 177.9 kn | 91.6 m/sec | 178.2 kn | 91.7 m/sec | 176.2 kn | 90.7 m/sec |
| | Δ EPNL, EPNdB[b] | –12.9 | –12.9 | –13.5 | –13.5 | –12.7 | –12.7 | –16.0 | –16.0 | –15.5 | –15.5 |
| | EPNL, EPNdB | (96.6) | (96.6) | (94.7) | (94.7) | (87.3) | (87.3) | (91.4) | (91.4) | (84.4) | (84.4) |
| | FAR 36, EPNdB | 104.4 | 104.4 | 104.4 | 104.4 | 99.0 | 99.0 | 99.0 | 99.0 | 104.4 | 104.4 |

[a] Configuration 3 requires mixer development

[b] From JT8D-9 hardwall baseline; see calculation method-paragraph 4.8.3.1

## TABLE 31.–727/JT8D NOISE COMPARISON AT FAR PART 36 MEASURING STATIONS, INCREASED BRGW

| Nacelle configuration (a) | Condition | Approach 1 nmi (1.85 km) | | | | Takeoff (with cutback) 3.5 nmi (6.48 km) | | Takeoff (without cutback) 3.5 nmi (6.48 km) | | Sideline 0.25 nmi (0.46 km) | |
|---|---|---|---|---|---|---|---|---|---|---|---|
| | | English units | SI units | English units | SI units | English units | SI units | English units | SI units | English units | SI units |
| 1 (JT8D-109 refan) | BRGW | – | – | – | – | 181 990 lb | 82 532 kg | 181 990 lb | 82 532 kg | 181 990 lb | 82 532 kg |
| | LGW | 142 500 lb | 64 624 kg | 150 000 lb | 68 025 kg | – | – | – | – | – | – |
| | Flaps, deg | 40 | 40 | 30 | 30 | 5 | 5 | 5 | 5 | 5 | 5 |
| | Altitude | 370 ft | 112.8 m | 370 ft | 112.8 m | 1310 ft | 399.3 m | 1440 ft | 438.9 m | 800 ft | 243.8 m |
| | Sideline | – | – | – | – | – | – | – | – | 1520 ft | 463.3 m |
| | Thrust/δ | 6310 lb | 28 269 N | 4560 lb | 20 429 N | 8490 lb | 38 035 N | 12 870 lb | 57 658 N | 12 790 lb | 57 299 N |
| | Velocity, TAS | 139 kn | 71.6 m/sec | 145 kn | 74.7 m/sec | 182 kn | 93.7 m/sec | 182 kn | 93.7 m/sec | 180 kn | 92.7 m/sec |
| | ΔEPNL, EPNdB[b] | -9.8 | -9.8 | -10.9 | -10.9 | -8.3 | -8.3 | -9.8 | -9.8 | -9.9 | -9.9 |
| | EPNL, EPNdB | – | – | (97.3) | (97.3) | (91.7) | (91.7) | (97.6) | (97.6) | (90.0) | (90.0) |
| | FAR 36, EPNdB | 104.6 | 104.6 | 104.6 | 104.6 | 99.4 | 99.4 | 99.4 | 99.4 | 104.6 | 104.6 |
| 2 (JT8D-109 refan) | BRGW | – | – | – | – | 182 500 lb | 82 781 kg | 182 500 lb | 82 781 kg | 182 500 lb | 82 781 kg |
| | LGW | 142 500 lb | 64 624 kg | 150 000 lb | 68 025 kg | – | – | – | – | – | – |
| | Flaps, deg | 40 | 40 | 30 | 30 | 5 | 5 | 5 | 5 | 5 | 5 |
| | Altitude | 370 ft | 112.8 m | 370 ft | 112.8 m | 1225 ft | 373.4 m | 1345 ft | 409.9 m | 800 ft | 243.8 m |
| | Sideline | – | – | – | – | – | – | – | – | 1520 ft | 463.3 m |
| | Thrust/δ | 6310 lb | 28 269 N | 4560 lb | 20 429 N | 8490 lb | 38 035 N | 12 575 lb | 56 336 N | 12 490 lb | 55 955 N |
| | Velocity, TAS | 139 kn | 71.6 m/sec | 145 kn | 74.7 m/sec | 182 kn | 93.7 m/sec | 182 kn | 93.7 m/sec | 180 kn | 92.7 m/sec |
| | ΔEPNL, EPNdB[b] | -11.8 | -11.8 | -13.0 | -13.0 | -8.5 | -8.5 | -10.3 | -10.3 | -10.9 | -10.9 |
| | EPNL, EPNdB | – | – | (95.2) | (95.2) | (91.5) | (91.5) | (97.1) | (97.1) | (89.0) | (89.0) |
| | FAR 36, EPNdB | 104.6 | 104.6 | 104.6 | 104.6 | 99.4 | 99.4 | 99.4 | 99.4 | 104.6 | 104.6 |
| 3[b] (JT8D-109 refan) | BRGW | – | – | – | – | 182 500 lb | 82 781 kg | 182 500 lb | 82 781 kg | 182 500 lb | 82 781 kg |
| | LGW | 142 500 lb | 64 624 kg | 150 000 lb | 68 025 kg | – | – | – | – | – | – |
| | Flaps, deg | 40 | 40 | 30 | 30 | 5 | 5 | 5 | 5 | 5 | 5 |
| | Altitude | 370 ft | 112.8 m | 370 ft | 112.8 m | 1210 ft | 368.8 m | 1315 ft | 400.8 m | 800 ft | 243.8 m |
| | Sideline | – | – | – | – | – | – | – | – | 1520 ft | 463.3 m |
| | Thrust/δ | 6310 lb | 28 269 N | 4560 lb | 20 429 N | 8485 lb | 38 013 N | 12 470 lb | 55 866 N | 12 400 lb | 55 552 N |
| | Velocity, TAS | 139 kn | 71.6 m/sec | 145 kn | 74.7 m/sec | 182 kn | 93.7 m/sec | 182 kn | 93.7 m/sec | 180 kn | 92.7 m/sec |
| | ΔEPNL, EPNdB[b] | -12.9 | -12.9 | -13.5 | -13.5 | -10.6 | -10.6 | -14.8 | -14.8 | -15.7 | -15.7 |
| | EPNL, EPNdB | – | – | (94.7) | (94.7) | (89.4) | (89.4) | (92.6) | (92.6) | (84.2) | (84.2) |
| | FAR 36, EPNdB | 104.6 | 104.6 | 104.6 | 104.6 | 99.4 | 99.4 | 99.4 | 99.4 | 104.6 | 104.6 |

[a] Configuration 3 requires mixer development

[b] From JT8D-9 hardwall baseline; see calculation method-paragraph 4.8.3.1

Results of the footprint studies are presented in three forms:

- Relative footprint contour areas versus EPNL
- Footprint contour percent area reductions versus EPNL
- Relative footprint noise index (RFNI) based on EPNL contours

Relative footprint contour areas are presented in figure 99 for the full-power operational profile and in figure 100 for the cutback certification profiles. Major results are as follows:

- The footprint areas of configuration 1 are considerably smaller than the areas of the baseline. This difference is due to the lower jet noise of the refanned engine cycle on takeoff and, to some degree, to the effect of acoustic treatment on approach.
- Configuration 2 is only slightly better than configuration 1. The additional lining material reduces the approach noise by approximately 2 EPNdB but has only a minor impact (less than 1 EPNdB) on the takeoff noise that dominates the overall footprint area.

## TABLE 32.—727-200 FULL POWER OPERATIONAL FLIGHT PROFILES

727-200 full power operational takeoff profiles for EPNL footprints—brake release gross weight = 172 500 lb (78 245 kg)

| Nacelle configuration | Distance from brake release | | Altitude | | Average power setting $F_N/\delta$ | | Average flight speed | | Flap position | Gear position |
|---|---|---|---|---|---|---|---|---|---|---|
| | ft | m | ft | m | lb | N | KTAS | m/sec | | |
| Hardwall baseline (JT8D-9) | 0 | 0 | 0 | 0 | 12 220 | 54 357 | 117.7 | 60.6 | 5 | Down |
| | 7 807 | 2 380 | 0 | 0 | 12 310 | 54 758 | 172.9 | 88.9 | ↓ | Down |
| | 21 110 | 6 434 | 1 500 | 457 | 12 270 | 54 580 | 200.2 | 103.0 | Retract | Up |
| | 27 840 | 8 486 | 1 500 | 457 | 12 030 | 53 512 | 241.2 | 124.1 | 0 | ↓ |
| | 33 840 | 10 314 | 1 500 | 457 | 9 520 | 42 347 | 265.0 | 136.3 | ↓ | ↓ |
| | 63 840 | 19 458 | 4 000 | 1219 | 9 780 | 43 504 | 275.1 | 141.5 | ↓ | ↓ |
| | 97 840 | 29 822 | 6 500 | 1981 | 10 110 | 44 972 | 287.4 | 147.9 | ↓ | ↓ |
| | 144 040 | 43 903 | 9 500 | 2896 | 10 480 | 46 617 | 301.0 | 154.8 | ↓ | ↓ |
| | 199 940 | 60 942 | 12 500 | 3810 | 10 930 | 48 619 | 317.0 | 163.1 | ↓ | ↓ |
| | 283 840 | 86 514 | 16 000 | 4877 | 11 640 | 51 777 | 337.6 | 173.7 | ↓ | ↓ |
| 1 (JT8D-109 refan) | 0 | 0 | 0 | 0 | 12 790 | 56 893 | 118.0 | 60.7 | 5 | Down |
| | 7 221 | 2 201 | 0 | 0 | 12 870 | 57 249 | 173.4 | 89.2 | ↓ | Down |
| | 19 660 | 5 992 | 1 500 | 457 | 12 670 | 56 359 | 200.7 | 103.2 | Retract | Up |
| | 26 120 | 7 961 | 1 500 | 457 | 12 200 | 54 268 | 241.6 | 124.3 | 0 | ↓ |
| | 31 900 | 9 723 | 1 500 | 457 | 9 300 | 41 368 | 265.0 | 136.3 | ↓ | ↓ |
| | 63 500 | 19 355 | 4 000 | 1219 | 9 830 | 43 726 | 275.1 | 141.5 | ↓ | ↓ |
| | 97 800 | 29 809 | 6 500 | 1981 | 10 430 | 46 395 | 287.4 | 147.9 | ↓ | ↓ |
| | 142 600 | 43 464 | 9 500 | 2896 | 11 080 | 49 286 | 301.0 | 154.8 | ↓ | ↓ |
| | 191 200 | 58 278 | 12 500 | 3810 | 11 730 | 52 178 | 317.0 | 163.1 | ↓ | ↓ |
| | 260 500 | 79 400 | 16 000 | 4877 | 12 400 | 55 158 | 337.7 | 173.7 | ↓ | ↓ |
| | 351 100 | 107 015 | 20 000 | 6096 | | | | | | |
| 2 (JT9D-109 refan) | 0 | 0 | 0 | 0 | 12 480 | 55 514 | 117.8 | 60.6 | 5 | Down |
| | 7 462 | 2 274 | 0 | 0 | 12 560 | 55 870 | 173.2 | 89.1 | ↓ | Down |
| | 20 360 | 6 206 | 1 500 | 457 | 12 370 | 55 025 | 200.4 | 103.0 | Retract | Up |
| | 26 980 | 8 224 | 1 500 | 457 | 11 850 | 52 711 | 241.3 | 124.1 | 0 | ↓ |
| | 33 110 | 10 092 | 1 500 | 457 | 8 990 | 39 990 | 265.0 | 136.3 | ↓ | ↓ |
| | 66 410 | 20 242 | 4 000 | 1219 | 9 520 | 42 347 | 275.1 | 141.5 | ↓ | ↓ |
| | 102 610 | 31 276 | 6 500 | 1981 | 10 110 | 42 972 | 287.4 | 147.9 | ↓ | ↓ |
| | 149 310 | 45 510 | 9 500 | 2896 | 10 740 | 47 774 | 301.0 | 154.8 | ↓ | ↓ |
| | 203 310 | 61 969 | 12 500 | 3810 | 11 400 | 50 710 | 317.0 | 163.1 | ↓ | ↓ |
| | 276 610 | 84 311 | 16 000 | 4877 | 12 130 | 53 957 | 337.7 | 173.7 | ↓ | ↓ |
| | 376 610 | 114 791 | 20 000 | 6096 | | | | | | |
| 3 (JT8D-109 refan) | 0 | 0 | 0 | 0 | 12 500 | 55 603 | 117.8 | 60.6 | 5 | Down |
| | 7 443 | 2 269 | 0 | 0 | 12 590 | 56 003 | 173.2 | 89.1 | ↓ | Down |
| | 20 320 | 6 194 | 1 500 | 457 | 12 430 | 55 291 | 200.3 | 103.1 | Retract | Up |
| | 26 920 | 8 205 | 1 500 | 457 | 11 960 | 53 201 | 241.2 | 124.1 | 0 | ↓ |
| | 32 950 | 10 043 | 1 500 | 457 | 9 040 | 40 212 | 265.0 | 136.3 | ↓ | ↓ |
| | 66 250 | 20 193 | 4 000 | 1219 | 9 600 | 42 703 | 275.1 | 141.5 | ↓ | ↓ |
| | 101 450 | 30 922 | 6 500 | 1981 | 10 200 | 45 372 | 287.4 | 147.9 | ↓ | ↓ |
| | 148 150 | 45 156 | 9 500 | 2896 | 10 830 | 48 174 | 301.0 | 154.8 | ↓ | ↓ |
| | 199 250 | 60 731 | 12 500 | 3810 | 11 470 | 51 021 | 317.0 | 163.1 | ↓ | ↓ |
| | 259 750 | 82 220 | 16 000 | 4877 | 12 160 | 54 090 | 337.7 | 173.7 | ↓ | ↓ |
| | 372 450 | 113 523 | 20 000 | 6096 | | | | | | |

727-200 approach conditions for EPNL footprints

| Nacelle configuration | Landing gross weight | | Approach speed 1.3 $V_{stall}$ + 10 kn (5.1 m/sec) | | Glide slope (degrees) | Flap position | Gear position | Power setting $F_N/\delta$ | |
|---|---|---|---|---|---|---|---|---|---|
| | lb | kg | KTAS | m/sec | | | | lb | N |
| All | 142 500 | 64 637 | 139.0 | 71.5 | 3 | 40 | Down | 6310 | 28 068 |
| All | 150 000 | 68 039 | 145.2 | 74.7 | 3 | 30 | Down | 4560 | 20 284 |

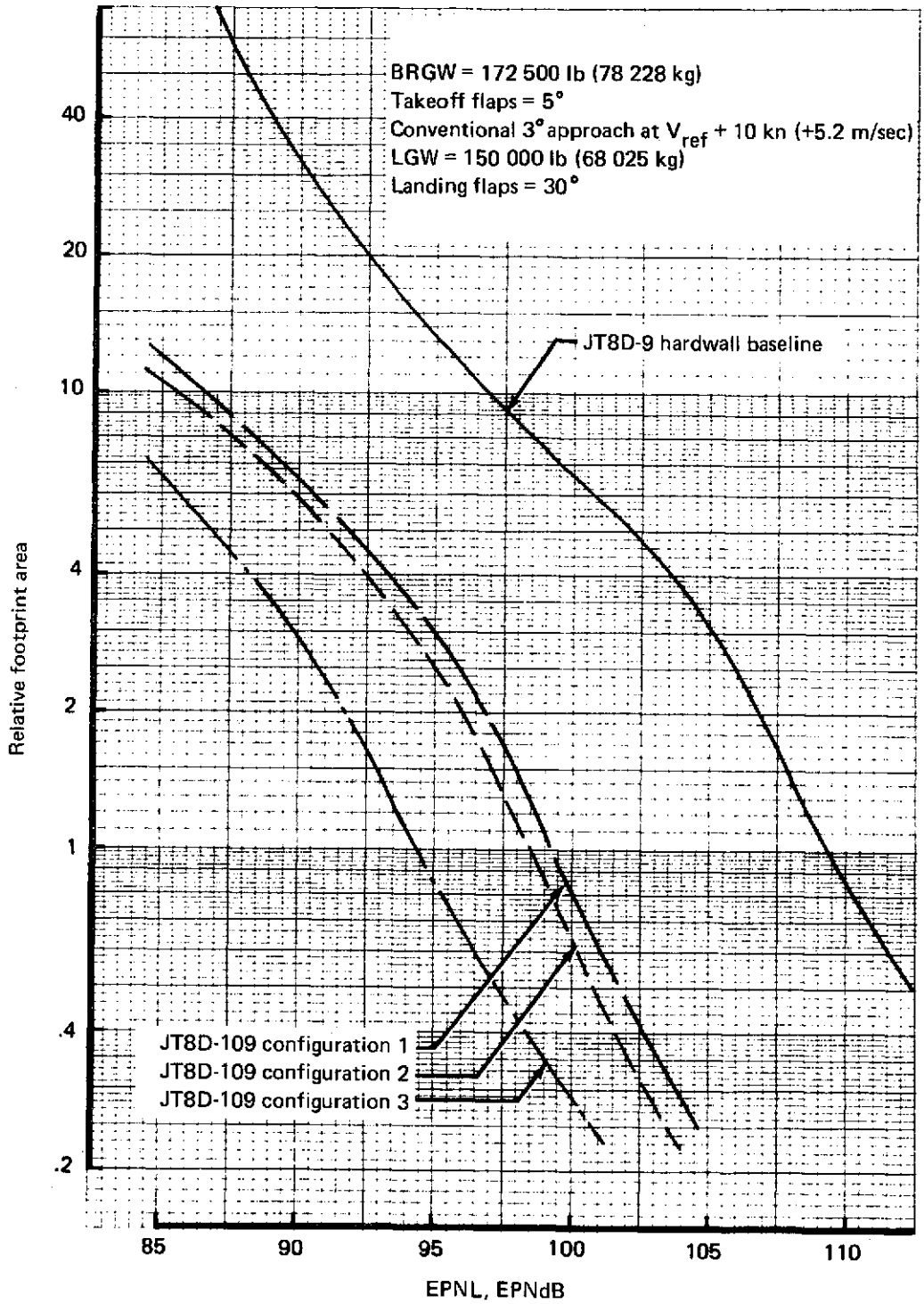


*FIGURE 99.—727/JT8D RELATIVE EPNL FOOTPRINT CONTOUR AREAS—FULL-POWER OPERATIONAL PROFILE*

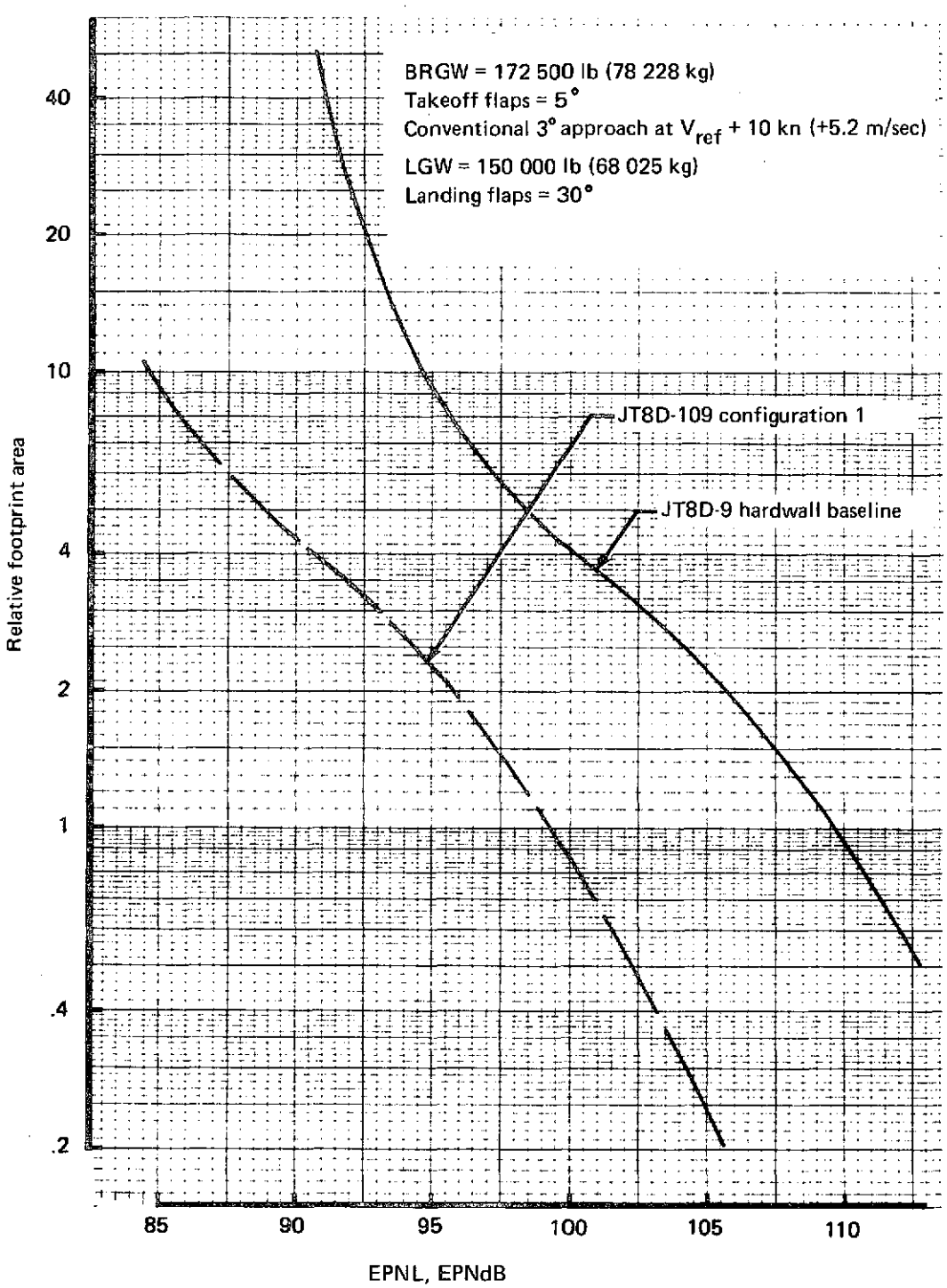


*FIGURE 100.–727/JT8D RELATIVE EPNL FOOTPRINT CONTOUR AREAS–CUTBACK CERTIFICATION PROFILE*

- The jet mixer of configuration 3 produces a significant additional area reduction. This is due to its strong attenuation of jet noise during takeoff.

In figure 101, the relative footprint-area-versus-EPNL curves of the two different profiles are compared. The graph can be divided into three segments:

- For small areas, footprint areas of the two profiles are practically identical. This is due to the fact that, in the proximity of the airport, the profiles, airplane speeds, and thrust settings are almost equal.

- For medium footprint areas, the cutback certification profile produces relatively smaller area and is therefore superior. This is primarily due to the lower thrust settings present in the corresponding segment of this profile.

- For large footprint areas, the trend reverses. The areas produced by the full-power operational profile are relatively smaller as a result of the higher altitude and greater aircraft speed.

Area benefits of the two profiles, therefore, depend on the EPNL of interest and the configuration. The percent of footprint area reduction for the different configurations is shown in figures 102 and 103. Both figures indicate at least a 75% reduction from the baseline footprint area. Variations in the shape of the footprint area reduction curves are due to the takeoff flight procedures (aircraft altitude, thrust, and velocity, as a function of distance from brake release) and the basic shape of the EPNL-thrust-distance curves.

The relative footprint noise index, as described in section 3.8.4.2, based on EPNL contours is presented for all three configurations in table 33. The RFNI values demonstrate the obvious benefits of the refanned-engine/modified-nacelle concept (85% for configuration 1) and the potential additional improvements (configuration 2 and, particularly, configuration 3).

*TABLE 33.—727/JT8D-9/JT8D-109 RELATIVE FOOTPRINT NOISE INDEX*

| Nacelle | RFNI (a) |
|---|---|
| JT8D-9 hardwall baseline | 1.000 |
| JT8D-109 configuration 1 | 0.145 |
| JT8D-109 configuration 2 | 0.124 |
| JT8D-109 configuration 3 | 0.042 |

[a]Based on 727-200 EPNL contours

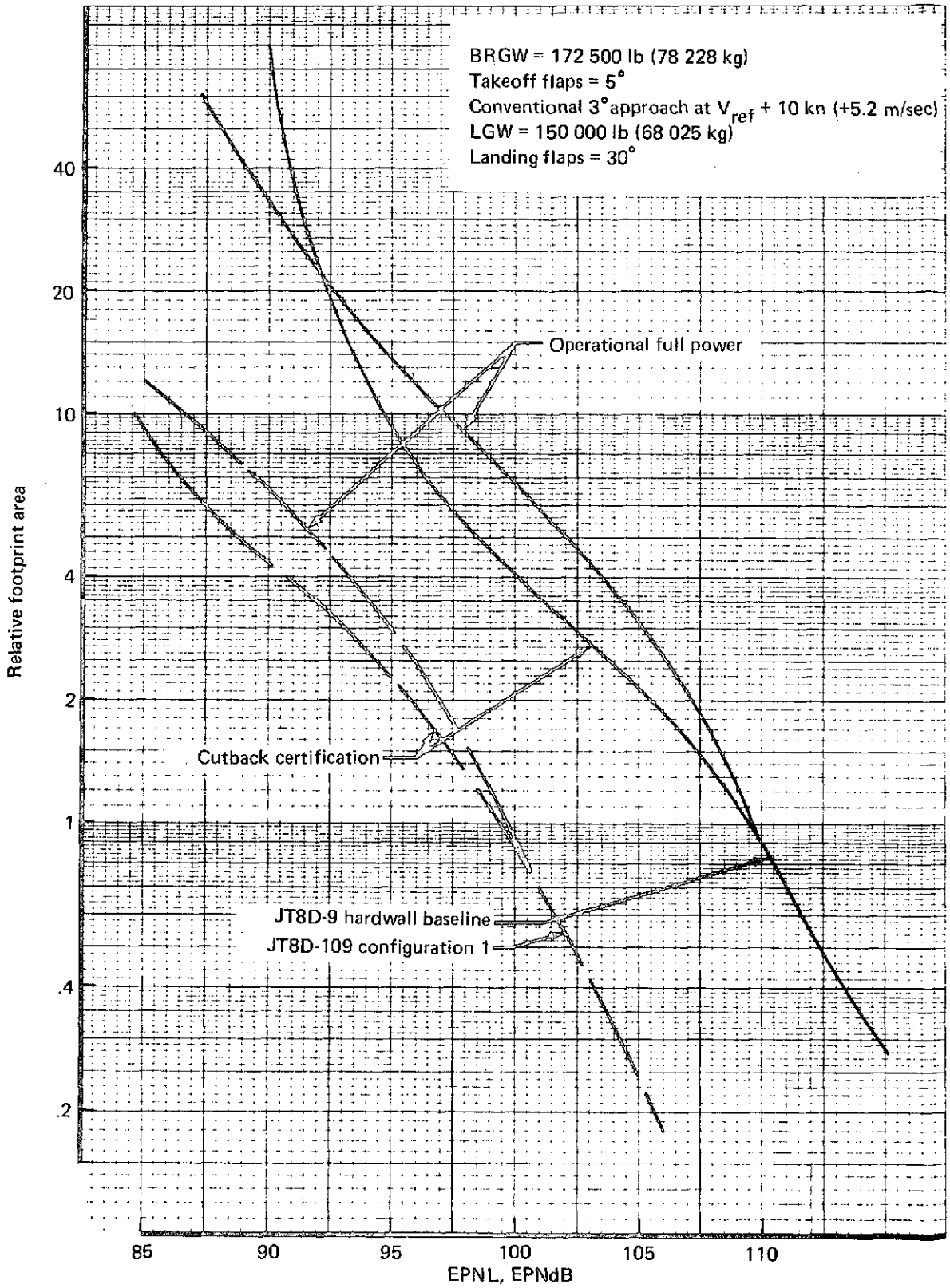


*FIGURE 101.–727/JT8D RELATIVE FOOTPRINT CONTOUR AREAS–TAKEOFF PROFILE COMPARISON*

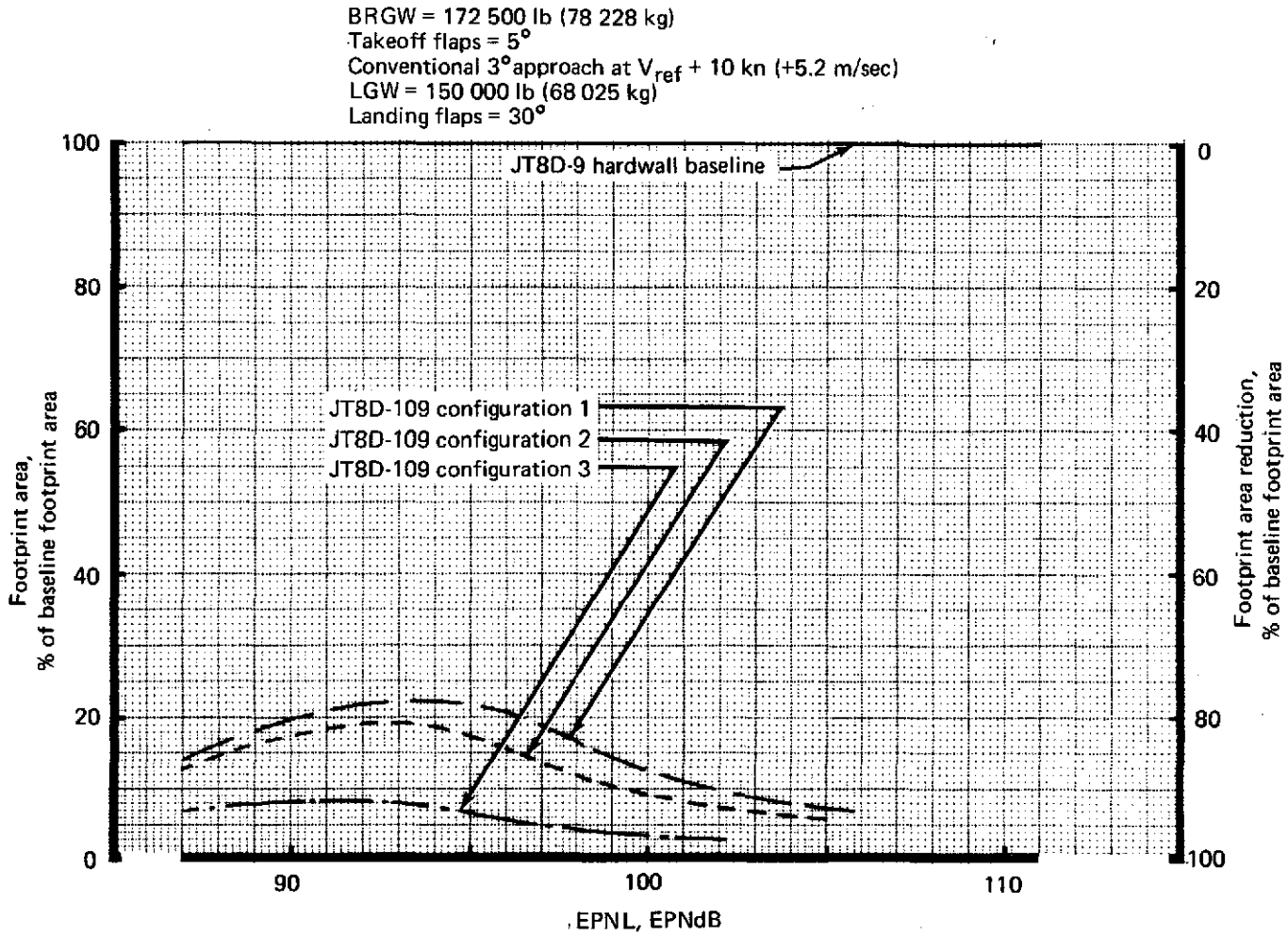


*FIGURE 102.—727/JT8D EPNL, FOOTPRINT AREA REDUCTION—FULL-POWER OPERATIONAL PROFILE*

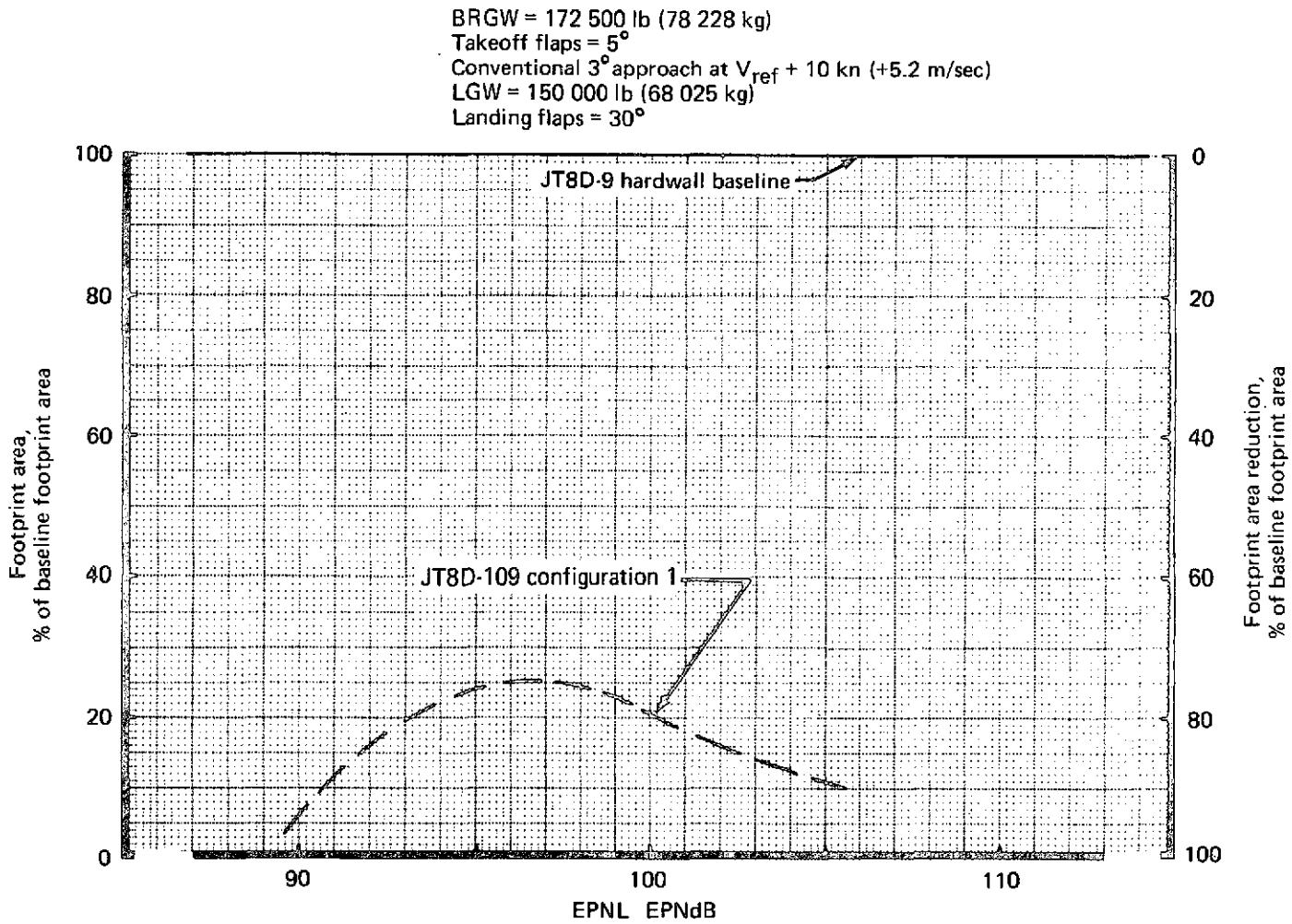


*FIGURE 103.—727/JT8D EPNL, FOOTPRINT AREA REDUCTION—CUTBACK CERTIFICATION PROFILE*

# 5.0 737 AIRPLANE

## 5.1 AIRPLANE DESCRIPTION

The 737 airplane is a low-wing, two-engine, commercial jet, with engines mounted under the wings and outboard of the fuselage. It has been manufactured in three versions—the -100 series, the -200 series, and the advanced -200 series. Figure 104 provides a weight/thrust growth history for the 737 airplane/JT8D engine combination.

The greatest number of 737s currently in airline service are of the -200 series; therefore, this version was selected as the baseline to consider for retrofit of refanned engines. The engine used on the 737-200-series airplane is the JT8D-9, of which approximately 380 are in 737 airline service. Figure 105 depicts the general arrangement of the 737-200 airplane.

The 737-200 is a 103 500-lb (46 948-kg) maximum brake release gross weight airplane. The JT8D-9 engines are rated at 14 500 lb (64 500 N) sea-level static thrust and have no acoustic treatment.

The major consideration involved in modifying the 737 airplane by installation of the JT8D-109 engine is the maintenance of nacelle-to-ground clearance. When the JT8D-9 engine is modified to the JT8D-109 configuration by adding a larger diameter front fan, the outer engine diameter will be increased by approximately 11 in. (0.279 m). This 11-in.-diameter increase will require a nacelle basic diameter close to 62 in. (1.575 m). The existing airplane configuration will not permit installation of a 62-in. (1.575-m) diameter nacelle with adequate ground clearance on the existing engine mounts.

Two methods can be used to modify the airplane to accept the refanned engines. One method is to lengthen the main landing gear to lift the entire airplane enough to provide the necessary under-wing ground clearance. The second method is to modify the engine attachment for installation of the engine with a minimal amount of clearance under the wing. With the second method, a small amount of additional landing gear length would still be required.

The critical areas for engine ground clearance are at the highlight of the nose cowl, at the deepest part of the nacelle (i.e., under the gear case or the precooler), and at the aft end of the tailpipe. (The aft end of the tailpipe defines the deployed position of the thrust reverser target doors.) Figure 106 shows the modified airplane retrofitted with refanned engines.

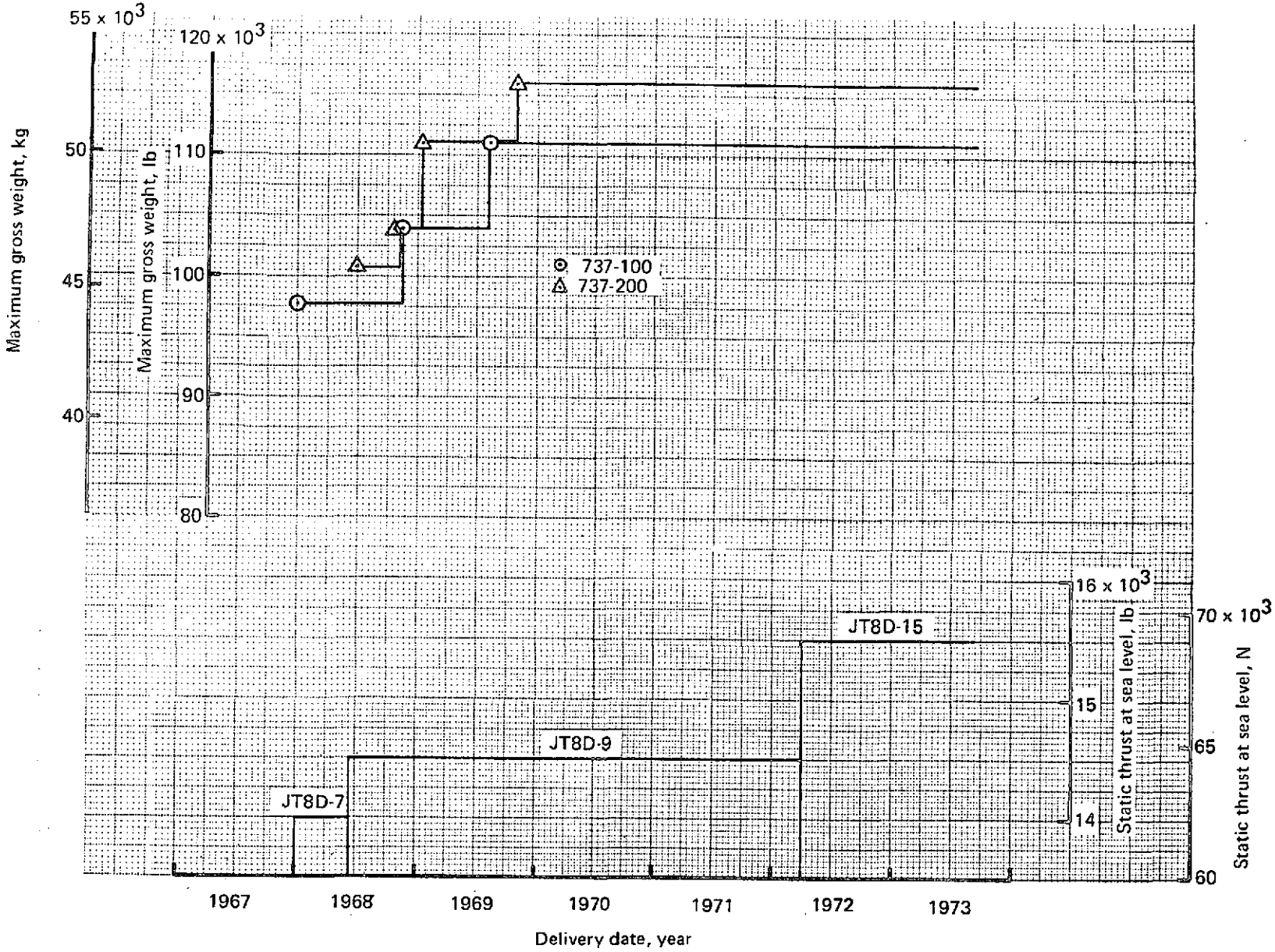


*FIGURE 104.—737/JT8D WEIGHT/THRUST GROWTH HISTORY*

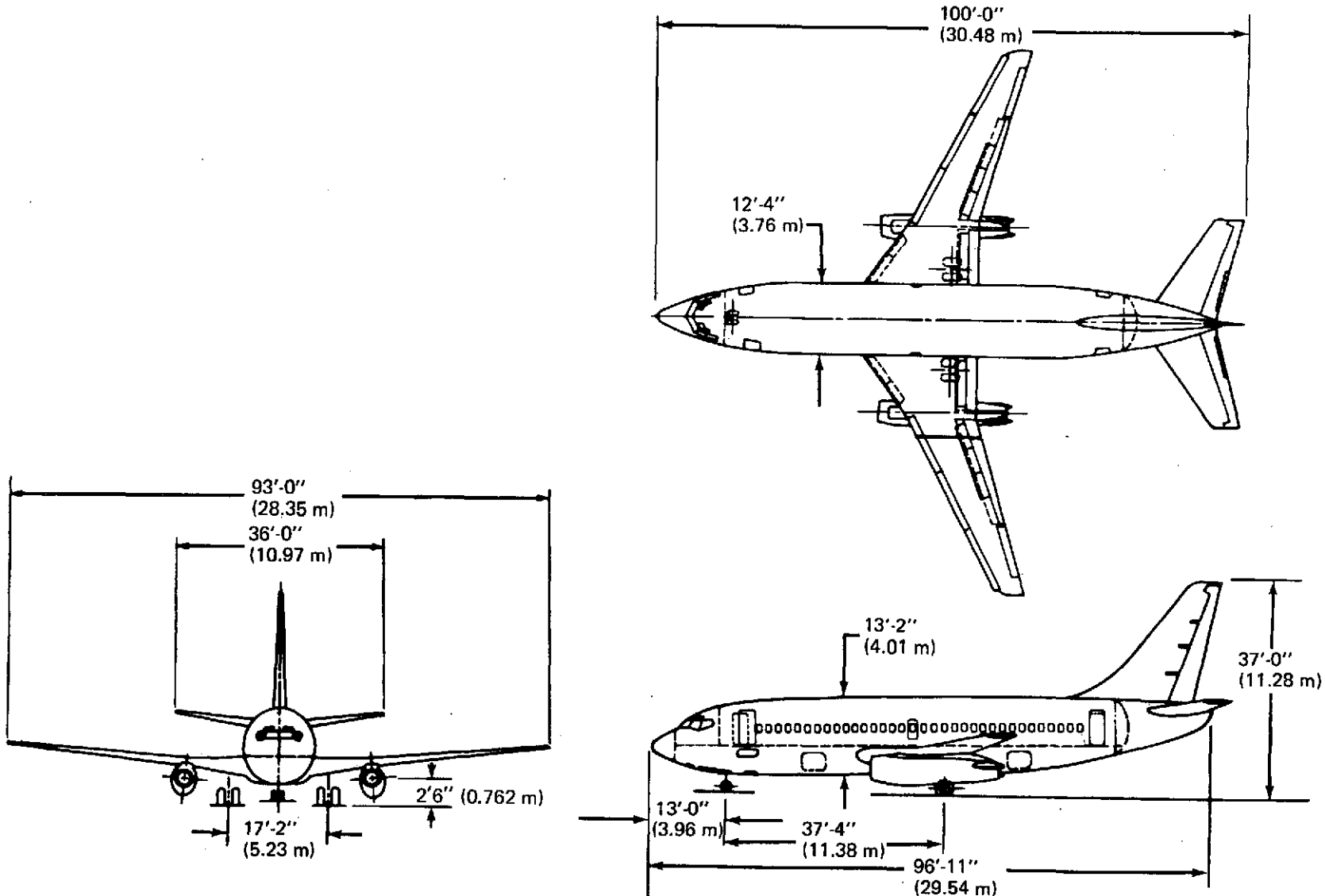


*FIGURE 105.—737-200/JT8D BASELINE AIRPLANE GENERAL ARRANGEMENT*

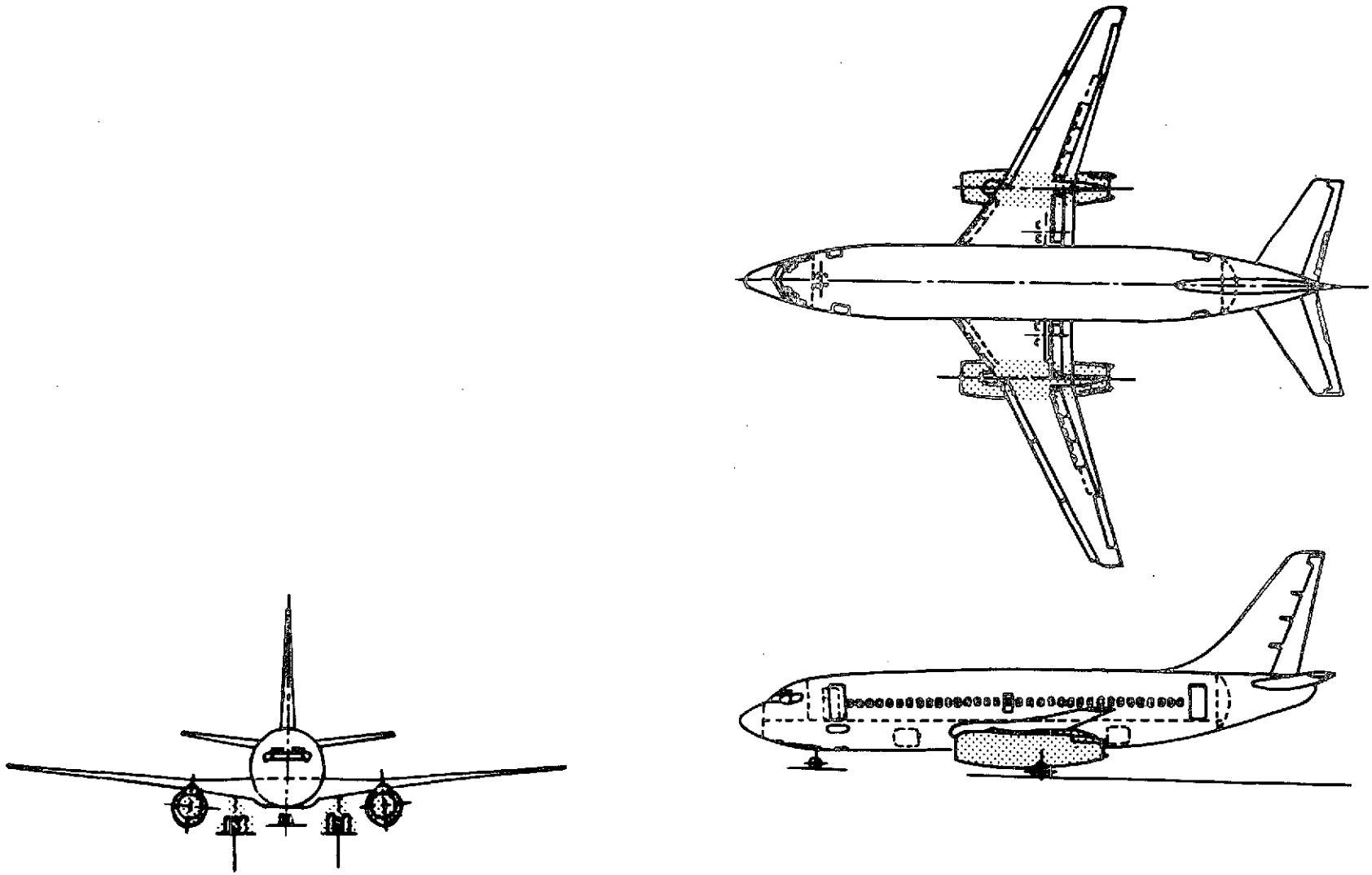

FIGURE 106.—737-200/JT8D-109 MODIFIED AIRPLANE GENERAL ARRANGEMENT

The clearance between the lowest part of the nose cowl highlight and the ground is critical, since this clearance defines the amount and size of foreign objects that can be picked up from the runway and passed through the engine. As an arbitrary parameter, the JT8D-109 highlight-to-ground clearance was kept as close as possible to the JT8D-9 highlight clearance. Even with the same height as the baseline engine maintained, some increase in foreign-object pickup would be expected due to the higher mass air flows. Some portion of any ingested objects would tend to go through the compressors; however, with the much higher bypass ratio, a considerably larger portion of the foreign objects would be discharged through the fan air duct.

The lowest point of the nacelle is critical from three aspects. The first requirement is to simplify installation of lower keel line drains, breather vents, etc.; the cowl doors would be built with one door extending some distance past nacelle bottom center. At the maximum taxi weight of the airplane, the doors would have to clear the ground when they are opened. The second requirement is the 15-in. (0.381-m) minimum ground clearance to clear airport ground lights, etc. Finally, ground clearance of the lower portion of the nacelle package would be a limiting factor on airplane roll when landing.

The exit nozzle location is critical in both fore-and-aft and height locations. These locations determine ground clearance for airplane rotation to tail skid contact. The exit nozzle also pre-positions the thrust reverser. If the target reverser is used, an actuation switch in the nose gear will be required to ascertain that the airplane is completely on the ground before the reverser is extended. Figure 107 illustrates nacelle ground clearance during taxi and during airplane rotation.

In consideration of the two methods that can be used to modify the airplane to accept the JT8D-109 engines, the following statement will describe the modification selected for discussion. Some of the different procedures that might have been selected will be discussed briefly later in this section.

The general configuration includes: 12-in. (0.305-m) landing gear length extension with a provision for shrinking to the present length when retracted to enable storage in the existing wheelwells; no nose wheel change; aft airstair change; reuse of existing engine mounts; reuse of portions of the wing-to-nacelle fairing; limited flap trim changes; minimal airplane system changes; and new engine buildup package, including nose cowls, larger nacelles, and thrust reversers.

The three different levels of acoustic suppression considered are described in section 5.4.

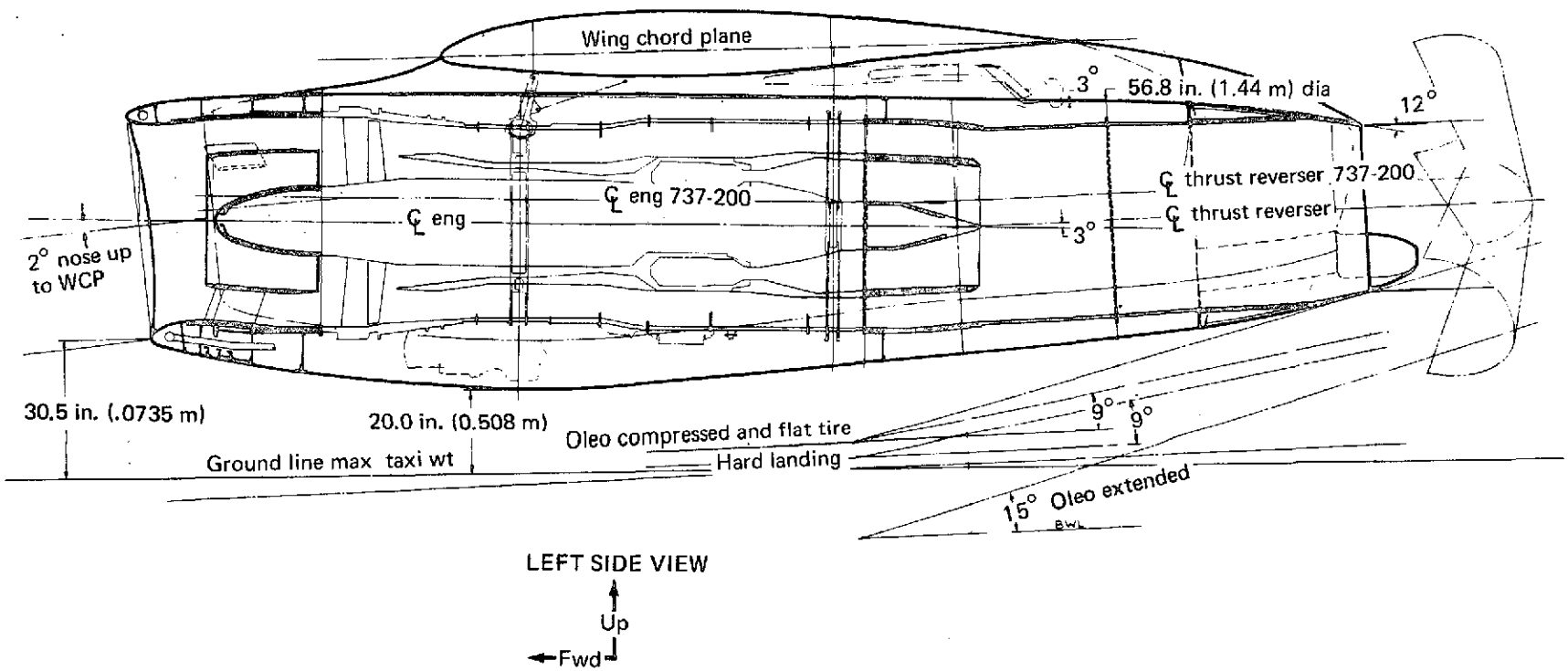


*FIGURE 107.—737/JT8D NACELLE GROUND CLEARANCE*

## 5.2 ENGINE DEFINITION

### 5.2.1 JT8D-9 (Baseline)

The JT8D-9 engine used on the 737-200 baseline airplane is also used on the 727-200 baseline airplane. Refer to section 4.2.1 for discussion of this engine.

### 5.2.2 JT8D-109 (Refanned)

The JT8D-109 engine to be used for the 737 modified airplane is also used on the 727 modified airplane. Refer to section 4.2.2 for discussion of this engine. Since the 737 airplane operating envelope is different from that of the 727 airplane, figures 108 and 109 show the pressure-altitude/speed and pressure-altitude/temperature envelopes for the JT8D-109 in the 737 airplane.

### 5.2.3 Uninstalled-Engine Performance

Uninstalled-takeoff performance for the JT8D-9 and the JT8D-109 is shown in section 4.2.3. The cruise condition for the 737 airplane is Mach 0.78 at 25 000 ft (7620 m) as compared to Mach 0.84 at 30 000 ft (9144 m) for the 727 airplane. Figure 110 illustrates the relationship between the JT8D-109 and JT8D-9 uninstalled cruise TSFC at this condition.

## 5.3 MODEL AND COMPONENT TESTS

Model tests proposed for the phase I program included airplane flutter, engine nozzle and inlet tests. Early evaluation of flutter was considered necessary if the nacelle wing location was changed. With the final recommendation locating the nacelle in the same position as on the current 737, the requirement for this model test was dropped.

Due to the requirement for commonality between the 727 and 737, the only difference in the two airplane exhaust system configurations would be the extension between the engine and the tailpipe assembly, which locates the thrust reverser aft of the flap system. It had, therefore, been proposed to conduct the 727 and 737 nozzle tests concurrently. This addition to the 727 model test program was canceled with termination of the 737 program.

An inlet model test was considered essential to determine that an acceptable pod-mounted inlet could be designed to meet the flow-field requirements of the 737 airplane and the operational requirements of the refanned JT8D engine. Inlets were considered that met the minimum,

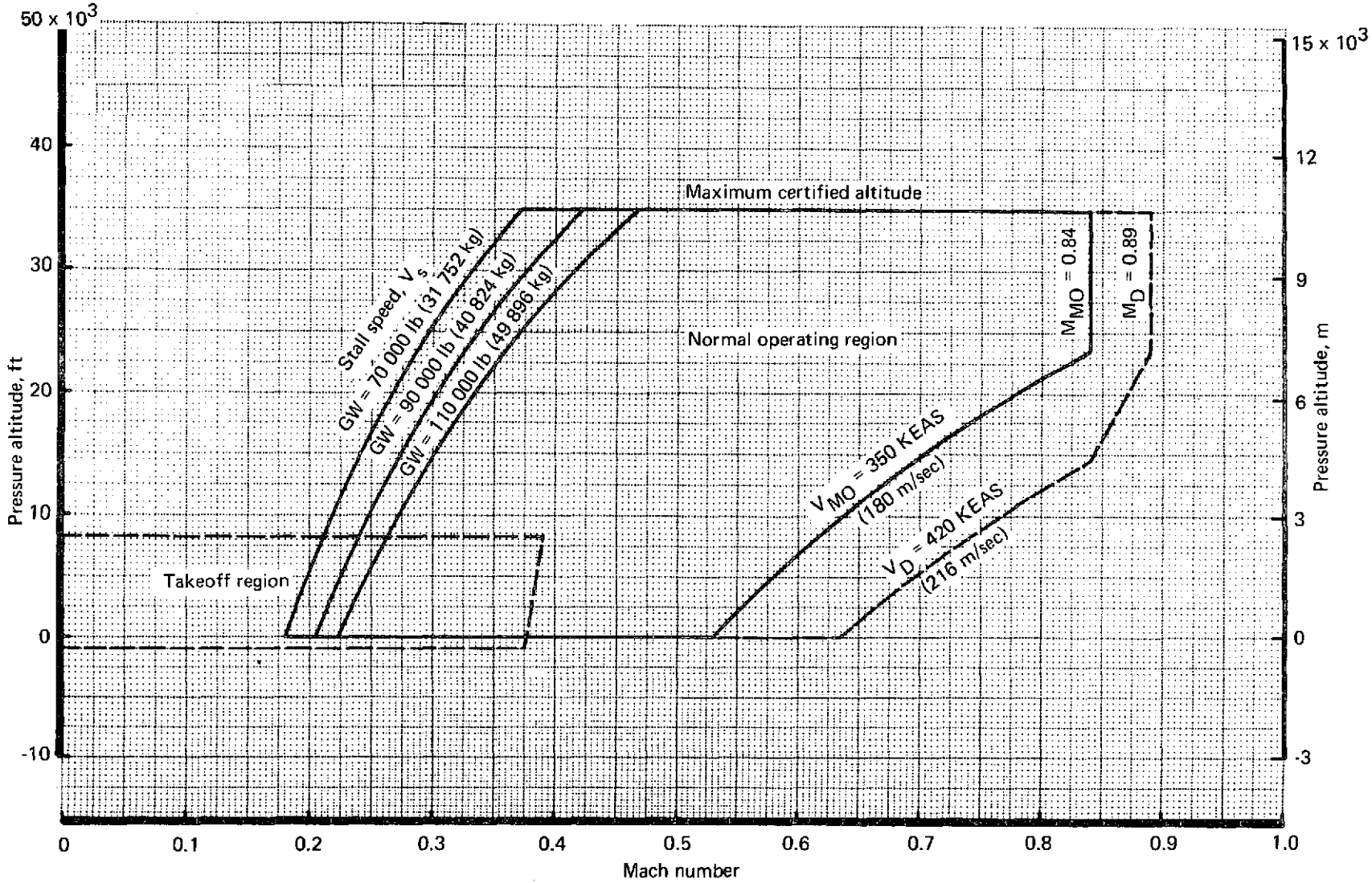


*FIGURE 108.—737/JT8D BASELINE AIRPLANE PRESSURE ALTITUDE/SPEED ENVELOPE—STANDARD DAY, FLAPS UP, GEAR UP*

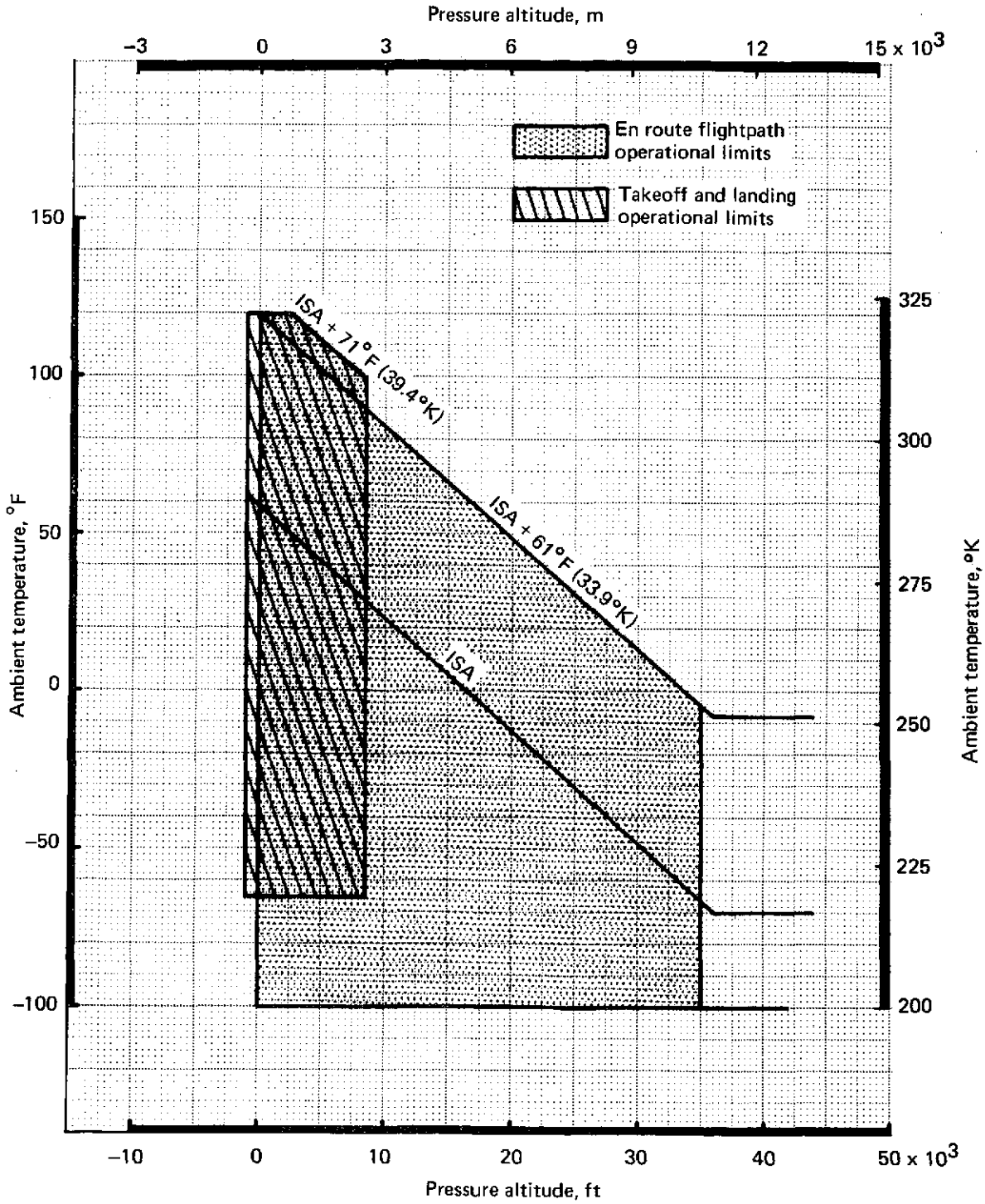


*FIGURE 109.–737/JT8D BASELINE–PRESSURE ALTITUDE/TEMPERATURE ENVELOPE*

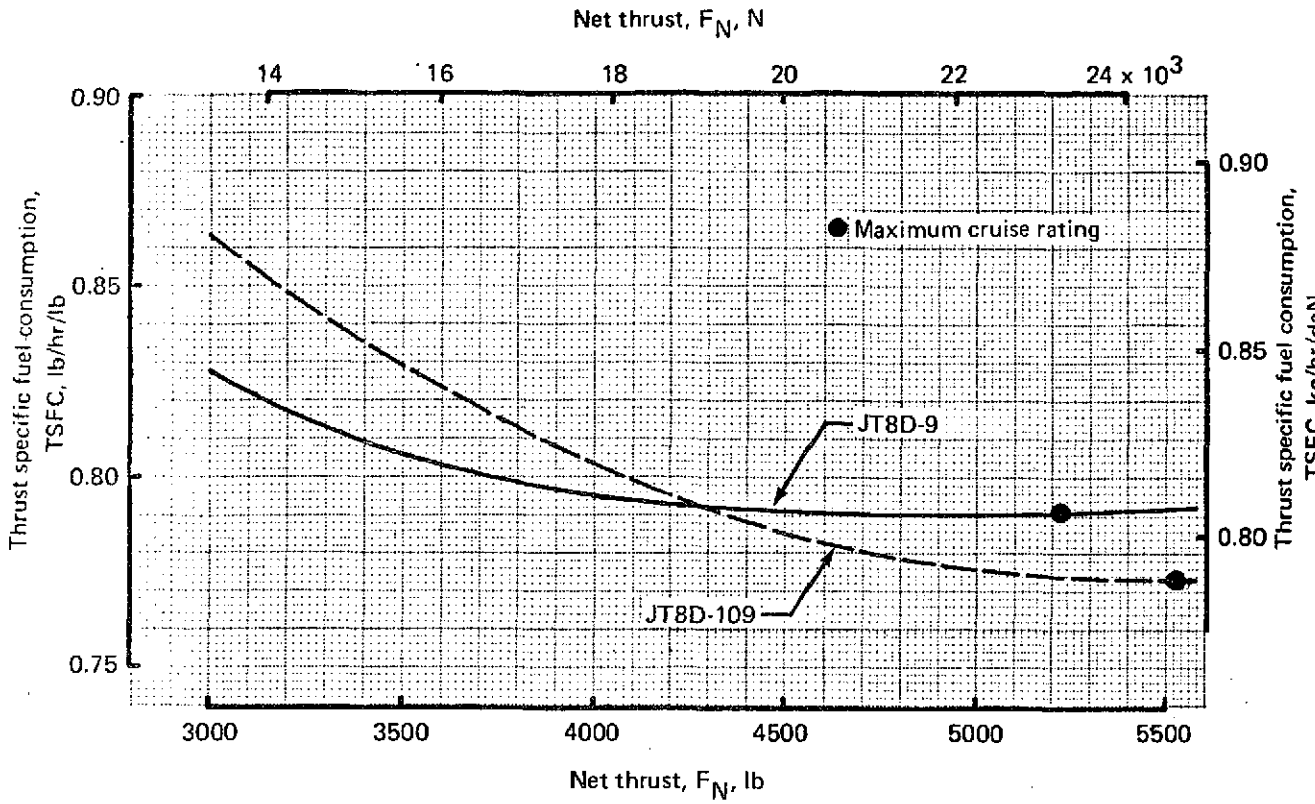


| Maximum cruise | JT8D-109 | JT8D-9 |
|---|---|---|
| Thrust at 25 000 ft (7620 m) and Mach 0.78 | 5520 lb (24 553 N) | 5220 lb (23 218 N) |
| TSFC at 25 000 ft (7620 m) and Mach 0.78 | 0.773 lb/hr/lb (0.788 kg/hr/daN) | 0.791 lb/hr/lb 0.807 kg/hr/daN) |

*FIGURE 110.–JT8D-9/JT8D-109 UNINSTALLED-ENGINE CRUISE PERFORMANCE COMPARISON– MACH 0.78, 25 000 FT (7620 M), STANDARD DAY*

intermediate, and maximum acoustic treatment requirements. Inlet models were designed to obtain parametric inlet pressure recovery and distortion performance for three levels of acoustic treatment at static, crosswind, and low-speed angle-of-attack conditions. The models consisted of one common diffuser, three lips (28%, 32%, and 36% contraction ratios), and one two-ring and three single-ring designs. The single-ring inlets were designed to determine the influence of the ring leading edge location relative to the inlet throat and the ring trailing edge location relative to the engine face. Model test measurements were to consist of surface static pressure, engine face steady-state total pressure, engine face dynamic total pressure, and inlet airflow. At the time of test cancellation, model design was 100% complete and model fabrication as 80% complete.

The acoustic tests reported for the 727 airplane in section 4.3 apply to the 737.

## 5.4 NACELLE PRELIMINARY DESIGN

This section is divided into four main parts. The first part relates to nacelle configuration 1, which was selected as the most logical design to be pursued for further development. The second and third parts relate to configurations 2 and 3; however, the scope of these discussions is limited to increased levels of acoustic treatment and noise attenuation and the nacelle changes that differ from the changes required for configuration 1. The fourth part of this section presents a very brief discussion of the trade studies investigated.

It is emphasized that the performance and noise results for configurations 1 and 2 reflect currently used treatment methods. On the other hand, performance and noise results for configuration 3 are primarily attributable to an idealized mixer design, which is not available at this time. Realization of the noise and performance results for configuration 3 will require an intensive mixer technology development program. Such a program would need to address both the propulsion performance and noise aspects of mixers. Therefore, the noise and installed-performance values quoted for configuration 3 are based on current best insight and must therefore be qualified as goals and not immediately practicable options.

Figure 111 shows the three different nacelle configurations that will be discussed in sections 5.4.1 through 5.4.3. In each case, the option of installing these engine configurations is based on the considered assumption that a 12-in. (0.305-m) extension to the main landing gear can be successfully accommodated by the wing and landing gear structure. This cannot be verified without extensive shimmy and load testing.

The existing installation for the JT8D-9 engine is shown in figure 112. The nacelle is suspended below the wing with the centerline canted up 3° with respect to the body. The front engine mount

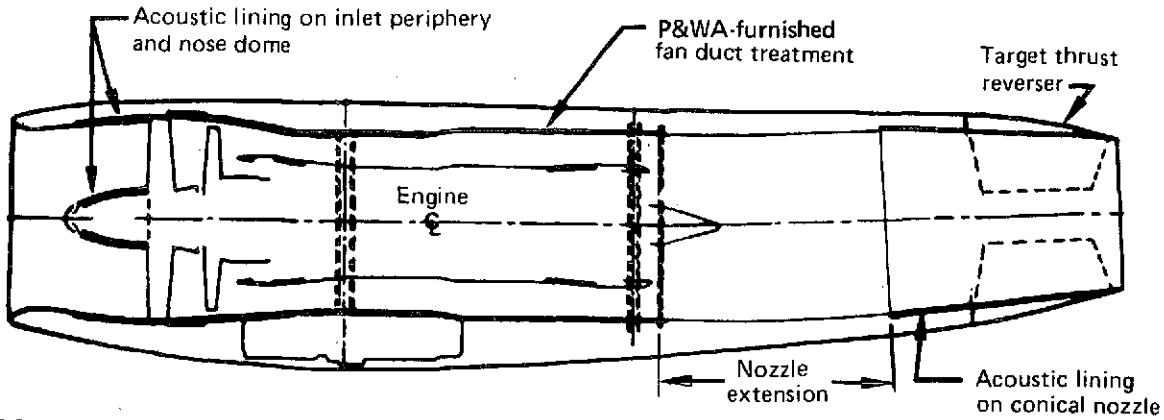


**737 CONFIGURATION 1**

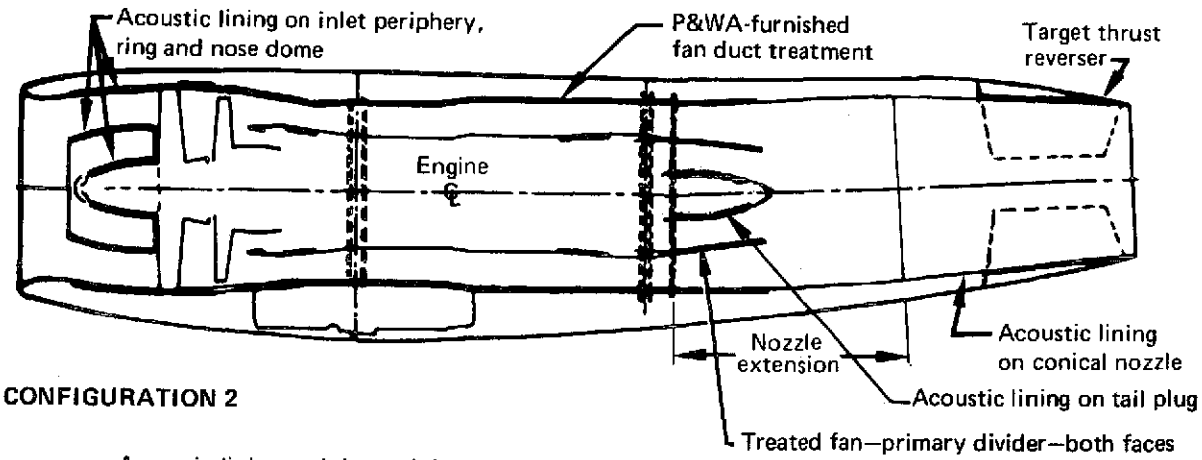


**737 CONFIGURATION 2**

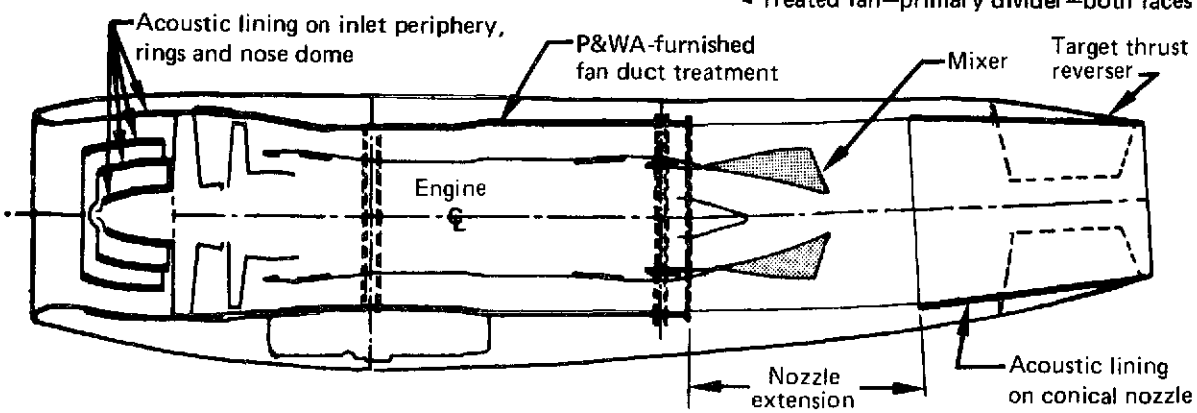


**737 CONFIGURATION 3**

*FIGURE 111.–737/JT8D-109 NACELLE CONFIGURATIONS*

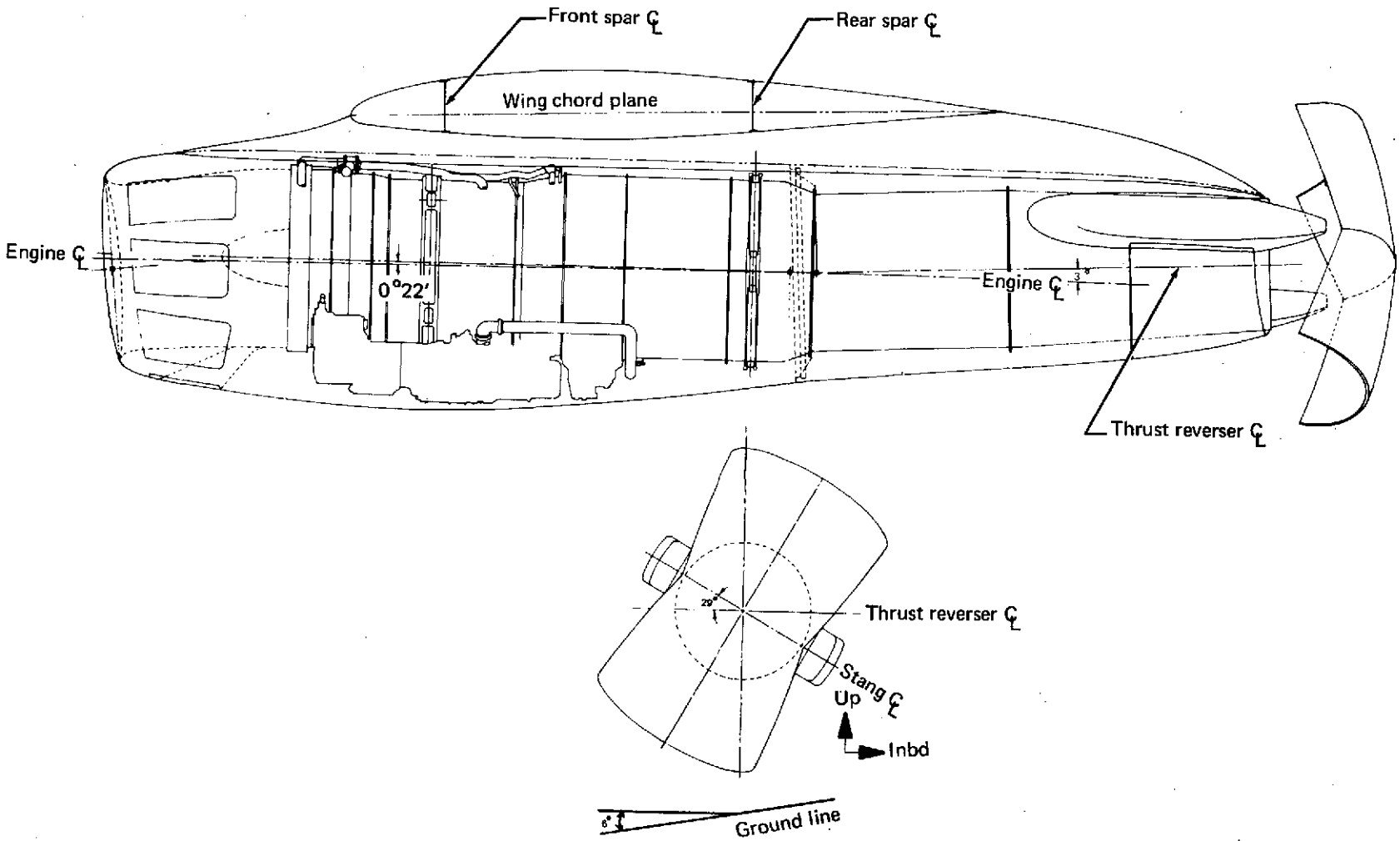


**REAR VIEW**

**THRUST REVERSER DEPLOYED**

*FIGURE 112.–737/JT8D-9 BASELINE NACELLE GENERAL ARRANGEMENT*

is attached to the wing near the front spar, and the rear mount is attached to the flap track under the rear spar. The inlet highlight plane is canted with toe-in and droop to match over-wing flow. Blow-in doors in the inlet provide supplementary airflow at takeoff. Two hinged side cowls provide access to the engine and accessories. A tailpipe extension is inserted between the aft engine face and the target-type thrust reverser to place reverse thrust gas flow behind the flaps.

### 5.4.1 Configuration 1

The nacelle general arrangement and aerodynamic design of configuration 1 are discussed in the following two sections.

#### 5.4.1.1 Nacelle General Arrangement

The installation designed for the JT8D-109 (fig. 113), retains the long fan duct integral with the engine. Configuration 1 also uses the wing-mounted concept from the baseline airplane and uses most of the existing wing/nacelle fairing with minor alterations.

The engine mounts were not redesigned, resulting in the engine centerline being relocated 5.5 in. (0.140 m) lower than on the baseline airplane while retaining the same inclination to the wing chord plane as before.

A longer landing gear, described in section 5.5.1, would keep ground clearances at the highlight plane and under the nacelle essentially the same as for the baseline airplane.

The nacelle design consists of an acoustically treated inlet of fixed geometry, two side cowls installed between the inlet and the tailpipe, a shrouded tailpipe extension, an acoustically treated conical tailpipe, and a target-type thrust reverser.

The engine mount concept was retained intact in the modified-configuration design. Due to higher loads generated by the heavier engines, the mount-to-wing attachment will have to be reviewed and the vibration isolators and cone bolts replaced with stronger units. To retain the existing geometry, the aft cone bolt length would be extended approximately 0.75 in. (0.019 m). The aft mount consists of only one suspension point. Figure 114 shows an exploded view of the forward mount.

One of the ways used to reduce noise levels was to install acoustic lining in the inlet. This required a complete new inlet design. Where the present design has a series of blow-in doors to supplement airflow at low Mach numbers, the new design used this internal area for the installation of sound-suppression material, thereby dictating a complete revision of the inlet lip and internal

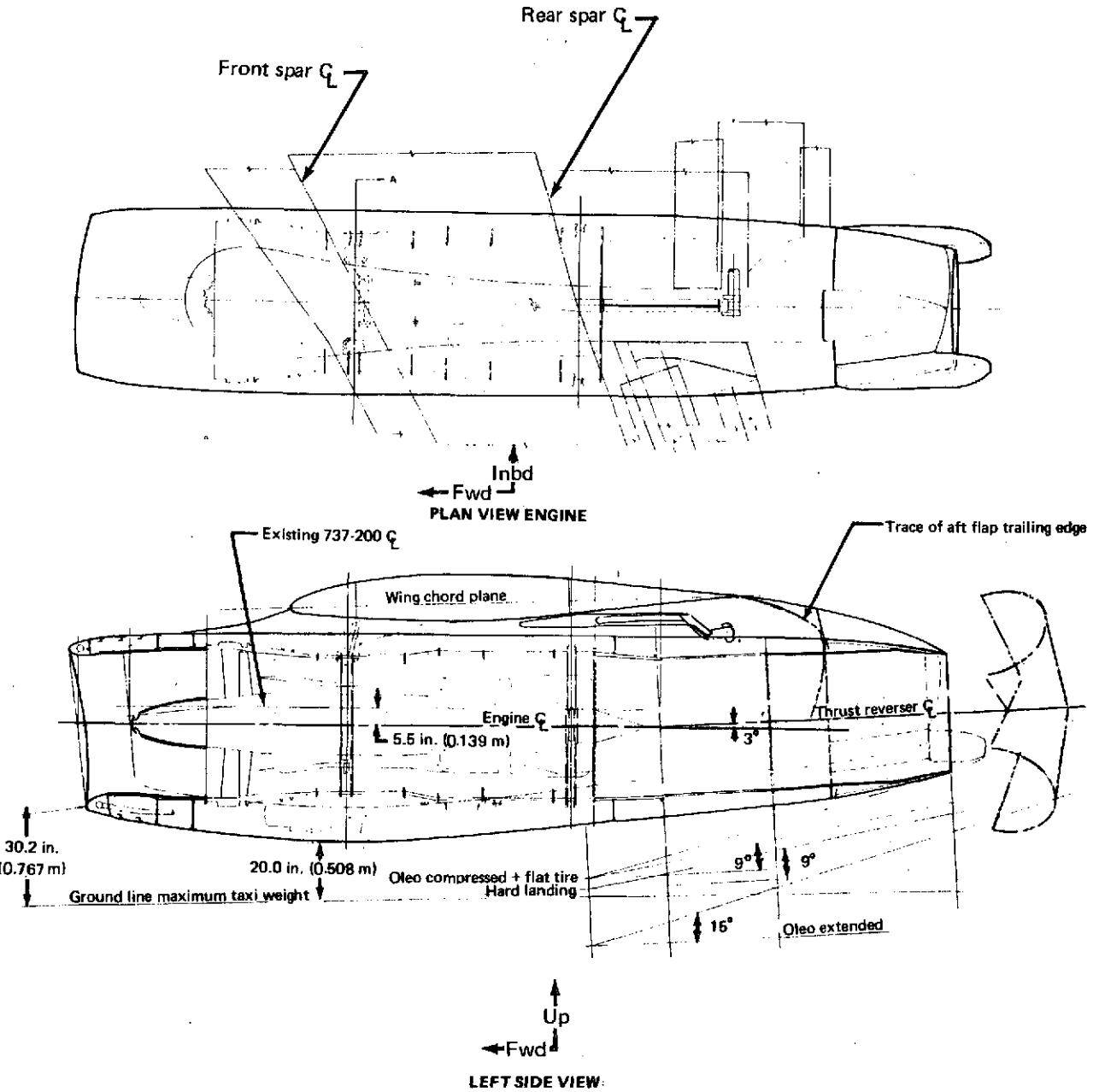


*FIGURE 113.—737/JT8D-109 CONFIGURATION 1 NACELLE*

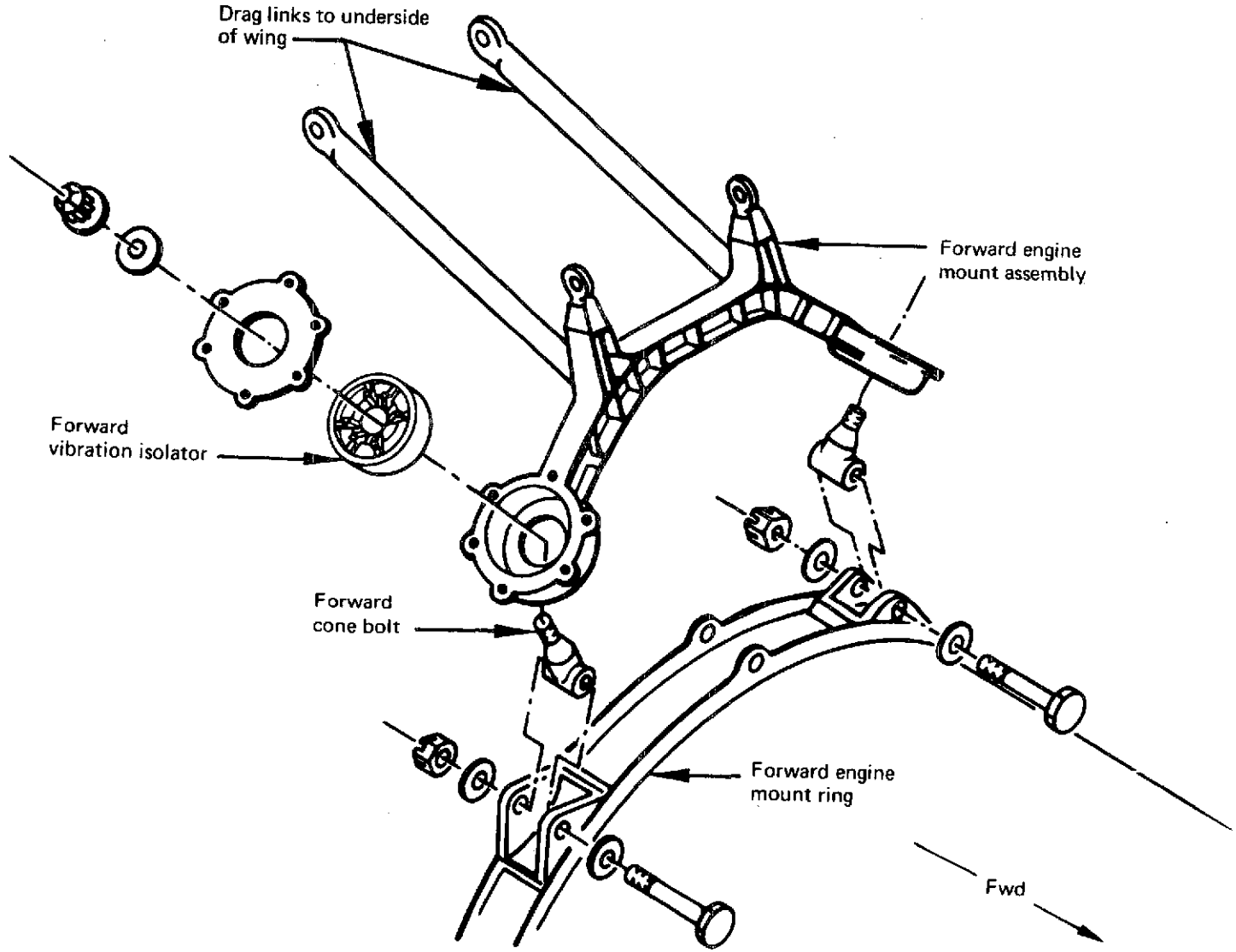


*FIGURE 114.—737/JT8D-109 FORWARD ENGINE MOUNT*

inlet geometry. Elimination of the blow-in doors required a change in the manner of picking up and discharging cooling air for the nose cowl thermal anti-ice (TAI) system.

The new inlet design retained the same highlight inlet position relative to the airplane and the same ground clearances as the existing model. The inlet ellipse and throat were sized for the larger basic engine and for the adjustments necessary to provide adequate low duct Mach number and high inflow angle airflows. Acoustic lining was designed to be installed aft of the inlet throat and aft of the TAI air exhaust ring on the nose dome. The inlet TAI system design was modified to approximately the same system as was used on the 727 JT8D-9 inlet. The remainder of the inlet would be aluminum skin and frame construction. See figure 115 for a cross-section view of the refanned engine inlet.

The JT8D-109 engine design incorporates a full-length fan bypass duct, which is similar to the fan duct on the JT8D-9. The two basic differences between the -9 and the -109 are higher bypass ratio and extensive sound absorption lining in the fan duct. In configuration 1, the engine primary air and the fan air would be free to mix through the full length of the tailpipe and the tailpipe extension.

The engine cowling, shown in figure 116, was designed in three sections. The upper section of approximately 120° was attached to the engine frames and included access panels for the forward-engine mount vibration isolators, the fuel heater valve, the bleed valve air filter, etc. The lower sections were hinged from the upper section and contained exit ports for engine accessory cooling air and heat exchanger exhausts, as well as fuel and oil drain sumps, the cowl vent, duct blowout doors, and an oil tank filler door.

The upper half of the engine cowling package was designed of fire-resistant construction. The lower portion would form an aerodynamic shape over the engine accessories. One of the lower two doors was designed to offset approximately 10° from bottom center to facilitate installation of drains along the keel line. Both the fixed and the hinged cowl panels would be of skin and stringer construction.

On the baseline airplane a tailpipe extension is inserted between the engine aft face and the exhaust-nozzle/thrust-reverser package. This is to ensure that the exhaust gas deflected by the thrust reverser doors will stay behind the wing trailing edge flaps when they are in the maximum-down position. A similar, but larger diameter, extension would be used on the JT8D-109 installation. The -109 tailpipe would be constructed of high-temperature perforated honeycomb to achieve the maximum sound attenuation.

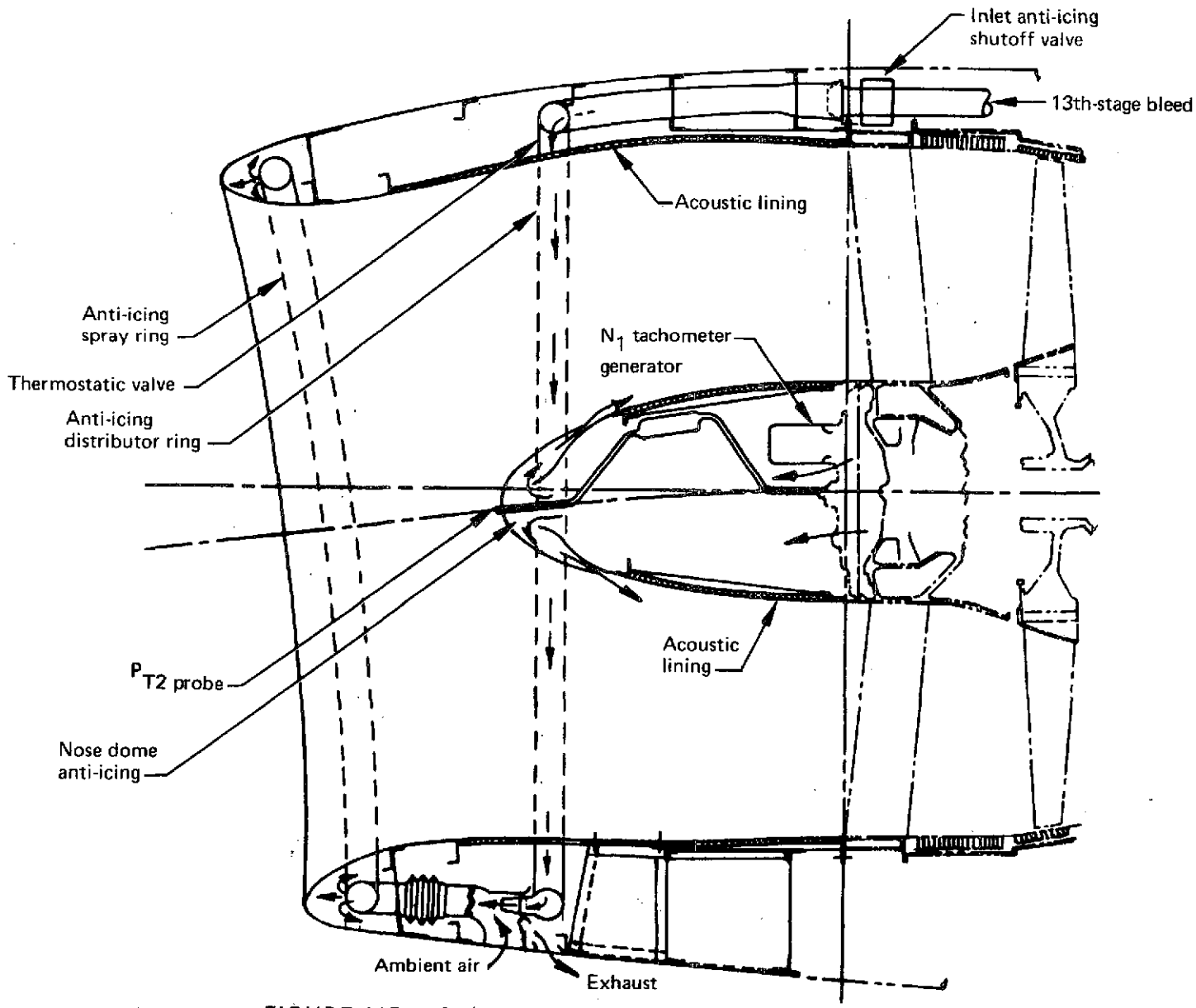


*FIGURE 115.–737/JT8D-109 CONFIGURATION 1 INLET CONSTRUCTION*

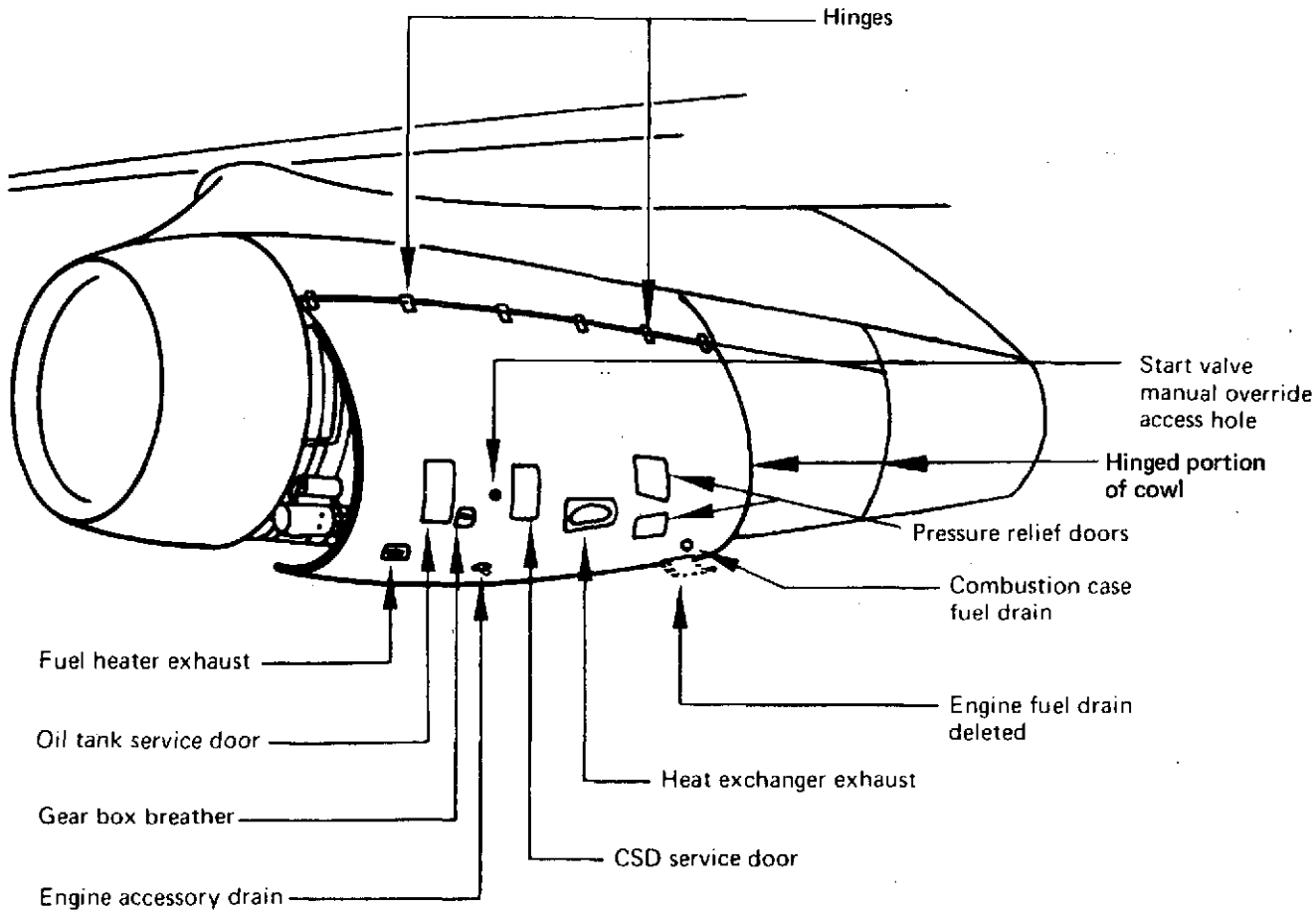


*FIGURE 116.—737/JT8D-109 COWL PANELS AND ACCESS DOORS*

To fair with the engine cowl package, a three-part shroud or cowl would be installed around the tailpipe. This shroud would be supported by two fire-resistant bulkheads, one at the aft engine flange and one near the forward flange on the nozzle/thrust-reverser package. This shroud would consist of a fixed upper section and two, hinged, lower sections. The upper half of this package would be of fire-resistant construction. The entire package would be of skin and stringer construction.

The design of the thrust-reverser to be used with the JT8D-109 engine was basically a scaled-up version of the target-type reverser in use on the baseline 737 aircraft (see fig. 112).

This same type of reverser was selected as the reverser for the 727 airplane with the JT8D-109 engine installation. For a discussion of the JT8D-109 reverser, see section 4.4.1. On the 737, the reverser design required door rotation from the vertical to prevent direct exhaust gas impingement on the fuselage and flaps.

The thrust reverser primary power source would be airplane hydraulic system A through the main landing-gear-down line, as shown on figure 117. Use of the landing gear hydraulic system as the power source allowed for isolation of the reverser system from the aircraft system during flight. An alternate source would be included from the aircraft standby hydraulic power system for emergency operation of the reverser.

The JT8D-109 installation design retained the same standard of interchangeability as that provided by the JT8D-9 installation on the 737. In particular, the tailpipe extension and the hinged cowl panels would be identical for both engine positions. The same thrust reverser would be used on either engine, but it would be clocked to a different angle on each installation to provide optimum flow characteristics. This requires change in the piggyback fairing location.

The total nacelle installation on either the left- or right-hand strut would be fully interchangeable, with the exception of the clocking requirements for the thrust reverser and the replacement of the inlet assembly and nose dome.

The exterior shape of the nacelle was selected to enclose the necessary components and yet present the least airflow resistance in flight. The inlet highlight diameter for the JT8D-9 engine is 41.74 in. (1.06 m), as compared to 52.98 in. (1.343 m) for the JT8D-109. The basic nacelle diameter was increased from 50 in. (1.27 m) to 62 in. (1.575 m).

The inlet design was sized to the available preliminary engine air requirements. The corrected airflow rates for sea level static takeoff thrust condition and 35 000-ft (10 668-m) altitude, Mach



(3

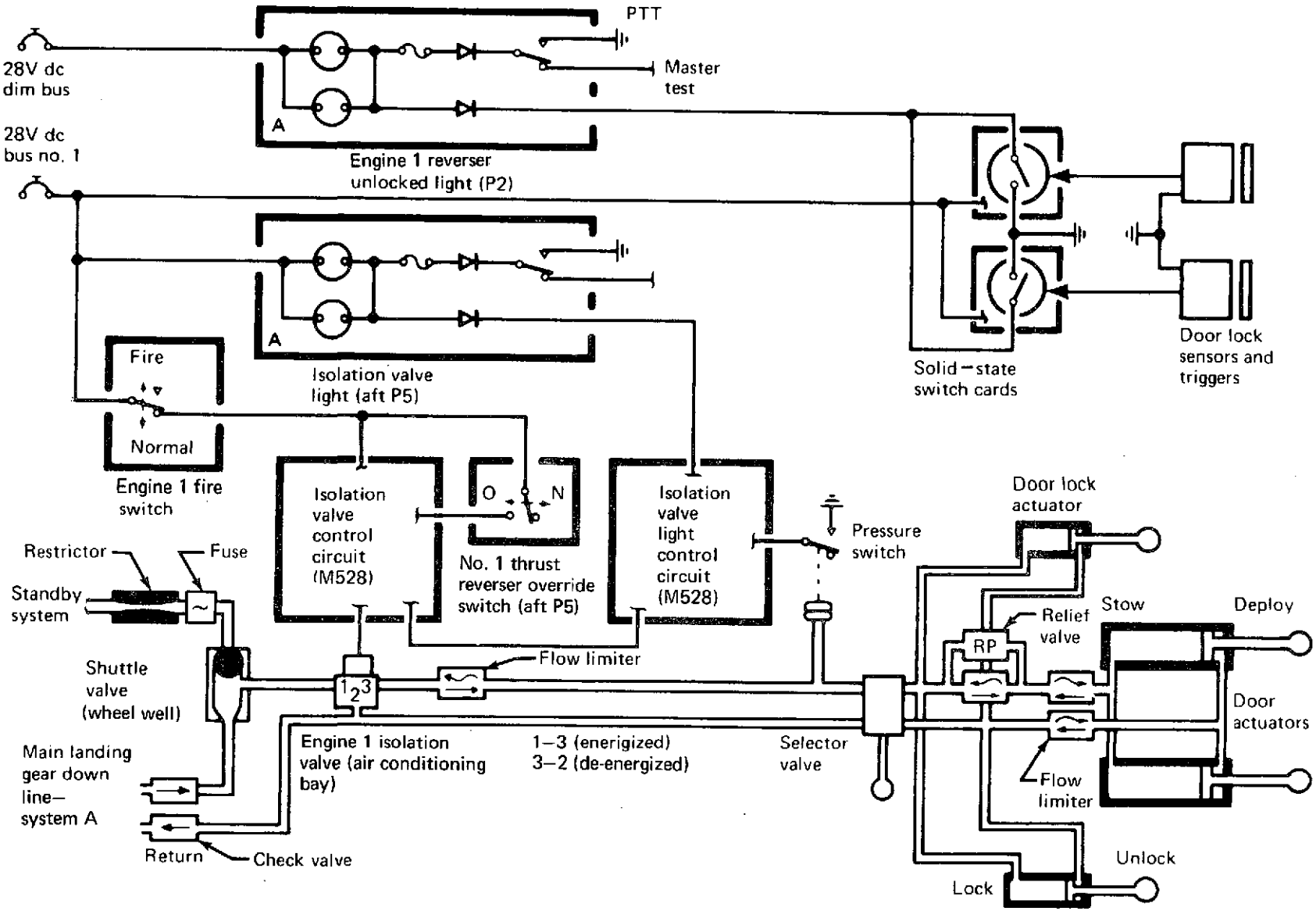


*FIGURE 117.–737/JT8D-109 THRUST REVERSER HYDRAULIC/ELECTRICAL SYSTEM DIAGRAM*

0.8 maximum continuous thrust conditions are 467 lb/sec (211.83 kg/sec) and 489 lb/sec (221.81 kg/sec), respectively. These flow rates correspond to inlet throat Mach numbers of 0.548 and 0.589, respectively. These flow rates also correspond to inlet pressure recovery ratios ($P_{T2}/P_{T0}$) of 0.990+ and 0.996+, respectively.

To agree with the 727 installation, a tailpipe length of 45 in. (1.143 m) was used. This was based on the use of a target-type thrust reverser. The tailpipe would be a conventional convergent conical nozzle that acts as a mixing chamber for the hot primary and the cold fan airflows. These then exit through the common nozzle.

A 73.5-in. (1.867-m) tailpipe extension would be inserted between the aft engine flange and the forward tailpipe flange to position the thrust reverser aft of the wing trailing edge flaps. This extension would provide additional mixing length for the primary and secondary airflows plus additional surface area that could be used for installation of acoustic absorption materials.

The engine and nacelle system design required was for the airframe equipment necessary to integrate the engine into the airplane. This included such items as cooling and ventilation, vents and drains, fire protection, lubrication and fuel systems, CSD/generator, controls and instrumentation, engine starting, engine bleed air, and ice protection, as shown in figure 118. All present systems would be retained to the maximum extent. In general, components would be retained, but ducting, plumbing, and bracketry would be redesigned.

The engine controls for the JT8D-109 would be identical to the JT8D-9. Therefore, no changes would be required other than those necessary to physically adapt to the greater engine size. The engine and engine equipment instrumentation would be similar to the existing JT8D-9 instrumentation with the only major changes being changes of limit values on readouts.

Figure 119 is a schematic of the engine bleed air system for the JT8D-109 engine. This system is schematically very similar to the existing JT8D-9 system; however, all ducting in the nacelle area would be new. Most of the present valves, etc., would be retained.

Figure 120 shows the three main fire-containment zones in the engine areas. One area includes the engine proper and uses two fire detectors. One fire detector would be installed below the under-wing firewall and the other would be run along the underside of the engine. The second area includes the full length of the tailpipe extension and a small part of the exhaust nozzle. One fire detector would be located under the tailpipe extension. The final protection zone is the reverser itself. There would be no detectors in this zone. The fire extinguishing system used on the JT8D-109 nacelle would be the same system presently being used on the JT8D-9 nacelle, with some minor changes to increase the system capacity to serve the larger volume of the JT8D-109 nacelle.

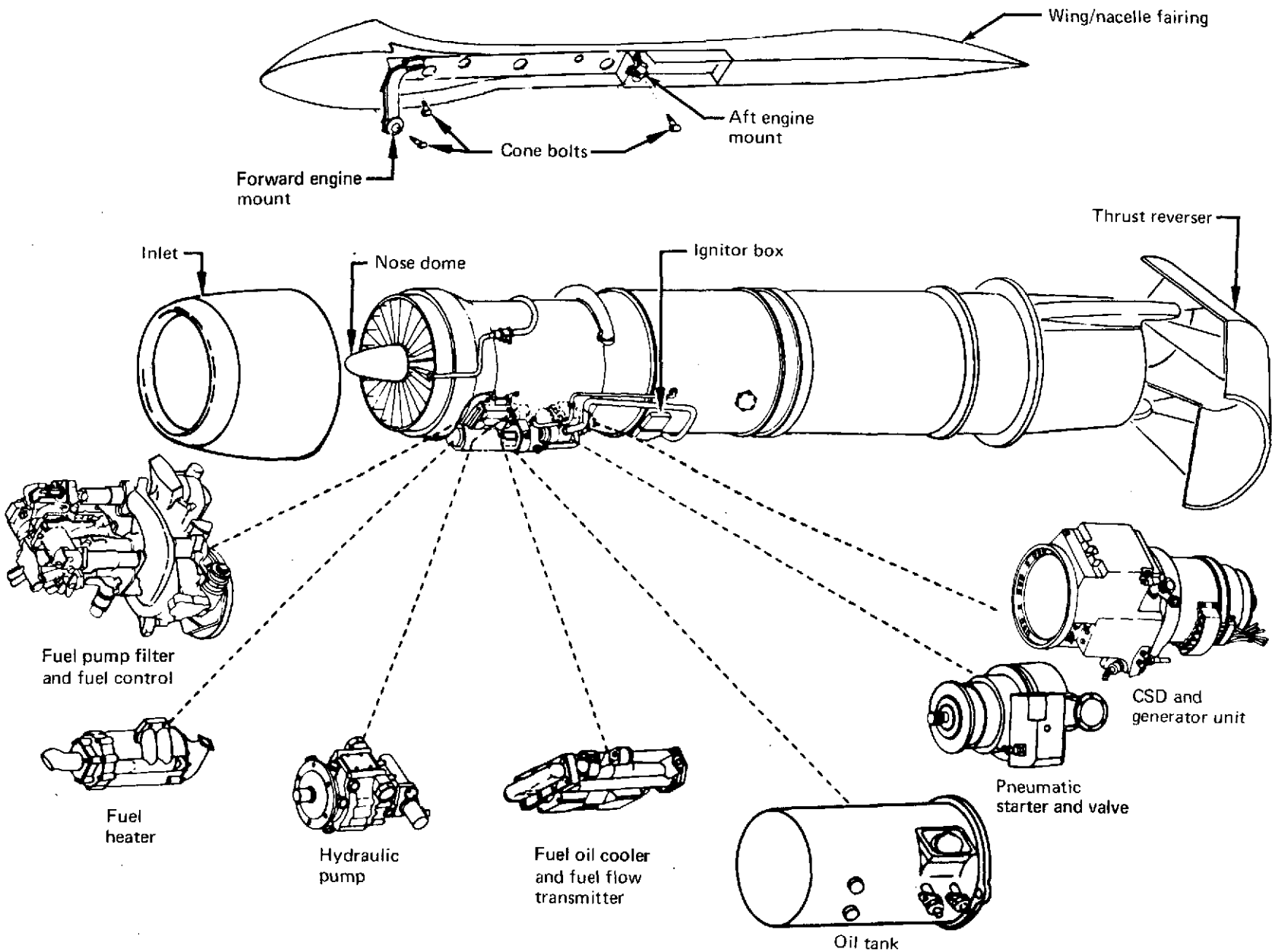


*FIGURE 118.–737/JT8D-109 POWER PLANT INSTALLATION*

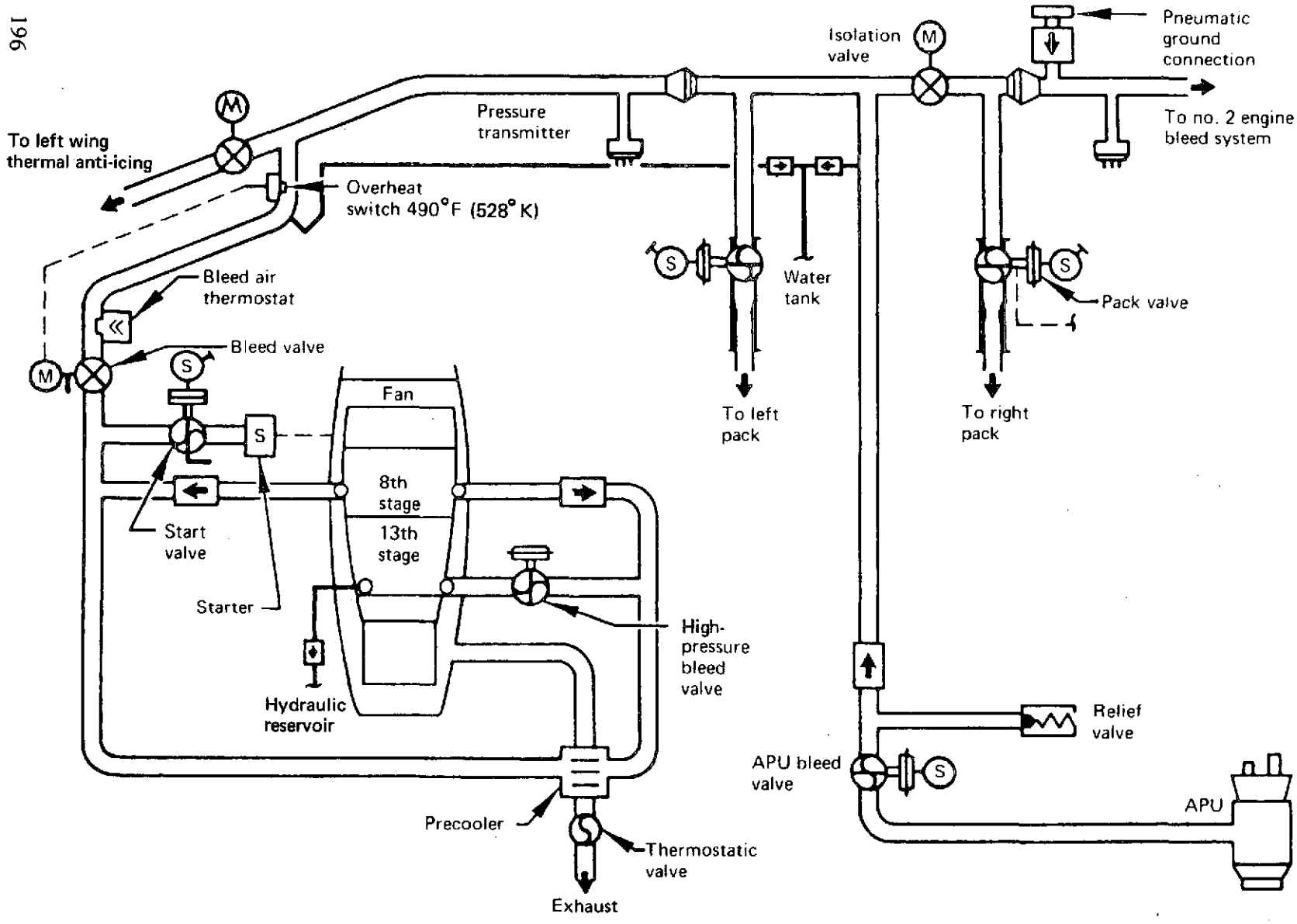


*FIGURE 119.—737/JT8D-109 PNEUMATIC SYSTEM BLOCK DIAGRAM*

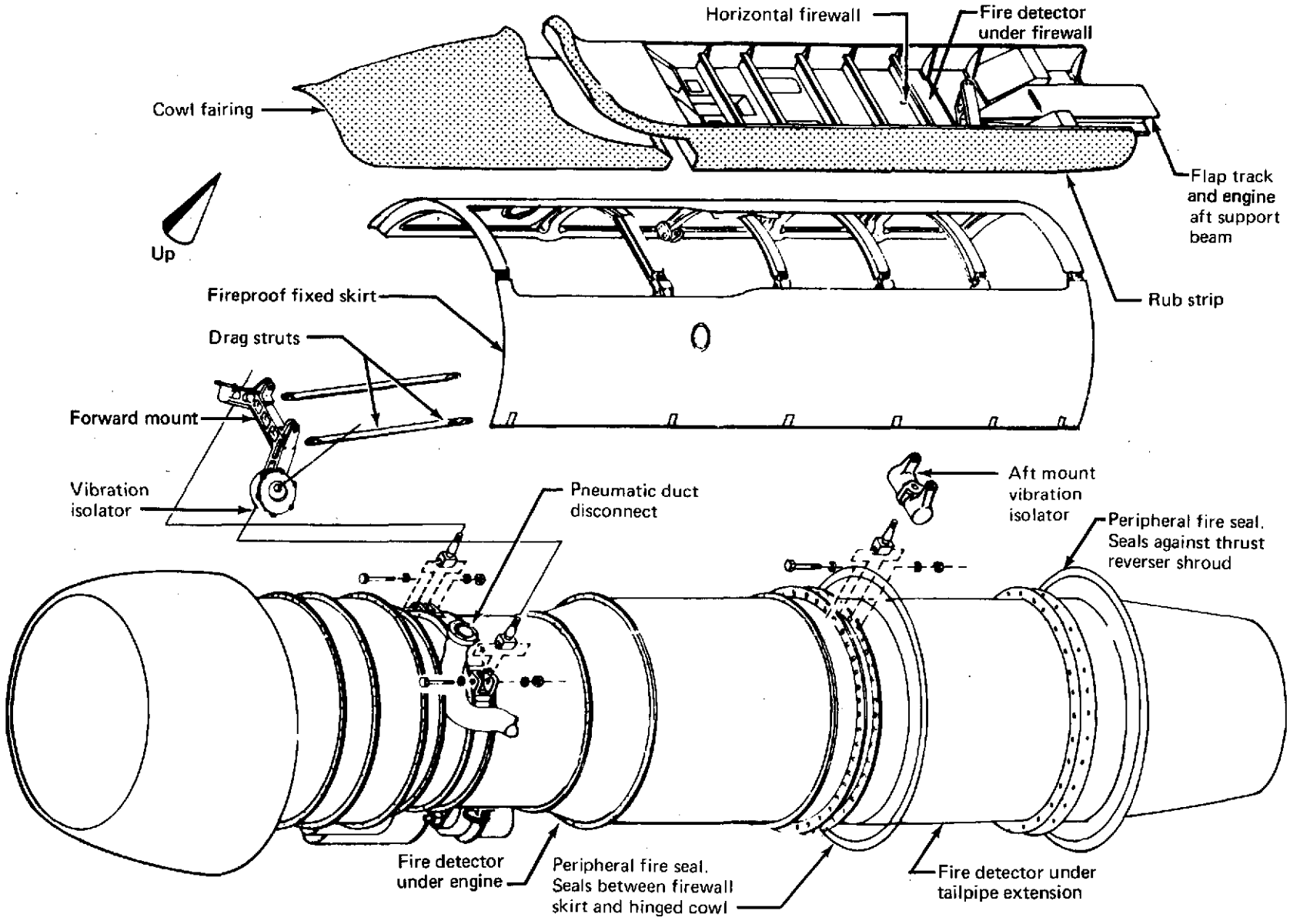


*FIGURE 120.—737/JT8D-109 FIRE ZONES AND DETECTORS*

### 5.4.1.2 Nacelle Aerodynamic Design

*External aerodynamics.*—The JT8D-109 nacelle is designed to enclose the engine and accessory package with the minimum increase in size from the current installation. A comparison of external geometric characteristics between the JT8D-109 and the JT8D-9 installations is shown in figure 121.

*Internal aerodynamics (inlet).*—The engine inlet, shown in figure 122, is of conventional design with acoustic lining on the diffuser periphery and the nose dome only. It has a contraction ratio (highlight area to throat area) that varies from 1.225 on the upper lip to 1.347 at the lower lip. These two extremes are located on a plane orientated 30° to the engine vertical centerline to satisfy the wing spanwise flow characteristics. An engine compressor face diameter of 50.10 in. (1.273 m) and a 42.60-in. (1.082-m) inlet centerline length result in an inlet length/diameter (L/D) ratio of 0.85.

The design requirements are:

a) Airflow—The engine inlet is sized from preliminary engine airflow data. These design inlet airflows and the resulting throat Mach numbers are shown below.

| Flight condition | Corrected airflow, $W_a$ lb/sec | Corrected airflow, $W_a$ kg/sec | Inlet throat Mach no. |
|---|---|---|---|
| Sea level static, takeoff thrust (standard day) | 467 | 211.8 | 0.548 |
| 13 000 ft (3962.4 m) static, takeoff thrust (standard day) | 491 | 222.7 | 0.593 |
| 35 000 ft (10 668 m), 0.8 M, maximum continuous thrust (standard day) | 489 | 221.8 | 0.589 |

b) Flow Field—The inflow angles relative to the body reference line are estimated to vary as much as 30° to 40° upflow, combined with a spanwise flow 2° to 3° at the inlet, depending on flap setting and forward speed at the takeoff condition.

Inlet aerodynamic losses can be subdivided into two categories: lip losses (a function of inlet velocity ratio, angle of attack, and lip geometry) and internal losses, which include acoustic treatment. The internal losses are only a function of wetted surface area and corrected airflow rate, provided that diffusion rates are low.

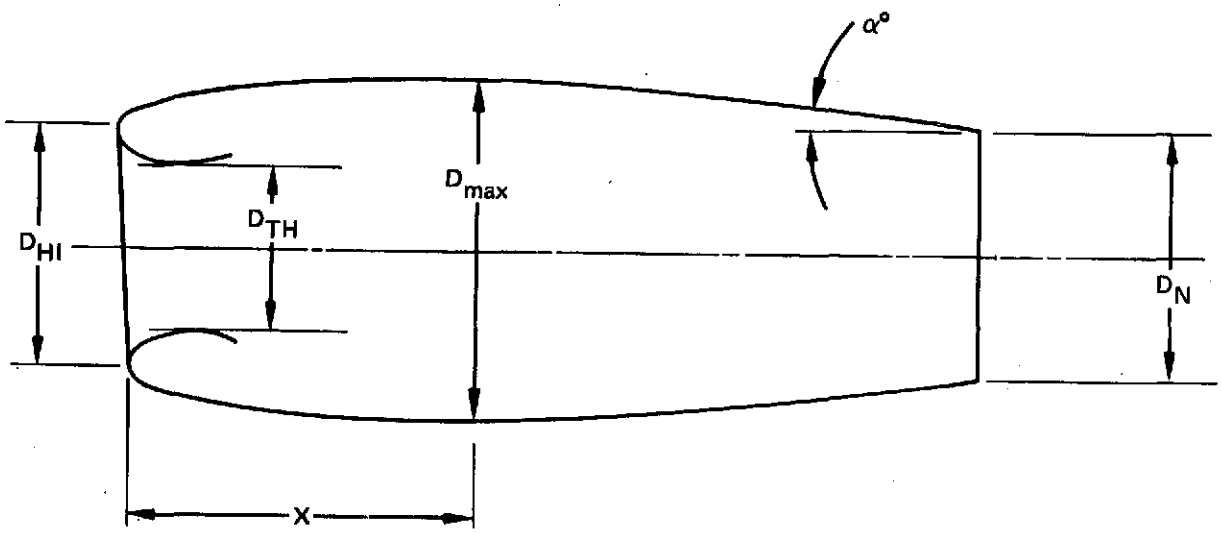


| | JT8D-9 | JT8D-9 | JT8D-109 | JT8D-109 |
|---|---|---|---|---|
| Nacelle length | 265.43 in. | 6.742 m | 289.15 in. | 7.344 m |
| Maximum diameter ($D_{max}$) | 50.0 in. | 1.27 m | 62.0 in. | 1.575 m |
| Maximum area ($A_{max}$) | 15.87 $ft^2$ | 1.474 $m^2$ | 23.0 $ft^2$ | 2.137 $m^2$ |
| Nozzle exit diameter ($D_N$) | 29.84 in. | 0.758 m | 38.544 in. | 0.584 m |
| Ratio ($D_{HI}/D_{max}$) | 0.854 | 0.854 | 0.855 | 0.855 |
| Length to maximum section (X) | 25.0 in. | 0.635 m | 58.57 in. | 1.488 m |
| Tailpipe boattail angle $\alpha$ | 12° | 12° | 12° | 12° |
| Throat diameter ($D_{TH}$) | 37.707 in. | 0.958 m | 46.70 in. | 1.186 m |
| Hilite diameter ($D_{HI}$) | 41.74 in. | 1.060 m | 52.98 in. | 1.346 m |

*FIGURE 121.–NACELLE AERODYNAMIC CHARACTERISTICS–737-200 AIRPLANE*

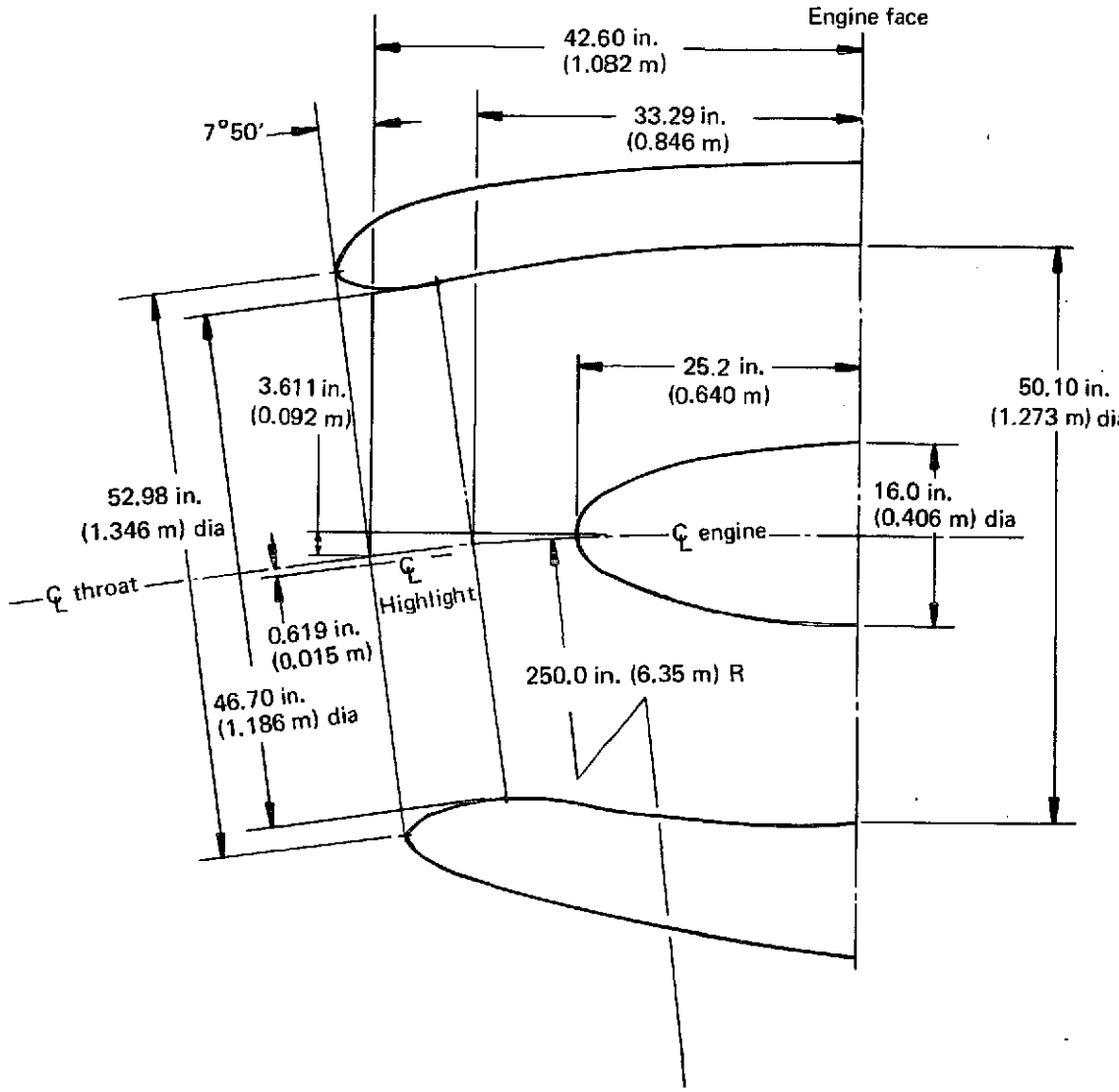


*FIGURE 122.–INLET GEOMETRY–737-200 AIRPLANE, CONFIGURATION 1*

The inlet pressure recovery, based on the above considerations, is estimated to be as shown below:

Estimated inlet performance

| Flight condition | Pressure recovery $P_{T2}/P_{T0}$* |
|---|---|
| Sea level static, takeoff thrust | 0.990 |
| Sea level, ⩾50 kn (25.72 m/sec), takeoff thrust | 0.996 |
| 35 000 ft (10 668 m), 0.8 M, maximum cruise thrust | 0.996 |

### 5.4.2 Configuration 2

The configuration 2 design was the same as configuration 1, except for the addition of an acoustically treated ring in the inlet, provision for hinging the inlet for access to the engine front face, an acoustically treated splitter ring and an elongated center plug in the tailpipe, and a revised thermal anti-icing system for de-icing the inlet splitter ring. Figure 123 shows a general arrangement of this configuration.

#### 5.4.2.1 Nacelle General Arrangement

The inlet splitter ring and the modifications to the inlet thermal anti-ice system are depicted in figure 124. A comparison of this figure with the cross-section of the configuration 1 inlet shown in figure 115 will show the additions. The method of hinging the inlet for access to the engine is shown in figure 125. Note that these hinges support the inlet only when the inlet is open. When operational, the inlet would be bolted to the front flange of the engine in the same manner as is the JT8D-9 inlet.

The tailpipe extension would house an acoustically treated splitter and an elongated, acoustically faced plug. The conical splitter would be located behind the aft engine face, the forward end forming a continuation of the flow divider between engine primary and fan air. The wetted areas on both sides of the splitter ring would be acoustically treated. The center plug would be elongated to provide an engine match to the splitter ring area and to include additional acoustic treatment.

*The tabulated pressure recovery must be corrected upwards by 0.003 to be consistent with the baseline JT8D-9 performance data, which is referenced to a bellmouth inlet, as this reference bellmouth already accounts for 0.003 boundary layer loss.

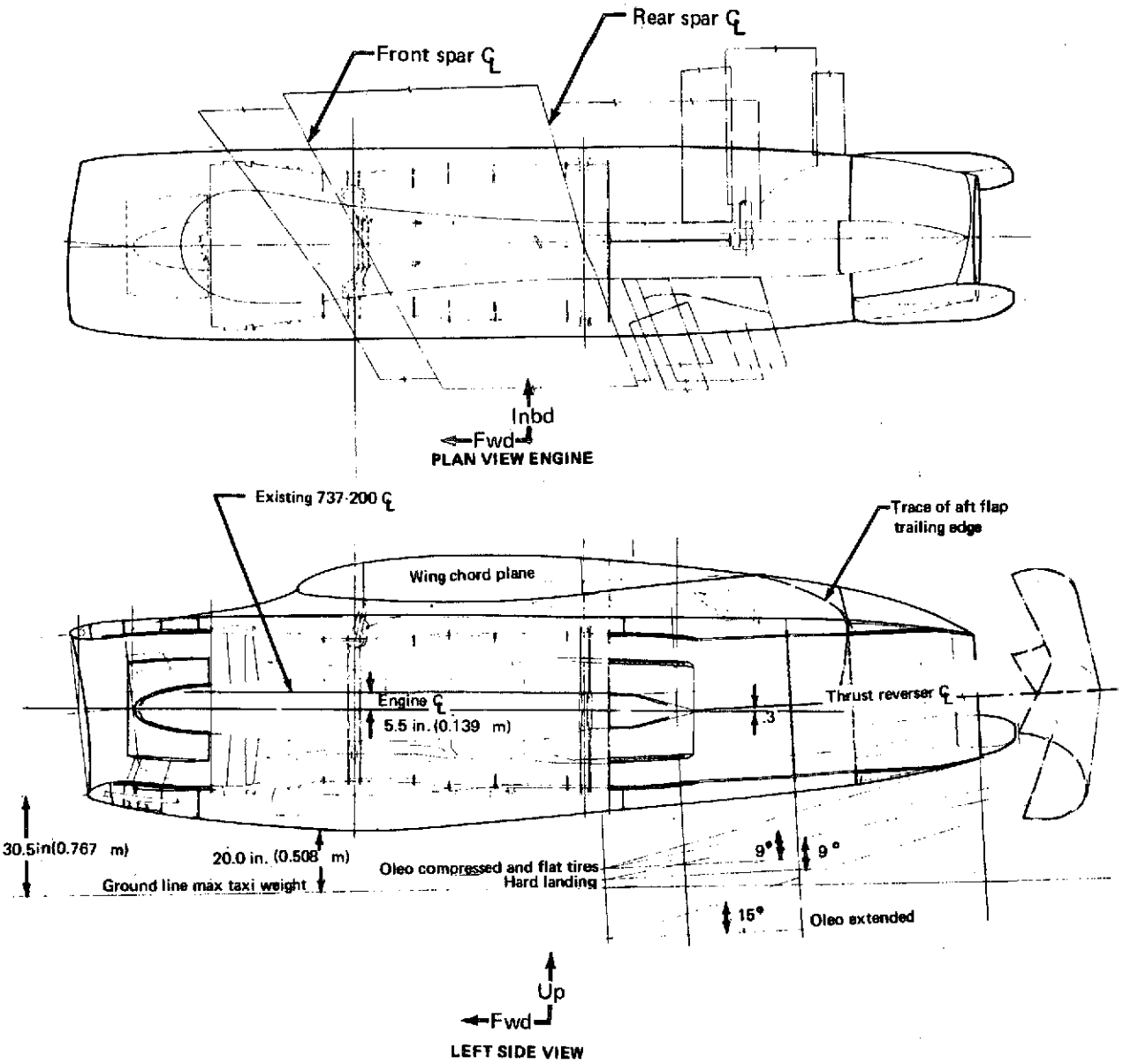


*FIGURE 123.–737/JT8D-109 CONFIGURATION 2 GENERAL ARRANGEMENT*

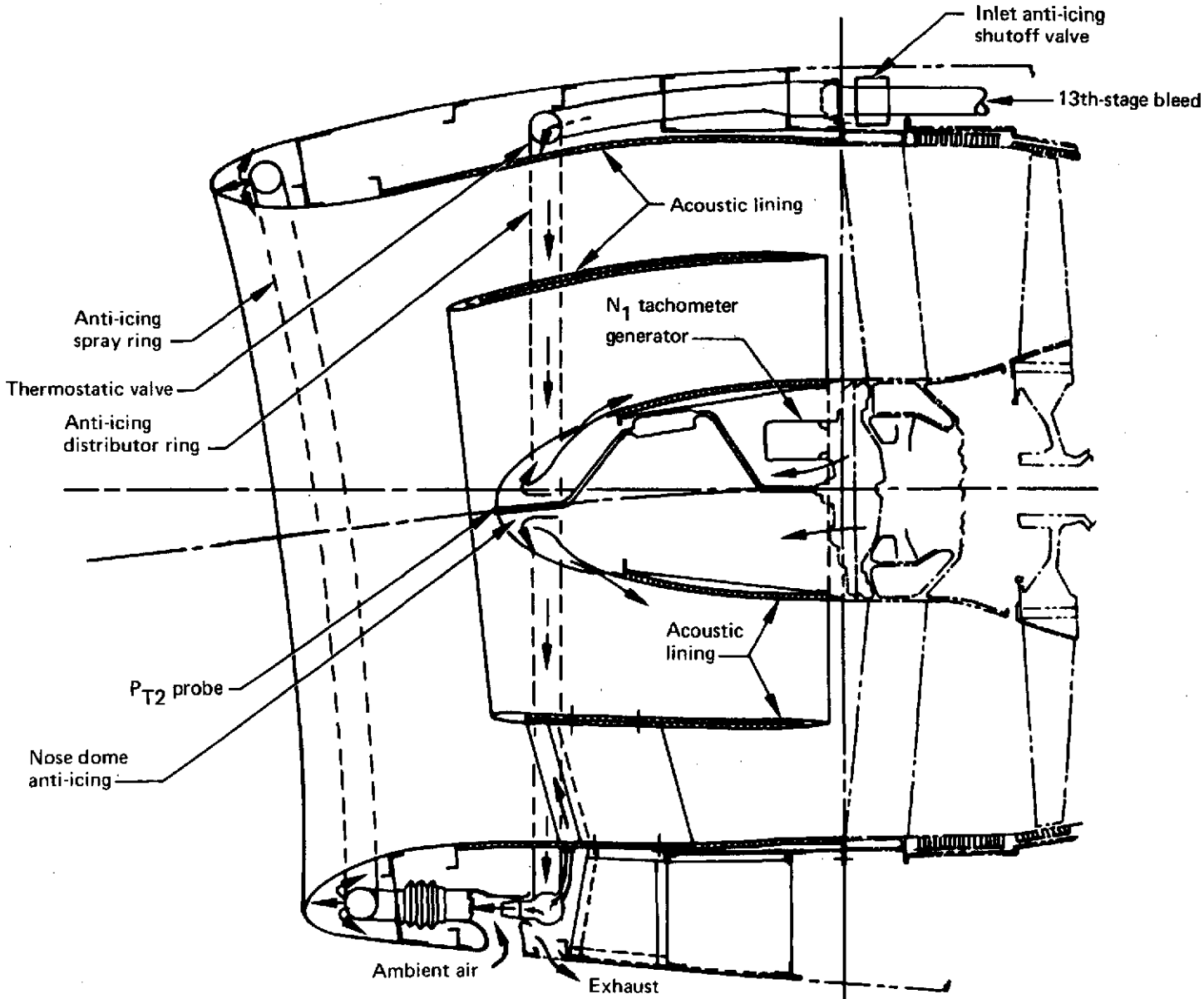


*FIGURE 124.—737/JT8D-109 CONFIGURATION 2 INLET CONSTRUCTION*

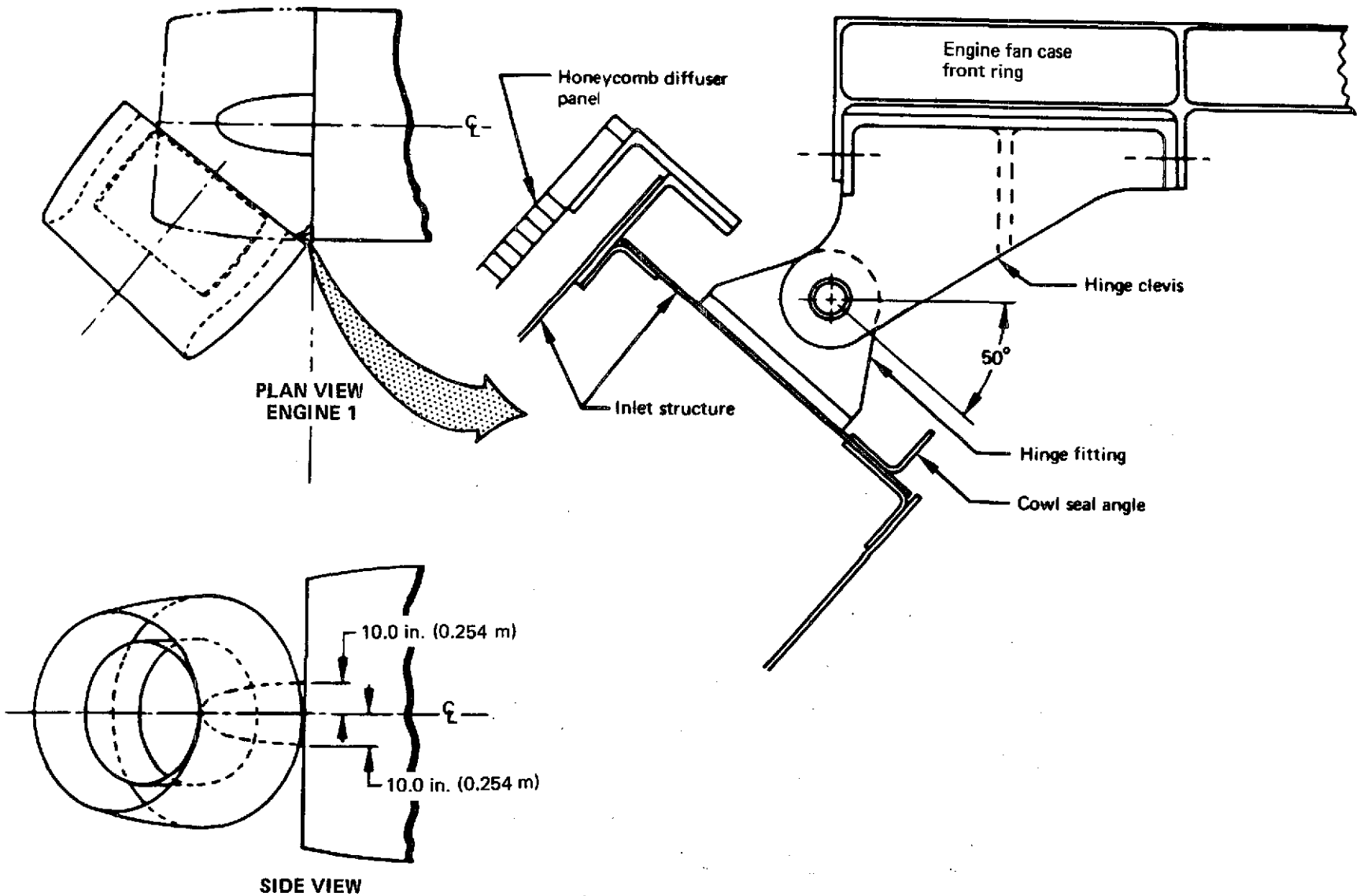


*FIGURE 125.—737/JT8D-109 NOSE COWL HINGE*

The internal airflow characteristics of configuration 2 would be very similar to configuration 1. The highlight would be the same size and would be installed in the same position relative to the airplane. The inlet lip and the throat diameter would be identical to configuration 1. The airflow through the inlet would be kept the same as configuration 1 by increasing the diffuser duct wall diameter in the area of the splitter. Accordingly, the corrected airflow and the throat Mach numbers would be identical to configuration 1.

Due to the greater wetted flow area generated by the splitter ring, the inlet pressure recovery ratio would be approximately 0.006 lower than the configuration 1 ratio. This would be true from sea-level static conditions to 35 000 ft (10 668 m) at Mach 0.8.

The sizing and flow area matching of the splitter ring and the extended tail cone in the tailpipe region would require analytical and model testing to finalize the design. The additions of the splitter ring and the elongated cone could result in some proportionate performance degradation.

#### 5.4.2.2 Nacelle Aerodynamic Design

The aerodynamic design for configuration 2 is the same as configuration 1. Installation of the single inlet ring did not necessitate any change in the inlet internal aerodynamics.

### 5.4.3 Configuration 3

The configuration 3 design was the same as configuration 1, except for the addition of two acoustically treated splitter rings in the inlet, provision for hinging the inlet for access to the engine front face, a forced primary-to-secondary air mixer in the tailpipe extension, and a revised thermal anti-icing system to provide for de-icing the two inlet splitter rings. (See fig. 126 for a general arrangement of the nacelle package.)

#### 5.4.3.1 Nacelle General Arrangement

The two inlet splitter rings and the modifications to the inlet thermal anti-ice system are depicted in figure 127. Comparison of this figure to the cross section of the configuration 1 inlet shown in figure 115 will show the additions. The method for hinging the inlet for access to the engine face would be the same as was used for configuration 2 and as shown in figure 125. As in configuration 2, the inlet would be peripherally bolted for flight operations.

The tailpipe design was the same as that used on configuration 1, except that it included an eight-lobe, primary-to-secondary air, forced mixer.

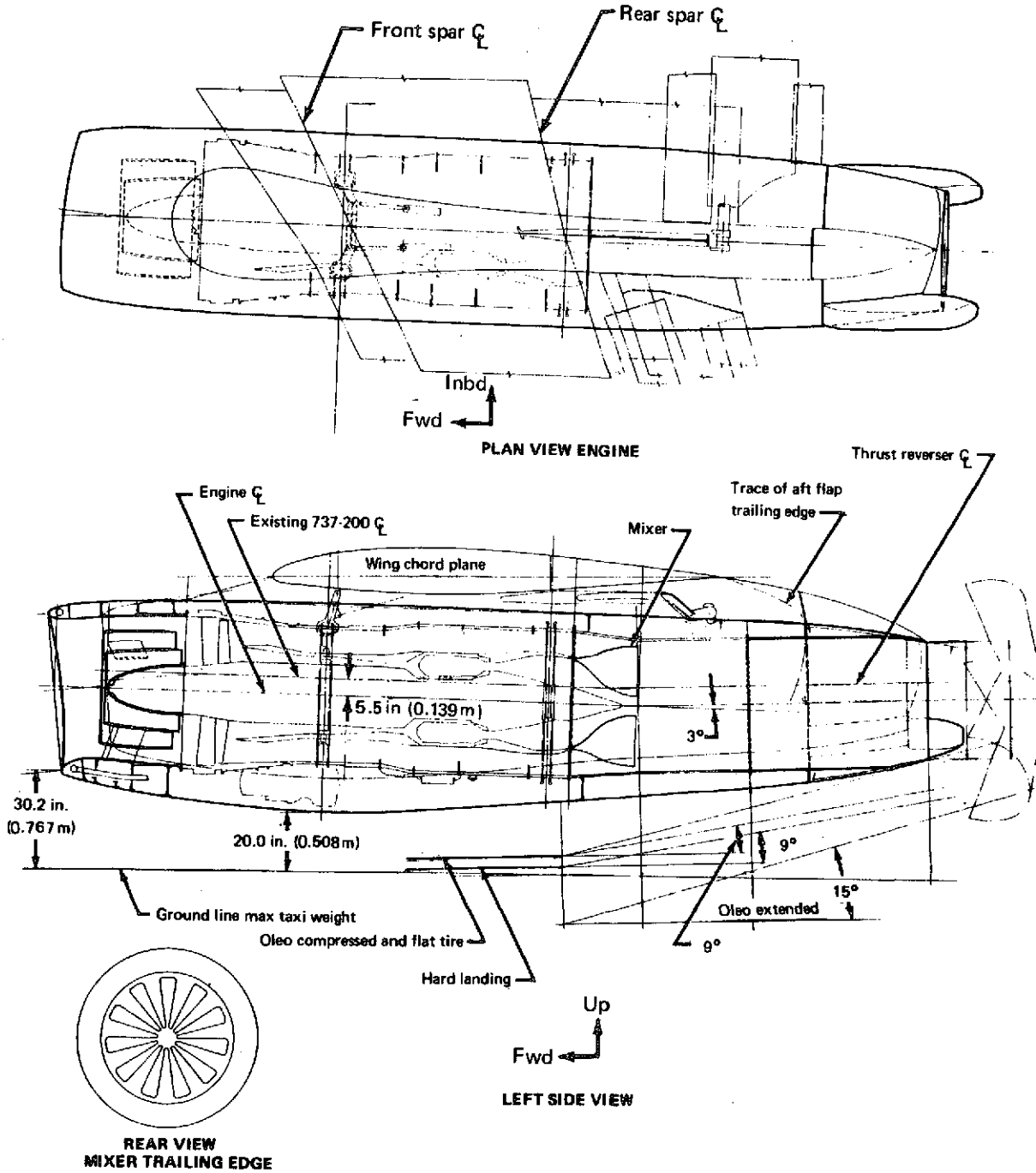


*FIGURE 126.—737/JT8D-109 CONFIGURATION 3 GENERAL ARRANGEMENT*

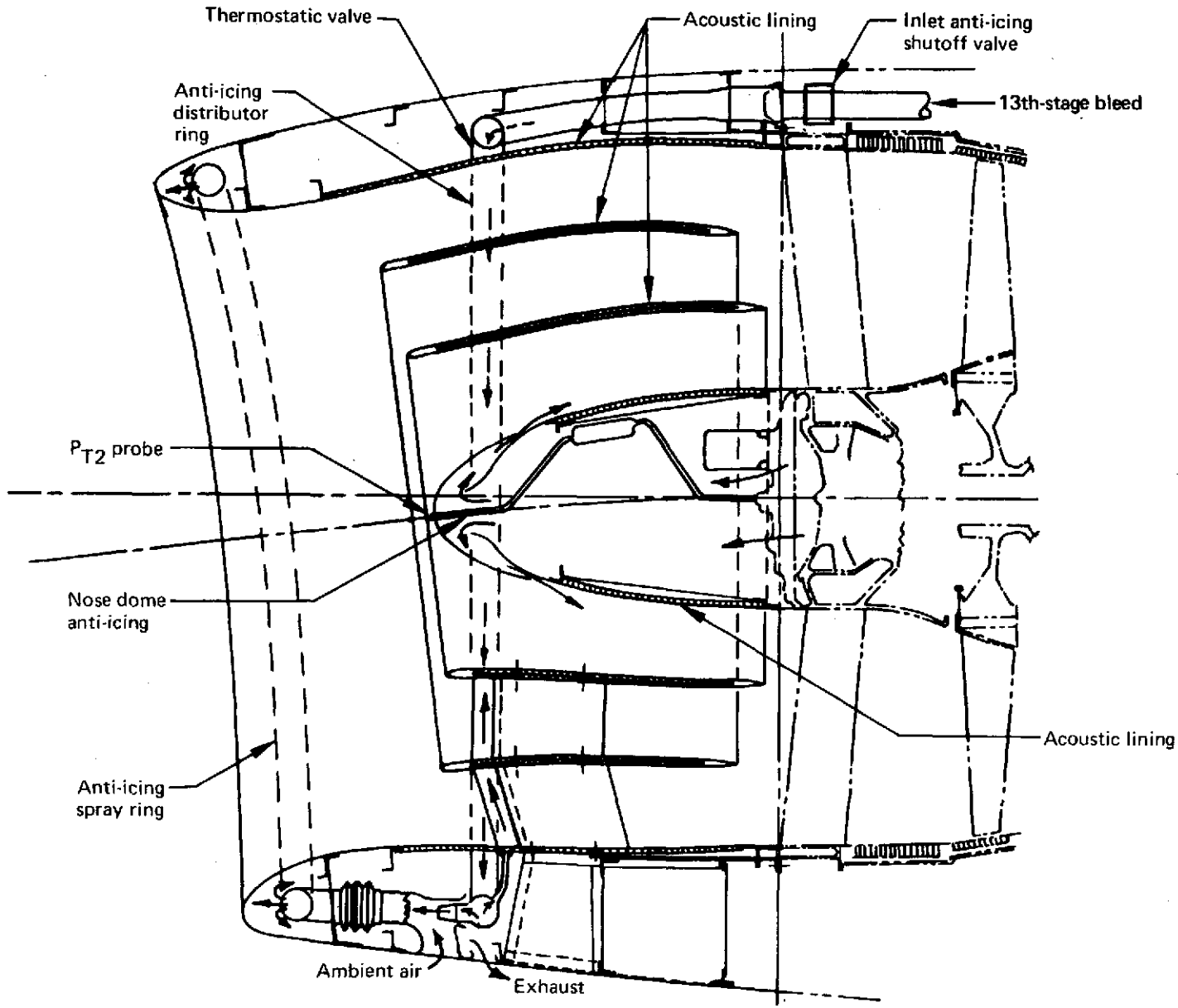


*FIGURE 127.—737/JT8D-109 CONFIGURATION 3 INLET CONSTRUCTION*

The inlet internal airflow characteristics for configuration 3 will be very similar to configuration 1. The highlight would be the same size and would be installed in the same position relative to the airplane. The throat ellipse and the throat diameter would be identical to configuration 1. The airflow through the inlet would be kept the same as configuration 1 by increasing the diffuser duct wall diameter in the area of the rings. Thus, the corrected airflow and the throat Mach numbers would be identical to configuration 1. Due to the much greater wetted flow area generated by the two splitter rings, the inlet pressure recovery ratio would be approximately 0.010 lower than the configuration 1 ratio. This is true for the full range of airplane operations.

The mixer in the tailpipe was designed to achieve the maximum amount of primary and secondary flow mixing possible using the length of the tailpipe and the tailpipe extension. This mixing would require a careful area match, both at the exit area of the mixer and at the nozzle. Extensive analytical studies, model testing, and full-scale testing would be required.

The purpose of a mixer in this application is to provide performance improvement and noise attenuation. With the extended mixing length in the 737 installation, a forced mixer at cruise should compensate for the penalties of weight and pressure loss associated with it. The performance of the mixer from a thrust augmentation aspect is a complex function of the design and thermodynamics of the hot and cold flows, but available mixing length is a strong positive function.

#### 5.4.3.2 Nacelle Aerodynamic Design

The aerodynamic design for configuration 3 is the same as for configurations 1 and 2. Installation of two inlet rings did not require any change in the inlet internal aerodynamics.

### 5.4.4 Studies

This section discusses the various studies conducted on the 737 airplane nacelle packages, the design considerations that preceded the particular studies, and the general reasons the airplane nacelle configuration discussed in section 5.4.1 (configuration 1) was chosen from the available options.

Airplane modification design studies are reviewed in section 5.5. The limiting factor to consider when installing a larger, heavier, more powerful engine on the 737 is the available space underneath the wing. Some factors that must be considered include: the fire integrity of the wing during an in-nacelle fire; adaptations to the leading and trailing edge flaps to retain the maximum flap area and to achieve the best seal against the fairing and nacelle package when in the extended position; and the general ease and simplicity of installing the total modification on the airplane.

The trade studies conducted before arriving at the airplane modification could be broken down into two groups: studies constrained either by a 12-in. (0.305-m) main landing gear extension or by a 4-in. (0.102-m) main landing gear extension. The configuration selected as the most promising for the 737 airplane program was the 12-in. (0.305-m) main landing gear extension.

A portion of the studies conducted on the various nacelle components were applicable only to the 4-in. (0.102-m) gear extension or only to the 12-in. (0.305-m) gear extension. The major portion were adaptable to either. Following is a very brief synopsis of the nacelle region studies conducted to assist in the selection of the 737 modification to be recommended.

#### 5.4.4.1 Inlet

The inlet was the first major subitem to be considered. Several different external and internal line combinations were investigated to check the feasibility of developing one basic inlet for both the 727 airplane and the 737 airplane. Coupled with this was a study of inlet length-to-diameter ratio to achieve the maximum performance recovery in various wind conditions. Due to the much different airflow patterns into the 727 and 737 inlets, no single inlet geometry would provide acceptable pressure recovery on both airplanes.

Several different types of acoustic materials were considered, both for noise attenuation and for internal strength. One of the principal considerations of the airplane operators is the service life of the acoustic absorption panels. This is also related to the ease of replacing the panels in case of irreparable damage.

Various methods of constructing the anti-ice plenum chambers were investigated. The primary consideration was to design a durable lip that would be heat resistant but would expand and contract with temperature fluctuations without materially affecting the adjoining aluminum structure.

Hinge types investigated for the nose cowls ranged from full clamping units to totally bolted units whose hinges supported the nose cowl only when open on the ground. Retention of the standard bolt circle with the hinges loaded only in the open position was selected.

#### 5.4.4.2 Engine Cowl Panels

The exterior lines of the cowl panels were defined by a combination of aerodynamic requirements and the physical requirements to clear engine equipment and to mate with existing engine-to-wing structure, which was to be reused.

The design parameters were lightweight structure for ease of handling, quick removal and replacement, minimum susceptibility to handling damage, stiff enough to provide a good base for all the engine access penetrations that would be required at the middle of the panel, and economical to produce.

The materials and construction methods evaluated included conventional aluminum skin and stringers, conventional titanium skin and stringers, formed panels of aluminum honeycomb with aluminum face sheets, and fiberglass face sheets with fiberglass honeycomb. Since the cowl construction above the engine horizontal centerline must be fire resistant, all of these materials, except the titanium, would require a partial lining of stainless steel sheet or a coating of intumescing paint. Considering both weight and recurring and nonrecurring costs, the fiberglass honeycomb construction would be the most attractive.

#### 5.4.4.3 Engine System Arrangement

The geometric arrangement and the size of the tailpipe and tailpipe extension were controlled by engine size and by location on the airplane. The trade studies, therefore, dealt with material only. The baseline selection was to use Inconel 625 sheet or Inconel 625 honeycomb. For the temperature environment, titanium could be used in all places, except where there would be a direct impingement of unmixed primary exhaust gas. For hardwall versions, titanium could be used in lieu of the Inconel 625. Thus, an extensive effort was made to determine whether a usable titanium honeycomb that would serve as a sound suppression panel was commercially available. If only titanium material were used, an airplane weight saving of approximately 290 lb (131.54 kg) could be realized.

#### 5.4.4.5 Mixers

The mixer discussion for the 727 airplane (sec. 4.4.4.5), is directly applicable to the 737 airplane.

#### 5.4.4.6 Thrust Reversers

The thrust reverser discussion for the 727 airplane (sec. 4.4.4.6) is directly applicable to the 737 airplane. Additional discussion concerning application to the 737 airplane follows.

One of the thrust-reverser configurations investigated was the exposed cascade type with internal clamshell doors in the tailpipe. This configuration could have a significant impact on the 737 airplane because of the possibility of gases being exhausted forward of the wing trailing edge flaps. Several methods of modifying a possible standard model (standard between the 727 and the

737 airplanes) of an exposed cascade reverser to exhaust half the gas through the nacelle aft fairing forward over the wing were evaluated. This modification would rotate the reverser package to discharge the remaining half of the exhaust gas forward, outward, and downward in relation to the nacelle.

If testing were to prove the feasibility of this approach, a considerable amount of the large overhung load of the 737 engine package could be avoided. A large weight saving could also be realized.

## 5.5 AIRPLANE MODIFICATION

Two general approaches were considered for determining required airplane modifications. One approach related to a 12-in. (0.305-m) main landing gear extension and the other to a 4-in. (0.102-m) main landing gear extension. The 12-in. (0.305-m) main landing gear extension was initially selected as the most likely approach to investigate. Sufficient work was completed on the 4-in. (0.102-m) main landing gear extension approach to verify the acceptability of the required modifications. A discussion of the shorter landing gear extension approach appears in section 5.5.7.

The airplane modifications necessary for the longer gear extension approach are explained in the following sections.

### 5.5.1 Landing Gear

#### 5.5.1.1 Landing Gear Extension

As discussed in section 5.1 reuse of the existing engine mount system would require lengthening of the landing gear approximately 12 in. (0.305 m) to maintain acceptable ground clearance under the nacelle. The new gear would be a levered suspension design that provides 12 in. (0.305 m) more body ground clearance than the existing gear, but which would shrink mechanically during retraction to stow within the existing wheelwall. The revised main landing gear is shown on figure 128 and would be operated as follows.

The inboard retraction motion of the main strut on its trunnion would cause an auxiliary collar with lever arms (G-H) to rotate in an opposite direction. The upper end of the shock strut attached at point H would thereby be moved upward and outboard to position the wheels and tires within the present wheelwell.

A more powerful actuator, associated with a strengthened actuation system, would be installed to accommodate the increased retraction load. Both the side strut and the reaction linkage would be

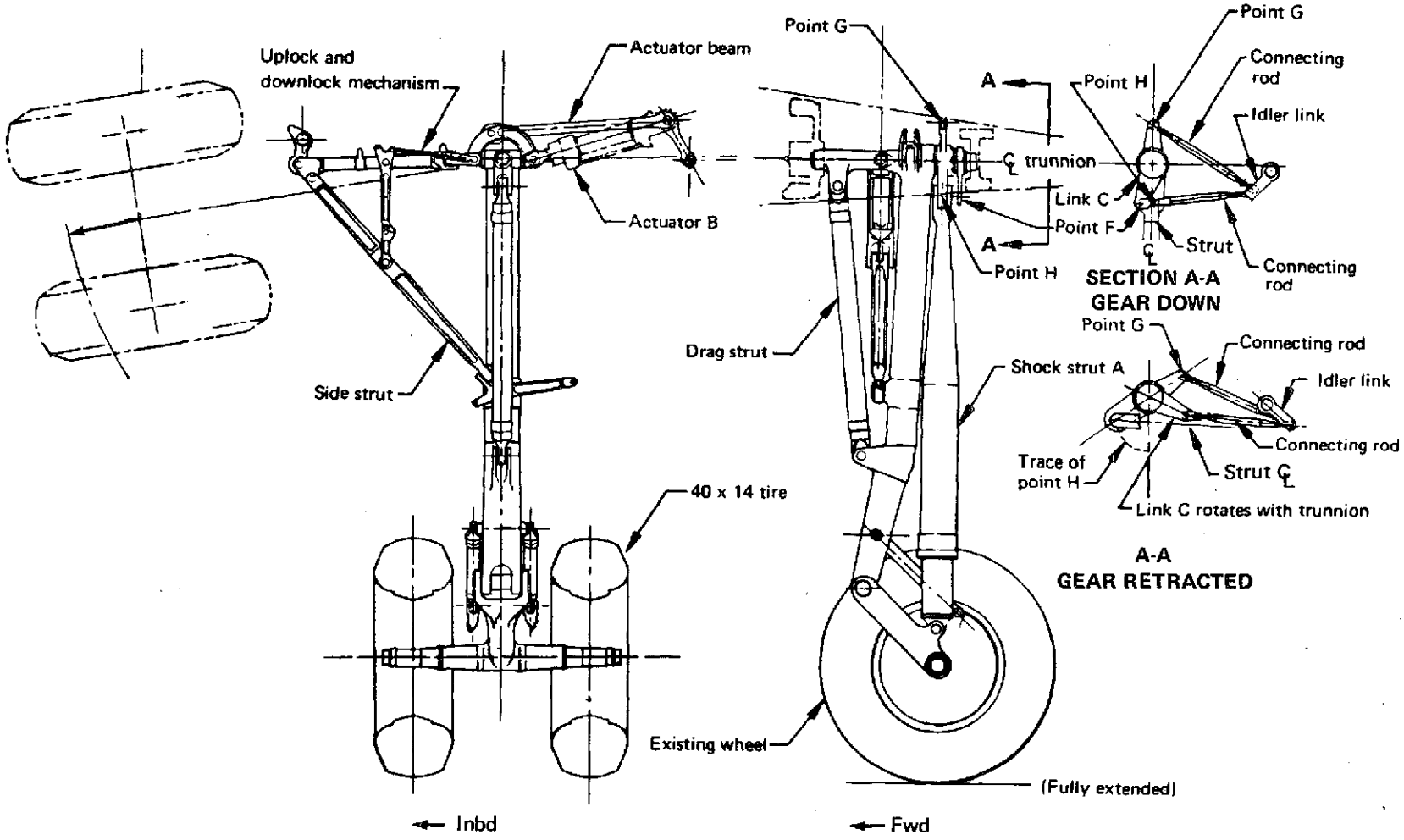


*FIGURE 128.—737-200 MODIFIED MAIN LANDING GEAR*

reinforced to accommodate the increased loads. The entry into the wheelwell would no longer be radial, and the external aluminum seal would be trimmed to provide an elongated opening. The internal aerodynamic flexible seal would remain unchanged.

The levered concept of gear extension was considered the most promising regarding shimmy characteristics; however, further analysis and testing would be required to obtain a final configuration.

5.5.1.2 Landing Gear Support Structure

The main landing gear extension of 12 in. (0.305 m) and its associated increased drag and side loads would produce an estimated 15% increase in loads on the landing gear beam and the forward trunnion support fitting.

The existing aluminum main landing gear support beam would be replaced by a new design titanium beam as shown in figure 129. New fore-and-aft trunnion bearings and fuse pins would be used, and the beam end fittings and the forward trunnion fitting would be reinforced.

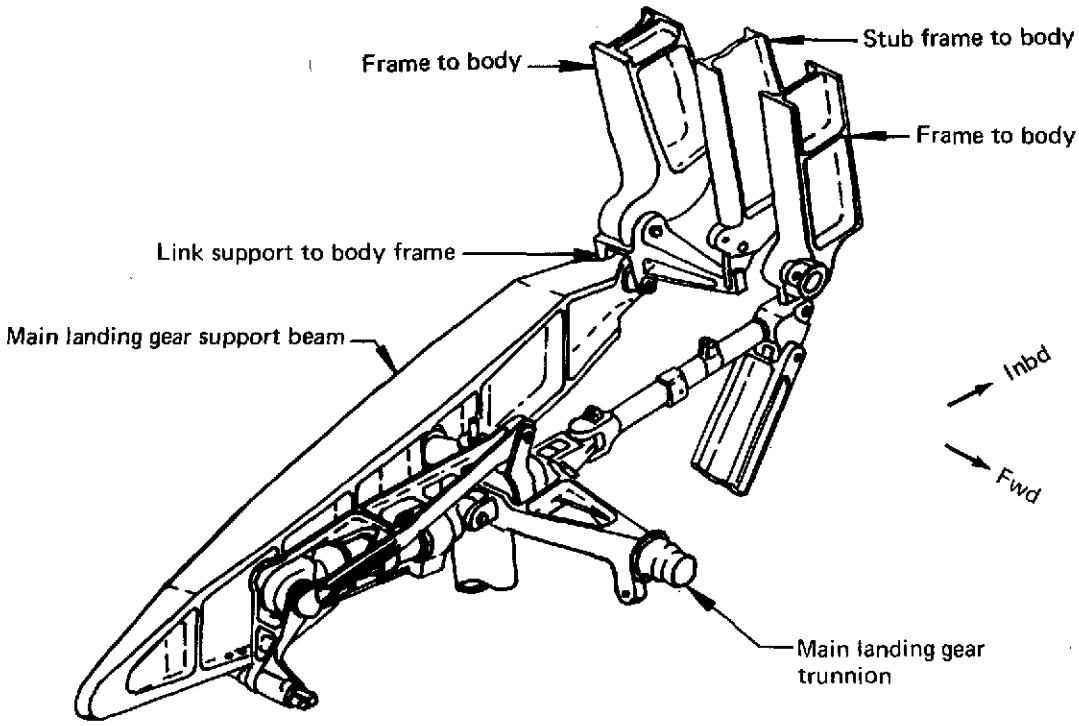


*FIGURE 129.–737-200 MODIFIED MAIN LANDING GEAR SUPPORT STRUCTURE*

Addition of the higher loaded beam would require some commensurate stiffening of the wing rear spar in the landing gear area, plus some strengthening of the fuselage attachment points.

### 5.5.2 Wing Flap System

#### 5.5.2.1 Leading Edge Flaps

The modified flap system is shown in figure 130. The leading edge flaps inboard of the nacelle would be existing parts with a minor trim at the outboard end to clear the new inlet contour. A matching change would be made in the fixed leading edge to fair with the stowed flap.

#### 5.5.2.2 Trailing Edge Flaps

On the baseline airplane, the trailing edge flap assemblies inboard and outboard of the nacelle consist of fore, mid, and aft flaps. The mid and aft flaps are trimmed to match the cowl contour when extended. In addition, a flipper flap is mounted adjacent to the nacelle aft fairing on each assembly to provide a continuous wing surface when the flaps were stowed and to provide an aerodynamic seal with the trimmed mid and aft flaps.

The installation designed for use with the JT8D-109 nacelle (see fig. 130 for location) would retain the identical fore flaps and use the existing mid and aft flaps, trimmed to match the increased nacelle diameter. New flipper flaps of similar design to the existing flipper flaps would be used with revised contours to match the mid and aft flap trim, but retain existing mounting components.

The flap actuation and control systems would not be changed.

### 5.5.3 Wing-to-Nacelle Fairings

Figure 131 shows the modified wing-to-nacelle fairings. These fairings would be similar to the existing fairings. Due to the revised contours of the larger engine, these fairings would be replaced, except for the aft fairing, which would be reused intact.

### 5.5.4 Wing Modification

No major wing modification was anticipated. Local stiffening at the engine-mount attachment points and at the attachment points for the landing gear and landing gear beam would be required. This conclusion assumes an adequate flutter margin for the wing, which was verified by analysis.

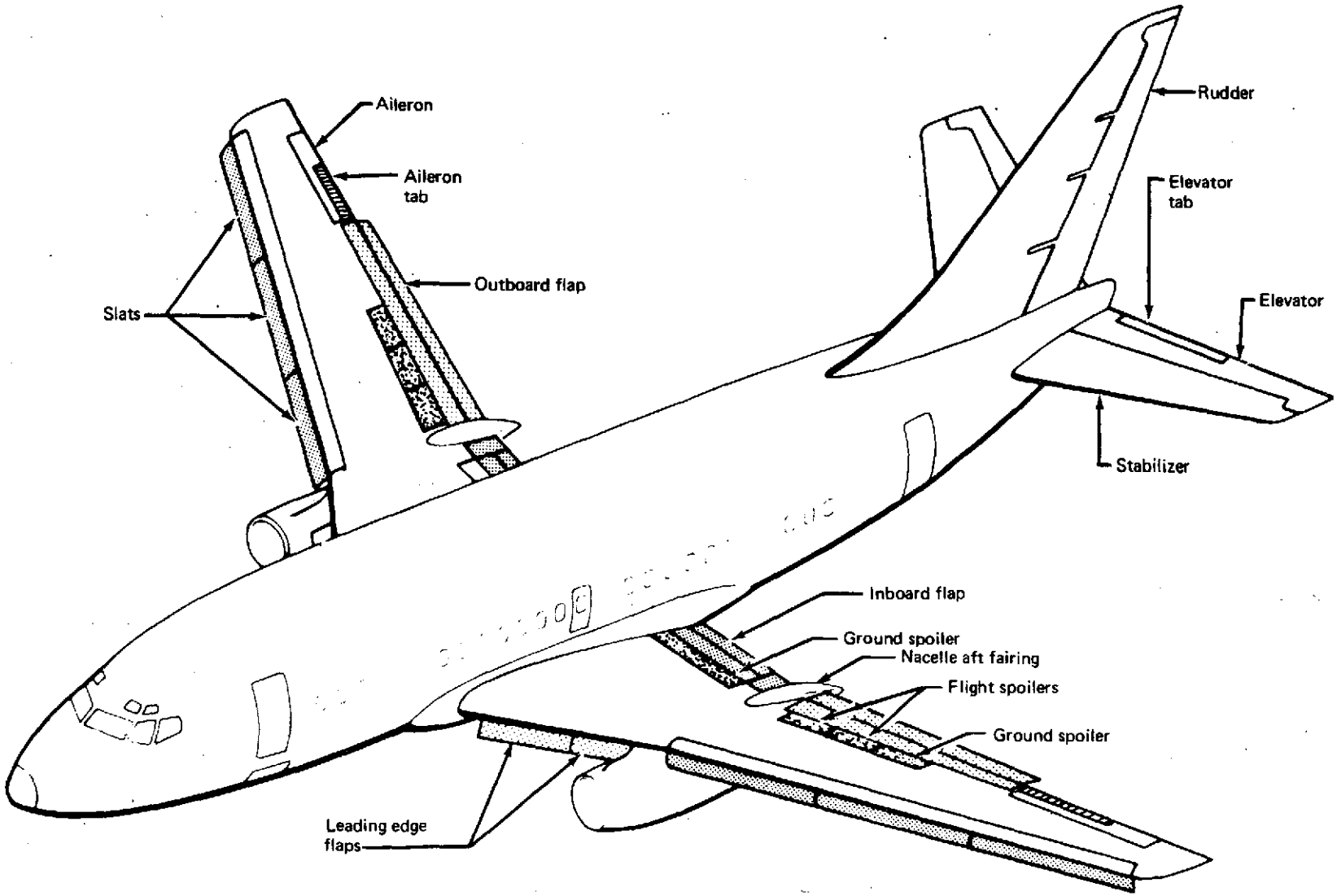


*FIGURE 130.–737-200 MODIFIED AIRCRAFT CONTROL SURFACES*

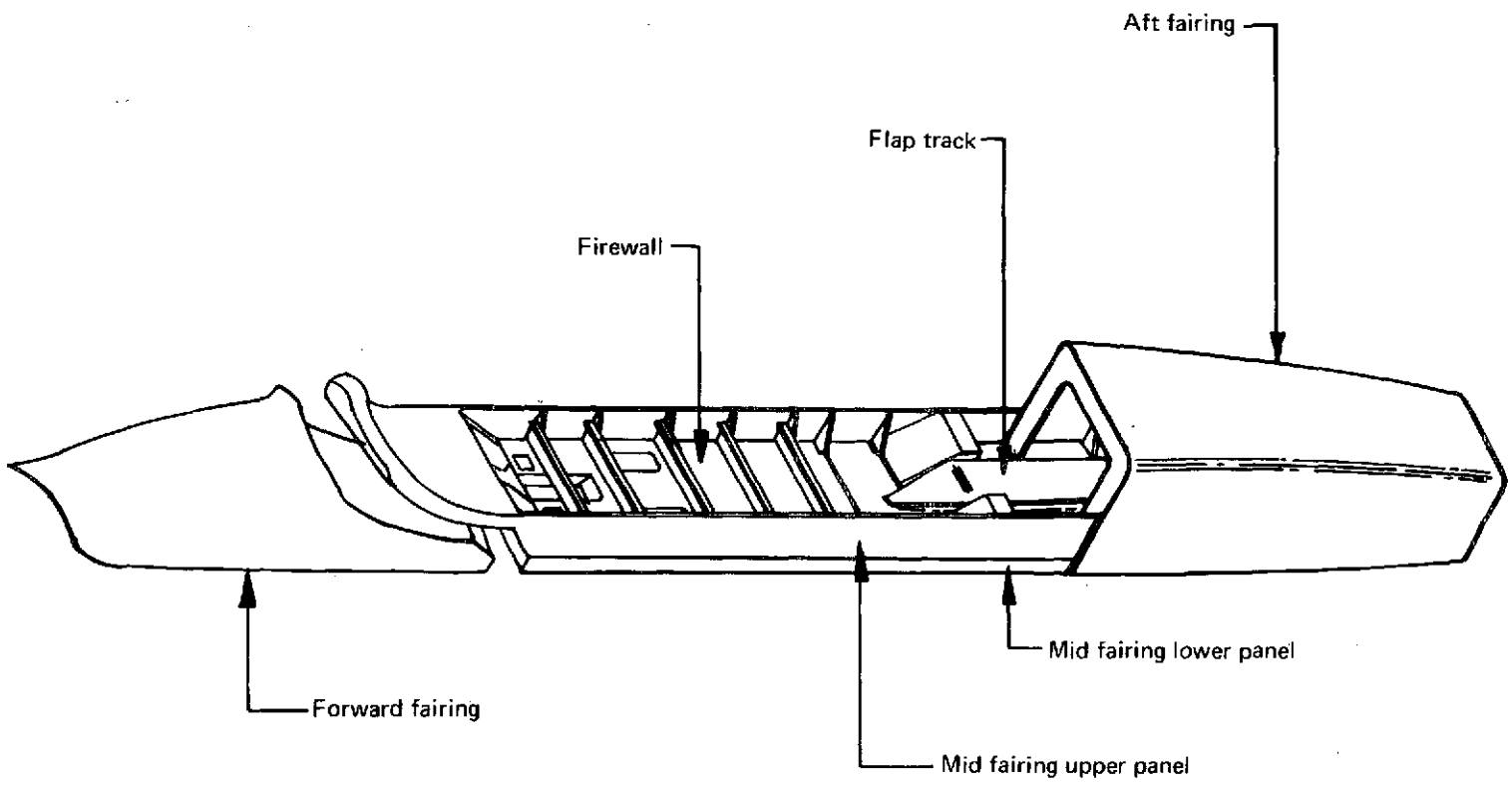


*FIGURE 131.–737-200 MODIFIED WING/NACELLE FAIRING*

### 5.5.5 Airplane Systems

Since the basic core engine and the basic engine accessories were so similar to the existing design, no changes, other than minor adjustments, were anticipated for the airplane systems. For better thrust-reverser control, the control panel would include two indicator lights for each thrust reverser to indicate thrust reverser "unlocked" and "deployed."

### 5.5.6 Airplane Airstairs

#### 5.5.6.1 Forward Airstairs

The existing forward airstairs are sufficiently flexible in height location to adapt to the 12-in. (0.305-m) main landing gear extension.

#### 5.5.6.2 Aft Airstairs

The lower unit of the existing aft airstairs is a four-step unit. To gain the necessary additional height, this unit would be replaced with a five-step unit. However, this modification would not require any accompanying changes in the housing or the related operational structure.

### 5.5.7 Studies

The following discussion considers the airplane modifications necessary to install a JT8D-109 engine on a 737 airplane with a 4-in. (0.102-m) main landing gear length increase.

This method would entail a major engine attachment change and a relatively minor landing gear change. Approximately 4 in. (0.102 m) of landing gear length increase could be attained by replacement of some internal strut components plus increasing the hydraulic pressure available to the strut.

This method of airplane modification would require the engines to be installed very close to the underside of the wing. To do this, the airplane would have to be modified by: major redesign of the leading edge and trailing edge flap systems, redesign for relocation of the inboard trailing edge flap support track approximately 22.6 in. (0.574 m) inboard, redesign for relocation of the flap drive gear box a like amount, design of a new engine mount system, design of a new wing-to-nacelle fairing and firewall system, redesign for stiffening of the existing landing gear beam, and numerous related small changes.

Weight and economic studies did not support further research into this airplane modification approach when a target-type thrust reverser is used. If future testing indicates an exposed cascade thrust reverser is feasible, the 4-in. (0.102-m) landing gear extension approach should be reconsidered.

## 5.6 MAINTENANCE ANALYSIS AND SUPPORT EQUIPMENT

### 5.6.1 Maintenance Analysis

The JT8D-109 installation design incorporated a majority of the JT8D-9 engine accessories, and the new items incorporated were designed to meet a standard of maintainability equivalent to that of the remainder of the installation.

The new engine installation would provide a standard of accessibility equal to (and, in some cases, better than) that of the baseline airplane. The longer landing gear and larger cowl doors would provide better engine accessibility.

The inlet was designed for the installation of an acoustic diffuser and an acoustic ring (or rings). The design would provide ease of inspection and replacement of the acoustic panels, when required. The airplane could be flown with the ring (or rings) removed, if necessary. The inlet was hinged to permit better access to the engine fan blades for inspection and maintenance.

The target-type thrust reverser was based on the design currently in use on the 737. This basic design has a minimum of moving parts, with none inside the tailpipe, and has demonstrated a high standard of reliability.

### 5.6.2 Support Equipment

There would be no change in the requirements for ground support equipment from those used for the present 737 airplane, except for dimensional changes.

The longer landing gear would change the airplane attitude relative to the ground, raising the aft passenger door 20 in. (0.508 m).

Existing equipment for the aft toilet connection and potable water connection could still be used but would not be as accessible from the ground. The majority of servicing connections are forward of the main landing gear and would be raised less than 12 in. (0.305 m), thereby requiring no change to the existing equipment. Galley servicing would be carried out at the forward door and would not be affected.

The increased weight and longer overall dimensions of the JT8D-109 engine and its nacelle would necessitate modification of the present equipment. No changes would be expected for tie-down or towing.

### 5.6.3 System Support

Little training would be required for certification of ground maintenance people, due to the high standard of commonality between the JT8D-9 and the JT8D-109 installations regarding accessories, instrumentation, and controls. The modified landing gear system would require some special training. A minimum of flight crew familiarization would be required since the flight and handling characteristics of the modified airplanes would be similar to the baseline airplane.

The modified thrust-reverser system incorporated the high-reliability features of the 737 thrust reverser.

Hardware was designed to the certification rules of FAR Part 25—the same rules in effect at the time of initial certification. Changes to the airplane would be confined to those required for installation of the refanned engines.

## 5.7 PERFORMANCE COMPARISON

The information contained in this section describes and details airplane characteristics that directly affect airplane operational capability.

The data deal primarily with a baseline airplane with a maximum taxi weight of 104 000 lb (47 174 kg). This airplane, following some modification, would be capable of operation at a higher gross weight of 110 000 lb (49 896 kg)—a gross weight more consistent with the increased thrust capability of the JT8D-109 engine. Performance at both gross weights is therefore shown.

A detailed weight breakdown is provided for the baseline and for each of the modified configurations. Performance comparisons on the basis of takeoff field length, payload versus range, and takeoff field length versus range are shown. The increase in airplane cruise drag for each of the modified configurations is approximately 1.6% at a typical midcruise condition. Possible changes in handling characteristics, stability and control, and flutter stability are also discussed.

Table 34 presents a summary of airplane performance, modification cost estimates, and predicted noise levels for each configuration as installed on an airplane with BRGW limited to that

*TABLE 34.–737-200 PERFORMANCE SUMMARY–CONSTANT BRGW*

| Parameter | 737-200 configuration | | | | | | | | | | |
|---|---|---|---|---|---|---|---|---|---|---|---|
| | Baseline | | 1 | | | 2 | | | 3[a] | | |
| OEW, lb (kg) | 59,700 (27,080) | | 62,080 (28 159) | | | (62 390 (28 300) | | | 62 460 (28 331) | | |
| ΔOEW, lb (kg) | | | 2380 (1080) | | | 2690 (1220) | | | 2760 (1252) | | |
| Change, % | | | +3.99 | | | +4.51 | | | +4.62 | | |
| Brake release gross weight,[b] lb (kg) | 103 500 (46 947) | | 103 500 (46 947) | | | 103 500 (46 947) | | | 103 500 (46 947) | | |
| Change, % | | | 0.0 | | | 0.0 | | | 0.0 | | |
| Takeoff field length, ft (m) | 6480 (1975) | | 5190 (1582) | | | 5650 (1722) | | | 5650 (1722) | | |
| Change, % | | | -19.9 | | | -12.8 | | | -12.8 | | |
| ATA range, nmi (km) | 745 (1380) | | 535 (991) | | | 490 (907) | | | 500 (926) | | |
| Change, % | | | -28.2 | | | -34.2 | | | -32.9 | | |
| Kit and installation cost, millions of dollars per aircraft | – | | 1.412 | | | 1.452 | | | 1.526 | | |
| Airplane quantity | – | | 169 | | | 169 | | | 169 | | |
| Cash DOC change from baseline, % | – | | 1.47 | | | 2.58 | | | 2.27 | | |
| Average range, nmi (km) | – | | 228 (422) | | | 228 (422) | | | 228 (422) | | |
| FAR Part 36 noise, EPNdB | Limit | Measured | Limit | Predicted | Δ[e] | Limit | Predicted | Δ[e] | Limit | Predicted | Δ[e] |
| Takeoff | 95.3 | 100.0 | 95.3 | 87.6 | -12.4 | 95.3 | 87.8 | -12.2 | 95.3 | 82.7 | -17.3 |
| Cutback | 95.3 | 96.7 | 95.3 | 86.2 | -10.5 | 95.3 | 86.3 | -10.4 | 95.3 | 84.4 | -12.3 |
| Approach[c] | 102.9 | 108.9 | 102.9 | 101.6 | - 7.3 | 102.9 | 100.6 | - 8.3 | 102.9 | 100.5 | - 8.4 |
| Sideline | 102.9 | 101.1 | 102.9 | 90.1 | -11.0 | 102.9 | 89.5 | -11.6 | 102.9 | 84.6 | -16.5 |
| 95-EPNdB contour area reduction[d],% | – | | -82.0 | | | -84.2 | | | -90.9 | | |
| Relative footprint noise index | 1.0 | | 0.161 | | | 0.147 | | | 0.044 | | |

[a]Design goals only; effort discontinued because of funding.
[b]Note constant BRGW
[c]Approach flaps–30
[d]At baseline BRGW
[e]Δfrom baseline measured noise levels

of the baseline airplane. Table 35 presents a similar summary in which the BRGW for the respective configurations is permitted to increase within presently authorized growth limits.

### 5.7.1 Installed Engine Performance

Installation losses and the effects of these losses on takeoff thrust and cruise fuel consumption for configurations 1, 2, and 3 are summarized in tables 36 and 37.

Takeoff lapse rates ($F_N$ vs TAS) for the three JT8D-109 nacelle configurations are compared with that for the JT8D-9 in figure 132 for an 84°F (302°K) day at sea level and at 5000 ft (1524 m). The JT8D-9 lapse rate is shown at both altitudes for comparison. The JT8D-109 would have considerably more thrust throughout the practical takeoff speed regime, which could be used to decrease takeoff field length requirements for a given airplane gross weight or to permit increased takeoff gross weight with a given runway length.

Thrust specific fuel consumption for the JT8D-109 for each of the configurations is compared with that for the JT8D-9 in figure 133. At the nominal midcruise thrust, TSFC for configuration 1 would be equivalent to that for the JT8D-9 engine. Configurations 2 and 3 show TSFC increases of 1.9% and 0.7%, respectively, when compared to the JT8D-9 in the same manner.

*TABLE 35.–737-200 PERFORMANCE SUMMARY–INCREASED BRGW*

| Parameter | 737-200 configuration | | | | | | | | | | |
|---|---|---|---|---|---|---|---|---|---|---|---|
| | Baseline | | 1 | | | 2 | | | 3[a] | | |
| OEW, lb (kg)<br>ΔOEW, lb (kg)<br>Change, % | 59 700 (27 080) | | 62 080 (28 159)<br>2330 (1080)<br>+3.98 | | | 62 390 (28 300)<br>2690 (1220)<br>+4.50 | | | 62 460 (28 332)<br>2760 (1252)<br>+4.62 | | |
| Brake release gross weight,[b] lb (kg)<br>Change, % | 103 500 (46 948) | | 109 000 (49 442)<br>+5.31 | | | 109 000 (49 442)<br>+5.31 | | | 109 000 (49 442)<br>+5.31 | | |
| Takeoff field length, ft (m)<br>Change, % | 6480 (1975) | | 6230 (1899)<br>-3.9 | | | 6550 (1996)<br>+1.1 | | | 6550 (1996)<br>+1.1 | | |
| ATA range, nmi (km)<br>Change, % | 745 (1380) | | 885 (1639)<br>+18.8 | | | 835 (1546)<br>+12.1 | | | 850 (1574)<br>+14.1 | | |
| Kit and installation cost, millions of dollars per aircraft | – | | 1.412 | | | 1.452 | | | 1.526 | | |
| Airplane quantity | – | | 169 | | | 169 | | | 169 | | |
| Cash DOC change from baseline, % | – | | 1.47 | | | 2.58 | | | 2.27 | | |
| Average range, nmi (km) | – | | 228 (422) | | | 228 (422) | | | 228 (422) | | |
| FAR Part 36 noise, EPNdB | Limit | Measured | Limit | Predicted | (Δ)[e] | Limit | Predicted | (Δ)[e] | Limit | Predicted | (Δ)[e] |
| Takeoff | 95.3 | 100.0 | 95.7 | 88.8 | -11.2 | 95.7 | 88.9 | -11.1 | 95.7 | 83.9 | -16.1 |
| Cutback | 95.3 | 96.7 | 95.7 | 87.7 | - 9.0 | 95.7 | 87.7 | - 9.0 | 95.7 | 85.8 | - 9.9 |
| Approach[c] | 102.9 | 108.9 | 103.1 | 101.6 | - 7.3 | 103.1 | 100.6 | - 6.3 | 103.1 | 100.5 | - 8.3 |
| Sideline | 102.9 | 101.1 | 103.1 | 89.9 | -11.2 | 103.1 | 89.3 | -11.8 | 103.1 | 84.4 | -16.7 |
| 95-EPNdB contour area reduction,[d] % | – | | 82.0 | | | 84.2 | | | 90.9 | | |
| Relative footprint noise index | 1.000 | | 0.161 | | | 0.147 | | | 0.044 | | |

[a]Design goals only-effort discontinued because of funding

[b]Note modified airplane gross weight increase—does not apply to all 737-200 airplanes

[c]Approach flaps–30

[d]At baseline BRGW

[e]Δ from baseline measured noise level

### 5.7.2 Weight and Balance

Installation of JT8D-109 engines would cause the airplane operating empty weight to increase. The operational weight breakdown for the baseline airplane is shown in table 38. Table 39 shows the items in the nacelle weight statement that would be modified by the refanned engine installation design. Airplane loadability is not degraded with installation of the JT8D-109 engines.

The 737-200 baseline airplane characteristics are listed in table 40. The baseline airplane has been selected as being typical of the 737 fleet.

Many of the 737 airplanes have the structural capability to increase the maximum taxi weight to 110 000 lb (49 896 kg). A kit is available to retrofit the 110 000 lb (49 896 kg) maximum taxi weight capability on those airplanes that do not currently have it. The kit consists of relatively minor changes to the leading edge flaps and slats and a tire ply rating increase.

The possibility of gross weight increases for all 737 models other than the baseline airplane will have to be studied to determine the extent of modifications required.

*TABLE 36.–737/JT8D-109 INSTALLED INCREMENTAL LOSSES $F_N/F_N$ AT TAKEOFF[a]*

| Item | Configuration | | | | | |
|---|---|---|---|---|---|---|
| | 1 | | 2 | | 3 | |
| | Loss | $\Delta F_N/F_N$, % | Loss | $\Delta F_N/F_N$, % | Loss | $\Delta F_N/F_N$, % |
| Inlet loss, $\Delta P/P$ | 0.007 | -2.0 | 0.013 | -3.6 | 0.017 | -4.7 |
| Power extraction | 60 hp (44.7 kW) | -0.4 | 60 hp (44.7 kW) | -0.4 | 60 hp (44.7 kW) | -0.4 |
| Nozzle velocity coefficient, $\Delta C_V$ | -0.002 | -0.2 | -0.008 | -0.8 | -0.001 | -0.1 |
| Total | | -2.6 | | -4.8 | | -5.2 |

[a]Sea level, standard day

*TABLE 37.–737/JT8D-109 INSTALLED INCREMENTAL LOSSES $\Delta TSFC/TSFC$ AT CRUISE[a]*

| Item | Configuration | | | | | |
|---|---|---|---|---|---|---|
| | 1 | | 2 | | 3 | |
| | Loss | ΔTSFC/TSFC,% | Loss | ΔTSFC/TSFC, % | Loss | ΔTSFC/TSFC, % |
| Inlet loss, $\Delta P/P$ | 0.001 | 0.1 | 0.007 | 0.8 | 0.011 | 1.3 |
| Power extraction | 60 hp (44.7 kW) | 0.5 | 60 hp (44.7 kW) | 0.5 | 60 hp (44.7 kW) | 0.5 |
| Bleed | 1.06 lb/sec (0.48 kg/sec) | 1.8 | 1.06 lb/sec (0.48 kg/sec) | 1.8 | 1.06 lb/sec (0.48 kg/sec) | 1.8 |
| Nozzle velocity coefficient, $\Delta C_V$ | 0 | 0.0 | -0.005 | 1.1 | +0.004 | -0.8 |
| Total | | 2.4 | | 4.2 | | 2.8 |

[a]Mach = 0.78, 25 000 ft (7620 m), net thrust = 4270 lb (18 992 N)

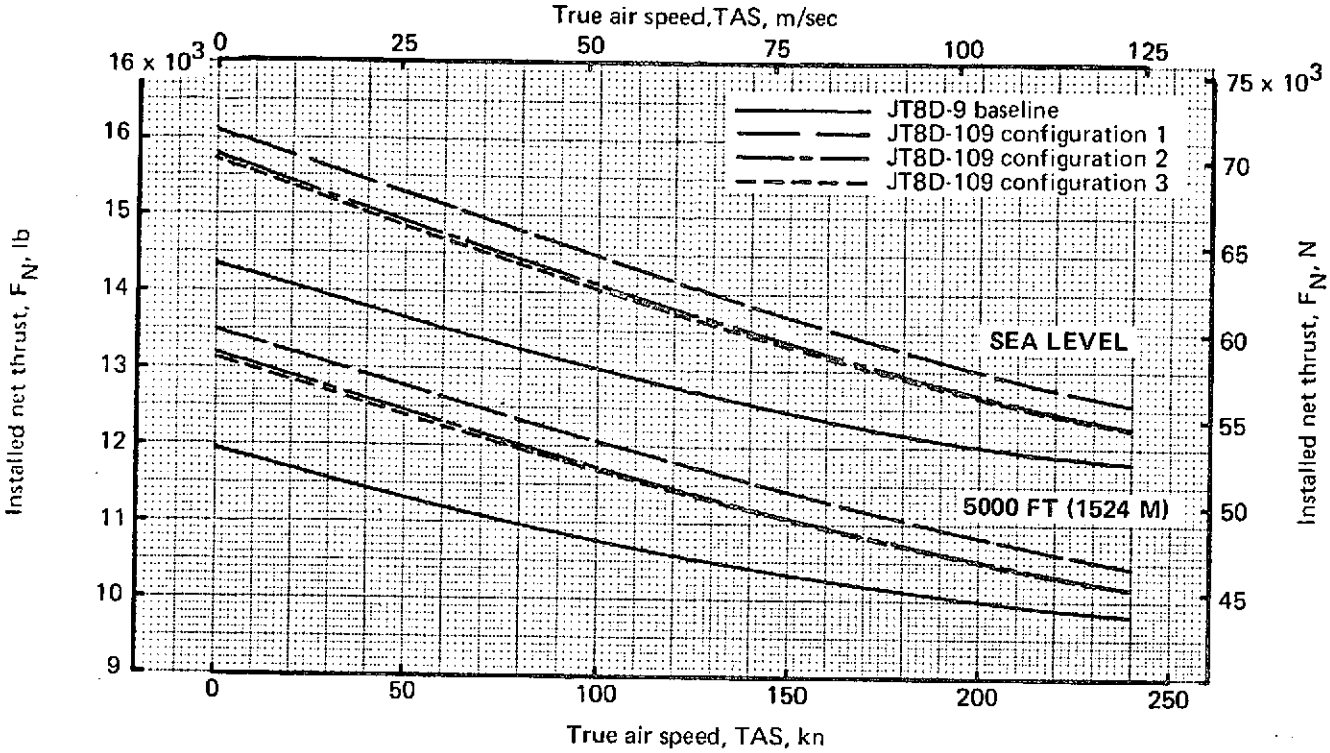


*FIGURE 132.—737/JT8D INSTALLED TAKEOFF THRUST LAPSE RATE COMPARISON—60 HP (44.7 KW) EXTRACTION, 84°F (302°K) DAY*

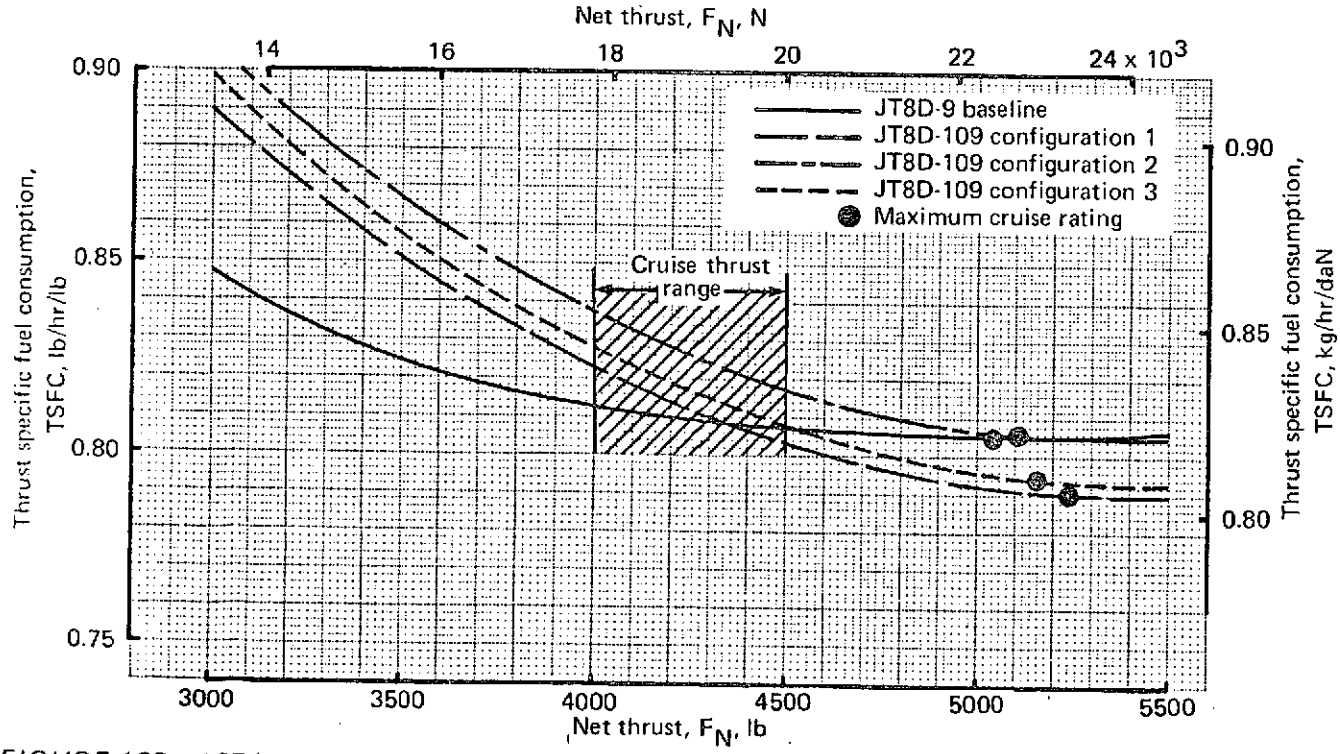


*FIGURE 133.—737/JT8D INSTALLED CRUISE TSFC PERFORMANCE COMPARISON—AIR CONDITIONING BLEED ON 60 HP (44.7 KW) EXTRACTION, MACH 0.78, 25 000 FT (7620 M), STANDARD DAY*

*TABLE 38.—737-200/JT8D BASELINE AIRPLANE WEIGHT BREAKDOWN*

| Component | lb | kg |
|---|---|---|
| Wing | 11 190 | 5 075 |
| Horizontal tail | 1 570 | 710 |
| Vertical tail | 1 150 | 520 |
| Body | 12 210 | 5 540 |
| Main landing gear | 3 690 | 1 675 |
| Nose landing gear | 520 | 235 |
| Nacelle and strut | 1 470 | 665 |
| Total structure | 31 800 | 14 425 |
| Engine | 6 460 | 2 930 |
| Engine accessories | 250 | 115 |
| Engine controls | 60 | 25 |
| Starting system | 80 | 35 |
| Fuel system | 560 | 255 |
| Thrust reverser | 1 020 | 460 |
| Total propulsion group | 8 430 | 3 825 |
| Instruments | 650 | 295 |
| Surface controls | 2 270 | 1 030 |
| Hydraulics | 600 | 270 |
| Pneumatics | 330 | 150 |
| Electrical | 1 310 | 595 |
| Electronics | 840 | 380 |
| Flight provisions | 640 | 290 |
| Passenger accommodations | 6 360 | 2 885 |
| Cargo handling | 710 | 320 |
| Emergency equipment | 370 | 170 |
| Air conditioning | 1 120 | 510 |
| Anti-icing | 180 | 80 |
| Auxiliary power unit | 830 | 375 |
| Total fixed equipment | 16 210 | 7 350 |
| Exterior paint | 60 | 25 |
| Manufacturer's empty weight | 56 500 | 25 630 |
| Standard and operational items | 3 200 | 1 450 |
| Operating empty weight | 59 700 | 27 080 |

*TABLE 39.—737-200/JT8D WEIGHT BREAKDOWN COMPARISON*

| Component | Configuration | | | | | | | |
|---|---|---|---|---|---|---|---|---|
| | Baseline (JT8D-9) | | 1 (JT8D-109) | | 2 (JT8D-109) | | 3 (JT8D-109) | |
| | lb | kg | lb | kg | lb | kg | lb | kg |
| Engine | 3 227 | 1464 | 3 797 | 1722 | 3 797 | 1722 | 3 797 | 1722 |
| Inlet | 166 | 75 | 181 | 82 | 266 | 121 | 308 | 140 |
| Cowl | 215 | 98 | 256 | 116 | 256 | 116 | 256 | 116 |
| Exhaust system | 557 | 253 | 873 | 396 | 944 | 428 | 937 | 425 |
| Strut | 259 | 118 | 244 | 111 | 244 | 111 | 244 | 111 |
| Engine mounts | 86 | 39 | 96 | 44 | 96 | 44 | 96 | 44 |
| Accessories | 527 | 239 | 512 | 232 | 512 | 232 | 512 | 232 |
| Total engine installation weight per side | 5 037 | 2285 | 5 959 | 2703 | 6 115 | 2774 | 6 150 | 2790 |
| Total engine installation weight per airplane | 10 074 | 4570 | 11 918 | 5406 | 12 230 | 5547 | 12 300 | 5579 |
| Propulsion weight change per airplane | Ref | Ref | +1 844 | +836 | +2 156 | +978 | +2 226 | +1010 |
| Airplane modifications | — | — | 534 | 242 | 534 | 242 | 534 | 242 |
| Ballast | — | — | 0 | 0 | 0 | 0 | 0 | 0 |
| Total OEW change | Ref | Ref | +2 380 | +1080 | +2 690 | +1220 | +2 760 | +1250 |

*TABLE 40.—737-200 CHARACTERISTICS*

| Characteristic | Baseline airplane | Growth option |
|---|---|---|
| Operating empty weight | 59 700 lb (27 080 kg) | 59 700 lb (27 080 kg) |
| Maximum taxi weight | 104 000 lb (47 200 kg) | 110 000 lb (49 900 kg) |
| Maximum landing weight | 98 000 lb (44 500 kg) | 98 000 lb (44 500 kg) |
| Maximum zero-fuel weight | 85 000 lb (38 600 kg) | 88 000 lb (39 900 kg) |
| Passenger seating capacity | 109 (TC) | 109 (TC) |
| Fuel capacity | 4232 gal (16 018 $m^3$) | 4232 gal (16 018 $m^3$) |
| Interior | All tourist class, typical galley and furnishings arrangement | All tourist class, typical galley and furnishings arrangement |
| Engine | JT8D-9 | JT8D-9 |

### 5.7.3 Airplane Performance

The takeoff and cruise performance for each of the modified configurations is compared to the baseline airplane performance in figures 134 through 136.

The performance loss due to the increased OEW of the modified configurations would be offset by the improved thrust of the refanned engines, which permits a heavier gross weight takeoff. Figure 134 shows that all three modified configurations can experience weight growth and require no increase in field length for takeoff. Figures 135 and 136 show the payload/range and range/field length trades. By taking advantage of the weight growth capability, all three configurations would have improved range over the baseline at the same field length.

This analysis applies only to the baseline 737-200, 104 000-lb (47 174-kg) gross weight airplane. Further study will be necessary to determine the extent of modifications required to other 737 models to achieve any desired gross weight increase.

### 5.7.4 Stability and Control

The ground and air minimum control speeds, $V_{MCG}$ and $V_{MCA}$, for the 737-200 airplane with JT8D-109 engines (configurations 1, 2, and 3) are given in table 41. The basic airplane minimum control speeds are also shown for comparison. All speeds are based on FAA-certified levels of airplane engine-out yawing moment capability.

Preliminary estimates of the effect of the modified nacelles on airplane speed stability indicate a 2% MAC reduction of the static stability margin due to the larger nacelles. Significant reductions in stability may require an aft center-of-gravity restriction and/or airplane modification, to ensure that aft center-of-gravity climb, cruise (Mach trim-off), and approach stability meet applicable levels for FAA certification. Wind tunnel tests would be required to confirm this estimated effect.

The refanned engine/nacelle/gear configuration is not expected to have a significant effect on nose wheel steering effectiveness at takeoff brake release or on takeoff rotation characteristics.

### 5.7.5 Flutter

Flutter analysis of the airplane with a modified nacelle has defined how sensitive flutter speed is to these design parameters:

- Nacelle and strut pitch frequency
- Nacelle and strut pitch inertia

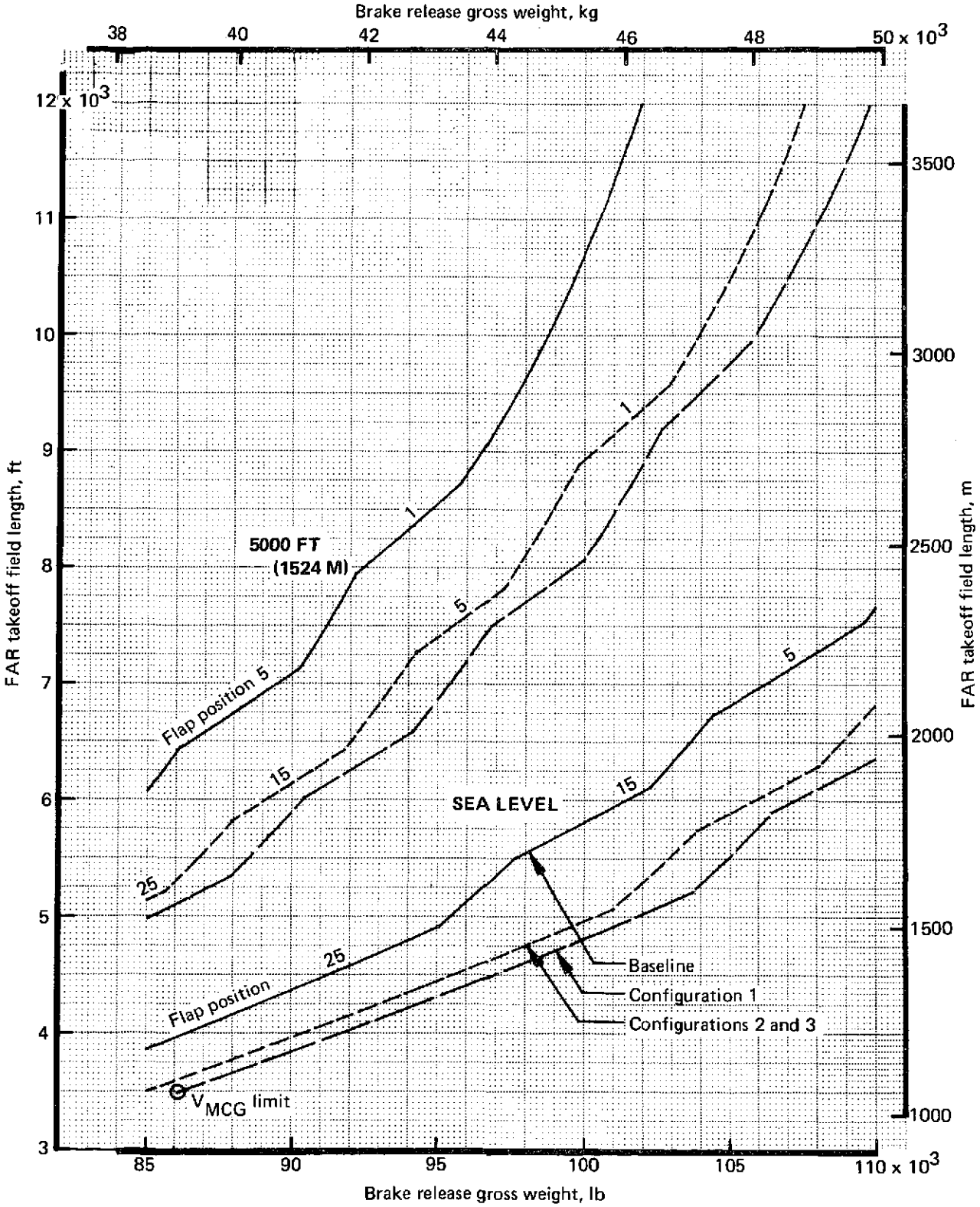


*FIGURE 134.–737/JT8D TAKEOFF FIELD LENGTH COMPARISON–84°F (302°K), NO AIR BLEED, ZERO WIND, ZERO SLOPE*

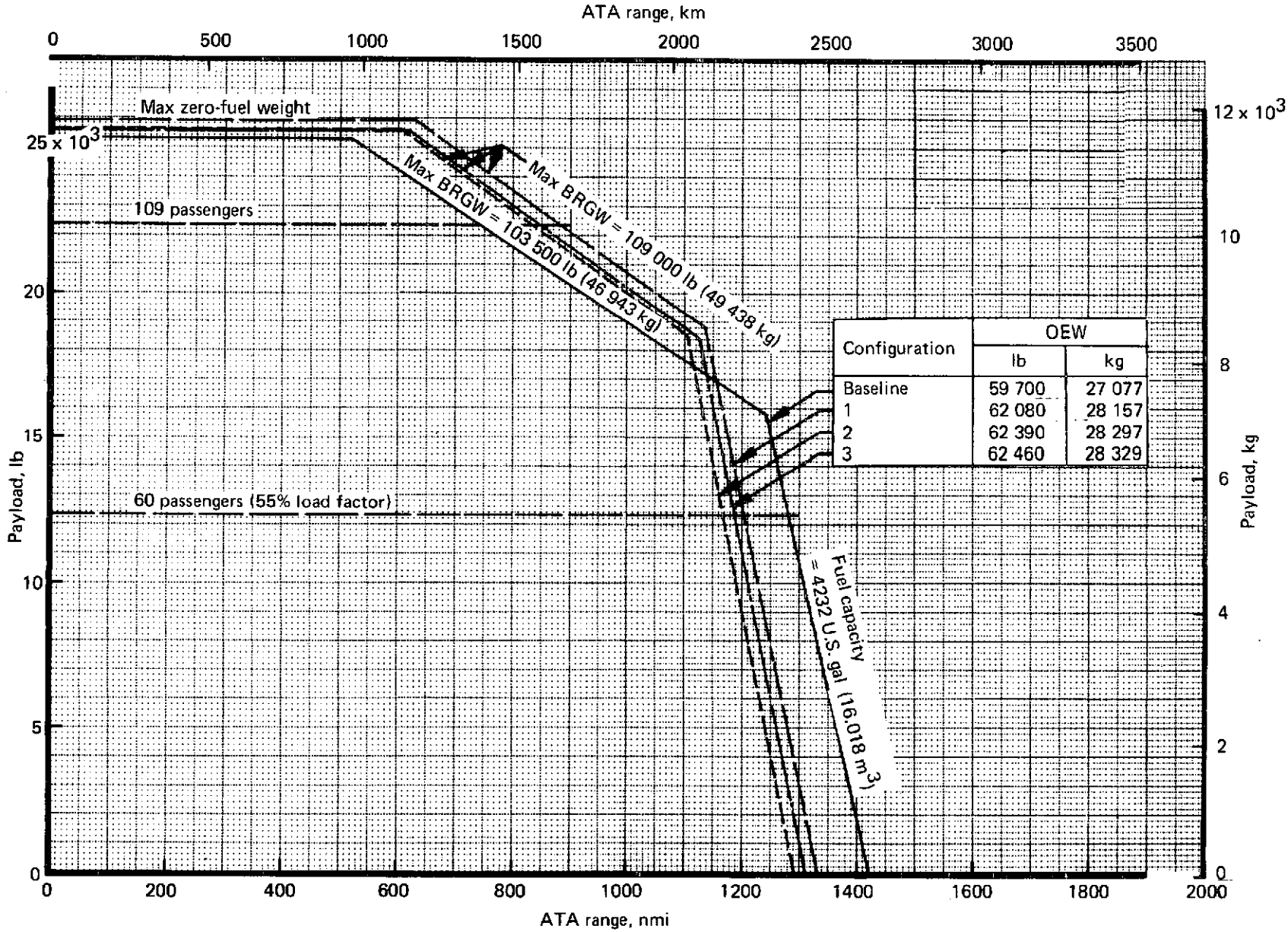


| Configuration | OEW | |
|---|---|---|
| | lb | kg |
| Baseline | 59 700 | 27 077 |
| 1 | 62 080 | 28 157 |
| 2 | 62 390 | 28 297 |
| 3 | 62 460 | 28 329 |

*FIGURE 135.—737/JT8D PAYLOAD/RANGE COMPARISON—MACH 0.78, 25 000 FT (7620 M), STANDARD DAY, ZERO WIND, ATA DOMESTIC RESERVES*

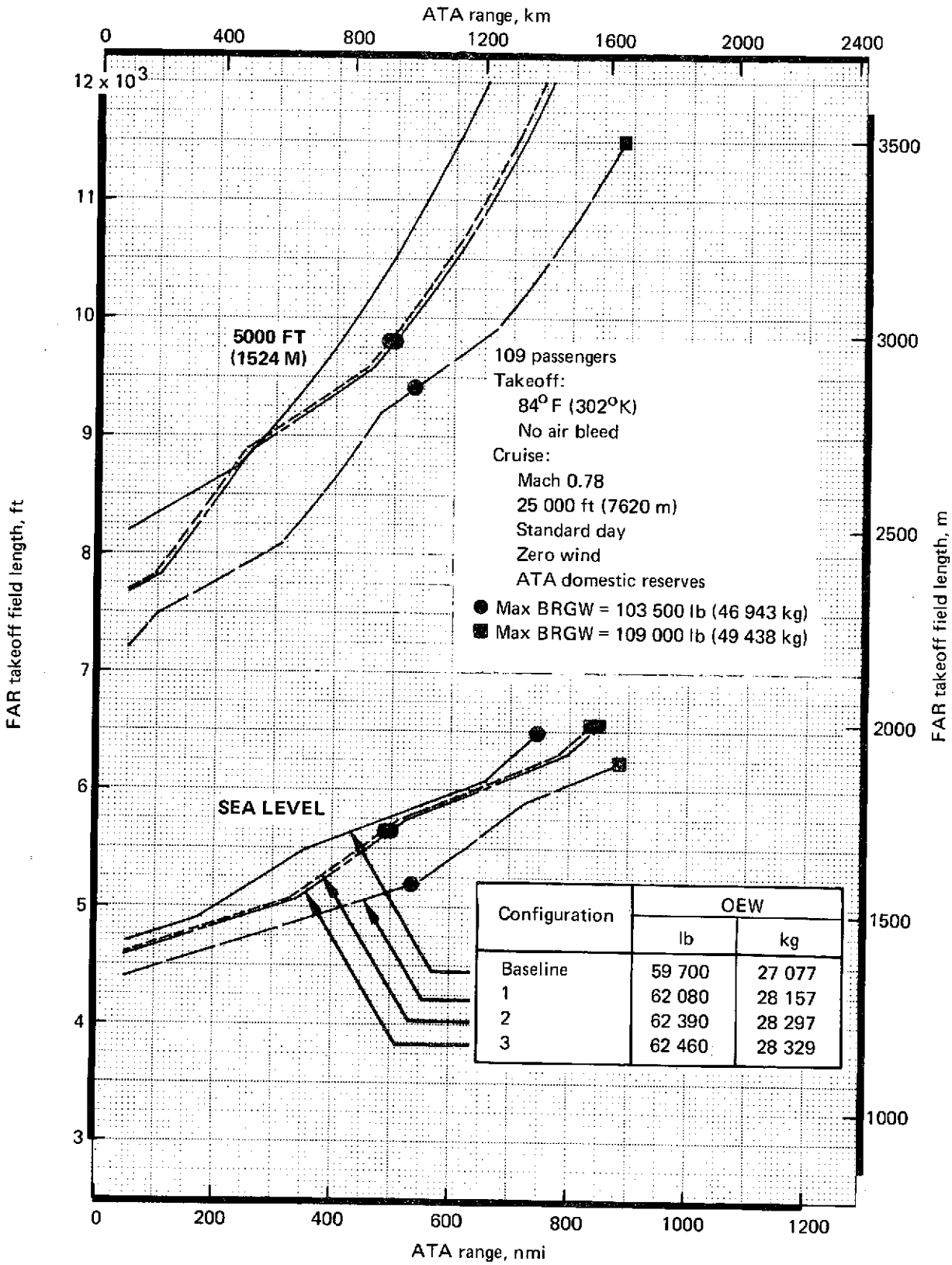


| Configuration | OEW | |
|---|---|---|
| | lb | kg |
| Baseline | 59 700 | 27 077 |
| 1 | 62 080 | 28 157 |
| 2 | 62 390 | 28 297 |
| 3 | 62 460 | 28 329 |

*FIGURE 136.—737/JT8D FIELD LENGTH/RANGE COMPARISON*

*TABLE 41.–MINIMUM CONTROL SPEED COMPARISON–737-200[a]*

| Engine | $V_{MCG}$ | | $V_{MCA}$ | |
|---|---|---|---|---|
| | KEAS | m/sec | KEAS | m/sec |
| JT8D-9 (baseline) | 102.5 | 52.7 | 92.0 | 47.3 |
| JT8D-109 (configuration 1) | 108.0 | 55.6 | 97.5 | 50.2 |
| JT8D-109 (configuration 2) | 106.5 | 54.8 | 96.5 | 49.6 |
| JT8D-109 (configuration 3) | 106.5 | 54.8 | 96.5 | 49.6 |

[a]Sea level, standard day

- Fore-and-aft location of the nacelle center of gravity
- Quantity of wing fuel.

Nacelle configuration 3 was analyzed for flutter, because this configuration results in the highest nacelle and strut pitch inertia, hence, the lowest flutter speed. For the flutter-critical fuel condition, configuration 3 shows satisfactory flutter stability. The nacelle and strut pitch frequency used in the analysis was based on supporting the nacelle on the existing strut and isolators.

## 5.8 AIRPLANE AND COMMUNITY NOISE CHARACTERISTICS

Initial noise design analyses for all three JT8D-109 refan configurations for the 737-200 airplane are presented in this section. These analyses have the same limitations as discussed in section 4.8 for the 727 airplane.

### 5.8.1 Nacelle Acoustic Preliminary Design

The three configurations investigated are the same as discussed for the 727 airplane in section 4.8.1, and the analytical methods are the same. Acoustic linings are shown in figures 137, 138, and 139. Lining attenuation spectra are shown in figures 140 and 141.

Designing the inlet and tailpipe acoustic treatment for the 727-200 approach power was consistent with maximum commonality between the 727 and 737. This JT8D-109 power setting for the 727 airplane is between the approach and cutback power for the 737.

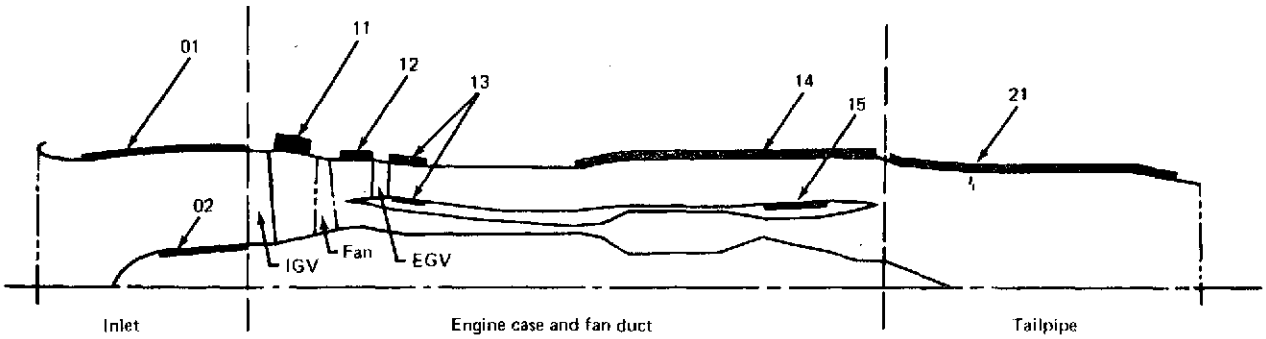


| Lining designation | Location | Face sheet type | Net active treatment area, $ft^2(m^2)$ | Core depth, in. (m) | Cell size, in. (m) | Design point, $R/\rho$ | Open area, % | Hole dia., in. (m) | Face sheet thickness, in. (m) |
|---|---|---|---|---|---|---|---|---|---|
| Inlet | | | | | | | | | |
| 1-01 | Diffuser | Polyimide | 31.6 (2.936) | 0.18 (0.0046) | 0.25 (0.0064) | 1.6 | | | |
| 1-02 | Nose dome | ↓ | 5.3 (0.492) | 0.18 (0.0046) | 0.25 (0.0064) | 1.6 | | | |
| Engine case fan duct | | | | | | | | | |
| 1-11 | Fwd of fan | Perforated sheet | 6.6 (0.613) | 1.00 (0.0254) | 0.375 (0.0095) | | 20 | 0.050 (0.0013) | 0.016 (0.0004) |
| 1-12 | Aft of fan | ↓ | 6.2 (0.576) | 0.50 (0.0127) | 0.375 (0.0095) | | 12 | 0.050 (0.0013) | 0.016 (0.0004) |
| 1-13 | Aft of EGV | ↓ | 8.8 (0.818) | 0.25 (0.0064) | 0.375 (0.0095) | | 12 | 0.050 (0.0013) | 0.015 (0.0004) |
| 1-14 | Outer wall aft | ↓ | 61.7 (5.732) | 0.50 (0.0127) | 0.375 (0.0095) | | 12 | 0.050 (0.0013) | 0.016 (0.0004) |
| 1-15 | Inner wall aft | ↓ | 7.0 (0.650) | 0.50 (0.0127) | 0.375 (0.0095) | | 12 | 0.050 (0.0013) | 0.016 (0.0004) |
| Tailpipe | | | | | | | | | |
| 1-21 | Outer wall | Perforated sheet | 48.0 (4.459 | 0.25 (0.0064) | 0.375 (0.0095) | | 3.5 | 0.040 (0.0010) | 0.020 (0.0005) |

*Allow up to 2 in. (0.0508 m) core depth for buzz-saw treatment.

*FIGURE 137.–737/JT8D ACOUSTIC LINING DEFINITION, CONFIGURATION 1*

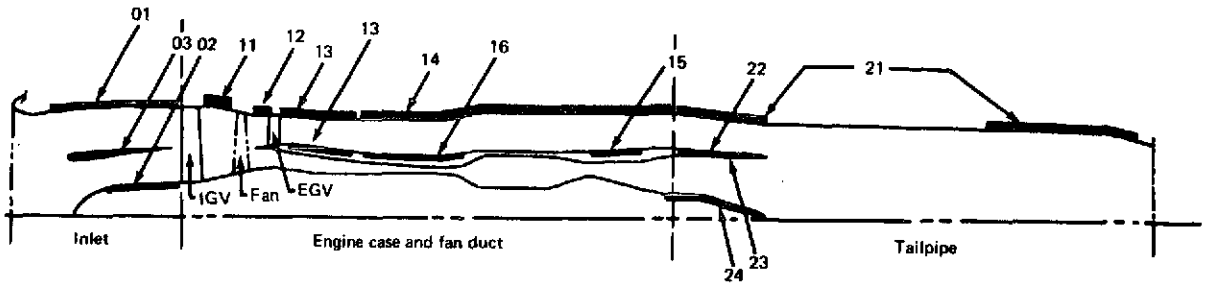


| Lining designation | Location | Face sheet type | Net active treatment area, ft$^2$ (m$^2$) | Core depth, in (m) | Cell size, in. (m) | Design point, $R/\rho c$ | Open area, % | Hole dia., in. (m) | Face sheet thickness, in. (m) |
|---|---|---|---|---|---|---|---|---|---|
| | | | Inlet | | | | | | |
| 1-01 | Diffuser | Polyimide | 31.0 (2.800) | 0.21* (0.0053) | 0.25 (0.0064) | 1.3 | | | |
| 1-02 | Nose dome | | 4.0 (0.372) | 0.21 (0.0053) | 0.25 (0.0064) | 1.3 | | | |
| 2-03 | Ring | | 11.0, 11.0 ++ (1.022) (1.022) | 0.21 (0.0053) | 0.25 (0.0064) | 1.3 | | | |
| | | | Engine case fan duct | | | | | | |
| 2-11 | Fwd of fan | Perforated sheet | 8.2 (0.762) | 1.0 (0.0254) | 0.375 (0.0095) | | 20 | 0.050 (0.0013) | 0.016 (0.0004) |
| 2-12 | Aft of fan | | 6.2 (0.576) | 0.50 (0.0127) | 0.375 (0.0095) | | 12 | 0.050 (0.0013) | 0.016 (0.0004) |
| 2-13 | Aft of EGV | | 21.8 (2.025) | 0.25 (0.0064) | 0.375 (0.0095) | | 12 | 0.050 (0.0013) | 0.016 (0.0004) |
| 2-14 | Outer wall aft | | 78.1 (7.255) | 0.50 (0.0064) | 0.375 (0.0095) | | 12 | 0.050 (0.0013) | 0.016 (0.0004) |
| 2-15 | Inner wall aft | | 7.0 (0.650) | 0.50 (0.0064) | 0.375 (0.0095) | | 12 | 0.050 (0.0013) | 0.016 (0.0004) |
| 2-16 | Inner wall | | 11.7 (1.087) | 0.50 (0.0064) | 0.375 (0.0095) | | 12 | 0.050 (0.0013) | 0.016 (0.0004) |
| | | | Tailpipe | | | | | | |
| 2-21 | Outer wall | Perforated sheet | 48.0 (4.459) | 0.35 (0.0089) | 0.375 (0.0095) | | 6 | 0.040 (0.0010) | 0.020 (0.0005) |
| 2-22 | Splitter out | | 21.9 (2.035) | 0.35 (0.0089) | 0.375 (0.0095) | | 6 | 0.040 (0.0010) | 0.020 (0.0005) |
| 2-23 | Splitter in | | 19.4 (1.802) | 0.55 (0.0140) | 0.375 (0.0095) | | 6 | 0.040 (0.0010) | 0.020 (0.0005) |
| 2-24 | Tail plug | | 5.5 (0.511) | 0.55 (0.0140) | 0.375 (0.0095) | | 6 | 0.040 (0.0010) | 0.020 (0.0005) |

++ Treatment on both sides of ring.
* Allow up to 2 in. (0.0508 m) core depth for buss-saw treatment

*FIGURE 138.–737/JT8D-ACOUSTIC LINING DEFINITION, CONFIGURATION 2*

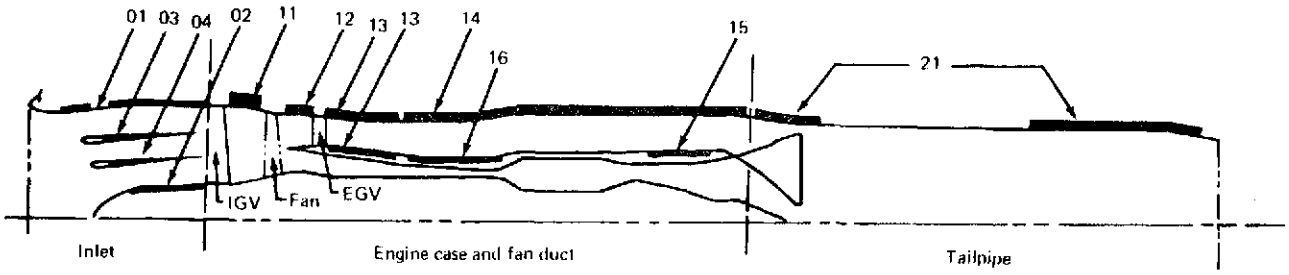


| Lining designation | Location | Face sheet type | Net active treatment area, ft² (m²) | Core depth, in. (m) | Cell size, in (m) | Design point, $R_s/\rho c$ | Open area, % | Hole dia., in. (m) | Face sheet thickness, in. (m) |
|---|---|---|---|---|---|---|---|---|---|
| Inlet | | | | | | | | | |
| 3-01 | Diffuser | Polyimide | 31.0 (2.880) | 0.23* 0.0058) | 0.25 (0.0064) | 1.1 | | | |
| 3-02 | Nose dome | | 4.0 (0.372) | 0.23 (0.0058) | 0.25 (0.0064) | 1.1 | | | |
| 3-03 | Outer ring | | 12.0, 12.0++ (1.115) (1.115) | 0.23 (0.0058) | 0.25 0.0064) | 1.1 | | | |
| 3-04 | Inner ring | | 8.0, 8.0++ (0.743) (0.743) | 0.23 0.0058) | 0.25 (0.0064) | 1.1 | | | |
| Engine case fan duct | | | | | | | | | |
| 3-11 | Fwd of fan | Perforated sheet | 8.2 (0.762) | 1.0 (0.0254) | 0.375 (0.0095) | | 20 | 0.050 (0.0013) | 0.016 (0.0004) |
| 3-12 | Aft of fan | | 6.2 (0.576) | 0.50 (0.0127) | 0.375 (0.0095) | | 12 | 0.050 (0.0013) | 0.016 (0.0004) |
| 3-13 | Aft of EGV | | 21.8 (2.025) | 0.25 (0.0064) | 0.375 (0.0095) | | 12 | 0.050 (0.0013) | 0.016 (0.0004) |
| 3-14 | Outer wall aft | | 78.1 (7.255) | 0.50 (0.0127) | 0.375 (0.0095) | | 12 | 0.050 (0.0013) | 0.016 (0.0004) |
| 3-15 | Inner wall aft | | 7.0 (0.650) | 0.50 (0.0127) | 0.375 (0.0095) | | 12 | 0.050 (0.0013) | 0.016 (0.0004) |
| 3-16 | Inner wall | | 11.7 (1.087) | 0.50 (0.0127) | 0.375 (0.0095) | | 12 | 0.050 (0.0013) | 0.016 (0.0004) |
| Tailpipe | | | | | | | | | |
| 3-21 | Outer wall | Perforated sheet | 48.0 (4.459) | 0.25 (0.0064) | 0.375 (0.0095) | | 4 | | |

++ Treatment on both sides of rings.
* Allow up to 2 in. (0.0508 m) core depth for buzz-saw treatment.

*FIGURE 139.–737/JT8D ACOUSTIC LINING DEFINITION, CONFIGURATION 3*

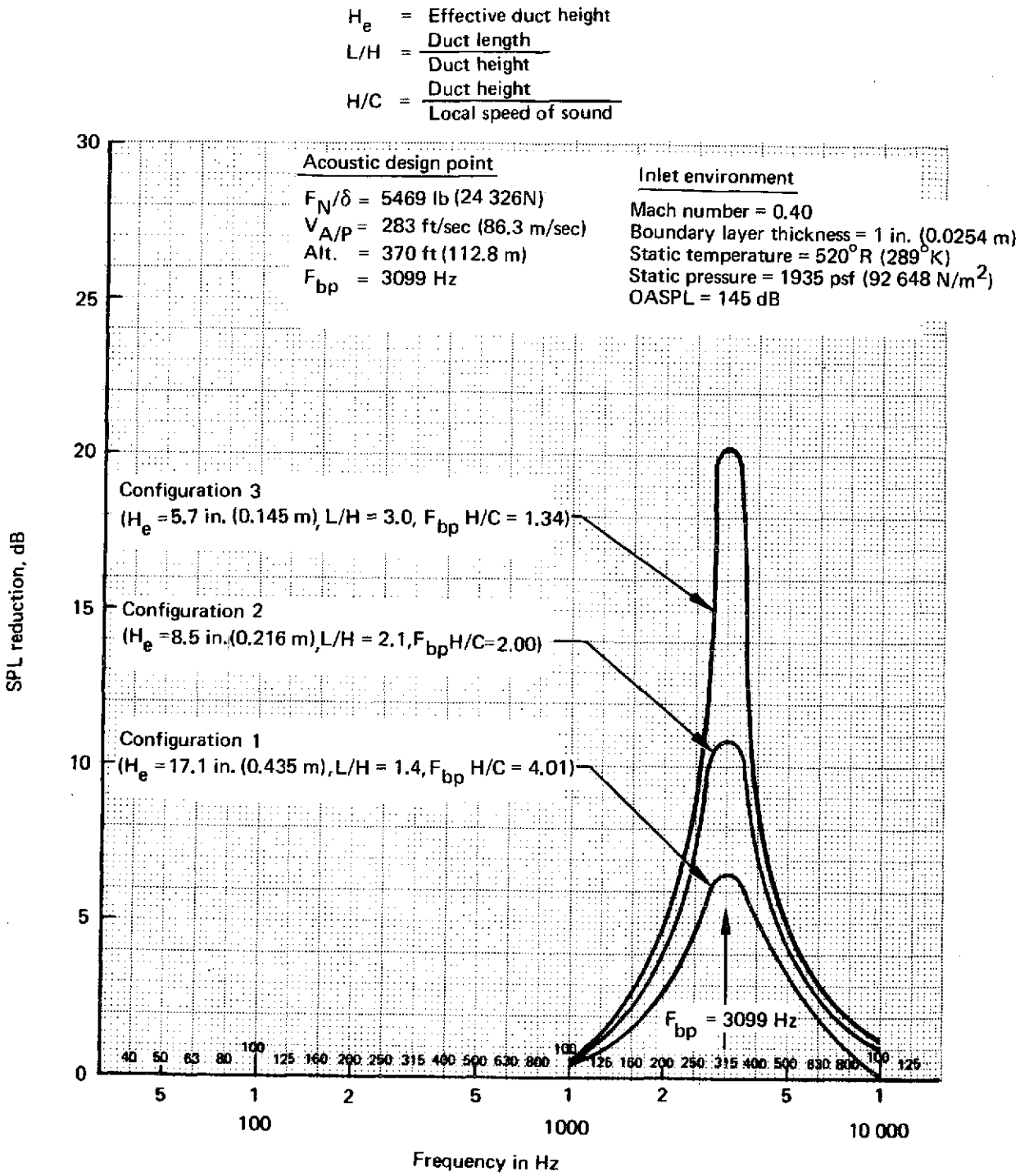


*FIGURE 140.—737/JT8D INLET LINING DESIGN ATTENUATION SPECTRA*

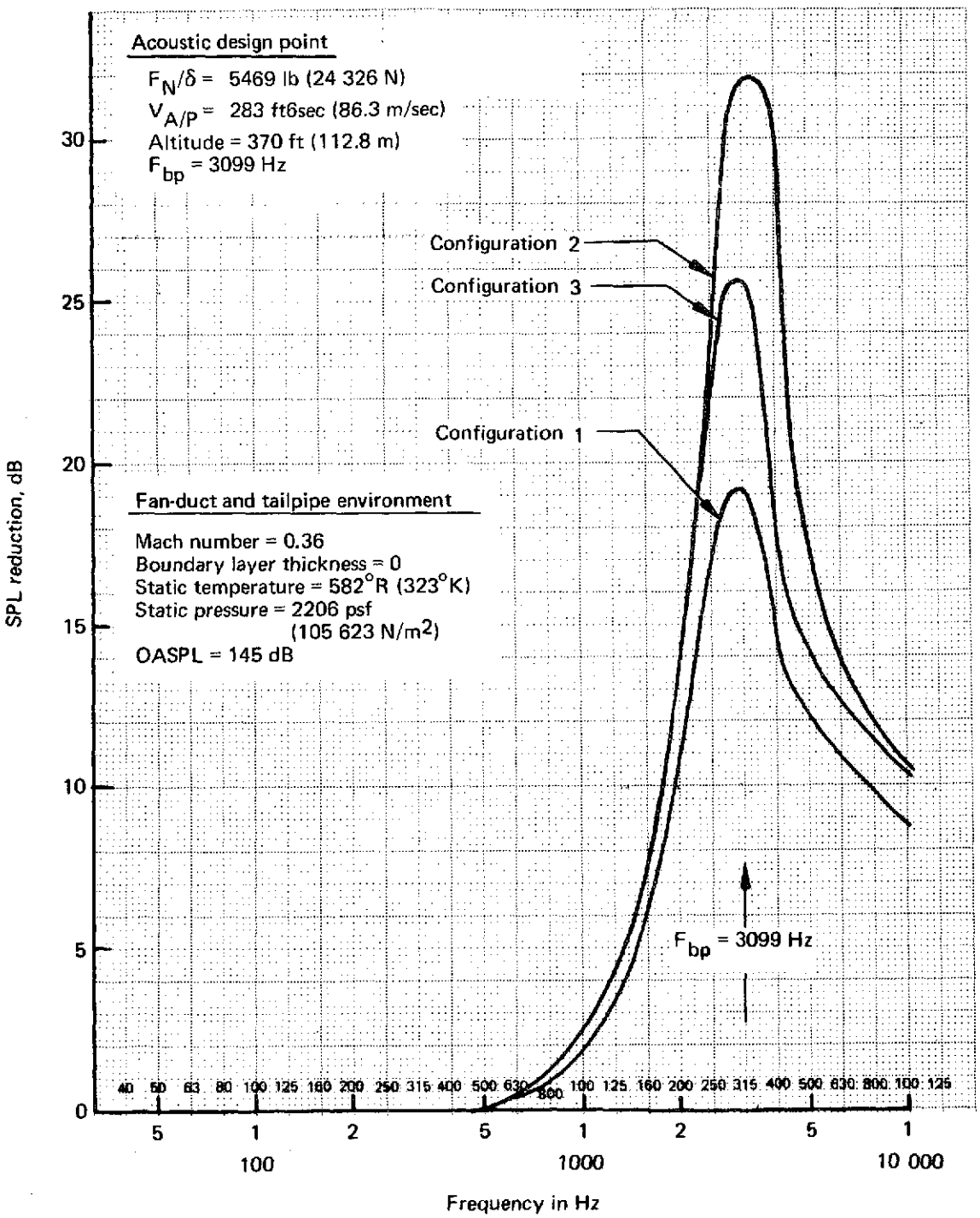


*FIGURE 141.–737-JT8D AFT FAN AND TAILPIPE LINING DESIGN ATTENUATION*

### 5.8.2 Noise/Thrust/Altitude Curves

EPNL levels were predicted as a function of altitude and thrust setting for the various configurations investigated. To provide a common basis for comparisons, all calculations were performed at constant true airspeed and each altitude corresponded to an airplane level flyover.

#### 5.8.2.1 Calculation Method

See section 4.8.2.1 for this method.

#### 5.8.2.2 Results

EPNL versus altitude plots were developed for a number of corrected thrust values and are presented in figures 142 through 146. Comparing figures 142 and 143 shows substantial EPNdB noise reduction due to the change in engine cycle without acoustic treatment. The addition of nacelle and engine acoustic treatment results in further reductions depending on thrust, altitude, and configuration.

Comparisons of the noise levels for the three configurations with acoustic attenuation (fig. 144, 145, and 146) show that, at low altitude, configuration 2 is 1 to 2 EPNdB lower than configuration 1, and configuration 3 is 0 to 2 EPNdB lower than configuration 2. At high altitudes, configuration 2 has a higher noise level than configuration 1, because configuration 2 requires higher jet velocities than configuration 1 to achieve the same corrected net thrust. Comparisons of configuration 1 or 2 and configuration 3 at high altitudes show reductions as large as 6 EPNdB resulting from the jet noise reduction attributed to the mixer. However, the mixer technology implied is subject to the limitations previously described in section 4.8.2.2.

### 5.8.3 Noise Levels at FAR Part 36 Conditions

#### 5.8.3.1 Calculation Method

The FAR Part 36 EPNLs were calculated with the method described in section 4.8.3.1.

#### 5.8.3.2 Results

The FAR Part 36 condition noise levels for the 737-200 at a maximum takeoff gross weight of 103 500 lb (46 937 kg) for the baseline and modified configurations are shown in table 42. Table 43 presents the same information for the modified configurations with the maximum brake release

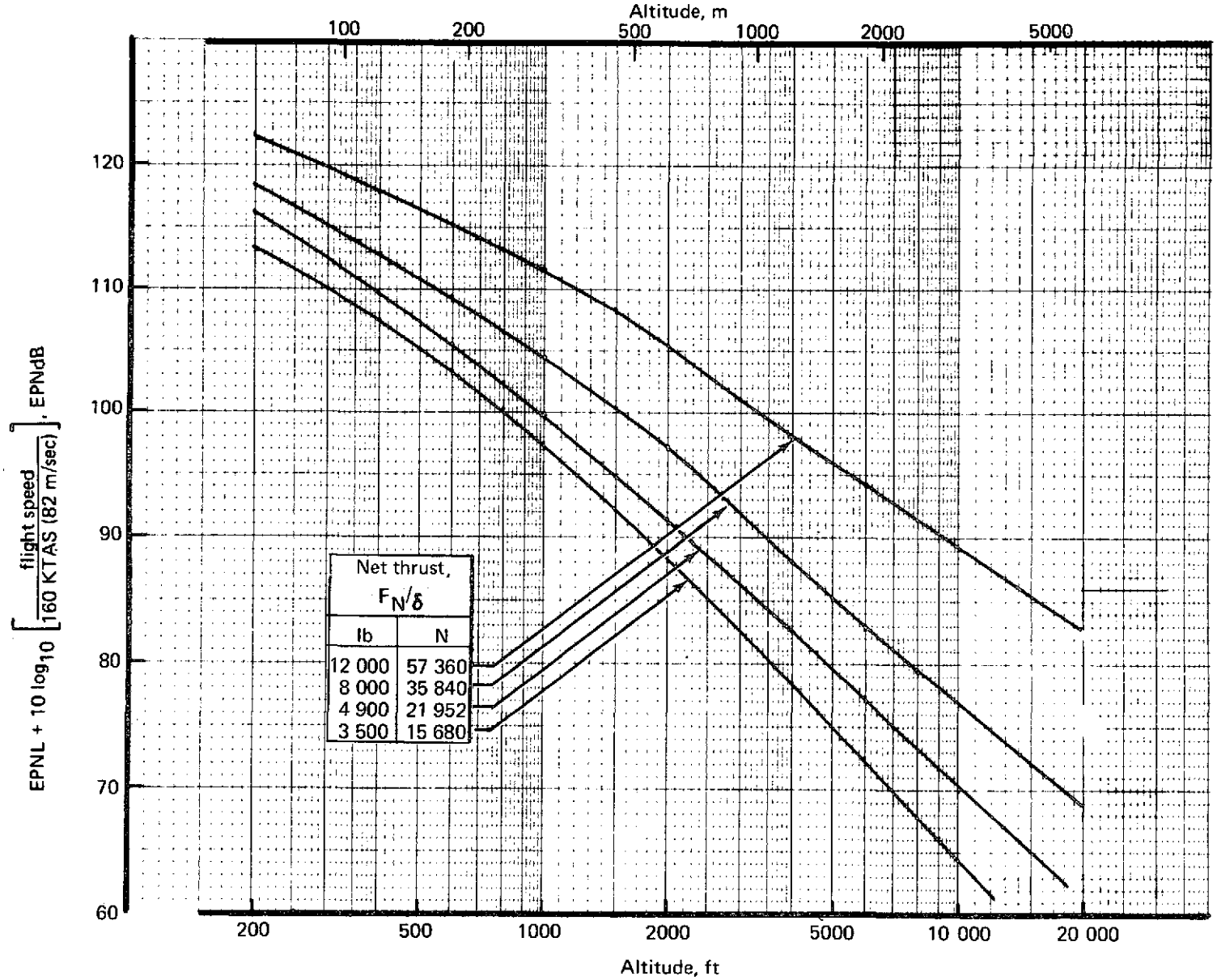


*FIGURE 142.–737/JT8D BASELINE (HARDWALL) NOISE/THRUST/ALTITUDE CURVES– NOISE EXTRAPOLATION CONDITIONS, 77°F (298°K), RELATIVE HUMIDITY 70%*

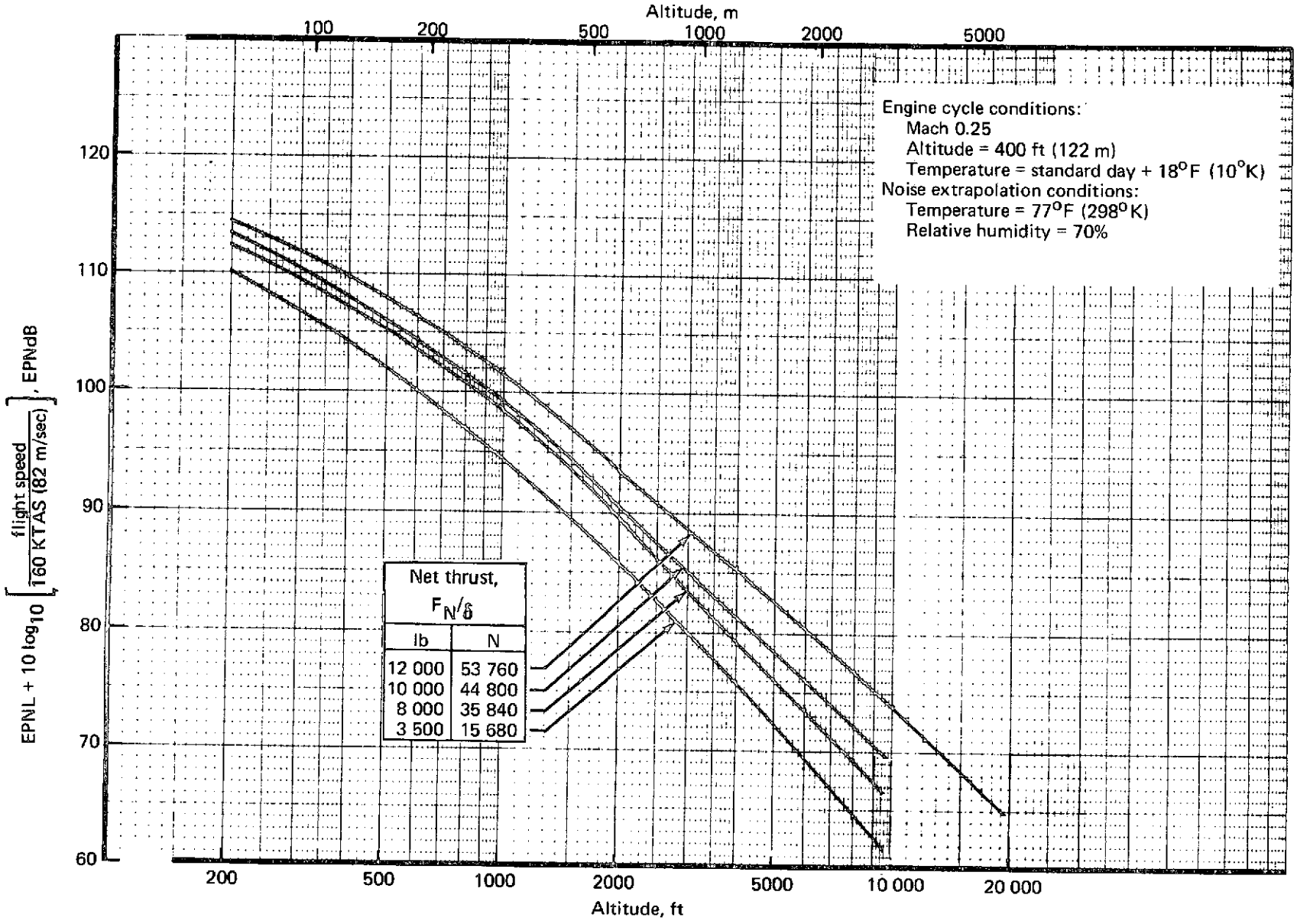


*FIGURE 143.—737/JT8D-109 CONFIGURATION 1 (HARDWALL) NOISE/THRUST/ALTITUDE CRUISE*

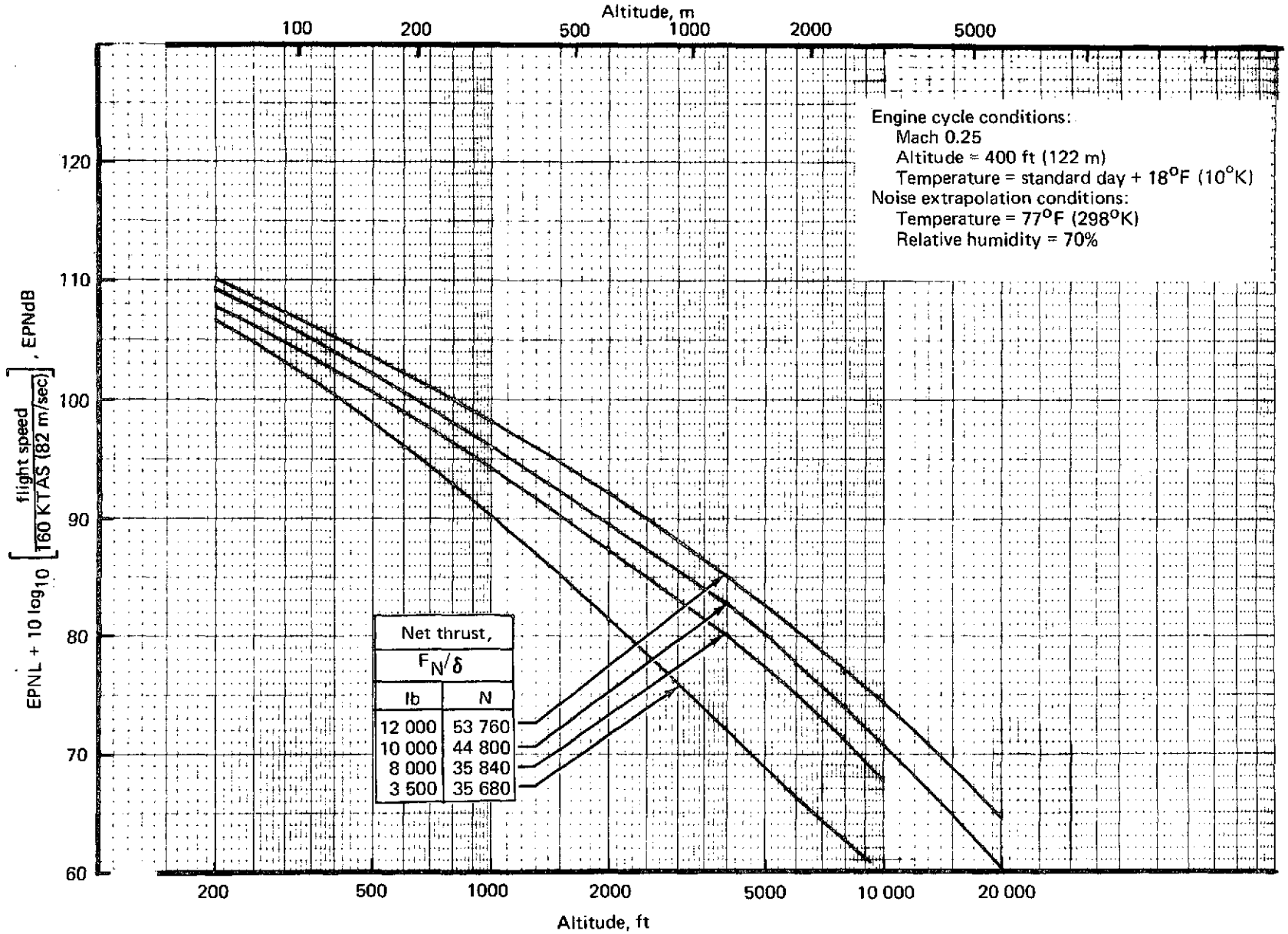


*FIGURE 144.–737/JT8D-109 CONFIGURATION 1–NOISE/THRUST/ALTITUDE CURVES*

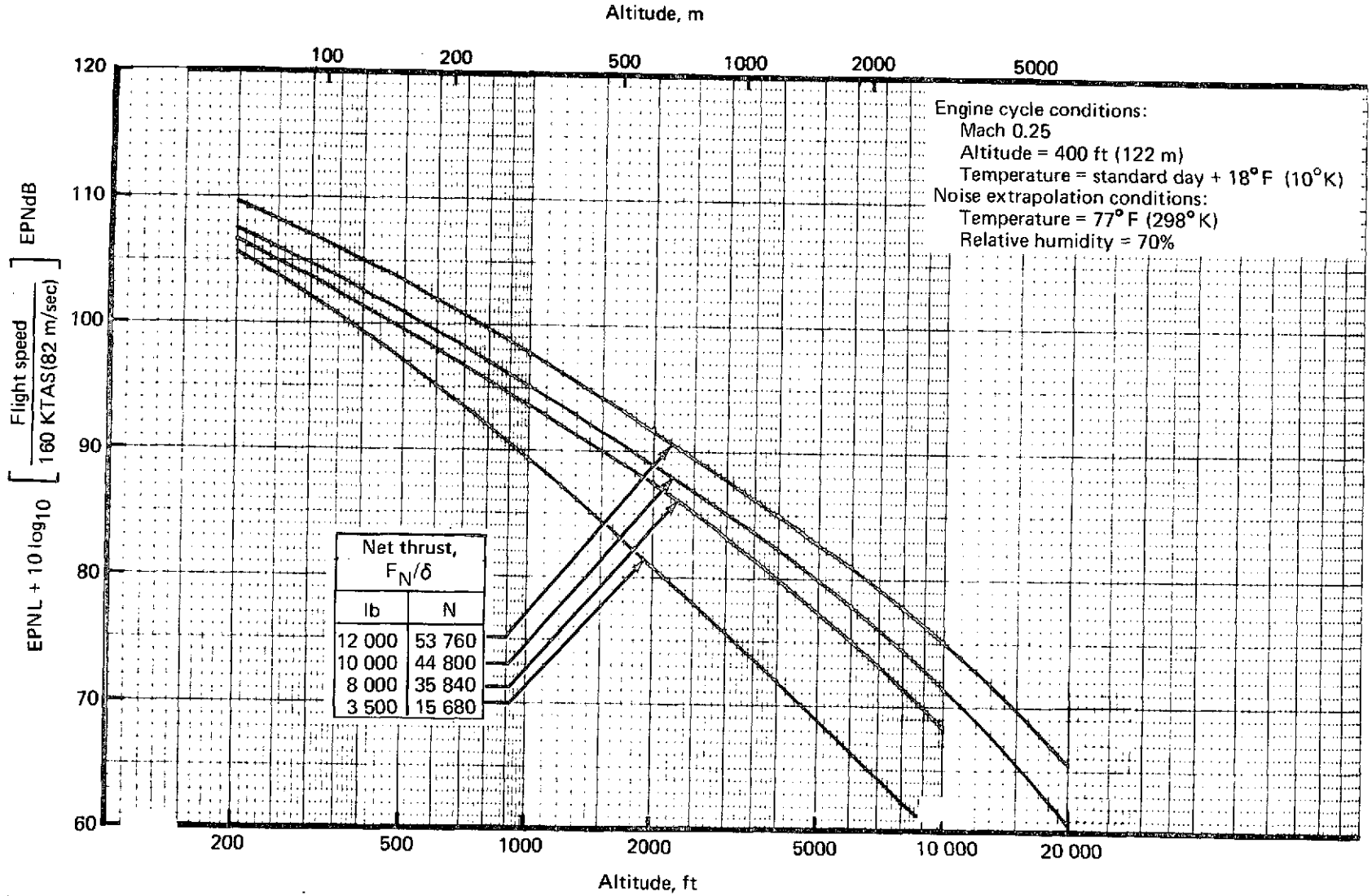


*FIGURE 145.–737/JT8D-109 CONFIGURATION 2–NOISE/THRUST/ALTITUDE CURVES*

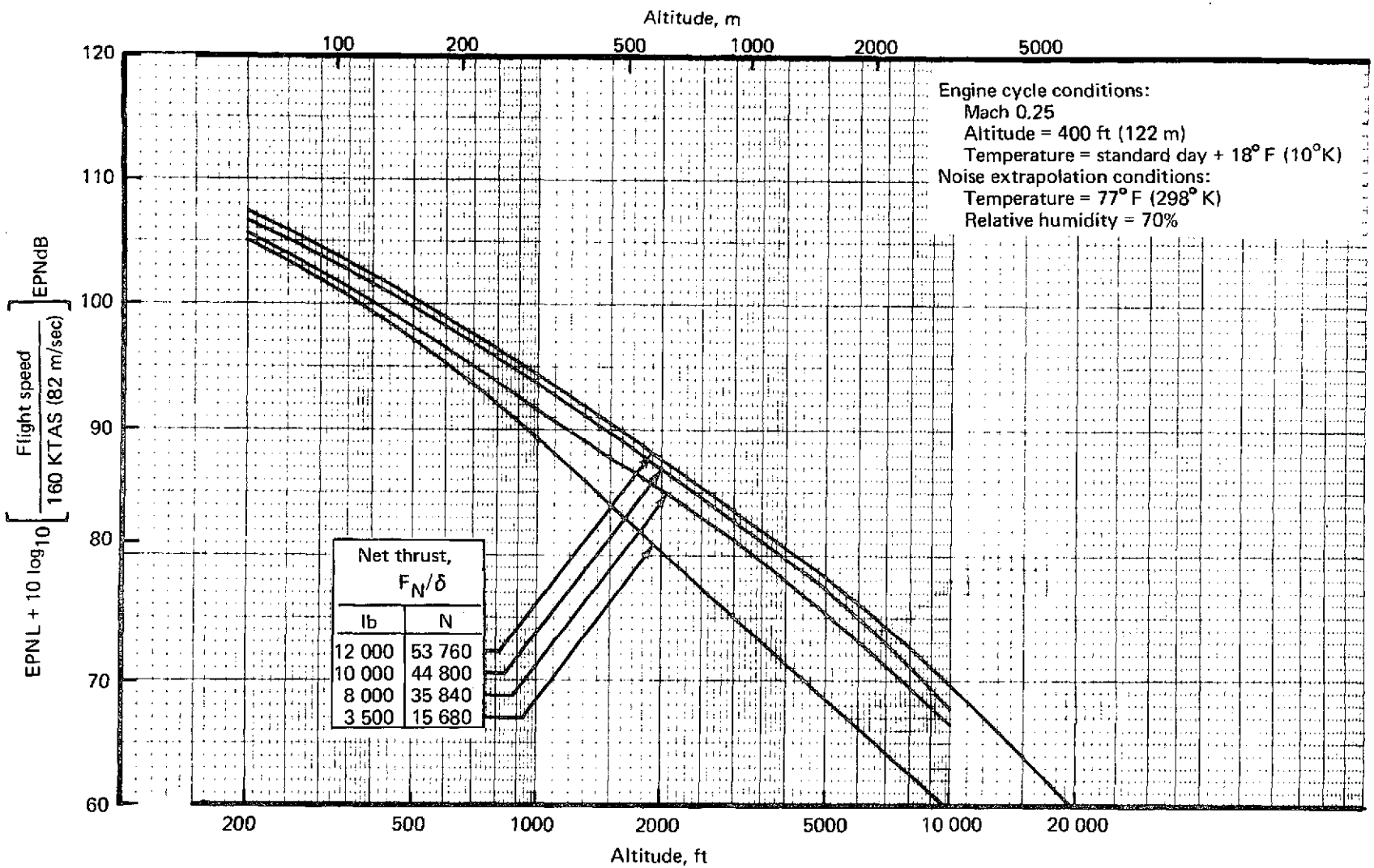


*FIGURE 146.–737/JT8D-109 CONFIGURATION 3–NOISE/THRUST/ALTITUDE CURVES*

*TABLE 42.–737/JT8D NOISE COMPARISON AT FAR PART 36 MEASURING STATIONS, BRGW = 103 500 LB (46 947 KG)*

| Nacelle configuration (a) | Condition | Approach 1 nmi (1.85 km) | | | | Takeoff (with cutback) 3.5 nmi (6.84 km) | | Takeoff (without cutback) 3.5 nmi (6.84 km) | | Sideline 0.25 nmi (0.46 km) | |
|---|---|---|---|---|---|---|---|---|---|---|---|
| | | English units | SI units | English units | SI units | English units | SI units | English units | SI units | English units | SI units |
| Hardwall baseline (JT8D-9) | BRGW | – | – | – | – | 103 500 lb | 46 937 kg | 103 500 lb | 46 937 kg | 103 500 lb | 46 937 kg |
| | LGW | 98 000 lb | 44 443 kg | 98 000 lb | 44 443 kg | – | – | – | – | – | – |
| | Flaps, position | 40 | 40 | 30 | 30 | 1 | 1 | 1 | 1 | 1 | 1 |
| | Altitude | 370 ft | 112.8 m | 370 ft | 112.8 m | 2244 ft | 684.0 m | 2400 ft | 731.5 m | 800 ft | 243.8 m |
| | Sideline | – | – | – | – | – | – | – | – | 1520 ft | 463.3 m |
| | Thrust/δ | 5450 lb | 24 416 N | 3720 lb | 16 666 N | 8326 lb | 37 300 N | 12 790 lb | 57 299 N | 12 570 lb | 56 314 N |
| | Velocity, TAS | 141 kn | 72.6 m/sec | 146 kn | 75.2 m/sec | 167 kn | 86 m/sec | 167 kn | 86 m/sec | 164 kn | 84.4 m/sec |
| | EPNL, EPNdB | 110.9 | 110.9 | 108.9 | 108.9 | 96.7 | 96.7 | 100.0 | 100.0 | 101.1 | 101.1 |
| | FAR 36, EPNdB | 102.9 | 102.9 | 102.9 | 102.9 | 95.3 | 95.3 | 95.3 | 95.3 | 102.9 | 102.9 |
| 1 (JT8D-109 refan) | BRGW | – | – | – | – | 103 500 lb | 46 937 kg | 103 500 lb | 46 937 kg | 103 500 lb | 46 937 kg |
| | LGW | 98 000 lb | 44 443 kg | 98 000 lb | 44 443 kg | – | – | – | – | – | – |
| | Flaps, position | 40 | 40 | 30 | 30 | 1 | 1 | 1 | 1 | 1 | 1 |
| | Altitude | 370 ft | 112.8 m | 370 ft | 112.8 m | 2525 ft | 769.6 m | 2695 ft | 821.4 m | 800 ft | 243.8 m |
| | Sideline | – | – | – | – | – | – | – | – | 1520 ft | 463.3 m |
| | Thrust/δ | 5450 lb | 24 416 N | 3720 lb | 16 666 N | 8410 lb | 37 677 N | 13 650 lb | 61 152 N | 13 420 lb | 60 122 N |
| | Velocity, TAS | 141 kn | 72.6 m/sec | 146 kn | 75.2 m/sec | 168 kn | 86.5 m/sec | 168 kn | 86.5 m/sec | 164 kn | 84.4 m/sec |
| | ΔEPNL, EPNdB[b] | -9.1 | -9.1 | -7.3 | -7.3 | -10.5 | -10.5 | -12.4 | -12.4 | -11.0 | -11.0 |
| | EPNL | (101.8) | (101.8) | (101.6) | (101.6) | (86.2) | (86.2) | (87.6) | (87.6) | (90.1) | (90.1) |
| | FAR 36, EPNdB | 102.9 | 102.9 | 102.9 | 102.9 | 95.3 | 95.3 | 95.3 | 95.3 | 102.9 | 102.9 |
| 2 (JT8D-109 refan) | BRGW | – | – | – | – | 103 500 lb | 46 937 kg | 103 500 lb | 46 937 kg | 103 500 lb | 46 937 kg |
| | LGW | 98 000 lb | 44 443 kg | 98 000 lb | 44 443 kg | – | – | – | – | – | – |
| | Flaps, position | 40 | 40 | 30 | 30 | 1 | 1 | 1 | 1 | 1 | 1 |
| | Altitude | 370 ft | 112.8 m | 370 ft | 112.8 m | 2404 ft | 732.7 m | 2570 ft | 783.3 m | 800 ft | 243.8 m |
| | Sideline | – | – | – | – | – | – | – | – | 1520 ft | 463.3 m |
| | Thrust/δ | 5450 lb | 24 416 N | 3720 lb | 16 666 N | 8376 lb | 37 524 N | 13 250 lb | 59 360 N | 13 040 lb | 58 419 N |
| | Velocity, TAS | 141 kn | 72.6 m/sec | 146 kn | 75.2 m/sec | 167 kn | 86 m/sec | 168 kn | 86.5 m/sec | 164 kn | 84.4 m/sec |
| | ΔEPNL, EPNdB[b] | -10.1 | -10.1 | -8.3 | -8.3 | -10.4 | -10.4 | -12.2 | -12.2 | -11.6 | -11.6 |
| | EPNL | (100.8) | (100.8) | (100.6) | (100.6) | (86.3) | (86.3) | (87.8) | (87.8) | (89.5) | (89.5) |
| | FAR 36, EPNdB | 102.9 | 102.9 | 102.9 | 102.9 | 95.3 | 95.3 | 95.3 | 95.3 | 102.9 | 102.9 |
| 3[b] (JT8D-109 refan) | BRGW | – | – | – | – | 103 500 lb | 46 937 kg | 103 500 lb | 46 937 kg | 103 500 lb | 46 937 kg |
| | LGW | 98 000 lb | 44 443 kg | 98 000 lb | 44 443 kg | – | – | – | – | – | – |
| | Flaps, position | 40 | 40 | 30 | 30 | 1 | 1 | 1 | 1 | 1 | 1 |
| | Altitude | 370 ft | 112.8 m | 370 ft | 112.8 m | 2400 ft | 731.5 m | 2565 ft | 781.8 m | 800 ft | 243.8 m |
| | Sideline | – | – | – | – | – | – | – | – | 1520 ft | 463.3 m |
| | Thrust/δ | 5450 lb | 24 416 N | 3720 lb | 16 666 N | 8376 lb | 37 524 N | 13 240 lb | 59 315 N | 13 040 lb | 58 419 N |
| | Velocity, TAS | 141 kn | 72.6 m/sec | 146 kn | 75.2 m/sec | 167 kn | 86 m/sec | 168 kn | 86.5 m/sec | 164 kn | 84.4 m/sec |
| | ΔEPNL, EPNdB[b] | -10.8 | -10.8 | -8.4 | -8.4 | -12.3 | -12.3 | -17.3 | -17.3 | -16.5 | -16.5 |
| | EPNL | (100.1) | (100.1) | (100.5) | (100.5) | (84.4) | (84.4) | (82.7) | (82.7) | (84.6) | (84.6) |
| | FAR 36, EPNdB | 102.9 | 102.9 | 102.9 | 102.9 | 95.3 | 95.3 | 95.3 | 95.3 | 102.9 | 102.9 |

[a] Configuration 3 requires mixer development

[b] From JT8D-9 hardwall baseline; see calculation method in section 5.8.3.1

## TABLE 43.—737/JT8D NOISE COMPARISON AT FAR PART 36 MEASURING STATION, INCREASED BRGW

| Nacelle configuration (a) | Condition | Approach 1 nmi (1.85 km) | | | | Takeoff (with cutback) 3.5 nmi (6.84 km) | | Takeoff (without cutback) 3.5 nmi (6.84 km) | | Sideline 0.25 nmi (0.46 km) | |
|---|---|---|---|---|---|---|---|---|---|---|---|
| | | English units | SI units | English units | SI units | English units | SI units | English units | SI units | English units | SI units |
| 1 (JT8D-109 refan) | BRGW | – | – | – | – | 109 000 lb | 49 432 kg | 109 000 lb | 49 432 kg | 109 000 lb | 49 432 kg |
| | LGW | 98 000 lb | 44 443 kg | 98 000 lb | 44 443 kg | – | – | – | – | – | – |
| | Flaps, position | 40 | 40 | 30 | 30 | 1 | 1 | 1 | 1 | 1 | 1 |
| | Altitude | 370 ft | 112.8 m | 370 ft | 112.8 m | 2230 ft | 679.7 m | 2385 ft | 726.9 m | 1000 ft | 305 m |
| | Sideline | – | – | – | – | – | – | – | – | 1520 ft | 463.3 m |
| | Thrust/δ | 5450 lb | 24 416 N | 3720 lb | 16 666 N | 8740 lb | 39 155 N | 13 545 lb | 60 681 N | 3360 lb | 59 852 N |
| | Velocity, TAS | 141 kn | 72.6 m/sec | 146 kn | 75.2 m/sec | 172 kn | 88.6 m/sec | 172 kn | 88.6 m/sec | 169 kn | 87.0 m/sec |
| | ΔEPNL, EPNdB[b] | -9.1 | -9.1 | -7.3 | -7.3 | -9.0 | -9.0 | -11.2 | -11.2 | -11.2 | -11.2 |
| | EPNL, EPNdB | (101.8) | (101.8) | (101.6) | (101.6) | (87.7) | (87.7) | (88.8) | (88.8) | (89.9) | (89.9) |
| | FAR 36, EPNdB | 103.1 | 103.1 | 103.1 | 103.1 | 95.7 | 95.7 | 95.7 | 95.7 | 103.1 | 103.1 |
| 2 (JT8D-109 refan) | BRGW | – | – | – | – | 109 000 lb | 49 432 kg | 109 000 lb | 49 432 kg | 109 000 lb | 49 432 kg |
| | LGW | 98 000 lb | 44 443 kg | 98.000 lb | 44 443 kg | – | – | – | – | – | – |
| | Flaps, position | 40 | 40 | 30 | 30 | 1 | 1 | 1 | 1 | 1 | 1 |
| | Altitude | 370 ft | 112.8 m | 370 ft | 112.8 m | 2120 ft | 646.2 m | 2265 ft | 690.4 m | 1000 ft | 305 m |
| | Sideline | – | – | – | – | – | – | – | – | 1520 ft | 463.3 m |
| | Thrust/δ | 5450 lb | 24 416 N | 3720 lb | 16 666 N | 8710 lb | 39 021 N | 13 165 lb | 58 979 N | 12 980 lb | 58 150 N |
| | Velocity, TAS | 141 kn | 72.6m/sec | 146 kn | 75.2 m/sec | 172 kn | 88.6 m/sec | 172 kn | 88.6 m/sec | 169 kn | 87.0 m/sec |
| | ΔEPNL, EPNdB[b] | -10.1 | -10.1 | -8.3 | -8.3 | -9.0 | -9.0 | -11.1 | -11.1 | -11.8 | -11.8 |
| | EPNL, EPNdB | (100.8) | (100.8) | (100.6) | (100.6) | (87.7) | (87.7) | (88.9) | (88.9) | (89.3) | (89.3) |
| | FAR 36, EPNdB | 103.1 | 103.1 | 103.1 | 103.1 | 95.7 | 95.7 | 95.7 | 95.7 | 103.1 | 103.1 |
| 3[b] (JT8D-109 refan) | BRGW | – | – | – | – | 109 000 lb | 49 432 kg | 109 000 lb | 49 432 kg | 109 000 lb | 49 432 kg |
| | LGW | 98 000 lb | 44 443 kg | 98 000 lb | 44 443 kg | – | – | – | – | – | – |
| | Flaps, position | 40 | 40 | 30 | 30 | 1 | 1 | 1 | 1 | 1 | 1 |
| | Altitude | 370 ft | 112.8 m | 370 ft | 112.8 m | 2115 ft | 644.6 m | 2260 ft | 688.8 m | 100 ft | 305 m |
| | Sideline | – | – | – | – | – | – | – | – | 1520 ft | 463.3 m |
| | Thrust/δ | 5450 lb | 24 416 N | 3720 lb | 16 666 N | 8710 lb | 39 021 N | 13 160 lb | 58 956 N | 12 980 lb | 58 150 N |
| | Velocity, TAS | 141 kn | 72.6 m/sec | 146 kn | 75.2 m/sec | 172 kn | 88.6 m/sec | 172 kn | 88.6 m/sec | 169 kn | 87.0 m/sec |
| | ΔEPNL, EPNdB[b] | -10.8 | -10.8 | -8.4 | -8.4 | -11.0 | -11.0 | -16.1 | -16.1 | -16.7 | -16.7 |
| | EPNL, EPNdB | (100.1) | (100.1) | (100.5) | (100.5) | (85.7) | (85.7) | (83.9) | (83.9) | (84.4) | (84.4) |
| | FAR 36, EPNdB | 103.1 | 103.1 | 103.1 | 103.1 | 95.7 | 95.7 | 95.7 | 95.7 | 103.1 | 103.1 |

[a] Configuration 3 requires mixer development

[b] From JT8D-9 hardwall baseline; see calcualtion method in section 5.8.3.1

gross weight increased. The corresponding noise escalation on takeoff is from 0 to 1.5 EPNdB, depending on flight condition. It is seen that, based on the initial design analysis, all three configurations meet the FAR Part 36 requirements.

### 5.8.4 Noise Contour Area Analysis

This analysis was conducted in the same manner as the 707 analysis (sec. 3.8.4).

#### 5.8.4.1 EPNL Contour Areas

EPNL contour areas were calculated by using the method presented in section 3.8.4.1. The full power operational profile is shown in table 44.

#### 5.8.4.2 Relative Footprint Noise Index

Relative footprint noise index (RFNI) calculations were made by using the method described in section 3.8.4.2.

#### 5.8.4.3 Results

EPNL footprints for the 737-200 were calculated for both full power operational and cutback certification profiles. The full power operational profile is shown in table 44. From the footprints derived with these profiles, constant EPNL contour areas were calculated in the range of 85 to 110 EPNdB.

Four engine/nacelle configurations were investigated: the JT8D-9 hardwall baseline and nacelle configurations 1, 2, and 3 for the JT8D-109 refan engine for full power operational profiles. The JT8D-9 hardwall baseline and JT8D-109 configuration 1 were also investigated using a cutback certification profile.

The results of the footprint studies are presented in three forms:

- Relative footprint contour areas versus EPNL
- Footprint contour percent area reductions versus EPNL
- Relative footprint noise index (RFNI) based on EPNL contours.

## *TABLE 44.—737-200 FULL POWER OPERATIONAL FLIGHT PROFILES*

737-200 full power operational takeoff profiles for EPNL footprints—brake release gross weight = 103 500 lb (46 947 kg)

| Nacelle configuration | Distance from brake release | | Altitude | | Average power setting $F_N/\delta$ | | Average flight speed | | Flap position | Gear position |
|---|---|---|---|---|---|---|---|---|---|---|
| | ft | m | ft | m | lb | N | KTAS | m/sec | | |
| Hardwall baseline (JT8D-9) | 0 | 0 | 0 | 0 | 12 400 | 55 158 | 113.0 | 58.1 | 1 | Down |
| | 6 010 | 1 832 | 0 | 0 | 12 530 | 55 736 | 163.3 | 84.0 | ↓ | Down |
| | 15 490 | 4 721 | 1 500 | 457 | 12 490 | 55 558 | 189.4 | 97.4 | ↓ | Up |
| | 20 520 | 6 254 | 1 500 | 457 | 12 210 | 54 313 | 236.8 | 121.8 | Retract | ↓ |
| | 26 420 | 8 053 | 1 500 | 457 | 9 630 | 42 836 | 265.0 | 136.3 | 0 | ↓ |
| | 51 420 | 15 673 | 4 000 | 1219 | 9 900 | 44 037 | 275.1 | 141.5 | ↓ | ↓ |
| | 79 120 | 24 116 | 6 500 | 1981 | 10 220 | 45 461 | 287.4 | 147.9 | ↓ | ↓ |
| | 116 720 | 35 576 | 9 500 | 2896 | 10 610 | 47 196 | 301.0 | 154.8 | ↓ | ↓ |
| | 161 220 | 49 140 | 12 500 | 3810 | 11 080 | 49 286 | 317.0 | 163.1 | ↓ | ↓ |
| | 221 920 | 67 641 | 16 000 | 4877 | 11 740 | 52 222 | 337.7 | 173.7 | ↓ | ↓ |
| | 307 920 | 93 854 | 20 000 | 6096 | | | | | | |
| 1 (JT8D-109 refan) | 0 | 0 | 0 | 0 | 13 250 | 58 939 | 113.6 | 58.4 | 1 | Down |
| | 5 448 | 1 661 | 0 | 0 | 13 370 | 59 473 | 163.8 | 84.3 | ↓ | Down |
| | 14 170 | 4 319 | 1 500 | 457 | 13 170 | 58 583 | 189.9 | 97.7 | ↓ | Up |
| | 18 950 | 5 776 | 1 500 | 457 | 12 590 | 56 003 | 237.3 | 122.1 | Retract | ↓ |
| | 24 500 | 7 468 | 1 500 | 457 | 9 580 | 42 614 | 265.0 | 136.3 | 0 | ↓ |
| | 49 800 | 15 179 | 4 000 | 1219 | 10 060 | 44 749 | 275.1 | 141.5 | ↓ | ↓ |
| | 77 100 | 23 500 | 6 500 | 1981 | 10 700 | 47 596 | 287.4 | 147.9 | ↓ | ↓ |
| | 112 500 | 34 290 | 9 500 | 2896 | 11 330 | 50 398 | 301.0 | 154.8 | ↓ | ↓ |
| | 151 800 | 46 269 | 12 500 | 3810 | 11 970 | 53 245 | 317.0 | 163.1 | ↓ | ↓ |
| | 205 100 | 62 514 | 16 000 | 4877 | 12 590 | 56 003 | 337.7 | 173.7 | ↓ | ↓ |
| | 280 500 | 85 496 | 20 000 | 6096 | | | | | | |
| 2 (JT8D-109 refan) | 0 | 0 | 0 | 0 | 12 870 | 57 249 | 113.3 | 58.3 | 1 | Down |
| | 5 656 | 1 724 | 0 | 0 | 12 990 | 57 782 | 163.6 | 84.2 | ↓ | Down |
| | 14 700 | 4 481 | 1 500 | 457 | 12 820 | 57 026 | 189.6 | 97.5 | ↓ | Up |
| | 19 600 | 5 974 | 1 500 | 457 | 12 250 | 54 491 | 237.0 | 121.9 | Retract | ↓ |
| | 25 410 | 7 745 | 1 500 | 457 | 9 220 | 41 013 | 265.0 | 136.3 | 0 | ↓ |
| | 52 210 | 15 914 | 4 000 | 1219 | 9 730 | 43 281 | 275.1 | 141.5 | ↓ | ↓ |
| | 81 010 | 24 692 | 6 500 | 1981 | 10 370 | 46 128 | 287.4 | 147.9 | ↓ | ↓ |
| | 118 510 | 36 122 | 9 500 | 2896 | 11 000 | 48 930 | 301.0 | 154.8 | ↓ | ↓ |
| | 160 310 | 48 862 | 12 500 | 3810 | 11 650 | 51 822 | 317.0 | 163.1 | ↓ | ↓ |
| | 216 210 | 65 901 | 16 000 | 4877 | 12 280 | 54 624 | 337.7 | 173.7 | ↓ | ↓ |
| | 295 610 | 90 102 | 20 000 | 6096 | | | | | | |
| 3 (JT8D-109 refan) | 0 | 0 | 0 | 0 | 13 020 | 57 916 | 113.5 | 58.4 | 1 | Down |
| | 5 575 | 1 699 | 0 | 0 | 13 140 | 58 450 | 163.7 | 84.2 | ↓ | Down |
| | 14 490 | 4 417 | 1 500 | 457 | 12 960 | 57 649 | 189.8 | 97.6 | ↓ | Up |
| | 19 340 | 5 895 | 1 500 | 457 | 12 370 | 55 025 | 237.2 | 122.0 | Retract | ↓ |
| | 25 050 | 7 635 | 1 500 | 457 | 9 350 | 41 591 | 265.0 | 136.3 | 0 | ↓ |
| | 51 250 | 15 621 | 4 000 | 1219 | 9 900 | 44 037 | 275.1 | 141.5 | ↓ | ↓ |
| | 79 350 | 24 186 | 6 500 | 1981 | 10 540 | 46 884 | 287.4 | 147.9 | ↓ | ↓ |
| | 115 650 | 35 250 | 9 500 | 2896 | 11 180 | 49 731 | 301.0 | 154.8 | ↓ | ↓ |
| | 156 050 | 47 556 | 12 500 | 3810 | 11 820 | 52 578 | 317.0 | 163.1 | ↓ | ↓ |
| | 210 750 | 64 237 | 16 000 | 4877 | 12 410 | 55 202 | 337.7 | 173.7 | ↓ | ↓ |
| | 286 150 | 87 219 | 20 000 | 6096 | | | | | | |

737-200 approach conditions for EPNL footprints

| Nacelle configuration | Landing gross weight | | Approach speed 1.3 $V_{stall}$ +10 kts. (5.1 m/sec) | | Glide slope (degrees) | Flap position | Gear position | Power setting $F_N/\delta$ | |
|---|---|---|---|---|---|---|---|---|---|
| | lb | kg | KTAS | m/sec | | | | lb | N |
| All | 98 000 | 44 452 | 141.2 | 72.6 | 3 | 40 | Down | 5450 | 24243 |

Relative footprint contour areas are presented in figure 147 for the full-power operational profile and in figure 148 for the cutback certification profiles. The two profiles are compared in figure 149. Percent area reduction of the different configurations is shown in figures 150 and 151. Relative footprint noise index based on EPNL is presented for all four configurations in table 45.

All three forms of EPNL footprint data show the same trends and lead to the same conclusions as for the 727 as discussed in section 4.8.4.2.

*TABLE 45.—737/JT8D-9/JT8D-109 RELATIVE FOOTPRINT NOISE INDEX*

| Nacelle | RFNI (a) |
|---|---|
| JT8D-9 hardwall baseline | 1.000 |
| JT8D-109 configuration 1 | 0.161 |
| JT8D-109 configuration 2 | 0.147 |
| JT8D-109 configuration 3 | 0.044 |

[a]Based on 737-200 EPNL contours

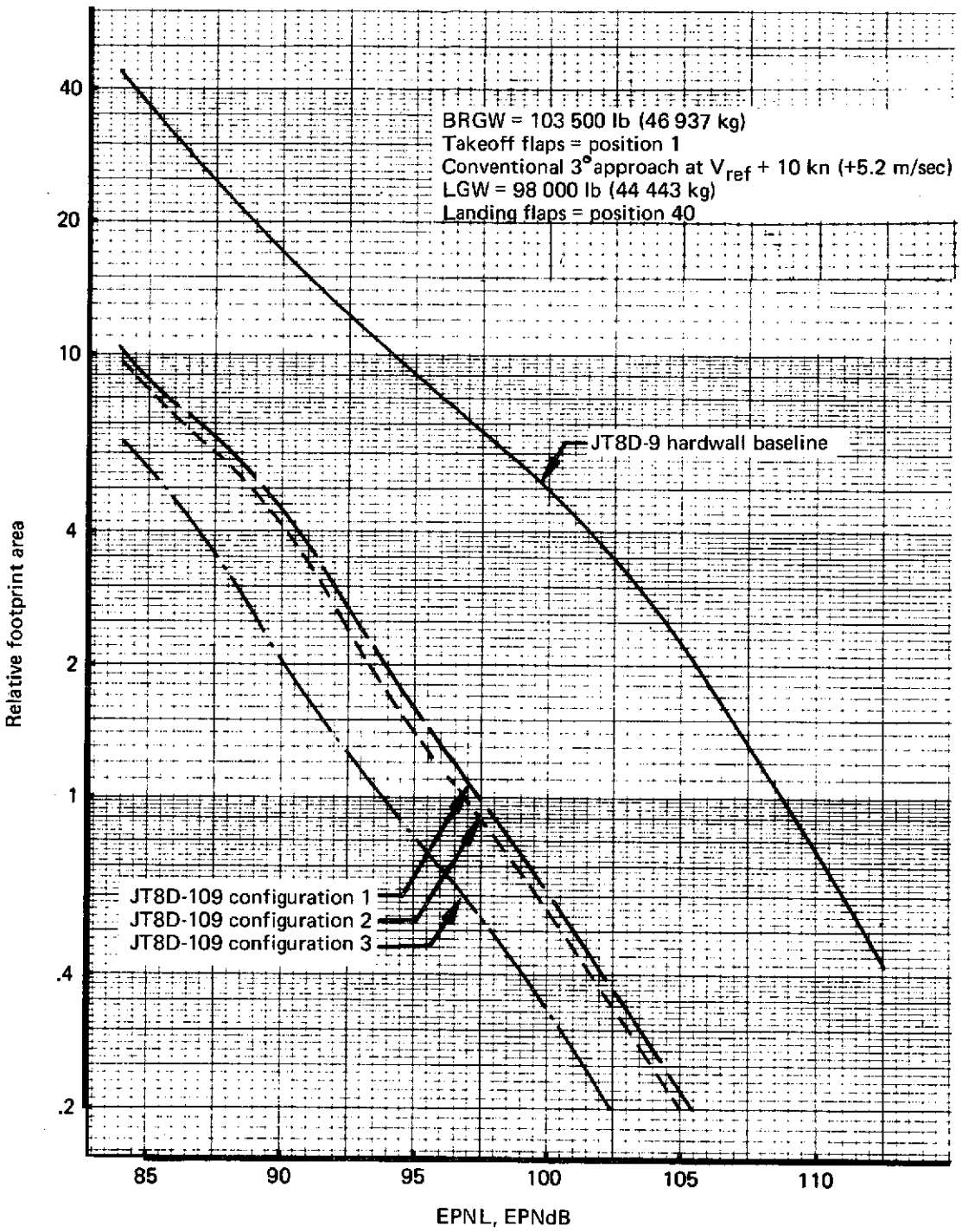


*FIGURE 147.–737/JT8D RELATIVE EPNL FOOTPRINT CONTOUR AREAS–FULL POWER OPERATIONAL PROFILE*

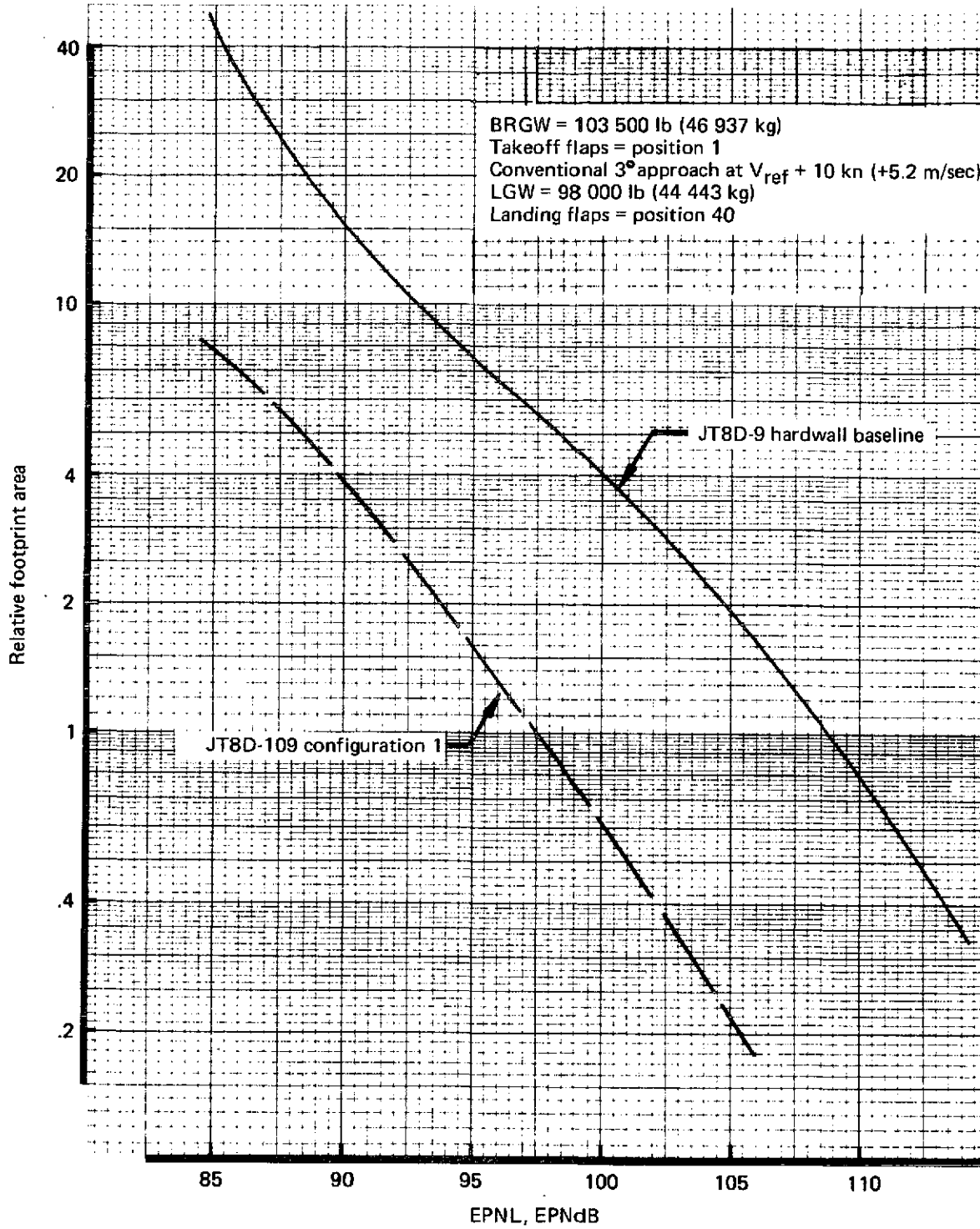


*FIGURE 148.—737/JT8D RELATIVE EPNL FOOTPRINT CONTOUR AREAS—CUTBACK CERTIFICATION PROFILE*

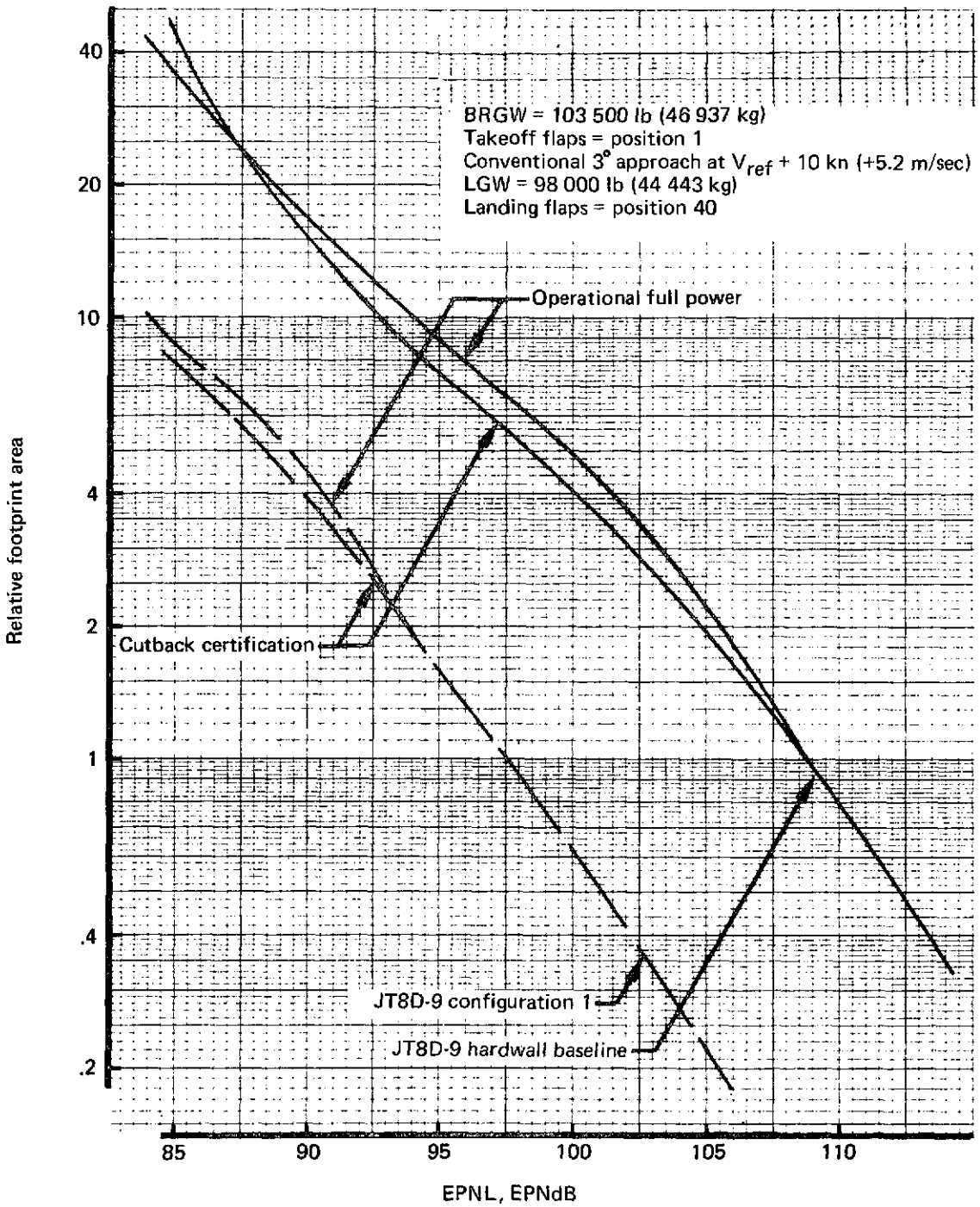


*FIGURE 149.—737/JT8D RELATIVE EPNL FOOTPRINT CONTOUR AREAS—TAKEOFF PROFILE COMPARISON*

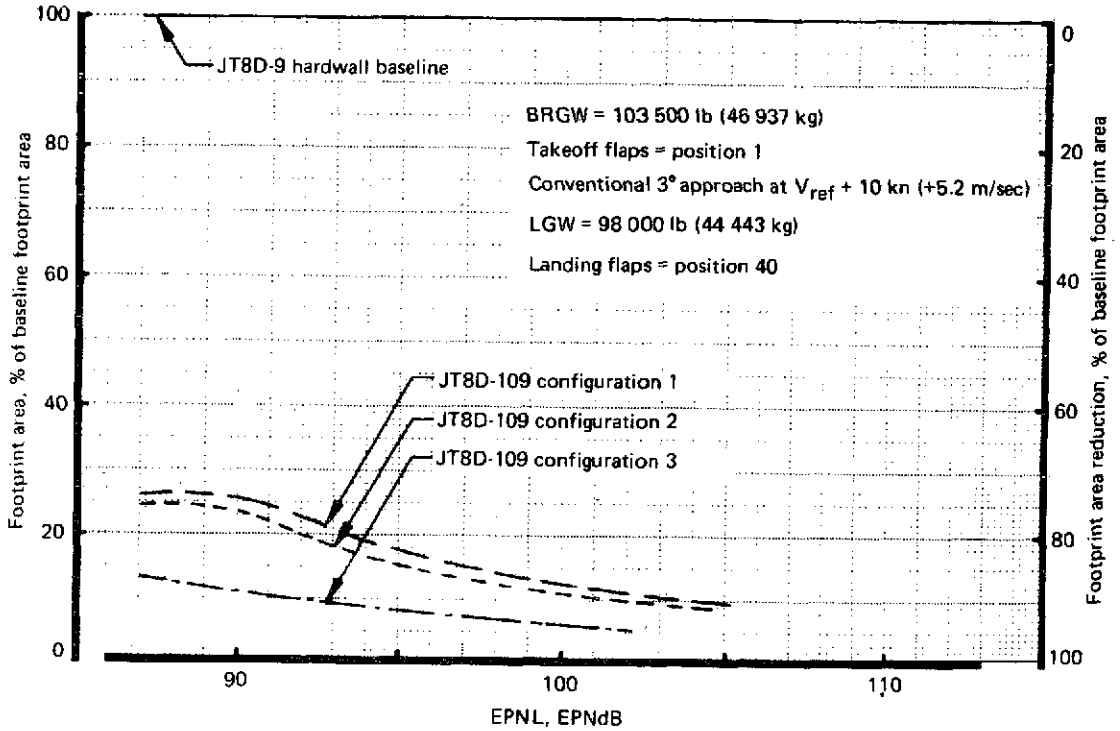


*FIGURE 150.–737/JT8D EPNL FOOTPRINT AREA REDUCTION–FULL POWER OPERATIONAL PROFILE*

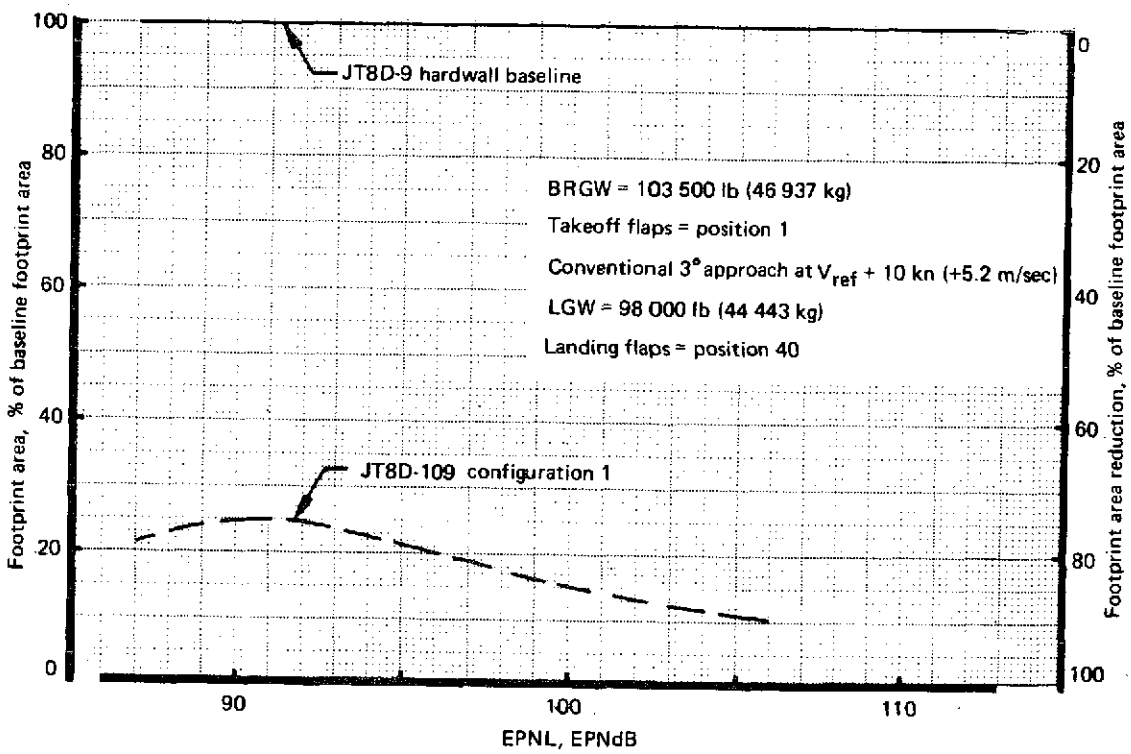


*FIGURE 151.–737/JT8D FOOTPRINT AREA REDUCTION–CUTBACK CERTIFICATION PROFILE*

# 6.0 ECONOMIC STUDIES

## 6.1 OBJECTIVES

The objective of the phase I refan program economic study was to analyze the cost consideration and noise reduction trades in the application of refanned JT3D and JT8D turbofan engines on their respective airplanes. The turbojet-powered 707/720 aircraft delivered early—representing about 20% of the domestic fleet of 707/720 aircraft—were not considered within the scope of this cost study.

In addition, one of the primary purposes of phase I of the refan program was to select the most likely refanned engine and nacelle configuration for further detailed design and analysis. This section presents results of studies centered around evaluating three nacelle configurations with different levels of treatment and evaluating these configurations in terms of noise reduction, performance impact on the airplane, and associated costs. Noise and performance data were based on the practical weight growth configurations defined in sections 3.0, 4.0, and 5.0.

This economic study is preliminary in nature, and, in the final analysis, detailed assessments must be made by each airline to determine the most cost-effective solution to meet Federal Aviation Regulations associated with community noise levels.

## 6.2 AIRPLANE/FLEET OPERATIONAL CHARACTERISTICS

This section defines the fleet size, mix, and operational characteristics that form the common baseline about which the study trades were conducted. Even though the contractor-produced fleet consists of many variants within each model series, it was possible to study only one currently delivered baseline model for each airplane.

Noise characteristics around airports can be categorized into two groups, depending upon whether the traffic is JT3D or JT8D engine dominated; hence, one short and one long runway were postulated as being representative for airport operations dominated by JT8D- and JT3D-powered aircraft, respectively. Fleet mix and operational characteristics were then based on historical data for a typical domestic short-haul airport served by 727, 737, and DC-9 aircraft and a coastal international airport served by 707 and DC-8 as well as 727, 737, and DC-9 airplanes. These typical airports reflect the nature of different classes of airports with all operations from one runway. Takeoffs and landings were assumed to occur in the same direction, and the takeoff and approach paths were straight. The airports were considered to be at sea level with an airport temperature of 77° F (298° K) and no wind.

A flight profile, assuming a full-power operational takeoff procedure, as shown in figure 152, was used. A single-segment, 3° approach path was used in all cases.

Typical standard-body fleet mixes for the domestic short-haul and coastal international airports were assumed. For the noise exposure forecast estimates, the modified fleet was based on JT8D-109-powered 727, 737, and DC-9 airplanes and refanned JT3D-9-powered 707 and DC-8 airplanes. The total fleet was considered to be modified to nacelle configuration 1 and the fleet mix was held constant for each airport. Takeoff gross weights were based on 100% and 55% load factors and sufficient mission fuel to fly typical routes from each of the two assumed airports. As a simplifying assumption, wide-body aircraft were not considered in the NEF estimates. Currently these wide-body aircraft comprise few operations, ranging from zero at some short- to medium-haul airports to less than 20% at some major hubs, and their noise signatures are small. It was assumed for this analysis that exclusion of the wide-body fleet would not invalidate the results.

The size of the JT3D/JT8D-powered fleet in operational inventory is constantly changing. New standard-body airplanes are being added, and older aircraft are being transferred among operators, leasing agents, and brokers. For this study, it was assumed that the size of the U.S. airline fleet of late 1972 would provide a representative base for modification cost assessment, while recognizing that foreign aircraft and future airplane deliveries could increase the modification quantity. Hence, the kit and modification costs (in 1973 dollars) were based on the fleet sizes of fan-powered aircraft shown in table 46.

*TABLE 46.—FAN-POWERED AIRCRAFT FLEET SIZES*

| Airplane | Quantity |
|---|---|
| 707-320B/C | 222 |
| 707-120B | 103 |
| 720B | 60 |
| Total 707 | 385 |
| 727-100 | 414 |
| 727-200 | 255 |
| Total 727 | 669 |
| 737-100 | 0 |
| 737-200 | 169 |
| Total 737 | 169 |
| Total all models | 1,223 |

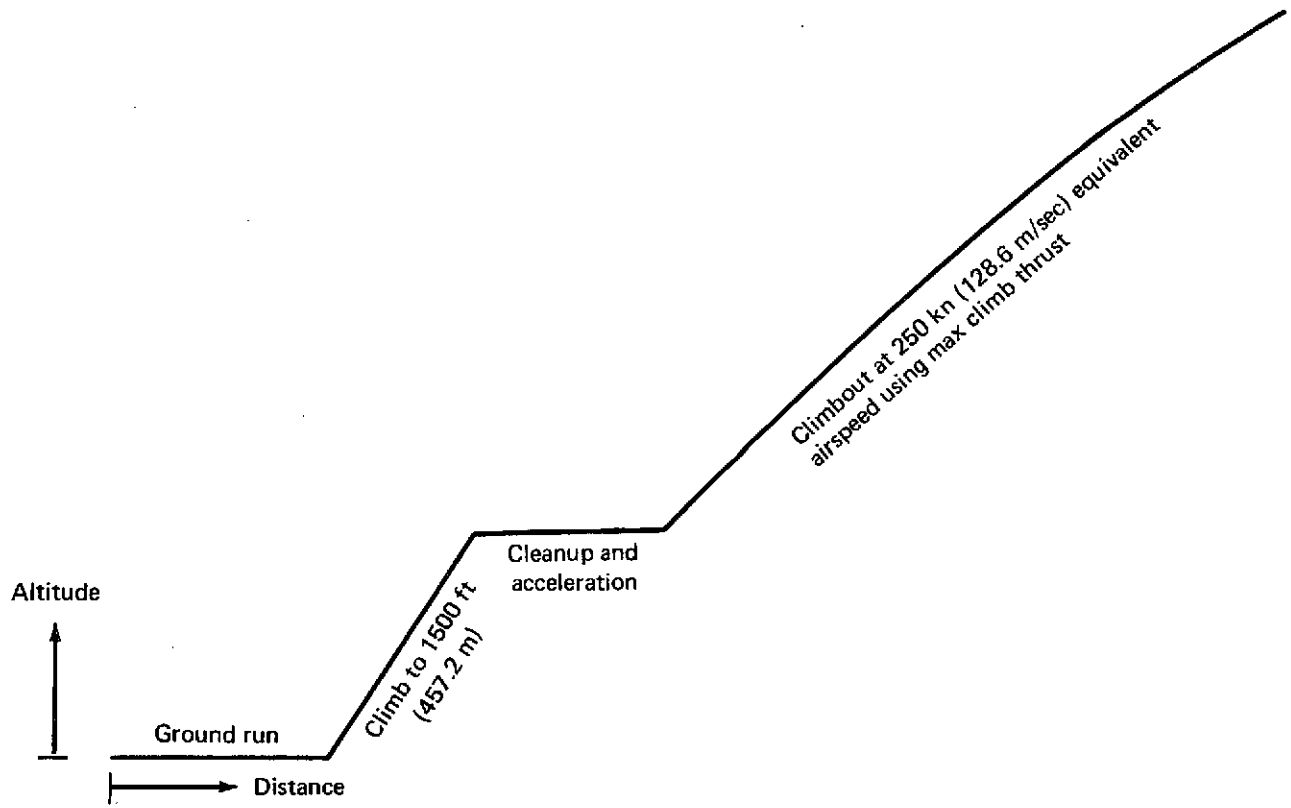


*FIGURE 152.—FULL-POWER OPERATIONAL TAKEOFF PROCEDURE*

Two modification cost trade cases for the 707- and 727-series of aircraft were established. The first case was for the total fleet, modified to configuration 1 (or 1A) for the 707. The second case was for the older aircraft (707-120B, 720B, and 727-100), modified to configuration 1 (or 1A) and the younger aircraft (707-320B and 727-200), modified to either configuration 2 or configuration 3. In both examples, the total fleet of 385 aircraft in the 707 series and 669 aircraft in the 727 series were considered to be modified. The total 737-200 fleet of 169 aircraft was considered modified to either configuration 1, 2, or 3.

## 6.3 OPERATING COSTS

Direct operating costs for the baseline airplanes were determined from a modified version of the 1967 ATA direct operating cost formula. The modification reflects service experience through 1971. The ATA DOC equations were developed statistically from composite airline operations data and are useful in comparing airplane configurations to the same performance rules by a standardized technique. The costs developed by the equations are statistical averages and parametric rather than absolute; therefore, they do not necessarily represent a specific airline's operational costs. However, for purposes of nacelle configuration comparisons, the cost differences established from these equations are valid.

When the 707, 727, and 737 aircraft have been equipped with refanned engines, there will be a modest OEW growth in relation to the baseline aircraft, however, the performance of the refanned engines will permit gross weight growth. Associated performance improvements for the modified configurations could in some models provide a capability for exceeding basic airplane performance. The resulting airplane performance is shown in sections 3.7, 4.7, and 5.7.

For this study, the direct cash items that changed were identified as fuel, insurance, and engine and nacelle maintenance. Crew pay could show changes on alternatives with increases in maximum gross weight of the aircraft. Changes in fuel expense were due to block fuel changes resulting from the change in performance. Insurance expense changes were the direct result of an increase in the value of the aircraft resulting from the additional cost of modification. Identifiable maintenance expense changes reflected only those changes resulting from the engine modifications and new nacelles, as established by maintainability analysis and as opposed to using the modified ATA parametric equations of the modified-configuration designs. Nacelle maintenance was included with airframe maintenance according to ATA categories.

Incremental trip cost elements, based on analysis of the preliminary modified nacelle configurations, are shown in tables 47, 48, and 49. The changes are shown in dollars and percent increase of each element relative to the corresponding baseline value. The cash items affected by airplane performance reflect small changes, primarily in fuel consumed. The principal cash changes were due to insurance.

## 6.4 FLEET MODIFICATION COSTS

### 6.4.1 Kit and Installation Costs

Airplane kit and installation cost estimates were based on preliminary definitions of the subject configurations and are subject to change. A Government surcharge was included for research and development cost payback to the limit of Government involvement. No credit was allowed for replaced parts. Modification program cost, expressed in 1973 dollars, was assumed to be expended over a 3-year period. No cost impact was included for gross weight increases proposed to achieve the quoted performance improvements; however, many of the airplanes in service are currently certified to cover the weights presented.

Refan program cost estimates were based on all available contractor engineering work statement information plus documented cost for engine modification kits supplied by Pratt & Whitney Aircraft. Similar work on related programs, such as the FAA quiet nacelle, was considered in preparation of the cost estimates.

Nacelle kit costs included airplane parts and assemblies, associated with the refanned engines, which could be installed by the operator or by a modification contractor. Struts, nacelles, thrust reversers, engine buildup, airplane changes, and a distribution of the cost of flight testing were included. Airplane changes included items such as wing attachment points for the 707, the center-engine duct and firewall changes for the 727, and landing gear and flap changes for the 737.

All pertinent modification kit nonrecurring and recurring costs were included, based on modifying 385 model 707s, 669 model 727s, and 169 model 737s, using a learning curve in accordance with commercial practices. Due to the commonality of many modification components within the model family, such as the 727 (414 model 727-100s and 255 model 727-200s), kit costs for each 707/727 model cannot be evaluated separately. Learning curves were based on cumulative quantities of 255, 414, and 669, depending on the item. Therefore, in the case of the 727 example, the cumulative program value for 669 applicable kit configurations must be totaled before calculating the average shipset cost. This requirement does not apply to the 737 because there are

## TABLE 47.—707-320B MODIFIED AIRPLANE TRIP COST COMPARISON 1515 NMI (2805 KM)[a]

| Direct cash items | Basic airplane trip costs | Configuration | | | | | | | |
|---|---|---|---|---|---|---|---|---|---|
| | | 1 | | 1A | | 2 | | 3 | |
| | | Δ $ | Δ % | Δ $ | Δ % | Δ $ | Δ % | Δ $ | Δ % |
| Crew pay | 892.41 | 0 | 0 | 0 | 0 | 0 | 0 | 0 | 0 |
| Fuel | 681.45 | -4.50 | -0.66 | 0 | 0 | -2.66 | -0.39 | -2.66 | -0.39 |
| Maintenance | | | | | | | | | |
| Airframe | 257.16 | -2.42 | -0.94 | -2.42 | -0.94 | -2.42 | -0.94 | -2.42 | -0.94 |
| Engine | 182.46 | -4.39 | -2.40 | -4.39 | -2.40 | -2.56 | -1.40 | -2.01 | -1.10 |
| Burden | 447.68 | -6.82 | -1.52 | -6.82 | -1.52 | -5.50 | -1.22 | -4.98 | -1.11 |
| Insurance | 92.72 | 14.37 | 15.49 | 14.63 | 15.77 | 20.56 | 22.17 | 20.69 | 22.31 |
| Total | 2553.88 | -3.76 | -0.14 | 1.00 | 0.03 | 7.42 | 0.29 | 8.62 | 0.33 |

[a]Average range based on CAB 1970 data

Note: Airframe maintenance includes nacelle

## TABLE 48.—727-200 MODIFIED AIRPLANE TRIP COST COMPARISON 473 NMI (876 KM)[a]

| Direct cash items | Basic airplane trip costs | Configuration | | | | | |
|---|---|---|---|---|---|---|---|
| | | 1 | | 2 | | 3 | |
| | | Δ $ | Δ % | Δ $ | Δ % | Δ $ | Δ % |
| Crew pay | 255.75 | 0 | 0 | 0 | 0 | 0 | 0 |
| Fuel | 254.28 | 6.78 | 2.66 | 10.97 | 4.31 | 7.58 | 2.98 |
| Maintenance | | | | | | | |
| Airframe | 77.83 | 0 | 0 | 0 | 0 | 0 | 0 |
| Engine | 49.06 | 0.08 | 0.16 | 0.13 | 0.26 | 0.17 | 0.34 |
| Burden | 123.44 | 0 | 0 | 0.14 | 0.11 | 0.25 | 0.20 |
| Insurance | 33.30 | 7.28 | 21.86 | 7.75 | 23.27 | 7.95 | 23.87 |
| Total | 793.68 | 14.12 | 1.77 | 18.69 | 2.35 | 15.43 | 1.94 |

[a]Average range based on CAB 1970 data

Note: Airframe maintenance includes nacelle

## TABLE 49.—737-200 MODIFIED AIRPLANE TRIP COST COMPARISON 228 NMI (422 KM)[a]

| Direct cash items | Basic airplane trip costs | Configuration | | | | | |
|---|---|---|---|---|---|---|---|
| | | 1 | | 2 | | 3 | |
| | | Δ $ | Δ % | Δ $ | Δ % | Δ $ | Δ % |
| Crew pay | 108.72 | 0 | 0 | 0 | 0 | 0 | 0 |
| Fuel | 107.24 | 0.67 | 0.62 | 4.33 | 4.03 | 2.54 | 2.36 |
| Maintenance | | | | | | | |
| Airframe | 44.04 | 0 | 0 | 0 | 0 | 0 | 0 |
| Engine | 22.40 | 0.06 | 0.26 | 0.22 | 0.98 | 0.41 | 1.83 |
| Burden | 65.69 | 0 | 0 | 0.09 | 0.13 | 0.31 | 0.47 |
| Insurance | 16.80 | 4.65 | 27.67 | 4.78 | 28.45 | 5.03 | 29.94 |
| Total | 364.89 | 5.38 | 1.47 | 9.42 | 2.58 | 8.29 | 2.27 |

[a]Average range based on CAB 1970 data

Note: Airframe maintenance includes nacelle

no 737-100s in the domestic fleet of 169 airplanes. It is believed that up to 50% of the foreign fleet will be candidates for such kits; therefore, it may be possible to spread the nonrecurring costs over a larger base than noted above.

Kit installation costs included labor and overhead for an assumed single modification facility. The total program quantities of 385 model 707s, 669 model 727s, and 169 model 737s were assumed to be completed over a 3-year period. The establishment of a master phasing plan was not within the scope of the phase I program. Therefore, only preliminary installation flow times were established assuming that the modification would be made at a single central facility. Average flow times for installation of the modification kits for production methods of performing the installation were estimated as follows:

| | |
|---|---|
| 707 | 16 days |
| 727 | 21 days |
| 737 | 18 days |

The flow times are working days from receipt of the airplane at a constant rate commensurate with an efficient modification cycle, to acceptance by the customer after modification, based on a 5-day week, two-shift operation. The modification kit and installation costs are shown in tables 50, 51, and 52.

Out-of-service costs are dependent on individual airline operational flexibility and would vary greatly between airlines. For reference, typical estimates, based on dry lease costs, are as follows:

| Model | $/Day |
|---|---|
| 707-320C | $3,333 |
| 727-100 | 2,100 |
| 737-200 | 1,666 |

### 6.4.2 Spares Cost

Spares provisioning philosophy and requirements vary greatly among airlines. Generally, the smaller the airline, the greater the spares provisioning. Foreign airlines, relative to the U.S. airlines, maintain a higher percentage of spares. Since spares allocations for the refanned engines and quiet nacelles would be established by each individual airline, only typical estimates were established in this study.

*TABLE 50.—707 MODIFICATION COSTS 385-AIRPLANE QUANTITY (THOUSANDS OF DOLLARS PER SHIPSET)*

| Item | Configuration | | | | | |
|---|---|---|---|---|---|---|
| | 1 | 1A | [a]1 | [a]1A | [a]2 | [a]3 |
| | Model dash numbers | | | | | |
| | 120B 720B 320B | 120B 720B 320B | 120B 720B | 120B 720B | 320B | 320B |
| | Airplane quantity | | | | | |
| | 385 | 385 | 163 | 163 | 222 | 222 |
| | Thousands of dollars per shipset | | | | | |
| Strut | 105 | 105 | 105 | 105 | 105 | 105 |
| Nacelle | 361 | 389 | 388 | 439 | 722 | 737 |
| Thrust reverser | 131 | 131 | 146 | 146 | 409 | 409 |
| Engine buildup | 59 | 59 | 67 | 67 | 70 | 70 |
| Airplane changes | 21 | 21 | 21 | 21 | 21 | 21 |
| Flight test | 17 | 21 | 17 | 25 | 23 | 23 |
| Total nacelle kit | 694 | 726 | 744 | 803 | 1350 | 1365 |
| Engine kit | 800 | 800 | 800 | 800 | 800 | 800 |
| Total nacelle and engine kit | 1494 | 1526 | 1544 | 1603 | 2150 | 2165 |
| Nacelle kit installation | 50 | 50 | 50 | 50 | 50 | 50 |
| Engine kit installation | 5 | 5 | 5 | 5 | 5 | 5 |
| Total nacelle and engine kit installation | 55 | 55 | 55 | 55 | 55 | 55 |
| Total cost per airplane | 1549 | 1581 | 1599 | 1658 | 2205 | 2220 |

[a]Modification consists of configuration 1 or 1A plus either configuration 2 or 3 option.

Estimates of the cost for spares to support the modified aircraft were based on the configuration definitions provided in sections 3.0, 4.0, and 5.0. In determining spares costs for modifying spare engines and QEC kits, it was assumed that only the number of each engine required to support the 707/727/737 fleets of the U.S. airlines under current maintenance and overhaul intervals would be modified. The estimated spares costs are presented in table 53.

## 6.5 NOISE COMPARISONS

The community noise comparisons at the FAR Part 36 conditions for the 707-320B/C, 727-200, and 737-200 airplanes are presented in sections 3.8, 4.8, and 5.8. Further comparisons of the modified-airplane community noise impact are included here. The unit of measure used in this section is the noise exposure forecast (NEF) area at an NEF value of 30.

*TABLE 51.–727 MODIFICATION COSTS 669-AIRPLANE QUANTITY (IN THOUSANDS OF DOLLARS/SHIPSET)*

| Item | Configuration | | | |
|---|---|---|---|---|
| | 1 | 1[a] | 2 | 3 |
| | Model dash nos. | | | |
| | 100<br>200 | 100 | 200 | 200 |
| | Airplane quantity | | | |
| | 669 | 414 | 255 | 255 |
| | Thousands of dollars per shipset | | | |
| Strut | 19 | 19 | 19 | 19 |
| Nacelle | 280 | 315 | 379 | 424 |
| Thrust reverser | 174 | 174 | 174 | 174 |
| Engine buildup | 77 | 77 | 77 | 77 |
| Airplane changes | 244 | 244 | 244 | 244 |
| Flight test | 8 | 6 | 15 | 15 |
| Total nacelle kit | 802 | 835 | 908 | 953 |
| Engine kit[b] | 750 | 750 | 750 | 750 |
| Total nacelle and engine kit | 1552 | 1585 | 1658 | 1703 |
| Nacelle kit installation | 78 | 78 | 78 | 78 |
| Engine kit installation | 4 | 4 | 4 | 4 |
| Total nacelle and engine kit installation | 82 | 82 | 82 | 82 |
| Total cost per airplane | 1634 | 1667 | 1740 | 1785 |

[a]Modification consists of configuration 1 plus either configuration 2 or 3 option.

[b]With new intermediate case assembly, otherwise engine kit cost is $645,000.

The NEF area is similar to a single-event footprint EPNL area, except that it reflects the accumulation of the noise from a mix of airplanes over a 24-hr period. The NEF footprint areas were based on the following assumptions:

- A single short runway typifying a U.S. domestic airport
- A single long runway typifying an international airport
- Current standard-body, peak-day jet transport operations
- Takeoff gross weight (flight profile) variations representative of mission requirements
- Aircraft payload based on 100% and 55% load factors.

*TABLE 52.–737 MODIFICATION COSTS 169-AIRPLANE QUANTITY (IN THOUSANDS OF DOLLARS/SHIPSET)*

| Item | Configuration | | |
|---|---|---|---|
| | 1 | 2 | 3 |
| | Model dash nos. | | |
| | 200 | 200 | 200 |
| | Airplane quantity | | |
| | 169 | 169 | 169 |
| | Thousands of dollars per shipset | | |
| Strut | 32 | 32 | 32 |
| Nacelle | 197 | 237 | 311 |
| Thrust reverser | 121 | 121 | 121 |
| Engine buildup | 77 | 77 | 77 |
| Airplane changes | 396 | 396 | 396 |
| Flight test | 23 | 23 | 23 |
| Total nacelle kit | 846 | 886 | 960 |
| Engine kit[a] | 500 | 500 | 500 |
| Total nacelle and engine kit | 1346 | 1386 | 1460 |
| Nacelle kit installation | 63 | 63 | 63 |
| Engine kit installation | 3 | 3 | 3 |
| Total nacelle and engine kit installation | 66 | 66 | 66 |
| Total cost per airplane | 1412 | 1452 | 1526 |

[a]With new intermediate case assembly, otherwise engine kit cost is $430,000.

*TABLE 53.–ESTIMATED SPARES COST (THOUSANDS OF DOLLARS PER AIRPLANE)*

| Airplane | Spares item | Configuration | | | |
|---|---|---|---|---|---|
| | | 1 | 1A | 2 | 3 |
| 707 | Nacelle kit | 58 | 60 | 130 | 131 |
| | Engine kit | 136 | 136 | 136 | 136 |
| | Total | 194 | 196 | 266 | 267 |
| 727 | Nacelle kit | 80 | | 83 | 86 |
| | Engine kit | 135 | | 135 | 135 |
| | Total | 215 | | 218 | 221 |
| 737 | Nacelle kit | 87 | | 90 | 97 |
| | Engine kit | 115 | | 115 | 115 |
| | Total | 202 | | 205 | 212 |

Figure 153 presents the NEF 30 relative areas around a domestic, short-haul airport for each aircraft model and for the total aircraft mix. The area reduction attributed to configuration 1 replacing the baseline airplanes for the total fleet is about 75%. Larger area reductions for other model aircraft exist; however, the total NEF 30 area was dominated by the 727 aircraft. As noted, the effects of load factor are minimized.

Figure 154 presents the NEF 30 relative areas around a coastal international airport for each aircraft model and for the total aircraft mix. The area reduction attributed to configuration 1 for the total fleet is about 80%. Here, however, the 707 and DC-8 models dominated. The results were again insensitive to load factor.

Configurations 2 and 3 would be expected to provide further NEF contour reduction.

## 6.6 MARKET CHARACTERISTICS

As a result of the introduction of jet-powered aircraft, which offered significant improvements in speed, ride comfort, operating economics, and cruise altitude, the airlines experienced very significant passenger traffic growth. Large capital investments in jet-powered equipment were made. Recently, the airline industry has recovered from the lowest traffic growth rates in its history; consequently, the depressed profits are showing a sluggish recovery, as indicated by tables 54 and 55. Premature retirement or major modification of 707/DC-8/727/737/DC-9 aircraft, due to noise legislation, would be financially disastrous, because of the magnitude of the capital investment required, unless a scheme for financial assistance was developed. This scheme could include such possibilities as:

- Guaranteed loan
- Government subsidy
- Passenger or ticket tax
- A combination of the above.

One possible scheme proposed as an equitable solution to financing would be to set up a Government-administered trust fund to be paid back by passenger (and cargo) ticket taxes. It has also been proposed that any additional ticket taxes to finance refan program capital expenditures should be applied through the Government trust fund taxes currently on the tickets.

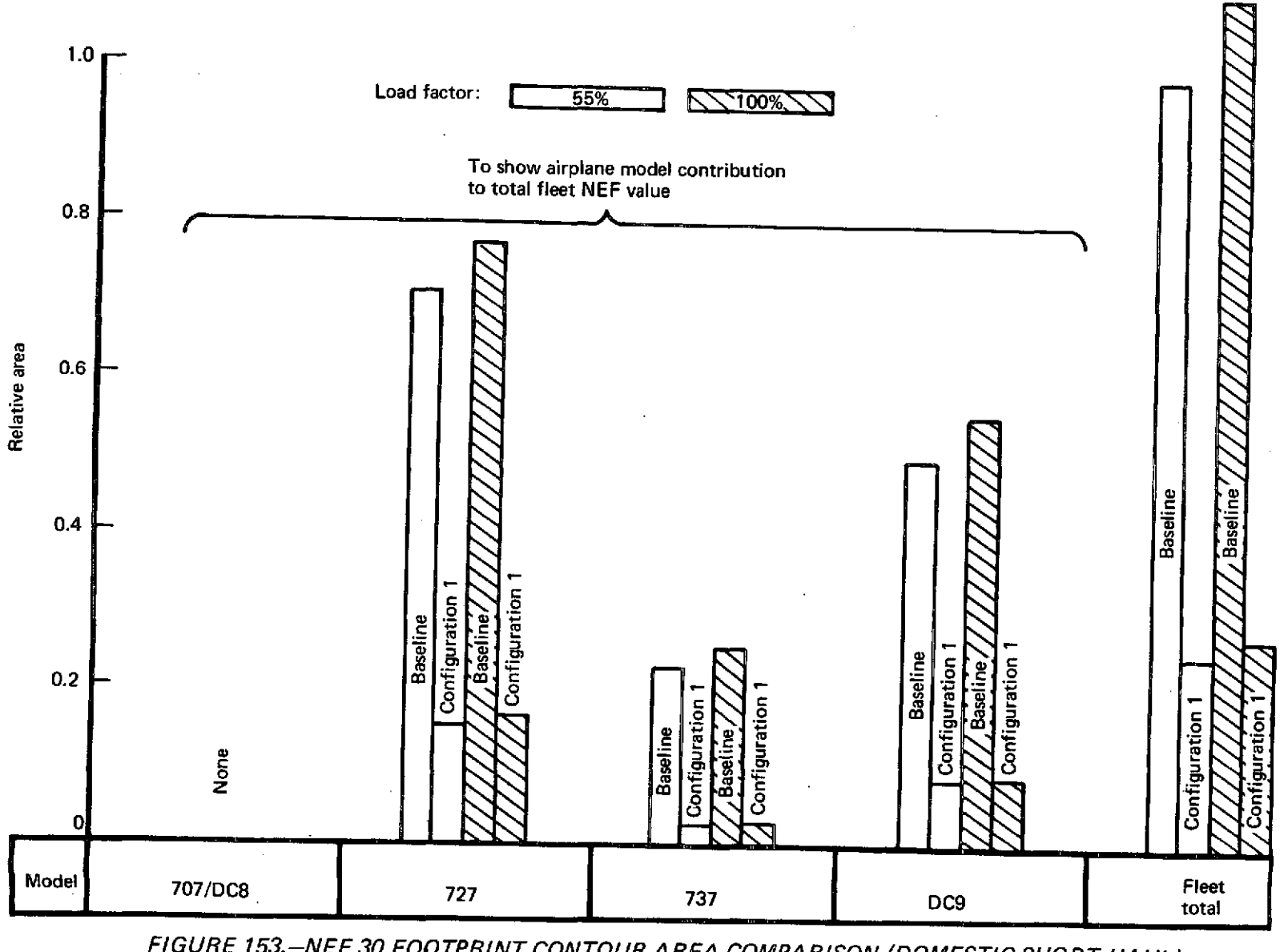


*FIGURE 153.—NEF 30 FOOTPRINT CONTOUR AREA COMPARISON (DOMESTIC SHORT HAUL)—*

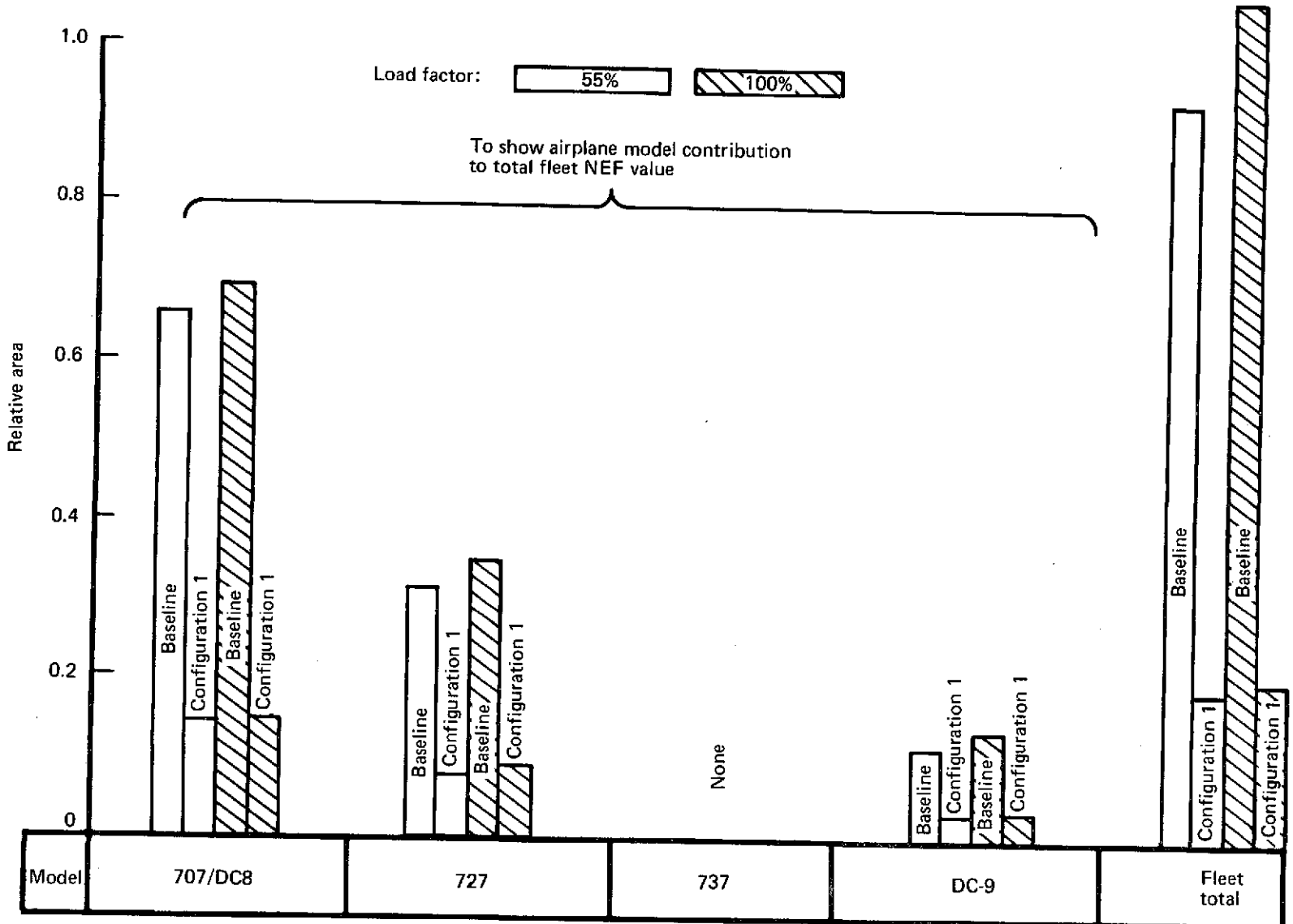


*FIGURE 154.–NEF 30 FOOTPRINT CONTOUR AREA COMPARISON (INTERNATIONAL)–FULL POWER OPERATIONAL TAKEOFF PROFILE, STANDARD BODY FLEET MIX*

*TABLE 54.–NET EARNINGS AFTER TAX*[a]

| Year | 1968 | 1969 | 1970 | 1971 | 1972 |
|---|---|---|---|---|---|
| Earnings, millions of dollars | 262 | 152 | –103 | 38 | 189 |

[a]U.S. trunks and Pan American Airways–all services

*TABLE 55.–ANNUAL REVENUE PASSENGER MILE GROWTH RATES*[a]

| Year | 1968 | 1969 | 1970 | 1971 | 1972 |
|---|---|---|---|---|---|
| Growth rate, % | 13.8 | 9.2 | 2.9 | 1.3 | 10.9 |

[a]U.S. trunks and Pan American Airways–all services

The 707 and 727 aircraft have demonstrated that they can satisfy existing markets and future markets, as evidenced by the resurgence of 707 and 727-200 sales in the last 18 months. As a result of route proliferation, point-to-point service expansion, extensive market competition, and expanding frequency demand, a continuing need for the standard-body aircraft is predicted.

Figures 155, 156, and 157 indicate the fleet age and a minimum projected 20-year use of the world airline fleets of 707, 727, and 737 airplanes. The assumed use of at least 20 years was based on a utilization rate of 3000 hr per year and a design life of 60 000 hr. The 20-year example is used solely for purposes of this study and is not intended as a structural life forecast. Airline retirement schedules and forecasts are beyond the scope of this study. Additional sales beyond those presented indicate that many standard-body aircraft would be in service during the 1990-2000 time period.

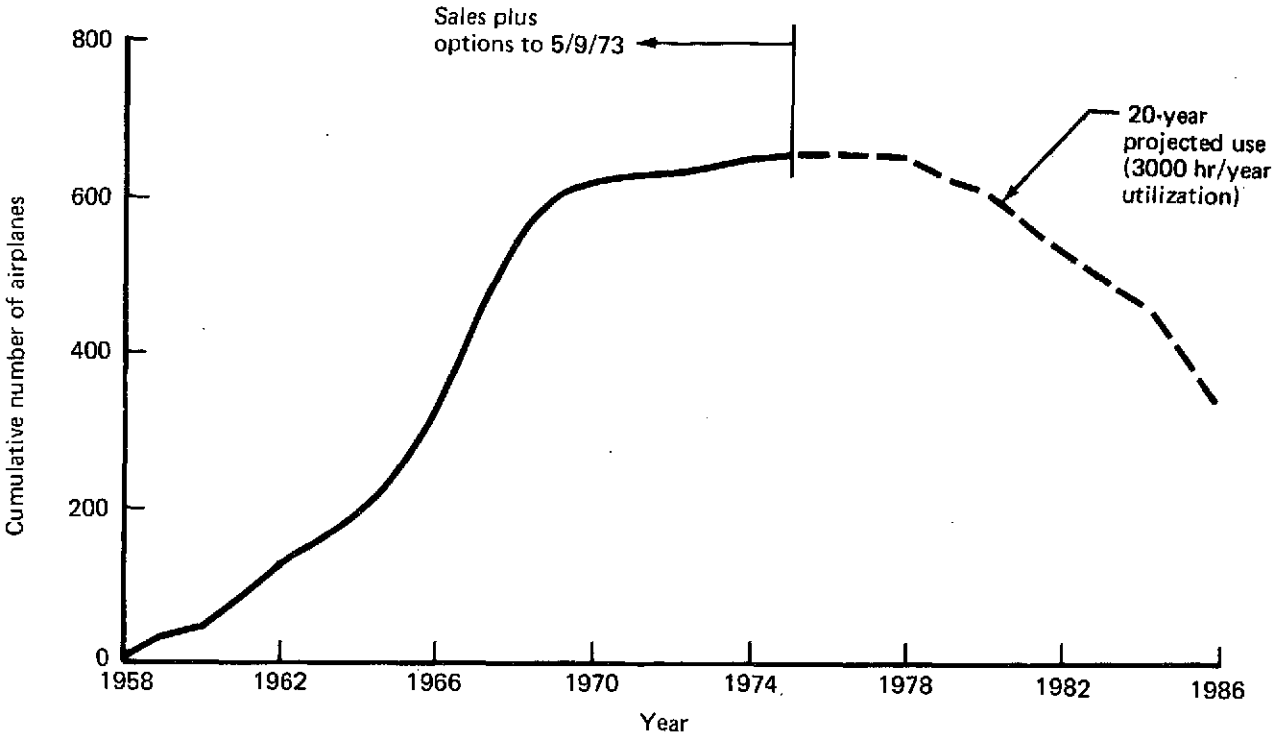


*FIGURE 155.–PROJECTED USE OF 707 CURRENT WORLD FLEET*

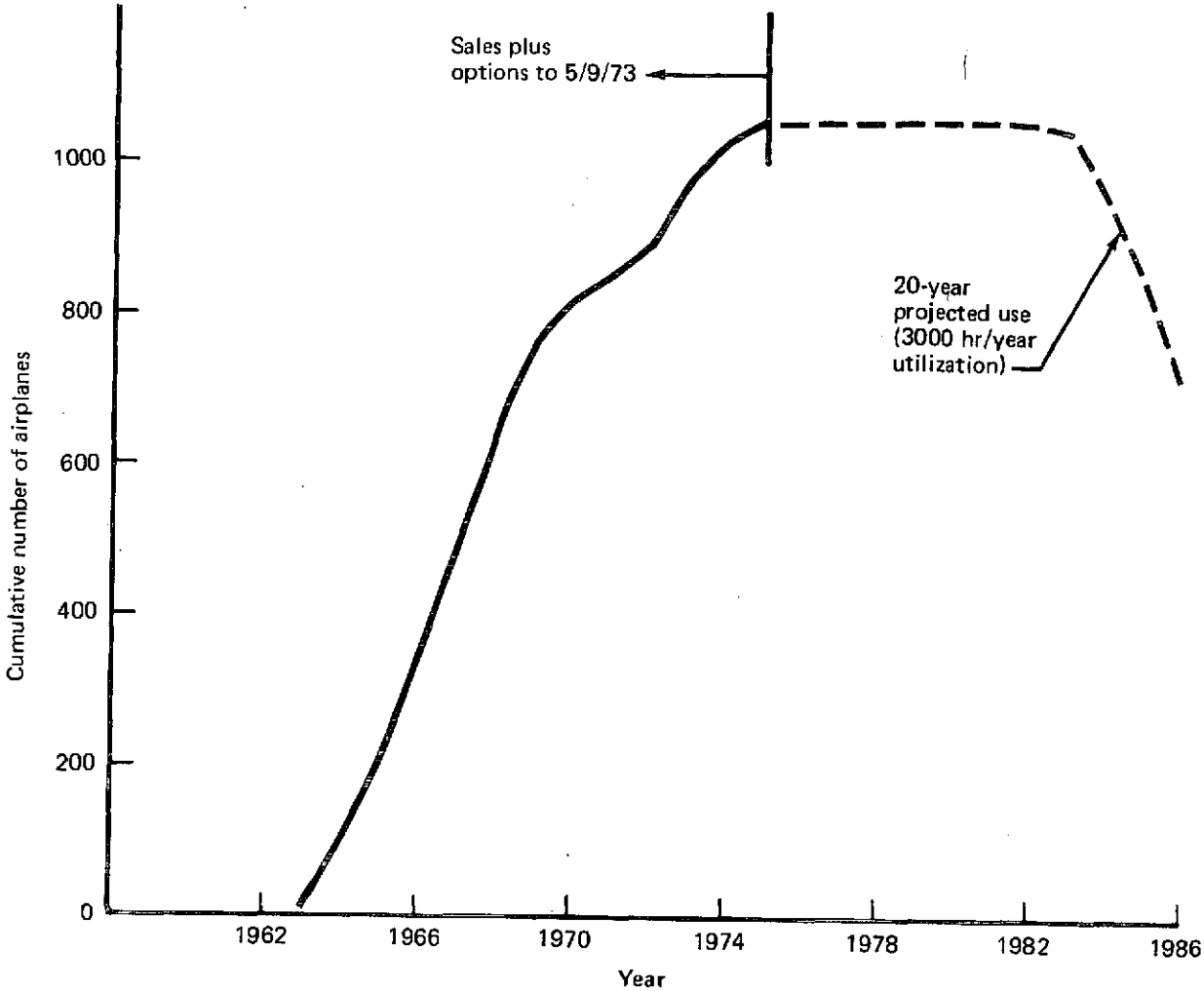


*FIGURE 156.–PROJECTED USE OF 727 CURRENT WORLD FLEET*

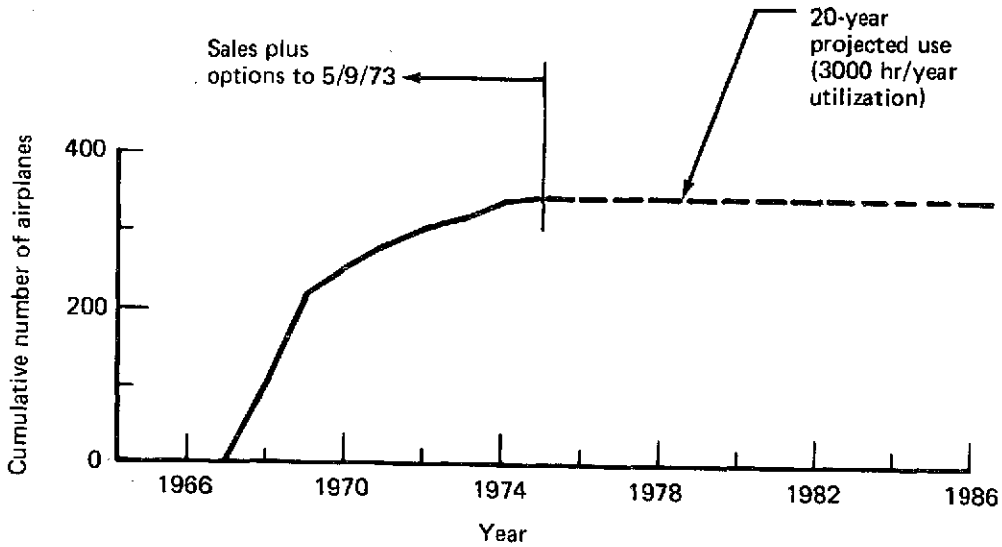


*FIGURE 157.–PROJECTED USE OF 737 CURRENT WORLD FLEET*

# 7.0 SUMMARY OF RESULTS AND CONCLUSIONS

This phase I of the refan program covered investigation of two different engine series as installed in three airplane series built by this contractor. Accordingly, no single result or conclusion can be reached. It is possible, however, from the work completed to date, to reach the general conclusion that the refan concept is technically feasible as well as economically practical and that development of the concept should be continued. Specific results and conclusions pertaining to the individual airplane series will be found in the subsequent subsections.

## 7.1 707 AIRPLANE

It was determined by model testing that flutter characteristics of all models of 707 airplanes with JT3D modified nacelles would be satisfactory with a suitable choice of nacelle frequencies and streamwise location of outboard nacelles.

The nacelle configuration considered most attractive for further development would be configuration 1A. This configuration would have a treated inlet with one treated splitter-ring, a treated short-fan duct, a new simplified cascade-type fan thrust reverser, and a modified primary thrust reverser. The inlet would be translatable forward on tracks to provide clearance at the engine front flange for ground maintenance.

Configuration 1A noise level reduction at FAR Part 36 conditions is predicted to be up to 13 EPNdB (sideline) and up to 20 EPNdB (takeoff-cutback) if engine noise sources are as predicted.

707-320B aircraft modified with configuration 1A and no increase in BRGW would show a range loss of 1.3%. The same airplane with a BRGW increase of 1.35% would have a range increase of 0.8%.

It was found that the JT3D refanned engines could be installed on 707 series airplanes with no problems which cannot be solved by normal design practices.

## 7.2 727 AIRPLANE

Exploratory model testing of a new larger center duct and inlet indicated that compatibility between the center duct and engine will be obtainable and that vortex generators will be necessary.

The required airflow was achieved with acceptable pressure recovery. Angles of attack within the 727 operating regime (-15° to +5°) had little effect on center-duct inlet pressure recovery and distortion.

Nacelle configurations 1 and 2 were found to be candidates for further development. Configuration 1 would have a treated inlet and treated tail pipe; configuration 2 would have a treated inlet with one treated ring and a treated tail pipe with a treated fan-primary splitter-ring. Both configurations would have target-type thrust reversers.

The additional weight of the modified propulsion installation will pose problems in airplane balance and ground handling requirements. Possible methods for alleviation of the problem include: (1) fixed ballast installed on the radome bulkhead, (2) selective loading of passengers and baggage, and (3) airplane configuration change to move weight forward. Other methods have been considered that are basically variations of the above. Case by case analysis of the requirements of each airline will be required to determine the most cost effective solution for that airline's routes.

Based on fan and exhaust jet noise only, noise reductions of configurations 1 and 2 at FAR Part 36 conditions are predicted to be up to 8 EPNdB (takeoff-cutback) and 13 EPNdB (approach) if the engine noise sources are as predicted. Low frequency noise from sources inside the engine are a matter of concern.

The 727-200 aircraft modified with configuration 2 and with no increase in BRGW would show a range loss of 21.4%, although the same airplane with a BRGW increase of 5.8% would show a range increase of 9.2%. Presently certified airplane modifications allow the airplane BRGW to increase this 5.8% [from 172 500 lb (78 245 kg) to 182 500 lb (82 781 kg)], which would permit recovery of range performance for those airlines for which this is necessary. These modifications are available at a relatively small cost. Other 727 models will require additional analysis to determine range-recovery options.

## 7.3 737 AIRPLANE

Installation of refanned JT8D engines on 737 airplanes would require installation of a new 12 in. (0.305 m) longer landing gear to maintain ground clearance. For stowage, this gear would have to be reduced in length during retraction. This gear configuration was defined only in preliminary layouts.

The same configurations (1 and 2) chosen for the 727 would be considered for the 737 airplane. The 737 configurations would be different in that the inlet would be drooped and an extension would be installed in the tailpipe.

Based on fan and exhaust noise only, noise reductions of configurations 1 and 2 at FAR Part 36 conditions are predicted to be up to 8 EPNdB (approach) and up to 12 EPNdB (takeoff) if the engine noise sources are as predicted. Low frequency noise from sources inside the engine are a matter of concern.

The 737-200 aircraft modified with configuration 2 and with no increase in BRGW would show a range loss of 34.2%, although the same airplane with a BRGW increase of 4.5% would show a range increase of 12.1%. Many of the 737-200 airplanes have the structural capability for this 4.5% BRGW increase [from 103 500 lb (46 948 kg) to 109 000 lb (49 442 kg)] which would permit recovery of range performance by the operator if desired. A kit is available for those airplanes not presently equipped with this structural capability. Other 737 models will require additional analysis to determine range-recovery options.

## 7.4 NOISE

The noise benefits that may be derived from the refanned engine and modified nacelle concept were found to be extensive. Noise Exposure Forecast (NEF 30) footprint contours for configuration 1 would be reduced by 75% for a domestic airport and by 80% for an international airport based on standard-body current fleet mix and single runway operation.

## 7.5 ECONOMICS

The 707, 727, and 737 fleets are relatively young and have the potential of being in commercial service for at least 20 years, based on a projected use of 60 000 to 70 000 flight-hours.

Airplane and engine modification costs were projected at $1.5 to $2.2 million for the 707 series, depending upon the model; approximately $1.6 to $1.8 million for the 727 series; and approximately $1.4 to $1.5 million for the 737 series. Estimates of the cash (out-of-pocket) direct operating costs at representative average airplane range were less than a 2.5% increase in DOC over the baseline airplanes. Total refanned engine/airplane costs, if amortized over the remaining depreciation period of an in-service aircraft, would represent a disproportionate increase in the direct operating cost of the aircraft. It becomes obvious that the cost of the refanned engine and airplane modification could not be expected to come out of normal airline profits. Other means of financing would have to be developed and include such possibilities as:

- Guaranteed loan
- Government subsidy
- Passenger or ticket tax
- A combination of the above.

# APPENDIX A

## REFERENCES

1. Mechtly, E.A. *The International System of Units–Physical Constants and Conversion Factors*, NASA SP-7012, (revised 1969).

# APPENDIX B

## DEFINITIONS

| | |
|---|---|
| Accessories | Components necessary for engine and airplane systems operation (i.e., starter, filters, fuel heaters, etc.) |
| Baseline Airplanes | Model 707-320B standard airplane—Brake release weight of 333 600 lb (151 321 kg); powered by Pratt & Whitney Aircraft JT3D-3B engines with 17 000 lb (75 616 N) thrust and no acoustic treatment.<br><br>Model 727-200 standard airplane—Brake release weight of 172 500 lb (78 246 kg); powered by Pratt & Whitney Aircraft JT8D-9 engines with 14 500 lb (64 496 N) maximum thrust and no acoustic treatment.<br><br>Model 737-200 airplane—Brake release weight of 103 500 lb (46 948 kg); powered by Pratt & Whitney Aircraft JT8D-9 engines with 14 500 lb (64 496 N) maximum thrust and no acoustic treatment. |
| Commonality | The application of parts or accessories to similar systems or to different airplane models with the objective of cost savings in production and total ownership. |
| Engine | The Pratt & Whitney Aircraft JT3D-9 or JT8D-109 (as appropriate) dry engine as supplied by the engine contractor for installation in the nacelle. |
| Inlet Cowl | That portion of the nacelle structure forward of the fan case which provides proper aerodynamic airflow direction to the engine and around the external nacelle. |
| Interchangeability | That quality in a part which will allow it to substitute for, or be substituted for, another part without changing the physical, functional, and structural requirements and by using the normal attaching means only (bolts, screws, nuts, washers, pins, etc.); this specifically |

precludes alteration of the part by trimming, cutting, filing, reaming, drilling, or forming during installation; no tools other than those normally available to service mechanics are required for installation; no operations or alterations, except designed-in adjustments, are required on supporting or surrounding structure in order to install the part.

Modified Baseline Nacelle

Model 707—The modified nacelle for the Pratt & Whitney Aircraft JT3D-9 engine; designed to meet the lower goal in noise suppression.

Model 727—The modified nacelle for the Pratt & Whitney Aircraft JT8D-109 engine; designed to meet the lower goal in noise suppression.

Model 737—The modified nacelle for the Pratt & Whitney Aircraft JT8D-109 engine; designed to meet the lower goal in noise suppression and differing from the 727 side-engine nacelle only in those components necessary to meet 737 requirements.

Nacelle

The nacelle consists of those components of an externally mounted propulsion package, including the engine, all engine-mounted accessories, the inlet cowl, side cowls, thrust reverser, and any other components suspended from the engine mounts.

Replaceability

That quality in a part which will allow it to substitute for, or be substituted for, another part, thereby meeting all physical, functional, and structural requirements, but which may require other than normal operations for installation; such operations may include shimming, drilling, reaming, filing, cutting, sawing, or forming—all of which operations are performed by the use of hand tools normally available to service mechanics.

Rudder Blowdown Speed

The speed at which the rudder hinge moment exceeds the capability of the rudder actuator.

| | |
|---|---|
| Strut | That structure necessary to separate and support the nacelle externally from the airframe; it includes primary and secondary structure and may contain provision for installation of airplane and engine systems components. |
| Thrust Reverser | The structure and mechanisms required to change the direction of flow of the engine exhaust gases, thereby providing a selective aerodynamic braking action. |

# APPENDIX C

## SYMBOLS AND ABBREVIATIONS

| | |
|---|---|
| A/C | air conditioning |
| AGD | axial gear differential |
| Alt | altitude |
| APU | auxiliary power unit |
| ARP | aerospace recommended practice |
| ATA | Air Transport Association |
| BL | buttock line |
| BRGW | brake release gross weight |
| BWL | body waterline |
| CAB | Civil Aeronautics Board |
| CAR | Civil Air Regulations |
| CSD | constant-speed drive |
| $C_V$ | velocity coefficient |
| $C_{VD}$ | velocity coefficient fan nozzle |
| $C_{VE}$ | velocity coefficient primary nozzle |
| Dan-Air | Dan-Air Services, Limited, London, England |
| dB | decibels |

| | |
|---|---|
| DOC | direct operating cost |
| EPNdB | effective perceived noise level, decibels |
| EPNL | effective perceived noise level |
| FAA | Federal Aviation Administration |
| FAR | Federal Aviation Regulations |
| $F_N$ | net thrust |
| GSE | ground support equipment |
| GW | gross weight |
| hp | horsepower |
| IAS | indicated air speed |
| IGV | inlet guide vane |
| ISA | international standard atmosphere |
| K | degrees Kelvin |
| KEAS | knots equivalent air speed |
| KTAS | knots true air speed |
| LGW | landing gross weight |
| M | Mach number |
| MAC | mean aerodynamic chord |
| $M_D$ | airplane maximum design Mach number |
| $M_{mo}$ | airplane maximum operating Mach number |

| | |
|---|---|
| NEF | noise exposure forecast |
| N | newton |
| $N_1$ | low-speed rotor rpm |
| $N_2$ | high-speed rotor rpm |
| OASPL | overall sound pressure level |
| OAT | outside air temperature |
| OEW | operating empty weight |
| P | pressure |
| PNdB | perceived noise decibels |
| PNLT | tone-corrected perceived noise level |
| $P_T$ | total pressure |
| $P_{T2}$ | engine compressor face total pressure |
| P&WA | Pratt & Whitney Aircraft |
| QEC | quick engine change |
| °R | degrees Rankine |
| RFNI | relative footprint noise index |
| SAE | Society of Automotive Engineers |
| SFC | specific fuel consumption |
| SLS | sea level static |
| SPL | sound pressure level |

| | |
|---|---|
| T | temperature |
| TAI | thermal anti-icing |
| TAS | true air speed |
| TC | tourist class |
| TE | trailing edge |
| T/R | thrust reverser |
| TSFC | thrust specific fuel consumption |
| $V_2$ | takeoff safety speed |
| $V_D$ | airplane maximum design speed |
| $V_{j\ rel}$ | relative jet velocity |
| $V_{MC}$ | airplane minimum-control speed |
| $V_{MCA}$ | airplane minimum control speed, air |
| $V_{MCG}$ | airplane minimum control speed, ground |
| $V_{MO}$ | airplane maximum operating speed |
| $V_{ref}$ | reference airplane speed |
| $V_S$ | airplane stall speed |
| $W_a$ | airflow |
| $\delta$ or $\delta_A$ | relative altitude ambient pressure, psia/14.7 |
| $\Theta$ or $\Theta_A$ | relative altitude ambient temperature, °R/518.7 |